10-6-2023

The geology, tectonic evolution, critical minerals, and glaciation of the Appalachians in northern Maine and western New Brunswick

Chunzeng Wang

Allan Ludman

David Lentz

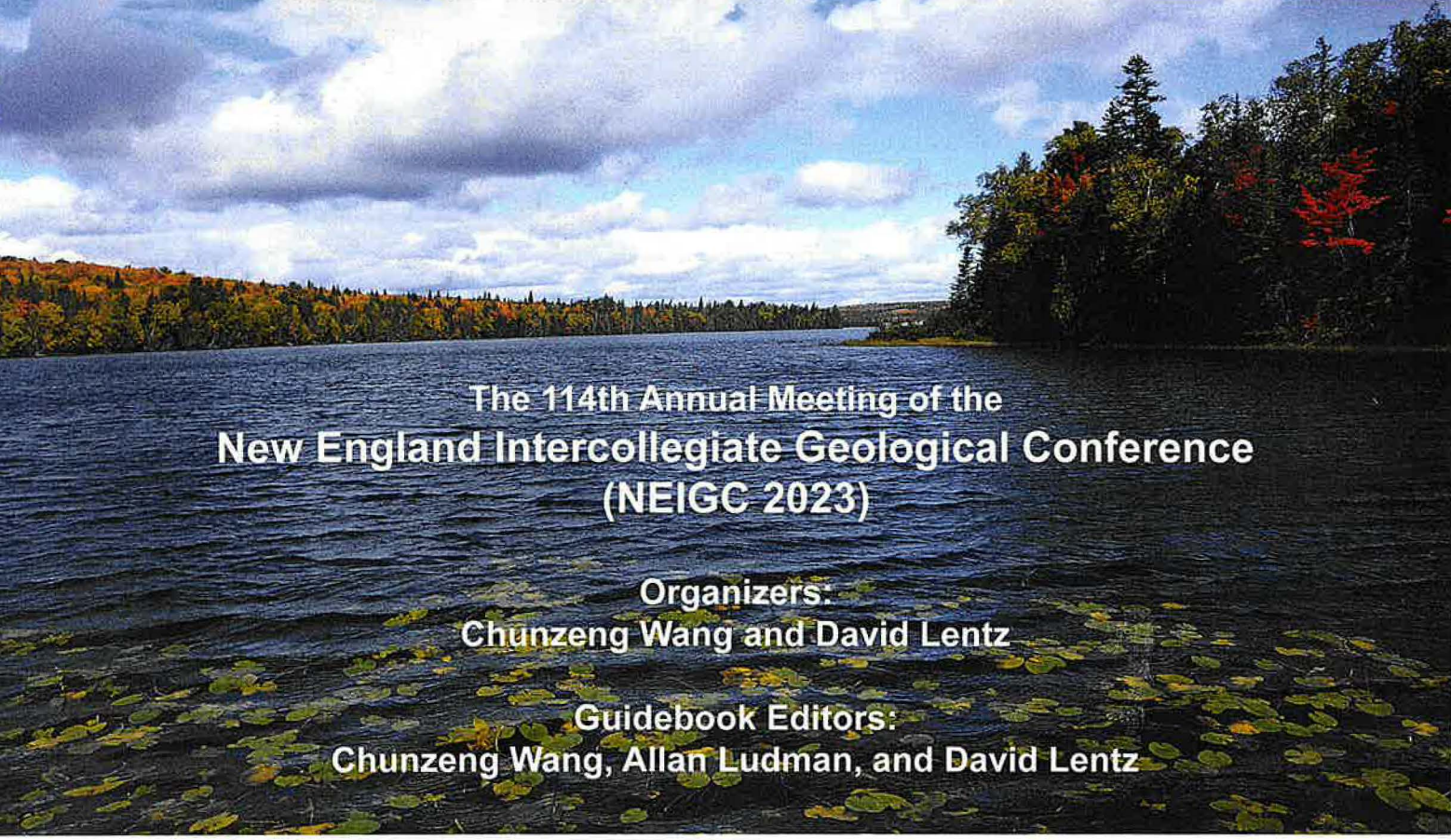

The 114th Annual Meeting of the
New England Intercollegiate Geological Conference
(NEIGC 2023)

Organizers:
Chunzeng Wang and David Lentz

Guidebook Editors:
Chunzeng Wang, Allan Ludman, and David Lentz

THE GEOLOGY, TECTONIC EVOLUTION, CRITICAL MINERALS, AND GLACIATION OF THE APPALACHIANS IN NORTHERN MAINE AND WESTERN NEW BRUNSWICK

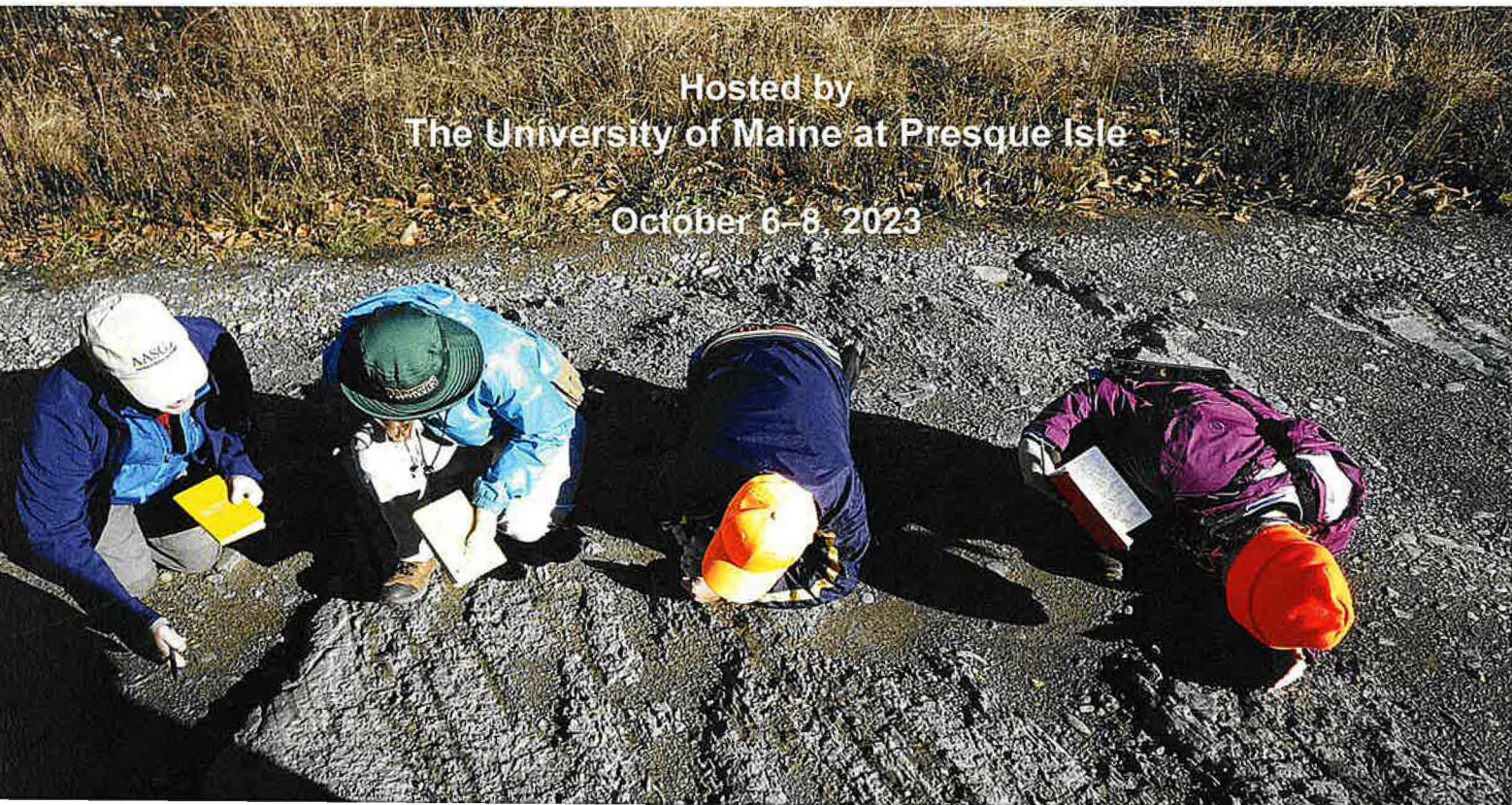

Hosted by
The University of Maine at Presque Isle

October 6–8, 2023

The 114th Annual Meeting of the
New England Intercollegiate Geological Conference
(NEIGC 2023)

THE GEOLOGY, TECTONIC EVOLUTION, CRITICAL MINERALS, AND GLACIATION OF THE APPALACHIANS IN NORTHERN MAINE AND WESTERN NEW BRUNSWICK

Organizers

Chunzeng Wang (University of Maine at Presque Isle)
David Lentz (University of New Brunswick)

Guidebook Editors

Chunzeng Wang (University of Maine at Presque Isle)
Allan Ludman (Queens College, CUNY)
David Lentz (University of New Brunswick)

Contributors

Trip A1: Allan Ludman (Queens College, CUNY)
Trip A2: Leah Page, Jeremy Ouellette, and Don Dudek (Wolfden Resources Corp.)
Trip A3: Bryan Way (Canadian Manganese Company)
Trip A4: Chunzeng Wang (University of Maine at Presque Isle) and Stephen Pollock (University of Southern Maine (Emeritus))
Trip B1: David Lentz (University of New Brunswick), Kathlee Thorne (New Brunswick Geological Survey Branch), Leslie Fyffe (Geological Consultant), James Walker (New Brunswick Geological Survey Branch), and Fazilat Yousefi (University of New Brunswick)
Trip B2: David Putnam (University of Maine at Presque Isle) and Aaron Putnam (University of Maine)
Trip B3: Chunzeng Wang (University of Maine at Presque Isle)
Trip B4: Robert Johnston and Lindsay Theis (Maine Geological Survey)
Trip C1: Adam Schoonmaker (Utica University)
Trip C2: Robert Marvinney (Former Maine State Geologist)
Trip C3: Chunzeng Wang (University of Maine at Presque Isle) and Lauren Madsen (University of Maine)
Trip C4: David Lentz (University of New Brunswick), Kathlee Thorne (New Brunswick Geological Survey Branch), and Fazilat Yousefi (University of New Brunswick)

Hosted by

The University of Maine at Presque Isle
Presque Isle, Maine
October 6 – 8, 2023

IN DEDICATION

Dr. Gary Boone
(1929–2023)

Dr. Robert Marvinney
(still busy)

IN HOHORING NORTHERN MAINE PIONEER GEOLOGISTS

Dr. Bill Forbes
(1931–2011)

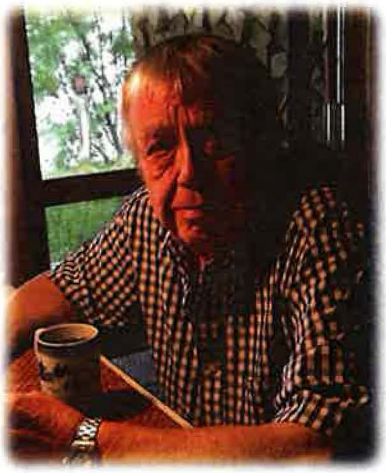

Dr. Brad Hall
(1933–2016)

Dr. David Roy
(1937–2008)

Remembering Gary McGregor Boone (1929–2023)

Mark Van Baalen (Harvard University)

When Gary Boone was a young man, his family owned a camp on Shin Pond, in the shadow of Katahdin. The adjacent camp was owned by the Brown family. Lifetime friend Bonnie Brown Potter reports that Gary was always bringing rocks back to the camp and piling them up. Gary was born in 1929 at Presque Isle, Maine, the son of well-known local doctor Storer Boone. As a teenager, he spent much time exploring the mountains and woods of Maine, including ascents of Ktaadn and The Traveler that stimulated his interest in geology. During WW II Gary became interested in aviation, living near the active Army Air Force base at Presque Isle. After a brilliant career in geology he returned to his roots. This year's 114th annual NEIGC meeting honors his contributions to our science.

After completing his undergraduate studies at Bowdoin College, Gary received a Master's degree at Brown University with a thesis entitled *Petrology of the metamorphic and igneous rocks in the vicinity of Farmington, Maine*. He continued his education at Yale University, studying under Matthew Walton and John Rodgers. His Ph.D. thesis (1958) was entitled *The geology of the Fish River Lake - Deboullie area, northern Maine*, thus firmly establishing his credentials as a Maine field geologist. Gary then took a position at the University of Western Ontario before moving to Syracuse University, where he spent much of his career. He is known as a petrologist and consummate field geologist, as well as a mentor for the next generation of scientists. Early in his career he also was influenced on petrologic issues by fellow Mainer Jim Thompson. Gary is best known for his work in the 1960's with colleagues Bob Moench and Gene Boudette on the metamorphic stratigraphy of rocks in the Rangeley region. This work led to the publication of a new paradigm for the stratigraphy of rocks in western Maine published initially in the 1970 NEIGC guide: *Bedrock geology of the Rangeley Lakes - Dead River basin region, western Maine.* It is difficult to overestimate the significance of this contribution. This paradigm, generally known as the Rangeley sequence, continues to be the standard model for understanding the stratigraphy of western Maine, New Hampshire, and even central Massachusetts.

The previous stratigraphic model for western New Hampshire was developed by Marland Billings in the 1930s and forms the basis for the 1956 NH state map. However, it proved difficult to extend this model eastward into Maine, where deformation and high-grade metamorphism made the trail hard to follow. Once the Boone/Boudette/Moench model gained acceptance it became possible to follow the Rangeley sequence westward across the border into New Hampshire, and following along strike, down into Massachusetts and Connecticut. Thus the new paradigm has withstood the test of time, as it complements the Billings stratigraphy in the western and southern areas.

Gary, however, always had a particular affinity for the rocks of the Carrabassett Valley, where his 1973 publication of the map of the Little Bigelow quadrangle is still considered a landmark contribution. Much later work on the complex Devonian Carrabassett Formation has been undertaken, for example, by Dwight Bradley and Lindley Hanson, as reported in the field guide for the 2013 NEIGC meeting. Gary co-edited the 1985 Bedrock Geologic Map of Maine, together with his late colleagues Phil Osberg and Art Hussey.

In addition to his numerous accomplishments in the field, Gary also served as a teacher and mentor, watching with pride as the careers of younger geologists emerge. The best known of these former students is Bob Marvinney, recently retired as State Geologist. Bob studied Maine geology under Gary at Syracuse, receiving a Master's degree in 1982 and his Ph.D. in 1986. Another Boone student at Syracuse, shown in a graduation photo taken in 1988, is Linda Ivany. Linda reports that she was almost persuaded by Gary to become a metamorphic petrologist, but ultimately turned to paleontology. After receiving her Ph.D. at Harvard, Linda returned to Syracuse where she is now a Professor in the geology department. Other successful students include Peter Lyttle, who had a long and successful career at USGS. In addition, Gary inspired Ellen Metzger now Professor at San Jose State, and Glenn Koller, who did a geophysical investigation of the Lexington batholith in western Maine for his 1979 Ph.D. thesis.

In retirement, as he returned to Presque Isle, Gary spent more time in the field and otherwise encouraged Chunzeng Wang, the organizer of this year's NEIGC meeting. Recalling his early interest in WW II aviation, Gary was also instrumental in the creation of the Presque Isle Air Museum, an historical gem. Gary remained intellectually active and always appreciated visitors, including the writer, to his home in Presque Isle. His last publication, with coauthor Barbara Bentley, was a 2018 map of the Wassataquoik River basin. He passed away on August 1, 2023, after a long struggle with cancer.

(The author thanks Bob Marvinney, Henry Berry, and Wally Bothner for their helpful additions to this memoir.)

Robert G. Marvinney: Field Geologist, State Geologist, Citizen Geologist

Henry Berry (Maine Geological Survey)

Field Geologist

Bob's geologic story begins in 1980 in a remote region of Maine northwest of Moosehead. The 1967 Preliminary Geologic Map of Maine shows a generalized swath of **Dss**, a purported sandy facies of the Seboomook Formation, based on "only vague generalities regarding the geology of this area" (Marvinney, 1981). Bob went to investigate. The field project involved solitary work. Bob had to rely on whatever resources he brought with him. There were no cell phones or internet, so geologic features were interpreted from his classroom training and a few textbooks in the truck. Description was paramount. This was pioneering geology, exploration and discovery. As one of Gary Boone's graduate students, he was visited in the field by his advisor, and he talked with other students.

The tangible impact of this mapping project is that it fundamentally changed our understanding of the stratigraphy and tectonics of that segment of the Appalachian orogen. We now know that the Frontenac Formation with its volcanics are in a Silurian extensional basin, the Second Lake Rift, related to a series of faults connected through southern Quebec into northern New Hampshire, and that this extensional event pre-dates deposition of the Devonian Seboomook Group (Moench et al., 1995; Marvinney et al., 2001). There was also an intangible impact, on Bob – developing his skills of patience, observation, fact-based analysis, perseverance, self-sufficiency, and interpretation from incomplete data. Bob became known as an adept stratigrapher.

The ensuing technological revolution in geologic map production is recounted well by Bob himself in his series of State Geologist messages published in the Geological Society of Maine newsletter. I refer you to those 63 messages, compiled by Amber Whittaker as a special edition of The Maine Geologist (2012, vol. 47, no. 3). When Walter Anderson hired Bob in 1987 to begin a GIS program at the Maine Geological Survey (MGS), it was because Bob had both GIS knowledge, hard-won at Exxon in Houston, and Maine geology experience. Bob is a field geologist at heart. In his first years at MGS, in addition to implementing (pioneering) the state's first GIS system he continued to do field work, and visited field geologists in many parts of Maine, gleaning wisdom from the likes of Gates, Ludman, Hussey, Moench, Boudette, Hanson, and Roy. He reviewed and edited maps for publication and supported the bedrock mapping program. A major scientific contribution during this time was co-editing with Bob Tucker the "Jackson Volumes," a set of six volumes of peer-reviewed technical articles on Maine geology.

State Geologist

When Walter retired as State Geologist in 1995, Bob's decision to apply was swayed by Walter's assurance that "it will be fun." That line was to be repeated around the office on various occasions for years. It took a while to appreciate Walter's sense of humor. Yes, there are rewarding opportunities to guide policy, to solve problems, to educate the public, but it is a demanding job. While Bob's 26 years of service in the position are impossible to encapsulate, some important themes emerged.

The State Geologist is a geologist. Even while fulfilling his role as chief executive of MGS, Bob remained engaged in field mapping, publishing bedrock maps for the Augusta and Readfield quadrangles. He conducted field reviews with contract mappers and attended formal and informal field trips. He co-authored 21 technical presentations at professional meetings on a variety of topics.

Facts matter. Whatever the issue under public discussion, Bob responded with research, facts, analysis, and synthesis to arrive at a simple, defensible declarative statement to be repeated as many times as necessary. Here are a few examples.

- Since 1912, sea-level in Portland has risen at 8.7 inches per century.
- The likelihood of a damaging earthquake is small (but not zero).
- One inch of Sebago Lake contains 800 million gallons of water.
- Annual groundwater recharge in Maine is about 2 to 5 trillion gallons.
- Test your water for arsenic.
- The Gulf of Maine north of Georges Bank has no potential for hydrocarbon accumulations.
- The reason Maine has no oil or gas production is because our rocks have no oil or gas.

Such statements have calmed fears and avoided unnecessary and irrelevant legislation.

Seeing is believing. When there were assertions that groundwater levels were being depleted by extraction for bottled water, Bob visited all of Poland Spring's well sites and saw flowing springs at each one. In response to a constituent complaint about environmental damage at the Pickett Mountain mineral exploration site, Bob assured the legislative committee that he had visited the site with DEP, and that regulations were being followed. At the

catastrophic Rockland landslide in 1996, Bob not only appeared on camera for the TV interviews, but he also met off-camera with city officials to discuss options.

Sometimes facts don't matter. This was a frustrating realization. Politics or other factors can override science and logic. That Bob was reappointed by 4 governors of three political parties is a testament to his even temper and professionalism.

Technology is good. A proponent of GIS, online maps and data, LiDAR imagery, Bob continually sought to improve the way geologic information is collected, analyzed, stored, and distributed. MGS has been among the national leaders in using and providing digital geologic information.

Let's get together. On many important issues, Bob organized panel discussions, meetings, or field trips for stakeholders to understand geologic issues and to listen to each other. Water resources, coastal dune regulation, coastal erosion, mining regulations, mineral resources, and more. He had formal leadership roles on the Maine Climate Council, Water Resources Planning Committee, and Ocean Energy Task Force, bringing reliable scientific information into the conversation.

On the national stage, Bob was an active member of the Association of American State Geologists (AASG), including a term as president from 2005-06. He participated in policy-making discussions and served on review panels for grant proposals under the National Cooperative Geologic Mapping Program. He advocated for small state geological surveys who depend on federal funding to supplement their operating budgets. Bob visited the offices of the Maine congressional delegation in Washington many times, even as the occupants changed. He helped secure funding for geologic mapping, coastal process management, resource investigations, and geologic hazard studies. When there were proposals to consider offshore oil and gas leases off the Maine coast, Governor Baldacci sent Bob to testify before Congress on our behalf.

Every state agency expects a certain amount of administrative adjustment. During Bob's years as State Geologist, the MGS faced unprecedented budgetary reductions and department reorganizations. Through it all, Bob's focus was on trying to preserve the scientific integrity of the programs and care for the staff as much as possible. His dedication to the mission of the survey and to the geologists did not go unnoticed, even as his own administrative workload increased substantially. His management style was to shield the staff from the bureaucracy so the geologists could do science. Before retiring he began the process of separating the State Geologist from the Bureau Director position so that no one would ever again have to try to do both jobs. He left MGS poised for the future.

Citizen Geologist

His final message as State Geologist to the GSM Newsletter (vol. 47, no. 2, p. 2) is entitled *Signing Off*. This is a typical closing when someone is going off duty. It was clear that Bob needed a break, but he was not going away. If anything, his freedom from administrative duties has renewed his passion for geology and its importance in public decision-making. In his retirement, Bob is serving on the Maine Board of Environmental Protection, helping MGS review and edit new bedrock maps, providing consultation on MGS's northern Maine projects, participating in a New England regional stratigraphy project, and was seen on the Geological Society of Maine field trip this summer.

Keep an eye out for Bob. If you see him around, say thanks from the people of Maine!

Chunzeng Wang, Amber Whittaker (MGS), Bob Marvinney, and pillow basalt in Fish River Lake area, Aroostook County, September 30, 2021. (Photo courtesy Steve Pollock)

William H. "Bill" Forbes – Maine Paleontologist (1931–2011)

Gary M. Boone

(Note: Gary wrote this tribute for the Bill Forbes memorial at the 2012 Geological Society of Maine spring meeting held at the University of Maine at Presque Isle on April 13, 2012)

Bill Forbes was born in Bingham and grew up in Caribou, Maine. He attended Caribou primary and secondary schools and graduated from Caribou High School in 1949. It was in primary school that he began his life-long love of searching for and finding fossils. A sister of Bill's recalls that after school Bill would walk down Main Street toward his father's garage, but often would stop to visit with Olof Nylander, an elderly, grandfatherly figure.

There he fell under the spell of Olof O. Nylander, an emigré from Sweden who made his way to Aroostook County in the 1890s, making a name for himself with finds of Silurian and Devonian shelly faunas in company with U.S. Geological Survey (USGS) geologists H.S. Williams and H.E. Gregory. He eventually became a teacher of courses in natural history at Caribou High School. The Caribou city-sponsored Nylander Museum is dedicated to his collections. Bill emulated Nylander in his interest in Natural History, collecting – especially fossils – and later, in a love of teaching. In addition, the two were similar in that each had only a high school formal education; they each received honorary degrees: Nylander, an M.Sc. from U. of Maine in 1938, and Bill, as described below.

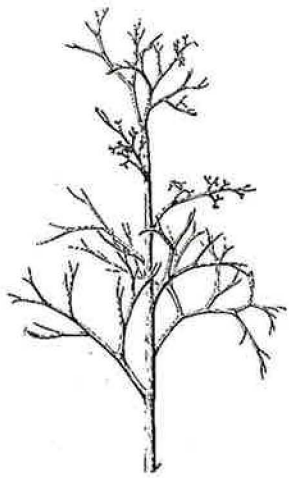

Psilophyton forbesii

Bill was a scholar in the traditional sense. He had a voracious interest not only in earlier geological books, journals and maps, but in many areas of the natural sciences worldwide. Two thick volumes listing his hundreds of holdings are in the Special Collections of the University of Maine at Presque Isle (UMPI). He became self-educated in the biological science of classifying fauna and flora, as well as how to prepare them for preservation in scientific collections. He eventually was invited to apprentice under a specialist in that field at the U.S. Natural History Museum in Washington.

After Bill's graduation from high school in 1949, Bill needed to find work. All the more necessary as he was soon to marry his life-long companion, Warrena Bugbee of Washburn. He landed a job with the National Cash Register Co. (NCR), commissioned to travel to stores around the County to sell or upgrade their counter-top sales - - - "Catch-Ching!" He was obliged to use the family vehicle, which Warrena says was an elderly gray & tan station wagon.

Bill was a persuasive salesman, and in his extensive travels throughout the County, he managed to find himself at his hour-long lunch break at a roadside outcrop, where he could 'work' the upturned folded strata inch by inch, and thereby discover new fossil finds. He thus began his outcrop-by-outcrop coverage, in road-cuts, on logging roads, and river- and stream-exposures in the woods, and his remarkably detailed geologic-paleontological analysis of Aroostook geologic history.

One day, probably early 1950s, he stopped for his lunch break at a roadside outcrop between Presque Isle and Ashland, pre-occupied as usual, when a large USGS van pulled up behind Bill's old station wagon. Out piled several geologists, in the vanguard was Prof. Henry N. Andrews, Jr., paleobotanist at the University of Connecticut, Prof. Eli Mencher, of Massachusetts Inst. of Technology (MIT), and Dr. James Schopf, of the USGS. When asked what he was doing, Bill replied that he was collecting fossil plants. Bill is then believed to have said: "This is nothing; you should see what I have in my basement." The field party spent the rest of the afternoon with Bill. Later he invited them to his home in Washburn where he showed them his extensive collection of fossils. And so began Bill's lasting association and friendship with many paleontologists at the USGS, the U.S. National Museum of the Smithsonian, and especially with Henry Andrews of the Univ. of Connecticut. Andy Kasper adds: "As a new graduate student in Andrews's laboratory, I worked with Henry on the publication of a new species of early Devonian vascular plant from Baxter State Park named after Bill Forbes, i.e., *Psilophyton forbesii*."

Then began a remarkable turn of events for Bill. Brad Hall recalls that around 1968–1969 when Bill went for a teaching position at the then Aroostook State College of the University of Maine, Brad and a number of his colleagues at Orono "provided a written, signed testimonial to the fact that Bill was in our minds qualified. The list of signers was impressive: Art Boucot and Robert Shrock of MIT, Bob Neuman and Ellis Yochelson of the National Museum, and I believe Marland Billings of Harvard." And so Bill Forbes was appointed a part-time lecturer beginning Sept. 1, 1970. He quickly advanced to full-time instructor in geology at about the time of the college's change of name to the University of Maine at Presque Isle, in 1971. He was promoted from Associate to full Professor of Geology in 1985.

When Bill began teaching at UMPI, an honorary D.Sc. degree was bestowed upon him by Ricker College, of Houlton, in April of 1970. From then until his retirement with emeritus status in the early 1990s, his students always referred to him with affection as Doc Forbes.

In the latter half of the 20th Century there was hardly another person, armed only with a high school education, who became a self-taught leader in the field of paleontology and paleobotany. He has had a number of fossil species named after him, among which is *Psilophyton forbesii*, already mentioned.

He also was a co-discoverer of one of the earliest sporangia-bearing small trees, *Pertica quadrifaria*, in the shales of the Early Devonian (late Emsian) Trout Valley Formation (c. 395 Ma) in northern Baxter State Park.

In Andy Kasper's words: "In July 1968, Henry [Andrews] and I headed for Baxter State Park. . . and the "Crossing" on Trout Brook in the Trout Valley Formation. . ." On the 18th of July, they discovered fossils that ultimately would be named *Pertica quadrifaria*. "In . . . July of 1971 Bill Forbes and I were slogging up Trout Brook. . . it was a bright sunny day and Bill and I were slipping and sliding on the algal-covered rocks." They were about to head back for lunch, ". . .but I suggested we just turn the bend up ahead. A minute later I spotted a large block in the middle of the brook . . . some 2 1/2′ × 3′ and about 10″ thick with three large vertical bands, [which] I knew immediately were plant stems, and put a chisel to the edge of the block. . . the rock split perfectly into two magnificent halves – bluish matrix with maroon, inch-wide plant stems. . . How to transport two such heavy blocks? After lunch we returned with ropes, cut a tree, tied one block to the tree, and Bill and I carried the block with the tree extended from his shoulder to mine – slipping and sliding all the way back. We did the same for the other. . . Later that day Bill traced the loose blocks in the brook to the actual outcrop – which provided abundant [pieces] of *Pertica quadrifaria*. Because of the spectacular size and appearance of this fossil plant, Bill Forbes promoted it as suitable for the State Fossil."

Upon an act of the state legislature, it now is designated as Maine's official fossil. An artist's reconstruction of *Pertica* is on display in the Maine State Museum.

In the 1950s the quest to map Maine's geology, both bedrock and surficial, was at a fever pitch. The USGS hatched the grandiose scheme to map 15′ quadrangle transects across strike, starting at Maine's western boundary and over the next few years, to "march" toward the coast – quadrangle by quadrangle. We dubbed it the "Lemming Project."

From time to time, great conclaves were held to review field-work-in-progress. Such it was, around 1956, that a Great Gathering of us lowly grad students, profs, and survey geologists congregated at Presque Isle's Northeastland Hotel. Assembled were the High and Mighty from Harvard, Yale, MIT, the USGS from Washington and the Maine Survey. Plans had been for breakfast the next morning at 4:30 to allow time for all concerned to travel in caravan-style to the Munsungan region to view some spectacular finds made by Brad Hall in his mapping there, and to return to Presque Isle for the night.

By this time Bill's fame was growing, and he was invited along. In the pre-dawn darkness, Bill walked along Main Street toward the hotel. Suddenly he spotted a sleeping bat clinging to the brick façade of a building. He stopped, took off his floppy field hat, lifted the bat to the top of his head, replaced his hat, and walked through the hotel's main entrance. Art Boucot of MIT spotted Bill and told him he should meet the Mightiest of All, Professor Marland Pratt Billings of Harvard University. As Bill was introduced to Marland Billings, he started to shake hands, and with his other hand, removed his field hat – and out flew the bat. Jackets, hats and rolled-up newspapers were aimed at the bat, light fixtures swinging, draperies coming down. Bill's love of a practical joke was enjoyed by a now-fully awakened two-dozen or so geologists.

Ever after, people knew Bill Forbes for both his humor and his ability as a field investigator and internationally known researcher of Devonian paleobotany.

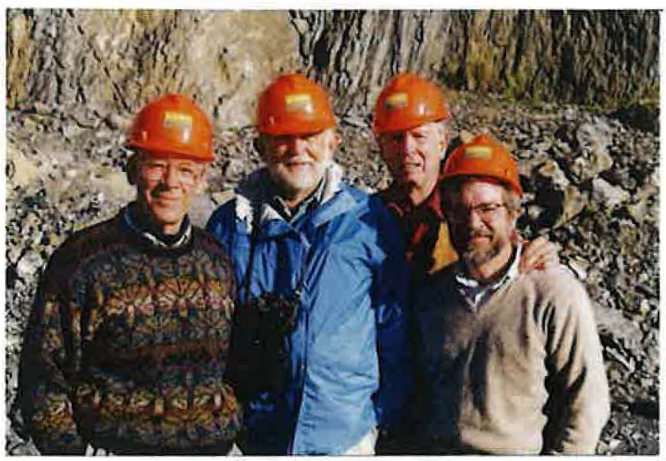

Bill Forbes, Art Hussey (Bowdoin College), Gary Boone, and Bob Marvinney at Lane quarry, Presque Isle, 1998.

Remembering Bradford A. Hall (1933–2016)

Stephen Pollock (University of Southern Maine (Emeritus))

Bradford Hall, or Brad as he preferred, established himself as a major contributor to northern Appalachian geology with the release of Maine Geological Survey Bulletin 22 "*Stratigraphy of the Southern End of the Munsungun Anticlinorium, Maine*" in 1970. The bulletin with the wonderful color map was published just three years after the release of the "Preliminary Geologic Map of Maine". The release of Brad's bulletin immediately made a large area of the 1967 map obsolete. Brad always spelled Munsungun with a "u" as opposed to Munsungan with an "a" as shown on the topographic map. When asked about this he replied, "We always spelled it with a "u"". Brad's father operated Bradford Camps on the north shore of Munsungun Lake for years. Bradford Camps on Munsungun Lake were named for Brad. Brad was a registered Maine Guide and private pilot. The time came when Brad was faced with a choice whether to be a sporting camp owner and operator or continue as a college professor. Brad chose the latter and Bradford Camps were sold. Bradford Camps continues operation to this day, but Brad retained a camp on the perimeter of Bradford Camps until his passing.

Brad was drafted into the army in the 1950s and stationed in Germany. Brad liked to tell a story about his deployment in cold war Europe. He and his squad while on field maneuvers came up to a farmhouse in Germany where they were invited to lunch. The farmer offered them cheese and bread. He said the farmer took them to a large block of farmer made cheese. The cover was laden with chicken droppings. The farmer scraped off the chicken droppings and removed the cover. With laughter Brad declared that it was the best cheese he ever ate.

After his stint in the U.S. Army Brad studied geology at Yale with John Rodgers as his mentor. Rodgers in his later years was considered the "Dean of Appalachian Geology". Brad earned his PhD in 1964 and took an Assistant Professorship at the University of Maine. Brad's dissertation was the map of the Spider Lake 15' quadrangle. During the 1960s through the 1980s geology departments such as Yale considered the mapping of a 15' quadrangle in New England worthy of a dissertation.

Brad mapped beyond the Spider Lake quadrangle into Umsaskis Lake, Musquacook Lakes, Churchill Lake, Chesuncook and Telos Lake 15' quadrangles for MGS Bulletin 22. It is easy to forget that his mapping was done without the benefit of GPS, LiDAR and geophysical surveys. Brad mapped at a time when orienteering was done by pace and compass. As an example, this is Brad's location description for fossil collection BH 156 – 66. *"LOCATION: Intersection of 1160 foot contour line with S2°E bearing from triangulation point on hill (Spider Lake quadrangle) north of Little Leadbetter Pond (Telos Lake quadrangle).* Brad accessed the more remote areas by float plane or long traverses. Woods roads by today's standards were primitive at best. Today's logging practices together with a plethora of wide woods roads has opened up the north Maine woods. Construction of these roads necessitated opening borrow pits for road materials. This construction created outcrops unavailable to Brad at the time of his mapping and compilation. The number and quality of these pits was unimagined during his mapping and compilation efforts. An examination of Brad's Munsungun map shows just how few roads there were. Brad told of being flown onto a lake by his father, he made his traverses and then would picked up at a designated time. His choice of water transportation was an Old Town 20-foot cedar and canvas guide canoe. The canoe served Brad well on the large lakes such as Spider, Telos, Clear, Pleasant, Matagamon and others. His map shows substantial outcrop locations, but also shows the limited control he had on contacts as well as uncertainty of formational assignments. Experienced mappers know that detailed first time on foot mapping has its own set of challenges. Brad's generation mapped at the 15' scale while our generation maps at the 7.5' scale and larger. Brad never confided about his choice of structural terms to describe the complex belt of rocks, but the 1985 Bedrock Map of Maine as well as his Yale mentor liberally used the terms "synclinoria" and "anticlinoria". Plate tectonics had not been "invented" during Brad's time at Yale and mapping for his bulletin. The gospel during his time at Yale was the Geosyncline. Brad's work established the Late Ordovician volcanic complex. These volcanics are now recognized as an island arc. The distribution of these felsic volcanic rocks in MGS Bulletin 22 has been used in many peer-reviewed papers seeking to define orogen scale tectonic models.

The lasting importance of Bulletin 22 was the recognition of complex volcanics of Ordovician age together with the mafic volcanic belt of Silurian volcanics with associated Siluro – Devonian sedimentary rocks together with Early Devonian slate and sandstone. Of considerable importance was the 73 fossil localities that Brad collected. Brad successfully networked with the leading invertebrate paleontologists of 20th century North America. The prolific brachiopod specialist Arthur Boucot and the leading graptolite specialist W.N.B. Berry were members of Brad's network. Brad's 1969 paper extended the idea of the pre-Late Ordovician Penobscot Orogeny west of the type area defined by Bob Neuman. Bob was a close colleague of Brad.

A National Science Foundation award together with funding from the Maine Geological Survey allowed Brad to fund graduate students to study Early Devonian rocks in the vicinity of Matagamon Lake. Work here resulted in several

publications defining the nature of a delta – prodelta complex. The short paper in a 1976 Geological Society of America Memoir was an important contribution to Maine Geology and has been cited by multiple authors.

Brad was a compiler to the Bedrock Geologic Map of Maine and most of his compilation responsibilities were in the area covered in MGS Bulletin 22. However, his compilation extended formations in Bulletin 22 to the northeast. Some of this extension of formations was partially driven by the location of Maine Forest Service fire towers whose trails provided easier access. One of these fire towers was on Norway Bluff adjacent to Munsungun Lake and another on Round Mountain, northeast of Munsungun Lake.

Brad's emphasis was on rocks, but he used his field work to supplement his other interests. On a geology field trip during hunting season, Brad used his deer rifle to harvest a Ruffed Grouse. On a fossil collecting trip Brad spotted oyster mushrooms growing about 12 feet above the forest floor. After acquiring an appropriate harvesting device (aka a long stick) he secured the mushrooms. Newspapers intended to wrap fossils quickly became wrapping paper for the mushrooms. Fresh oyster mushrooms lightly sauteed with onions are a gourmet delight. Along the shore of Bradford Camps Brad and his father collected "Indian artifacts" made from chert which crops out in the Munsungun Lake Formation. Brad showed these artifacts and chert outcroppings along Norway Bluff and Round Mountain to Rob Bonnichsen, a newly hired anthropologist and archaeologist at UMO. Bonnichsen, seizing upon the importance of the chert artifacts and the outcrop sources, acquired NSF funding for archaeological investigations. Chert, which crops out in the Munsungun Lake Formation from Round Mountain southwest to Line Brook Mountain (which is in the southern portion of MGS Bulletin 22) is now recognized as one of the most important, if not the most important, source for stone tools used by indigenous cultures in northeastern North America.

Chunzeng Wang, Don Zillman (UMPI President 2006–2012), Art Hussey (Bowdoin College), Walter Anderson (former State Geologist), Brad Hall, and Gary Boone at the 2012 Geological Society of Maine spring meeting held at UMPI. A Bill Forbes memorial was part of the program. Zillman and Wang hold well-preserved plant fossil specimens collected by Bill.

Brad Hall in the Munsungun Lake area in middle 1950's.

Remembering David Chalmer Roy (1937–2008)

Stephen Pollock (University of Southern Maine (Emeritus))

Dave's father and mother were both geologists. Hence Dave was exposed to geology throughout his formative years. Dave spent his career as a faculty member at Boston College, and his obituary notes that he was an excellent teacher. In 1979, he was profiled in Boston College's internal publication "Boston College Colleague" (Volume 4, Number 5, January 1979). Early in his life Dave felt the call to ministry, but, as stated in his profile, he had "my road-to-Damascus experience." Here Dave was quoted as saying: "I was pounding around the Rockies, and I was standing on Bighorn Mountain, looking out at the Bighorn Basin, and suddenly, for the first time, I saw systematics in rocks—all the things my parents had been showing me for years! Goodbye ministry; hello geology." Dave understood what it was to be a "GK" (geologist's kid). In April 1997, our son Seth was five weeks old when Dave wrote Seth a letter on Boston College letterhead. This is part of the letter:

Dear Seth;

".... There is one small problem that you may now be aware of. Your father is a geologist. I can tell you that his professional nature is not as bad as it sounds. Both my father and mother were geologists and on the whole, they treated me and my brother very well. One difficulty that I warn you of, however, is the tendency for geologists to make frequent stops along highways and road cuts. This will slow down your arrival to a fun place or lengthen the time until you have lunch. Once you stand on your own two feet your father will start using you as a "scale" in pictures. It is very embarrassing because people driving by will think that you have a crazy father. They simply don't understand that you have a father who loves you and wants to have a record of your growth. He will also use pictures in class and at professional meetings. This is good because lots of folks will know who you are once you have grown up. ..."

Yours truly,

David C. Roy

Geologist and Father – of – Three

After serving in the U.S. Army and graduating from the Iowa State University, Dave earned his PhD in 1971 from the Massachusetts Institute of Technology. The title of his dissertation was: *The Silurian of Northeastern Aroostook County, Maine.* Dave was a sedimentologist and sedimentary geologist, but, above all, a field geologist. His professional interests were broad and extended well beyond the geology of northern Maine, but it was in northern Maine geology that he made a significant impact. Dave's 483-page dissertation was condensed into a paper in Geological Society of America (GSA) Memoir 148 with Ely Mencher as his co-author. This article formally introduced one new group, three new formations, revised the names of three formations and introduced "provisional members" of one formation. Details were still incompletely known at the beginning of Dave's dissertation work, but Dave benefited from Henry Shaler Williams 1916 USGS Bulletin 89, *The Fauna of the Chapman Sandstone, Maine*, and the multiple publications (mostly USGS Bulletins) by Louis Pavlides and a few other publications of the 1960s. Dave's dissertation provides details of paleontology, and, by looking at the dissertation's appendix, Dave had significant support from noted paleontologists of the era. In the late 1970s and early 1980s, Dave continued his contributions to northern Maine geology by mapping several 15' quadrangles for the Maine Geological Survey which spanned the distance from Houlton westward to the Quebec boundary and south to Sherman. In addition, Dave with Dorothy Richter described the prehnite-pumpellyite very-low-grade metamorphism of northeastern Aroostook County in GSA Memoir 146 (1976).

As a result of his deep knowledge, Dave was the compiler of eastern Aroostook County for the 1985 Bedrock Geologic map of Maine. Gary Boone along with Dave co-compiled the Early Devonian of central Aroostook County, and he co-compiled with Gary Boone, Eugene Boudette, and Bradford Hall the northwestern portion of Aroostook County.

During the late 1980s, Dave, Lindley Hanson and I did detailed mapping along the Quebec border in northwestern Maine. Dave and I had different opinions about the contact between the Little East Lake Formation and the St. Daniel mélange. There was less than a stone's throw between two outcrops. Driving through the little village of St. John I passed a business that built and maintained logging roads. I turned around and inquired what would be the cost to rent a bulldozer and excavate a trench about 50 feet long along one of the roads west of Allagash. I called Walter Anderson, Maine State Geologist, and told him I wanted to excavate the contact and that the cost would be $1100. Walter provided the money. On a drizzly cold day in October 1988, a large bulldozer dug a trench about 8 feet deep, 12 feet wide and about 50 feet long. The contact was exposed, and it was a fault. The fault is shown on our 1991 map of the St. John region.

Dave, with Richard Naylor, organized the 1980 NEIGC trips in northern Maine, the first ever in the region.

Sponsors

CLWH

Clayton Lake Woodlands Holdings, LLC.

LandVest®

REAL ESTATE · FOREST RESOURCES

maine DEPARTMENT OF Agriculture Conservation & Forestry

GEOLOGY

IRVING

IRVING WOODLANDS, LLC

KINROSS

FREEMAN RESOURCES

WOLFDEN

North Maine Woods, Inc.

P. O. Box 421, 45 Main Street, Ashland, Maine 04732

"Experience the Tradition"

7 ISLANDS LAND COMPANY

FIELD TRIPS
(TABLE OF CONTENTS)

Friday, October 6

Saturday, October 7

Sunday, October 8

Supplementary

A TRANSECT ACROSS THE SOUTHERNMOST SEGMENT OF THE CAMBRO-ORDOVICIAN MIRAMICHI TERRANE IN EAST-CENTRAL MAINE

Allan Ludman
School of Earth and Environmental Sciences (emeritus)
Queens College (CUNY), Flushing, NY 11367. Allan.Ludman@qc.cuny.edu

INTRODUCTION

The Miramichi terrane is the largest belt of pre-Late Ordovician rocks in the Northern Appalachians, extending nearly 450 km from Chaleur Bay in northern New Brunswick to east-central Maine where it narrows dramatically and terminates abruptly south of the town of Greenfield (Fig. 1). The terrane is separated everywhere along its length by faults from Late Ordovician through late Silurian to early Devonian strata– in eastern and east-central, Maine, the Central Maine/Aroostook-Matapedia (CMAM) basin to the northwest and the Fredericton trough to the southeast (Fig 1). Its continuity is interrupted by large Devonian granitoid bodies, first by the polyphase Pokiok complex at the Maine/New Brunswick border. To the southwest, the Whitney Cove and Passadumkeag River plutons of the Bottle Lake complex separate a broad Danforth segment from a smaller Greenfield segment (Fig. 2).

This trip is a transect across the Greenfield segment, until recently the least studied part of the Miramichi terrane. It focuses mostly on the Cambro-Ordovician Miramichi stratigraphy, chiefly its Early Ordovician volcanic rocks, and on the cause of its termination, and looks only briefly at the flanking cover rocks. Glacial deposits limit outcrops to <1% of the study area. Rocks visited on the trip were metamorphosed regionally to only lower greenschist facies conditions (chlorite zone) and most primary volcanic and sedimentary features are preserved well.

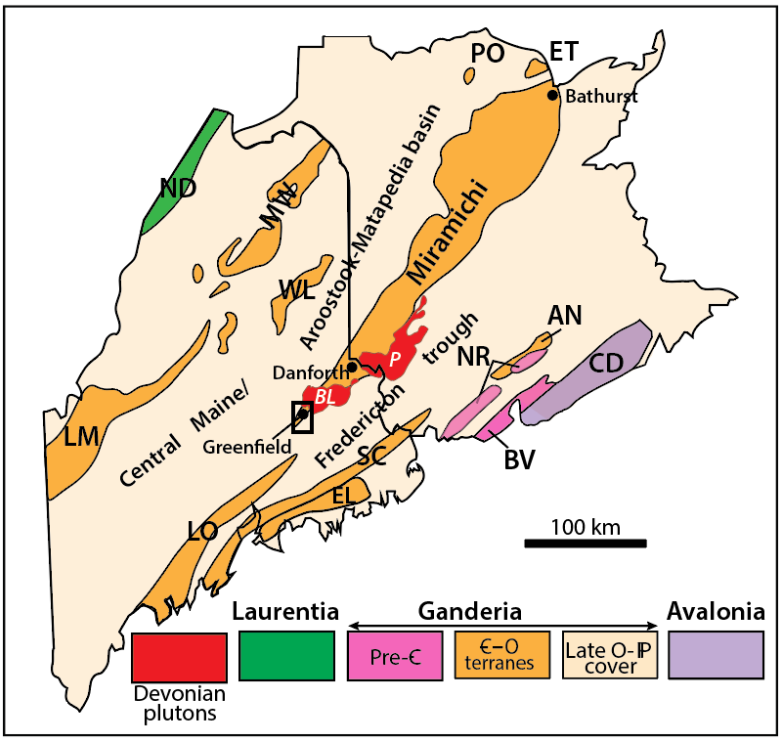

Figure 1. Lithotectonic framework of Maine and New Brunswick. Small rectangle shows field trip location. **Terranes**: AN-Annidale; BV-Brookville; CD-Caledonia; EL-Ellsworth; ET-Elmtree; LM-Lobster Mountain; LO-Liberty-Orrington; MW-Munsungun-Winterville; ND-Notre Dame; NR-New River; PO-Popelogan; SC-St. Croix; WL-Weeksboro-Lunksoos Lake. **Plutons**: P-Pokiok; BL-Bottle Lake complex.

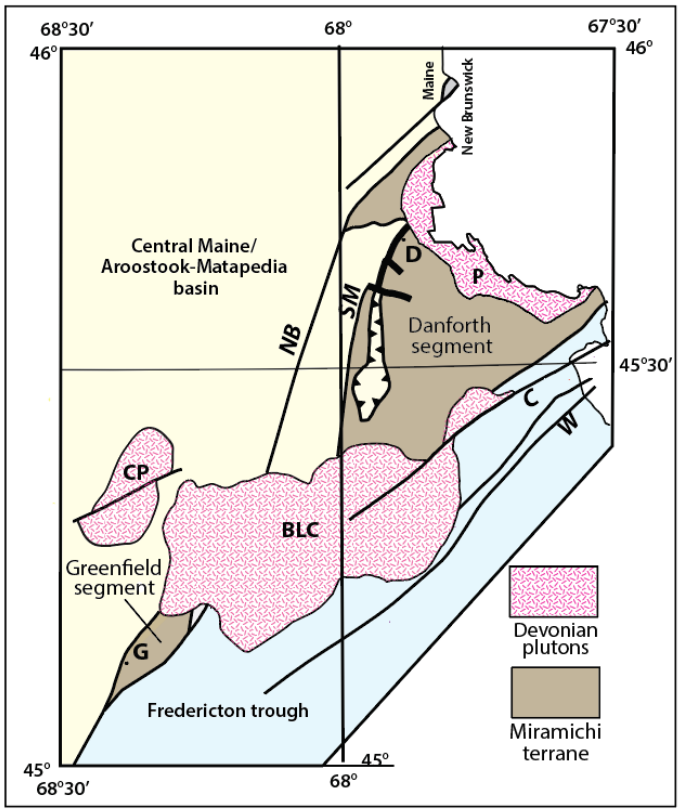

Figure 2. The Danforth and Greenfield segments of the Miramichi terrane in Maine. D=Danforth; G=Greenfield. *Plutons*: P= Pokiok plutonic complex; BLC = Bottle Lake plutonic complex; CP = Center Pond pluton. *Faults:* NB=North Bancroft; SM=Stetson Mountain; C = Codyville and W=Waite strands of the Norumbega fault system.

PREVIOUS WORK

The Miramichi terrane has been studied extensively in northern New Brunswick where it hosts volcanogenic massive sulfide deposits (e.g., Wilson, 1993; Wilson et al., 2015; Whalen et al, 1998; van Staal et al. 2003), and in west-central New Brunswick in the Benton-Eel River area (Venugopal 1978, 1979; Fyffe 2001; Fyffe and Wilson 2012). Early reconnaissance of the Danforth segment by Larrabee et al. (1965) and my compilation for the Maine Bedrock map (Osberg et al., 1985) were followed over the next forty years by detailed mapping (Sayres, 1986; Ludman, 1978, 1991, 2003; Hopeck, 1998; Ludman and Berry, 2003; Ludman and Hopeck, 2020). Until recently, however the only studies of the Greenfield segment were an unpublished University of Maine Master's thesis (Olson, 1972) and reconnaissance (Griffin, 1976a, b) that covered small portions of the Greenfield and Otter Chain Ponds 7½' quadrangles. The geologic map in Figure 3 incorporates more recent detailed mapping, geochemical, and geochronological studies (Ludman, 2020, 2023; Ludman et al., 2021) that revealed similarities and differences among Miramichi stratigraphy and rock types in the Greenfield, Danforth, and Benton-Eel River areas.

STRATIGRAPHY

Figure 4 shows the current interpretation of the stratigraphy of the Greenfield segment and adjacent cover rocks. There are significant unresolved issues within each of the three belts and/or correlation with rocks along strike to both northeast and southwest, so this should be viewed as the latest evolutionary stage rather than the final word. These issues are outlined briefly here and detailed in Ludman (2020, 2023. Feedback from trip participants is most welcome.

GEOLOGY OF THE GREENFIELD SEGMENT

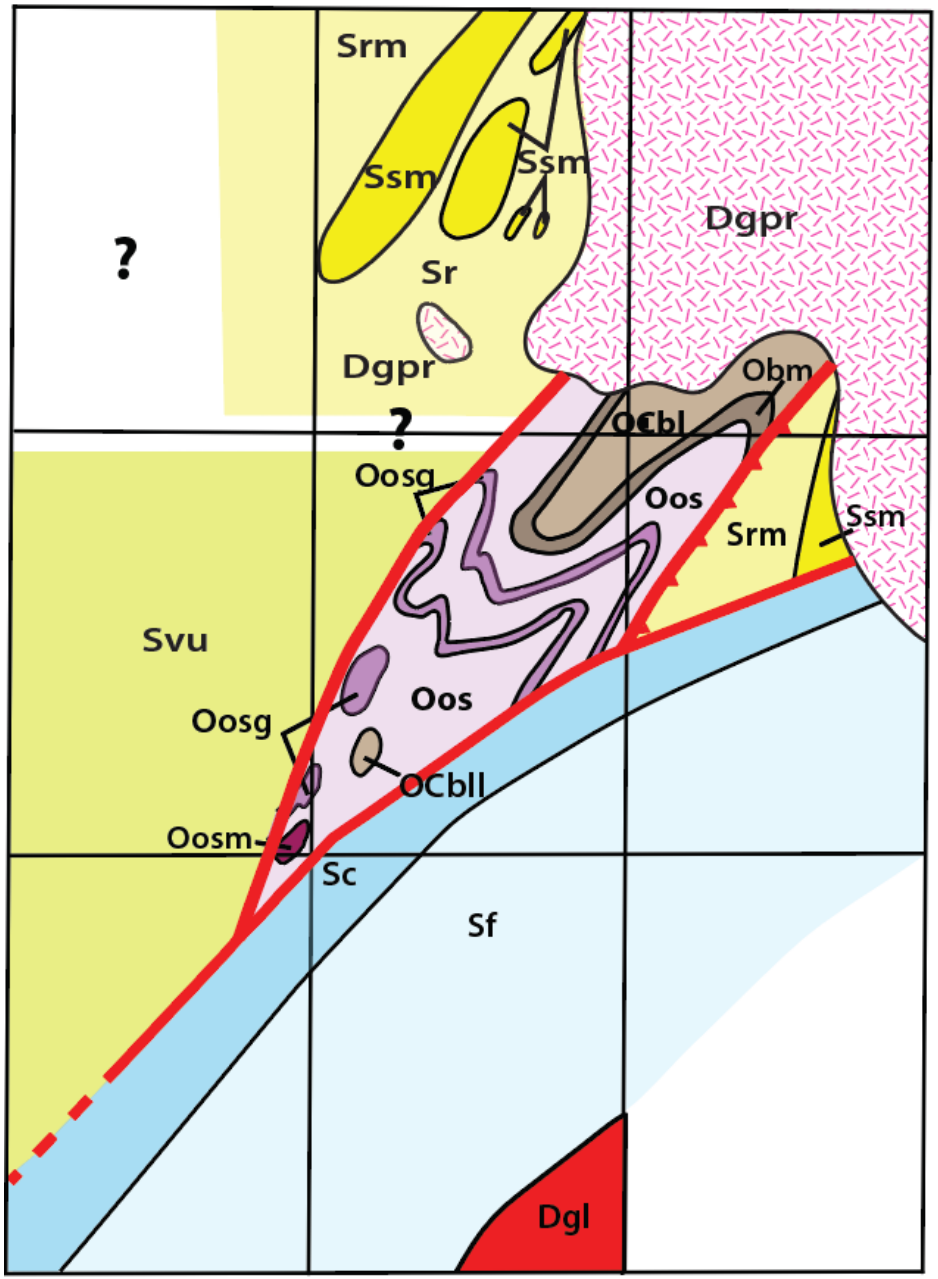

EXPLANATION

Igneous rocks
Dgpr: Passadumkeag River pluton (Bottle Lake complex)

Stratified rocks
CMAM Basin
Srm: Rollins Mountain Formation
Ssm: Smyrna Mills Formation
Ssu: Undifferentiated Silurian sandstones

Fredericton trough
Sfr: Flume Ridge Formation
Scr: County Road Formation

Miramichi terrane
Oo: Olamon Stream Formation
Oou Upper volcanic member
Oog Greenfield member
Ool Lower volcanic member
Oom Mafic member (stratigraphic position unknown)
Obm: Bowers Mountain Formation
O€b: Baskahegan Lake Formation
Obl Lazy Ledges Road member

Figure 3. Simplified geologic map of the Miramichi terrane Greenfield segment (shaded) and adjacent cover rocks.

Miramichi terrane: differences between northern and southern parts of the Greenfield segment; correlation with the Danforth segment; relationships with the nearest Miramichi volcanic rocks in the Eel River-Benton area in west-central New Brunswick.

CMAM basin: subdivision of sandstone-rich turbidites adjacent to the Miramichi terrane; correlation with CMAM strata near Danforth to the northeast and Bangor to the southwest.

Fredericton trough: Correlation with CMAM and Fredericton trough strata in the Bangor-Veazie area.

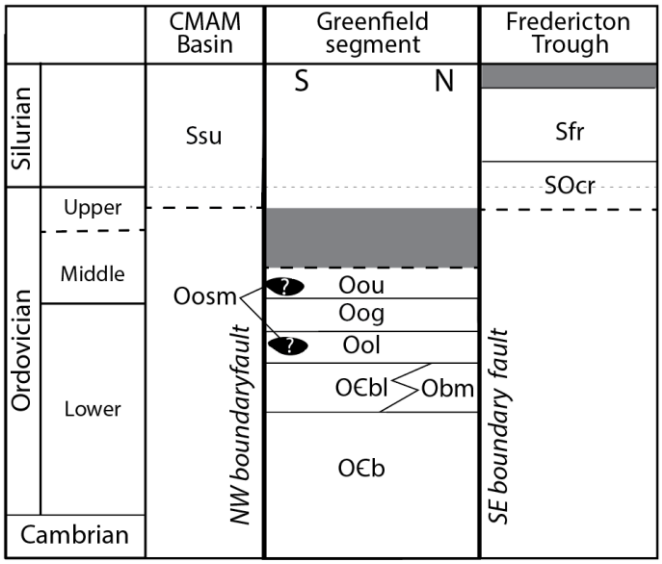

Figure 4. Stratigraphy of the Greenfield segment and adjacent cover rocks. Symbols as in Figure 3.

Miramichi terrane

The northern part of the Greenfield segment, adjacent to the Bottle Lake complex (Figs. 3, 4), is underlain by a continuation of units from the Danforth segment— an apparently conformable sequence with the basal Cambrian to earliest Ordovician Baskahegan Lake Formation overlain by the Bowers Mountain Formation, and capped by volcanic rocks. It is logistically impractical to visit this area during today's trip; hopefully the description here will suffice. The southern part of the segment is different, as described below.

Northern Greenfield segment: The Baskahegan Lake Formation (Ludman, 1991) comprises moderate- to thick-bedded turbidites (15 cm to > 2 m) composed mostly of gray-weathering quartzose arenites and chalky white weathering quartzofeldspathic wackes that typically grade upward to subordinate shales. Arenites and wackes are dominantly light to medium gray, the pelites somewhat darker, but are dark to light maroon, respectively, in a distinctive hematite-rich lower member. Partial to nearly complete Bouma sequences indicate deposition by turbidity currents, and features including graded bedding, load casts, flame structures, and rip-up clasts are common (Figs. 5a, b). Cordierite porphyroblasts characterize both wackes and pelites in the innermost parts of the contact aureole (Fig. 5c).

Fossils have not been found in the Baskahegan Lake Formation in Maine, but a Cambrian to earliest Ordovician (Tremadocian) age is assigned based on fossils in correlative units in Maine and New Brunswick. The trace fossil *Oldhamia* in the equivalent basal Grand Pitch Formation in the Weeksboro-Lunksoos Lake terrane (Neuman, 1984) suggests a Cambrian age for at least part of the formation. The formation may extend to the lowest Ordovician based on the trace fossil *Circulichnus montanus* near Woodstock, New Brunswick, below Tremadocian graptolites in the overlying Bright Eye Brook Formation (Pickerill and Fyffe, 1999).

The Bowers Mountain Formation overlies the Baskahegan Lake Formation conformably in the Danforth segment and on Passadumkeag Mountain in the northern part of the Greenfield segment. The base of the formation consists of rusty weathering, sulfidic, carbonaceous black pelite with subordinate quartz arenite that pass upward into thinly interbedded medium to dark gray siltstone and shale. An earliest Ordovician (Tremadocian) age is assigned based on graptolites in the equivalent Bright Eye Brook Formation in the Eel River-Benton area of New Brunswick.

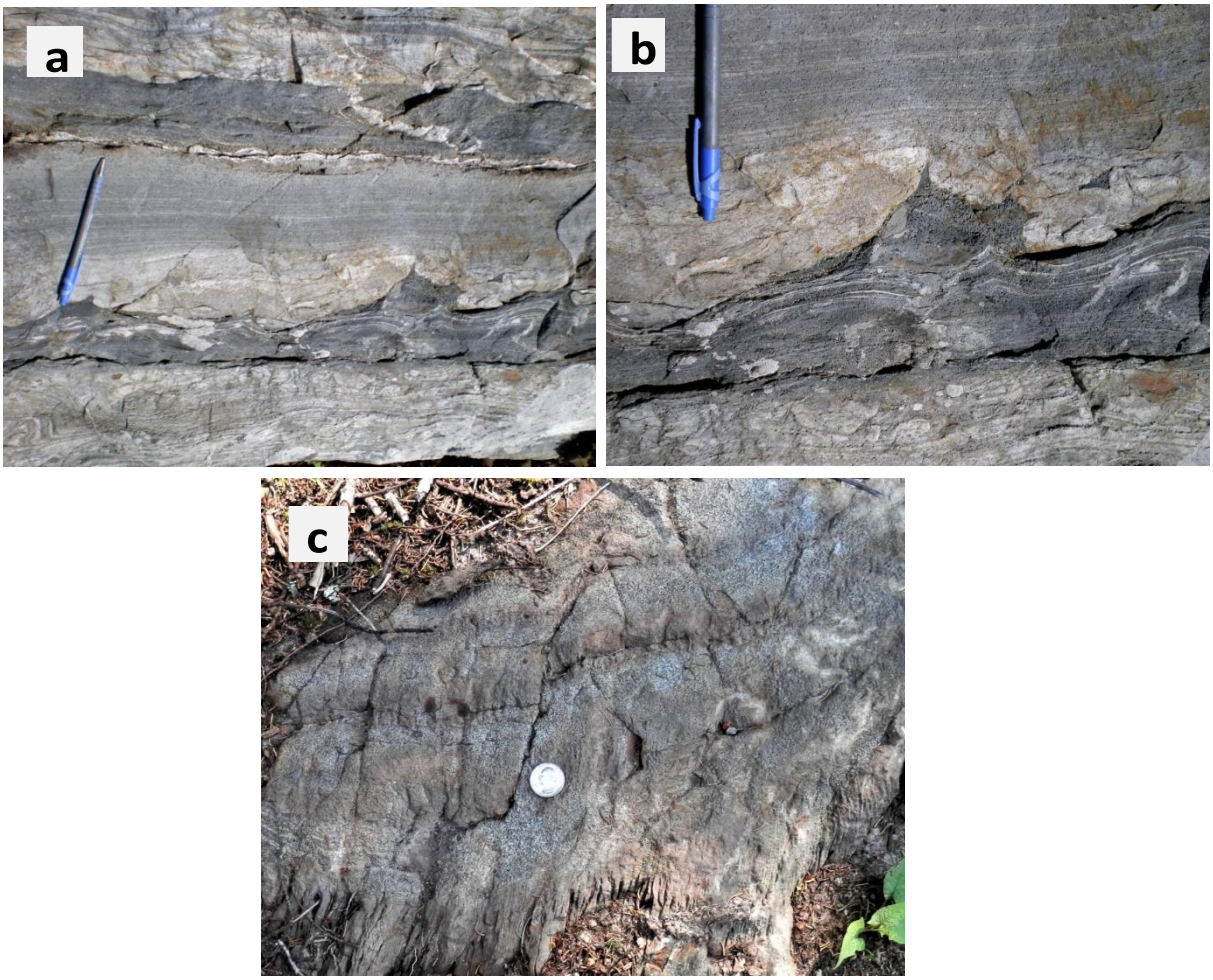

Figure 5. Thermally metamorphosed Greenfield segment Baskahegan Lake turbidites in the contact aureole of the Passadumkeag River pluton. (a) Graded beds with sandstones (pale gray) exhibiting soft-sediment deformation, sandstone/siltstone laminae (medium gray), and aluminous pelite (dark gray). Note large load casts and flame structure at the base of the central bed. (b) Closeup of flame structure showing abundant cordierite crystals in the pelite and laminated siltstones. (c) Closeup of graded wacke and pelite with abundant circular pits resulting from weathering of cordierite porphyroblasts.

Stetson Mountain Formation: The youngest Miramichi unit in the Danforth segment is the Stetson Mountain Formation, a thick pile of felsic and intermediate tuffs, lava flows, and agglomerates with rare black shale horizons and a unique medial ferromanganiferous horizon. Similar volcanic rocks in the northern part of the Greenfield segment are continuous with the Olamon Stream Formation in the southern part and will be described below.

***Southern Greenfield segment*:** Neither the typical Baskahegan Lake nor Bowers Mountain Formation crop out in the southern part of the Greenfield segment, which is underlain almost entirely by the dominantly volcanic rocks of the Olamon Stream Formation. Two oval areas of metasedimentary rock are surrounded by Olamon Stream volcanics in the southwestern part of the Greenfield quadrangle (Fig. 3). These ovals result from erosion of an interference pattern involving two generations of folds (see below), but the identity of the rocks was initially problematic. The more northerly (Oog) is now recognized as the medial Olamon Stream Greenfield member, but the other has been enigmatic, possibly a unique horizon in either the Baskahegan Lake or Olamon Stream Formation.

Rocks in the southern oval differ from the Greenfield member in that they are lighter colored and lack the manganese oxides and hydroxides that give that member a matte black appearance. They are also coarser

grained than the dominant Greenfield member mudstones, generally thicker bedded, and much more feldspathic. They differ from Baskahegan Lake quartzofeldspathic sandstones in the northern part of the Greenfield segment by their thinner, more regular bedding and finer grains.

Detrital zircon data (Ludman et al., 2019) were informative. And surprising. The age of the youngest zircon population in the southern oval is 555 Ma (latest Neoproterozoic— Ediacaran), the oldest of any Miramichi rocks in Maine. These are much older than the youngest zircons in Bowers Mountain Formation quartz arenites (485 Ma) and even older than the youngest zircons in the lower member of the Baskahegan Lake Formation (538 Ma). They are older still than the 468–470 Ma Olamon Stream volcanic rocks (Ludman et al., 2021). The complete detrital zircon age spectrum is most similar to that of the lower Baskahegan Lake Formation, and these rocks are now assigned to the Baskahegan Lake Formation (O~~C~~bl) as its Lazy Ledges Road member.

Baskahegan Lake Formation, Lazy Ledges Road member (Stop 6): The Lazy Ledges Road member is exposed in large pavement outcrops on and adjacent to that road. The large pavement outcrop at Stop 6 exhibits all the characteristics of the unit, and will be the type locality when the name is formalized. The Lazy Ledges Road member consists of chalky white weathering, generally thin- to medium-bedded, medium gray sandstones and coarse siltstones (Fig. 7). Bed thickness varies (Fig. 7B, C), and most sandstones and siltstones are medium to dark gray. The chalky weathering suggests high feldspar content, possibly including a component of volcanic ash. The rocks are tightly folded and graded beds suggest that at least some of the folds are inverted.

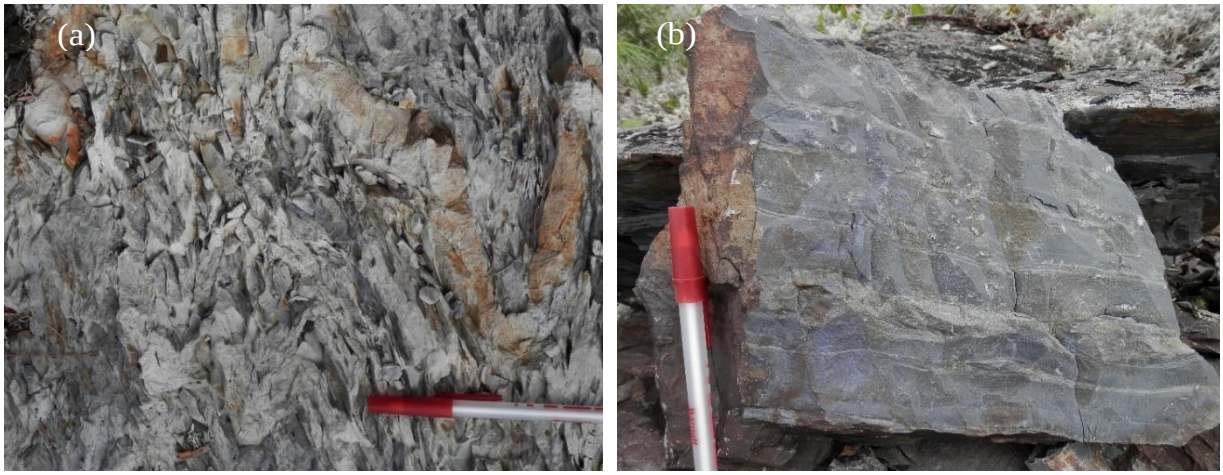

Figure 6. Baskahegan Lake Formation Lazy Ledges Road member. (a) Thinly interbedded, tightly folded chalky white weathering feldspathic siltstone and fine-grained sandstone. (b) Thicker bedded finely laminated siltstone and fine-grained sandstone. Compare with Figure 5a.

Olamon Stream Formation: The Olamon Stream Formation consists of upper and lower volcanic members separated by the sedimentary Greenfield member, interpreted as a hiatus in volcanic activity. The upper and lower members are indistinguishable, identifiable only by position relative to the Greenfield member. U/Pb zircon crystallization ages and chemical compositions of Olamon Stream volcanic rocks visited on this trip are shown in Table 1, and their classification in Figure 7.

Upper and Lower members (Stops 8, 9, 10). Chemically, the upper and lower members of the Olamon Stream Formation are an andesite-dacite-rhyolite suite. Each compositional type exhibits a wide range of rock types, with several pyroclastic textures (Fig. 8) including porcelaneous, cryptocrystalline (now devitrified) and microporphyritic tuffs, fine- to medium grained crystal, lithic, and crystal-lithic tuffs, along with porphyritic lava flows with fine-grained crystalline matrices, volcanic breccias, and coarse to very coarse grained agglomerates. Some outcrops are homogeneous chemically and lithologically, but many contain mixtures of chemical and/or textural types (Table 1, Fig. 7).

Table 1. Age and major element composition of Olamon Stream volcanic rock at trip stops. See Ludman et al., 2021 for complete analyses of all Greenfield and Danforth samples

Stop	Age (Ma)	SiO_2	Al_2O_3	TiO_2	FeO*	MnO	MgO	CaO	Na_2O	K_2O	P_2O_5	LOI	Total
1		46.73	18.17	1.309	10.49	0.161	4.80	7.11	3.33	0.22	0.22	5.28	99.2
		49.08	16.47	2.313	10.50	0.135	5.55	8.53	3.12	.027	0.27	3.22	99.8
8	467 ± 4	78.25	11.59	0.183	2.54	0.081	0.57	0.15	2.02	3.02	0.03	1.85	100.3
		78.49	11.35	0.178	2.32	0.101	0.65	0.17	0.75	3.87	0.03	2.06	100.0
9		78.34	10.11	0.226	2.33	0.449	0.52	1.58	3.36	1.36	0.05	2.25	100.6
10	470 ± 4	56.97	15.55	0.416	9.05	0.165	5.11	5.00	5.46	0.55	0.07	2.41	100.8
		58.11	15.38	0.407	8.44	0.187	4.52	3.61	5.88	0.61	0.07	2.42	99.62

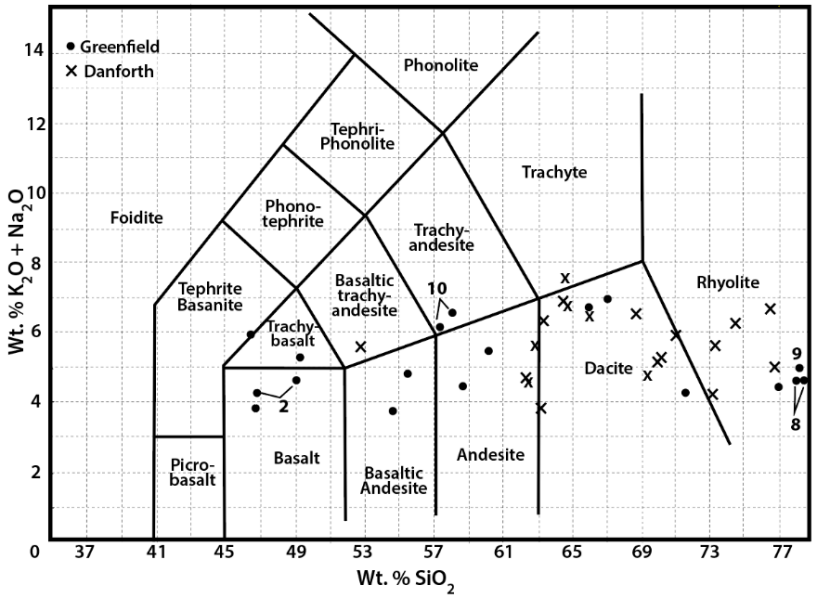

Figure 7. Classification of Maine Miramichi volcanic rocks (after LeBas et al., 1986). Numbers indicate samples from trip stops.

Primary layering is rare in most exposures, especially very fine-grained felsic ashfall tuffs in which the only planar features are broadly spaced joints (Stop 8). This severely hampers stratigraphic and structural interpretations. Sayres (1986) reported a general upward transition in the Danforth segment (Stetson Mountain Formation) from basal cryptocrystalline ashfall tuffs to a medial manganiferous iron formation, and then to upper coarser ashflow tuffs, agglomerates, and lava flows. The Meductic Group, nearest Miramichi volcanic rocks in the Eel River-Benton area, also shows systematic stratigraphic control – in composition rather than texture – with basal rhyolites of the Porten Road Formation grading upward into andesites and minor basalts of the Eel River Formation, and capped by basalts of the Oak Mountain Formation (Fyffe, 2001). However, with the *caveat* of the first sentence of this paragraph in mind, neither textural nor chemical variations appear to be related to stratigraphic position in the Greenfield segment (but see discussion of the Olamon Stream mafic member, below).

Where present, layer thickness and style vary considerably, even within individual outcrops (Fig. 9). Many cryptocrystalline felsic tuffs occur in massive homogeneous outcrops with uniform grain size and color, and no visible fabric. Slightly coarser microporphyritic tuffs have quartz phenocrysts barely visible even with a hand lens. Both are interpreted as ashfall tuffs comparable, perhaps, to the thick tuff that buried Pompeii. Coarser medium-grained tuffs with weakly foliated phenocrysts and coarse agglomerates with aligned and locally imbricated lithic fragments are interpreted as ash flows. Lava flows are best identified in thin section, by their crystalline rather than devitrified matrices (Fig. 8b) not visible in hand specimen. Most flows are also homogeneous, but one flow with a scoriaceous top has been observed (Fig. 9d).

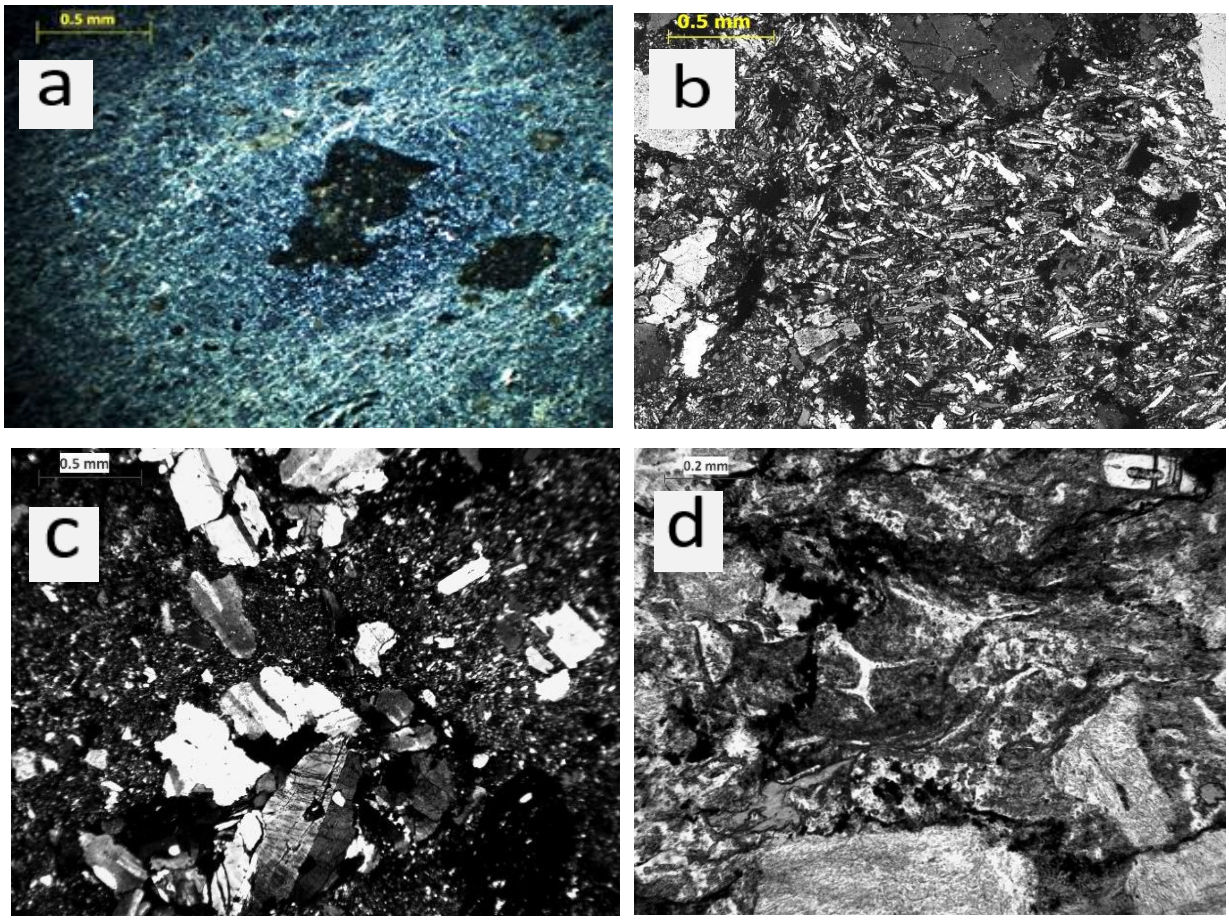

Figure 8. Photomicrographs (crossed polarizers) showing textures of Olamon Stream volcanic rocks. (a) small lithic fragments in devitrified lithic felsic tuff; (b) dacite lava flow with weakly aligned crystalline plagioclase matrix and plagioclase feldspar and partially resorbed quartz phenocrysts. (c) hornblende, quartz, and plagioclase phenocrysts in andesitic crystal tuff; (d) andesite crystal tuff with shard outlines, saussuritized plagioclase phenocrysts, and chloritized matrix.

Greenfield member (Stops 8, 9). The medial Greenfield member is a distinctive combination of thin (5 mm –5.0 cm), rhythmically graded couplets of dark gray to black mudstone and subordinate medium gray siltstone and fine sandstone, although some couplets reach 15 cm. Mudstone/siltstone:sandstone ratios range from 10:1 to 1:1 (Fig. 10a. Stop 7). The dark color is caused by manganese oxides rather than carbon and, because there is little carbon or sulfide, the mudstones are neither sooty nor rusty weathering. Siltstone/sandstone horizons are more resistant to erosion, resulting in a characteristic ribbed appearance shown in Figure 10a. Close to the contact with Olamon Stream volcanic rocks, the Greenfield member beds become thicker and are accompanied by, homogeneous quartzofeldspathic volcaniclastic sandstones and light gray, very fine grained to cryptocrystalline tuff layers a few centimeters thick (Fig. 10b, Stop 7), suggesting a gradational transition to the volcanic members.

Mafic member (Oosm) (Stops 2, 3). The southwesternmost rocks in the Miramichi terrane are basaltic tuffs, agglomerates, lava flows, and possible sub-volcanic intrusives that crop out in the Olamon and Otter Chain Pond quadrangles. These mafic rocks are separated from adjacent Olamon Stream volcanic rocks and the Greenfield member by a large area with no outcrop control, so their stratigraphic position relative to the rest of the formation is unknown.

The mafic member contains three dominant rock types: featureless, massive porphyritic basalt; porphyritic lava flows locally with basaltic fragments (Fig. 11a), in some instances possibly autobrecciated; and coarse-grained highly altered agglomerates with fine grained tuffaceous matrices. The massive basalts occur in large rounded knobby outcrops with unaltered fresh clinopyroxene phenocrysts in a similarly

unaltered fine-grained plagioclase-pyroxene matrix. These rocks exhibit widely spaced joints, and lack evidence for primary volcanic layering. They are interpreted as either massive basalt lava flows or hypabyssal sub-volcanic intrusives.

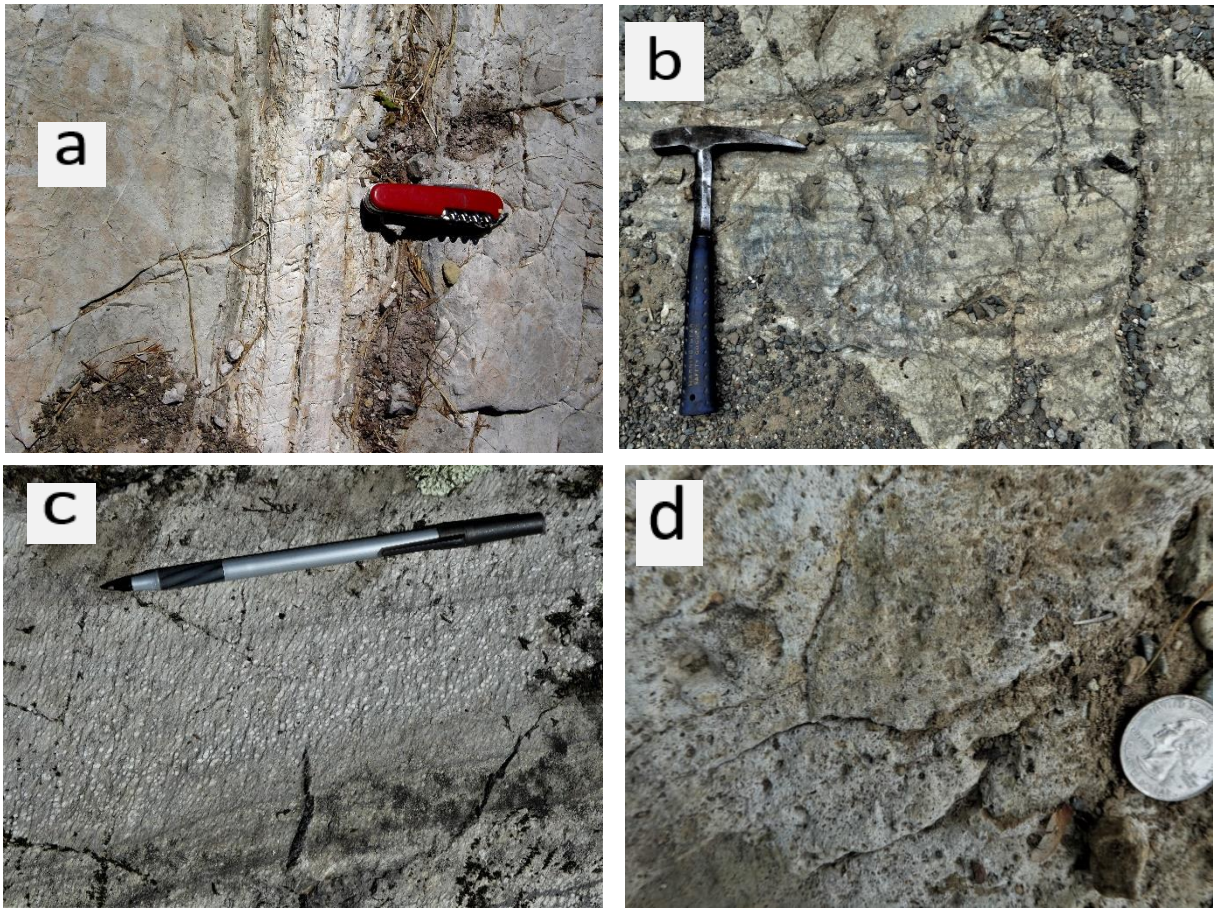

Figure 9. Primary volcanic layering in the Olamon Stream Formation. (a) variable bedding thickness in microporphyritic felsic tuff. (b) thinly layered andesite tuff. (c) strongly cleaved eruptive units of porphyritic rhyolitic tuff (Stop 10); (d) scoriaceous top of andesitic lava flow.

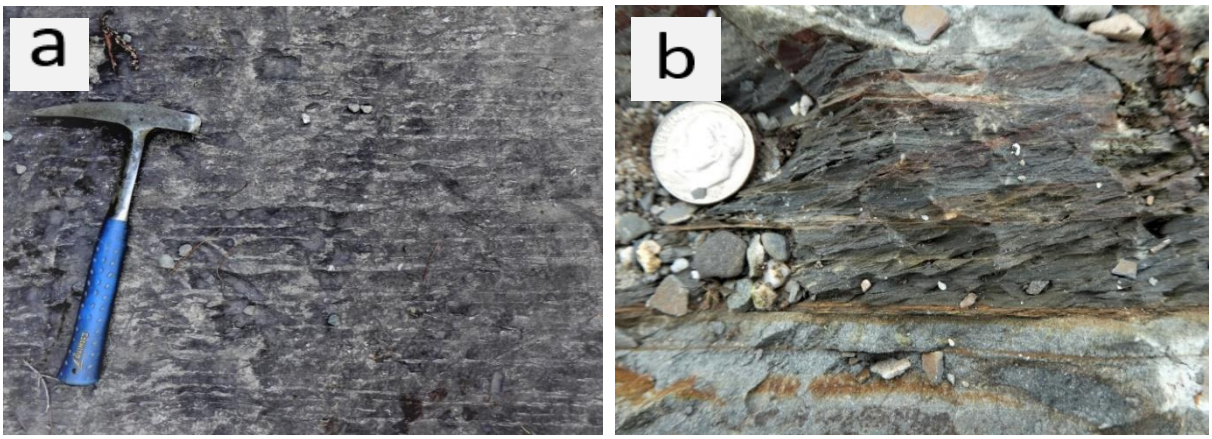

Figure 10. Olamon Stream Greenfield member. (a) Rhythmically interbedded sandstone (resistant ribs) and black mudstone (less resistant) couplets. (b) Closeup of sandstone and mudstone above microporphyritic tuff layer (Stop 7).

Rocks interpreted as lava flows also contain clinopyroxene phenocrysts, but in a plagioclase-pyroxene matrix, also have some endogenous basalt fragments (Fig. 11a), and show varying degrees of phenocryst and matrix grain alignment (Fig. 11b). Pyroxene and plagioclase feldspar crystals are slightly more altered than those in the massive basalts. Agglomerates have large, commonly rounded lithic fragments (Fig. 11c), in some outcrops only endogenous fine-grained basalt, in others exotic rhyolite or andesite, and in some a combination of both. Although pyroxene crystals are only slightly altered, the tuffaceous matrix is commonly converted to a green chlorite-epidote-bearing greenstone (Fig. 11d) and feldspars are typically strongly saussuritized.

Age and tectonic significance: The two ages shown in Table 1 are from the lower member of the Olamon Stream Formation. An additional age of 469.3 ± 4.6 Ma (Ludman et al., 2019) was obtained from a dacite lava flow that turned out to be a large float block whose origin is clearly the Olamon Stream Formation but whose position within the formation is unknown. Attempts to date the basalt were unsuccessful; one contained no zircons, another not enough for a reliable age although there is an indication that they may also be around 470 Ma (Ludman et al., 2021). These ages cluster around the boundary between the Lower (Floian) and Middle (Dapingian) Ordovician. Although the Olamon Stream and Stetson Mountain formations have been correlated with the Meductic Group in New Brunswick, recent dating of the Olamon Stream Formation shows that it is ~10 million years younger (Ludman et al., 2021). Several additional samples were collected in the summer of 2023 from both the Danforth and Greenfield segments and two from the Meductic Group, but dating has not been completed yet.

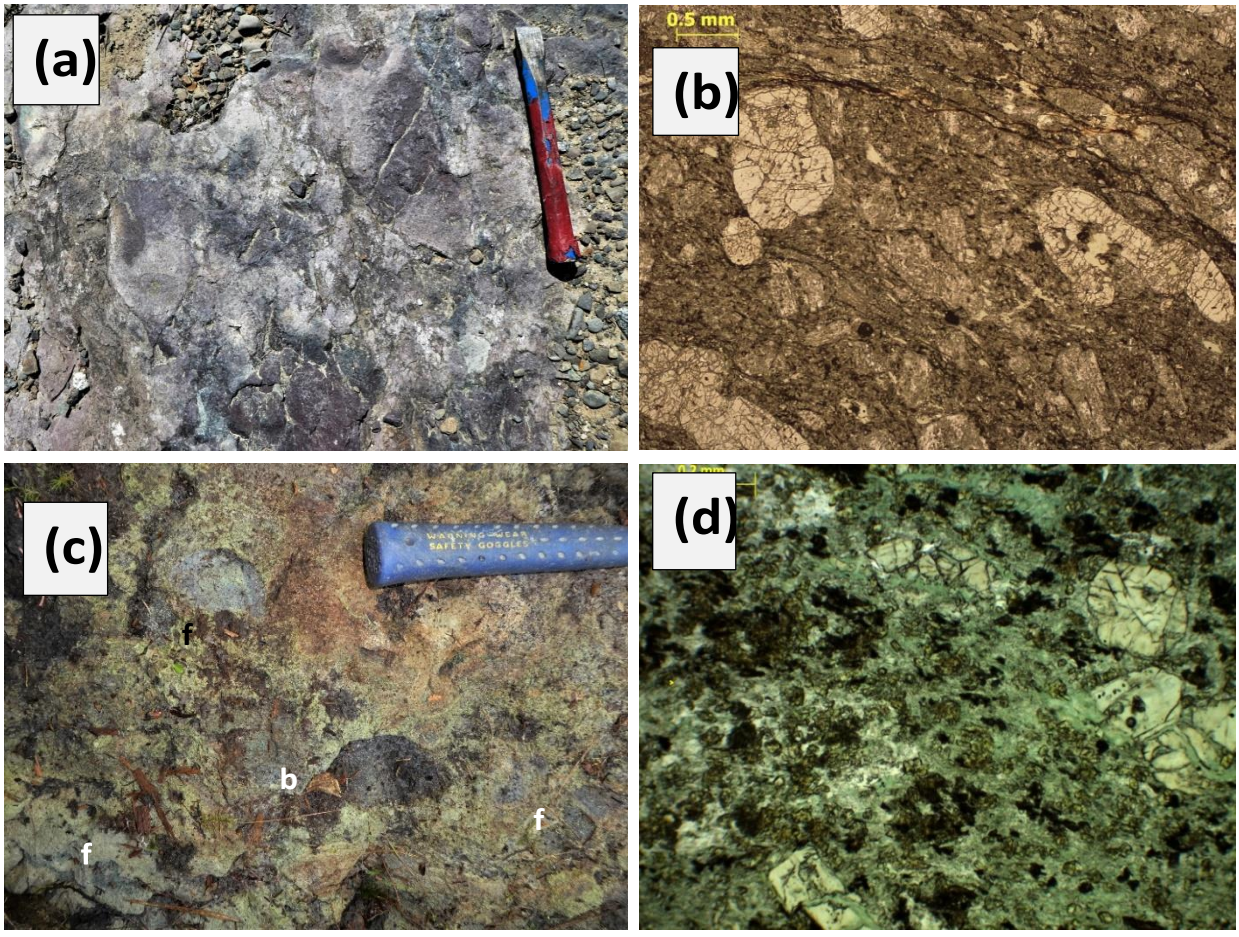

Figure 11. Olamon Stream mafic lava and agglomerate. (a) Outcrop of lava flow with basaltic fragments and a possible pillow; (b) Photomicrograph (uncrossed polarizers) showing weak alignment of clinopyroxene phenocrysts and matrix; (c) Outcrop of greenstone agglomerate with basalt (b) and felsic/intermediate (f) fragments; (d)Photomicrograph (crossed polarizers) of greenstone with slightly altered clinopyroxene and saussuritized feldspar crystals in chlorite-epidote matrix.

Tectonic setting**:** Major and trace element analyses (Ludman et al., 2021) show that Olamon Stream and Stetson Mountain Formation volcanic rocks are calc-alkaline (Fig. 12a) and erupted in a subduction-related volcanic arc (Fig. 12b) on a continental basement (Fig.12c). Although precise correlation with New Brunswick Miramichi volcanic rocks is uncertain, the tectonic setting is the same as proposed for what has been called the Popelogan-Meductic volcanic arc (van Staal et al., 2003, 2016; Fyffe et al., 2023).

Cover rocks

In the most recent Maine bedrock map (Osberg et al., 1985), Silurian turbidites northwest and southeast of the Miramichi terrane were assigned to a single formation, the Vassalboro Formation, based on tentative correlation with that unit in the Waterville area. Today, these flanking rocks are attributed to two separate depocenters, the CMAM basin to the northwest and Fredericton trough to the southeast. Logistics and the short autumn day limit our ability to visit rocks in these belts.

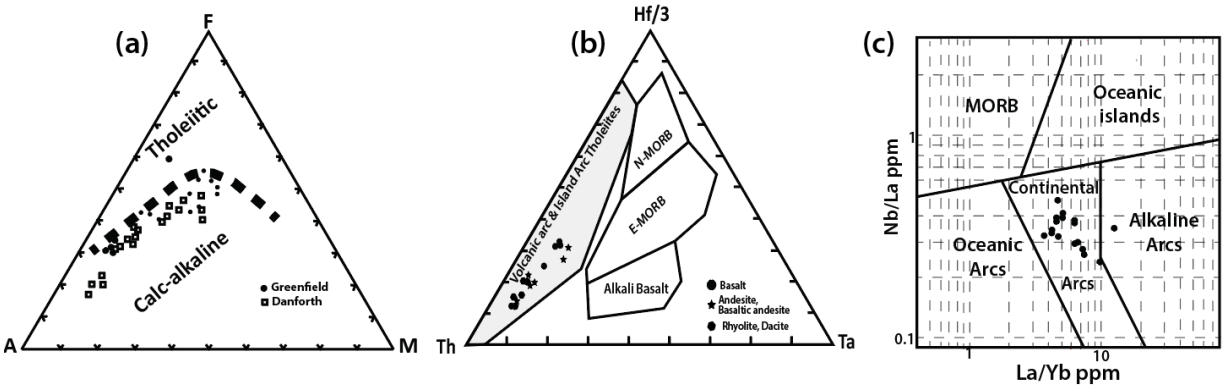

Figure 12. Tectonic setting of Maine Miramichi volcanic rocks. After Ludman et al., 2021. (a) AFM diagram after Irvine and Baragar, 1971); (b) Th-Hf-Ta discrimination diagram after Woods, 1979; (c) Nb-La-Yb discrimination diagram after Pearce et al., 1984.

CMAM basin (Stop 1): Sand-rich turbidites northwest of the Miramichi terrane exhibit a range of bedding styles and thicknesses, but extremely poor outcrop control makes it impossible to map different units. Based on their extensions to the northeast and southwest, and following the terminology of Marvinney et al. (2010), these rocks are assigned to the Vassalboro *Group,* undifferentiated. Stop 1, in the south-central part of the Olamon quadrangle, is in moderately thick bedded sand-silt and sand-silt-mud turbidites. Rocks in the same structural position in the northwest corner of the Greenfield and northeast corner of the Olamon quadrangle are finer grained, contain more aluminous pelite, and exhibit extensive small- and outcrop-scale soft-sediment deformation. There are, unfortunately, no outcrops between these widely separated areas.

No fossils have been discovered in either area, but 422 Ma detrital zircons (Pridoli) in the latter area indicate a maximum late Silurian age (Ludman et al., 2018). This is supported by relationships to the north where similar rocks with the same detrital zircon age are demonstrably younger than the Waterville Formation and are therefore assigned to the Mayflower Hill Formation of the Vassalboro Group.

Fredericton Trough Stops (4, 5): Turbidites east of the Miramichi terrane can be traced to Fredericton trough strata at the New Brunswick border (Kingsclear Group) and are divided into the County Road and Flume Ridge formations based on abundance of aluminous pelite and carbonate content. The contact appears to be gradational, and acritarchs and Silurian spores indicate that the County Road Formation (no younger than Homerian) is older than the Flume Ridge (Ludman, 2023).

Both formations consist dominantly of turbiditic sandstone with similar bedding styles, but are distinguished by subtle differences. The two units differ in the color of their fresh surfaces – medium gray for County Road sandstones vs light gray for the Flume Ridge, and their weathered surfaces – buff to orange-brown for the Flume Ridge vs medium gray (quartz-rich) or chalky-white quartzofeldspathic) for the County Road. County Road sandstones are also typically non- to only slightly calcareous, lack ferroan carbonate, have few or no detrital muscovite flakes, and are, in general, coarser grained. Flume Ridge sandstones effervesce typically and more vigorously, and contain abundant ankerite and detrital muscovite

flakes up to 3 mm across. Aluminous pelites make up as much as 40% of County Road turbidites but are scarce in the Flume Ridge except for the transition zone.

Deformation history

Deformation of rocks visited on this trip included Middle Ordovician and late Silurian folding separated by a newly proposed episode of NW-over-SE thrusting, and brittle dip-slip and strike-slip faulting on the faults that separate the Miramichi terrane from adjacent cover rocks (Figure 13). Additional soft-sediment deformation is exhibited by CMAM turbidites adjacent to the NW Boundary Fault.

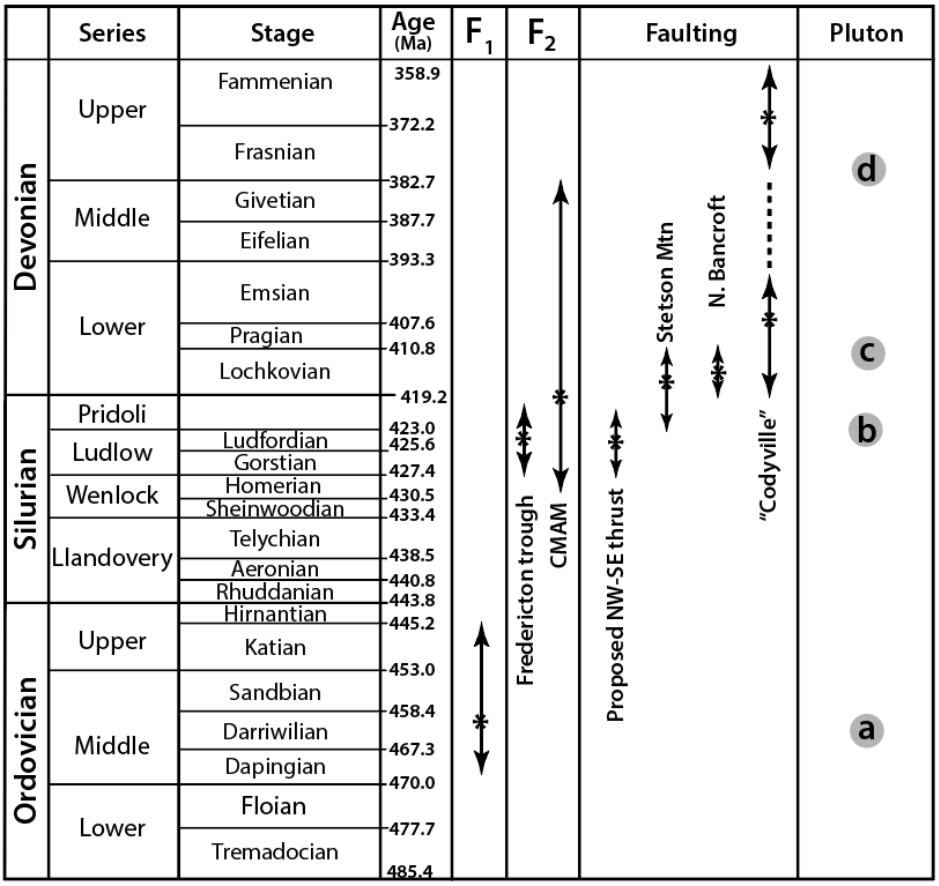

Figure 13. Deformation timeline. Double arrows indicate range constrained by microfossils and ages of detrital zircons and cross-cutting plutons. Asterisks indicate preferred timing. Plutons: (a) Benton pluton (467 ±1.6 Ma; Fyffe et al. 2023); (b) Pocomoonshine gabbro-diorite (421.9 ±2.4 Ma; Ludman et al., 2018); (c) Pokiok complex, Skiff Lake pluton (409 ± 2 Ma; Bevier and Whalen, 1990); (d) Bottle Lake complex, Whitney Cove pluton (381 ±3 Ma; Ayuso et al., 1984)

Cambro-Ordovician rocks of the Miramichi terrane were folded twice, first (F_1) in the Middle Ordovician into large recumbent structures, and later (F_2) refolded in the late Silurian into regionally pervasive tight to isoclinal upright folds. The resulting interference outcrop pattern in the Miramichi terrane is shown in Figure 14. Adjacent Silurian rocks were only deformed by F_2, but the lack of marker horizons prevents mapping individual folds.

The recumbent nature of F_1 is evidenced directly in the Danforth segment by a 3-dimensional outcrop showing recumbently folded (F_1) Stetson Mountain volcanic rocks deformed by upright F_2 folds, and by an overturned limb of a mesoscale fold. Indirect evidence includes upright and inverted F_2 folds, indicating positions on the upright and overturned limbs, respectively, of F_1 structures throughout the Danforth segment and in the northern part of the Greenfield segment. The distinctive Greenfield member of the

Olamon Stream Formation defines the basic outcrop pattern, but the scarcity of primary layering in the volcanic rocks precludes tracing structures of either generation in the upper and lower members.

Proposed thrust faulting: Anomalous relationships between CMAM rocks and the Miramichi terrane are observed in both segments. In the Danforth segment, intermediate facies CMAM rocks are isolated within the main Miramichi outcrop belt (Figs. 2, 15b, iv). In the Greenfield segment, two distinctive CMAM units crop out in a fault-bounded block east of the eastern Miramichi boundary fault and in contact with Fredericton trough strata (Fig. 15a, b-iv). These relationships were initially puzzling (e.g., Ludman, 2020) but are now interpreted as allochthonous, remnants of an eastward-directed thrust sheet that brought the CMAM strata at least *onto* (Danforth segment) and locally *over* (Greenfield segment) their Miramichi terrane source (Ludman, 2023). Thrusting must have occurred after F_1; upright folds in both autochthonous Miramichi and cover rocks and the allochthonous rocks in the thrust sheet indicate that it occurred before F_2.

The thrust sheet was later dissected by steep north-trending dip-slip faults and eroded. In the Danforth segment, remnants of the thrust sheet were preserved between the Northwest Boundary and Stetson Mountain faults as two klippen on and adjacent to Dill Hill (#s 2 and 3 in Fig. 15b-iv). In the Greenfield area, erosion isolated the CMAM rocks between the Stetson Mountain and southeast boundary fault, exposing the entire Greenfield segment as a window through the thrust sheet.

Miramichi boundary faults: The faults that separate the Greenfield segment from the CMAM basin and Fredericton trough post-date F_2 and are the most recent structural features in the area. Unfortunately, they are cut by the Bottle Lake and Pokiok complexes, obscuring their relationships with faults in the Danforth segment and possible connections with structures in New Brunswick. The Northwest Boundary fault is intruded to the northeast by the ~380 Ma Passadumkeag River pluton, from which it *appears to* emerge as the North Bancroft fault and then continues into New Brunswick as the Woodstock-Catamaran fault. Two small outcrops of the Northwest Boundary fault reveal brittle deformation and dextral strike-slip offset. In its type locality, the North Bancroft fault experienced initial dip-slip offset but was reactivated with dextral strike-slip movement. A similar history is proposed in the Greenfield area.

The Eastern Boundary fault (EB on Fig. 15a) is inferred to separate the Miramichi terrane from Fredericton trough rocks to the east. It is not exposed in the Greenfield segment, and could be either the thrust itself or a later high-angle fault that cuts it. The fault is intruded by the Passadumkeag River pluton, but *may* connect with the Stetson Mountain fault north of the pluton. Like the North Bancroft fault, the Stetson Mountain fault experienced initial dip-slip offset followed by a second strike-slip event, and was later intruded by the Skiff Lake pluton of the Pokiok intrusive complex.

The Southeast Boundary fault is a brittle dextral strike-slip fault that separates the Miramichi terrane from the Fredericton trough. It cuts the East Boundary fault and is probably the youngest boundary fault, although it is *probably* also intruded by the Passadumkeag River pluton. "*Probably"* because it is on strike with the northernmost strand of the Norumbega fault system – the dextral Codyville fault – which was reported by Ayuso to cut the Whitney Cove pluton of the Bottle Lake pluton. Ayuso mapped the fault as ending at the essentially coeval Passadumkeag River pluton, but the potential connection between the two faults passes through an area within the pluton in which no outcrops were discovered.

MORE WORK NEEDED: ANY VOLUNTEERS?

The state of current dating is such that relationships are uncertain among dated volcanic rocks of the Greenfield segment and as yet undated rocks of the Danforth segment, as well as with the Meductic Group, the nearest New Brunswick Miramichi volcanic rocks. Similarly, connections of the Miramichi boundary and internal faults between Maine segments and then with the Meductic Group in New Brunswick are unresolved. Correlation of CMAM strata adjacent to the Miramichi terrane with turbidites in the Bangor area (Pollock, 2011 a, b) and farther southwest is problematic, and is obstructed by poor outcrop control. Comparison of detrital zircon age spectra may be useful – see me if you're interested.

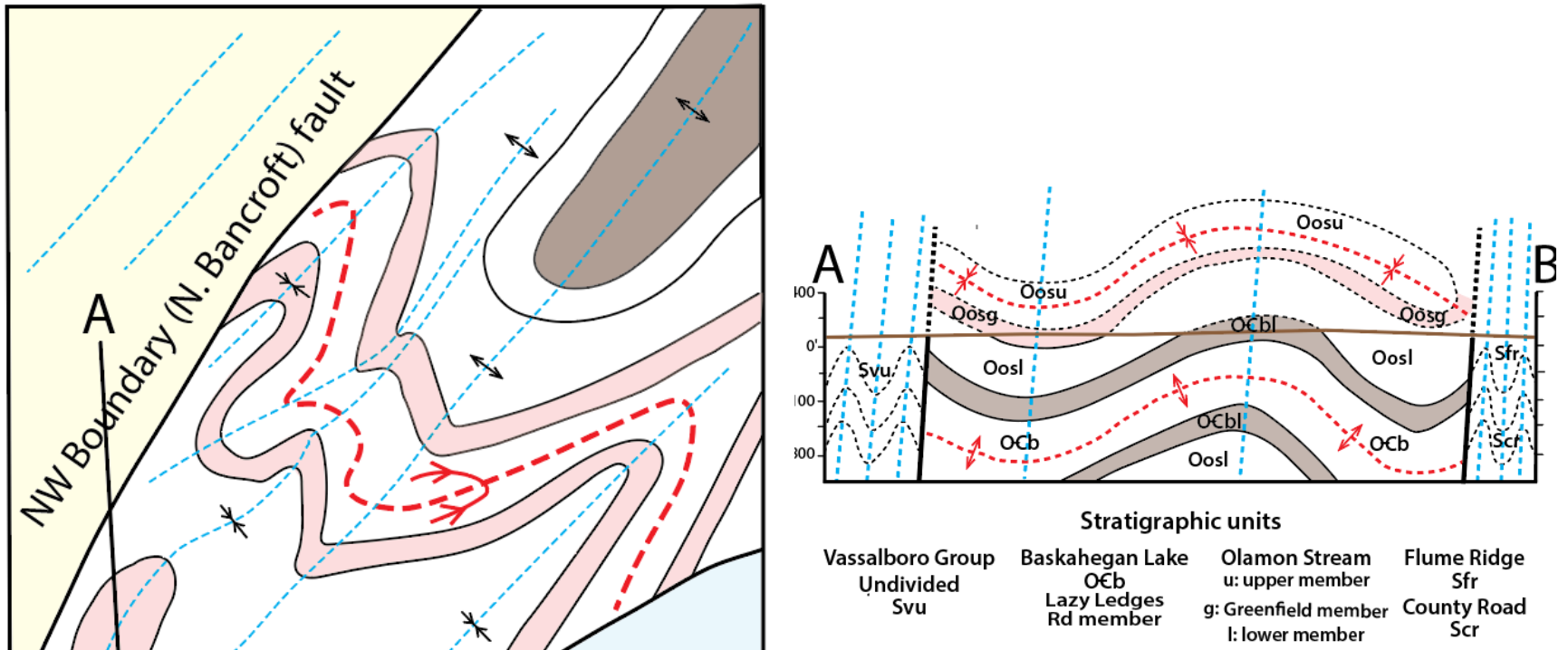

Figure 14. Structural framework of the Miramichi terrane and adjacent rocks in the Greenfield quadrangle (after Ludman, 2023). Left, Map showing F_1 and F_2 hinge surfaces. F_2 shown accurately in Miramichi terrane, schematically in CMAM basin and Fredericton trough. Right, Cross-section along line A-B, not to scale. O$\in$bl=Lazy Ledges Road member, Baskahegan Lake Formation; Oos = Olamon Stream Formation: l, u = lower and upper members, g=Greenfield member. SOvu= undifferentiated Vassalboro Group; Scr=County Road Formation

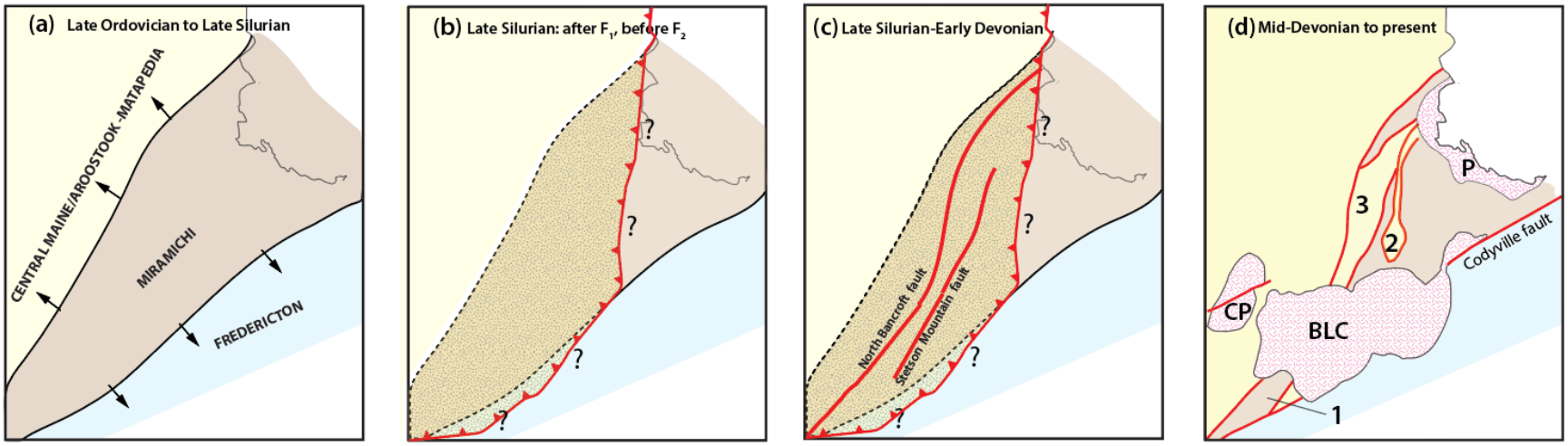

Figure 15. Evolution of the late Silurian (pre-F_2) thrust (vertical ruling).

(a) Sediment eroded from emergent Miramichi terrane deposited in adjacent Fredericton trough and CMAM basin.

(b) Early late Silurian: CMAM strata thrust eastward onto, and locally over, their Miramichi source rocks. Question marks indicate uncertainty about eastward extent of the thrust sheet.
Late Silurian: F_2 upright folding deforms allochthonous thrust sheet and autochthonous Miramichi and cover rocks.

(c) Late Silurian-early Devonian: Initiation of dip-slip NW boundary and Stetson Mountain faults. Possible early dip-slip motion on SE boundary fault.

(d) Upper Devonian: Intrusion of Bottle Lake and Pokiok igneous complexes. Dextral strike-slip offset on Codyville fault and SE boundary fault.

Carboniferous to present: Dip-slip reactivation of Codyville and other boundary faults. Erosion isolates klippen in the Danforth segment [2-Dill Hill klippe; 3-unnamed thrust fragment] and exposes the Greenfield segment as a "window" through the thrust.

TRIP ROUTE

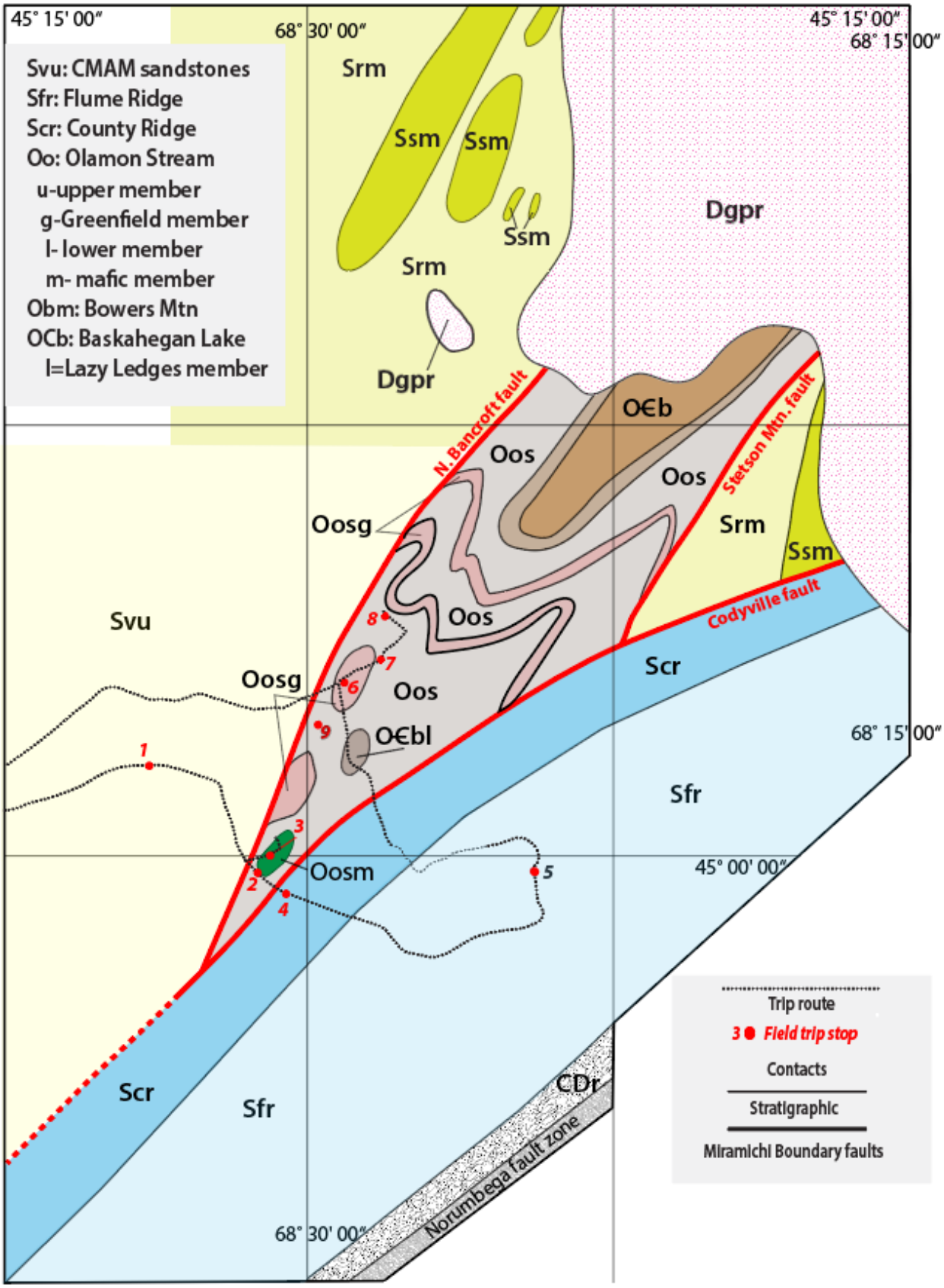
45° 15' 00"
68° 30' 00"
45° 15' 00"
68° 15' 00"
Svu: CMAM sandstones
Sfr: Flume Ridge
Scr: County Ridge
Oo: Olamon Stream
u-upper member
g-Greenfield member
l- lower member
m- mafic member
Obm: Bowers Mtn
OCb: Baskahegan Lake
l=Lazy Ledges member
Srm
Ssm
Ssm
Ssm
Srm
Dgpr
Dgpr
O€b
N. Bancroft fault
Oos
Oos
Stetson Mtn. fault
Srm
Ssm
Oosg
Oosg
Svu
Oos
Oos
Codyville fault
Scr
O€bl
68° 15' 00"
Sfr
Oosm
45° 00' 00"
Scr
Sfr
CDr
Norumbega fault zone
68° 30' 00"
Trip route
3 Field trip stop
Contacts
Stratigraphic
Miramichi Boundary faults

ROAD LOG

Note: UTM coordinates are NAD 27. Mileages are estimated from Google Earth, partly because the odometer in my field vehicle is in kilometers and partly in order to complete the trip guide in a timely fashion.

Cumulative mileage	**Description**
0.00	Exit Costigan boat ramp parking lot, cross Route 2, and head east on Greenfield Road.
0.33	Turn right onto St. Regis Road.
0.34	Turn left onto Stud Mill Road.
1.21	Pass Chip Mill.
3.21	Whitney Brook.
3.74	Stop for outcrop.

Stop 1: Pavement outcrop on south side of Stud Mill Road. CMAM Vassalboro Group undifferentiated [0534884E, 4985420N]. Participants are encouraged to continue peeling moss to expose more bedding features. This outcrop consists of thin-bedded (1–4 cm), light gray weathering siltstone (30%) that most commonly grades upward into medium to dark gray mudstone (70%). A few thicker turbidite units (15–20 cm) consist mostly of fine-grained sandstone that grades upward to finely laminated mudstone/siltstone tops. Some pinch-and-swell features, stretched and truncated siltstone beds, and a few quartz veins suggest bed-parallel shearing. *Possible correlation with the dominant Brewer Formation lithology to be seen on tomorrow's field trip?*

5.16	Sunkhaze Stream.
6.61	Park at gated road to left. Walk to large 3-dimensional outcrop on the north side of the Stud Mill Road just east of the gated road.

Stop 2: **Massive basalt of the Olamon Stream mafic member**. The rocks here are medium-grained basalts with clinopyroxene phenocrysts a few millimeters across embedded in a finer grained plagioclase crystal matrix. Here, and at nearby areas where the basalt is well exposed, both minerals exhibit only slight alteration. The prominent planar features here are broadly spaced joints; the absence of primary layering and the unaltered nature of the rock compared with greenstones at Stop 3 suggest that these may be shallow intrusives into the volcanic pile rather than lava flows. An attempt to date these rocks failed because they contained no zircon, and a nearby sample was slightly more productive but still didn't yield enough zircons on Concordia to give a reliable date. Those that were present suggested an age of 470 Ma, in agreement with the rest of the Olamon Stream dated rocks shown in Table 1. An additional sample was collected prior to the trip and will hopefully produce a publishable age.

Turn left onto gated road. ***Permission (and combination for lock) needed to enter the road.*** *Small outcrops of Olamon Stream mafic member on the road and in the woods just to the right as slope steepens.*

7.28	Bear left around sharp turn, following access road.
7.43	Turn left at fork.
7.65	Park at side road on right.

Stop 3a: Olamon Stream mafic member exposed in a small but interesting pavement outcrop. The rock here is a coarse-grained volcanic agglomerate with rounded fragments up to 20 cm of basalt and maroon sedimentary rocks embedded in a fine-grained tuffaceous matrix. Fragments are slightly imbricated, suggesting primary layering and flow direction.

Return to cars, turn around and head back toward Stud Mill Road.

Park along access road. Follow flagging to an outcrop a short distance into the woods on the left (east).

Stop 3: Olamon Stream Formation mafic member volcanic agglomerate [0538451E, 4982737N]. This is the largest of several Olamon Stream mafic member greenstone outcrops along the access road. **17A53.** As at Stop 1, participants are cordially invited to enlarge the outcrop by peeling moss. Volcanic agglomerate containing rounded and angular fragments up to 25 cm in diameter in a fine-grained gray-green matrix. Most fragments are black, fine-grained basalt but lighter colored exogenous clasts are also present but the

maroon sedimentary rock fragments seen at Stop 3a are absent. The greenstone matrix was mostly volcanic ash, now highly altered to epidote and chlorite but contains a few visible feldspar crystals.

Continue south to gate.

8.69 Pass through gate and turn left (east) on Stud Mill Road.

9.56 Park along Stud Mill Road just west of intersection with County Road. Walk to intersection, turn right to Stop 4.

Stop 4: County Road Formation (Fredericton trough) [0538693E, 4981537N]. Otter Chain Ponds quadrangle. Large pavement and low 3-dimensional outcrops on the Stud Mill Road at the northwest corner of the intersection are deeply weathered, but fresh exposures typical of the County Road Formation are visible around the corner to the south. Most of the outcrop (~85%) consists of chalky weathering, medium gray, non-calcareous fine-grained feldspathic sandstone in featureless beds 20-30 cm thick. Subordinate (15%) dark gray aluminous pelite occurs in strongly cleaved horizons 5-15 cm thick. A phyllitic sheen on cleavage surfaces suggests bed-parallel shearing.

Numerous outcrops along County Road to the south exhibit the same thick bedding and dominant sandstone. Pelite-dominant horizons, like those seen at Stop 1 have not been observed. Some sandstone is slightly calcareous, particularly close to the inferred gradational contact with the Flume Ridge Formation to the southeast. We will discuss the similarities and differences of the two formations at Stop 4.

Cross County Road and continue east on Stud Mill Road.

10.20 Unnamed road to right.

10.45 Pickerel Pond Road to left.

11.55 Titcomb Pond (22-22-00 Road to right.

12.18 Horseback Road to right.

12.68 01-05-0 road to left.

13.04 01-06-6 road to left.

13.49 Unnamed road to right.

14.50 Turn left onto Myra Road.

15.88 Park along Myra Road next to large pavement outcrop on the right.

Stop 5: Flume Ridge Formation (Fredericton trough) [0547343E, 4983543N] (The Horseback quadrangle). This outcrop shows typical Flume Ridge bedding and lithologic proportions. Quartzofeldspathic sandstone makes up ~80% of the outcrop and most commonly occurs in homogeneous beds ranging in thickness from 15 cm to over 1.5 m. Graded beds in which sandstone passes upward into darker siltstones are abundant but less common. Sandstone beds are generally at least slightly calcareous and in addition to calcite also contain diagenetic ferroan carbonate (ankerite or siderite). A distinctive punky orange weathering rind results from a combination of weathered feldspar and ferroan carbonate. This rind is so thick in deeply weathered outcrops that fresh material is not available for testing with hydrochloric acid. The siltstones are rarely calcareous, and unlike shales or slates in other units, are neither closely cleaved nor highly aluminous. As a result, the aluminous index minerals cordierite and andalusite common in other formations are absent from the Flume Ridge in the inner parts of contact aureoles.

Continue northwest on Myra Road.

20.24 Stay on main road (now Crocker Turn Road) at crossroad (County Road to west, Webber Road to east).

21.75 Lazy Ledges Drive on left. Continue north on Crocker Turn Road to its end at Greenfield Road.

22.86 Turn right onto Greenfield Road.

23.01 Park along Greenfield Road at a long driveway to the right through a blueberry field. Walk along the driveway to the first outcrops on right and left.

Permission needed.

Stop 6: Gradational contact between Olamon Stream volcanic and Greenfield members. [0541004E, 4988020N]. This stop is in a gradational contact zone between the Olamon Stream Greenfield member and either the upper or lower volcanic member. The Greenfield member crops out extensively across Greenfield Road to the north, but all outcrops in the blueberry field to the south and for 250 m beyond, across the northern crest of Lamb Hill, are Olamon Stream tuffs. *One goal of our visit is to determine whether it is the upper or lower member – there should be enough evidence to determine which.*

The first outcrop on the right side of the driveway is typical of the Greenfield member: thin graded couplets of interbedded gray siltstone and dark gray to black manganiferous mudstone, but here with unusual thicker beds of quartzofeldspathic sandstone and layers 15-30 cm thick of fine-grained crystal-lithic tuff (Fig. 10a, b). More tuff crops out across the driveway just to the south. Outcrops farther south, in and beyond the blueberry field, are dacitic and andesitic crystal-lithic tuffs commonly with crystals and clasts up to 1.5 mm but with some reaching 2 cm on Lamb Hill.

Continue NE on Greenfield Road.

23.76 Cross Olamon Stream and park along Greenfield Road before houses on both sides. Walk east into woods before the first house to large 3-D outcrops. Park along Greenfield Road before houses on both sides of road. Walk south into the lowland next to Olamon Stream to large three-dimensional outcrops.

Stop7: **Massive microporphyritic rhyolite tuff** 19A60, 61 [0542225, 4989032]. This outcrop is typical of Olamon Stream cryptocrystalline and microporphyritic rhyolitic and dacitic tuffs, in that fresh surfaces are light to medium gray, weathered surfaces chalky white; they commonly break with conchoidal fractures; contain tiny phenocrysts that can barely be seen with a 20X hand lens; primary layering is difficult to identify; and the most prominent planar features are widely spaced joints. These are the most siliceous Olamon Stream lithologies, rhyolites with more than 78% SiO_2 and, at 467 ± 4 Ma, are the youngest dated volcanic rocks in the Miramichi terrane in Maine and southwestern New Brunswick.

Two samples from this outcrop yielded almost identical compositions but, in other outcrops of apparently the same lithology, seemingly identical samples proved to be rhyolites and andesites. These tuffs are smooth to the touch and appear almost vitreous. In thin section they contain quartz microphenocrysts less than 1 mm across and the cryptocrystalline matrix is interpreted to be devitrified ash particles. Primary layering may be revealed in a few places by light and dark gray color banding and one strongly cleaved horizon.

Continue east on Greenfield Road.

24.23 Side road to left.

24.32 Outcrop on left side. *This was going to be a stop that preserved eruptive units in porphyritic rhyolite (Fig. 8a) but has been deeply weathered. It is unusual in that the rocks are strongly cleaved – but the primary layering seen in Fig. 8a is no longer visible.*

Continue east on Greenfield Road.

24.52 Gilbert Way on right side.

24.62 Turn left (N) onto Will White Road. Small pavement outcrops between the entrance and Stop 8 are medium to coarse-grained felsic and intermediate crystal-lithic tuffs and agglomerates.

25.22 Park along road at large 3D outcrop on left.

Stop 8: **Trachyandesite crystal-lithic tuff and agglomerates** [0542191, 4990331]. Large 3D outcrop on the west side of the road and small polished pavement outcrops along the road south of Ledge Brook are andesitic crystal, lithic, and crystal-lithic tuffs and coarse agglomerates. **18B70** Angular, rounded, and irregular fragments in the agglomerate are mostly of what appear to be endogenous crystal and lithic tuff similar to the agglomerate matrix. The matrix is medium to dark gray, with abundant 2 mm feldspar crystals, and was dated at 470 ± 4 Ma (Ludman et al., 2021).

Turn around and return to Greenfield Road. Turn right (southwest) and retrace route past Crocker Turn Road.

28.36 Hawk Hollow Road entrance on the right. If time permits, we can run a short traverse along the unlocked gated road to the south, opposite the entrance to Hawk Hollow Road. ***If not, continue southwest on Greenfield Road to the Costigan assembly point (Passing the only general store on the trip).***

Consolidate cars and drive a short distance to see a unique lithology in the Olamon Stream Formation.

Optional Stop 9: Maroon sandstones, siltstones, and mudstones (Fig. 17a): In southwestern New Brunswick, these maroon sedimentary rocks are important stratigraphic markers, occurring at the boundary between volcanic formations of the Lower Ordovician Meductic Group. The position of this horizon within the Olamon Stream Formation is not known, and correlation with the Meductic Group would be very helpful. However, correlation is unlikely as the only rock dated thus far (from the base of the Meductic

Group) is 10 million years older than those of the Olamon Stream Formation reported above. Several additional samples were collected from New Brunswick and Maine earlier this summer, so stay tuned for the results.

Figure 17. Only Olamon Stream Formation outcrop of maroon sandstone and siltstone horizon

END OF TRIP

Take Greenfield Road to US Route 2 and the Costigan boat launch ramp. *There will be a general store along the route for those who are hungry or thirsty.*

To reach Presque Isle:

(a) Turn south on Rte 2 to Old Town and follow signs to I-95 N.
(b) Turn north on Rte 2 then turn left at flashing light (WEST) on Rte 155 toward Howland.
(c) At Howland, follow signs to I-95 North.
(d) Take I-95 N to its end in Houlton, then north on US Rte 1 to Presque Isle.

REFERENCES

Ayuso, R. (1984). Field relations, crystallization, and petrology of reversely zoned granitic plutons in the Bottle Lake Complex, Maine. U.S. Geological Survey Professional Paper 1320, 58 pp and 1:125,000 scale geologic map.

Bevier, M. & Whalen, J. (1990). U-Pb geochronology of Silurian granites, Miramichi terrane, New Brunswick. *In* Radiogenic age and isotopic studies, Report 3. Geological Survey of Canada, Paper 89-2, 93–100.

Fyffe, L., 2001. Stratigraphy and geochemistry of Ordovician volcanic rocks of the Eel River area, west-central New Brunswick. Atlantic Geology, 37, pp. 81–101.

Fyffe, L. and Wilson, R. A. 2012. An ancient volcanic environment in the Benton-Meductic area of West-Central New Brunswick, Canada. New Brunswick Department of Natural Resources, Geological Surveys Branch, Field Guide No. 5, 31 p.

Fyffe, L., Ludman, A., and McFarlane, C. 2023. Composition, age and tectonic significance of the Benton granite, Eel River area, west-central New Brunswick, Canada. Atlantic Geosciences v. 59, p. 87–108.

Fyffe, L., van Staal C., Wilson R., and Johnson C. 2023. An overview of Early Paleozoic arc systems in New Brunswick, Canada, and eastern Maine, USA. Atlantic Geosciences 59, 1–28.

Griffin, J. 1976a, Reconnaissance bedrock geology of the Saponac [15-minute] quadrangle, Maine: Maine Geological Survey, Open-File Map 76-19, map, scale 1:62,500.

Griffin, J., 1976b, Reconnaissance bedrock geology of the Orono15' quadrangle, Maine. Maine Geological Survey Open File Map 76–21 (Scale 1:62,500).

Irvine, T. and Baragar, W. 1971. A guide to the chemical classification of the common volcanic rocks. Canadian Journal of Earth Science, 8, p. 523–548.

Larrabee, D, Spencer, C., and Swift D. 1965. Bedrock geology of the Grand Lake area, Aroostook, Hancock, Penobscot, and Washington Counties, Maine. United States Geological Survey Bulletin 1201, 38 pp.

Ludman, A., 1978, Stratigraphy and structure of Silurian and pre-Silurian rocks in the Brookton-Princeton area, eastern Maine; in Ludman, A., editor, *New England Intercollegiate Geological Conference Guidebook for trips in southeastern Maine and southwestern New Brunswick*; pp. 145–161.

Ludman, A., 1991, Stratigraphy of the Miramichi terrane in eastern Maine; in A. Ludman, editor, *Geology of the Coastal Lithotectonic Belt and neighboring terranes, eastern Maine and southern New Brunswick*; New England Intercollegiate Geological Conference Guidebook, p. 338–357.

Ludman, A., 2003, Bedrock Geology of the Dill Hill 7½' quadrangle, Maine; Maine Geological Survey Open File Report OF 03-93 (1:24,000 map plus16 page report).

Ludman, A., and Berry, Henry IV, 2003, Bedrock Geologic Map of the Calais 1:100,000 quadrangle; Maine Geological Survey Open File Report, OF 03-97

Ludman, A., 2020. Bedrock geology of the Greenfield quadrangle, Maine: Maine Geological Survey, Open-File Report 20-10, 43 pp. and map, scale 1:24,000. *Superseded by Ludman, 2023*.

Ludman, A., 2020. Bedrock geology of the Lincoln Center quadrangle, Maine; Maine Geological Survey Open File Report 20-24.

Ludman, A., Aleinikoff, J., Berry, H.N. IV, and Hopeck, J., 2018, SHRIMP U-Pb zircon evidence for age, provenance, and tectonic history of early Paleozoic Ganderian rocks, east-central Maine. Atlantic Geology 54, pp 335-387.

Ludman, A., McFarlane, C., and Whittaker, A., 2021. Chemistry, age, and tectonic setting of Miramichi terrane volcanic rocks in eastern and east-central Maine. Atlantic Geology v. 57, p. 239–273.

Ludman, A., 2023, Bedrock geology of the Greenfield quadrangle, Maine (revised): Maine Geological Survey, Open-File Report 23-1, 31 p. report and color map, scale 1:24,000.

Marvinney, R.G., West, D.P. Jr., Grover, T. W., and Berry, H.N. IV, 2010, A stratigraphic review of the Vassalboro Group in a portion of central Maine; *in* Gerbi, C., Yates, M, Kelley, A., and Lux, D., eds., *Guidebook for field trips in coastal and interior Maine*; New England Intercollegiate Geological Conference Guidebook, p. 61-76.

Neuman, R. 1984. Geology and paleobiology of islands in the Ordovician Iapetus Ocean: Review and implications. Geological Society of America Bulletin, 95, pp. 1188–1201.

Olson, R. 1972. Bedrock geology of the southwest one sixth of the Saponac quadrangle, Penobscot and Hancock counties, Maine; Unpublished M.S. thesis, University of Maine, Orono, ME, 60 p.

Pearce, J., Harris, B., and Tindle, A. 1984. Trace element discrimination diagrams for the tectonic interpretation of granitic rocks. Journal of Petrology, 25, pp. 956–983.

Pickerill, R., & Fyffe, L. 1999. The stratigraphic significance of trace fossils from the Lower Paleozoic Baskahegan Lake Formation near Woodstock, west-central New Brunswick. Atlantic Geology, 35, pp. 215–224.

Pollock, S., 2011a. Stratigraphy and structural geology of the Bangor and Veazie 7.5' quadrangles, Maine. Maine Geological Survey Open File Report 11-147, 8 pp.

Pollock, S., 2011b. Bedrock geology of the Bangor quadrangle, Maine. Maine Geological Survey Open File Report 11-57, Scale 1:24,000.

van Staal, C., Wilson, R., Rogers, N., Fyffe, L., Langton, J., McCutcheon, S., McNicoll, V., and Ravenhurst, C., 2003, Geology and tectonic history of the Bathurst Supergroup, Bathurst Mining Camp, and its relationships to coeval rocks in southwestern New Brunswick and adjacent Maine – A synthesis, *in* Goodfellow, W. D., McCutcheon, S. R., and Peter, J. M., editors: Economic Geology Monograph 11, p. 37–60.

Venugopal, D.V. 1978. Geology of Benton-Kirkland, Upper Eel River Bend map-area G-22. New Brunswick Department of Natural Resources, Geological Surveys Branch, Map Report 78-3, 16 p.

Venugopal, D.V. 1979. Geology of Debec Junction-Gibson Millstream-Temperance Vale- Meductic region, map-areas G-21, H-21, I-21, and H-22 (Parts of 21 J/3, 21 J/4, 21 G/13, 21 G/ 14). New Brunswick Department of Natural Resources, Geological Surveys Branch, Map Report 79-5, 36 p.

Whalen, J.B., Rogers, N., van Staal, C.R., Longstaffe, F.J., Jenner, G.A., and Winchester, J.A. 1998. Geochemical and isotopic (Nd, O) data from Ordovician felsic plutonic and volcanic rocks of the Miramichi Highlands: petrogenetic and metallogenic implications for the Bathurst Mining Camp. Canadian Journal of Earth Sciences, 35, pp. 237–252.

Wilson, R.A. 1993. Geology of Heath Steele-Halfmile Lakes area; Northumberland County, New Brunswick (Part of NTS 21 O/8). New Brunswick Department of Natural Resources and Energy, Mineral Resources, Report of Investigation 25, 98 p.

Wilson, R., van Staal, C., and McClelland, W., 2015. Synaccretionary sedimentary and volcanic rocks in the Ordovician Tetagouche backarc basin, New Brunswick, Canada: Evidence for a transition from foredeep to forearc basin sedimentation

Wood, D., Joron, J-L., and Treuil, M. 1979. A re-appraisal of the use of trace elements to classify and discriminate between magma series erupted in different tectonic settings.
Earth and Planetary Science Letters, 45, pp. 326–336.

PICKETT MOUNTAIN PROJECT: A RESPONSIBLE PATHWAY TO THE DEVELOPMENT OF MAINE'S CRITICAL METALS

Leah Page, Jeremy Ouellette, and Don Dudek
Wolfden Resources Corp., Patten, Maine 04765. lpage@wolfdenresources.com

ADENDA

9:00 am	PowerPoint presentation at Wolfden's Patten Office (coffee and donuts provided) 20 Main St., Patten
10:00 am	Core review at Core Shed, 9 Potato Row, Patten
12:00 noon	Lunch (sandwiches and coffee/tea provided)
1:00 pm	Travel from Patten to Field Stop 1 on Pickett Mountain Property
3:30 pm	Travel back to Wolfden office for additional discussion or travel to Presque Isle

INTRODUCTION

The Pickett Mountain Property (the "Property" or the "Project") is located in northeastern Maine, USA, in the southeast quarter of Township 6, Range 6, Penobscot County (Fig. 1). It is about 153 kilometers ("km") north of Bangor and approximately 53 km from the Canadian border. The Property consists of 2,887 hectares (7,135 acres) of private land that was acquired in 2017 by Wolfden Mt. Chase LLC (a wholly owned subsidiary of Wolfden Resources Corporation) ("Wolfden" or the "Company") and included all the mineral, timber, oil, and surface rights, exclusive of the surface area of any lakes greater than 10-acres in size (i.e., great ponds).

The Project is located within the Gander Terrane ("Ganderia") of the northern Appalachian orogenic belt, formed during the Paleozoic orogenies. The area is underlain by Late Neoproterozoic to Early Ordovician rocks that have undergone multiple stages of deformation, metamorphism, and plutonism and record the development and destruction of a continental margin. Ganderia hosts various metallic mineral deposits and prospects from New Hampshire, trending northeast through Maine and New Brunswick, to Newfoundland (Fig. 2), including world-class volcanogenic massive sulphide ("VMS") deposits of zinc, lead, copper, and silver, as well as significant gold deposits.

The Property covers a portion of the southeast limb of the southwest-plunging Weeksboro-Lunksoos Lake Belt that is cored by Early Cambrian shale and siltstone with interbedded quartzite of the Grand Pitch Formation. Unconformably overlying the Grand Pitch Formation is a sequence of quartz-feldspar crystal tuff, rhyolite, volcanic breccia, and lapilli tuff, a massive sulphide horizon that varies from 0 to about 15 meters thick dominated by sphalerite-galena-chalcopyrite-pyrite mineralization, hanging wall tuffs, mafic flows, and shale.

The mineralized zone at Pickett Mountain is a stratabound VMS deposit that has been traced by drilling approximately 1,000 meters along strike and 850 meters down dip. It consists of three primary lenses (West, East and Footwall) with the West and East zones located at the stratigraphic top of the host felsic volcanic unit. The Footwall Zone ("FW") is situated at the base of the host felsic unit in contact with a porphyritic quartz+feldspar±hornblende intrusive unit ("QFP") and conformable sediments. VMS deposits are a major source of Cu, Zn, and to a lesser extent Pb, Ag, Au, Cd, Se, Sn, Bi, and minor amounts of other metals. This style of mineralization typically has a high value due to its multi-element character and concentrated value per tonne mined.

EXOLORATION TIMELINE

Between 1978 and 1989, the Property was explored by Getty Mineral Company ("Getty") and then by Chevron Resources Company ("Chevron"). Over this period, 135 holes totalling 34,058 meters were drilled. A historical resource estimate was prepared by Getty and estimated the deposit to contain approximately 3.15 million metric tons with an average grade of 9.66% Zn, 4.30% Pb, 1.24% Cu, 2.96 opt Ag, and 0.029 opt Au. In 1989, Chevron completed another historical resource estimate using an updated geological interpretation and more rigorous controls. This estimate was 2.5 million metric tons averaging 11.42% Zn, 4.94% Pb, 1.62% Cu, and 3.3 opt Ag. Wolfden does not consider these historical estimates to represent current Mineral Resources and the historical estimates are not NI 43-101 compliant.

Since acquiring the Property in December 2017, Wolfden's exploration activities include an airborne geophysical survey ("VTEM"), ground Time-Domain electromagnetic surveys ("TDEM"), bore-hole TDEM electromagnetic surveys, ground induced polarization surveys ("IP"), and geological mapping as well as diamond drilling. To date,

135 historical drill holes and 69 drill holes completed by Wolfden in 2017-2021, have tested the Pickett Mountain deposit and other regional exploration targets. Total footage for these combined drilling campaigns is 67,860 meters.

In 2019, Wolfden completed an updated resource estimate followed by a Preliminary Economic Assessment ("PEA") in 2020. The resource estimate employed a 9% ZnEq cut-off which resulted in Indicated Mineral Resources of 2.05 million tonnes grading 19.32% ZnEq and Inferred Mineral Resources of 2.03 million tonnes grading 20.61% ZnEq (see Table 1 for details). No Mineral Reserves have been estimated at this time.

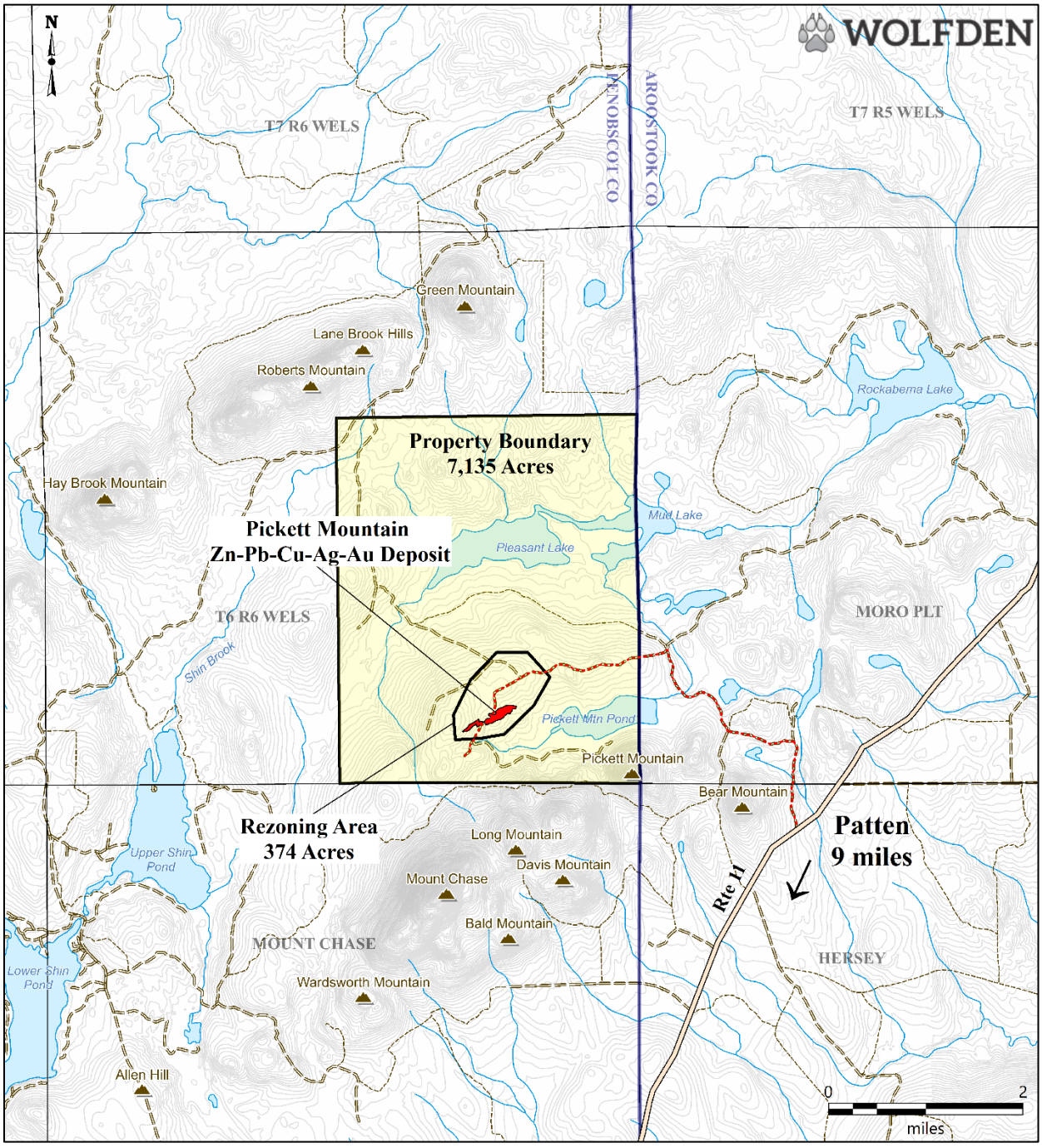

Figure 1. Property location map (Wolfden, 2023).

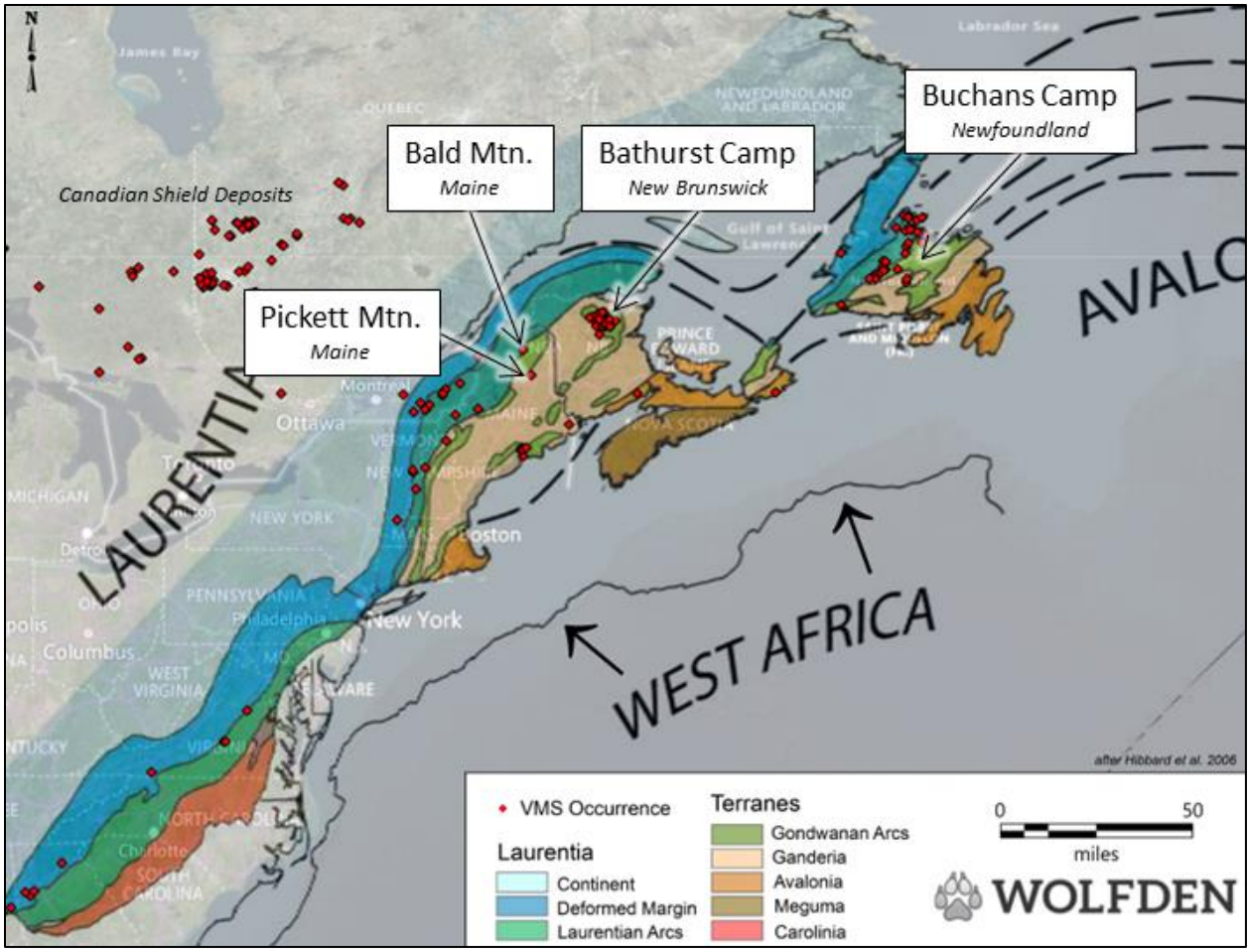

Figure 2. Generalized tectonic map of the Appalachian orogenic belt and volcanogenic massive sulphide deposits (after Hibbard et al, 2006 and USGS).

Table 1. Mineral Resource Estimate using a 9% ZnEq cutoff (A-Z Mining Professionals Ltd., 2019)

MINERAL RESOURCE STATEMENT – JANUARY 7, 2019								
Category	**Tonnes**	**% Zn**	**% Pb**	**% Cu**	**g/t Ag**	**g/t Au**	**Density**	**% ZnEq**
Indicated	2,050,000	9.88	3.93	1.38	101.58	0.92	3.99	19.32
Inferred	2,030,000	10.98	4.35	1.20	111.45	0.92	4.00	20.61

Based on this resource, Wolfden completed a PEA which showed a robust project as follows.
The Base Case Financial Model Yields (A-Z Mining Professionals Ltd., 2020):

- After-tax IRR of 37%
- After-tax NPV8% of US$198 million to Wolfden for an underground mine plan scenario
- Initial capital expenditure of US$147.4 million including 20% contingency and closure costs
- Payback 2.4 years

The PEA financial model used consensus metal prices assumptions of $1.15/lb Zinc, $1.00/lb Lead, $3.00/lb Copper, $18.00/oz Silver and $1,500/oz Gold. Full details of the Preliminary Economic Assessment in the form of a technical report for the purposes of NI 43-101 was filed on SEDAR. All financial figures are in US dollars.

Subsequent to the PEA, Wolfden continued testing the West and East zones with more focus on the FW Zone. This drilling, along with an updated geologic model, resulted in an improved resource estimate, at a 7% ZnEq cut-off, comprising Indicated Mineral Resources of 2.7 million tonnes grading 17.72% ZnEq and Inferred Mineral Resources of 3.6 million tonnes grading 17.65% ZnEq (see details in Table 2).

Table 2. Mineral Resource Estimate Sensitivity Analysis (A-Z Mining Professionals Ltd., 2021)

SENSITIVITY TO CUT-OFF GRADES - INDICATED MINERAL RESOURCE - November 17, 2021								
% ZnEq Cut-off Grade	Tonnes	% Zn	% Pb	% Cu	g/t Ag	g/t Au	Density	% ZnEq
3 % ZnEq	5,539,000	5.25	2.22	0.92	64.0	0.6	3.85	11.12
4 % ZnEq	4,723,000	5.95	2.52	0.99	71.2	0.6	3.84	12.44
5 % ZnEq	3,752,000	7.10	3.02	1.09	81.5	0.7	3.83	14.50
7 % ZnEq	2,724,000	8.91	3.83	1.22	97.2	0.8	3.84	17.72
9 % ZnEq	2,393,000	9.69	4.17	1.28	103.9	0.9	3.84	19.08

SENSITIVITY TO CUT-OFF GRADES - INFERRED MINERAL RESOURCE – November 17, 2021								
% ZnEq Cut-off Grade	Tonnes	% Zn	% Pb	% Cu	g/t Ag	g/t Au	Density	% ZnEq
3 % ZnEq	6,471,000	5.88	2.42	0.82	71.7	0.6	3.83	11.83
4 % ZnEq	5,426,000	6.79	2.79	0.87	81.9	0.6	3.81	13.44
5 % ZnEq	4,479,000	7.90	3.25	0.92	93.5	0.7	3.79	15.33
7 % ZnEq	3,593,000	9.27	3.83	1.00	105.4	0.7	3.81	17.65
9 % ZnEq	3,003,000	10.46	4.32	1.05	114.2	0.8	3.82	19.57

There is significant exploration upside and potential for additional resources to be added to the deposit in known mineralized zones due to the following:

- The West Zone is oriented nearly vertical and is open at depth, having been drill tested to 850-meters (vertical depth below surface).
- Additional massive sulphide mineralization intersected below the East Zone requires follow-up.
- The FW Zones in both the East and West zones require significant drilling to define the extents of the mineralization and near-surface folded geometry in the West FW Zone.
- There are indications of additional massive sulphide mineralization located approximately 400 metres north of the West Zone.

Since the completion of the PEA, Wolfden has been working with local communities, the Maine Land Use Planning Commission ("LUPC" or the "Commission"), and other state agencies to advance the Project with a first step of re-zoning a portion of the property to allow for the development of a small footprint, state of the art underground mine, that is protective of Maine's environment, recreational activities, and social fabric.

PICKETT MOUNTAIN DEPOSIT GEOLOGY SUMMARY

The local stratigraphy documented proximal to the Pickett Mountain deposit is thought to be equivalent to the Ordovician-age Shin Brook Formation (see Figs. 3 and 4).

In 2018, geological mapping was completed in the deposit area as well as in the northwest portion of the Property. Outcrop exposure is quite poor; mapping was augmented with the logged drill-hole geology in the deposit area. Eight principal rock units were observed in the outcrop and in drill core: footwall mudstones to pebble conglomerates, felsic volcanic rock, massive sulphide, hanging wall mudstone-siltstone, hanging wall massive mafic rock and mafic debris flows, quartz+feldspar±hornblende phyric felsic hypabyssal intrusions, gabbro dikes and fine to medium grained diorite intrusions. An updated map, based on mapping, drilling and geophysical data, is in progress.

The host felsic volcanic rock unit varies from 50 to 200 meters wide and is thickest in the deposit area. The fragmental rock in the deposit area is commonly felsic volcanic breccia, consisting of rounded, oblate fragments in a matrix of similar composition and texture, but a slightly different color. Quartz and more commonly, feldspar phenocrysts, are generally round and less than 1 mm. Sections of the breccia contain abundant blocky patches of dark, fine-grained felsic rock with scattered 0.5 mm plagioclase phenocrysts thought to be fiamme, although wall rock rip-ups have also been reported. The fragmental rock also includes sections of tuff and lapilli tuff, which are compositionally similar to the volcanic breccia. More massive felsic rock has been noted in drill logs and observed as massive to lobate flows footwall to both the West and East zones and to the west and east of the mineralized zones. Flows and fragmental units underlying the West Zone locally contain finely disseminated magnetite. Thin aplite dikes are reported in the drill logs. The foliation is usually penetrative, and the aspect ratio of the fragments is 2:1:1. Sericitization is almost always present and commonly minor, but increases to strong in the deposit area, especially below the West Zone.

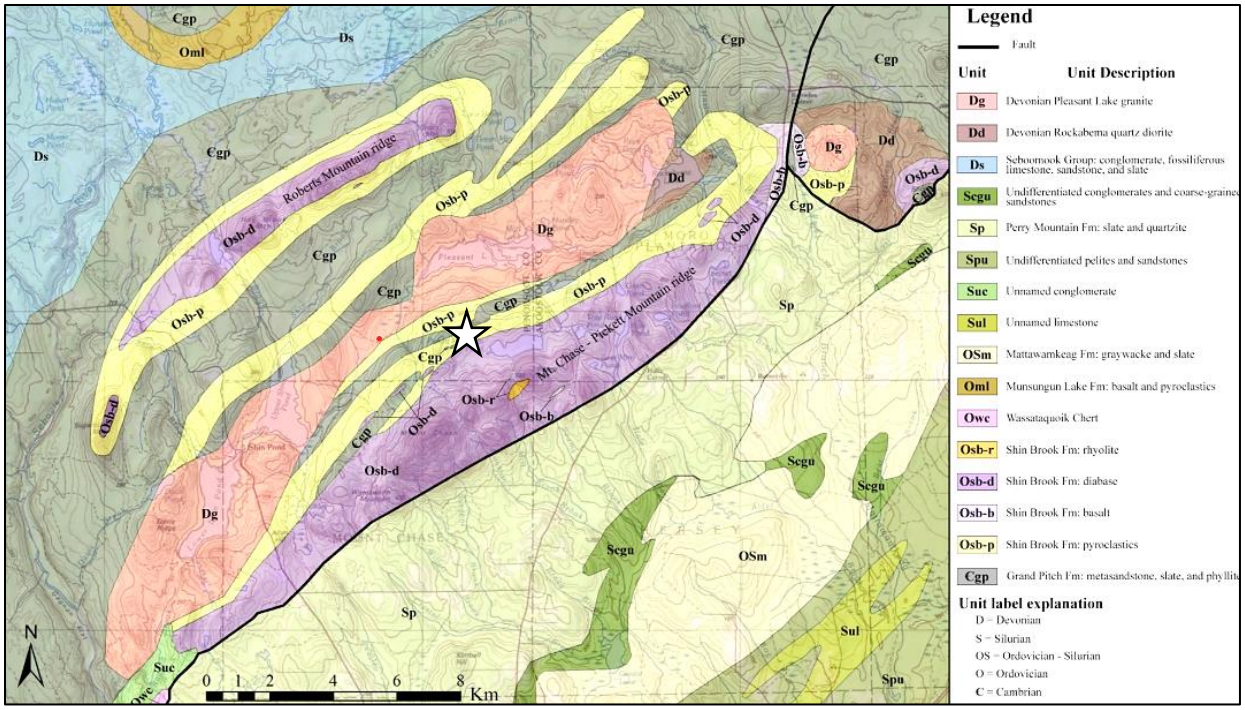

Figure 3. Revised regional bedrock geologic map of the Weeksboro-Lunksoos Lake Belt, northern Maine (after Neuman, 1967; McCormick, 2021).

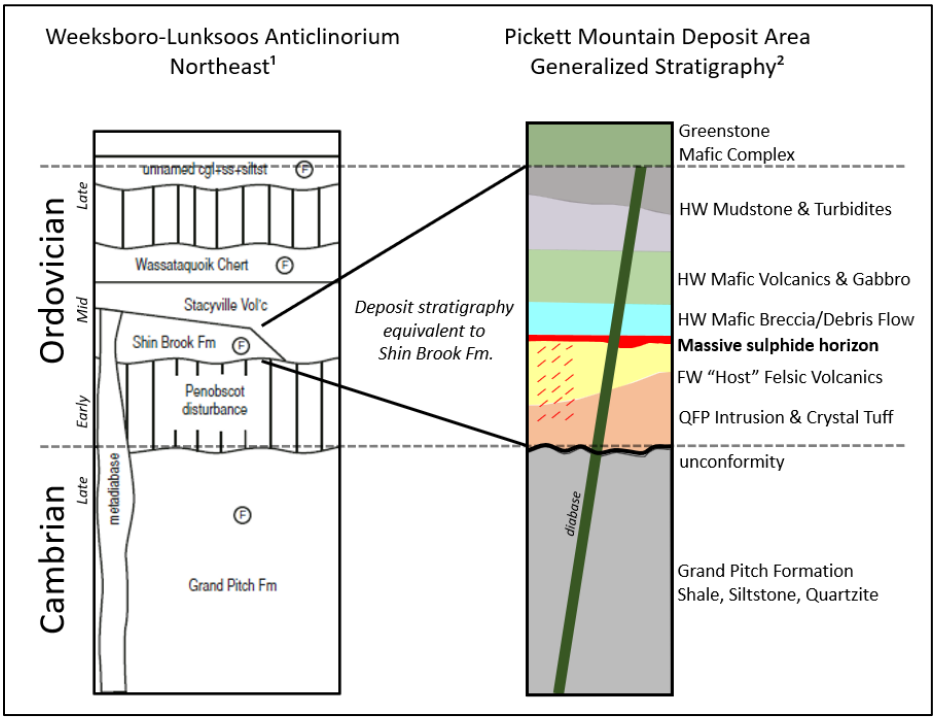

Figure 4. Stratigraphic Section of Weeksboro-Lunksoos Lake Belt and Pickett Mountain Deposit (after Neuman, 1967; Scully, 1989).

In the deposit area, the contact between the footwall and hanging wall rocks is occupied by massive sulphide which is capped by a debris flow (see Figs. 8 and 9). The debris flow is dominated by tuffaceous mafic material and includes clasts and potentially rafts of sulphide and altered felsic volcanics. Generally, contacts and bedding strike

northeast and dip steeply to the southeast. Repetitions of the contact between the footwall and hanging wall rocks are common due to Z-shaped folds.

The West Zone is planar to Z-folded and steeply dipping. The East Zone is similarly oriented at its west edge, but the strike rotates clockwise and the dip shallows eastward, as it becomes affected by an interpreted quartz feldspar phyric felsic intrusion at depth and a later diorite intrusion at the deposit's eastern edge.

The FW Zone lies near the base of the felsic volcanic unit, very proximal to, or contiguous to, the altered quartz feldspar porphyry with silver enrichment extending laterally along the basal felsic volcanic-sediment contact. Locally, boiling-like textures and breccias, potentially phreatic to hydrothermal, along with carbonate enrichment, occur at the stratigraphic location of the FW Zone, especially under the West Lens, proximal to talc-altered zones. Along strike, the FW Zone time horizon can be traced geochemically through its elevated silver content and carbonate-enrichment.

As part of the mapping and drill hole program data collection, a total of 1,849 samples were collected and analyzed for major oxides and select trace elements. These samples were collected to geochemically document the different geological units and alteration features. Below is a Zr (ppm) vs TiO2 (%) diagram which clearly documents the major rock types (Fig. 5). Of particular note, the host felsic volcanics (yellow triangles) and hypabyssal QFP (±hornblende) units form distinct rock types. As well, the hanging wall mafic rocks and gabbro dikes/sills, and associated sediments display a significant enrichment in TiO_2, thus denoting a completely separate provenance as compared to the felsic volcanics and related felsic intrusions.

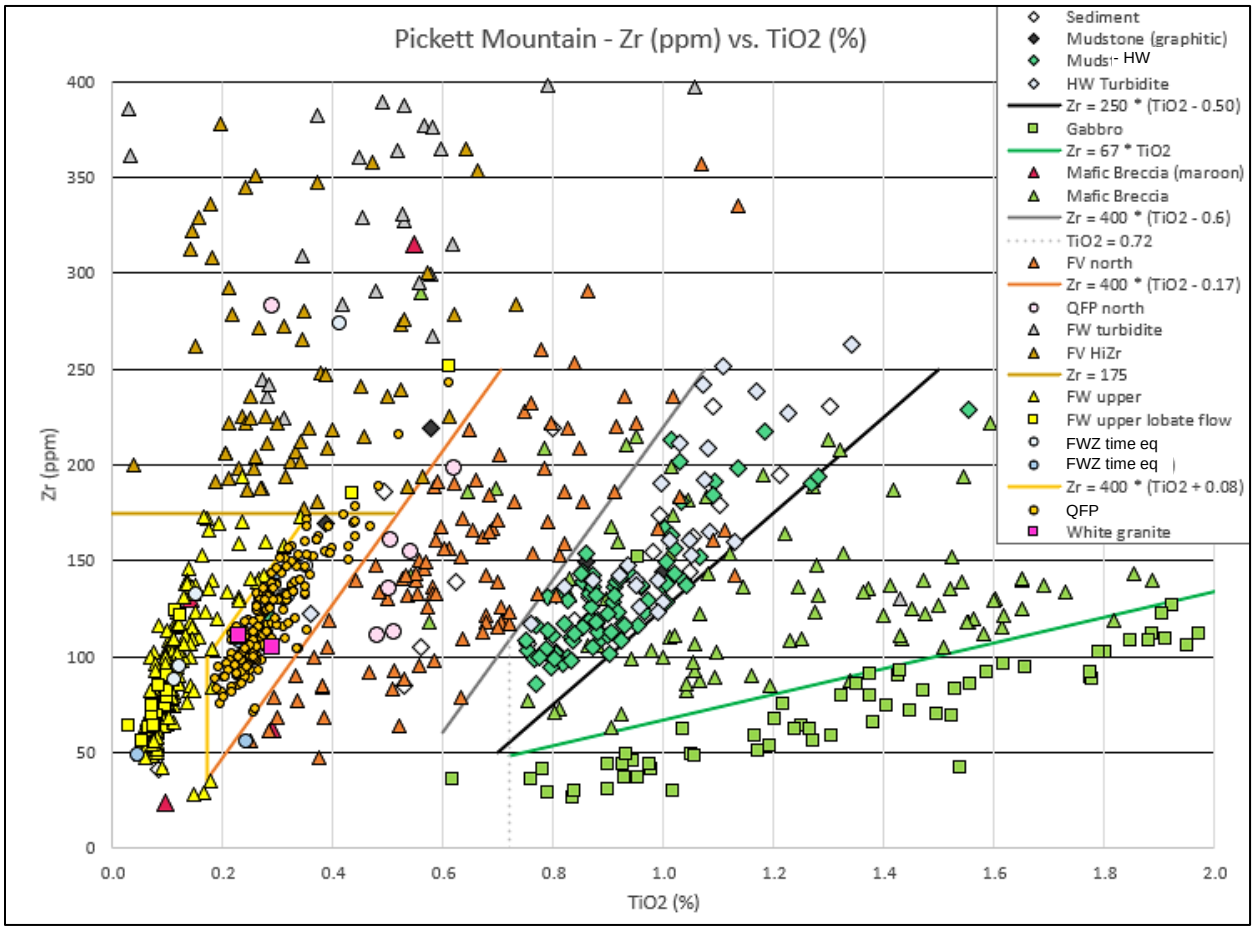

Figure 5. Zr-TiO_2 Lithogeochemical plot (created by J. Grant, Wolfden).

EXPLORATION

Exploration in Maine for massive sulphides commenced soon after 1953 when the Brunswick #6 deposit was discovered in neighboring New Brunswick, Canada. This early work concentrated on the volcanic rocks known to exist along the Maine coast and resulted in two deposits being found and developed: Cape Rosier and Blue Hill.

Intermittent exploration continued in northern and western Maine through to the 1970s. In 1967, a consortium of exploration companies operated under the name "The Northeast Joint Venture". This group, amalgamated and managed by J.S. Cummings, eventually discovered the base metal deposit at Bald Mountain in 1977 along with several other metallic mineral prospects ranging from the Quebec border to northeastern Maine (Cummings, 2012).

In 1978, Getty Mineral Company explored the area using a regional geochemical sampling program and identified an anomalous area of base metal enrichment close to Pickett Mountain. The first step of the program involved collecting stream, seep, and soil samples averaging about 30 samples per square mile. This was followed by a more detailed soil sampling program that further defined the geochemical anomaly. During the summer of 1979, a Max-Min horizontal loop electromagnetic ("HLEM") survey and magnetic surveys were conducted. A bedrock conductive source that was identified and drilled in the fall resulted in the initial discovery hole. Since that time, approximately 68,000 meters of drilling, including hole extensions, totalling 204 holes have been completed. The FW Zone was discovered in 2019 after recognition of the exhalative horizon by Art Hamilton, a well-known geologist from the Bathurst mining camp, under the supervision of Don Hoy, who was the Vice President of Exploration of Wolfden at the time.

Soil sample results, which were the catalyst for the original discovery, have proven to be an effective exploration technique as the overburden thickness is generally thin. Combined Zn+Pb+Cu soil anomalies, in excess of 500 ppm, clearly highlight the discovery area. The image below presents a color-contoured map of combined Zn-, Pb- and Cu-in-soils overlain by the surface projections of the FW (dashed red line), West and East zones (Fig. 6). The strongest anomalies, at greater than 2,000 ppm combined Zn+Pb+Cu, lie under the westernmost surface projection of the FW zone and western portion of the East Zone. These strong responses generally correlate with areas of shallow overburden. Anomalous zones that extend to the southeast, from the zones, are likely due to glacial dispersion and drainage. The anomalous zone located to the north of the zones, appears to be a fold repetition of the sequence, and represents a future exploration opportunity.

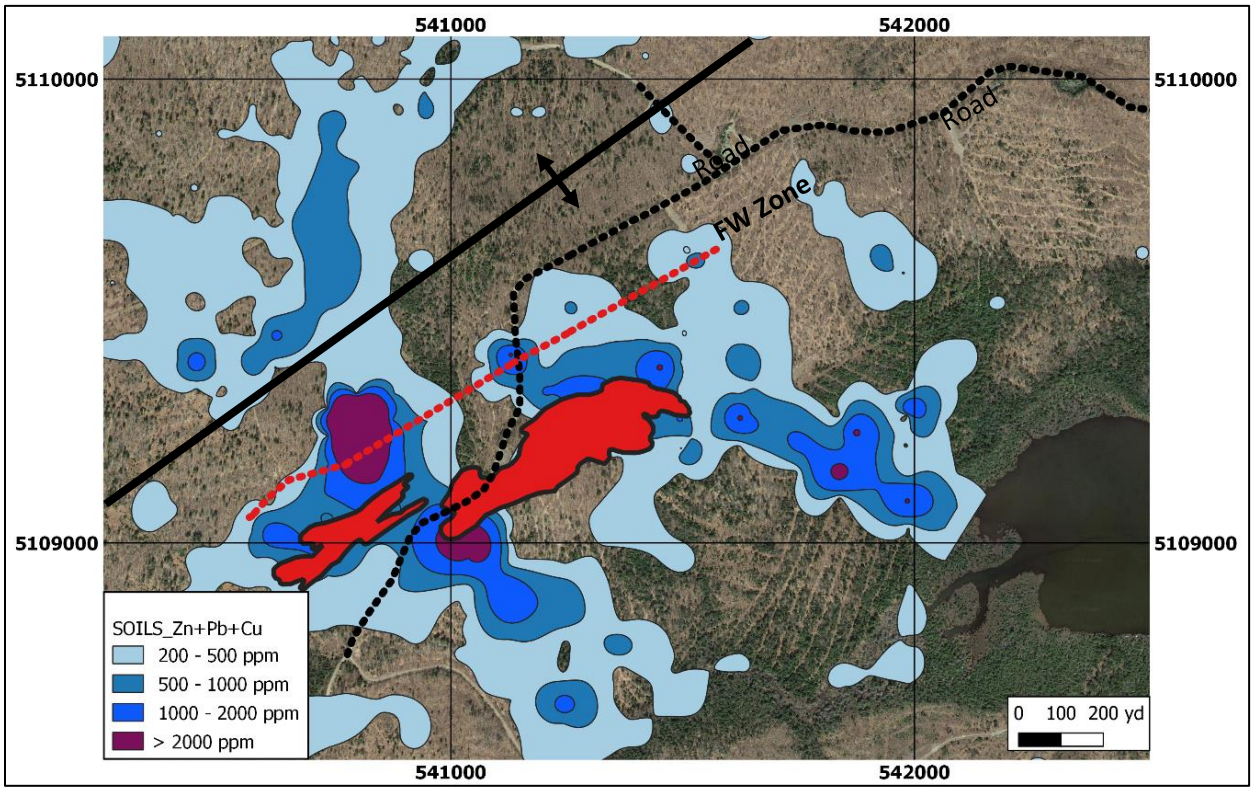

Figure 6. Summarized soil sample results for the Pickett Mountain Deposit.

Geophysical surveys, including electromagnetic ("EM"), induced polarization ("IP"), gravity and magnetics have also been effective exploration tools. The massive sulphide bodies are modest-strength EM conductors. IP surveys have been effective, especially for delineating the FW Zone. Magnetic surveys have been useful in defining stratigraphy. Both IP and magnetic data have been subjected to data inversion to provide a 3D view of the magnetic,

chargeability and resistive character of the rocks, which in turn, led to more effective drill targeting.

DEPOSIT GEOLOGY

The Pickett Mountain Deposit consists of three zones, West, East, and Footwall (FW).

The FW Zone occurs at the onset of the felsic volcanism with mineralization located within carbonate-rich, locally pebbly sediments, adjacent or proximal to, the top of, what is interpreted to be, a hypabyssal quartz feldspar (±hornblende) porphyry (QFP) intrusion. This intrusion is generally medium to coarse grained with quartz 'eyes' to 1 cm in size, specifically under the West Zone. Locally, QFP fragments have been observed at the contact along with a carbonate- and silver-enriched 'exhalite' unit, which hosts the FW Zone mineralization. Locally, breccia textures suggest that the QFP breached or was emplaced just under the sea water/rock interface. Regionally, quartz felspar crystal felsic tuffs, suggest that the QFP-equivalent rocks are extrusive. Alteration within the QFP comprises ubiquitous weak to intense sericitization, locally strong silicification, disseminated pyrite, local sphalerite, galena, pyrite and chalcopyrite stringers and local disseminated to massive talc (underlying the FW mineralization beneath the West Zone). FW Zone mineralization varies from disseminated to massive sulphide comprising a mixture of sphalerite, galena, pyrite, chalcopyrite and, locally, tetrahedrite (Fig. 7).

Figure 7. FW Zone sulphide mineralization below the East Zone.

The West and East zones lie at, or near, the top of the felsic volcanic package and occupy the same time-equivalent stratigraphic position. The massive sulphide mineralization can be traced for approximately 1,000 meters along strike and to a depth of 850 meters, where the West Zone, and potentially the East Zone, is still open. On the western end of the deposit, the West Zone mineralization becomes thinner and more pyrite dominant. The East Zone is cut off to the east by a younger diorite intrusion. No mineralization has been found to the east of the diorite body. Overall, the West Zone is higher grade than the East Zone. As well, the West Zone exhibits strong footwall alteration versus weak alteration under the East Zone. Both zones are overlain by an eastward-thickening, mafic tuff dominant, debris flow that contains occasional massive sulphide/altered felsic volcanic fragments and local rafts. The current interpretation is that the East Zone is a slumped and/or faulted portion of the West Zone and that both zones were capped by a debris flow that marks the onset of mafic volcanism. The debris flows resulted in the preservation of the massive sulphide zones.

Sections through the West and East zones, including the FW Zone, are presented in Figures 8 and 9, respectively. Note that the FW Zone interpretation may change with additional drilling. Also note that the FW zone ranges from disseminated to massive sulphide, in character.

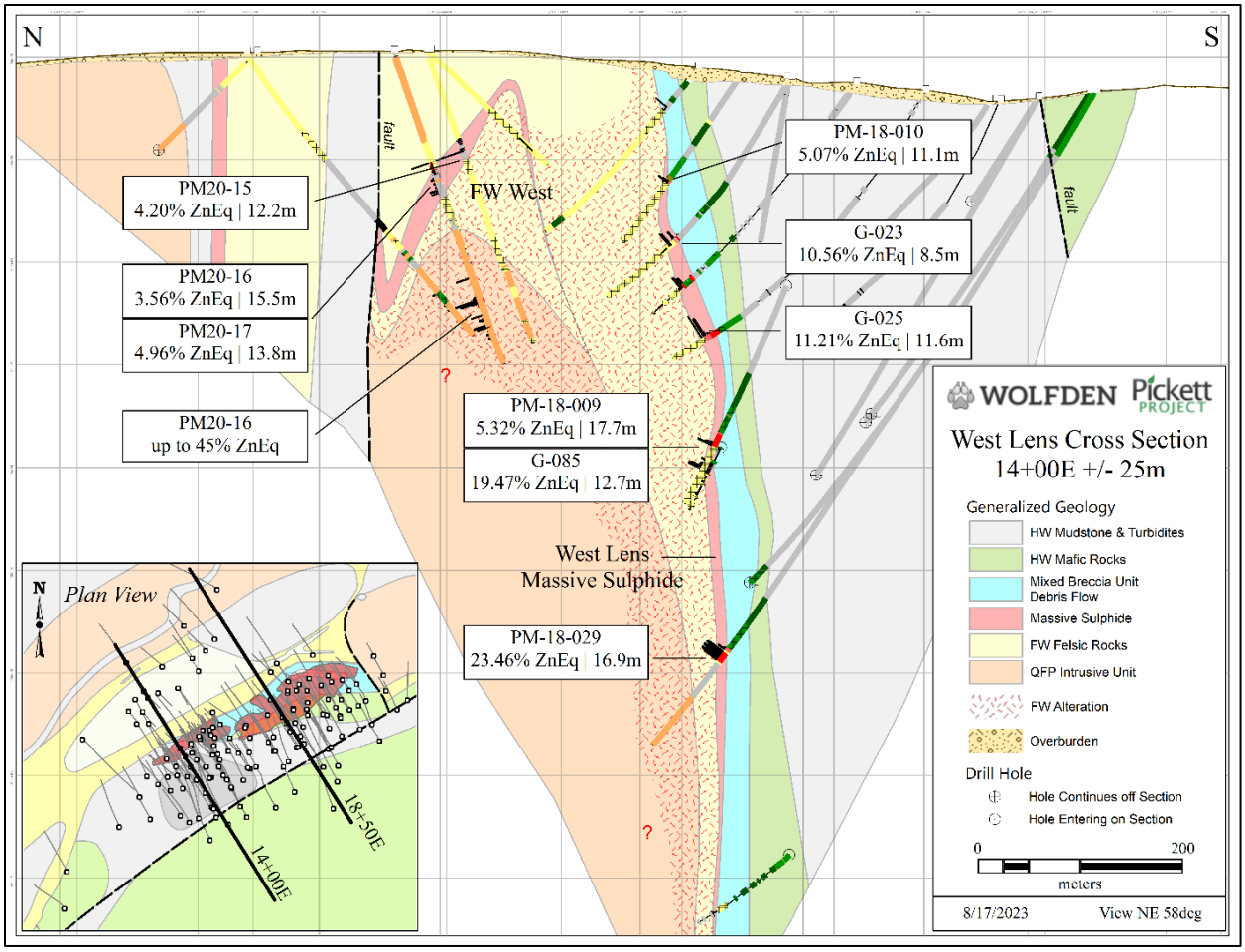

Figure 8. Cross sectional view of the West Zone and western portion of the Footwall Zone stratigraphy.

The West Zone is planar to locally Z-folded and steeply dipping. The East Zone is similarly oriented at its western edge, but the strike rotates clockwise and the dip shallows eastward, as it becomes affected by the interpreted quartz feldspar phyric felsic intrusion at depth and a later diorite intrusion at the deposit's eastern edge. The West and East zones are horizontally offset by 60 to 80 meters. This offset occurs across a less than 50 m wide band at the eastern edge of the West Zone, where the West Zone is Z-folded, in an accordion-like fashion, with up to seven repetitions of the massive sulphide time horizon noted in drill core. This folding was first observed by Jerry Grant and later validated by two, well-placed drill holes. As a result of this updated interpretation, several (previously interpreted) separate massive sulphide lenses and a couple of unexplained massive sulphide intercepts became part of the West Zone, resulting in an increased deposit tonnage estimate in 2021.

The grade x thickness contouring of the Zones shows that the deposits are relatively well constrained and are not expected to materially change in shape to the east and west. The West Zone's elongate shape supports the interpretation that the location of this deposit is controlled by basin-margin faults with orthogonal cross structures that focused ascending, metal-rich hydrothermal brines (see Fig. 10). Higher % ZnEq grades appear to be more common at depth in the West Zone. The West Zone is clearly open to depth.

The FW Zone is more silver rich and pod-like in nature (see Fig. 11). The silver-rich character of the FW zone is evident with individual samples returning over 200 oz/t Ag. Since the FW Zone is closely related to the QFP, the poddy nature of the zone could be related to proximity to the QFP. Another possibility is that the FW Zone time horizon exhibits unequal preservation as there is no clear deposit-capping geology. As with the West Zone, the FW Zone, especially below the East Zone, is clearly open.

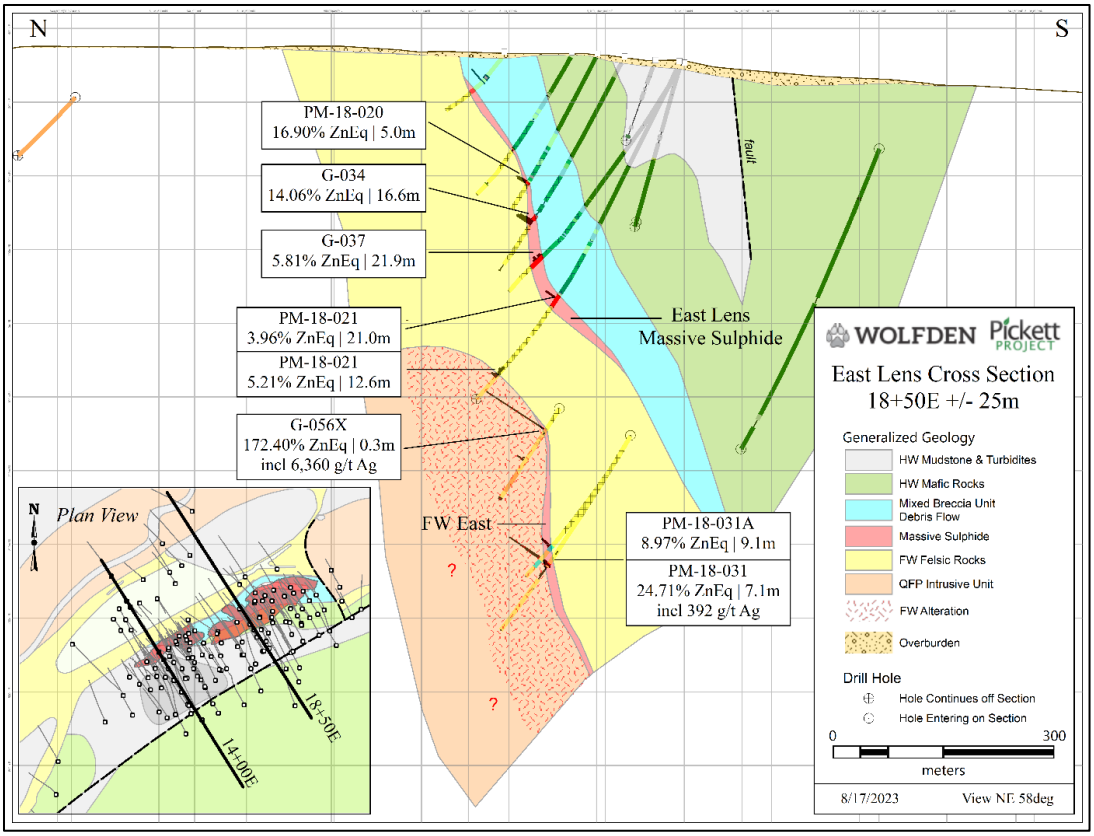

Figure 9. Cross sectional view of the East Zone and eastern portion of the Footwall Zone stratigraphy.

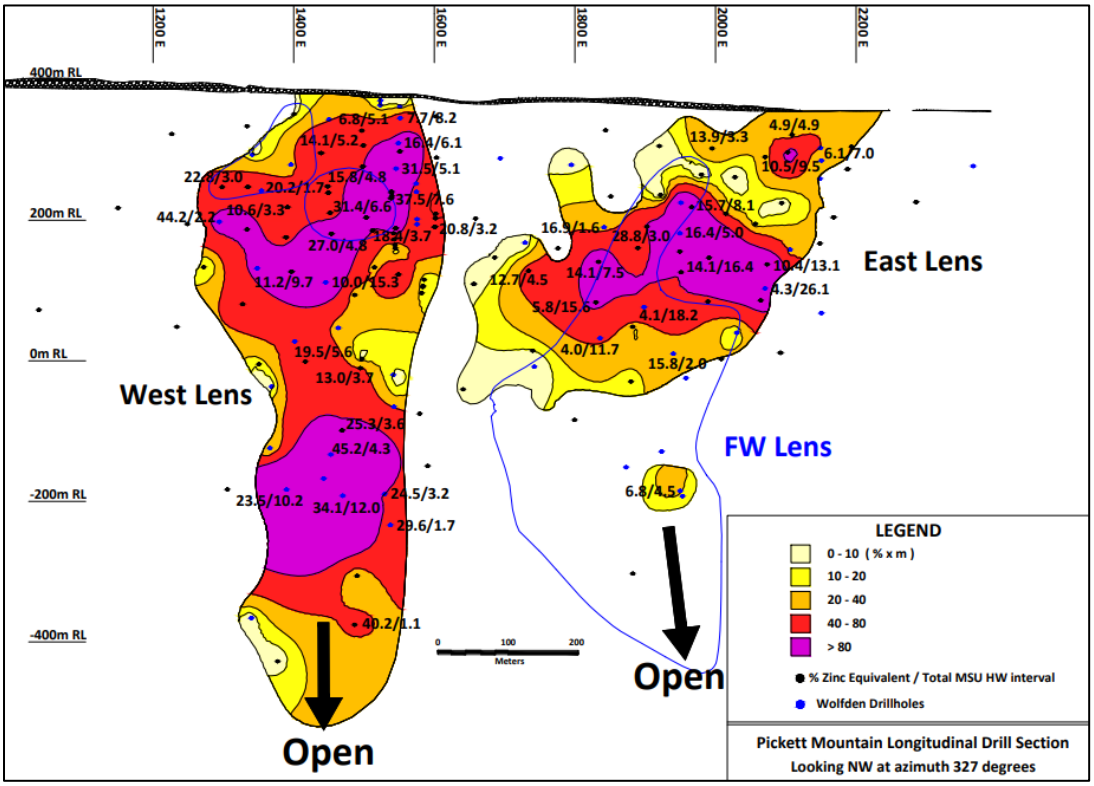

Figure 10. Color contoured % ZnEq grade x width West and East Zones (Wolfden, 2023).

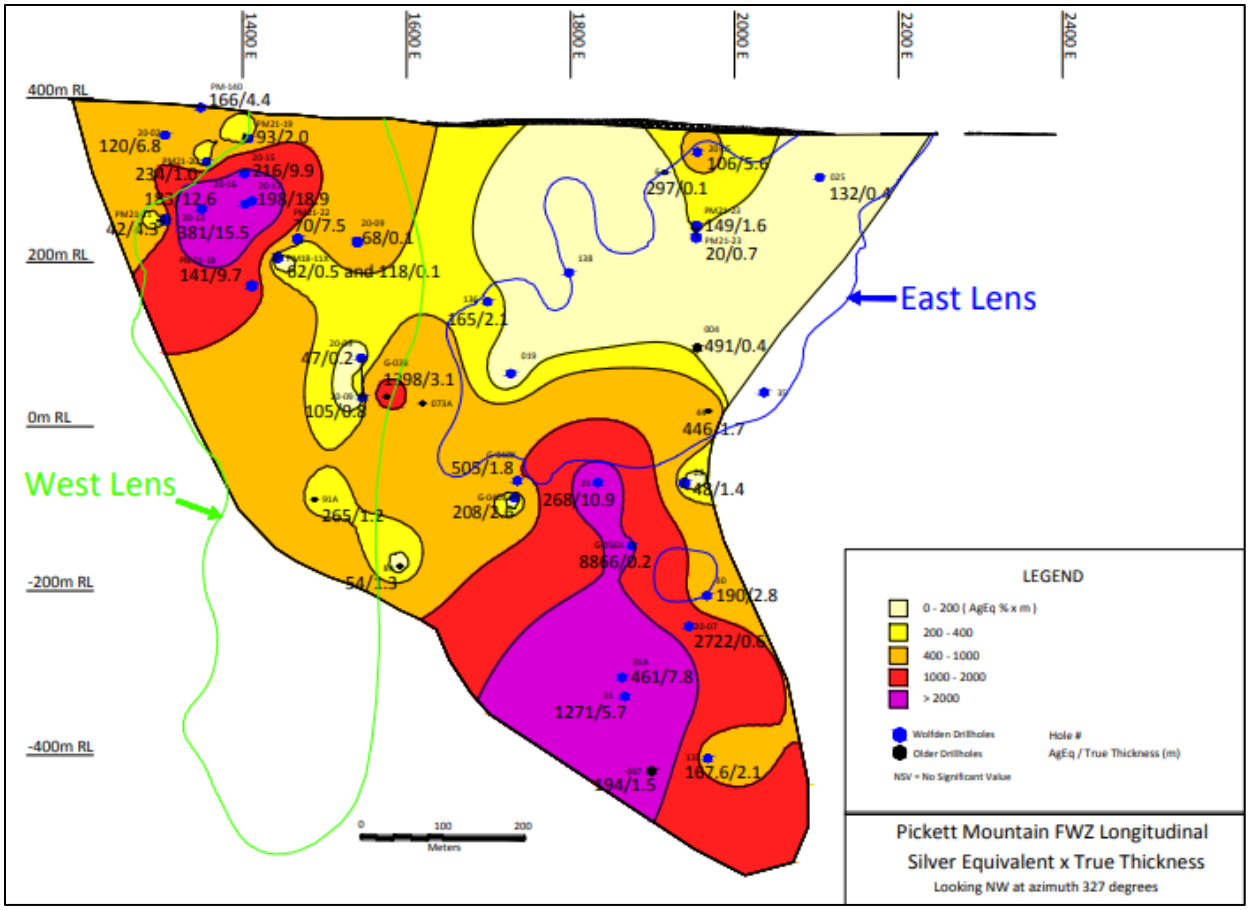

Figure 11. Color contoured g/t AgEq grade x width FW Zone (Wolfden, 2023).

DEPOSIT MODEL

Figure 12 synthesizes most of the drill core, mapping and lithogeochemical observations collected to date. Of note, is the relationship with the QFP and the FW zone and the QFP's relationship with the West Zone. Higher grade at deeper portions of the West Zone correlate with the QFP stoping up into the stratigraphy. Strong alteration is noted in the felsic volcanics below the West Zone and in the QFP, suggesting a strong genetic link. It is likely that this model will be updated in the future as additional observations from in-fill drilling and additional interpretations are incorporated.

PERMITTING AND NEXT STEPS

In early 2023, Wolfden submitted a rezoning application to the LUPC for a 374-acre portion of the Company's 7,135-acre, wholly owned property. An approval from the LUPC to rezone the mine area from a General Management (M-GN) subdistrict to Planned Development (D-PD) would allow Wolfden to proceed with baseline and feasibility studies to present to the Maine Department of Environmental Protection ("MDEP").

The proposed Project is a 1,200 tonne per day underground mining operation with a 10–15-year mine life, located five miles off of State Route 11, in an area of very low population density, north of the Town of Patten. The mine and other supporting infrastructure will require a steady-state work force of roughly 272 direct employees and contractors. An image of the proposed site, including a portal/decline, water treatment facility and storage ponds, and a solar array, shows the infrastructure that is currently planned (Fig. 13). The mined ore from the Project will be processed at a different location (not in T6 R6) and therefore is outside of the scope of the LUPC rezoning application. Moreover, the technical analysis for each aspect of the Project, including proposals for the protection of natural resources, demonstrate that the Project is economically feasible and consistent with Chapter 200 and the values prioritized by the LUPC in its Comprehensive Land Use Plan.

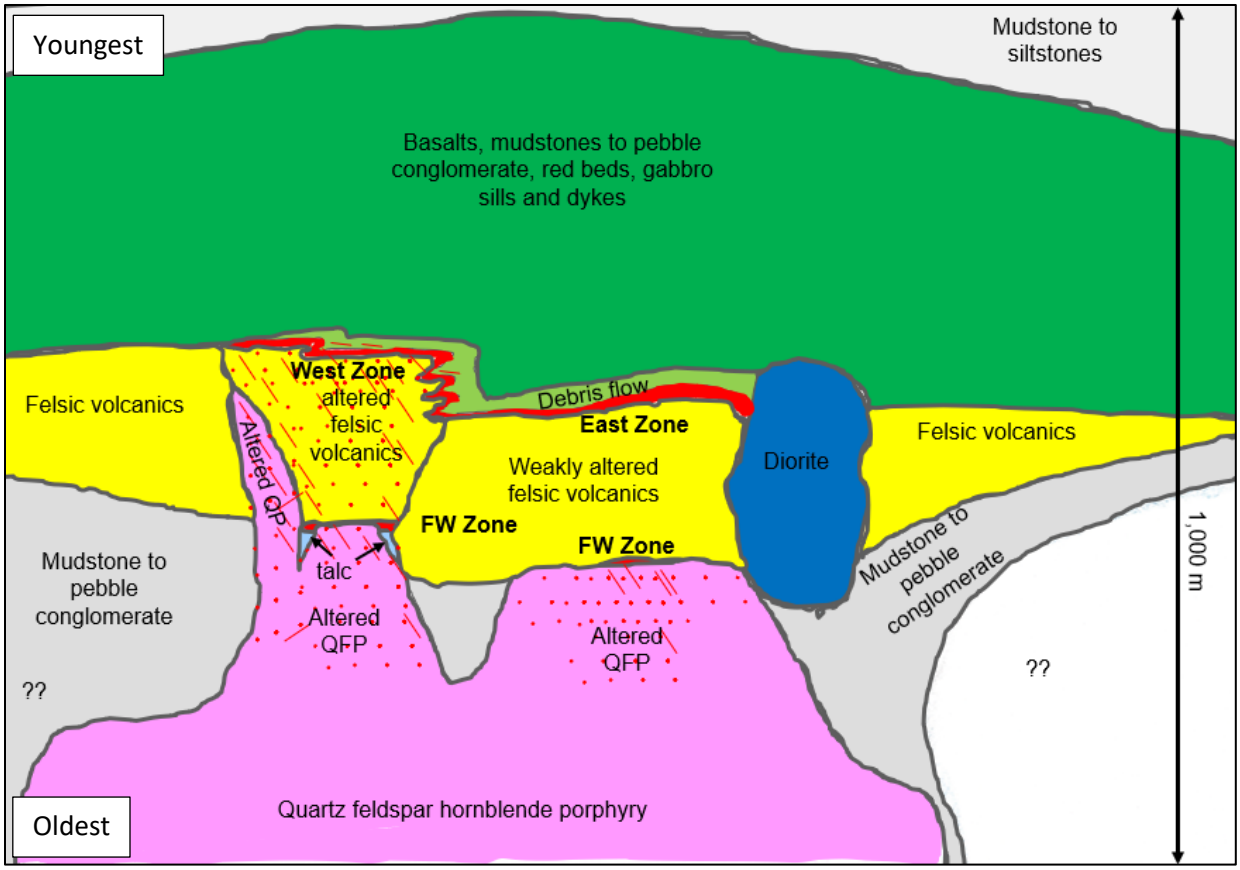

Figure 12. Pickett Mountain Geological Model (Wolfden, 2023).

Upon completion of the rezoning process, Wolfden plans to commence a feasibility study including the collection of additional environmental baseline characterization data, a drill program to convert Inferred to Indicated Mineral Resources, design of the various operational components (including the ore processing and tailings management facilities) and a complete estimate of costs. This data will all be used as input to a mining permit application for MDEP review under Maine's Chapter 200 Regulations (*Metallic Mineral Exploration, Advanced Exploration and Mining*). Approval would allow for the construction, operation, closure, and reclamation of a state of the art, small footprint underground mine in a manner that is fully protective of the environment.

The rezoning application is subject to and will be reviewed under the Commission's Chapter 10 and Chapter 12 Rules. Chapter 12 and Chapter 5 (*Rules for the Conduct of Public Hearings*) require a public hearing to be held by the Commission at a location in close proximity to, or significantly affected by, the Project before a final decision on the application.

A copy of the rezoning application along with related correspondence with the LUPC, and more information about the process, is available for download from the LUPC project-specific webpage and the Company's website.

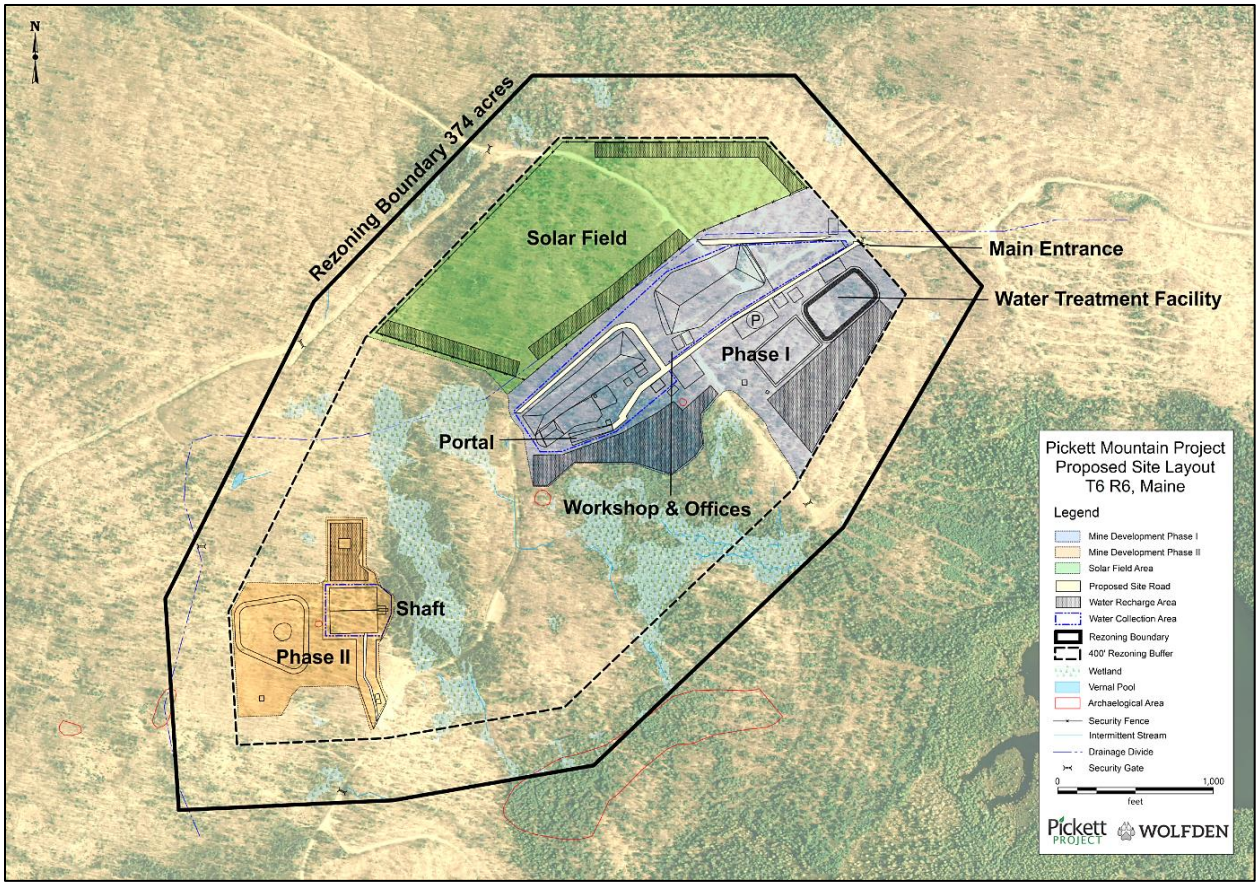

Figure 13. Proposed mine-site layout.

FIELD TRIP DETAILS

Meeting point – Debbie's Deli or Wolfden's office at 20 Main St. in Patten. Wolfden's office is located across the street from Debbie's Deli and adjacent to the south side of the Post Office. Parking is available in the lot on the east side of Debbie's Deli or behind the Wolfden office building.

9 am – Stop 1: PowerPoint presentation at Wolfden's Patten office
The presentation will provide an overview of the Pickett Mountain Deposit's location, geologic setting, geologic model, mineralization long sections, permitting and mine plan.

10 am – Stop 2: Review of drill core at the Core Shed
Hole PM20-04:
This hole exhibits seven repetitions of the West Zone time horizon along the eastern side of this Zone.
Hole PM-18-031:
This hole presents the FW Zone discovery below the East Zone and its proximity to the altered QFP. Core from this hole from 729 m to 800 m, down-hole depth, will be reviewed.
Hole PM20-17:
This hole presents the FW zone beneath the West Zone that displays fragmental and possible boiling textures demonstrating a potentially important relationship with the underlying QFP unit. Core from this hole from 120 m to 190 m, down-hole depth, will be reviewed.

12 noon – Stop 3: Lunch at Wolfden's office

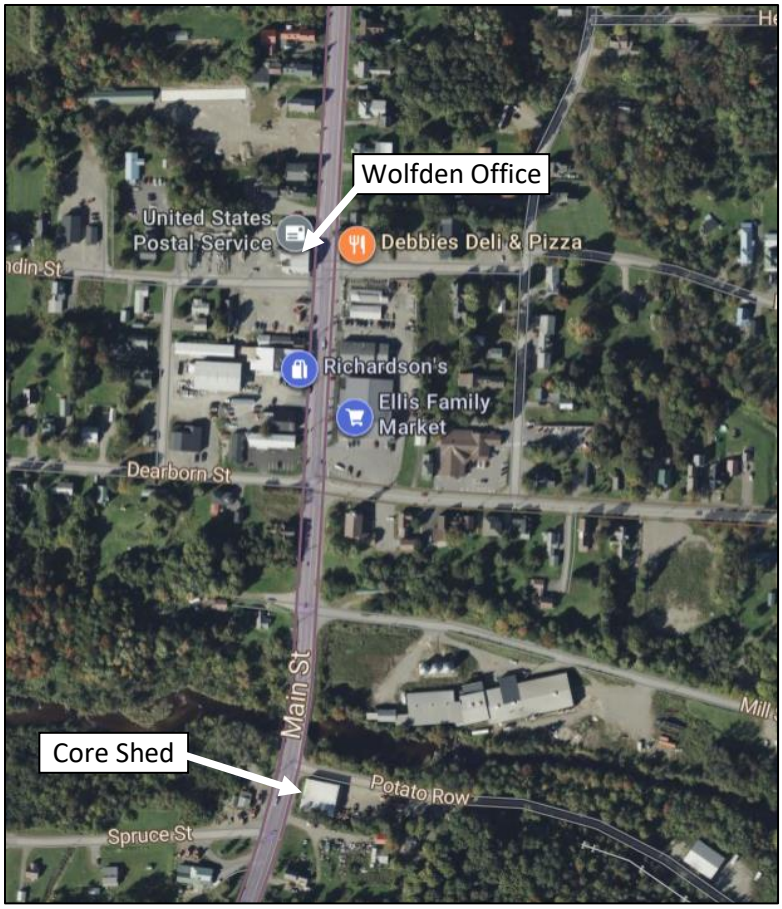

Figure 14. Location map of Wolfden's office and Core Shed, Stops 1 and 2.

1:00 pm – Leave Wolfden's office for Pickett Mountain Project site

1:30 pm – Stop 4: Z-folded West Zone outcrop – UTM coordinates 540,816E / 5,109,075N
Stop 4 displays an area that has been stripped of overburden where the West Zone massive sulphide time horizon has been subject to Z-folding. Figure 17 is a generalized clip of the mapping completed by Jerry Grant in 2020 for Wolfden.

Stop 5: Magnetic lobate FW Felsic volcanic flows - UTM coordinates 540,765E / 5,109,151N
This stop lies along an area of overburden stripping in the footwall to the West Zone. Magnetic, massive to lobate felsic flows occur in several areas.

Stop 6: Possible surface expression of FW Zone - UTM coordinates 541,585E / 5,109,846N
Stop 6 lies along a drill access trail. Felsic volcanic rocks exposed along the trail are locally pyritic and correspond with elevated base metals in the soils. Additional sampling should be completed at this site to determine if the characteristic silver-enrichment of the FW Zone occurs at this location.

Stop 7: Outcrop of QFP in contact with FW sediments - UTM coordinates 541,509E / 5,109,667N
The weakly pyritic QFP intrusion at this location is in contact with the footwall sedimentary rocks. Within the deposit area, the QFP occurs immediately below the FW Zone and locally stopes up into the felsic volcanics, to lie immediately below the West Zone.

3:30 pm – return to Patten for additional discussion or drive to Presque Isle to prepare for dinner

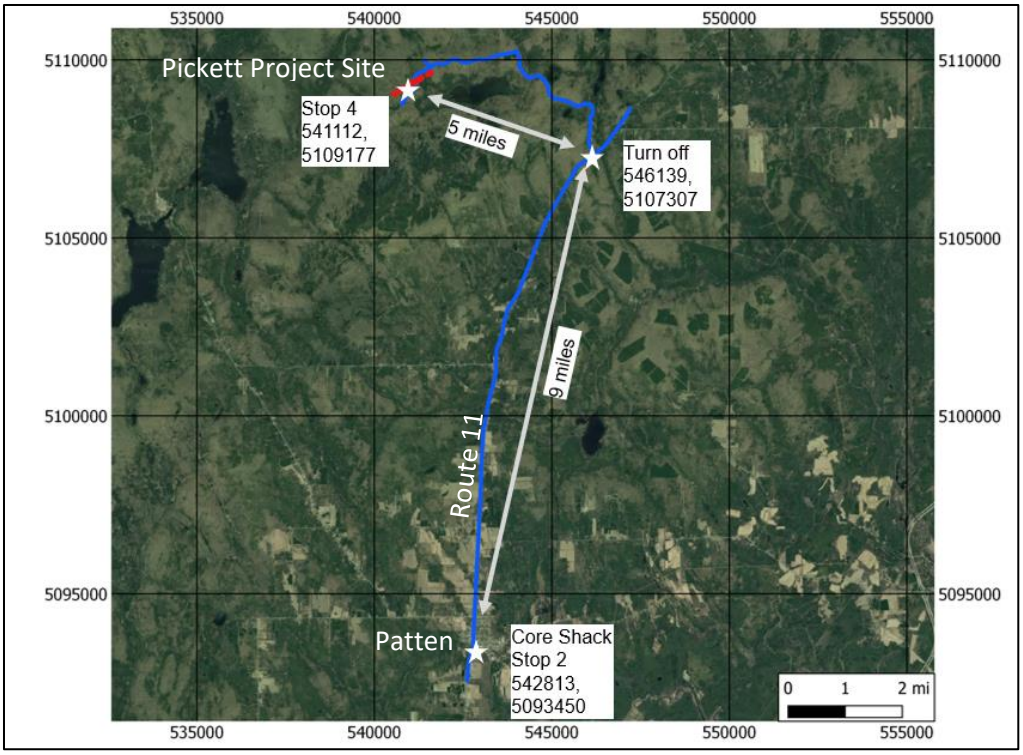

Figure 15. Route form Patten to Pickett Mountain Project site

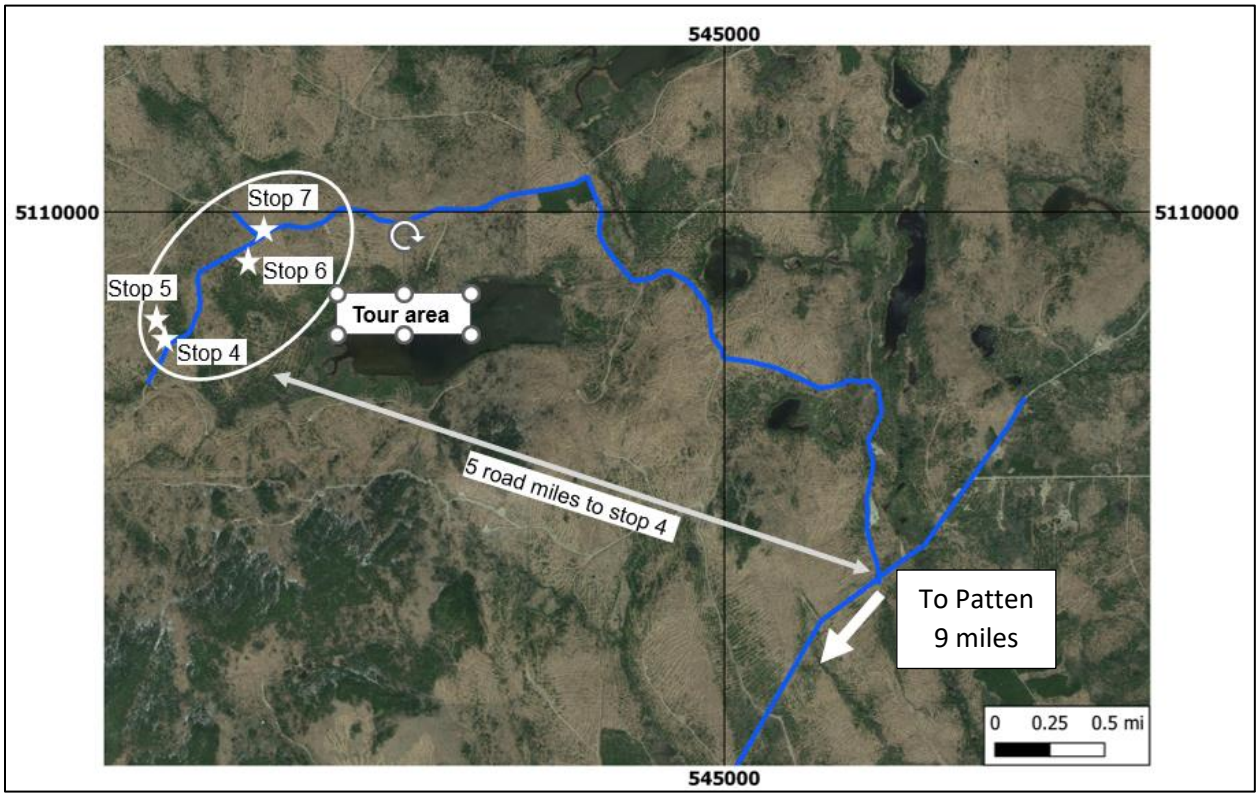

Figure 16. Route from Highway 11 to Pickett Mountain Project site

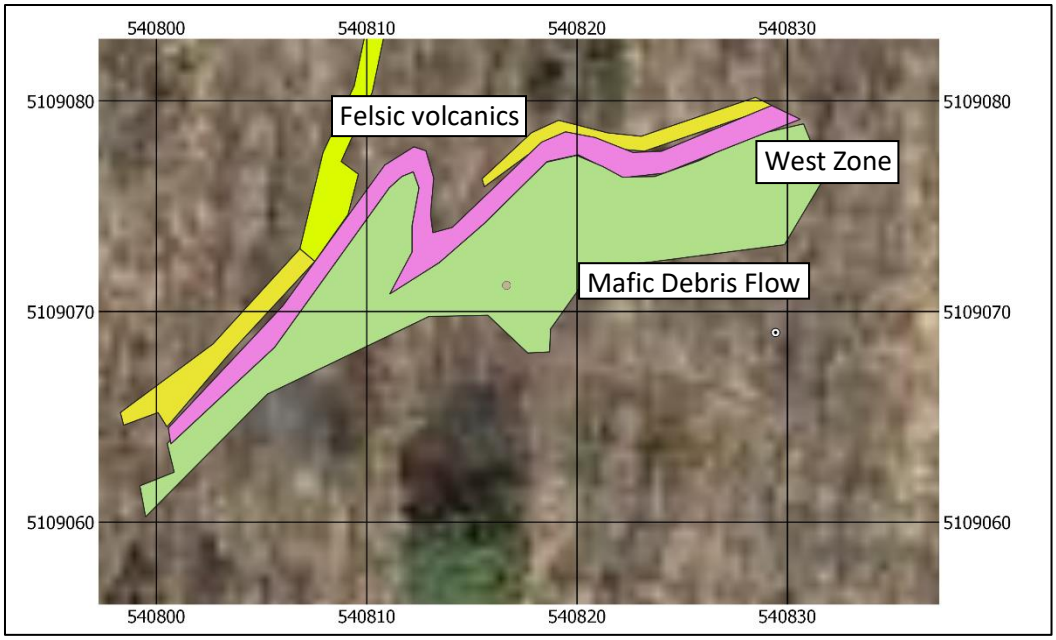

Figure 17. Simplified plan view of Z-folded West Zone outcrop at Stop 4.

REFEERNCES

A-Z Mining Professionals Ltd., 2019, Pickett Mountain Project Resource Estimation Report, Penobscot County, Maine, USA: NI 43-101 Mineral Resource Estimate, 98 p.

A-Z Mining Professionals Ltd., 2020, Preliminary Economic Assessment Pickett Mountain Project, Penobscot Couty, Maine, USA: NI 43-101 Preliminary Economic Assessment, 205 p.

A-Z Mining Professionals Ltd., 2021, Updated Mineral Resource Statement for the Pickett Mountain Deposit: Wolfden Resources Corporation News Release – November 17, 2021, 4 p.

Cummings, J.S., 2012, The Lost Promise of Golconda: Metals in the Maine Earth: RE-BOOKS, 89 p.

Hibbard, J.P. et al, 2006, Lithotectonic map of the Appalachian orogen, Canada – United States of America [2 Sheets]: Geological Survey of Canada Map 2096A.

McCormick, M.J., 2021, Geology and Lithogeochemistry of the Pickett Mountain Volcanogenic Massive Sulfide Deposit, Northern Maine: M.Sc. thesis, University of Maine, 204 p.

Neuman, R.B., 1967, Bedrock geology of the Shin Pond and Stacyville quadrangles Penobscot County, Maine: United States Geological Survey Professional Paper 524-I, 37 p., 3 plates.

Scully, M., 1989, Geology and Petrogeochemistry of the Mount Chase Massive Sulfide Prospect, Penobscot County, Maine: M.Sc. thesis, University of Missouri-Rolla, 117 p.

MANGANESE GIANTS IN THE MARITIMES, WOODSTOCK, NEW BRUNSWICK

Bryan Way
Canadian Manganese Company, 55 University Avenue, Suite 1805, Toronto, Ontario, Canada, M5J 2H7
Email address: bryan.way1@gmail.com

INTRODUCTION

Iron was first discovered within the Woodstock area back in the 1820's by early settlers. In 1836, Charles T. Jackson of the Maine Geological Survey produced the first geological report of the Woodstock area. In his report, he noted the occurrence of iron deposits having a thickness of almost 274.3 m (900 ft) and unknown in length, with the greatest thickness of the beds and accessibility in Jacksontown, near Jacksonville, New Brunswick. The rocks were described as compact rocks of red hematite with a blocky cleavage with a surface crust of manganese oxide (Jackson, 1837). From 1848 to 1884, these deposits served as a source of armor plating for British Naval warships. With mining and smelting operations untaken by the Woodstock Iron and Charcoal Company. The high manganese content in the iron deposits produced a material that was hard (similar to steel when struck) but not brittle (Hind, 1865; Sidwell, 1964; Potter, 1983). Within that time, approximately 70,000 tonnes of Fe-Mn mineralized rock were mined and smelted from the Jacksonville mines (Figs. 1 & 2). At the time, rising costs and diminishing known sources of the iron ore and charcoal in the area caused the deposits to be abandoned shortly after the smelting operations had ceased. (Bailey, 1898; Sidwell, 1964; Anderson, 1968; Potter, 1983; Way, 2012). Bailey (1898) suggested that the Woodstock deposits could be a source of manganese if more cost-effective methods were adopted.

In 1954 a gravimetric survey identified several gravimetric anomalies southwest of the known iron deposits. A diamond drilling program in 1957 indicated six Fe-Mn deposits (Fig. 3;) that had an estimated combined tonnage of 194,000,000 metric tonnes with an average grade of 13% iron and 9% manganese. Due to the rising energy costs and difficulties of extracting the manganese ore at the time, mining of the deposits never took place. Much of the information on these deposits became lost over time once the major exploration efforts had ceased (Sidwell, 1954; Sidwell, 1957; Way, 2012).

Exploration occurred sporadically over the next 50 years until August of 2010 when Buchans Minerals Corporation (BMC) acquired the claims on several mineral properties west of the town of Woodstock. Globex Mining also staked several claims of several mineral properties at the locations of the original Jacksonville mines in 2010. These claims were then optioned to Manganese X Energy Corp in 2016. As of 2023, four drilling programs have been completed by Buchans Minerals, one by Globex Mining, and three by Manganese X Energy Corp (Way, 2012; Teniere et al., 2021). A PEA (Preliminary Economic Assessment) by the Canadian Manganese Corporation (CMC) has been completed on the Plymouth Fe-Mn Deposit in 2022 and a PEA was completed by Manganese X Energy Corp on the nearby Battery Hill (Iron Ore Hill, Moody Hill, and Sharpe Farm) Fe-Mn Deposits in May of 2022 (Canadian Manganese Company Inc, et al., 2022). Most recently, the tonnage and grade amounts have been recalculated to 216,840,000 metric tonnes with an average grade of 12.32% iron and 8.31% manganese (Fig. 3).

WOODSTOCK STRATIGRAPHY

The regional stratigraphy of the Woodstock area (Figs. 4 & 5) is largely composed of deformed quartzite, quartz wacke, and silty shale of the basal Cambrian to Ordovician Woodstock Group. The Woodstock Group (locally the Baskahegan Lake Formation) is intruded by the Ordovician Gibson Granodiorite and Benton Granite. The Woodstock Group is then disconformably superimposed by the Meductic Group, composed of Lower Ordovician felsic and mafic volcanic and volcaniclastic rocks, that are visible east of the Woodstock Fault (van Staal and Fyffe, 1991; Fyffe, 2001). West of the Woodstock Fault, structurally separated, and unconformable on the Woodstock Group, is the argillaceous limestone and calcareous shale of the Upper Ordovician to Lower Silurian Matapedia Group (Fyffe, 1982; Ludman, 1988; Smith and Fyffe, 2006). None of the areas located west of the Woodstock Fault expose outcrops of the Meductic Group, Woodstock Group, or the base of the Matapedia Group. Some areas west of the United States/Canada border (near Bridgewater, Maine) display the Matapedia Group conformably underlain by Meduxnekeag Group (Pavlides, 1966). Conformably and depositional on top of the Matapedia Group is the Perham Group, as identified in drill core sections near Plymouth, NB. The Perham group is dominated by noncalcareous siltstone, noncalcareous and calcareous sandstone, and associated ferromanganiferous siltstone. The uppermost formation in the study area is the Lower Carboniferous Carlisle Formation, comprised red sedimentary rock, which lies unconformably on top of the

Woodstock Group, east of the Woodstock Fault, and is terminated sharply on the western side by the Woodstock Fault. (Fig. 5; Way, 2012).

Figure 1. Remains of an abandoned open pit mine at Iron Ore Hill (circa 1860's)**.**

Figure 2. Remains of an abandoned open pit mine at Moody Hill (circa 1860's)**.**

Plymouth ***Recalculated 2023****	51,000,000 ***56,700,000***	13.3 ***14.01***	10.9 ***10.7***
North Hartford	50,000,000	12.0	8.0
South Hartford	50,000,000	12.0	8.0
Moody Hill	26,740,000	10.36	6.21
Iron Ore Hill	25,000,000	14.0	10.0
Sharpe Farm	8,400,000	11.56	6.96
Total	216,840,000	12.32	8.31

Figure 3. Tonnage and grade of each of the Woodstock Fe-Mn deposits. *Includes new inferred tonnage for the Plymouth Fe-Mn at a 5% cut-off grade as of March 2023 (Sidwell, 1957; Potter 1983; Ténière et al., 2021; Canadian Manganese Company Inc, et al., 2022, Canadian Manganese Company Inc press release, 2023).

LITHOLOGY OF THE ROUTE 95 AREA

Much of the bedrock exposure within western New Brunswick and eastern Maine is limited to small irregularly situated outcrops and roadcuts. Expansion of Route 95 from the Woodstock, New Brunswick/Houlton, Maine border-crossing station to Woodstock, New Brunswick, has led to several large new roadcuts (Fig. 6) that can aid to a better understanding of the local stratigraphy as first mapped in detail by Hamiliton-Smith in 1972. This recent bedrock

exposure also lies perpendicular to the general northeast strike of bedrock and nearby to the largest of the Woodstock Fe-Mn deposits. Within this area there are two formations, the Upper Ordovician to Lower Silurian White Head Formation and the Silurian Smyrna Mills Formation (Pavlides and Berry, 1966; Sidwell, 1957; Anderson, 1968; Hamiliton-Smith, 1972; Fyffe, 1982; Smith and Fyffe, 2006; Way, 2012).

Matapedia Group – White Head Formation

East of the town of Woodstock, the Upper Ordovician to Lower Silurian White Head Formation (formerly the Cary Mills Formation) lies structurally separate from the Cambrian to Ordovician Baskahegan Lake Formation (Fyffe, 1982). These two formations are divided by the south southwest-trending Woodstock Fault (Anderson, 1968; Fyffe, 1982; Smith and Fyffe, 2006). The White Head Formation is present locally as a series of tightly folded antiforms and synforms associated with localized D_1 and D_2 events and conformably underlies the Silurian Smyrna Mills Formation. The White Head Formation is composed of dark grey to blue-grey, massive and laminated argillaceous limestone, with interbedded calcareous shale and medium-grained calcareous sandstone and siltstone with an estimated thickness of over 750 m in areas west of Woodstock (Figures 4 & 5; Hamilton-Smith, 1972, Way, 2012).

Perham Group – Smyrna Mills Formation

The Smyrna Mills Formation lies conformably on the White Head Formation. This was identified in outcrops and drill cores near Plymouth, New Brunswick. This formation has been biostratigraphically dated as late Wenlockian to Ludlovian in age. In general, the Smyrna Mills Formation is a vertical to near vertical dipping sequence of interbedded siltstone and sandstone with a northeast strike (Pavlides and Berry, 1966; Hamilton-Smith, 1972; Fyffe, 1982; Roberts and Prince, 1990; Smith and Fyffe, 2006). Locally, this formation also contains silvers of interbedded mafic volcanic rocks, and felsic tuffs are also present within this formation (Fig. 4; Venugopal, 1981; Fyffe, 1982; Smith and Fyffe, 2006).

Hamilton-Smith (1972) subdivided the Smyrna Mills Formation into lower and upper members. The lower member is estimated to be 200 to 450 m in thickness and is composed of finely laminated dark grey noncalcareous siltstone and mudstone with minor green and red siltstone and associated Fe-Mn siltstone (Hamilton-Smith, 1972; St. Peter, 1982). The conformably lying upper member is composed of dark grey calcareous shale and siltstone interbedded with grey, calcareous, quartzose sandstone displaying flute and load casts with an overall thickness of 600 to 900 m in the McKenzie Corner. In areas near Glassville, New Brunswick it has been found with a thickness of more than 1500 m (Fig. 5; Pavlides and Berry, 1966; Hamilton-Smith, 1972; St. Peter, 1982; Smith and Fyffe, 2006; Way, 2012).

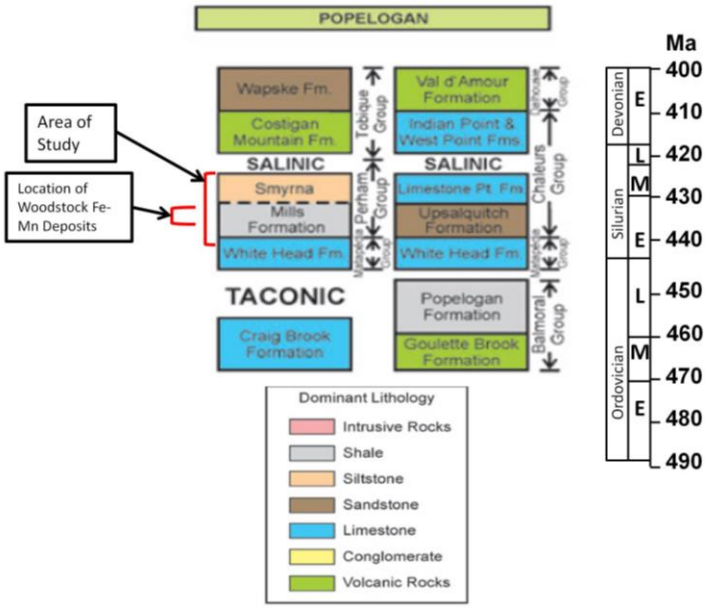

Figure 5. General Stratigraphy of the Popelogan Terrane that hosts the Woodstock Fe-Mn Deposits (Modified from Fyffe et al., 2011 and Ogg et al., 2008).

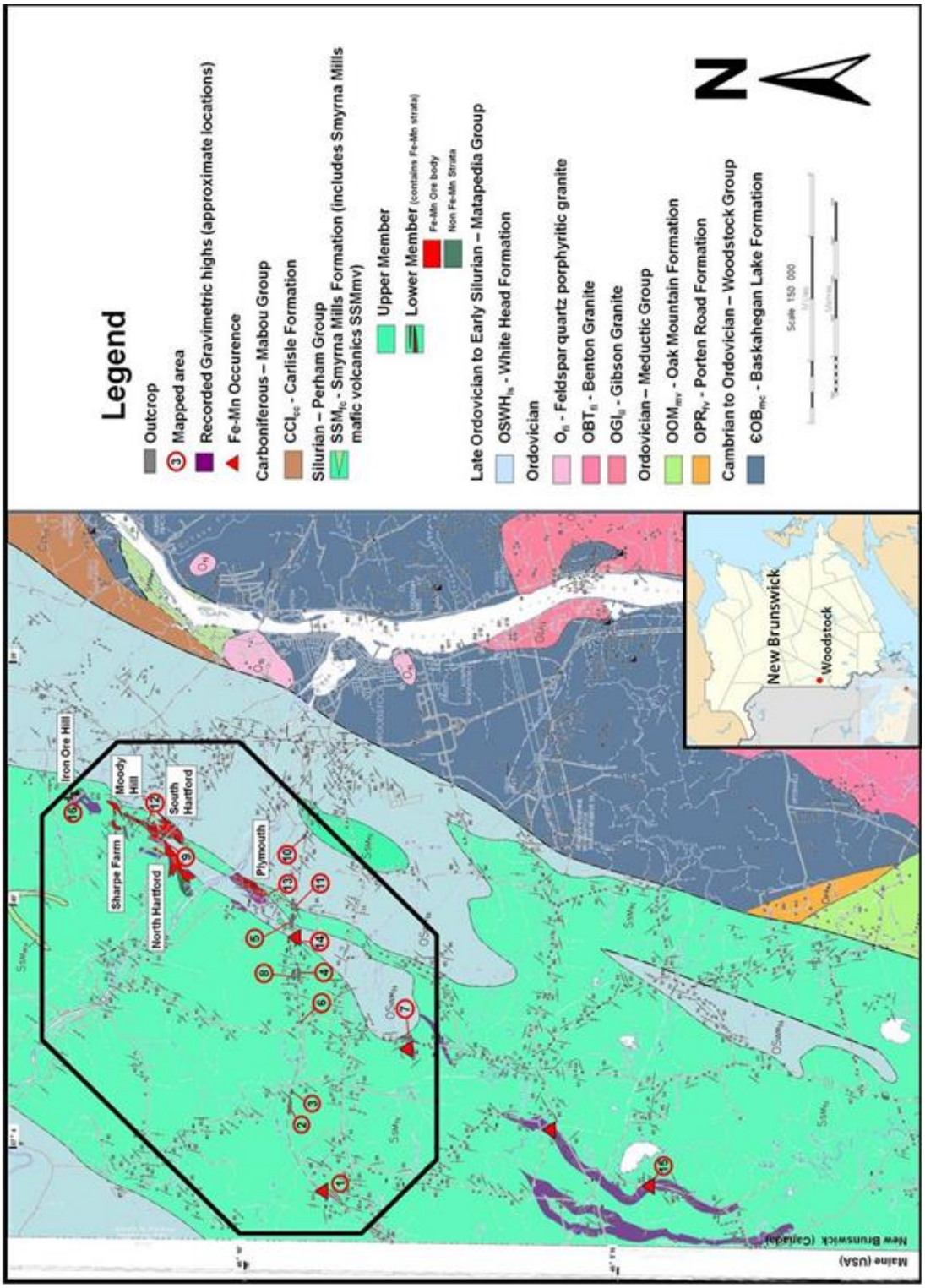

Figure 4. Bedrock Geological Map of the Woodstock Area displaying mapped outcrops, historical gravimetric anomalies, locations of Fe-Mn mineralization west of the Woodstock

Figure 6. Large outcrop along the Plymouth Road as part of the expansion to Route 95.

LITHOFACIES ASSOCIATIONS

Recent geological mapping, based on the methodology of Miall (1978), identified a total of six lithofacies associations (Fig.7; LA O, I, II, III, VI, V). It is also possible that there is another Lithofacies Association that has been dubbed the Transitional Zone (LA T) that is sandwiched in between LA O and LA I (Way, 2014). Folding and interbedding of the lithofacies have complicated the succession of the Lithofacies Associations within the Woodstock area, but in general, the lithofacies associations lie in stratigraphic succession and can range from tens to hundreds of metres in thickness. Many of these lithofacies have only minor changes in grain size lacked obvious bedding features and thus are classified by subtle changes in colour and mineralogy (Way, 2012).

Lithofacies Association O

Lithofacies Association O (LA O; Fig. 8) forms the upper part of the White Head Formation and is measured to be at least 43.3 m in thickness near Plymouth, New Brunswick. This unit is composed of blue-grey calcareous sandstone, interbedded blue-grey calcareous siltstone, with lesser limestone and contains abundant coarsening and fining up turbidite sequences. Geochemical analysis displayed elevated amounts of CaO and Sr in this lithofacies association. These anomalies are not present in the other lithofacies associations (Way, 2012).

The presence of turbidite sequences and overall coarsening upward of LA O might be associated with a progression more energetic turbidity currents associated with sea level regression. The location of LA O, at the time of deposition, is interpreted to be located on outskirts of the continental shelf where turbidity currents would have been commonplace (Pickerill, 1980; St. Peter, 1982). The lack of Fe-Mn beds suggests the seawater was not saturated in Fe^{2+} ions, or, alternately, did not experience changes in redox potential (Way, 2012). Within the regional context, LA O was accreted on the Laurentian margin during the uplift of the Popelogan terrane (Fig. 5) within a late Taconic tectonic event that marked the complete closure of the Iapetus Ocean (Fyffe et al., 2011).

Transitional Zone

The Transitional Zone (Figs. 7 & 8) is a depositional layer of massive blue-grey calcareous siltstone (*Fbuc*) that transitions into green calcareous siltstone (*Fgnc*). The upper and lower contacts between lithofacies *Fbuc* and *Fgnc* are found to be gradual and depositional and likely form the boundary between LA O and LA I as well mark the transition between the White Head and the Smyrna Mills formations and is occasionally present in outcrops and drill core. The Transition Zone varies in thickness near Plymouth, New Brunswick and appears to have a maximum thickness of 32.5 m (Way, 2014).

Lithofacies Association I

Lithofacies Association I (LA I) is the bottom section of the Smyrna Mills Formation. It is composed of green calcareous siltstone (*Fgnc),* green and grey interbedded laminated siltstone *(Fgngyib*), black to grey laminated mudstone *(Fbkpl),* grey and minor greenish laminated siltstone *(Fgyl*), greyish green siltstone *(Fgygn*), and green laminated siltstone with rare white microspheroidal limestone (*Fgnl*) (Fig. 8) Near Plymouth, New Brunswick it has an overall thickness of 253 m. Structurally, Lithofacies Association I displays F_1 and F_2 folds that may be associated with events from the Salinic Orogeny (Fyffe et al., 2011) and regional subgreenschist grade metamorphism (Roberts

and Prince, 1990). S_1 fabrics are parallel to bedding (S_0 fabrics), whereas S_2 fabrics, that are present as kink banding are perpendicular to the S_1 fabrics. Quartz veins, which appear to be associated with the D_1 events, may attribute some of the localized Cu and Co anomalies found in the area (Way, 2012). Geochemical analysis of Lithofacies Association I displays an enrichment in Al_2O_3, K_2O, Fe_2O_3, MnO, and P_2O_5 and decreases of CaO in comparison with the conformably underlying White Head Formation. Increases of Cu, Pb, S, As, Ba, Co, and V with decreases in Sr relative to SiO_2 are also present in LA I when compared to LA O (Way, 2012).

The LA I is largely composed of medium silt-sized grains and it remains largely consistent throughout the stratigraphic sequence. However, the variety of different lithofacies within LA I suggests a depositional environment was rapidly changing geochemically but still remained in a state of anoxia. Evidence of a Transition Zone (LA T), observed in drill core, upsection from LA O implies a slow change from an energetic carbonate-rich continental shelf to a stagnant silicate-rich anoxic shelf environment. Black pyritic mudstone beds (Figs. 5 & 7; lithofacies Fbkpl), suggests there were infrequent inductions of organic material deposited within the marine environment. Optical analysis of several thin sections displayed layers of framboidal pyrite within the seafloor which are locally present in outcrops and drill cores as identified by optical and XRF analysis (Way, 2012).

Within the regional context of this paleoenvironment, the closure of the Iapetus Ocean would in consequence produce restricted ocean circulation allowing localized ocean anoxia (Fyffe et al., 2011). Where substantial amounts of organic matter would amass and be deposited as grey siltstone (*Fgyl*) and black pyritic mudstone (*Fbkpl*) (Way, 2012). Lithofacies Fbkpl suggests it formed during early diagenesis (Berner, 1974; Wilkin and Barnes, 1997, Way, 2012). The decomposition of organic matter could in turn produce a fractionation of soluble Mn and Fe in the seawater and allow localized precipitation of iron sulfides and manganese carbonates onto the seafloor (Way, 2012).

Lithofacies Description	Code	Interpretation of sedimentary process(es)	Lithofacies Association(s)
Blue-grey laminated calcareous sandstone. May contain calcareous concretions	Sbuc	Deeper marine environment possibly associated with turbidity flows.	O
Blue-gray calcareous laminated siltstone. May contain calcareous concretions	Fbuc	Deeper marine environment possibly associated with turbidity flows.	O
Blue-grey limestone	Lbu	Deeper marine biogenic environment	O
Green calcareous siltstone	Fgnc	Anoxic marine environment	I
Green and grey interbedded laminated siltstone (tiger-striped)	Fgngyib	Marine anoxic environment with minor organic input	I
Black to grey laminated mudstone with authigenic pyrite	Fbkpl	Marine stagnant organic-rich anoxic environment.	I, II
Grey and minor greenish laminated siltstone	Fgyl	Marine anoxic marine organic environment with less sulfur.	I, II, V
Greyish green siltstone	Fgygn	Marine anoxic environment with minor organic input	I, II, IV, V
Green laminated siltstone with rare white microspheroidal limestone	Fgnl	Marine anoxic environmental with less sulfur with rare possible biogenic limestone	I, II, III, IV, V
Dark green to black laminated mineralized siltstone	Fgnz	(Detailed further)	II, rare III
Green to greyish green and tan calcareous and noncalcareous massive or laminated sandstone	Sgnl	Shallow marine environment.	II, III, IV
Red and maroon, variably arenaceous siltstone. Massive or with asymmetric cross-laminations	Frml	Oxic marine environment.	III, rare II
Red and maroon mineralized siltstone	Frmz	(Detailed further)	III
Grey laminated, asymmetrically cross-laminated, cross-bedded, or massive sandstone. Locally bioturbated, locally with crinoid hash. Bases may be intruded with flame structures	Sgyce	Shallow marine environment with macroscopic organisms present.	IV, V

Figure 7. Tabulation of each observed lithofacies along the Route 95 area west of Woodstock, New Brunswick. The codes of each lithofacies coincide with the following descriptions based on Miall (1978). S = Sandstone, F = Siltstone, L = Limestone, bu = blue-grey, bk = black, gy = grey, gn = green, rm = red and maroon, wh = white, c = calcareous concretions, p = pyritic, z = mineralized, l = laminated, o = microspheriodal, e = cross-bedded or massive, m = massive, ib = interbedded.

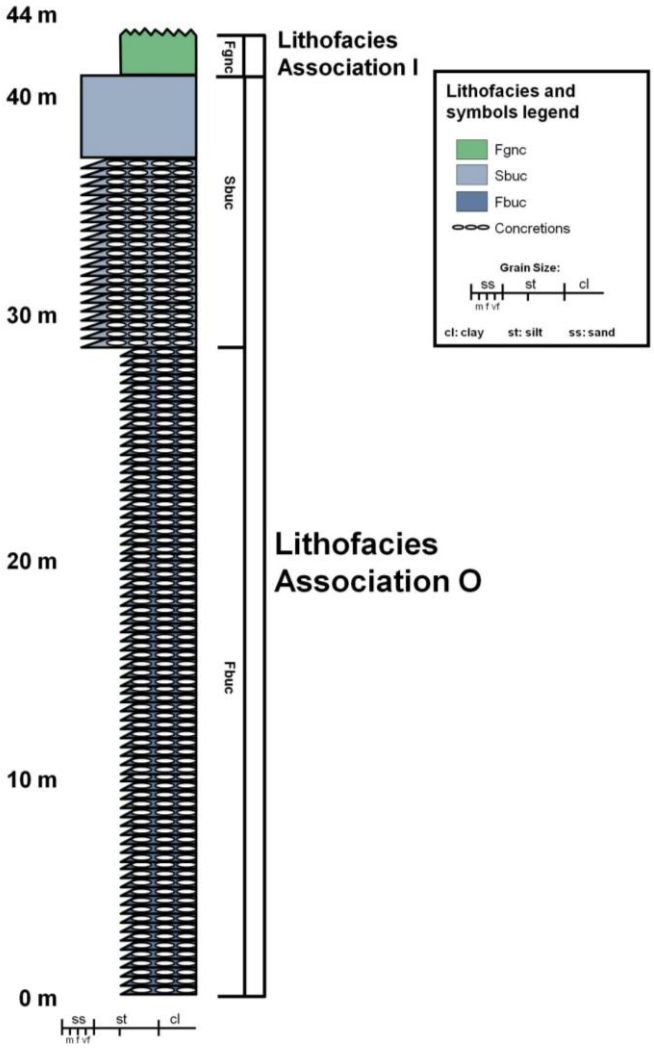

Figure 8. Stratigraphic column of Lithofacies O that forms the topmost section of the White Head Formation (e.g., Site 11) (Way, 2012).

Lithofacies Association II

Lithofacies Association II (LA II) lies upsection from LA I and is the middle section of the lower member of the Smyrna Mills Formation. It is composed of greyish green siltstone (*Fgygn*), green laminated siltstone with rare white microspheroidal limestone (*Fgnl),* green to grayish green and tan calcareous and noncalcareous massive or laminated sandstone *(Sgnl),* and minor dark green to black mineralized siltstone (*Fgnz*), grey and minor greenish laminated siltstone (*Fgyl*), black pyritic mudstone (*Fbkpl*) and red and maroon mineralized siltstone *(Frmz*). It is calculated to be at least 279 m thick in areas near Plymouth (Fig. 10; Way, 2012). Lithofacies Association II collectively displays decreased K_2O, TiO_2, V, S, Cr, As, Zn, and Cu, and increased Fe, Mn, and REEs in relation to Lithofacies Association I (Way, 2012).

The presence of dark green to black mineralized siltstone (*Fgnz*) and rare red and maroon mineralized siltstone *(Frmz*) suggests a change in redox potential at the time of deposition. The increase and presence of sandstone beds may be associated with a greater storm-wave depth, or close proximity to a river mouth, and hence, a nearer to shoreline setting within a continental shelf environment. Minor amounts of black mudstone lithofacies (*Fbkpl)* interbedded with lithofacies *Fgygn,* exclusive of areas proximal to Fe-Mn mineralized strata, proposes the idea of a lower relative rate of organic matter input or preservation. This further suggests only a minor fractionation of Fe^{2+} from the water column or pore waters took place when compared to that in LA I. In rare localities, white microspheroid, non-fossiliferous, calcareous laminae are present. Sometimes these calcareous beds are stratigraphically close to beds of Fe-Mn mineralization. Zoned pyrite is occasionally interbedded within these beds and are possibly the remains of

organic-rich carbonates that were chelated by bacteria. It is possible that these bacteria were associated with the changes in redox that lead to the precipitation of Fe-Mn-rich strata (Way, 2012). Regionally, this continual closure of the Iapetus Ocean (Fyffe, et al., 2011), the deposition of sediments, further decrease the depth of the seawater, and an increase in the redox potential would allow Fe-Mn minerals to precipitate more easily from the seawater (Way, 2014).

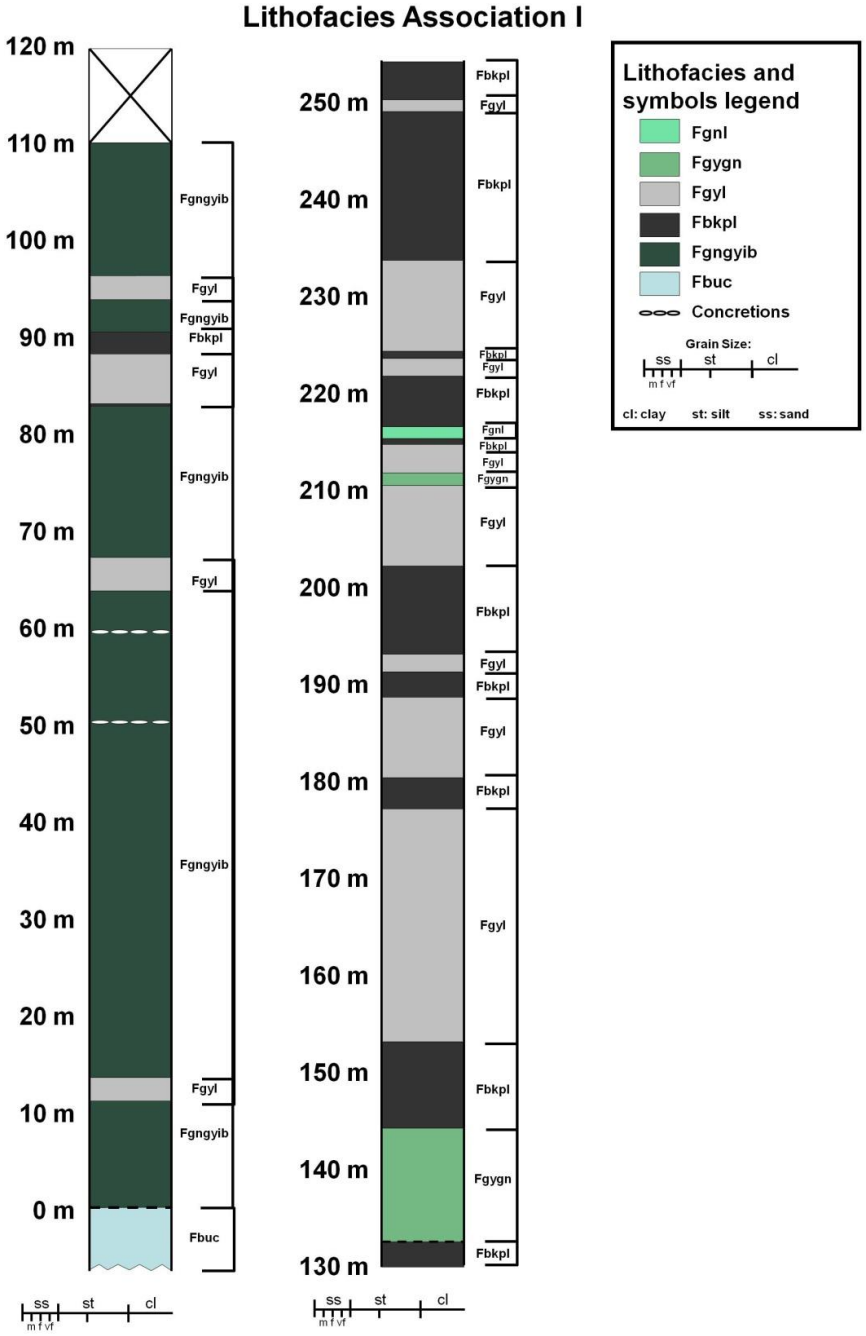

Figure 9. A stratigraphic column of Lithofacies Association I (Site 5) (Way, 2012).

Lithofacies Association III

Lithofacies Association III forms the topmost unit of the lower member of the Smyrna Mills Formation (Fig. 11). It is composed of red and maroon siltstone (*Frml)* with increasing interbeds of green to grayish green and tan calcareous and noncalcareous massive or laminated sandstone (*Sgnl*) upsection, green laminated siltstone with rare white microspheroidal limestone *(Fgnl),* and red and maroon mineralized siltstone (*Frmz*). LA III is often close to

major localities of Fe-Mn mineralization such as those seen at the Plymouth, North Hartford, South Hartford, and Iron Ore Hill, Moody Hill, and Sharpe Farm deposits (Sidwell, 1957, 1964; Hamilton-Smith, 1972; Roberts and Prince, 1990; Way, 2012). Overall, Lithofacies Association III has higher mean values of Fe_2O_3, MnO, P_2O_5, Cu, Co, Pb, As, Sb, Sr, and Ba, and lower K_2O, TiO_2, and MgO in comparison to Lithofacies Association II (Way, 2012).

LA III is occasionally found to be interbedded with LA II, possibly associated with redox changes during deposition. The increasing abundance of sandstone beds upsection in the stratigraphy may be associated with greater storm-wave depth, lowered sea-level, and (or) closer proximity to the base of a delta or fan slope and (or) river mouth. The high Mn and Fe content, and microbanding of Fe oxides and Fe-Mn carbonates of lithofacies *Frmz* implies these were formed in shallower, oxygen-rich marine paleoenvironment (van der Weijden, 1992). The early Salinic regression within the anoxic Iapetus Ocean (Fyffe et al., 2011), decrease in seawater depth, and mixing of currents would allow anoxic Fe and Mn saturated waters to mix with oxic top waters allow massive precipitation of Fe-Mn oxide-carbonate (*Frmz*) to be deposited onto the seafloor (Way, 2012).

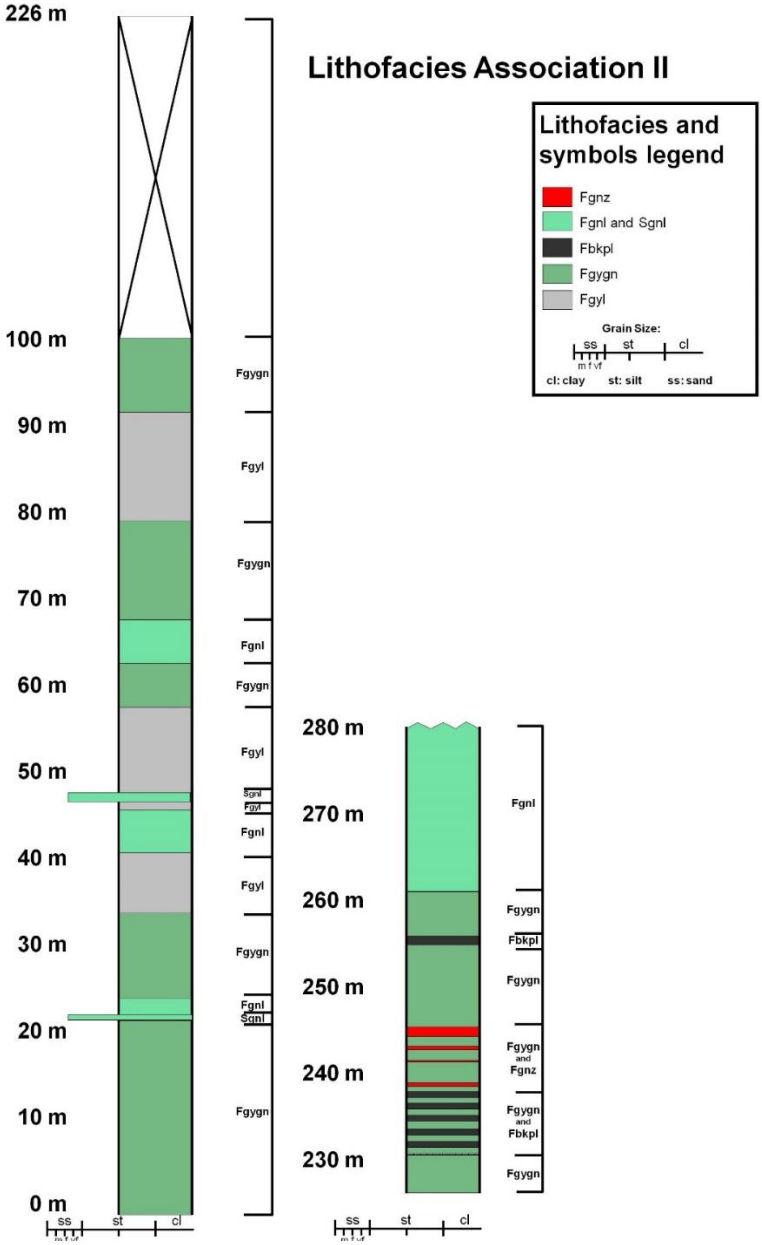

Figure 10. A stratigraphic section of Lithofacies Association II (lower member, Smyrna Mills Formation) present within the Route 95 study area that is a composite section of Sites 5 and 14. The leftmost column is Site 5 and the rightmost column Site 14. Some beds of Fe-Mn mineralization were present within this association (Way, 2012).

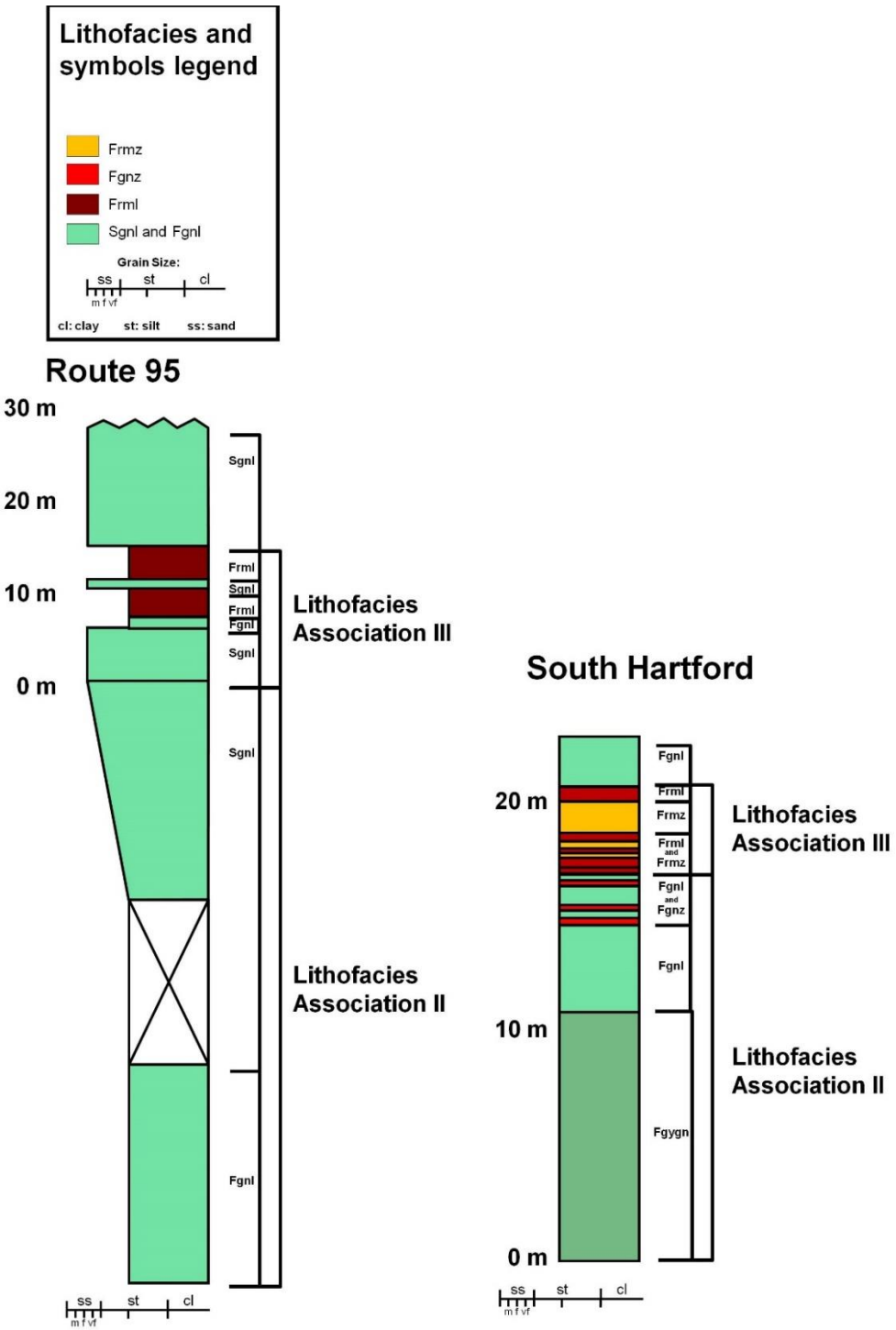

Figure 11. A stratigraphic section of Lithofacies Association III (lower member, Smyrna Mills Formation) from the Route 95 (Site 6) study area and from a Fe-Mn mineralized section from the South Hartford Fe-Mn deposit (Site 12). Fe-Mn mineralization was also present in outcrops northeast of Plymouth (Way, 2012).

Lithofacies Associations IV and V

The upper member of the Silurian Smyrna Mills Formation is composed of Lithofacies Associations IV and V that are collectively composed of lithofacies Sgyce (grey laminated, bedded, bioturbated, and massive sandstone), Sgnl (green to greyish green and tan calcareous and noncalcareous sandstone), Fgnl (green laminated siltstone with rare white microspheroidal limestone), Fgyl (grey and minor greenish laminated siltstone), and Fgygn (greyish-green

siltstone) (Figs. 12 & 13). Both LA IV and LA V are found to lack any Fe-Mn mineralization and therefore are just briefly mentioned in this guidebook. This member of the Smyrna Mills Formation is represented by beds of massive green quartz-chlorite-carbonate sandstone and rare occurrences of ripple marks, crinoidal debris, and bioturbidated sediments. This suggests a higher energy shallow marine environment for the upper member of the Smyrna Mills Formation (Way, 2012).

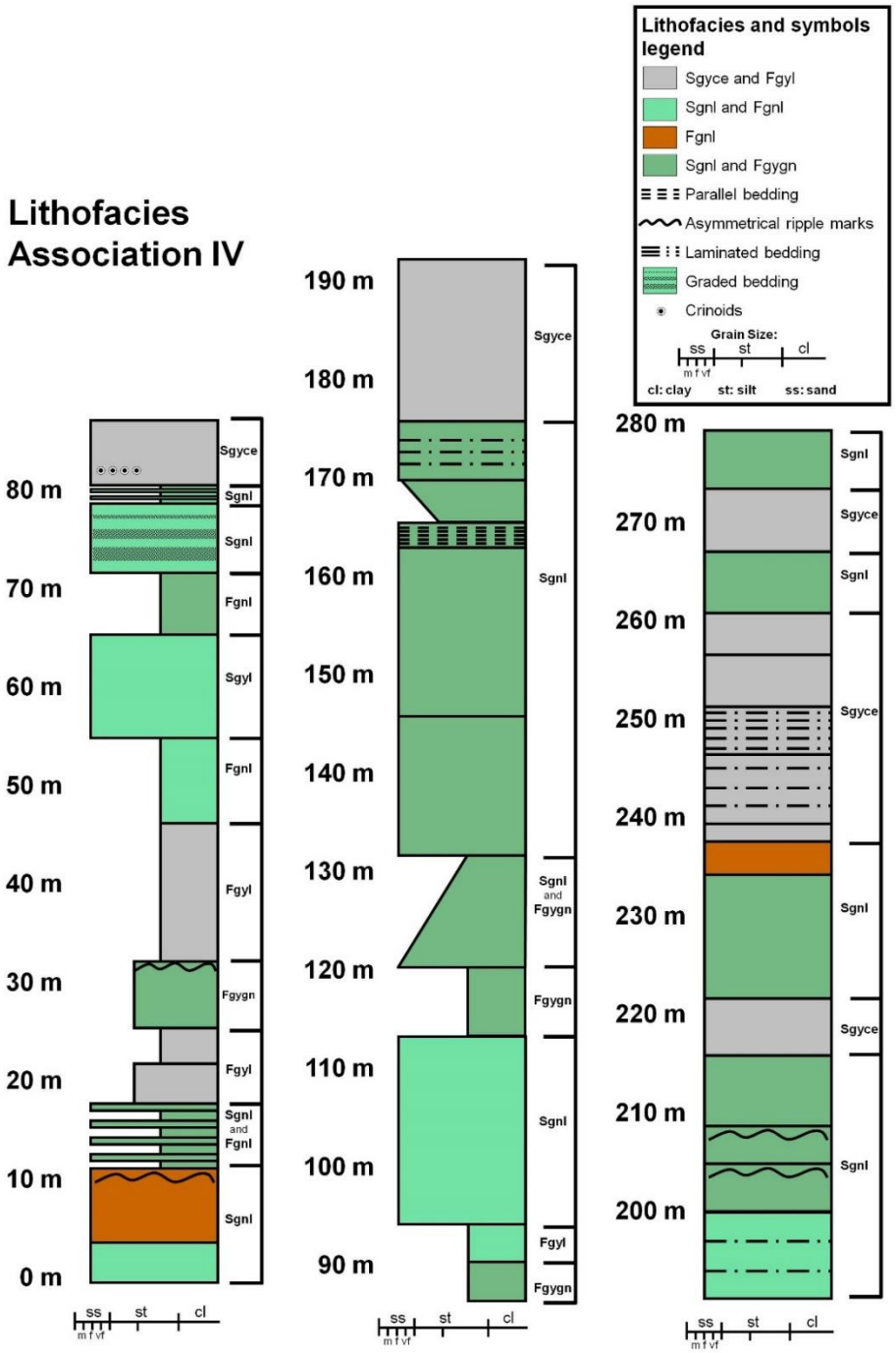

Figure 12. A composite stratigraphic section of Lithofacies Association IV composed of Sites 4 and 8 as present within the Route 95 study area. This Lithofacies Association was largely composed of lithofacies *Sgyce, Sgnl, Fgnl,* and *Fgygn* that occasionally containe asymmetrical ripple marks, graded and laminated bedding and minor cross-bedding with rare fossil and trace fossil horizons. The trace fossil horizons were found in the talus piles and not in outcrop (Way, 2012).

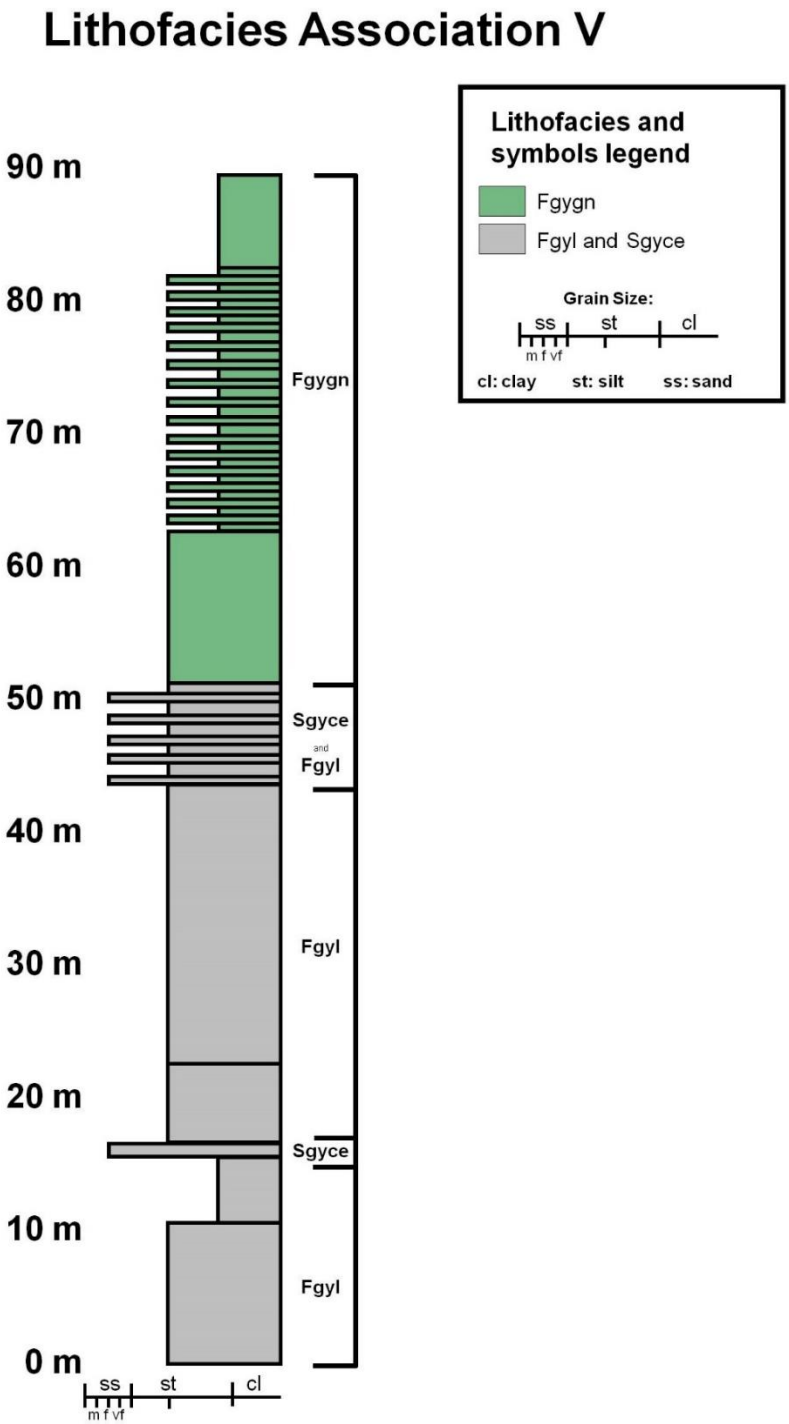

Figure 13. Stratigraphic section of Lithofacies Association

FERROMANGANESE DEPOSITS

Iron Ore Hill Deposit

The Iron Ore Hill Deposit (Fig. 14) is the northernmost Fe-Mn deposit in the Woodstock area (Fig. 3). It was mined during the mid-1850's and approximately 70,000 tonnes of ore were quarried by the Woodstock Iron and

Charcoal Company (Sidwell, 1957). The trenches within the deposit were excavated from 1848 to 1864 and in general followed the strike of the Fe-Mn mineralization with the base of each the trench roughly level with the surrounding road. It has 25,000,000 metric tonnes averaging 14.0% Fe and 10% Mn.

During the 1950's, 2 drill holes were sunk into the gravimetric anomaly during the 1950's southwest of the trenches. The first drill hole intersected a Fe-Mn mineralized section composed of silicified siltstone, zones of manganiferous hematite, and red siltstone over a length of 225 m. The second drill hole intersected the same mineralized section over a length of 53 m, indicating stratigraphic thinning of the mineralization (Sidwell, 1957). A large portion of the bedrock exposed at this locality as red and green siltstone with interbedded layers of manganiferous hematite. Pyrite and chalcopyrite are locally present within the hinges of folded manganiferous hematite layers (Way, 2012).

Five DDHs (totaling 1,051 m) were sunk into Iron Ore Hill by Manganese X in 2016 and estimate the Iron Ore Hill deposit at 9,550,000 metric tonnes grading at 9.44% Fe and 5.74% Mn at a 1.5% Mn cutoff grade. This estimate, published in a 2022 NI 43-101 PEA, is based on a limited drilling and sampling program of the historically mapped Fe-Mn deposit. Magnetic anomalies and historical data suggest a larger area of Fe-Mn mineralization (Fig. 15; MacKinnon, 2012; MacKinnon, 2020; Canadian Manganese Company Inc, et al., 2022).

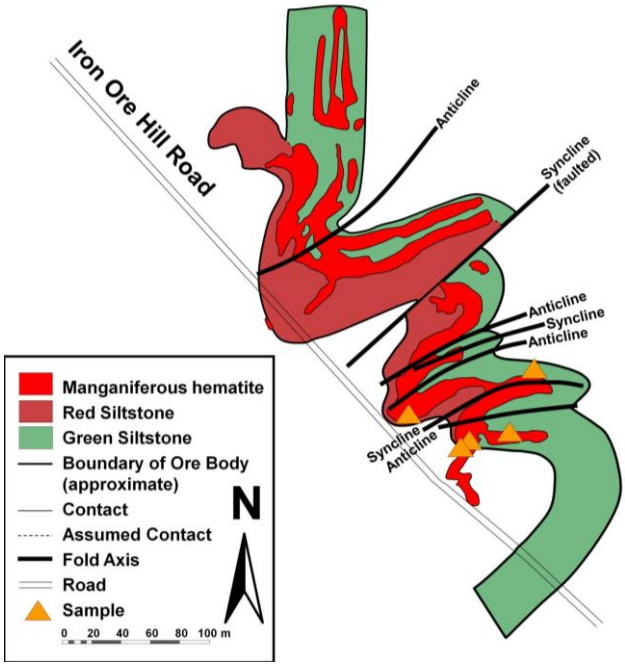

Figure 14. Geologic map of Iron Ore Hill deposit (modified from Baldwin, 1954). The strike of the Fe-Mn mineralization follows the trenches excavated in the mid 19th century (Baldwin, 1954; Anderson, 1968, Way, 2012).

Moody Hill Deposit

In 1954, 3 holes were drilled into the Moody Hill Deposit (Fig. 15), indicating 10,000,000 metric tonnes of low-grade ore averaging 9.5% Mn with an unknown percent of Fe and a width of 252 m and unknown strike length. The Fe-Mn mineralization was found as lenticular beds of manganiferous hematite within red, green, and grey siltstone (Sidwell, 1957). Moody Hill served as an iron source in 1848–1864 (Sidwell, 1964; Anderson, 1968; Potter, 1983).

Manganese X completed 38 DDHs on the Moody Hill deposit (6532 m) between 2016 and 2020 to further map extent of Fe-Mn mineralization and structure of the deposit. Continuous Fe-Mn mineralization on Moody Hill was identified over a strike length of 500 m from surface to a drill depth of 150 m. An updated PEA has estimated of mineral resource of the Moody Hill Fe-Mn Deposit with a measured and indicated metric tonnage of 26,740,000 at a grade of 10.36% Fe and 6.21% Mn at a 1.5% cutoff grade (MacKinnon, 2020; Canadian Manganese Company Inc, et al., 2022). V as present within the Route 95 study area (Way, 2012).

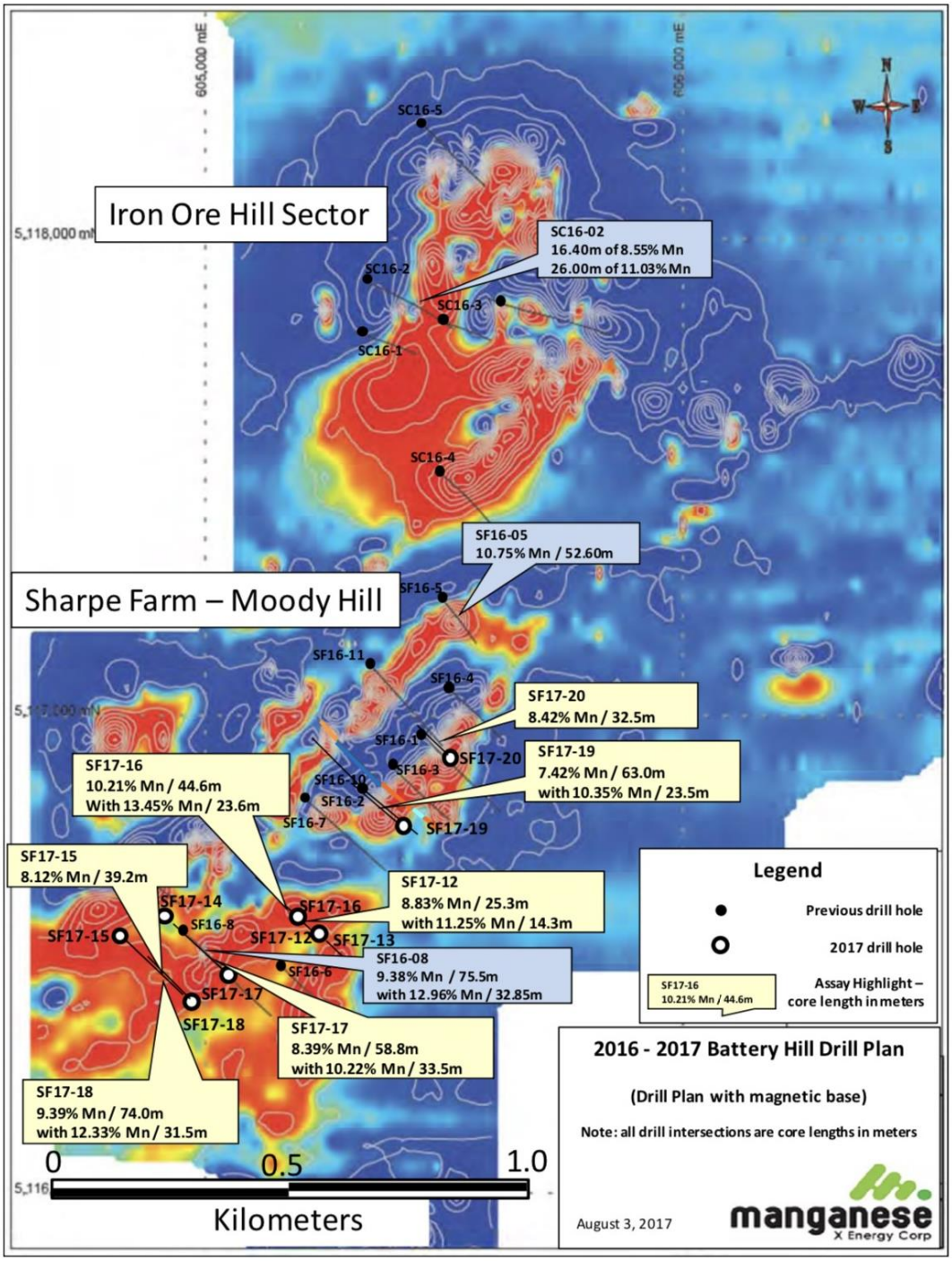

Figure 15. Magnetic map of the Iron Ore Hill, Moody Hill, and Sharpe Farm Fe-Mn Deposits (MacKinnon, 2020).

Sharpe Farm Deposit

The Sharpe Farm Deposit is located between the Moody Hill and Iron Ore Hill deposits (Fig. 15). It is the smallest of the six Fe-Mn deposits. It has 8,000,000 metric tonnes at 9% Mn and an unknown grade of Fe. In 1954, 2 drill holes intersected a Fe-Mn mineralized zone about 46 m in width. The deposit was found to be manganiferous silicified siltstone within grey siltstone (Sidwell, 1957; Anderson, 1968).

A ground magnetic survey by Manganese X identified a moderate to strong magnetic anomaly northeast towards Iron Ore Hill over 400 m in diameter second only to Iron Ore Hill. During 2016 and 2017, Manganese X completed

10 DDHs (2,804 m) with Fe-Mn mineralization associated with grey to black siltstone and minor green, grey, and buff siltstone. An updated PEA has estimated a measured and indicated tonnage of 8,400,000 at 11.56% Fe and 6.96% Mn, at a 1.5% cut-off grade (MacKinnon, 2020; Canadian Manganese Company Inc, et al., 2022).

Plymouth Deposit

The Plymouth deposit (Fig. 16) was first discovered by gravimetric surveys in 1954 (Sidwell, 1954). Currently, it is the largest of the Woodstock Fe-Mn deposits in both tonnage and grade. 23 drill holes were sunk into the deposit during the early to mid 1950's. Drilling during the 1950's indicated that the Fe-Mn deposit was continuous for a length of 945 m southwest of the Meduxnekeag River to the Plymouth Road with an average width of 99 m and to a depth of about 200 m of continuous Fe-Mn mineralization (Sidwell, 1957). The western side of the orebody is cut by a fault that is identified by highly chloritized rocks (Roberts, 1985; Roberts and Prince, 1990), and fault gouge in drill cores. The relatively large size of the deposit set initial plans for open-pit mining during the 1960's but due to high energy costs at the time it was never put into production.

Fe-Mn mineralization within the Plymouth deposit is composed of both beds of red Fe-Mn oxide-carbonate siltstone and green Fe-Mn oxide-silicates-carbonate siltstone (Nickel, 1957; Sidwell, 1957; Heinrich, 1962; Roberts and Prince, 1990; Way, 2012). Roberts and Prince (1990) reported high anomalous concentrations of copper and cobalt within areas of Fe-Mn mineralization at this deposit. Copper was reported of having a maximum concentration of 410 ppm, whereas Co had a maximum concentration of 250 ppm.

In 2013, Buchans Minerals Corporation sunk 16 DDH into the Plymouth Fe-Mn Deposit to follow up their 5 DDH 2011 exploration project to produce a PEA. At a 5% cutoff grade the deposit is calculated to be 43,710,000 metric tonnes at 14.29% Fe and 9.98% Mn. In 2022, a 25 DDH drilling project completed by the Canadian Manganese Company upgraded the deposit to have a measured and indicated tonnage of 56,700,000 tonnes at 14.01% Fe and 10.7% Mn. These grade and tonnage estimates are based off a pit constrained model with a 4.75% Mn cut-off grade (Canadian Manganese Company, 2023).

North Hartford Deposit

The North Hartford Deposit (Fig. 17) is northwest of the Plymouth Fe-Mn Deposit and is estimated at 50,000,000 metric tonnes (12% Fe and 8% Mn) based on 13 DDH totalling 1640 m (Sidwell, 1957). Some of the Fe-Mn mineralization is present in outcrop and previous drilling indicated beds of Fe-Mn carbonate with a general strike of 045° and dipping 80° SE and an overall thickness of 152 m (Sidwell, 1957; Gilders, 1976; Way, 2012). Fe-Mn mineralization associated with this deposit is exposed as a ~4 m wide jet black outcrop with beds of ellipsoidal rhodochrosite concretions, minor interbedded hematite, and Fe-Mn carbonates, locally in conformable contact with green siltstone. Macroscopic euhedral sulfides are found locally within some of the Fe-Mn mineralized talus at the outcrop (Way, 2012). Currently, 33 DDH have been sunk into the North Hartford Deposit to help produce 3-dimensional georeferenced map of the deposit, and determine the tonnage and grade of the deposit.

South Hartford Deposit

The South Hartford Deposit (Fig. 17) is a horseshoe shaped deposit about 0.25 km southeast of the North Hartford Deposit (Fig. 3). In the 1950's it was calculated to be the same tonnage and grade as the North Hartford Deposit (50,000,000 metric tonnes at 12% Fe and 8% Mn). In contrast to the North Hartford Deposit, previous drill data suggest that South Hartford is composed mainly of manganiferous hematite (Sidwell, 1957). Previously, 9 drill holes were into the deposit and displayed a highly folded and contorted Fe-Mn mineralized body composed of red siltstone, maroon interbedded manganiferous hematite siltstone, and minor green siltstone (Sidwell, 1957). A small portion of the South Hartford deposit is partially exposed in an abandoned quarry displaying interbedded hematite, and Fe-Mn carbonates, locally in conformable contact with red siltstone (c.1950's; Way, 2012).

MINOR Fe-Mn OCCURRENCES

There are several minor Fe-Mn occurrences along and south of the highway 95. Sidwell (1954) had identified two large gravimetric anomalies about 18 km southwest of Woodstock adjacent to the US/Canada border (Fig. 3). Early geologic maps (c. 1936; Baldwin, 1954) identified areas of Fe-Mn mineralization. Two 50-foot holes were sunk into the anomalies during the 1950's but no follow exploration was conducted within that time. A general lack of outcrops in the area makes it difficult to identify the full extent of Fe-Mn mineralization (Way, 2012).

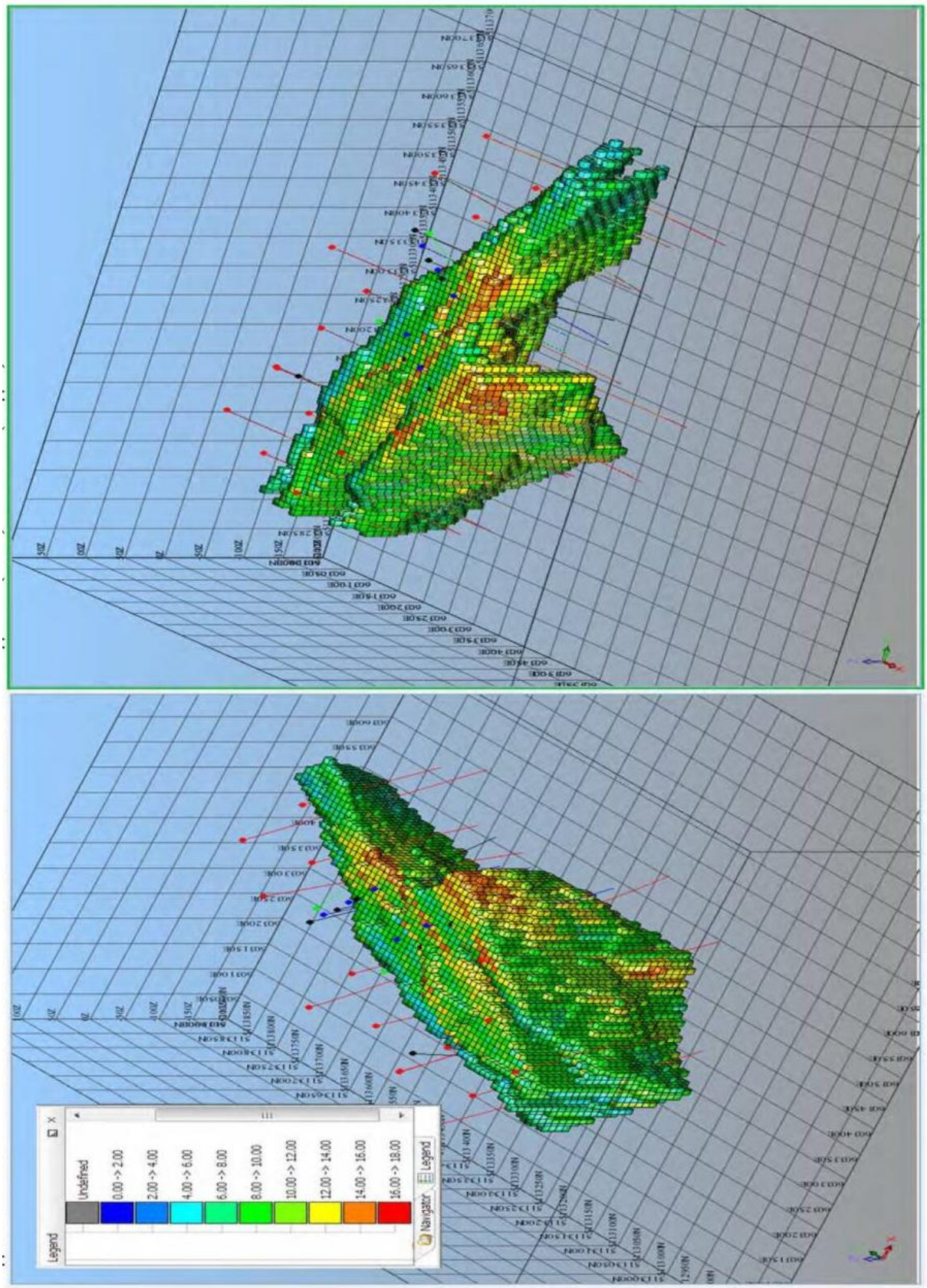

Figure 16. 2013 Resource map of the Plymouth Fe-Mn Deposit at a 5% cut off grade Looking NW (Left) and SW (Right) (Cullen et al., 2013).

Union Corner Fe-Mn occurrence

The Union Corner Fe-Mn occurrence is a 4.7-m wide roadcut that is largely hidden by dense overgrowth. It is composed largely of heavily Fe-hydroxide stained manganiferous green and brown siltstone that is composed largely of interbedded oligonite and rhodochrosite with minor quartz-chloride-sulfide, and sulfide veinlets. The extent of the Fe-Mn mineralization is unclear within this area due to the lack of exposure (Way, 2012).

Irish Settlement Fe-Mn occurrence

The Irish Settlement Fe-Mn occurrence is located at 1 km east of the US/Canada border on Route 95 lies a large fault-cut roadcut 430 m in length. Most of the outcrop is unmineralized siltstone but does contain minor Fe-Mn mineralization in its northeast corner as Fe-Mn mineralized beds (Way, 2012). In 2011, Globex mining sunk a DDH into a strong magnetic anomaly in the area but found only minor Fe-Mn mineralization (MacKinnon, 2011).

BASE METAL MINERALIZATION

Base metal mineralization associated with the Woodstock Fe-Mn Deposits was first recorded by Robb (1870). Minor Cu-Fe-S and Co-As-S mineralization was found to occur within several areas associated with Fe-Mn mineralization. The base metal mineralization is commonly found within quartz-chlorite-sulfide and quartz-sulfide veinlets, euhedral crystals, and (or) as inclusions. It is possible that some of this base-metal mineralization was formed during precipitation of Fe-Mn minerals and recrystallized during diagenesis. The presence of the veinlets and overprinting sulfides in relation to the Fe-Mn mineralization has suggested that there were two periods of minor Cu-Fe-S and Co-As-S mineralization within the Woodstock Fe-Mn deposits. It is likely that some of the original depositional base-metals were remobilized by the introduction of fluids and caused by late epigenetic base-metal mineralization during regional scale subgreenschist-grade metamorphism in the Woodstock area. (Way, 2012).

ACKNOWLEDGEMENTS

We would like to thank the University of Maine at Presque Isle and following people for help making this fieldtrip possible: Chunzeng Wang, Dave Lentz, Jim Walker, Matt Allas, and the staff at Canadian Manganese and Manganese X Energy Corp.

ROAD LOG

Assembly place and time: 8:30 am EST at Irving gas station in Houlton, Maine and depart at 9:00 am EST. Those arriving from Canada will meet at 10:30 am AST at Stop 1 on the Plymouth Road at the intersection of Route 95.

Mileage

0.4	Head south on US-1 S/North St toward Katahdin Ln
3.5	Turn left to merge onto I-95 N
7.5	Continue onto NB-95 E
7.8	Take exit 7 for NB-540 toward Richmond Corner/Belleville
8.4	Turn right onto NB-540 S
10.1	Turn left onto NB-555 E
11.0	Turn left onto Plymouth Rd

Stop 1. (Site 11; E 602982.97, N 5112309.64): Outcrops near the Plymouth Fe-Mn Deposit. Exposures of both the White Head Formation and the Smyrna Mills Formation in outcrop showcase the changes in the paleoenvironment from a turbidite-rich setting to an anoxic environment. This outcrop displays two of the Lithofacies Associations (LA O and LA I).

Continue on the road.

11.5	Follow the Plymouth Rd. Destination will be on the right.

Stop 2. (Site 14; E 603011.40, N 5113168.67): Plymouth Fe-Mn Deposit. There will be a short hike to the deposit (0.5 km). Here we will be visiting one of the trenches where there is Fe-Mn mineralization in outcrop. Remains of the rock crusher are also visible here.

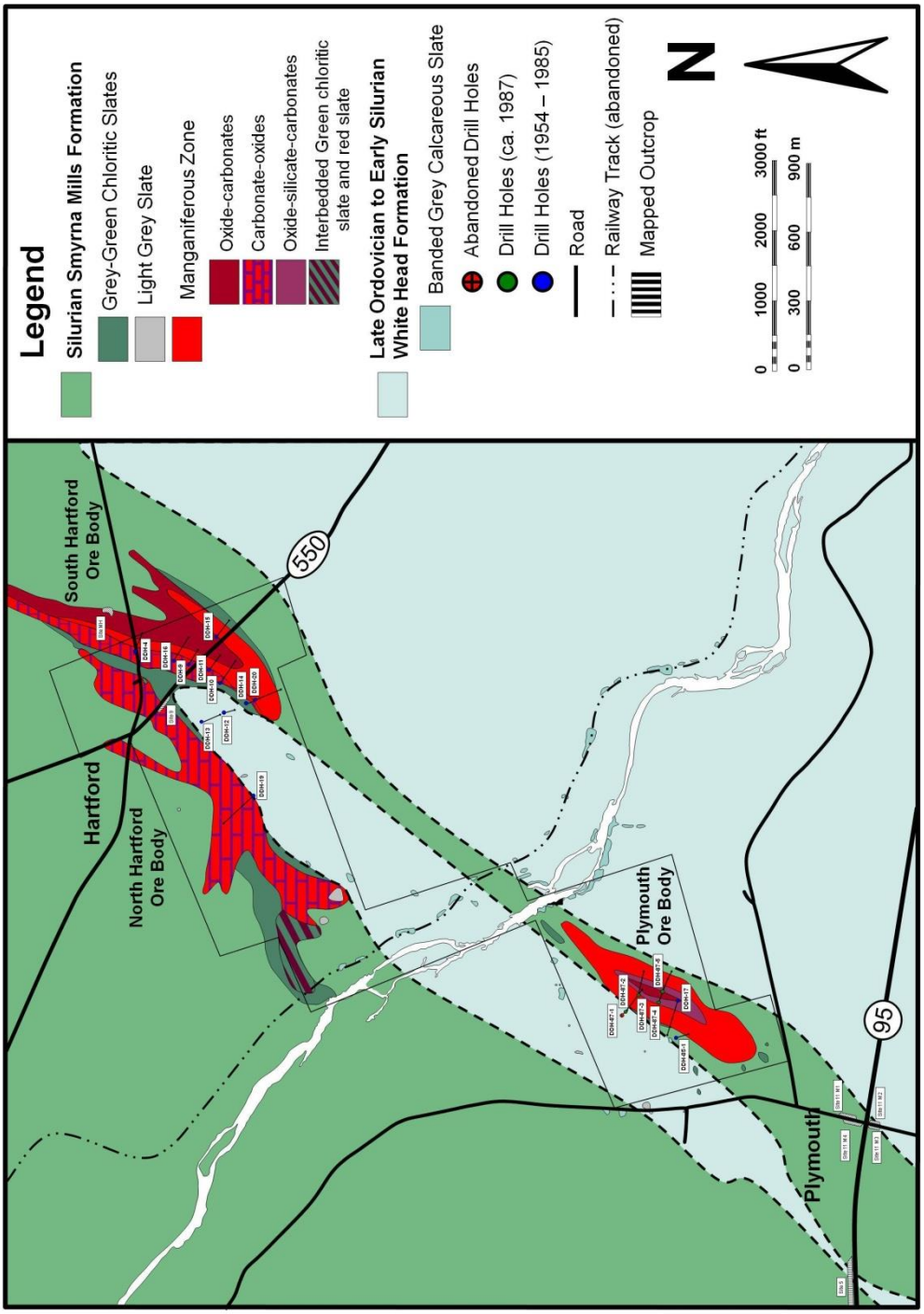

Figure 17. Geologic Map of the Plymouth, North Hartford, and South Hartford deposits in location with surrounding bedrock units (modified from Gilders, 1976; Roberts and Prince, 1990).

Turn around.

13.0 Head south on Plymouth Rd toward Simcox Rd
13.9 Turn left onto NB-555 E
15.7 Turn right onto Bedell Settlement Rd
17.5 Turn left onto Beardsley Rd/Beardsley Rd
18.0 Continue onto Tamarack Rd

Stop 3. (E 607262.61, N 5108910.80): Drill Core Shed. There will be a short stop here for a look at the recent drill cores from the Plymouth Deposit.

18.3 Head west on Tamarack Rd toward Aubrie Ct
18.9 Turn left onto Beardsley Rd
19.2 Take the NB-2 W/TC ramp toward Edmundston
19.9 Turn left onto the NB-2 W/TC ramp toward Edmundston
25.1 Merge onto Trans-Canada Hwy/NB-2 W
25.4 Take exit 184 for NB-560 toward Jacksonville/Upper Woodstock/Ch Lockhart Mill Rd
26.3 Turn left onto NB-560 N
26.9 Turn left onto Iron Ore Hill Rd
27.7 Turn left onto a dirt road

Stop 4. Moody Hill (E 605349.42, N 5116659.58): There will be a short walk to the (0.1 mi) mine site. Please use caution when near the trenches.

28.5 Head north toward Iron Ore Hill Rd
29.3 Sharp left onto Iron Ore Hill Rd

Stop 5. Iron Ore Hill (Lunch Stop; E 605731.94, N 5117812.72): This bedrock exposure will serve as the lunch stop for field trip participants. There are several Fe-Mn mineralized outcrops at this site. Minor walking will be involved. Please use caution when near the trenches.

30.3 Head southeast on Iron Ore Hill Rd toward NB-560 S
31.5 Turn right onto NB-560 S
35.0 Turn right onto Lockhart Mill Rd
35.3 Turn left onto NB-550 S

Stop 6. North Hartford deposit (E 604708.65, N 5115635.54): Small outcrop of Fe-Mn mineralized siltstone within green siltstone beds. Fe-Mn carbonate concretions are common at this locality. Cobaltite and other sulfides are occasionally found in outcrop talus.

35.8 Head west on Lockhart Mill Rd toward NB-550 N
36.1 Take the 1st left onto NB-550 S

Stop 7. South Hartford Quarry (E 605284.04, N 5115888.13): This quarry serves as the final stop for the field trip. There is a short hike to the quarry (~0.5 km). It will consist of four different stops each displaying different features of the deposit. Please use caution near the quarry walls.

Depart onto Lockhart Mill Road and take Trans-Canada Hwy west towards Houlton exit for people going back to Maine.

REFERENCES

Anderson, F.D., 1968, Woodstock, Millville, and Coldstream Map-Areas, Carleton and York Counties, New Brunswick: Geological Survey of Canada Memoir 353, 69 p.

Bailey, L.W., 1898, The mineral resources of the province of New Brunswick: Geological Survey of Canada, Summary Report 1897, v. 10, part. M, p. 128.

Baldwin, A.B., 1954, The Nature and Genesis of the Iron Ores of the Hayot Lake Area, Labrador-New Quebec in Comparison with those of New Brunswick: unpublished MSc. Thesis, University of New Brunswick, Fredericton, NB, 92 p.

Cullen, M., Hilchey, A., Goodine, S., 2013, Mineral Resource Estimate Technical Report for the Plymouth Mn-Fe Deposit Woodstock Property, New Brunswick, Canada, Buchans Minerals and Centrerock Mining Limited, 145 p.

Canadian Manganese Company Inc, Manganese X Energy Corp., University of New Brunswick, New Brunswick Geological Survey, 2022, Metallogeny of the Woodstock Area, New Brunswick Department of Natural Resources, 75 p.

Canadian Manganese Company, 2023, "Canadian Manganese Announces Updated Mineral Resources Estimate for Plymouth Deposit at Woodstock Including M&I Resource of 56,700,000 tonnes grading 10.07% Manganese", Press Release, March 3, 2023.

Fyffe, L.R., 1982, Geology of Woodstock (sheet 21 J): New Brunswick Department of Natural Resources, Map NR-4.

Fyffe, L.R., 2001, Stratigraphy and geochemistry of the Ordovician volcanic rocks of the Eel River area, west-central New Brunswick: Atlantic Geology, v. 37, p. 81 – 101.

Fyffe, L.R., Johnson, S.C., and van Staal, C.R., 2011, A review of Proterozoic to Early Paleozoic lithotectonic terranes in the northeastern Appalachian orogen of New Brunswick, Canada, and their tectonic evolution during Penobscot, Taconic, Salinic, and Acadian orogenesis: Atlantic Geology, v. 47, p. 211 – 248.

Gliders, R., 1976, Geology of the Woodstock Manganese Claim Group for R.S. Boorman, Assessment Report #470389, Open File Report, New Brunswick Department of Natural Resources, Mineral Development Branch, 17 p.

Hamilton-Smith, T., 1972, Stratigraphy and structure of Silurian rocks of the McKenzie Corner area New Brunswick. New Brunswick Department of Natural Resources, Mineral Development Branch, Report of Investigation 15, 26 p.

Hind, H.Y., 1865, A preliminary report of the Geology of New Brunswick, Queen's Printer, Fredericton, p. 161-165.

Jackson, C.T., 1837, First report on the geology of the State of Maine: Augusta, Smith and Robinson, 128 p.

Ludman, A., 1988, Revised bedrock geology of central-eastern and southeastern Maine: Maine Geological Survey, Open File Report, 36 p.

MacKinnon, R.P., 2011, Assessment Report on the Preliminary Reconnaissance and Sampling, Claim Unit 5816, Globex Mining Enterprises Inc., Woodstock Area of New Brunswick Manganese-Iron Deposit, Assessment Report Number 477479, 24 p.

MacKinnon, R.P., 2012, Globex Mining Enterprises Inc. Irish Settlement New Brunswick July 11-14, 2011 Diamond Drill Program Right Number 5745, Assessment Report Number 477263, 23 p.

MacKinnon, R.P. 2020. NI 43-101 Technical Report on the Woodstock Manganese Occurrence Exploration Licenses 5816 and 5745 Near Jacksonville and Irish Settlement Carlton County New Brunswick. Prepared for Manganese X Energy Corp, effective date of June 30, 202, 143 p.

Miall, A.D., 1978, Lithofacies types and vertical profile models in braided river deposits: a summary, *in* Miall, A.D. ed, Fluvial Sedimentology, Canadian Society of Petrology: Geol. Memoir 5, p. 597 – 604.

Ogg, J.G, Ogg, G., and Gradstein, F.M. 2008, The Concise Geological Time Scale, International Commission on Stratigraphy, 14 p. URL <http://www.stratigraphy.org/bak/GTS2008.pdf> December 2010.

Pavlides, L., 1966, Meduxnekeag Group and Sprague ville Formation of Aroostook County, northeast Maine, in Cohee, G.V., and West, W.S., Changes in stratigraphic nomenclature in the U.S. Geological Survey - 1965: U.S. Geological Survey Bull. 1244-A, p. 52-60.

Pavlides, L., and Berry, W.B.N., 1966, Graptolite-bearing Silurian rocks of the Houlton-Smyrna Mills area, Aroostook County, Maine: United States Geological Survey, Professional Paper 550-B, p. B51 – B61.

Pickerill, R. K., 1980, Phanerozoic flysch trace fossil diversity-observations based on an Ordovician flysch ichnofauna from the Aroostook-Matapedia Carbonate Belt of northern New Brunswick: Canadian Journal of Earth Sciences, v. 17, p. 1259 – 1270.

Potter, R.R., 1983, The Woodstock iron works Carleton County, New Brunswick: CIM Bulletin, v. 76, p. 81 – 83.

Robb, C., 1870, Report on the geology of northwestern New Brunswick, Geological Survey of Canada, Report of Progress for 1866-1869, Part N, p. 173-209.

Roberts, G.C., 1985, Exploration Report of M.R.R.'s Woodstock Mn Property, Carleton County, New Brunswick: Assessment File #473168, New Brunswick Department of Natural Resources, Mineral Development Branch Open File Report, 28 p.

Roberts, G.C., and Prince, J.D., 1990, Further Characterization of Plymouth Mn Deposit: New Brunswick, Department of Natural Resources and Energy, Minerals, and Energy Division, Open File Report 90-4, 362 p.

Sidwell, K.O.J., 1954, Preliminary report on the National Management Ltd. Property (N.B. Group 24), Woodstock, N.B.: New Brunswick Department of Natural Resources, Mineral Development Branch, Open file report, 10 p.

Sidwell, K.O.J., 1957, The Woodstock, N.B., Iron – Manganese Deposits: Transactions of the Canadian Institute of Mining & Metallurgy, v. 50, p. 411 – 416.

Sidwell, K.O.J., 1964, Manganese ore occurrences in New Brunswick: New Brunswick Resources Development Board, New Brunswick Department of Natural Resources, Minerals Division, Reference 26, 172 p.

Smith, E.A., and Fyffe, L.R., (Compilers) 2006, Bedrock Geology of the Woodstock Area (NTS 21 J/04) Carleton county, New Brunswick, New Brunswick Department of Natural Resources, Minerals, Policy and Planning Division, Plate 2006 – 5.

St. Peter, C., 1982, Geology of Juniper-Knowlesville-Carlisle area, map-areas I-16, I-17, I-18 (Parts of 21 J/11 and 21 J/06): New Brunswick Department of Natural Resources, Geological Surveys Branch, Map Report 82-1, 82 p.

Ténière, P., Harrington, M, Warkentin, D., Elgert., L, 2021, NI 43-101 Battery Hill Project Mineral Resource Estimate Woodstock Area New Brunswick, Canada, 133 p.

van der Weijden, C.H., 1992, Early Diagenesis and marine water, *in* Wolf, K.H. and Chilinger, G.V., eds., Diagenesis III, Elsevier Science Publishers B.V., p. 13 – 134.

van Staal, C.R., and Fyffe, L.R., 1991, Dunnage and Gander zones; New Brunswick. Canadian Appalachian Region: New Brunswick Department of Natural Resources and Energy, Mineral Resources, Geoscience Report 91-2, 39 p.

Venugopal, D.V., 1981, Geology of Hartland-Woodstock-Nortondale region, map-areas H-19, H-20, 1-20 (Parts of 21 J/03, 21 J/04, 21 J/05, 21 J/06): New Brunswick Department of Natural Resources, Mineral Resources Branch, Map Report 81-6, 37 p.

Way, B.C., 2012, Geology and Geochemistry of Sedimentary Ferromanganese Ore Deposits, Woodstock, New Brunswick, Canada, Unpublished MSc. thesis, University of New Brunswick, Fredericton, 276 p.

Way, B.C., 2014, Stratigraphic and Paleoenvironmental setting of the Woodstock Fe-Mn deposits in Woodstock, New Brunswick, GAC-MAC 2014 guidebook, GAC-MAC, 175th meeting of the Geological Association of Canada, 37p.

GEOLOGY OF THE MUNSUNGUN–WINTERVILLE BELT: THE MUNSUNGUN INLIER

Chunzeng Wang[1] and Stephen Pollock[2]
[1]University of Maine at Presque Isle, Presque Isle, Maine 04769. chunzeng.wang@maine.edu
[2]Wilmington, North Carolina 28412

INTRODUCTION

The Munsungun–Winterville Belt (MWB) of Maine is a major early Paleozoic lithotectonic belt in the Northern Appalachians. The belt includes two major inliers, the Munsungun inlier in the southwest and the Winterville inlier in the northeast, along with nine geologically similar but smaller inliers – the Portage Lake, Castle Hill, and York Ridge inliers, and the much smaller ones in the headwaters of the East Branch Penobscot River and Aroostook River (Fig. 1). The inliers are composed predominantly of Ordovician volcanic and sedimentary rocks.

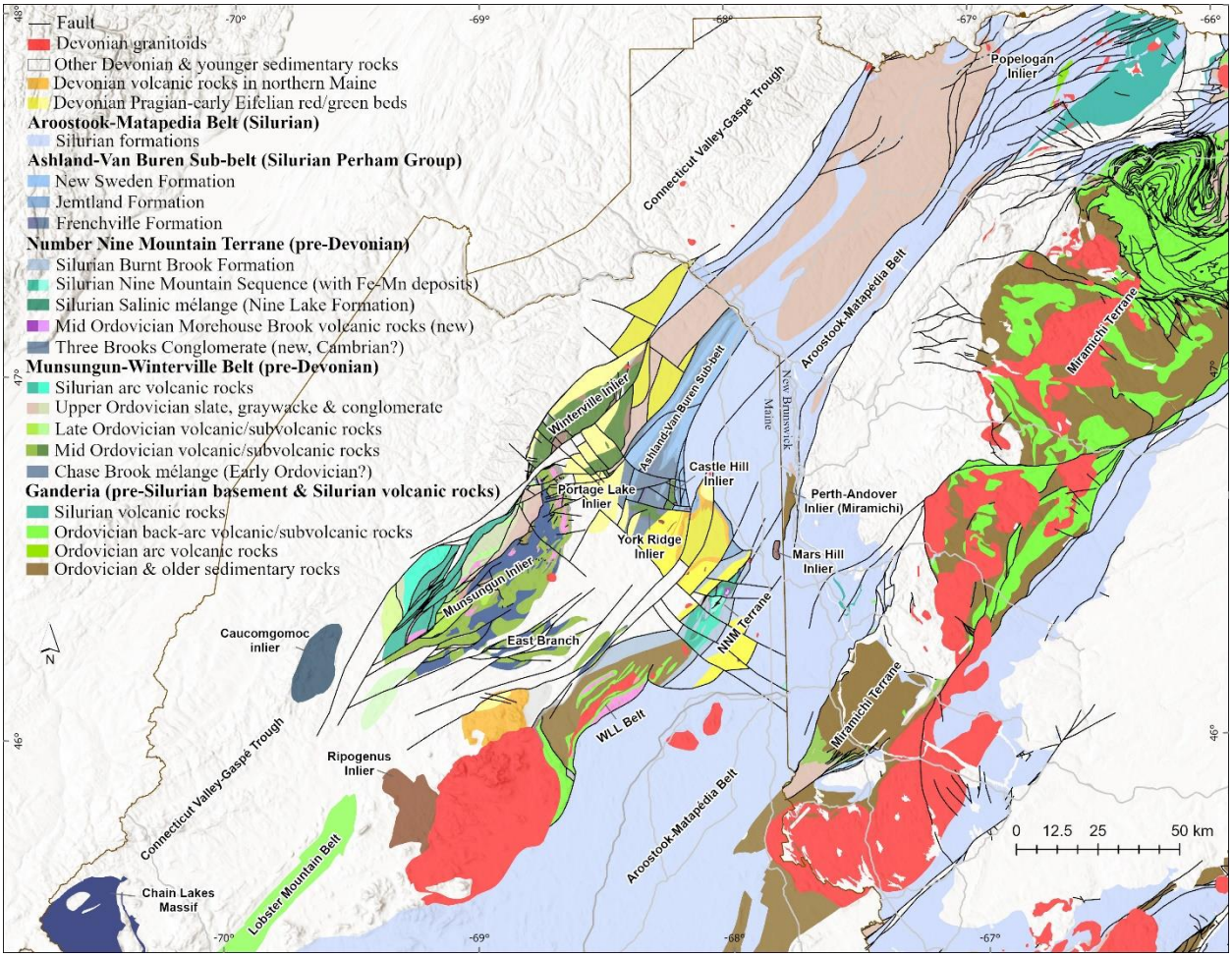

Figure 1. Simplified lithotectonic and regional geologic map of northern Maine and northern New Brunswick. Maine side is based on recent detailed and reconnaissance mapping. NNM Terrane – Number Nine Mountain Terrane. WLL Belt – Weeksboro-Lunksoos Lake Belt.

Our studies of the MWB since 2016 are based on the pioneer foundational work performed by Gary Boone who mapped the area around Fish River Lake and Winterville, as well as the Deboullie syenite complex in the 1950's (Boone, 1958, 1970) and Brad Hall who mapped the southwestern Munsungun inlier in the 1950–1960's (Hall, 1970). Several other small projects for master's degrees were also performed in certain areas in both inliers, for example, Supkow (1965) mapped the Spider Lake Formation in the Churchill and Spider Lake quadrangles, Horodyski (1968)

conducted reconnaissance mapping in the area around Greenlaw, Mooseleuk Lake, Winterville, and Fish River Lake quadrangles, and Fitzgerald (1991) did a geochemical study on the Spider Lake and West Branch Penobscot volcanic suites.

Exploration of base metals in volcanic rocks in both Munsungun and Winterville inliers peaked in the late 1970's and the early 1980's with discovery of the Bald Mountain volcanic massive sulfide (VMS) deposit and several occurrences, including Bull Hill VMS and "New Gold Prospect" at Chandler Mountain by application of soil sampling, airborne magnetic and radioactive surveys, and borehole drilling (Cummings, 1988) (Fig. 2). In the late 1990's the United States Geological Survey (USGS) studied the Bald Mountain VMS deposit, with focus on its volcanic and tectonic settings, lithogeochemistry, geochronology, and metallogenesis (e.g., Ayuso and Schulz, 2003; Ayuso et al., 2003; Busby et al., 2003; Schulz and Ayuso, 2003; Slack et al., 2003).

Our recent and current mapping funded by the USGS STATEMAP Program shows that northern Maine, including the WMB, has experienced significant faulting with considerable vertical and horizontal displacement, and the faulting took place mostly during the Acadian and Neoacadian orogenies. The majority of the faults strike southwest (dip northwest) or northeast (dip southeast) and are reverse-thrust faults with mostly southeast-oriented reverse faulting. They have produced the northern Maine stacked, domino-style imbricate fault system. Multiple generations of the faulting have produced numerous fault slivers or blocks; the imbricate fault pattern and the fault sliver/block system construct the structural framework of northern Maine (Fig. 1).

The Munsungun inlier is characterized by two volcanic belts, the dominant Middle-Late Ordovician belt on the southeast and the Silurian (Ludlow) volcanic belt to the northwest (Figs. 1 and 2). Both occur as fault blocks or slivers of the imbricate fault system. The Middle-Late Ordovician volcanic formations show west-northwestward younging direction, including, from the east to west, the Munsungun Lake (463 – 470 Ma), Round Mountain (465 Ma), Bluffer Pond (455 Ma), Ragged Mountain (458 Ma), and Ingalls Brook Road (455 Ma) formations, as a result of west-northwestward arc migration associated with a possibly retreating southeast-dipping subduction system during the Middle – early Late Ordovician time. The Silurian Spider Lake and Churchill Ridge formations are dated 424 – 427 Ma and probably associated with the New Brunswick subduction during the Salinic orogeny. Detrital zircon spectra of several Upper Ordovician sedimentary formations (e.g., Rowe Lake, Blind Brook, and Ferguson Brook formations) in the Munsungun inlier indicate a Laurentian provenance, suggesting their adjacency to the Laurentia margin after producing the composite Laurentia terrane due to accretions.

The WMB has long been considered as an Ordovician arc developed on the leading edge of the peri-Gondwanan Ganderia terrane, and as part of the Bronson Hill–Popelogan arc. New detrital zircon data (of 252 grains) from the Chase Brook mélange of the Munsungun inlier demonstrate a typical Laurentia spectrum with the youngest zircon grains dated to 556 Ma, suggesting that the MWB is a peri-Laurentia terrane.

REGIONAL GEOLOGY OF NORTHERN MAINE

Northern Maine has several northeast-trending lithotectonic belts. From northwest to southeast, these are the Notre Dame belt, the Connecticut Valley-Gaspé trough, the Munsungun-Winterville belt, the Weeksboro-Lunksoos Lake belt, the Aroostook-Matapedia basin, and the Miramichi terrane (Fig. 1). The Notre Dame terrane or subzone of the Dunnage zone occurs along the Maine-Quebec border in the northwesternmost Maine. It is composed of Ordovician volcanic and sedimentary rocks and likely even older rocks. The Connecticut Valley-Gaspé trough generally represents a major, orogen-scale Silurian–Devonian basin of the Northern Appalachians. In northern Maine, it is composed entirely of the Lower Devonian Seboomook Group that is tightly folded and faulted by southwest-striking or northeast-striking reverse faults.

The Munsungun-Winterville belt generally consists of two major inliers, the Munsungun inlier and the Winterville inlier, with a number of much smaller inliers. The inliers are composed of Cambro-Ordovician volcanic-subvolcanic and sedimentary rocks, as well as Silurian volcanic-subvolcanic rocks (for the Munsungun inlier). The Weeksboro-Lunksoos Lake belt is composed of Cambro-Ordovician volcanic-subvolcanic and sedimentary rocks with the oldest being the Cambrian Grand Pitch Formation. A recent detrital zircon geochronological work confirmed the age of the Grand Pitch Formation to be Cambrian and its provenance from Gondwana (see Trip C3 for details). The Lower Ordovician Shin Brook Formation of volcanic-subvolcanic rocks unconformably overlies the Grand Pitch Formation. The Aroostook-Matapedia basin is the northeastern extension of the Central Maine basin. It is comprised predominantly of Silurian sedimentary rocks, for example, the Perham Group, Carys Mills Formation, Smyrna Mills Formation, etc. The Aroostook Manganese District is hosted by the Silurian formations in the basin (see trip C3 for details). The Miramichi terrane is the largest Cambro-Ordovician terrane in the New Brunswick-Maine Appalachians, with complicated composition, structural patterns, and tectonic history. The terrane becomes narrower toward Maine and disappeared in the Greenfield area, northeast of Old Town (see trip A1 for details). The Miramichi terrane is well

known for producing all types of mineral deposits, in particular the volcanic sulfide massive (VMS) deposits hosted by Ordovician volcanic rocks (see trip B1 for details), and well represented by the world-class Bathurst Mining Camp.

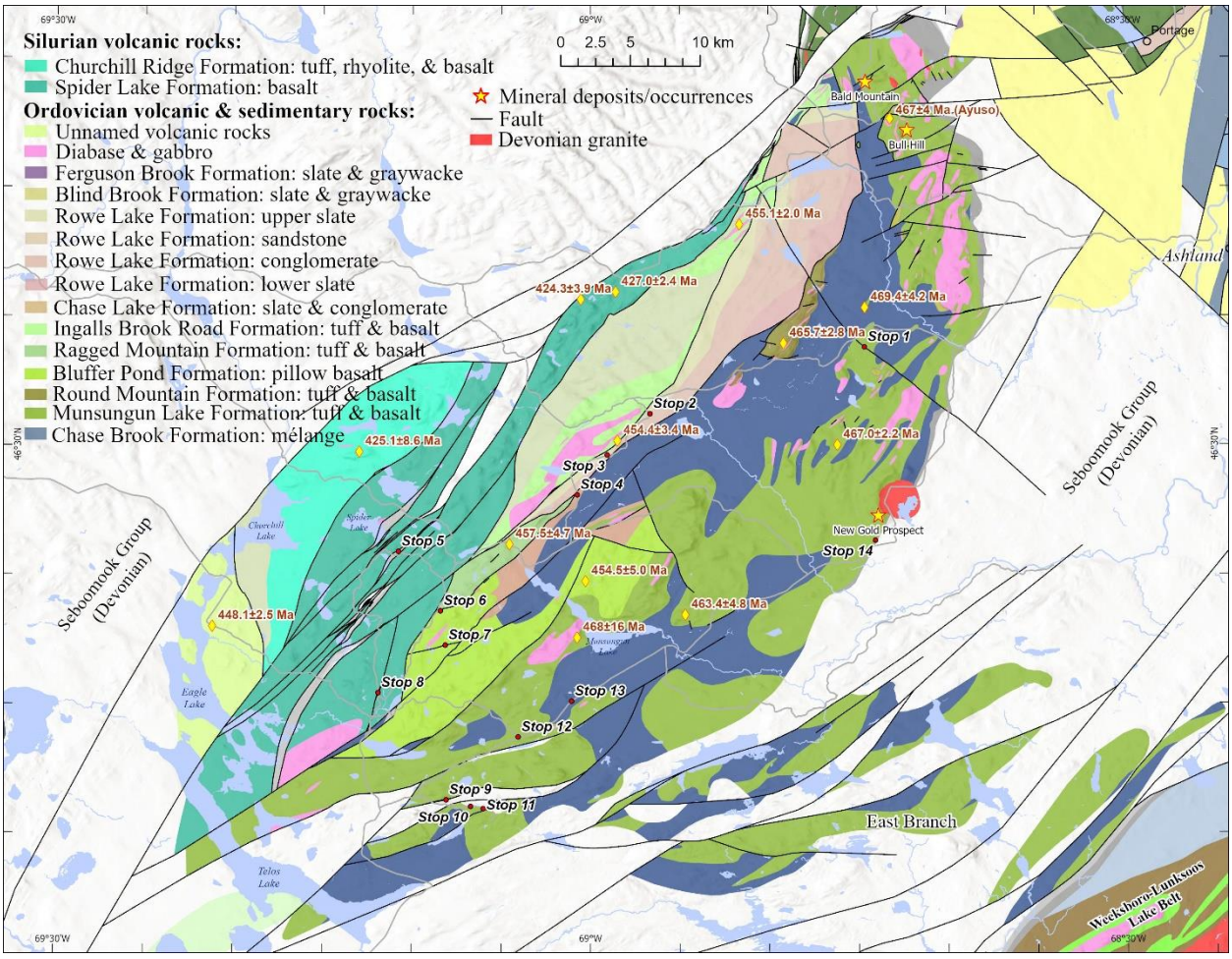

Figure 2. Geologic map of the Munsungun inlier based on recent detailed and reconnaissance mapping. Stops for this trip are marked on the map. The map also shows igneous zircon U-Pb ages of all the volcanic formations in the Munsungun inlier obtained in our projects, as well as major metallic deposits/occurrences.

Early Devonian	Seboomook Group: slate, sandstone, limestone, c& onglomerate
	Salinic C
Silurian (Ludlow)	Churchill Ridge Formation (new): volcanic rocks, 425 Ma
	Spider Lake Formation: volcanic rocks, 424-427 Ma
	Salinic A
Late Ordovician	Ferguson Brook Formation (new): slate & conglomerate
	Rowe Lake Formation: slate & conglomerate
	Blind Brook Formation: slate & sandstone
	Chase Lake Formation: slate & conglomerate
	Taconic 3
	Ingalls Brook Road Formation: volcanic rocks, 455 Ma
	Bluffer Pond Formation: volcanic rocks, 455 Ma
	Ragged Mountain Formation (new): volcanic rocks, 458 Ma
Mid Ordovician	Round Mountain Volcanic Suite (new): volcanic rocks, 466 Ma
	Munsungun Lake Formation: volcanic rocks, 463-470 Ma
	Taconic 2
Early Ordovician	Chase Brook Formation: mélange

Figure 3. Revised stratigraphic column of the Munsungun inlier.

STRATIGRAPHY OF THE MUNSUNGUN INLIER

Stratified volcanic and sedimentary rocks within the Munsungun inlier include, from the oldest to the youngest, the likely Early Ordovician Chase Brook Formation mélange, the Middle-Late Ordovician volcanic-subvolcanic rocks of the Munsungun Lake, Round Mountain, Bluffer Pond, Ragged Mountain, and Ingalls Brook Road formations, the Late Ordovician sedimentary rocks of the Chase Lake, Rowe Lake, Blind Brook, and Ferguson Brook formations, and the Silurian volcanic-subvolcanic rocks of the Spider Lake and Churchill Ridge formations. The Early Devonian Seboomook Group is the most widespread component of the Connecticut Valley–Gaspe trough in northern Maine. It unconformably overlies the Ordovician and Silurian formations. The following descriptions of the formations are in the order from the oldest to the youngest.

The Ordovician Formations

Chase Brook Formation: The Chase Brook Formation (Hall, 1970) occurs to the east-southeast side of the northeast-striking Round Mountain and Bluffer Ridge faults along with Ordovician volcanic formations; it is underlain mostly in valleys and lowlands. Hall (1970) recognized "blocks" of cross bedded calcareous siltstone and medium to coarse grained quartz and feldspathic wacke within slate of the Chase Brook but made no interpretations regarding the nature of its origin. Because of the "blocks in matrix" character the Chase Brook was later interpreted as a mélange (Neuman and Max, 1989; Pollock, 1993, 2020, 2023; Wang 2018). The mélange consists of crumbly gray to dark gray slate and intraclasts (Fig. 4a). The intraclasts include isolated blocks or rounded pieces of dominantly light-brown, calcareous metasiltstone and sandstone, with some slate. The mélange is nearly entirely pyritic and contains ubiquitous ball-shaped pyrite concretions as large as 10 centimeters in diameter (Fig. 4b). Oxidation of pyrite makes the formation distinctively rusty. Fresh slate is dark gray to black and graphitic. The formation is pervasively and strongly cleaved by the Acadian foliation event. Cleavages could be straight but mostly irregular and produce biconvex phacoidal fragments, referred to as phacoidal cleavage as seen throughout the Munsungun inlier.

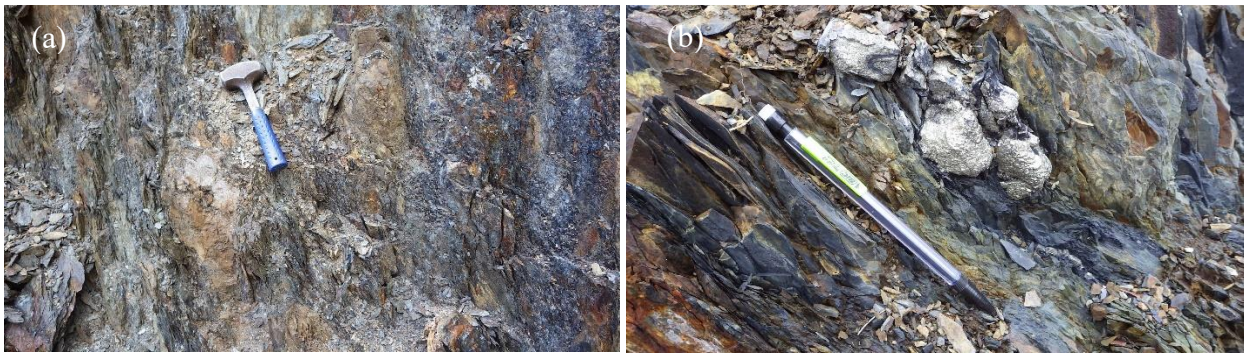

Figure 4. Mélange of the Chase Brook Formation. (a) Sandstone intraclasts and phacoidal cleavage; (b) Ball-shaped pyrite concretions common in the mélange.

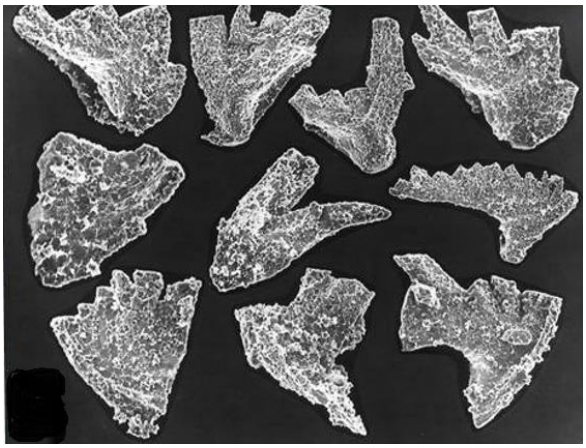

Figure 5. Conodont elements *Periodon flabellum* (Linstrom) from the Chase Brook mélange. Image by John Repetski. No scale included.

Hall (unpublished) collected a sample from a limestone and calcareous siltstone block in the Mooseleuk Mountain 7.5' quadrangle, along the access road to Bradford Camps, in the late 1980's. John Repetski of the USGS analyzed the sample and identified several conodont elements as *Periodon flabellum* (Lindstrom) (Fig. 5). *P. flabellum* is known only from the middle and upper Arenig series (Early Ordovician) and is typical of the deep cold water North Atlantic conodont faunal province. Pollock (1993) initially reported this result.

The Chase Brook Formation has long been considered the oldest formation in the Munsungun inlier. A sandstone sample collected from the Machias River valley in the Jack Mountain quadrangle yielded more than 250 detrital zircon grains. U-Pb LA-ICP-MS dating of the zircon grains at the Arizona LaserChron Center (ALC) shows a typical Laurentia spectrum with the youngest zircon grains at around 556 Ma (Fig. 6), suggesting that the Chase Brook mélange was developed on a tectonically active margin of a peri-Laurentia terrane. Because the mélange is overlain by the Middle Ordovician volcanic rocks of the Munsungun Lake and Round Mountain formations and it does not contain any zircon grains younger than 556 Ma, the mélange should pre-date Middle Ordovician. From Ediacaran to Cambrian, the eastern Laurentia margin was a passive margin going through rifting and shelf sedimentation of clasts and carbonate. The margins of the rifted peri-Laurentia terranes, for example, the Chain Lakes massif (or microcontinent or block) (Gerbi et al., 2006) became tectonically active and associated with Iapetus oceanic subduction from the beginning of the Early Ordovician (White and Waldron, 2022). Therefore, it is suggested that the Chase Brook mélange was associated with a peri-Laurentian terrane in the Early Ordovician, which is also supported by the conodont data (Fig. 5).

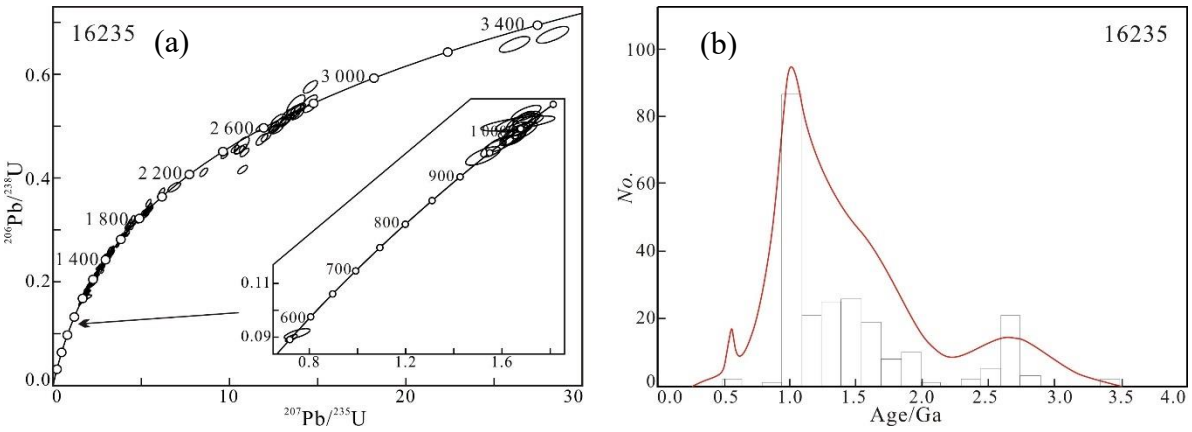

Figure 6. Detrital zircon age spectrum showing Laurentia affinity for the Chase Brook mélange.

Munsungun Lake Formation: The Munsungun Lake Formation (Hall, 1970) refers to the volcanic rocks that are widely distributed along the eastern-northeastern half of the Munsungun inlier, north to the Bald Mountain–Greenlaw Pond area and south to the Chamberlain Lake area, for near 80 kilometers. The formation includes voluminous explosive facies of pyroclastic rocks, effusive facies of predominantly basalt with minor rhyolite, andesite, and dacite, and subvolcanic facies of diabase sills and dikes. The pyroclastic rocks include all types of submarine tephra such as tuff, lapillistone, and volcanic breccia, with minor volcaniclastic tuffite that occurs only locally. The formation in the central and southern Munsungun area is dominated by pyroclastic rocks, particularly gray and red tuff. Coarse tuff and lapillistone are generally composed of mixed crystal (quartz and feldspar) and lithic (tuff, pumice, and scoria) fragments, with minor devitrified glass shards; some contain more crystal fragments than others or vice versa. About 80 vol% of the tuff is gray and the remainder maroon, purplish red, or bright green, with changes between the colors either knife sharp or gradational (Fig. 7a). Tuff is generally foliated by the regional prevailing northeast-southwest Acadian foliation event. Poorly sorted volcanic breccia, tuffaceous breccia, and block-bearing lapillistone generally consist of gray cherty tuff fragments, with some containing blocks of maroon tuff and/or red jasper. Fine tuff can be cherty (Fig. 7b, c). Some very fine and cherty rocks shown in different colors from gray to red have been called chert (Fig. 7d). They show quartz spherules as seen in Figure 44 and interpreted to be radiolarians. The chert layers or lenses are commonly interbedded with volcanic rocks, mostly coarse tuff and breccia. Whole-rock geochemical analysis shows their volcanogenic origin, as initially reported by Pollock (1987a). In other words, the chert was made predominantly of volcanic material like ash, being originally tuff (or tuffite). This type of chert is radiolarian tuff or radiolarian-bearing tuff due to its volcanogenic origin and composition of primarily tuff; it is not typical sedimentary radiolarian chert. For both cherty tuff and radiolarian tuff, hydrothermal silicification has always made them even more cherty and sharp due to addition of more silica. The chert of the best quality, the glassy one, is almost always

silicified with fine and microscopic quartz veinlets (Figs. 7d and 44d) and/or disseminated quartz. For more information of the "Munsungun chert", please refer to Pollock (1987a, 2020) and Pollock et al. (1999).

Basalt is another major component of the Munsungun Lake Formation and dominates in the northern Munsungun inlier. It is predominantly unfoliated, aphyric, and fine grained, and composed of plagioclase and augite with minor olivine and hornblende. Phyric basalt occurs only locally. Agglomerate and hyaloclastite are common. Pillow basalt is less common (Fig. 7e). Basalt flows with vesicular and/or amygdaloidal textures (with amygdales of calcite, zeolite, quartz, and opal) suggest a shallow-water depositional environment. Red hematitic chalcedony veins or aggregates (called "red jaspers") are common in basalt, as a result of low-temperature silica and iron-rich hydrothermal activities. Red jasper can occur as blocks in volcanic breccia (Fig. 7f). Most of the basalts have experienced hydrothermal alteration with resulting abundant secondary minerals such as chlorite, calcite, epidote, and iron oxides.

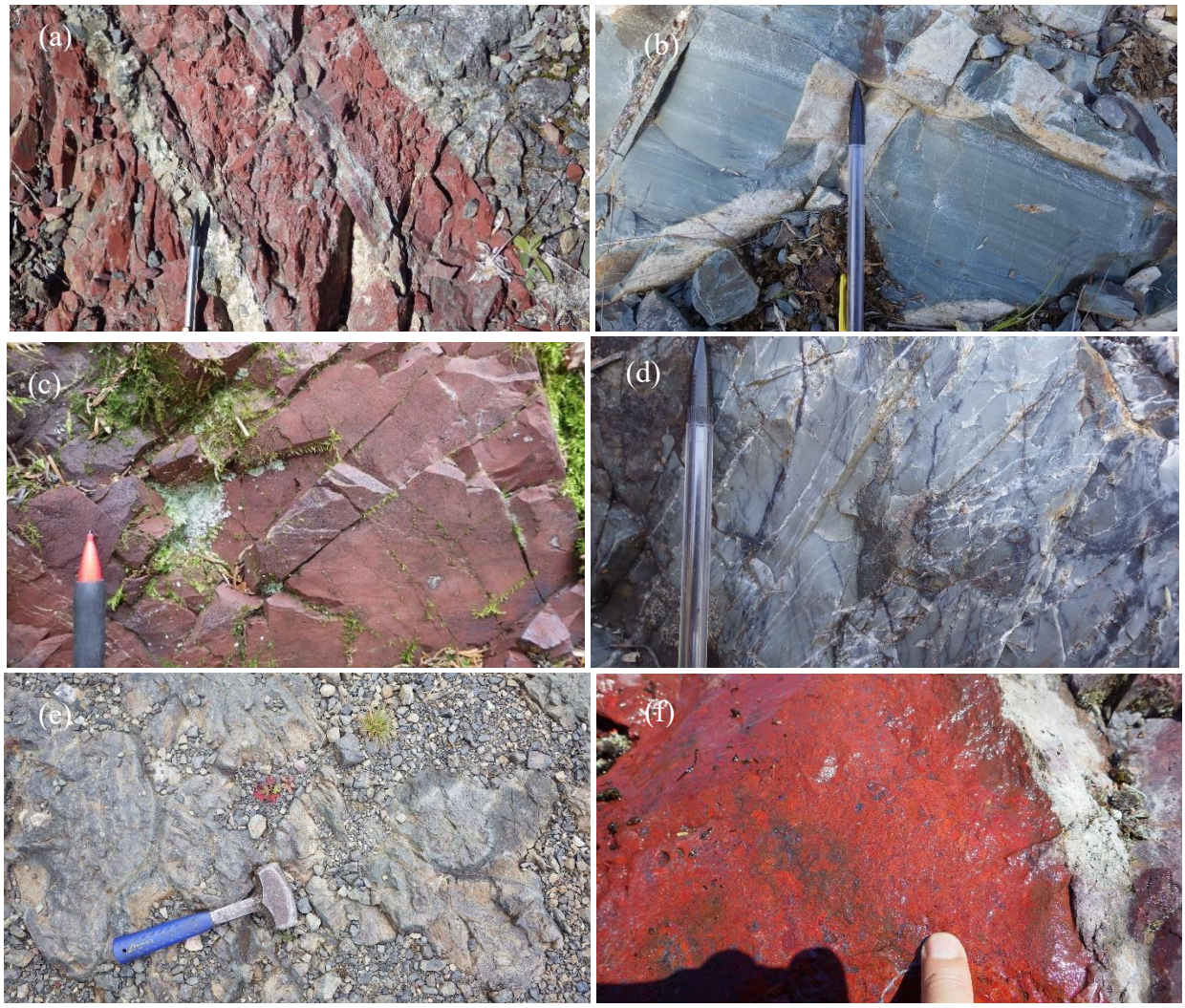

Figure 7. Munsungun Lake Formation. (a) Alternating layers of gray and red fine tuff. (b) Gray cherty fine tuff and coarse tuff. (c) Red cherty fine tuff. (d) Silicified gray chert. (e) Pillow basalt at Williard Ridge. (f) A red jasper block in volcanic breccia.

Twenty-five samples of basalt, andesite, diabase, and tuff have been collected for whole-rock major and trace elemental analysis and several of them for Nd isotopic analysis. Samples vary from tholeiitic E-MORB-like (rifted arc) basalt and diabase with enriched LREE (light rare earth elements) & LILE (large ion lithophile elements) and positive εNd values (1.3 to 5.3), to transitional and calc-alkaline basalt, andesite, and andesitic tuff that are depleted in Ta, Nb, and Ti and enriched in LILE with negative Eu anomaly and negative εNd values (-16.3 to -18) (Fig. 8a, b, c). On the tectonic discrimination diagrams such as Nb/Yb vs. Th/Yb (Pearce 2008) and La/10–Y/15–Nb/8 (Cabanis and Lecolle, 1989) diagrams (Fig. 8d, f), the transitional and calc-alkaline basalt and diabase, as well as the andesite

and andesitic tuff plot in the "volcanic arc array" or "orogenic domains", whereas the tholeiitic basalt plots in the "E-MORB array" or "late to post-orogenic intra-continental domains".

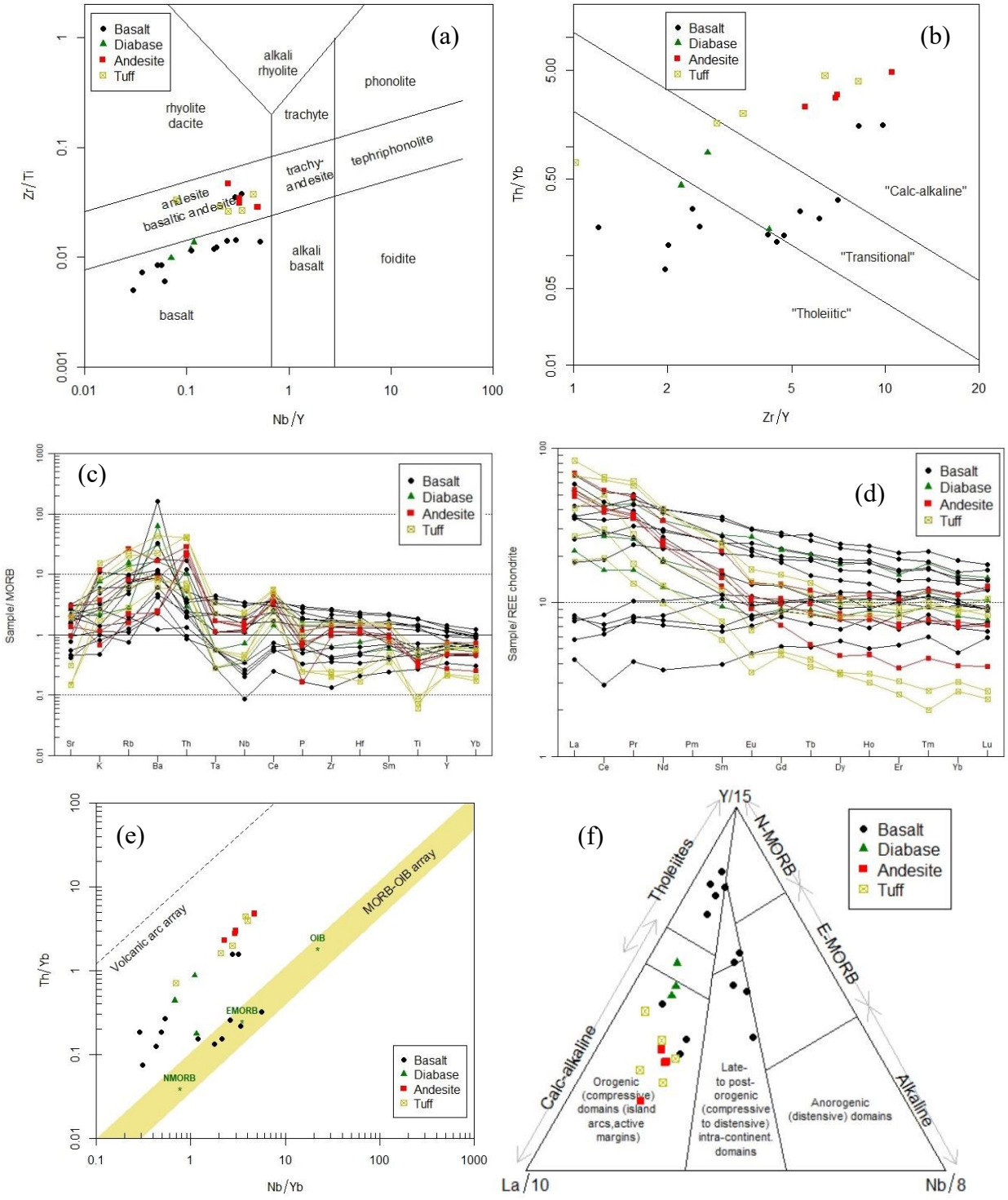

Figure 8. Geochemistry and tectonic discrimination of the Munsungun Lake Formation. (a) Classification of the samples (Pearce, 1996). (b) Zr/Y vs. Th/Yb diagram (Ross and Bedard, 2009); (c) MORB-normalized spider diagram (Pearce, 1983); (d) Chondrite-normalized REE pattern (Nakamura, 1974); (e) Nb/Yb vs. Th/Yb discrimination diagram (Pearce, 2008); (f) La/10–Y/15–Nb/8 discrimination diagram (Cabanis and Lecolle, 1989).

Four tuff samples have been analyzed by using zircon U-Pb LA-ICP-MS method at the University of New Brunswick ICP-MS Laboratory by Dr. Christopher McFarlane and the Arizona LaserChron Center (ALC). They yielded weighted mean ages of 463.4 ± 4.8 Ma (Willard Ridge; Fig. 9), 467.0 ± 2.2 Ma (Center Mountain), 468 ± 16 Ma (Munsungun Ridge), and 469.4 ± 4.2 Ma (Jack Mountain) (Fig. 2). Before this geochronological work, the only radiometric age obtained in the Munsungun inlier was the U-Pb zircon SHRIMP age of 467 ± 4 Ma for a tuff sample collected from Bull Hill, south of Bald Mountain (Ayuso et al., 2003). The unconformable contact with the underlying Chase Brook mélange may well represent one of the three circles of Tectonic orogeny, Taconic 2 (van Staal and Barr, 2012). However, it must be noted that the contact was faulted by a low-angle thrust fault, at least in the northern Munsungun inlier.

The variations in geochemistry and tectonic settings and the age gap indicate that the Munsungun Lake Formation should be subdivided into multiple formations when more detailed mapping and analyses are available in the future.

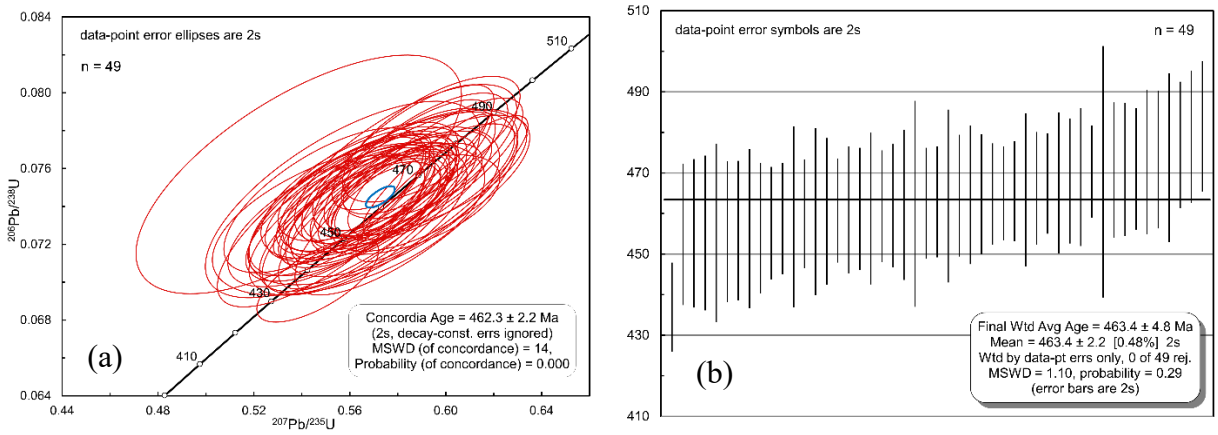

Figure 9. Zircon U-Pb concordia diagram (a) and weighted mean age (b) of a tuff sample from the Munsungun Lake Formation at Willard Ridge.

Round Mountain Volcanic Suite: The Round Mountain Volcanic Suite (Wang, 2018) is a volcanic sequence made of alternating layers of eruptive pyroclastics (fine tuff, coarse tuff, lapilli tuff, lapillistone, and tuffaceous breccia) and effusive basalt (dominantly porphyritic basalt). The formation was constructed from multiple cycles of submarine volcanic eruptions during which each cycle began with explosive eruption and ended with effusive basaltic lava flows. Diabase occurs as either sills or dikes – they are medium-coarse-grained with typical ophitic texture. Layers of fine or very fine tuff can be very silica rich and cherty (Fig. 10a). The artifacts found around Round Mountain were believed to be largely sourced from the cherty fine tuff and/or radiolarian-bearing (suspected) fine tuff layers of Round Mountain (Wang, 2018). The cherty fine tuff and radiolarian-bearing fine tuff are mostly gray or dark gray. Some are in red or pink or purple color. Color may change gradually between both gray and red/pink/purple colors. The basalt flows are characterized by porphyritic texture with plagioclase as major phenocrysts (Fig. 10b).

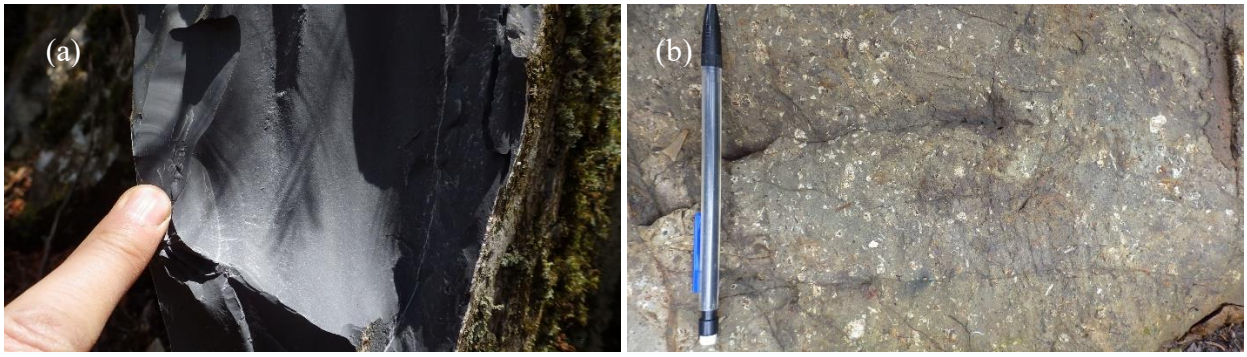

Figure 10. Round Mountain Volcanic Suite. (a) Gray cherty fine tuff with conchoidal fracture. (b) Porphyritic basalt.

The basalt shows transition to calc-alkaline series whereas the andesitic and dacite tuff are calc-alkaline (Fig. 11a). They are enriched in LREE and LILE with the tuff samples showing negative Eu and Ta, Nb anomalies (Figs. 11b, c).

However, the basalt does not show any Eu anomaly and only slight Ta and Nb negative anomalies. The basalt samples plot in the "late to post-orogenic intra-continental domains" (Fig. 11d).

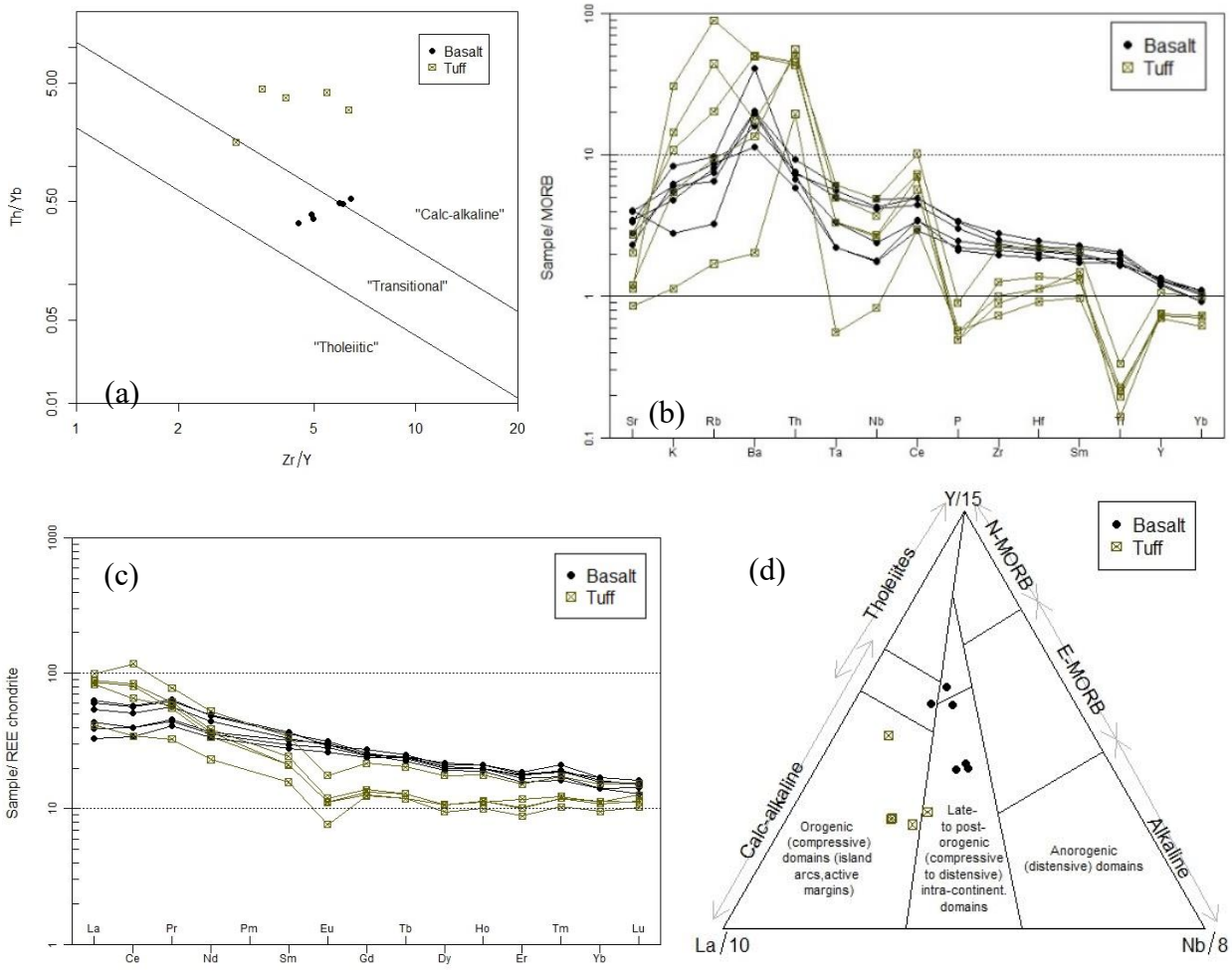

Figure 11. Geochemistry and tectonic discrimination of the Round Mountain Volcanic Suite. (a) Zr/Y vs. Th/Yb diagram (Ross and Bedard, 2009); (b) MORB-normalized spider diagram (Pearce, 1983); (c) Chondrite-normalized REE pattern (Nakamura, 1974); (d) La/10-Y/15-Nb/8 tectonic discrimination diagram (Cabanis and Lecolle, 1989).

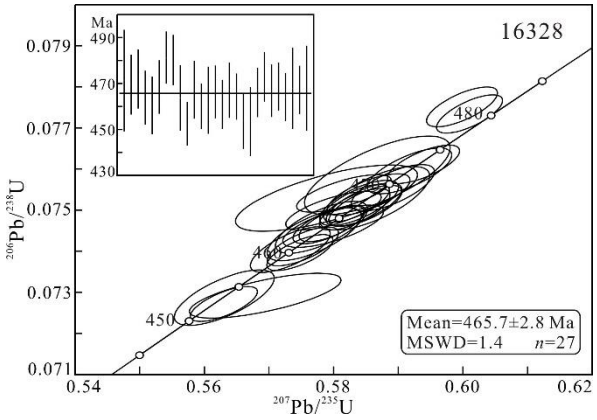

Figure 12. Zircon U-Pb concordia diagram and weighted mean age of the Round Mountain Volcanic Suite.

The Round Mountain Volcanic Suite was developed within a well-preserved half-graben. The alternating pyroclastic and basaltic layers within the half-graben form a homocline dipping toward west-northwest. The half-graben structure confirms a rifting, extensional environment for the formation, which is consistent with the geochemical characteristics. This extensional environment might be related to an arc-rifting phase during arc evolution.

A coarse tuff sample collected from the Peaked Mountain analyzed by zircon U-Pb LA-ICP-MS U-Pb method at ALC yielded a weighted mean age of 465.7 ± 2.8 Ma age (Fig. 12).

Bluffer Pond Formation: The Bluffer Pond Formation (Hall, 1970) is composed nearly entirely of basalt and characterized by pillow basalt (Fig. 13a), with very minor gray tuff and subvolcanic diabase sills and dikes. Basalt may be non-vesicular or vesicular or amygdaloidal with generally small vesicles. Hyaloclastite basalt occurs locally. Despite minor, some gray fine tuff can be very cherty (Fig. 13b). The formation is unconformable with both the underlying Chase Brook and the overlying Chase Lake formations.

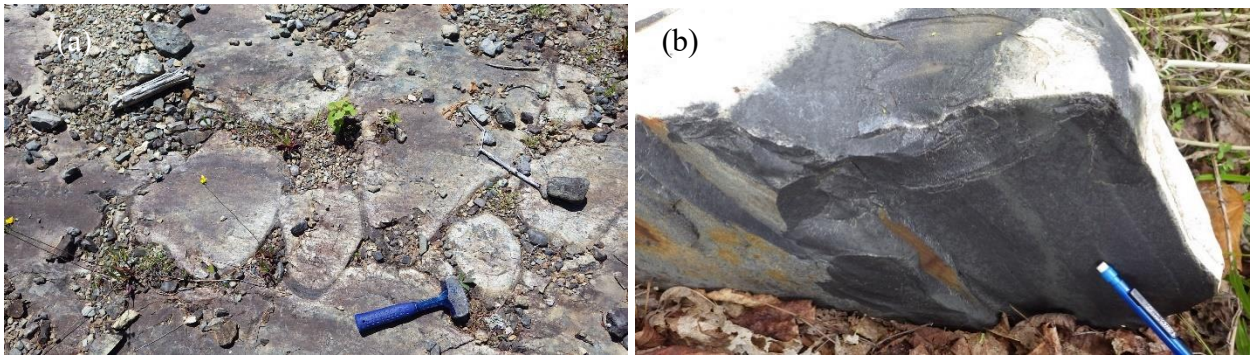

Figure 13. Bluffer Pond Formation. (a) Pillow basalt. (b) Cherty gray fine tuff with conchoidal fracture.

Seven basalt samples show a transitional to calc-alkaline series (Fig. 14a). The basalt is depleted in Ta, Nb, and Ti and enriched in LILE with slightly higher LREE than HREE (Fig. 14b, c). The tectonic discrimination diagrams show "volcanic arc array" (Fig. 14d) and "late to post-orogenic intra-continental domain" (Fig. 14e). It seems the basalt was emplaced in a subduction related arc setting.

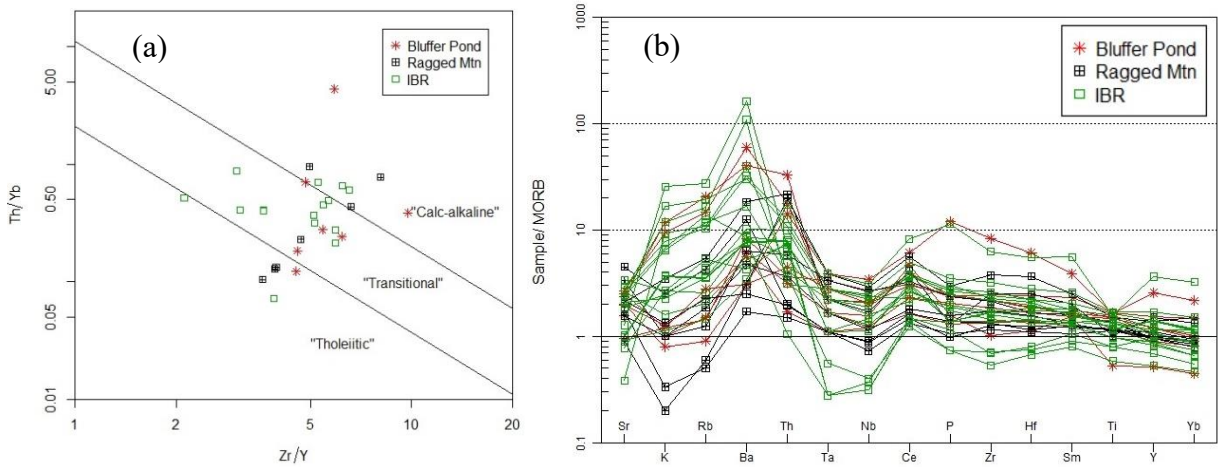

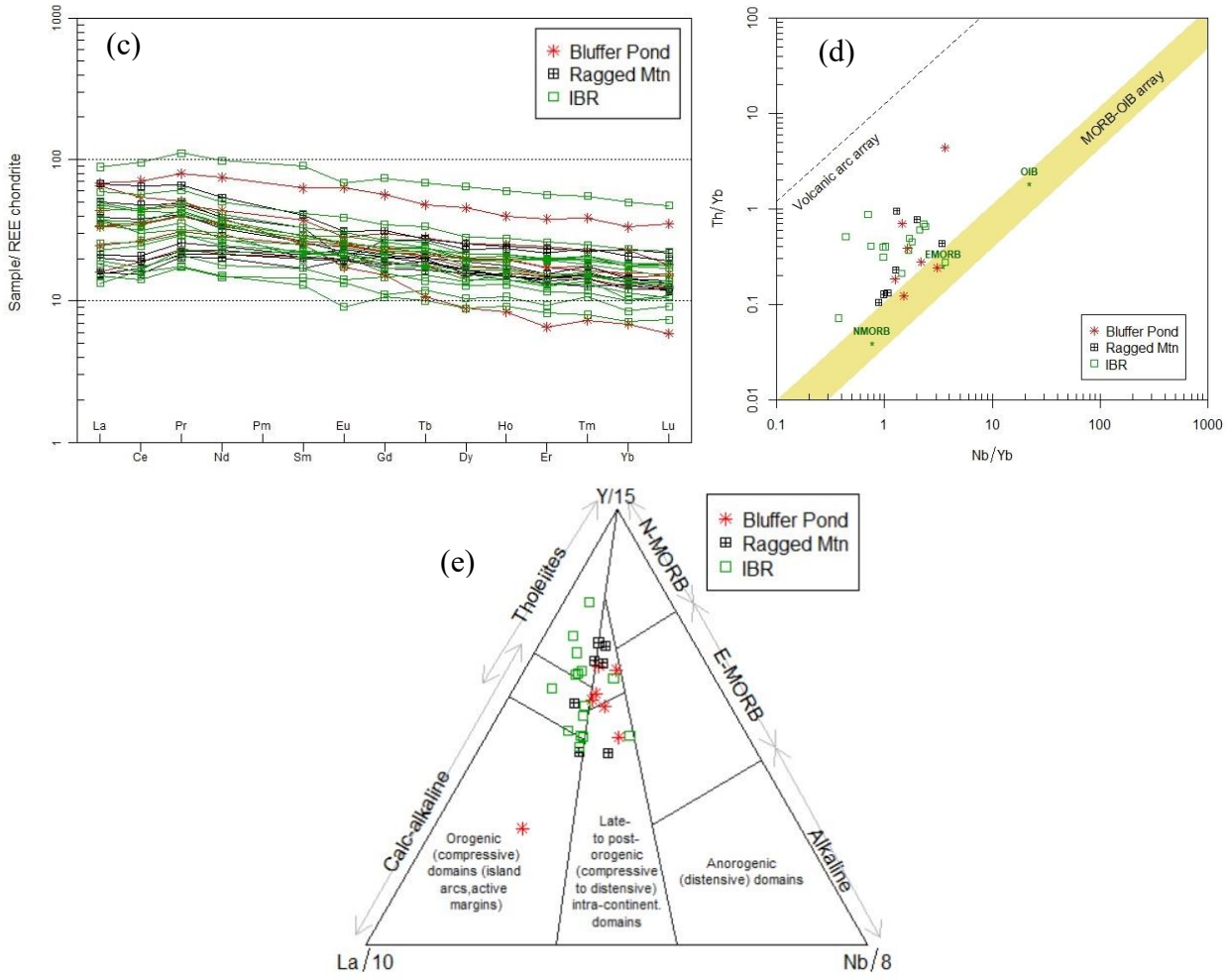

Figure 14. Geochemistry and tectonic discrimination of the Bluffer Pond, Ragged Mountain, and Ingalls Brook Road (IBR) formations. (a) Zr/Y vs. Th/Yb diagram (Ross and Bedard, 2009); (b) MORB-normalized spider diagram (Pearce, 1983); (c) Chondrite-normalized REE pattern (Nakamura, 1974); (d) Nb/Yb vs. Th/Yb discrimination diagram (Pearce, 2008); (e) La/10–Y/15–Nb/8 discrimination diagram (Cabanis and Lecolle, 1989).

A tuff sample yielded a weighted mean age of 454.5 ± 2.7 Ma for the Bluffer Pond Formation (Fig. 15). It indicates that the "Munsungun-Winterville arc" was still volcanically active in the Sandbian stage of the Late Ordovician time.

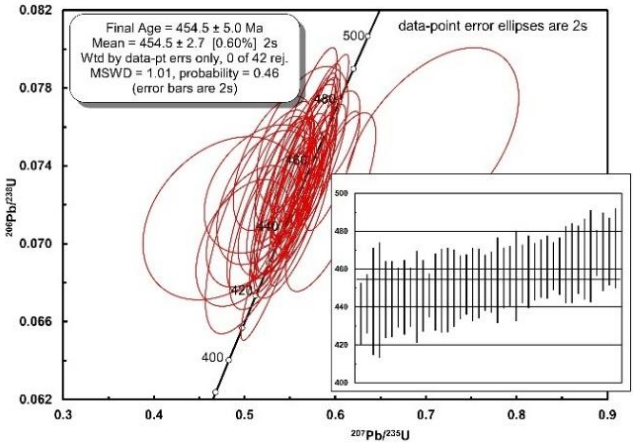

Figure 15. Zircon U-Pb concordia diagram and weighted mean age of the Bluffer Pond Formation.

Ragged Mountain Formation: Recently named (Wang, 2023a), the formation occurs as a southwest- or northeast-striking fault block. The formation is composed of nearly half basalt and half pyroclastics of mostly gray tuff and red/maroon rhyolitic crystal tuff along the Ragged Mountain ridge and in the area around First Currier Pond and Second Currier Pond. The basalt is predominantly aphyric with only some basalts being vesicular/amygdaloidal with relatively small vesicles and amygdales. Pillow basalt, agglomerate, and hyaloclastite basalts are less common. The tuff is generally dominated by gray and dark gray coarse and fine tuff with lesser amounts of volcanic breccia and lapillistone. Fine tuff, in particular, the silicified fine tuff can be cherty or even glassy. Lapillistone is composed of either gray fine tuff fragments or felsic pumice fragments (pumice lapillistone or pumice flow). A rhyolitic and crystal tuff lens occurs along Ragged Mountain. Hall (1970) mapped it as "soda rhyolite" and named it the "Ragged Mountain Member" of the Bluffer Pond Formation. It is structureless and in red or maroon color. This distinctive unit was seen by the recent airborne radiometric survey as a K anomaly (Shah, 2022).

Similar to the basalt samples from the Bluffer Pond Formation, seven basalt samples collected from the Ragged Mountain Formation also show a transitional to calc-alkaline series (Fig. 14a). The basalt is depleted in Ta and Nb and enriched in LILE with slightly higher LREE than HREE (Fig. 14b, c). The tectonic discrimination diagrams show "volcanic arc array" (Fig. 14d) and "orogenic – late to post-orogenic intra-continental" domains (Fig. 14e). In summary, the geochemical data suggest a subduction related arc setting for the Ragged Mountain basalt.

Zircon U-Pb LA-ICP-MS analysis at ALC for a tuff sample yielded a weighted mean age of 457.5 ± 2.1 Ma (Fig. 16). It again shows that the "Munsungun-Winterville arc" was still volcanically active in the beginning of the Late Ordovician time.

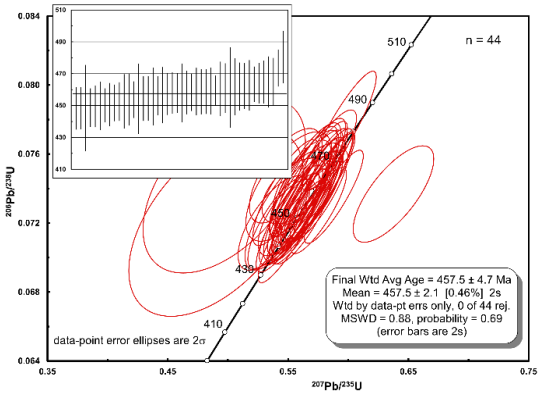

Figure 16. Zircon U-Pb concordia diagram and weighted mean age of the Ragged Mountain Formation.

Ingalls Brook Road Formation: This formation is fault-bounded with the upper slate unit of the Rowe Lake Formation by the northwest dipping Ingalls Brook reverse-thrust fault to the southeast. The formation is unconformably overlain by Blind Brook Formation to the west-northwest. The formation consists of pyroclastic rocks (of volcanic breccia, lapillistone, and gray and dark gray tuff), basalt, and diabase. However, from Little Ragged Mountain to the Mule Brook Mountain and McPherson Brook area, the formation is dominated by pyroclastic rocks. Tuff is gray and dark gray, massive or banded. The volcanic breccia and lapillistone are composed mainly of gray and dark gray cherty fine tuff blocks or fragments (Fig. 17a). Large subvolcanic diabase sills or dikes occur in the formation. Basalt may show excellent pillow structures (Fig. 17b). According to Pollock (2019), some gray chert layers are interbedded with pyroclastic rocks at Mule Brook Mountain.

Similar to the basalt samples from the Bluffer Pond and Ragged Mountain formations, fifteen basalt samples geochemically show predominantly transitional series (Fig. 14a, b). They are considerably depleted in Ta and Nb and some in Ti, enriched in LILE with slightly higher LREE than HREE (Fig. 14c, d). Some show negative Eu anomalies, others not. The tectonic discrimination diagrams show "volcanic arc array" (Fig. 14e) and "orogenic domains" (Fig. 14f). (Note: several tuff and rhyolite samples analyzed for whole-rock geochemistry are not included in the diagrams; they are calc-alkaline and strongly show subduction and arc setting.)

Two coarse tuff samples separately collected from the formation for zircon U-Pb LA-ICP-MS analyses at the University of New Brunswick ICP-MS Laboratory. One yielded a 454.4 ± 1.8 Ma weighted mean age and the other a 455.1 ± 2.0 Ma weighted mean age (Fig. 18); both are near identical and within error range. The ages again support the conclusion that there existed subduction and arc volcanism along the "Munsungun-Winterville arc" in the beginning (Sandbian) of the Late Ordovician time.

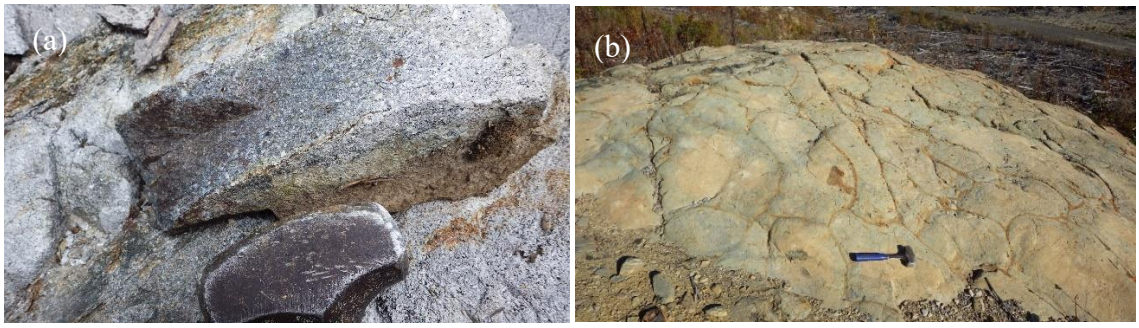

Figure 17. Ingalls Brook Road Formation. (a) Coarse tuff. (b) Pillow basalt.

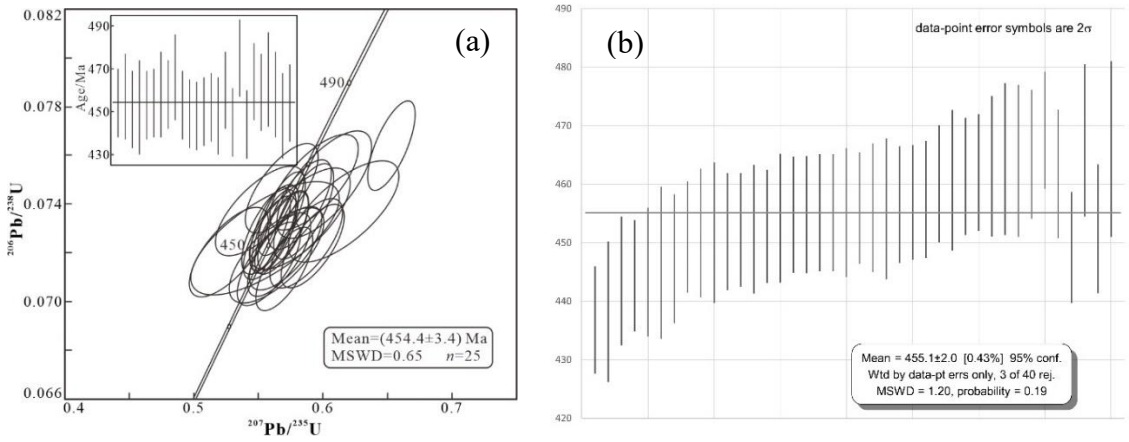

Figure 18. Concordia or weighted means ages of two tuff samples (a and b) of the Ingalls Brook Road Formation.

Chase Lake Formation: The Chase Lake Formation (Hall, 1970) is distributed mainly on the northwest side of Chase Lake and along the east flank of Ragged Mountain and Pell and Pell Road in the Chase Lake area. The formation is composed generally of interbedded gray and dark gray slate, siltstone, sandstone, graywacke, and granule, pebble, and cobble conglomerate with the conglomerate accounting for nearly one quarter of the formation. The conglomerate is generally very poorly sorted, matrix-supported, and composed predominantly of sedimentary rocks such as sandstone and siltstone, with much lesser amounts of volcanic rocks of mostly gray fine tuff and minor basalt. The sandstone beds range between 10 and 30 cm thick and most of the sandstones are lithic sandstone. The very poorly sorted conglomerate with predominantly irregularly shaped sandstone and siltstone clasts/chips and the dark or black coarse lithic sandstone are remarkable diagnostic features of the formation (Fig. 19a). Another distinctive diagnostic feature is the cleaved rhythmically interbedded thin (2 mm – 10 cm) pyritic siltstone (weathered to be tan rusty) and dark gray or black argillite throughout the formation (Fig. 19b). No sandstone made with abundant well sorted and mature quartz sand has ever been found. Parallel and graded bedding is common. No outcrops showing contact relationship with Chase Brook Formation have ever been found but based on the map pattern, it is likely that the Chase Lake Formation unconformably overlays the Chase Brook mélange and the volcanic rocks of the Bluffer Pond Formation.

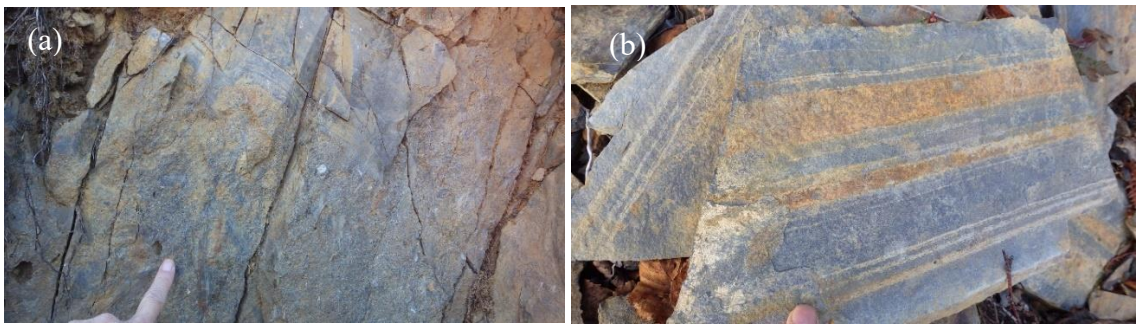

Figure 19. Chase Lake Formation. (a) Conglomerate. (b) Cleaved rhythmically interbedded thin, pyritic siltstone (weathered to be tan rusty) and dark gray or black argillite.

Blind Brook Formation: The Blind Brook Formation (Hall, 1970) is a distinctive but localized slate. It consists predominantly of dark gray or black rusty weathering slate, thin- to medium-bedded sandstone (or graywacke), and minor intercalated granule conglomerate. It is fault bounded with the basalt of the Spider Lake Formation by the northwest dipping Blind Brook reverse-thrust fault to the northwest and unconformably overlies the pyroclastics of the Ingalls Brook Road Formation to the southeast, with a thin layer of basal conglomerate and sandstone (Fig. 20a). The formation is characterized by ubiquitous pyrite sub-mm grains that are disseminated throughout the formation and occur as thin discontinuous bedding-parallel lamina up to 10 mm in thickness. Tan weathered coarse-grained metasiltstone to metasandstone is common due to oxidation of pyrite (Fig. 20b). Abundance of pyrite suggests that the formation was likely deposited in a restricted suboxic to anoxic basin which was free of current activity.

Figure 20. Blind Brook Formation. (a) West (left)-dipping unconformity between Blind Brook Formation (left; layered conglomerate and sandstone) and Ingalls Brook Road Formation (right; layerless gray cherty tuff). (b) Slate and rusty thin-medium-layerd sandstone (or graywacke).

The Blind Brook Formation is notably graptolitic (Fig. 21); one can find graptolite fossils at almost every outcrop. Several borrow pits show well-preserved graptolite fossils. The commonly found graptolites include *Orthograptus quadrimucronatus, Orthograptus calcaratus, Orthograptus truncates*, *Orthograpus amplexicaulis*, *Climacograptus bicornis, Climacograptus spiniferus, Dicranograptus ramosus,* and *Pseudoclimacograptus sp*. of Late Ordovician (slightly early late Sandbian age) (Identification by Henry Williams). Detrital zircon U-Pb dating of a sandstone collected from the Mooseleuk Lake quadrangle yielded ages clustered at 445.2 ± 1.8 Ma of all the 40 analyzed detrital zircon grains, confirming the Late Ordovician age of the formation and a limited source of clasts from either local volcanics or a Laurentia-associated terrain.

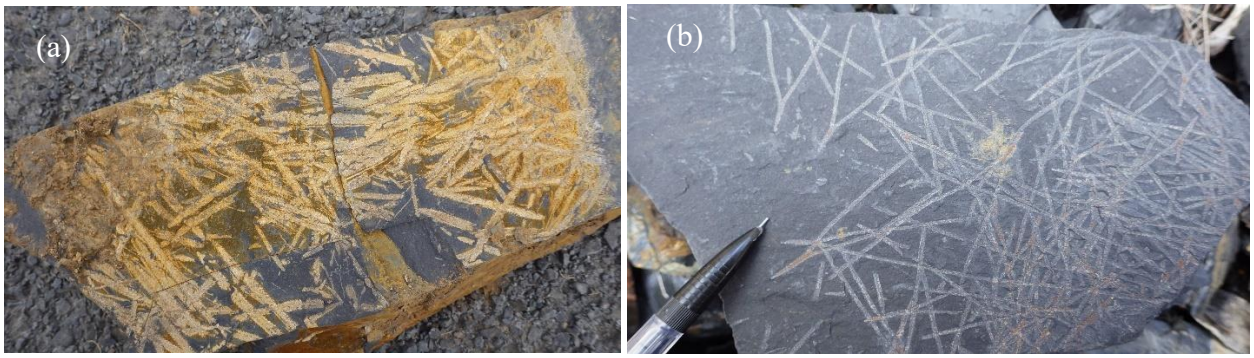

Figure 21. Graptolites of the Blind Brook Formation. (a) A layer of mostly *Orthograptus quadrimucronatus.* (b) A layer of *Dicranograptus ramosus.* Identifications by Henry Williams.

Rowe Lake Formation. The Rowe Lake Formation was initially named in the Round Mountain quadrangle (Wang, 2018). It consists of four conformable units. These are: (1) The lower slate unit – it is predominantly an argillic slate. It has a distinct fresh yellowish brown weathering. (2) The conglomerate unit – it is the thickest unit; it is predominantly a massive and thickly layered, clast-supported, pebble, cobble, and granule conglomerate, with lesser intercalated layers of sandstone and slate. The conglomerate is least polymictic and composed mainly of clasts of light gray tuff and dark gray cherty tuff pebbles (Fig. 22a). Interestingly it does not contain red or green pebbles of fine tuff commonly seen in the Munsungun Lake Formation, indicating that it was likely sourced from the early Late Ordovician Ragged Mountain and Ingalls Brook Road formations because both formations don't contain red or green

tuff. (3) The sandstone unit – it is characterized by medium-thick layers of coarse sandstone and silty sandstone with minor interbedded conglomerate and slate layers. The unit occurs as an intraformational lens only in the Big Machias Lake quadrangle. (4) The upper slate unit – it is nearly entirely a black or dark gray, lithologically homogenous, and non-pyritic argillic slate, with minor interbedded sandstone, siltstone, and rarely intercalated conglomerate. It is characterized by repeating thin (0.3 – 2 cm) layers of brown siltstone in 5 – 15 cm intervals (Fig. 22b). Generally, the formation is presented as a northwest-west-dipping homocline with an average dip angle of 40°.

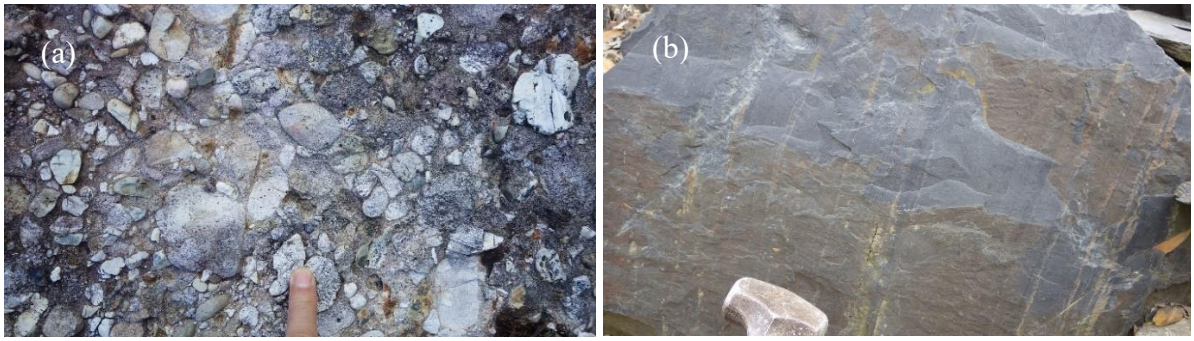

Figure 22. Rowe Lake Formation. (a) The conglomerate containing no red tuff pebbles. (b) The upper slate characterized by repeated thin seams of brown sandstone.

The upper slate contains Late Ordovician graptolite genera *Orthograptus sp*. and *Climacograptus spiniferus* (Fig. 23). Detrital zircon U-Pb dating of a sandstone sample collected from the conglomerate member at the University of New Brunswick ICP-MS Laboratory shows the youngest zircon grains clustered at 447.0 ± 3.2 Ma, indicating that the formation was deposited during the Late Ordovician time (Fig. 24). The age spectrum of the 39 analyzed detrital zircon grains clearly demonstrates a Laurentian provenance.

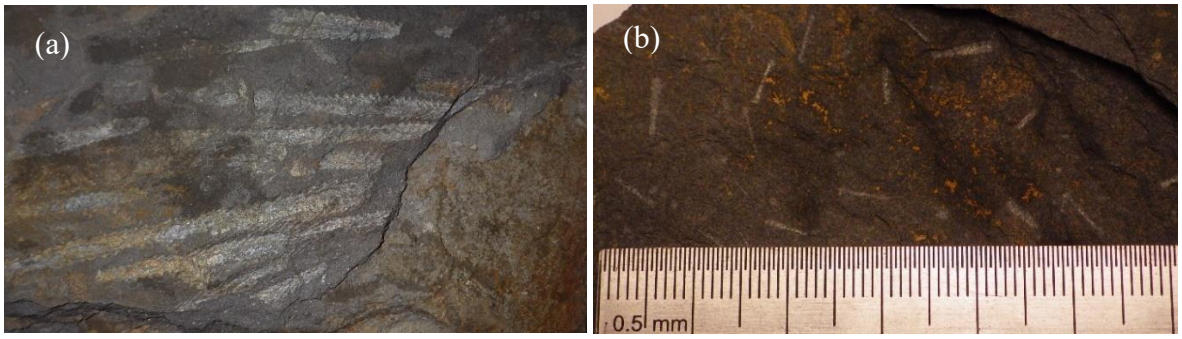

Figure 23. Graptolites in the upper slate of the Rowe Lake Formation. (1) *Orthograptus sp*. (b) *Climacograptus spiniferus*. (Identification by Henry Williams)

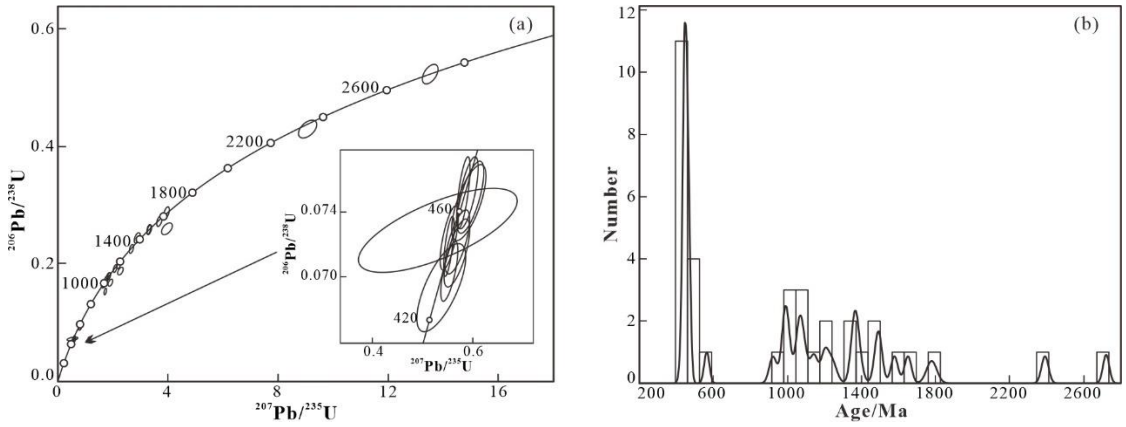

Figure 24. Detrital zircon age spectrum (a) and distribution histogram (b) of the Rowe Lake Formation.

Ferguson Brook Formation: The Ferguson Brook Formation was initially named in the Carr Pond quadrangle (Wang, 2022) and occurs mostly in the Winterville inlier. It occurs as only several small segments in the Jack Mountain and Greenlaw Pond quadrangles where it was initially mapped as "unnamed graywacke and slate" (Wang, 2019, 2021a) in the Munsungun inlier. The formation is predominantly medium to thickly layered dark gray graywacke, dark gray, black pyritic slate, and minor intercalated conglomerate (Fig. 25a, b) and black cherty siliceous mudstone. Some graywacke is turbiditic and characterized by horizontal lamination and cross ripples. The conglomerate is poorly sorted, angular, and polymictic with mostly cherty tuff and basalt clasts that were probably derived from the volcanic rocks of the Munsungun Lake (and Winterville) formations (Fig. 25b).

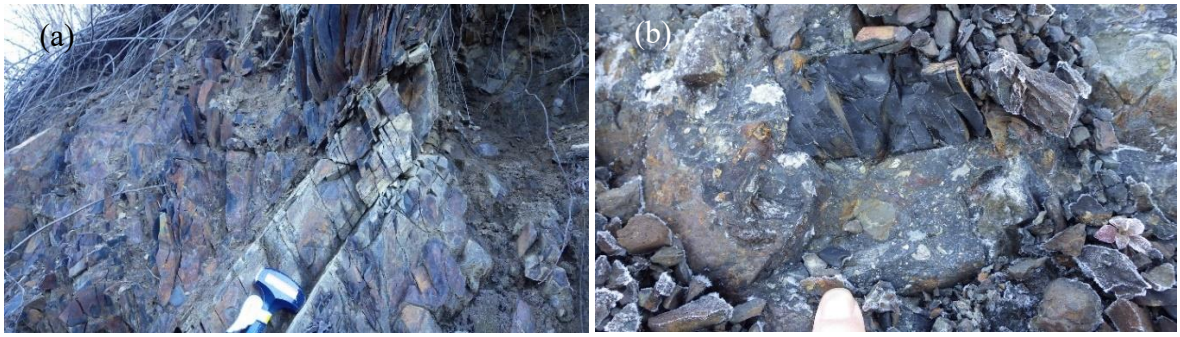

Figure 25. Ferguson Brook Formation. (a) Black slate and graywacke and the preliminary bedding. (b) Intercalated poorly sorted and matrix-supported conglomerate.

No fossils have been found in the formation. A detrital zircon analysis for a sandstone collected from the formation exposed in a pit next to American Realty Road, southwest of Greenlaw Mountain, yielded a typical Laurentian spectrum, with the youngest zircon grains clustered at 451 Ma (Fig. 26), albeit only 19 gains analyzed. The youngest age is indicative of a Late Ordovician age for the formation.

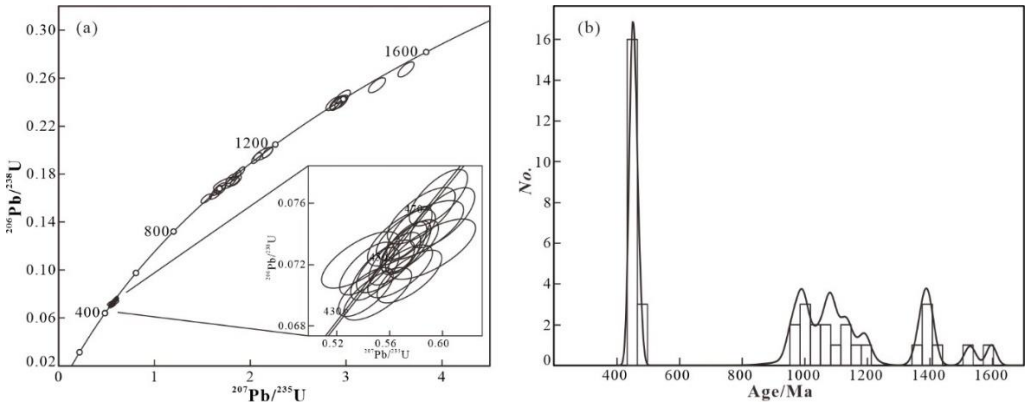

Figure 26. Detrital zircon age spectrum for the Ferguson Brook Formation.

The Silurian Formations

Spider Lake Formation: The Spider Lake Formation (Hall, 1970) is one of the major and widespread volcanic formations in the Munsungun inlier. The formation is dominated by basalt with very minor pyroclastics and subvolcanic diabase. Basalt is generally and distinctively characterized by vesicular and amygdaloidal textures with large vesicles and amygdales of commonly calcite, chlorite, epidote, zeolite, and quartz (Fig. 27a). Only a few of outcrops show pillow basalt, agglomerate basalt, and hyaloclastite. The basalt is dominantly aphyric and fine grained, with some show phyric texture with plagioclase phenocrysts. Phyric texture can be also found in vesicular basalt (Fig. 27b). Some basalt in the Horseshoe Pond area show excellent peperite (Fig. 27c). The formation is substantially faulted and displaced by mostly southwest-striking reverse faults into fault blocks and slivers, as part of the Munsungun imbricate fault system. It is important to point it out that the slivers also include Lower Devonian Seboomook Group, in particular its bottom succession of the so-called "trinity" in our study – the basal conglomerate, fossiliferous limestone and calcareous sandstone, and maroon slate/siltstone (Fig. 27d). The fossiliferous limestone and calcareous

sandstone are rich in marine invertebrate fossils typical of Early Devonian Helderberg fauna (please see the section below for the Lower Devonian Seboomook Group for more information of the fossils).

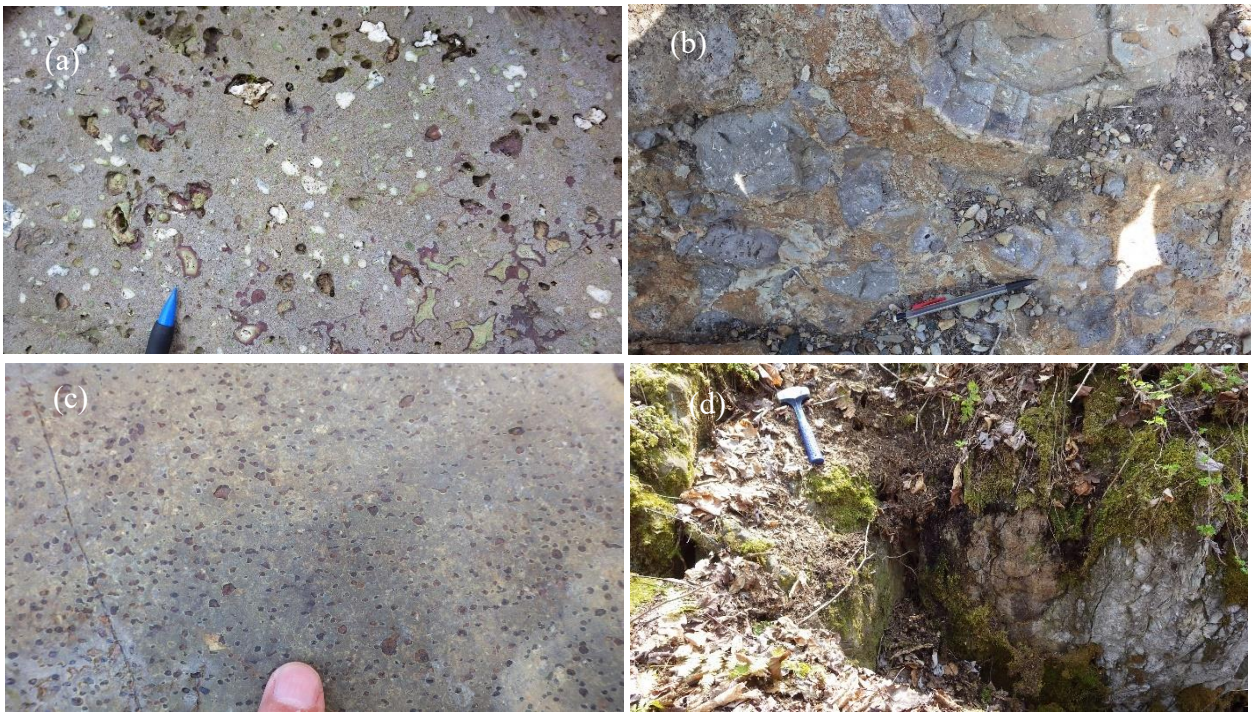

Figure 27. Spider Lake Formation. (a) The characterizing vesicular/amygdaloidal textures with large vesicles and amygdales. (b) Agglomerate of phyric and vesicular basalt. (c) Peperite. (d) Fault contact between the Spider Lake basalt (left side) and the Seboomook fossiliferous limestone sliver (right); viewer facing south; the fault slickenside dips toward northwest.

Twelve basalt samples plot mostly in andesite/basalt field and in the calc-alkaline series domain (Fig. 28a, b). The MORB-normalized spider and chondrite-normalized REE distribution patterns show considerably depleted Ta and Nb and enriched LILE, as well as higher LREE than HREE (Fig. 28c, d), which is typical of oceanic crust subduction in an active arc setting. The tectonic discrimination diagrams clearly demonstrate “volcanic arc array” and “continental arcs” settings (Fig. 28e, f).

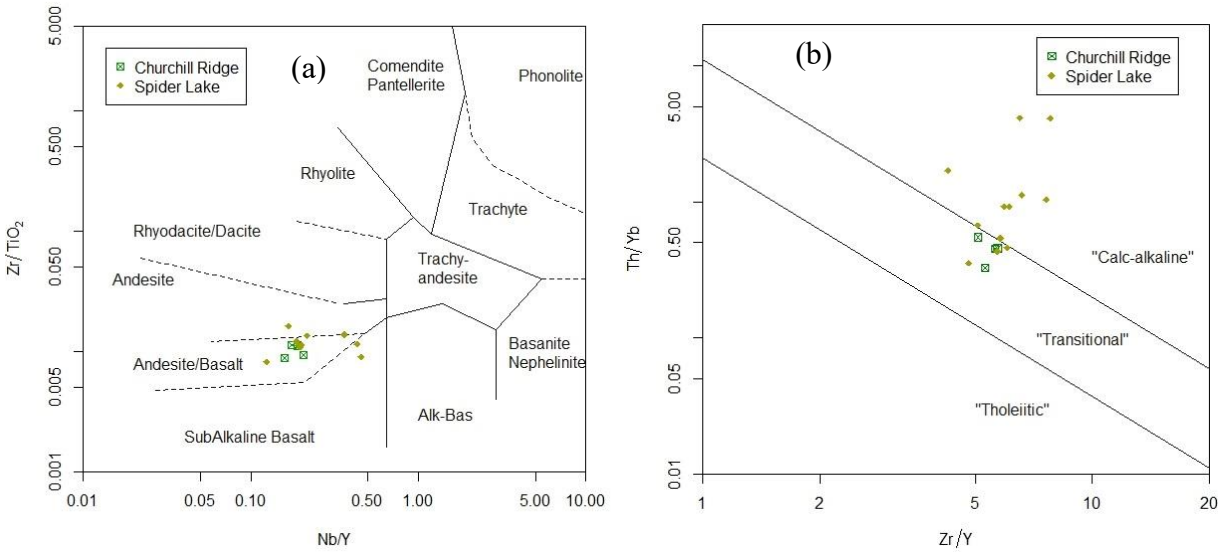

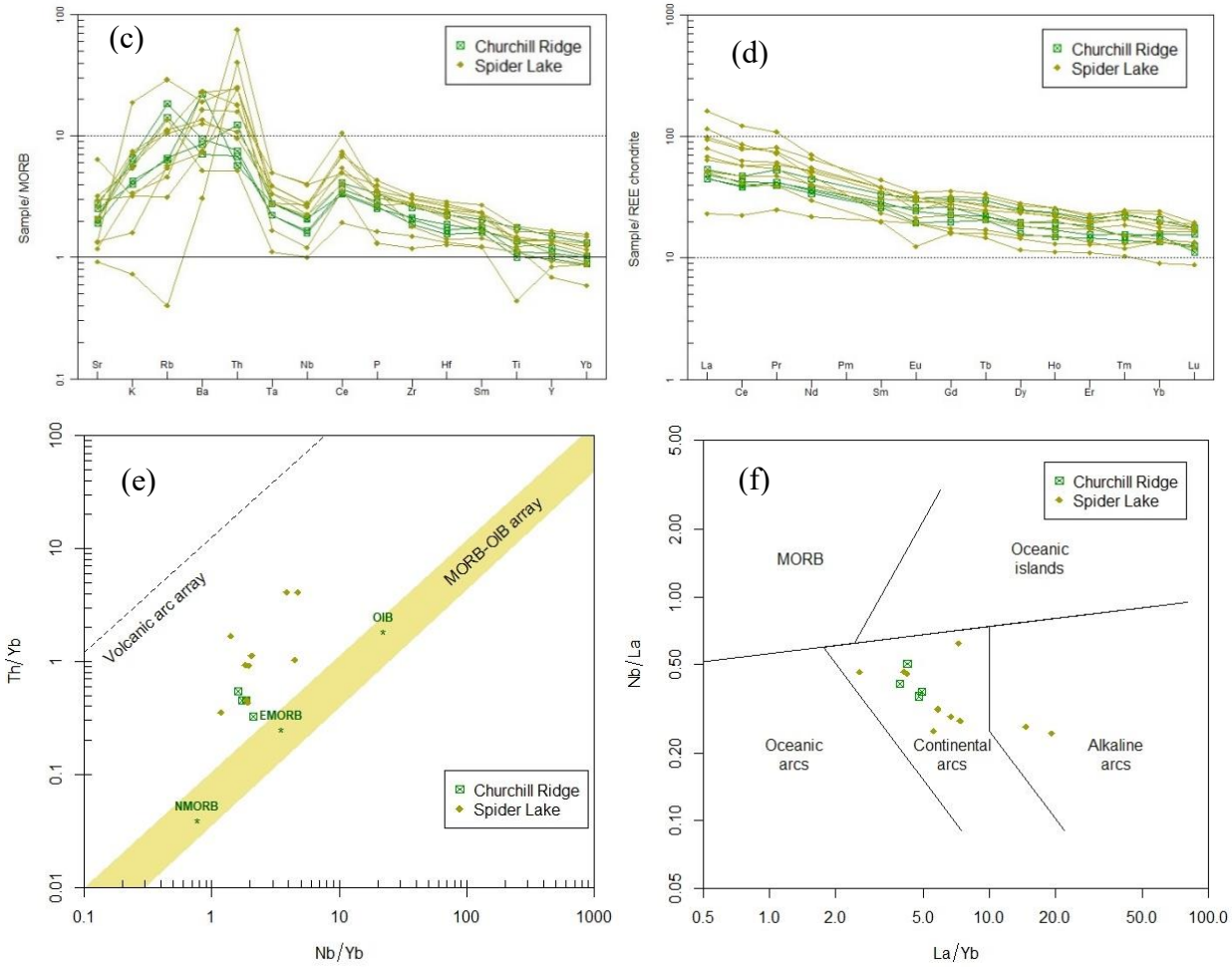

Figure 28. Geochemistry and tectonic discrimination of the Spider Lake and Churchill Ridge formations. (a) Classification; (b) Zr/Y vs. Th/Yb diagram (Ross and Bedard, 2009); (c) MORB-normalized spider diagram (Pearce, 1983); (d) Chondrite-normalized REE pattern (Nakamura, 1974); (e) Nb/Yb vs. Th/Yb discrimination diagram (Pearce, 2008); (f) La/Yb vs. Nb/La discrimination diagram (Hollocher et al. 2012).

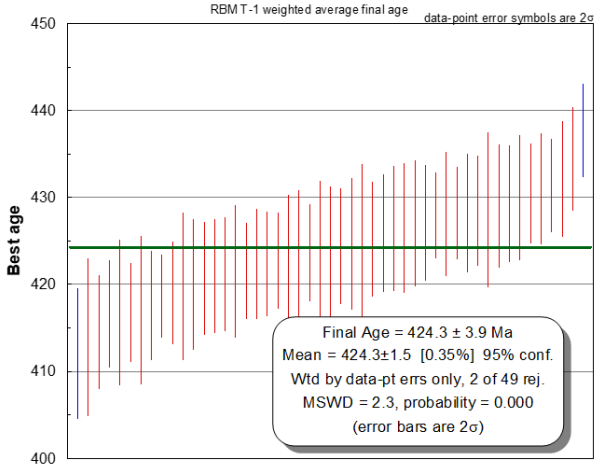

Figure 29. Zircon U-Pb dating of a tuff sample for the Spider Lake Formation.

Some brachiopod fossils have been found in a layer of volcaniclastic rocks (tuffaceous sandstone) sandwiched in basalt, on the south side of Fifth Musquacook Lake and the fossils indicate Silurian age (Hall, 1970; Pollock, 2023). Two samples of pyroclastic rocks were collected from the Spider Lake Formation at Rocky Brook Mountains for

zircon U-Pb dating at ALC. The dating yielded two similar ages: 424.3 ± 1.5 Ma and 427.0 ± 2.4 Ma, confirming that the Spider Lake Formation is Silurian Ludlow age (Fig. 29). With the volcanic rocks of the formation erupted in an active arc subduction setting based on their geochemistry, it is concluded that the Spider Lake Formation was resulted from subduction during the Silurian Ludlow time, and it was likely related to the Salinic Brunswick Subduction (van Staal, 1994).

Churchill Ridge Formation: The volcanic and subvolcanic rocks west-northwest of the Spider Lake Formation are shown as Devonian-Silurian or Devonian-Ordovician "un-differentiated" formations in Hall (1970) and Maine state (Osberg et al., 1985) geologic maps. Recent mapping demonstrates that these volcanic rocks are composed of basalt, pyroclastic and volcaniclastic rocks of volcanic breccia, lapillistone, tuff, tuffaceous "conglomerate", and tuffite (Fig. 30a), and rhyolite, with minor diabase sills and dikes. The basalt is generally either featureless or vesicular and amygdaloidal with vesicles generally smaller than that of the Spider Lake Formation basalt. Only a few outcrops show pillow basalt. Rhyolite flow layers can be as thick as 400 meters as the one along Harrow Mountain, referred to "Harrow Mountain rhyolite". The rhyolite is generally red or maroon in color and porphyritic with euhedral-subhedral potassium feldspar and anhedral quartz phenocrysts. Locally the rhyolite contains fiamme (Fig. 30b) that are likely pumice fragments but later devitrified. Rhyolite layers are characterized by well-developed flow bands (Fig. 30c). Pyroclastics rocks include volcanic breccia, lapillistone, and tuff/cherty tuff, and some intercalated volcaniclastic rocks, for example, tuffite and tuffaceous "conglomerate" that have more sedimentary features. Fragments or blocks are dominantly gray and dark gray cherty tuff. Some intercalated tuffaceous conglomerate contains rounded or near-rounded pebbles or granules of gray and dark gray cherty fine tuff (Fig. 30d). The thickest layer of pyroclastic rocks occurs along the entire length of the west-east-trending Churchill Ridge – it is 1400–1600 m thick and at least 7 km long. The pyroclastic and volcaniclastic rock beds strike 210º–270º and dip north-northwest at a dip angle of 54º–80º. All of them are foliated with the foliation generally striking at 230–270º, which is more westerly than the regional northeast- or southwest-striking foliation, indicating considerable rotation of the fault block as a result of probably large-scale transpressional faulting. These volcanic and subvolcanic rocks are compositionally and structurally distinct from the Spider Lake Formation and are newly named as Churchill Ridge Formation (Wang, 2023b).

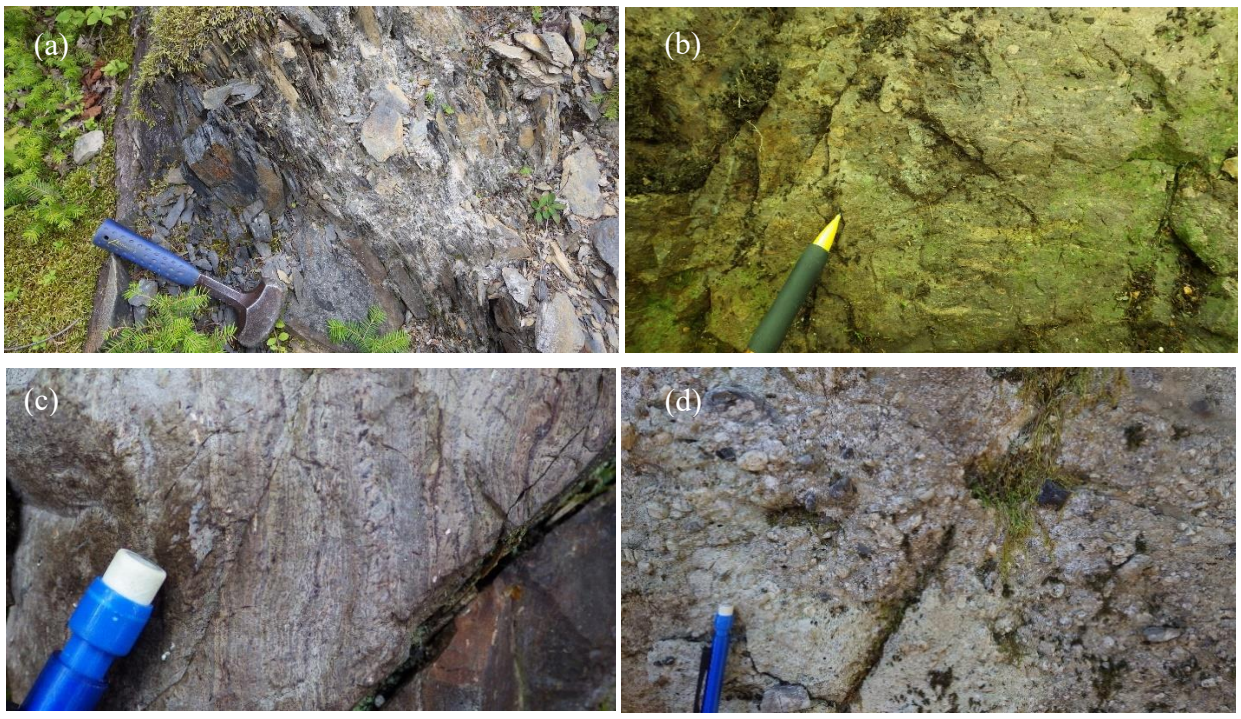

Figure 30. Churchill Ridge Formation. (a) Tuffite. (b) fiamme in rhyolite. (c) Flow bands in rhyolite. (d) Tuffaceous conglomerate.

Four basalt samples show that the basalt is transitional (Fig. 28b). The MORB-normalized spider and chondrite-normalized REE distribution patterns show considerably depleted Ta and Nb and enriched LILE, as well as higher

LREE than HREE (Fig. 28b, c), which is typical for oceanic crust subduction in an active arc setting. The tectonic discrimination diagrams clearly demonstrate "volcanic arc array" and "continental arcs" settings (Fig. 28c, d).

A rhyolite sample collected from the "Harrow Mountain rhyolite" was recently dated at ALC by using zircon U-Pb ICP-MS method. The dating gave a weighted mean age of 425.1 ± 8.6 Ma and a concordia age of 424.9 ± 4.5 Ma (Fig. 31). The whole-rock geochemical data and the U-Pb age indicate an active subduction and volcanic arc during the Silurian Ludlow time, which was likely related to the Salinic Brunswick Subduction (van Staal, 1994).

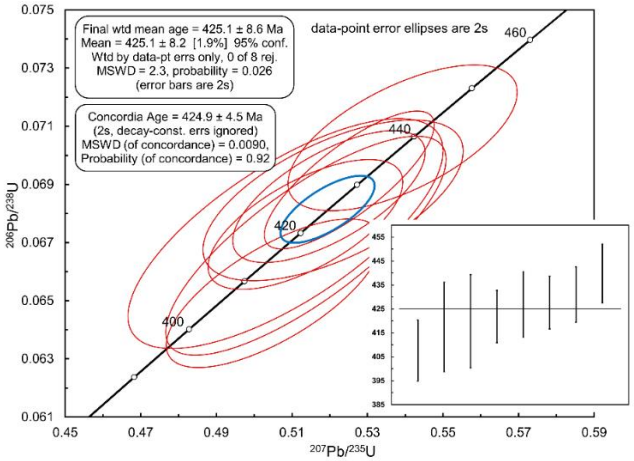

Figure 31. Zircon U-Pb concordia and weighted mean ages of the Churchill Ridge Formation.

The Related Devonian Formations

Seboomook Group: The Seboomook Group (Pollock, 1987) or initially Seboomook Slate (Perkins, 1925) in northern Maine is lithologically divided into four conformable units, from bottom to top: the basal conglomerate, fossiliferous limestone and calcareous sandstone, maroon slate, and turbiditic sandstone and slate units, with the last one dominating the group (Wang, 2019, 2021a, 2021b, 2022). Pollock (2023) recently proposed a separate unit of the slate, Musquacook Slate in the Musquacook lakes area. The lower three units are informally referred to as "Trinity". They had never been considered as part of the Seboomook Group prior to this study. The basal conglomerate unconformably overlies the Ordovician volcanic rocks and Chase Brook mélange along the Munsungun-Winterville belt (Fig. 32a); it is generally massive, matrix-supported, poorly sorted, and polymictic with clasts derived mostly from igneous and pyroclastic rocks found within the Munsungun and Winterville inliers, such as basalt, diabase, and gabbro, but predominantly gray tuff. The conglomerate is characterized by distinctive red, purplish red, and bright green tuff and red jasper pebbles (Fig. 32b). The fossiliferous limestone and calcareous sandstone unit is made of shelf-reef limestone and argillaceous limestone (Fig. 32c, d), and near-shore calcareous sandstone, siltstone, and mudstone of varying thickness. The medium-thin layers of the limestone and argillaceous limestone may occur as discontinuous but still layered and trackable boudins or lenses (so-called "limestone breccia"; Fig. 32e) that were probably caused by diagenetic solution and compaction. They contain abundant marine invertebrate fossils, including fragments of crinoid stems of at least three species, stromatoporoids, corals (e.g., *Favosites helderbergiae, Thamnopora sp., and Streptelasma sp.*), brachiopods (e.g., *Leptaena rhomboidalis, Strophonella sp., Howellella sp., Meristella sp., Acrospirifer sp., Atrypa sp., Athyris sp.*), bryozoans (e.g., *Fenestella sp*. and *Rhombopora Sp*.), and stromatolite. Small reef mounds made of mostly stromatoporoids, thamnopora, and favosites are common (Fig. 32c, d). Fossils indicate Helderberg fauna of the Early Devonian Lochkovian age. The maroon slate/siltstone unit is composed of argillaceous and micaceous slate, silty slate, siltstone, and minor sandstone, and characterized by distinctive maroon or bright red color due to the abundance of iron oxides hematite (Fig. 32f).

The Seboomook Group is pervasively cleaved by the regional, prevailing, Acadian foliation that strikes 225° (locally 045°; average) at 75° – 85°. It unconformably overlies the Munsungun and Winterville inliers. However, its unconformable contact with the Munsungun and Winterville inliers along their west flanks is significantly displaced by imbricate southwest-striking (west-northwest dipping), southeast-directed reverse faults, producing multiple, stacked fault blocks and slivers that can be composed of both Seboomook Group sedimentary rocks (mostly the "Trinity" or part of the "Trinity") and volcanic rocks. Similarly, the East Branch area has been also significantly displaced horizontally and vertically by multiple southwest- and west-striking reverse-thrust faults, producing a number of small-size Ordovician inliers that are made of the East Branch-type volcanic rocks and the Chase Brook mélange (Figs. 1 and 2).

Figure 32. The "Trinity" of the Seboomook Group: (a) The basal conglomerate and its unconformity with the basalt of the Munsungun Lake Formation. Amber Whittaker, Bob Marvinney, and Lauren Madsen. (b) The basal conglomerate characterized by red tuff pebbles. (c) Reef limestone composed of stromatoporoids (dominant) and thamnopora. (d) Reef limestone composed of thamnopora (dominant) and stromatoporoids. (e) "Limestone breccia" with breccias mostly eroded, leaving holes. Dave Putnam. (f) Maroon slate/siltstone.

FAULTS AND THE IMBRICATE FAULT SYSTEM

Northern Maine has experienced significant faulting with considerable vertical and horizontal displacement. Majority of the faults strike southwest or northeast and are reverse or reverse-thrust faults, showing as longitudinal faults parallel to the regional lithological and structural trends, with some striking southeast or northwest as transverse faults perpendicular to the regional lithological and structural trends. Due to northwest-southeast-directed compression and shortening (present coordinates), the southwest-striking (northwest-dipping) longitudinal faults have produced stacked, domino-style imbricate fault system with a large number of fault slivers or blocks. Most of them show southeast-oriented sense of faulting. The imbricate fault pattern and the fault sliver/block system constitute the structural framework of the region, making northern Maine structurally complicated and unique.

Several faults are pre-Acadian, likely Salinic, because they don't extend into Devonian Seboomook Group sedimentary rocks instead are truncated by the group. They occur in the pre-Devonian rocks. Most of them are small size, with only a couple to be long and regional, for example, the northeast-striking Round Mountain and Blind Brook reverse-thrust fault that show substantial displacement and that mark major structural boundaries.

Most of the faults are Acadian and post-Acadian (likely Neoacadian) because they have displaced the Devonian formations. Majority of them are indeed post-Acadian (Neoacadian) because they have displaced the Devonian Pragian and Emsian formations, the Scopan Lake (Pragian) and St. Froid Lake (Emsian) formations.

Structurally, the Munsungun inlier is dominated by this imbricate and stacked fault system, with significantly long fault blocks and slivers – the longest sliver stretches up to 70 kilometers. The multiple smaller inliers in the headwaters of the East Branch Penobscot River and Aroostook River, on the north-northeast side of the Baxter State Park, are the inliers probably displaced/detached from the Munsungun inlier.

All the Ordovician, Silurian, and Devonian formations in the region have been significantly faulted and displaced, causing the Acadian-Neoacadian fault system and producing fault blocks and slivers of various sizes and lengths. A fault block or sliver can be composed of any of the formations, including the oldest Chase Brook mélange and the youngest Emsian St. Froid Lake Formation red and green beds. In the Munsungun inlier, commonly, a fault block/sliver can be simply only Seboomook Group sedimentary rocks, or only Chase Brook mélange, or only Ordovician or Silurian volcanic-subvolcanic rocks, or a combination of any of the formations.

Because the "Trinity" (the basal conglomerate, fossiliferous limestone and calcareous sandstone, and maroon/red slate/siltstone) of the Lower Devonian Seboomook Group is the bottom succession of the group and directly unconformably overlies the older formations (Chase Brook mélange and Ordovician and Silurian volcanic-subvolcanic and sedimentary rocks) of the inlier, the fault slivers with Seboomook Group generally show either the entire Trinity or part of the Trinity. Only one sliver, the sliver sandwiched by Peaked Mountain fault and Cliff Lake fault, is composed dominantly of the slate and sandstone unit of the Seboomook Group.

We will visit two borrow pits for fault slivers and faults.

ACKNOWLEDGEMENTS

The Munsungun-Winterville mapping project has been funded by the USGS STATEMAP Program and Maine Geological Survey since 2016. Before Dr. Robert Marvinney retired from the State Geologist position in 2021, he was the coordinator for the project. He not only has played a critical leadership role but also has been very involved in the project by running trips and editing maps and reports each year. Bob keeps advising the project after retirement. Amber Whittaker has been cartographer and editor of our maps and reports. From 2021 Amber becomes the coordinator and oversees the project. David Putnam has provided Wang years of mentorship and field assistance in the woods. The early trips to the North Maine Woods led by Amanda Barker during 2013–2015 resulted in the decision made by the Maine Geological Survey to launch bedrock geology mapping project in North Maine Woods. Dr. Gary Boone provided constructive discussions and suggestions over the years. Dr. Christopher McFarlane helps zircon U-Pb ICP-MS geochronology. Dr. Henry Williams helps with the identification of graptolites fossils. Drs. Carleton Brett and Alex Bartholamew help with the identification of marine invertebrate fossils. Field assistants to Wang include Ethan Albair (2023), Preston Bass (2022), Liam Daniels (2022), Miranda Washinawatok (2021), Jesse Federico (2021), Eric Bagley (2020), Adam Weyeneth (2019), Dylan Damboise (2018), Caleb Ward (2016, 2017, 2018), and Daniel Swallow (2016). Field assistants to Pollock include Dinyi Jian (2016), Tyler Pollock (2017), Chandler Harris (2018), and Jeremy Braun (2019). Access and permissions granted by North Maine Woods, Clayton Lake Woodlands Holdings, LandVest, Irving Woodlands, Seven Islands Land Company, Huber Resources, and Prentiss & Carlisle are much appreciated.

ROAD LOG

Assembly time and location: Meet at the parking lot next to the soccer field/tennis court on UMPI campus. The departure time is 7:00 am ET. Other people may meet the group at Ashland One Stop at 7:30 am ET. Regular cars without sturdy tires are not recommended for the trip. Car-pooling is encouraged and appreciated. Bring whatever you plan to eat or drink. Wear warm clothes. Wear oranges if possible. Most stops are next to roads with only a couple require very short and light hiking. While driving in the woods, pay attention to logging trucks. They have absolute right of way.

Cumulative milage	**Description**
0.0	Start logging from UMPI south entrance; make left turn to Main St (Rte-1).
0.7	Left turn to State St. after two traffic lights.
0.9	Left turn to Rte-163 toward Mapleton/Ashland at the five-street intersection. Keep on Rte-163.
21.1	Stop by Ashland One Stop parking lot to pick up more people. 10 minutes for gas, coffee, restroom, etc.

Turn either left or right onto Rte-11 northbound.

21.4 Left turn and continue on Rte-11.
22.2 Left turn to Garfield Rd after passing the bridge.
22.8 Right turn to American Realty Rd. In a second it changes to dirt load. It is a major logging road in the woods.
27.8 ***Six-mile gate***. Slow down, stop, and say hi to the gate staff. You are now in the North Maine Woods. Take Pinkham Rd on the left at the fork.
36.2 Right turn to Jack Mountain Rd after passing Machias River bridge.
39.7 Bear left and take left turn.
40.2 Right turn to another logging road.
41.4 Stop at the ledge located on the left side of the road for Stop 1.

Stop 1. Volcanic breccia with jasper blocks of the Munsungun Lake Formation: This big ledge shows an excellent volcanic breccia with large blocks of beautiful red jasper (Fig. 33). The jasper is a chalcedony rich in red hematite. This jasper volcanic breccia is probably the only best one in the world. The matrix is composed mainly of pumice and quartz fragments. Similar red jasper volcanic breccia has been mapped at a number of places in the Munsungun Lake Formation. In the Munsungun inlier, in particular in the Munsungun Lake Formation, the jasper itself is commonly seen as red jasper chalcedony veins in basalt.

This red jasper volcanic breccia occurs within the andesite of the Jack Mountain dacite-andesite suite as a fault sliver along the South Branch Machias River Fault. The andesite crops out on the north side of the logging road; it is generally dark gray to greenish gray, massive and layer-less, and porphyritic or hyalopilitic with mainly euhedral or subhedral plagioclase feldspar and minor quartz phenocrysts.

No hammer on the jasper and no collecting please. Leave it like it is.

Figure 33. The red jasper volcanic breccia ledge at Stop 1. Caleb Ward (field assistant during 2015–2018) is peeling for a larger exposure on August 10, 2017.

Turn around to return to Jack Mountain Rd.

42.6 Left turn at the end of the road.
43.1 Left turn to Jack Mountain Rd at the end of the road. Keep on Jack Mountain Rd for the next 13 miles.
56.0 Left turn to Island Pond Rd at the fork.
57.2 Stop by a huge conglomerate ledge on the right side of the road.

Stop 2. Rowe Lake conglomerate: (504272, 5151938) This huge ledge shows the typical pebble conglomerate of the Upper Ordovician Rowe Lake Formation (Figs. 34 and 36). The conglomerate is clast-supported but the least polymictic and it is composed mainly of clasts of light gray tuff and dark gray tuff pebbles. Interestingly it does not contain pebbles of red or green fine tuff, indicating that it was likely sourced from the early Late Ordovician Ragged Mountain and Ingalls Brook Road formations because both formations don't contain red or green tuff (whereas red tuff is common in the Munsungun Lake Formation although green tuff is less common). Detrital zircon geochronological analysis of the Rowe Lake Formation showed a typical Laurentia zircon age spectrum.

Figure 34. The Rowe Lake pebble conglomerate ledge at Stop 2. Viewer facing south.

Continue on Island Pond Rd.

59.8 Park on the right side by the borrow pit.

Stop 3. Rowe Lake upper slate: (501209, 5148959) This pit shows the typical upper slate of the Rowe Lake Formation (Fig. 35) and is used as a type locality of the upper slate. It is near entirely a black or dark gray, lithologically homogenous, and non-pyritic slate and argillite, with minor interbedded sandstone, siltstone, and rarely intercalated conglomerate. It is characterized by repeating thin (0.3 – 2 cm) layers of brown siltstone in 5 – 15 cm intervals (Fig. 35b). Rowe Lake Formation (the conglomerate and upper slate) occurs as a fault sliver in this area (Fig. 36)

Figure 35. Stop 3 in a pit by Island Pond Rd with the upper slate of the Rowe Lake Formation.

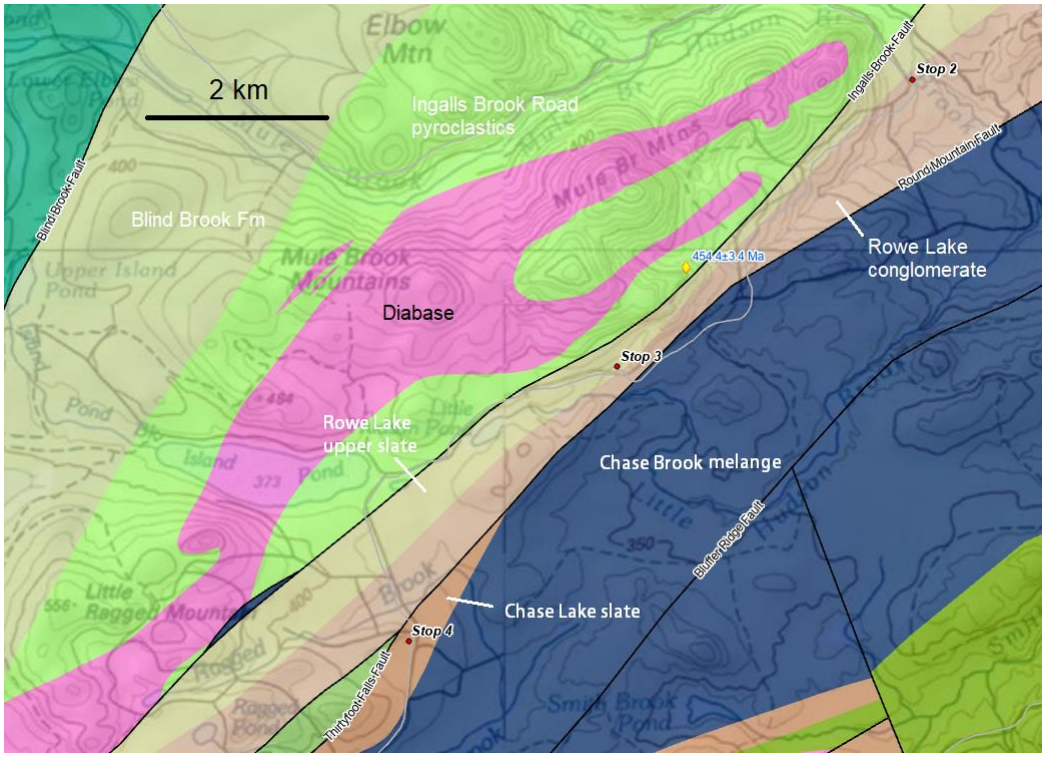

Figure 36. Geology map of the Mule Brook Mtn area.

Continue on Island Pond Rd.

61.6 Bear left and at the "end" of the road, make a left turn on to the road that is also Island Pond Rd.

62.8 Stop and park by a borrow pit on the right side of the road.

Stop 4. Chase Lake Formation slate: (499042, 5146120) This pit shows typical Chase Lake Formation (Figs. 36, 37). A major diagnostic feature of the Chase Lake Formation is the very poorly sorted conglomerate with predominantly irregularly shaped sandstone and siltstone clasts/chips and the dark or black coarse lithic sandstone. Another distinctive diagnostic feature is the cleaved rhythmically interbedded thin (2 mm – 10 cm) pyritic siltstone

(weathered to be tan rusty) and dark gray or black argillite throughout the formation. Parallel and graded bedding is common.

Figure 37. Slate of the Chase Lake Formation at Stop 4.

Continue on Island Pond Rd.

65.4 Right turn to Pell & Pell Road (also called Pelletier Rd). It is a major logging road.
71.5 Left turn to 522 Road at the fork (We are not going to Churchill Dam) It is another major logging road.
72.6 Right turn to Cliff Lake Rd, an old logging road.
75.3 Right turn to a logging road.
75.5 Stop and park in a turnaround area for Stop 5.

Stop 5. Fault sliver of Seboomook fossiliferous limestone and calcareous sandstone: (486214, 5142057) Here is one of the largest (with largest width and length) fault slivers (see Fig. 40) made entirely of sedimentary rocks of the Seboomook Group within the Leadbetter Pond fault (Wang, 2023b), in Spider Lake Formation. The sedimentary rocks of this sliver are mostly fossiliferous limestone with minor calcareous sandstone. The limestone is composed predominantly of stromatoporoids (a type of sea sponge; Fig. 38a) and thamnopora corals with minor favosites. Stromatoporoids were the most important reef builders in the Ordovician oceans. This site also shows the "limestone breccia" with the breccias/chunks being made of small fragments of shells and bones of marine invertebrate fossils such as crinoids. A red jasper vein (hematitic chalcedony) crosscuts the limestone on one of the ledges at this site (Fig. 38b).

Figure 38. Reef limestone at Stop 6. (a) Stromatoporoids. (b) Red jasper (hematitic chalcedony) vein in the limestone.

Turn around and go back to Cliff Lake Rd.

75.7 Left turn to Cliff Lake Rd eastbound.
78.4 Right turn to 522 Rd southbound.
79.9 left turn to a side logging road.
80.1 Stop for the pillow basalt ledge on the right side of the road.

Stop 6. Pillow basalt of the Bluffer Pond Formation: (489225, 5137796) The Bluffer Pond Formation is dominated by pillow basalt (Fig. 39). This site is not the best site for pillow basalt but still very good; it is close to the main road. Pillow basalt is known as mafic lava flows forming in subaqueous environment, in particular when eruption rate is low. The outer surface of a lava lobe would be quenched rapidly by water, but it is still fluidly inside the lobe and the

lobe continues to inflate as lava continues to supply so that it forms a bulging, pillow-like lobe. The lobe then breaks off and new pillow-like lobes keep forming as the flow advances. Pillows commonly have a spherical or bulbous shape, generally show convex (rounded) upper surface and a keel wedge projecting downward. The convex up surface and the keel wedge help tell the top or bottom of a pillow. What is the top of the pillows at this stop? A pillow generally also has a chill margin and radial vesicles.

Figure 39. Pillow basalt of the Bluffer Pond Formation at Stop 6.

Turn around and go back to 522 Rd.

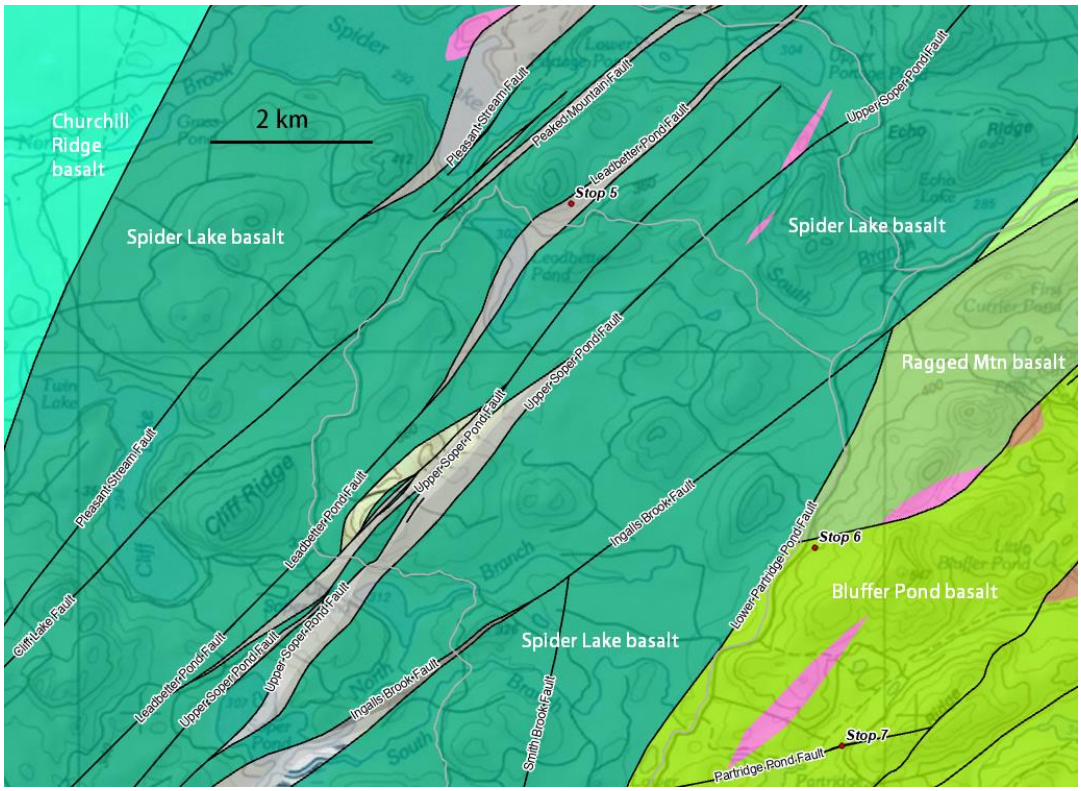

Figure 40. Geologic map of the Spider Lake and Bluffer Pond area showing multiple fault slivers of sedimentary rocks of the Seboomook Group (in light gray colors).

80.2 Left turn back to 522 Rd southbound.
81.6 Left turn to another old logging road toward Bluffer Pond. Bear right! Don't make any left turns!
84.7 Stop by an abandoned pit located on the left side of the road.

Stop 7. Fault and graptolitic slate fault sliver of Blind Brook Formation: (589570, 5135342) This pit shows excellent exposure of a large fault in Bluffer Pond Formation and a fault sliver within the fault (see Fig. 40 for location). The sliver is rusty, black graphitic and graptolitic slate and thin graywacke sandstone of the Blind Brook Formation

(Fig. 41a). The slate contains graptolite fossils, although there are not many at this site but you may find one. On the left side (northwest side) of the rusty slate is fault breccia with large fragments of vesicular basalt and even limestone. A cave is developed within a huge calcite vein in the fault. The fault strikes northeast and dips southeast with a steep dip angle (Fig. 41b). The hanging wall is diabase.

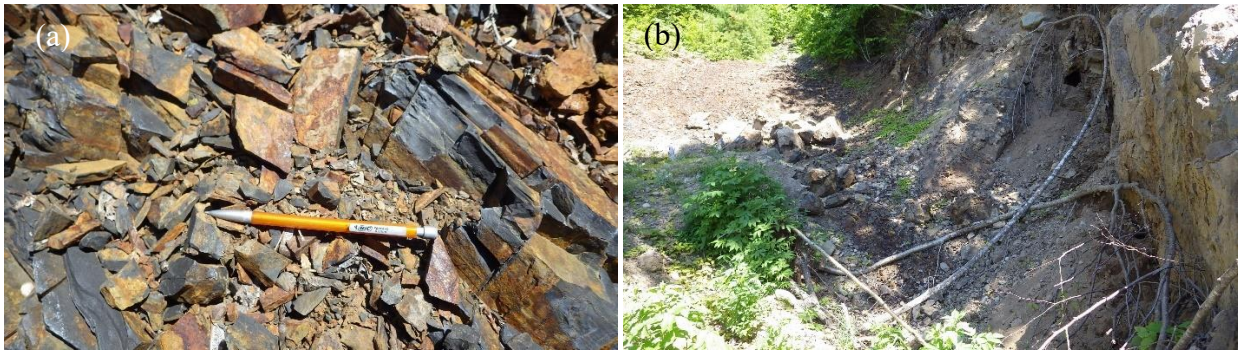

Figure 41. Fault and fault sliver of the Blind Brook graptolitc and graphitic slate (a) at Stop 7. Viewer facing northwest. The fault slickenside dips toward southeast (b). A cave is developed within a huge calcite vein in the fault (b). Viewer facing north.

Turn around back to 522 Rd.

87.7 Left turn to 522 Rd southbound.
91.7 Right turn to Cliff Lake Rd at the fork.
91.9 Stop and park next to the pit located on the left side of the road.

Stop 8. Maroon/red slate/siltstone/sandstone sliver (of the Seboomook Group): (484765, 5131945) This borrow pit shows a maroon/red micaceous slate/siltstone (with minor sandstone and granule conglomerate) fault sliver (Fig. 42a) and the fault contact between the sliver and vesicular basalt (Fig. 42b) of the Spider Lake Formation. The red/maroon slate/siltstone is one of the "Trinity" of the Seboomook Group. The fault contact strike 195º and dips toward northwest at a dip angle of 63º. The beds of the maroon/red slate/sandstone strike 215º and dip toward northwest at a dip angle of 25º. Red tuff of the Munsungun Lake Formation may look similar to the maroon/red slate/siltstone but the difference is the red tuff contains no mica flakes (i.e., muscovite) or a very few mica whereas the maroon/red slate/siltstone is rich in mica flakes. See Figure 44 for location.

Figure 42. The borrow pit at Stop 8 showing maroon/red slate/siltstone (a) and fault contact with vesicular basalt of the Spider Lake Formation (b).

Turn around back to 522 Rd.

92.1 Right turn to 522 Rd south bound. Passing Connector Rd.
96.8 Left turn to Pinkham Rd at the T junction (Continuation of 522 Rd is Telos Rd that leads to Golden Rd).
98.6 Right turn to Popple Rd, another logging road.
99.4 Left turn to Carpenter Rd, another logging road.
100.1 Stop and park by the pit located on the right side of the road.

Stop 9. Fault and fault sliver of Chase Brook mélange: (489626, 5124261) This big borrow pit shows another fault and fault sliver (Fig. 43). The fault strikes southwest-west and dips north-northwest. The footwall is the basal conglomerate of the Lower Devonian Seboomook Group and the hanging wall is the Chase Brook mélange (but only at around this pit; along the fault the hanging wall is mostly the Munsungun Lake Formation volcanic rocks). The Chase Brook mélange actually occurs as a narrow fault sliver within the fault, similar to several other faults in other places in the Munsungun region where the mélange also occurs as fault slivers. See Figure 44 for location.

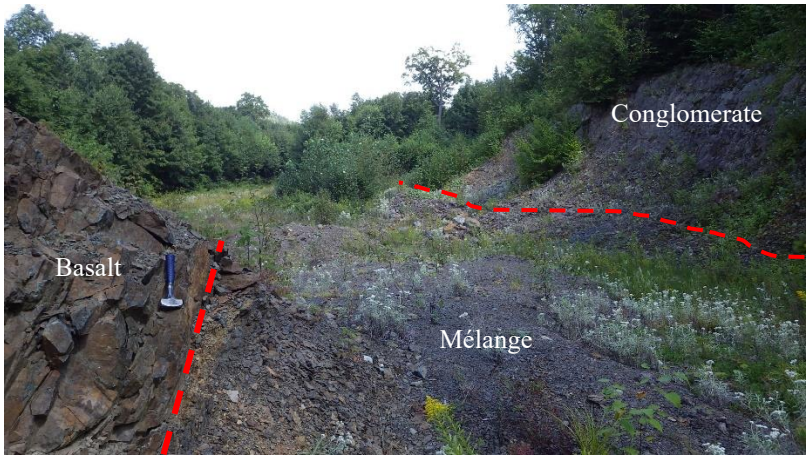

Figure 43. The fault and fault sliver at Stop 9. Viewer facing east. Chase Brook mélange occurs as a narrow fault sliver sandwiched by basalt of the Munsungun Lake Formation (left or north-northwest side, hanging wall) and basal conglomerate of the Seboomook Group (right or south side, footwall). Red dash lines show fault contacts.

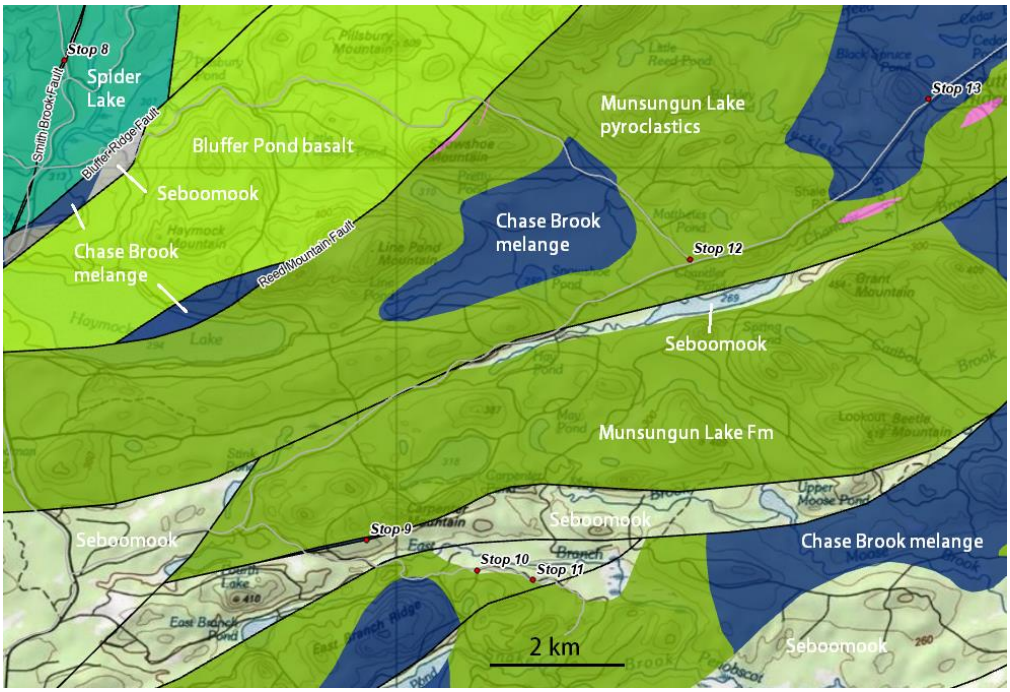

Figure 44. Geologic map of Haymond Lake and Beetle Mtn area showing faults, fault slivers, and stops.

Turn around back to Popple Rd.

100.7 Left turn to Popple Rd eastbound.
102.8 Stop by a small pit on the right side of the road for fossils.

Stop 10: Fossiliferous limestone and calcareous sandstone: (491392, 5123776) This small pit shows one of the "Trinity", the fossiliferous limestone and calcareous sandstone of the Seboomook Group (Fig. 45). This unit is rich in

marine invertebrate fossils of brachiopods, corals (thamnopora, favosites, rugosa, etc.), sponges, crinoids, etc., of the Early Devonian Helderberg fauna. The pit also shows the "limestone breccia" (Fig. 32e) that is a common feature of the unit throughout northern Maine. See Figure 44 for location.

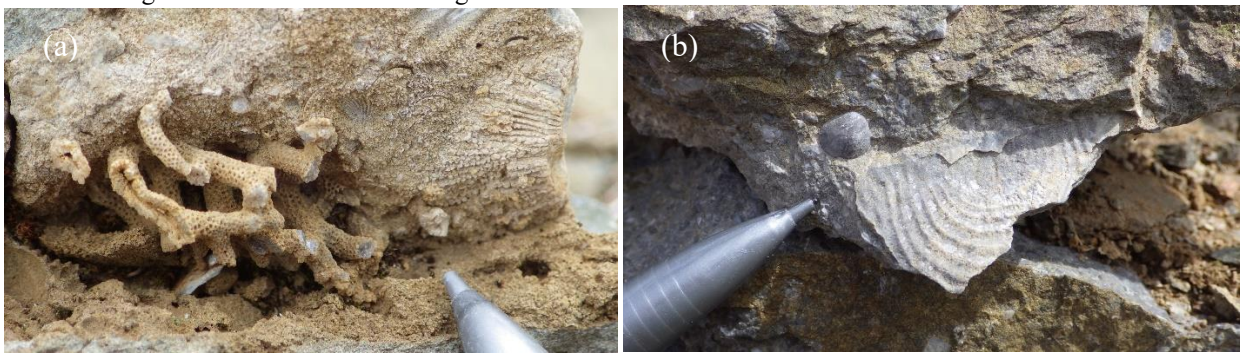

Figure 45. Some of the fossils at Stop 10. (a) Favosites and bryozoan and (b) *Leptaena rhomboidalis* (the big one) and *Meristella* (the small one*).* Both are common brachiopods in the unit.

Continue on Popple Rd eastbound.

103.4 Stop by a ledge located on the right side of the road.

Stop 11. Unconformity between Seboomook and Munsungun Lake formations and the basal conglomerate: (492294, 5123614) This outcrop probably shows you the best unconformity outcrop in Maine (or at least one of the best)! Here the basal conglomerate of the Lower Seboomook Group unconformably overlies the vesicular basalt of the Munsungun Lake Formation (Fig.46) – this type of unconformity is called "non-conformity" - it develops where sediments are deposited on top of an eroded surface of igneous or metamorphic rocks. The immediate conclusion to be drawn from this unconformity is that the Early Devonian Seboomook actually began with transgression, not like what's thought in the past that the Seboomook was continuation of in a Silurian sea. This unconformity represents the very last stage of the Salinic orogeny that started from Silurian time. Recognition of the Seboomook unconformity rewrites the tectonic evolution history of Maine Northern Appalachians. See Figure 44 for location.

Figure 46. Dr. Bob Marvinney at the unconformity outcrop. Photo taken on October 23, 2020.

Turn around back to Pinkham Rd.

107.0 Right turn to Pinkham Rd northbound.

112.6 Stop at the Connector Rd intersection. Watch for logging trucks.

Stop 12. Munsungun red chert (radiolarian tuff): (494814, 5128751) This roadside outcrop (Figs. 44, 47) shows a red chert (Fig. 47a, b) of the Munsungun Lake Formation. Petrographic analysis shows it to be primarily fine tuff (Fig. 47c). Whole-rock geochemical analysis of a sample collected from this site and several other sites with similar chert appearance show their volcanogenic origin, as initially reported by Pollock (1987a). In other words, the chert was made predominantly of volcanic material like ash, being originally tuff (or tuffite). The tuff contains quartz spherules mostly less than ¼ mm in diameter (Fig. 47c, d). These spherules are interpreted to be radiolarians. Due to the old age of the formation and subsequent metamorphism, for example, the tuff was foliated during the Acadian orogeny (Fig. 47c), and hydrothermal alteration and silicification, original structures and morphology of the radiolarians could have been completely changed. The chert layers or lenses in the Munsungun Lake Formation, thick or thin, are all interbedded in volcanic-subvolcanic rocks and show gradational change to or from pyroclastic rocks of coarse tuff or volcanic breccia. The chert is not typical sedimentary radiolarian chert but radiolarian tuff or radiolarian-bearing tuff.

Investigations over the entire Munsungun inlier also reveal that all the high quality (meaning sharp and glassy) chert has experienced significant silicification as evidenced by stockwork of fine quartz veinlets as seen at this site (Fig. 47b) – mostly microscopic (Fig. 47d). The silicification has enhanced the hardness and sharpness of the chert. The quartz veins crosscut the spherules, which indicates that the silicification post-dated the formation of the spherules. The spherules are shortened and elongated if foliated (Fig. 47c), suggestive of their pre-deformation existence, which can be evident for the spherules to be originally radiolarians.

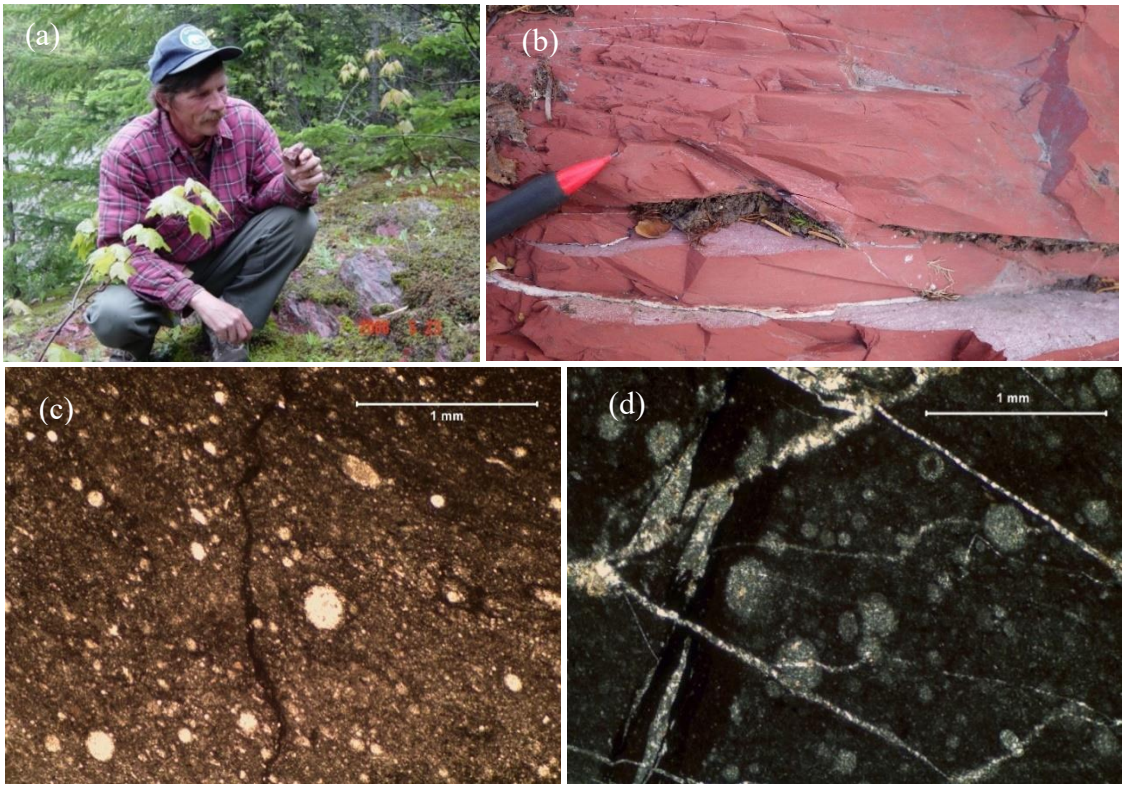

Figure 47. Red chert at Stop 12. (a) Dave Putnam at the site. Photo date May 23, 2006. (b) The red chert with fine quartz veinlets. (c) and (d) Photomicrographs of the red chert showing microscopic fragments of quartz and plagioclase and elongated quartz spherules due to foliation (c) and quartz veinlet stockwork crosscutting quartz spherules. Plane polarized light for (c) and cross polarized light for (d).

Continue on Pinkham Rd northbound.

115.7 Stop and park inside a large borrow pit located on the left side of the road.

Stop 13. Chase Brook mélange: (498643, 5131314) This huge pit shows the mélange of the Chase Brook Formation. The rusty pyritic olistostromal mélange contains blocks or intraclasts of mostly sandstone and limestone as seen in this pit (Fig. 48a). Some pyrite occurs as ball-shaped concretions (Fig. 48b). See Figure 44 for location.

Figure 48. Mélange of the Chase Brook Formation showing sandstone and limestone blocks (a) and pyrite balls/concretions (b) at Stop 13.

Continue on Pinkham Rd northbound.

132.2 Left turn on to a side logging road toward to a ledge.

132.5 Stop by the ledge located on the right side of the road.

Stop 14. Amanda's Ledge (Munsungun Lake Formation tuff): (520438, 5142868) This ledge is the well-known Amanda's Ledge in North Maine Woods. It took us two trips and the Maine Forest Service two full loads of water tank (fire truck) to clear up the originally much covered ledge. Amanda Barker was the forest ranger for the Maine Forest Service before 2017. She later became a science teacher at Ashland Community School. When she was a forest ranger, she would pay attention to new logging roads and new borrow pits for any interesting rocks or geology. She was curious. She would contact Dave Putnam and later me and took us to the woods to see her findings. This is how the Round Mountain archaeological site was discovered. The discovery of the Round Mountain archaeologic site led to a question about the source of the chert used to make the artifacts discovered at the site and vinity. State Geologist Dr. Bob Marvinney and State Archaeologist Dr. Art Spiess decided to fund Chunzeng Wang to investigate the Round Mountain ridge and Stephen Pollock to investigate the Mule Brook Mountains area in 2016. This is how we started mapping or remapping the Munsungun inlier. Amanda helped with our first attempt cleaning up the Ledge in fall 2015.

This ledge is made of tuff from the Munsungun Lake Formation. It shows lots of features that might be related to volcanic sedimentation, volcanic and seismic activities, rock deformation (or soft-rock deformation), even glaciers of the last ice age, etc. Feel free to explore and discuss.

Figure 49. (a) Amanda's Ledge seen from a drone – about 50 meters (~150 feet) high above the ground. (b) Forest Ranger Amand Barker in fall 2015. (c) Before we call it Amanda's Ledge.

Turn around and go back to Pinkham Rd.

132.8 Left turn to Pinkham Rd northbound.

153.0 ***The Six-mile gate***. Slow down, stop, and say hi to the gate staff. Bear right and turn right towards Ashland at the fork.

157.8 Bear left on Garfield Rd towards Ashland.

158.3 Right turn to Rte-11 toward the bridge and Ashland.

159.4 ***Ashland One Stop***. Left turn to Rte-163 towards Mapleton and Presque Isle.

179.5 Presque Isle.

End of road log

REFERENCES

Ayuso, R.A. and Schulz, K.J., 2003. Nd-Pb-Sr isotope geochemistry and origin of the Ordovician Bald Mountain and Mount Chase massive sulfide deposits, northern Maine. Economic Geology Monograph 11, p. 611–630.

Ayuso, R.A., Wooden, J.L., Foley, N.K., Slack, J.F., Sinha, A.K., and Persing, H., 2003. Pb isotope geochemistry and U–Pb zircon (SHRIMP–RG) ages of the Bald Mountain and Mount Chase massive sulfide deposits, northern Maine: Mantle and crustal contributions in the Ordovician. Economic Geology Monograph 11, p. 589–609.

Boone, G.M., 1958. The Geology of the Fish River Lake – Deboullie Area, Northern Maine: Ph.D. thesis, Yale University, 186 p.

Boone, G.M., 1970. The Fish River Lake Formation and its environments of deposition: in Shorter Contributions to Maine Geology: Maine Geological Survey, Bulletin 23, p. 27 – 41.

Cabanis, B. and Lecolle, M., 1989. Le diagramme La/10 – Y/15 – Nb/8: Un outil pour la discrimination des series volcaniques et en evidence des mélange et/ot de vontamination crustale. Comptes Rendus de l'Académie des Sciences, Série II, 309, p. 2023–2029.

Cummings, J.S., 1988. Geochemical detection of volcanogenic massive sulphides in humid-temperate terrain (using surficial methods): Bangor, Maine, J.S. Cummings, Inc., 298 p.

Busby, C.J., Kessel, L., Schulz, K.J., Foose, M.P., and Slack, J.F., 2003. Volcanic setting of the Ordovician Bald Mountain massive sulfide deposit, northern Maine. Economic Geology Monograph 11, p. 219–244.

Fitzgerald, J.P., 1991. Geochemistry of the Spider Lake and West Branch Penobscot volcanic suites, northern Maine: Tectonic implication from a complex petrogenesis: Boston, Massachusetts, Boston College, Master thesis, 254 p.

Gerbi, C., Johnson, S., Aleinikoff, J, Bedard, J.H., Dunning, G.R., and Fanning, C.M. 2006. Early Paleozoic development of the Maine-Quebec Boundary Mountains region. Canadian Journal of Earth Sciences, vol. 43, no. 3, pp. 367-389.

Hall, B., 1970. Stratigraphy of the southern end of the Munsungun anticlinorium, Maine. Maine Geological Survey Bulletin 22, 63 p.

Hollocher, K. E., 2012. Geochemistry of amphibolite-facies volcanics and gabbros of the Støren Nappe in extensions west and southwest of Trondheim, Western Gneiss Region, Norway: a key to correlations and paleotectonic settings. American Journal of Science*, 312.4*, p. 357–416.

Horodyski, R.J., 1968. Bedrock geology of portions of Fish River Lake, Winterville, Greenlaw, and Mooseleuk Lake quadrangles, Aroostook County, Maine. M.S. thesis, Cambridge, Massachusetts, Massachusetts Institute of Technology, 192 p.

Nakamura, N., 1974. Determination of REE, Ba, Mg, Na and K in carbonaceous and ordinary chondrites: Geochimica et Cosmochimica Acta, 38, p. 757–775.

Neuman, R.B. and Max, M.D., 1989. Penobscotian-Grampian-Finnmarkian orogenies of terrane linkages. Geological Society of America Special Paper 230, p. 31–42.

Osberg, P.H., Hussey, A.M., II, and Boone, G.M. (editors), 1985. Bedrock geologic map of Maine: Maine Geological Survey.

Pearce, J.A., 2008. Geochemical fingerprinting of oceanic basalts with applications to ophiolite classification and the search for Archean oceanic crust: Lithos 100, p.14–48

Pearce, J. A., 1983. Role of sub-continental lithosphere in magma genesis at destructive plate margins, in Continental Basalts and Mantle Xenoliths, edited by C. J. Hawkesworth and M. J. Norry, p. 230–249, Shiva, Nantwich, UK.

Perkins, E.H. and Smith, E.S.C., 1925. Contributions to the geology of Maine, No. 1: A geological section from the Kennebec River to Penobscot Bay: American Journal of Science, 5th series, v. 9, no. 51, p. 204–228.

Pollock, S.G., 2023. Bedrock Geology of the Fifth Musquacook Lake Quadrangle, Maine: Maine Geological Survey, Open-File Map, scale 1:24,000. (in press)

Pollock, S.G., 2020. Bedrock Geology of the Mooseleuk Mountain Quadrangle, Maine. Maine Geological Survey Open File Map 20–1.

Pollock, S.G., 2019. Bedrock Geology of the Mooseleuk Lake Quadrangle, Maine. Maine Geological Survey Open File Map 19–2.

Pollock, S.G., Hamilton, N.D., and Bonnichsen, R. 1999. Chert from the Munsungun Lake Formation (Maine) in Palaeoamerican archaeological sites in northeastern North America: Recognition of its occurrence and distribution: Journal of Archaeological Science, v. 26, p. 269–293.

Pollock, S.G., 1993. Terrane sutures in the Maine Appalachians, USA and adjacent areas. Geological Journal, v. 28, p. 45–68.

Pollock, S.G., 1987a. Chert Formation in an Ordovician Volcanic Arc. Journal of Sedimentary Petrology, 57, p. 75–87

Pollock, S.G., 1987b. The Lower Devonian slate problem of western and northern Maine revisited: Northeastern Geology, v. 9, no. 1, p. 37–50.

Ross, P.S. and Bédard, J.H., 2009. Magmatic Affinity of Modern and Ancient Subalkaline Volcanic Rocks Determined from Trace-Element Discriminant Diagrams: Canadian Journal of Earth Sciences, 46, p. 823-839.

Schulz, K. J. and Ayuso, R. A., 2003. Lithogeochemistry and paleotectonic setting of the Bald Mountain massive sulfide deposit, northern Maine. Economic Geology Monograph 11, p. 79–109.

Shah, A.K., 2022. Airborne magnetic and radiometric survey, Munsungun region in northern Maine, 2021: U.S. Geological Survey data release, https://doi.org/10.5066/P97VUIJS.

Slack, J.F., Foose, M.P., Flohr, M.J.K., Scully, M.V., and Belkin, H.E., 2003. Exhalative and subsea-floor replacement processes in the formation of Bald Mountain massive sulfide deposit, northern Maine. Economic Geology Monograph 11, p. 513–547.

Supkow, D.J., 1965. Stratigraphy and structure of the Spider Lake Formation, Churchill and Spider Lake quadrangles, Maine. M.S. thesis, Orono, University of Maine, 106 p.

Van Staal, C.R. and Barr, S.M. 2012. Lithospheric architecture and tectonic evolution of the Canadian Appalachians and associated Atlantic margin. Chapter 2 in Tectonic Styles in Canada: the LITHOPROBE Perspective. Edited by J.A. Percival, F.A. Cook, and R.M. Clowes. Geological Association of Canada, Special Paper 49, pp. 41–95.

Van Staal, C., 1994. Brunswick subduction complex in the Canadian Appalachians: Records of the Late Ordovician to Late Silurian collision between Laurentia and the Gander margin of Avalon. Tectonics, Vol. 13, Issue 4, p. 946–962.

Wang, C., 2023a. Bedrock Geology of the Northern Half of the Chase Lake Quadrangle, Maine: Maine Geological Survey, Geologic Map 23-19, scale 1:24,000.

Wang, C., 2023b. Bedrock Geology of the Northern Half of the Spider Lake Quadrangle, Maine: Maine Geological Survey, Geologic Map 23-18, scale 1:24,000.

Wang, C., 2022. Bedrock Geology of the Carr Pond Quadrangle, Maine: Maine Geological Survey, Open-File Map 22-6, scale 1:24,000.

Wang, C., 2021a. Bedrock geology of the Greenlaw Pond quadrangle, Maine. Maine Geological Survey Open-File No. 21-2.

Wang, C., 2021b. Bedrock Geology of the Big Machias Lake Quadrangle, Maine: Maine Geological Survey. Open-File Map 21-3, scale 1:24,000.

Wang, C., 2019. Bedrock geology of the Jack Mountain quadrangle, Maine. Maine Geological Survey Open-File No. 19–6.

Wang, C., 2018. Bedrock geology of the Round Mountain quadrangle, Maine. Maine Geological Survey. Open-File Map 18–8, scale 1:24,000.

ORDOVICIAN-AGED MINERALIZATION TYPES IN SOUTHWESTERN NEW BRUNSWICK

David R Lentz [1], Kathleen Thorne [2], Leslie Fyffe [3], James Walker[4], Fazilat Yousefi [1]

[1] Department of Earth Sciences, University of New Brunswick, Fredericton, NB E3B 5A3 Canada. dlentz@unb.ca
[2]Geological Surveys Branch, New Brunswick Department of Natural Resources and Energy Development, P.O. Box 6000, Fredericton, NB E3B 5H1 Canada
[3] Geological Consultant, former Director, New Brunswick Geological Surveys Branch, Fredericton, NB E3B 5H1, Canada
[4]Geological Surveys Branch, New Brunswick Department of Natural Resources and Energy Development, 2570 Route 180, Bathurst, NB E2A 7B8, Canada

This trip will examine the geologic context for various types and styles of Ordovician-aged mineralization associated with arcs and back arcs formed during the pre-Salinic orogeny subduction. The trip involves looking at roadside outcrops, as well as drill core of the various mineralized occurrences. These will include the unique vanadiferous slates of the Woodstock Group, Meductic volcanogenic massive sulfide occurrence (and other Cu-Zn-Pb massive sulfide drill cores from various parts of the famous Bathurst Mining Camp) of the Meductic Group, the subvolcanic porphyry and Gibson-related stock (Connell Mtn Cu-Mo-Au deposit; drill core) and the Sharp Mountain diatreme will be visited.

Assembly time and location: 9:30 am (Atlantic time, or 8:30 am Eastern time) at the Irving Oil (Gas station) in Meductic (45.994781, -67.487305). Use Exit 212 from the TransCanada Highway (#2). Americans going to the trip need to have their passport ready.

PART I
AN ANCIENT VOLCANIC ENVIRONMENT IN THE BENTON-MEDUCTIC AREA OF WEST-CENTRAL NEW BRUNSWICK

Les Fyffe and Reg Wilson
New Brunswick Department of Natural Resources and Energy Development, Geological Surveys Branch (retired), Fredericton, New Brunswick. email address: gabbro@nb.sympatico.ca

INTRODUCTION

This field guide describes several geological sites of interest in the Benton–Meductic area of west-central New Brunswick. The ancient sequence of volcanic and sedimentary rocks in this area was deposited along the southeastern margin of the Iapetus Ocean and today forms part of the Miramichi Terrane (Figs. 1, 2). The variety of features displayed by rocks in the Benton–Meductic area can be used to reconstruct the geological conditions that existed in this part of the Appalachian mMountain belt during the distant past.

The starting point for understanding the geological history of the Benton–Meductic area was bedrock mapping to determine the order in which the sedimentary and volcanic rocks were laid down (stratigraphic succession) and whether they were deposited in a marine or subaerial environment (depositional setting). During mapping, the observation of features such as bedding orientation, bedding gradation, pillow structures, and fossils (type and age) provided critical evidence for the reconstruction process. Additional studies such as geochronological dating of zircon and chemical analyses of bedrock units provided further data about the area's geological evolution. The combined field and laboratory evidence led to a fairly clear understanding of the tectonic setting of volcanic activity in and around the Benton–Meductic area.

The next step was to relate volcanic activity in the Benton–Meductic area to the broader plate tectonic processes that affected development of the Appalachian mountain belt as a whole. The overall mechanism controlling tectonic evolution of the northeastern Appalachians was the opening and subsequent destruction of the Paleozoic Iapetus Ocean. Vestiges of ancient oceanic crust associated with the opening of this ocean are preserved in the Bay of Chaleur region, northeastern New Brunswick (Fig. 1). Volcanic activity in the Benton–Meductic area occurred between 480 and 470 million years ago along the southeastern margin of this once extensive ocean. Younger volcanism took place between 470 and 455 million years ago in the Bathurst area near Bay of Chaleur. The contrasts in age and chemical composition of volcanic magmas from these two regions suggest that volcanic rocks in the Benton–Meductic area formed in an island arc at a converging plate boundary, whereas those in the Bathurst area formed in an extensional backarc basin.

Volcanic rocks generated in plate tectonic settings similar to those in the Benton–Meductic and Bathurst areas have a high potential to host economic deposits of base metals (lead, zinc, copper). Some 45 stratiform sulphide deposits containing ~500 Mt of base metal resources have been discovered in the Bathurst Mining Camp since the early 1950s (McCutcheon et al. 2003). During the 1990s the Benton–Meductic area became the focus of exploration following the discovery of a large sulphide clast in a roadcut along Benton Road. BHP Minerals Canada Ltd. subsequently drilled 12 holes along strike of the sulphide occurrence but intersected only minor sulphide mineralization. A sulphide clast from one drillhole assayed 16.7% Zn and 5.6% Pb; another drillhole intersected 1 m of pyrite mineralization with low base metal content. The sulphide mineralization most likely accumulated on the seafloor surrounding active hydrothermal vents, proximal to emerging felsic domes (McClenaghan et al. 2006).

REGIONAL GEOLOGY

New Brunswick is divided into several geological terranes that feature distinctive stratigraphic and tectonic characteristics (Fig. 1). These characteristics were determined largely by the terrane's original geographic position relative to the margin of the Iapetus Ocean, which opened in the northern Appalachians between the late Precambrian and early Paleozoic. After these terranes were deformed and uplifted during ocean closure in the later Paleozoic, sedimentary and volcanic rocks were deposited as cover sequences in a series of marine and terrestrial basins (Fyffe et al. 2011).

The Miramichi Terrane was situated along the southeastern margin of the Iapetus Ocean. It underlies the axial region of New Brunswick and includes early Paleozoic sedimentary and volcanic rocks that extend from the Benton–Meductic area near Woodstock to the Bathurst area near Bay of Chaleur (Fig. 1). In the former area, the Miramichi Terrane is flanked on the northwest by the Woodstock Fault and the Late Ordovician to Late Silurian Matapédia Basin (Fyffe 1982; Fyffe et al. 2011); and on the southeast by the Late Silurian to Early Devonian

Pokiok Batholith (Fig. 2). Younger sedimentary and volcanic rocks of the Early Devonian Tobique Group unconformably overlie the Miramichi Terrane along the batholith margin (Fig. 3). The Matapédia Basin contains deep-water limestone of the Late Ordovician to Early Silurian Matapédia Group and overlying clastic sandstone and shale of the Early to Late Silurian Perham Group (Fig. 2).

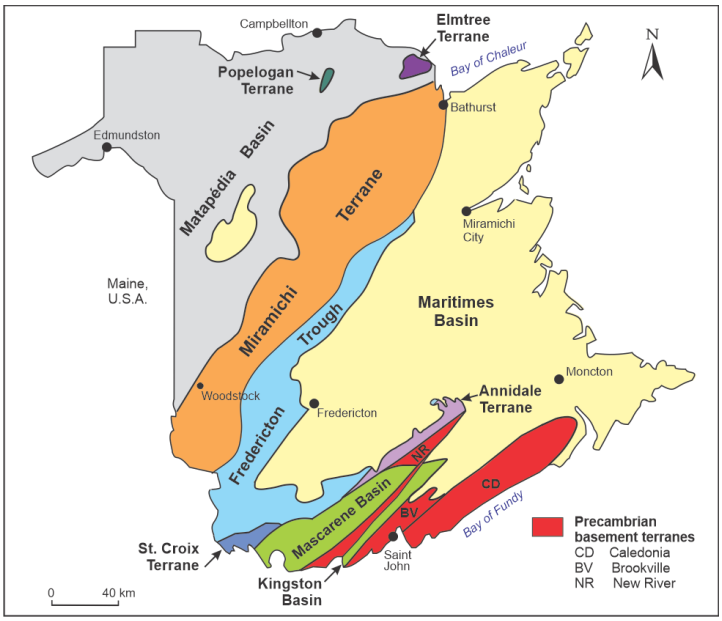

Figure 1. Regional geology of west-central New Brunswick and adjacent Maine.

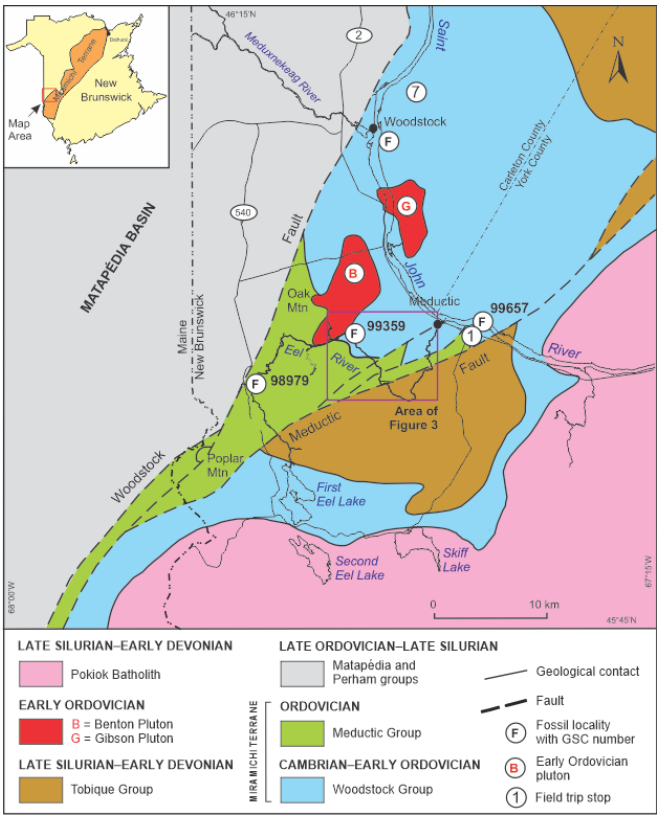

Figure 2. Regional geology of west-central New Brunswick and adjacent Maine.

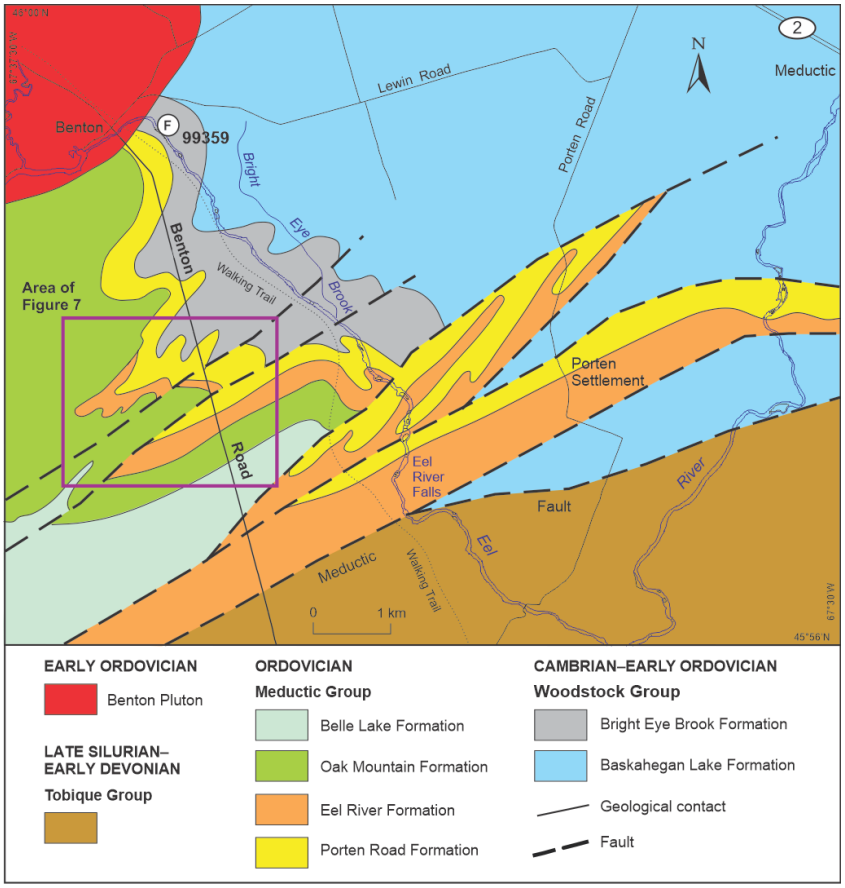

Figure 3. Geological map of the Benton-Meductic area (after Fyffe, 1999). Figure 2 shows the location of this map area in west-central New Brunswick.

The volcanic rocks in the Miramichi Terrane can be divided into compositionally distinct types on the basis of colour, hardness, mineral content, and texture. These characteristics are controlled largely by silica (SiO_2) content, which varies from relatively low in the dark, soft, mafic volcanic rocks, through intermediate values into relatively high silica content in the light-coloured, hard, felsic volcanic rocks. Volcanic rocks are named according to the SiO_2 content of the unaltered samples: basalt (<53%), andesite (53–63%), dacite (63–70%), and rhyolite (<70%) (Gill, 1981). Differences in the age and chemical composition between volcanic rocks of the Miramichi Terrane in the Benton–Meductic and Bathurst areas provide important clues for understanding the plate tectonic configuration of New Brunswick during the Ordovician.

Benton–Meductic Area

The sedimentary and overlying volcanic rocks in the Benton–Meductic area (Fig. 3) have been designated as the Woodstock and Meductic groups, respectively (Fig. 4; Fyffe 1999, 2001).

The ***Woodstock Group*** includes Cambrian to Early Ordovician quartzose sandstone and shale of the Baskahegan Lake Formation and overlying Early Ordovician silty mudstone and shale of the Bright Eye Brook Formation. The Baskahegan Lake Formation cannot be older than Early Cambrian according to the date of 525 ± 6 Ma on its youngest contained zircon population (Fyffe et al. 2009). It may be as young as Early Ordovician according to trace fossils found near Woodstock (Fig. 2; Pickerill and Fyffe 1999). Graptolites from two locations in black shale of the Bright Eye Brook Formation have been age-dated as Early Ordovician at two locations: those at Eel River near Benton (GSC loc. 99359 on Fig. 2, 3) are late Tremadocian (Bailey 1901; Fyffe et al. 1983), whereas those on Temple Road east of Meductic (GSC loc. 99657 on Fig. 2) are early Floian (Fyffe and Pickerill 1993; Pickerill and Fyffe 1999).

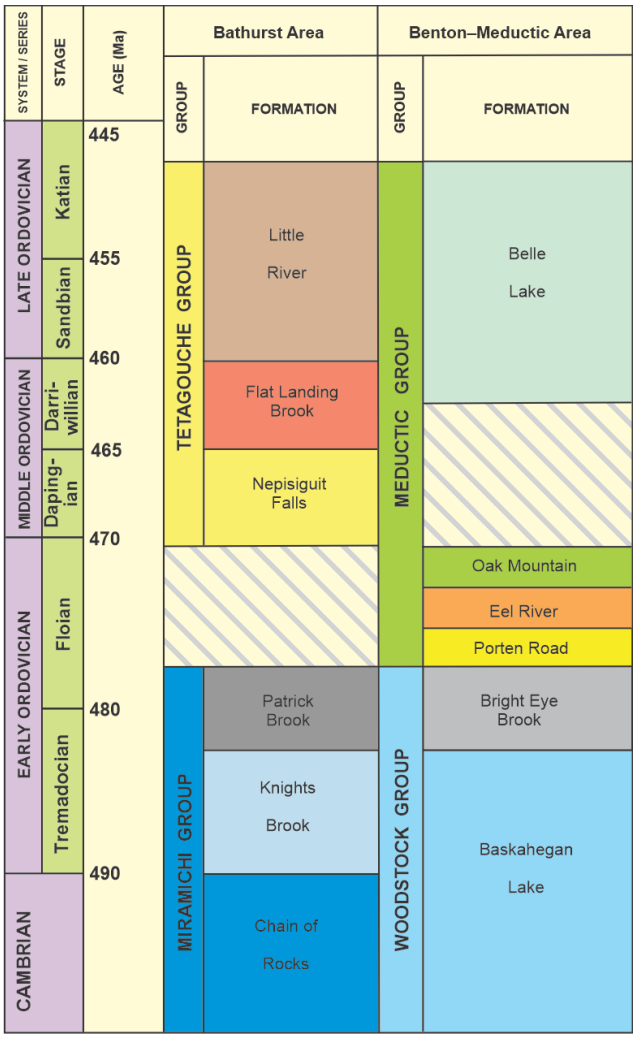

Figure 4. Stratigraphic columns comparing Cambrian and Ordovician sedimentary and volcanic rocks of the Miramichi Terrane in the Bathurst area of northwestern New Brunswick with those in the Benton-Meductic area of west-central New Brunswick.

Volcanic rocks in the ***Meductic Group*** range from rhyolite and dacite through andesite to basalt. From oldest to youngest, they comprise rhyolitic and dacitic rocks of the Porten Road Formation, andesitic rocks of the Eel River Formation, and basaltic rocks of the Oak Mountain Formation (Fig. 3, 4). Feldspathic sandstone and black shale overlying the volcanic rocks are included in the Belle Lake Formation, also of the Meductic Group. Graptolites from the Belle Lake Formation (GSC loc. 98979: Fig. 2, 5) indicate a Late Ordovician (Sandbian) age (Fyffe et al. 1983). Thus, fossils found below and above volcanic rocks of the Meductic Group restrict the time of eruption to between the Early Ordovician (early Floian) and Late Ordovician (Sandbian; Fig. 4).

Radiometric dating of the Gibson Pluton (Fig. 2) in the Woodstock area yielded a U–Pb zircon date of 473 ± 1 Ma (Bevier 1990), providing a tighter control on timing of this Meductic volcanic activity. The nearby, similar Benton Pluton (Fig. 2) intrudes basaltic volcanic rocks of the Oak Mountain Formation in the upper part of the Meductic Group. Thus, if the Benton Pluton is the same age as the Gibson Pluton, then all volcanic rocks of the Meductic Group are Early Ordovician (Floian). The Middle Ordovician (Dapingian–Darriwillian) gap in deposition between the Oak Mountain and Belle Lake formations (Fig. 4) marks the cessation of volcanic activity in the Benton–Meductic area.

The gradational nature of the lithological and geochemical profiles through silty mudstone of the Bright Eye Brook Formation (Woodstock Group) into overlying iron formation and felsic volcanic rocks of the Meductic Group (Fyffe and Pickerill 1993; Hennessy and Mossman 1996) suggests a conformable relationship. This is in contrast with the unconformity between the Miramichi and Tetagouche groups in the Bathurst area of the Miramichi Terrane (see below).

Figure 5. Graptolites from the Belle Lake Formation (GSC loc. 98979) in the Benton-Meductic area. Figure 2 shows the fossil locality.

Bathurst Area

In the Bathurst area, the sedimentary and overlying volcanic rocks of the Miramichi Terrane are referred to as the Miramichi and Tetagouche groups, respectively (Fig. 4). The ***Miramichi Group*** consists of a Cambrian to Early Ordovician sedimentary sequence (Fig. 4). It is subdivided into a lower unit of thick-bedded quartzite (Chain of Rocks Formation), a middle unit of medium-bedded quartzites and shales (Knights Brook Formation), and an upper unit of thin- to medium-bedded feldspathic wacke and shale (Patrick Brook Formation).

The Miramichi Group is unconformably overlain by Middle to Late Ordovician volcanic rocks of the ***Tetagouche Group*** (van Staal 1987; van Staal and Fyffe 1991, 1995; van Staal et al. 1991, 2003; Fyffe et al. 1997). The volcanic rocks are bimodal: that is, mafic and felsic in composition with none of intermediate composition. The Tetagouche Group (Fig. 4) is subdivided into a lower unit of coarse quartz–feldspar crystal tuff and iron formation (Nepisiguit Falls Formation); a middle unit of aphyric to sparsely feldspar-phyric rhyolite flows (Flat Landing Brook Formation); and an upper unit of pillow basalt, basaltic breccia, maroon ferromanganiferous siltstone, and black shale (Little River Formation).

Beds of conglomerate and sandy limestone at the base of the Nepisiguit Falls Formation contain rounded pebbles derived from the underlying Patrick Brook Formation (Miramichi Group). Conodonts from the limestone and brachiopods from the associated calcareous siltstone indicate that the Nepisiguit Falls Formation is Middle Ordovician (Dapingian). Graptolites from black shales of the Little River Formation are Late Ordovician (Sandbian) (Neuman 1984; Fyffe et al. 1997). The volcanic rocks in the Bathurst area yielded Middle to Late Ordovician (Dapingian to Sandbian) U–Pb zircon dates of 471 ± 3 Ma to 457 ± 1 Ma (Sullivan and van Staal 1996; van Staal et al. 2003).

Depositional Environment

The chemical variation from basalt through andesite, dacite, and rhyolite in volcanic rocks of the Meductic Group is similar to that seen in volcanic rocks known to have formed along present-day convergent plate boundaries. These Meductic rocks are therefore interpreted to represent an ancient island arc that formed above a subduction zone along the southeastern margin of the Iapetus Ocean (Dostal 1989; van Staal and Fyffe 1991, 1995; Fyffe 2001).

In contrast, the bimodal volcanic rocks of the Tetagouche Group are interpreted to have been generated in a continental intra-arc rift that eventually evolved into a wide, oceanic seaway referred to as the Tetagouche backarc basin (van Staal 1987; van Staal and Fyffe 1991, 1995; van Staal et al. 1991, 2003). Opening of this backarc basin can be understood in terms of northwesterly rollback of a subducting slab dipping to the southeast beneath the Meductic arc. As a result of this rollback, the Meductic arc was left behind to become a dormant remnant while the active Popelogan arc migrated to the northwest into the main Iapetus Ocean. Vestiges of this ocean are now largely covered by younger, Late Ordovician to Early Devonian sedimentary and volcanic rocks of the Matapédia Basin (Fig. 1, 6). However, in northeastern New Brunswick, oceanic crust of the Tetagouche backarc basin is well exposed in the Elmtree Terrane along Bay of Chaleur (Fig. 1).

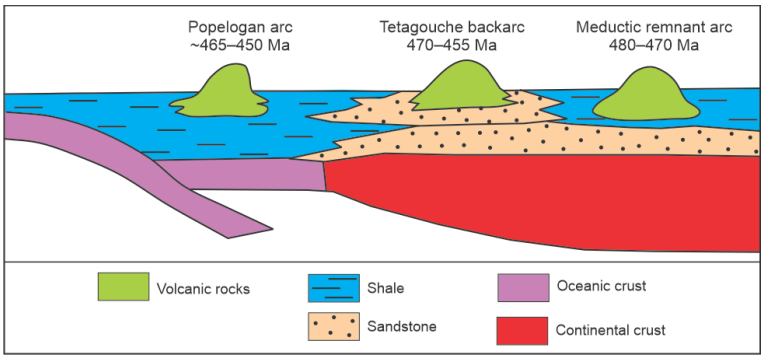

Figure 6. Plate tectonic model of New Brunswick in the Ordovician.

LITHOFACIES OF THE MEDUCTIC GROUP

Please note that Figures 8 to 30, cited throughout this **Lithofacies** *section, are grouped together on pages 13 to 24.*

Volcanic rocks in the three formations (Porten Road, Eel River, and Oak Mountain) of the Meductic Group are divided into several lithofacies that are defined on the basis of their compositional, textural, and bedding characteristics. These features in turn reflect their mode of eruption and deposition. For example, basaltic magma (low SiO_2 content) has a low viscosity and thus can flow overland as lava for several kilometres. If basaltic magma flows into seawater or erupts underwater, it typically cools quickly and either develops pillow structures or shatters into a glassy, fragmental and sometimes bedded rock known as 'hyaloclastite.'

In contrast, rhyolitic magma (high SiO_2 content) has a relatively high viscosity and does not flow far from the volcanic vent. More commonly, rhyolitic magma discharges explosively as ground-hugging, gas-rich, pyroclastic flows composed largely of broken mineral grains, volcanic rock fragments, and fine ash. These highly fluidized, subaerial, pyroclastic flows can travel many tens of kilometres downslope from the volcanic vent. Upon entering seawater, the denser pyroclastic material segregates from the overlying ash cloud and forms a massive to relatively thick-bedded, water-transported pyroclastic flow that may contain angular blocks of sediments eroded from the seafloor.

When unconsolidated pyroclastic material is transported deeper into the marine basin, it forms thinner, graded beds in which the grains become finer and more rounded as the material travels farther from the source area. Consolidated subaerial or submarine pyroclastic deposits are classified into ash tuff (<2 mm), lapilli tuff (2–64 mm), and tuff breccia (>64 mm), according to the predominant size of crystal and rock fragment clasts (Cole and DeCelles 1991).

The volcanic lithofacies in each formation of the Meductic Group are described below. Their specific characteristics are useful when reconstructing a depositional setting for Ordovician volcanic eruptions in the Benton–Meductic area. It should be noted that the area's complexity of folding and faulting (Fig. 3) and scarcity of exposed bedrock permit only a general interpretation of its volcanic history. However, good bedrock exposures of various lithofacies do exist here (Fig. 7) and are detailed under **Stop Descriptions** in the latter part of this field guide.

Porten Road Formation

Volcanic lithofacies in the Porten Road Formation consist of andesitic breccia, massive to brecciated porphyritic rhyolite, and rhyolitic and dacitic lapilli tuffs.

Andesitic breccia

A 250 m thick unit of andesitic breccia occurs locally at the base of the Porten Road Formation just above sedimentary rocks of the Bright Eye Brook Formation. The unit can be traced from the area of Benton Road eastward for 5 km to Eel River (Fig. 3, 7). Contacts with underlying black shale and silty mudstone of the Bright Eye Brook Formation (Fig. 8) and overlying felsic volcanic rocks of the Porten Road Formation are not exposed.

The breccia is typically composed mainly of dark grey to greyish green andesite fragments ranging from 1 cm to 7 cm across (Fig. 9). The jigsaw fit of the angular fragments suggests that brecciation took place in situ by lava-quenching in a subaqueous environment (Cas 1992; McPhie et al. 1993). Large clasts of grey siltstone are common in exposures east of Benton Road nearer the contact with the Bright Eye Brook Formation and presumably were incorporated into the breccia as it spread over the seafloor. The andesite fragments are generally

porphyritic; they contain up to 15% plagioclase phenocrysts that are 1 mm to 1.5 mm across and set in a fine-grained matrix of plagioclase crystals. Clinopyroxene phenocrysts ~0.7 mm across are preserved in some fragments. Sphene, calcite, epidote, and chlorite are common alteration products of both phenocrysts and groundmass. Table 1 shows the SiO_2 and MgO contents of this lithofacies.

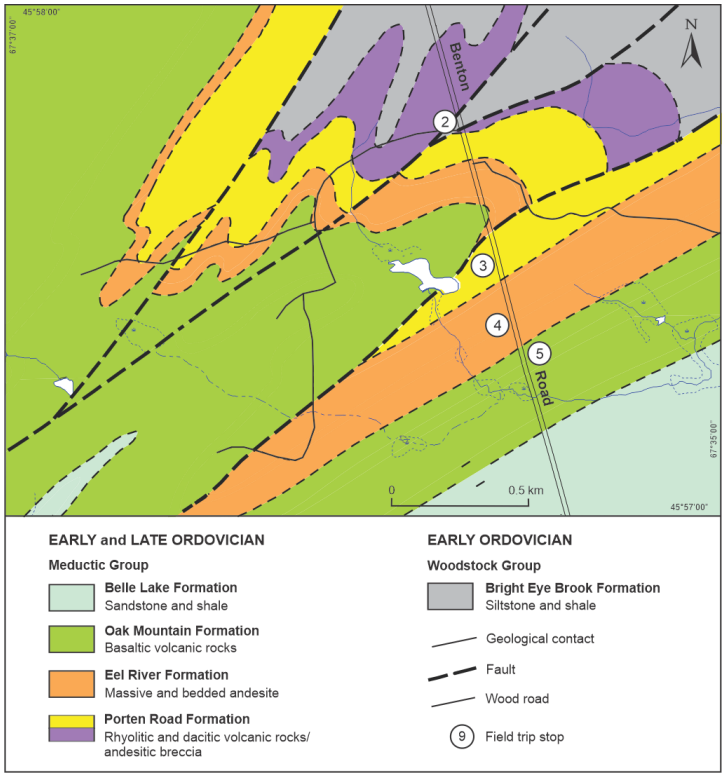

Figure 7. Geological map of the Benton Road area, showing field stop locations (geology after Fyffe, 1999). See Figure 3 for the location of this map area of west-central New Brunswick.

Massive to brecciated porphyritic rhyolite

The dominant lithofacies in the Porten Road Formation is massive, light greyish green to pale pink porphyritic rhyolite containing phenocrysts (1–3 mm across) of quartz and feldspar (Fig. 10, 11). The lithofacies underlies the southeastern part of the Eel River area from Eel River eastward to Porten Road and beyond (Fig. 3, 7). Its concordant nature with the overlying stratigraphy suggests that the massive rhyolite represents thick flows that extruded proximal to a volcanic dome.

The massive lithofacies varies locally to a brecciated rock containing angular porphyritic felsic fragments (2–10 cm across) that are barely discernable from the host rock (Fig. 11). The fragmentation is interpreted to have resulted from rapid solidification (quenching) of felsic lava as it was emplaced in a submarine environment, followed by shattering of the resultant volcanic glass to form an in situ autoclastic breccia (Cas 1992; McPhie et al. 1993). The rare, irregularly shaped mafic inclusions in the rock (Fig. 12) likely represent volcanic bombs deposited in a semi-molten, plastic state; their presence supports the interpretation that the rhyolite was discharged from a nearby volcanic vent. Total thickness of the massive rhyolite along Eel River is estimated at 300 m to 400 m. Table 1 shows the SiO_2 and MgO contents of this lithofacies.

Table 1. SiO_2 and MgO contents of lithofacies in formations of the Meductic Group, Benton–Meductic area, west-central New Brunswick (Fig. 3). Analyses are from Fyffe (2001).

Meductic Group		SiO_2 Content (wt %)		MgO Content (wt %)	
Formation	**Lithofacies**	**Range**	**Average**	**Range**	**Average**
Oak Mountain	Basaltic volcanic rocks	45.0–51.7	48.8	4.8–7.8	6.0
Eel River	Andesitic tuff	58.5–60.5	59.6	2.7–3.7	3.2
Porten Road	Rhyolitic and dacitic lapilli tuff	59.3–73.9	66.0	1.8–4.1	2.7
	Massive to brecciated porphyritic rhyolite	68.1–77.3	73.0	1.4–3.7	2.2
	Andesitic breccia	51.9–58.1	55.4	3.4–7.1	5.4

Rhyolitic and dacitic lapilli tuffs

This lithofacies comprises pale pink rhyolitic lapilli tuff and thick, poorly sorted, greyish green dacitic lapilli tuff (Fig. 13–15). It is exposed on Benton Road and along wood roads 3 km to 3.5 km south of the village of Benton (Fig. 3, 7).

Pyroclastic quartz grains constitute 10% to 20% of the rhyolitic tuff and ~5% of the dacitic tuff. They typically are from 1 mm to 2 mm across and range from round and embayed to angular, shattered remnants. Feldspar grains form 10% to 15% of the rhyolitic tuff and 30% to 40% of the dacitic tuff; they generally range from 1 mm to 1.5 mm long and are subhedral, commonly occurring in clusters. Lithic fragments in the tuffs are angular and from 1 cm to 15 cm across; they include abundant volcanic and sedimentary clasts and local massive sulphide clasts (Fig. 14). Feldspar crystals in some volcanic fragments commonly exhibit weak flow alignment, suggesting they were derived from lava flows. Table 1 shows the SiO_2 and MgO contents of this lithofacies.

The rhyolitic and dacitic lapilli tuffs are interlayered in exploration drillholes (McClenaghan et al. 2006), indicating that the two compositional varieties were emplaced essentially contemporaneously. An explosive, pyroclastic origin for the tuffs is suggested by the abundance of broken quartz crystals and the angularity of volcanic fragments (Cas 1992). Because none of the included sedimentary fragments exhibit features indicating derivation from either a shallow marine or a terrestrial source, the tuffs are interpreted to have been deposited as submarine pyroclastic flows along the flanks of a submerged volcanic vent (Cas 1992). Such a mode of deposition is consistent with the spatial and temporal relationship of these rocks with the massive and brecciated rhyolitic lithofacies described above.

The lack of pumice fragments is also consistent with deposition in a submarine rather than a subaerial environment: pumice is less dense than water and thus will not sink as readily to the seafloor. Laminated beds of greyish green siltstone are interstratified with the tuffs in intervals ranging from 50 cm to a few metres thick. These siltstone beds likely represent the finer fraction of pyroclastic material that was winnowed from the main flow during downslope transportation in a marine environment.

Eel River Formation

The Eel River Formation comprises a thick sequence of light grey to greyish green andesitic tuff interstratified with olive green siltstone, maroon ferromanganiferous siltstone and mudstone (Fig. 16, 17), and dark grey shale. Two lithofacies of andesitic tuff are recognized in the Benton–Meductic area: massive and well bedded. Grading in the bedded tuff indicates that the Eel River andesitic tuffs overlie the dominantly rhyolitic volcanic rocks of the Porten Road Formation.

The contact between the Porten Road and Eel River formations is defined by a narrow interval of siltstone or mudstone in the latter formation (Fig. 16). Good exposures of volcanic and sedimentary rocks of the Eel River Formation occur along Benton Road about 3.7 km south of the bridge over Eel River in Benton (Fig. 3, 7). The Eel River section along Benton Road dips ~75º S and has an estimated thickness of about 250 m.

Massive andesitic tuff:

Very thick, massive intervals of andesitic tuff are exposed along Benton Road and on adjoining wood roads to the east and west. The tuff contains about 20% light grey, fine-grained, angular, amygdaloidal, porphyritic to aphyric andesite fragments from 1 cm to 20 cm across set in a fine-grained, feldspathic matrix (Fig. 18). Rare porphyritic rhyolite fragments were likely derived from the underlying Porten Road Formation (Fig. 19). Crystal fragments consist predominantly of plagioclase feldspar with minor brown hornblende, clinopyroxene, and quartz and range in size from 0.4 mm to 2 mm. Table 1 shows the SiO_2 and MgO contents of this lithofacies.

The andesitic tuff was clearly deposited in a marine environment, as indicated by the intercalated ferromanganiferous sedimentary rocks (Fig. 17). The angularity of the fragments suggests deposition as syn-eruptive pyroclastic flows rather than as resedimented debris flows (Cas 1992; McPhie et al. 1993).

Bedded andesitic tuff

Medium- to thin-bedded andesitic tuff, typically in intervals several metres in thickness, are interlayered with massive andesitic tuff in the Benton–Meductic area. Individual beds range from 1 cm to ~1 m in thickness (Fig. 20). Grading in the thicker beds ranges from a coarse base to a fine, laminated top of 2 cm to 5 cm thick, whereas grading in the thinner beds is more subtle.

These bedded tuffs are very similar in mineralogy and chemical composition to the associated massive andesitic tuffs (Table 1); a sample of bedded andesitic tuff contained 56.5% SiO_2 and 3.6% MgO (Fyffe 2001). Thus, the bedded tuffs likely represent less voluminous pyroclastic flows that were transported into the marine basin by turbidity currents. Evidence for downslope resedimentation of these syn-eruptive deposits can be seen in tuff breccias containing large fragments of consolidated ash along Eel River southwest of Porten Settlement (Fig.

21); in slump folds within medium-bedded tuffs, also southwest of Porten Settlement (Fig. 22); and in mudflows containing volcanic clasts on Porten Road to the north of Porten Settlement (Fig. 23).

Oak Mountain Formation

Basaltic rocks of the Oak Mountain Formation are exposed about 4 km south of Benton on the east and west sides of Benton Road (Fig. 3, 7). These include abundant dark green, fine-grained, amygdaloidal, porphyritic basalt flows, basaltic breccia, pillow lava, and bedded basaltic tuff. The Oak Mountain Formation is estimated to be about 300 m thick in the Benton–Meductic area but apparently thickens greatly farther to the northwest (Venugopal 1978, 1979).

Tops from local pillow structures west of Benton Road indicate that basaltic rocks of the Oak Mountain Formation stratigraphically overlie andesitic rocks of the Eel River Formation. The contact between dark green basaltic volcanic rocks of the Oak Mountain Formation and the underlying massive to bedded, greyish green andesitic tuff of the Eel River Formation (Fig. 24, 25) is generally marked by a thin bed of greyish maroon, ferromanganifeous siltstone or mudstone that occurs at the top of the latter formation (Fig. 26).

Porphyritic basalt flows

Dark green, sparsely to highly porphyritic basalt flows of the Oak Mountain Formation (Fig. 26) are exposed in the northwestern part of the Benton–Meductic area (Fig. 3). The flows contain 5% to 20% dark green clinopyroxene phenocrysts from 1 mm to 7 mm long and 10% to 50% pale green plagioclase phenocrysts from 0.5 mm to 3 mm long. The phenocrysts are set in a groundmass that includes flow-aligned plagioclase crystals and amygdules infilled with chlorite, epidote, and calcite. The basalt flows locally contain scarce, irregularly shaped mafic volcanic fragments from 15 cm to 20 cm across. These fragments may represent bombs ejected from a nearby volcanic vent that likely rose well above sea level. The erosional remnant of this vent may be situated at Oak Mountain about 4 km northwest of Benton (Fig. 2).

Basaltic breccia and pillow lava

Massive basaltic breccia containing abundant, subrounded, mafic volcanic fragments from 10 cm to 20 cm across (Fig. 27) constitutes the dominant lithofacies of the Oak Mountain Formation in the southern part of the Benton–Meductic area (Fig. 3). This breccia likely was formed by quenching of basaltic lava upon entering a subaqueous environment. As a result of the rapid cooling by seawater, the solidified crust of the lava flow was shattered and fragments spalled off to form a hyaloclastic breccia.

A few bedrock exposures in this area contain well-developed pillow structures, further proof of deposition in a marine setting (Fig. 28). The pillows are typically about 50 cm in diameter with interpillow spaces infilled with green to greyish pink chert. Vesicles in the rock are formed by the release of gas from the cooling lava (Fig. 29). The association of hyaloclastic breccia with pillow lava indicates that a submarine basin once fringed the southern margin of the Oak Mountain volcanic vent.

Bedded basaltic tuff

Dark green, bedded basaltic tuff characterizes the Oak Mountain Formation in the southeastern part of the Benton–Meductic area (Fig. 3). The tuff beds vary from 3 cm to 1 m in thickness and are interlayered with maroon siltstone and mudstone beds that are 1 cm to 15 cm in thickness (Fig. 30). The tuff beds comprise an aggregate of tightly packed and elongated fragments (5 mm–1 cm long) of porphyritic basalt and lesser aphyric basalt.

The bedded tuff presumably represents resedimented volcanic detritus that was remobilized by turbidity currents and deposited in deeper parts of a marine basin. The source of this material was likely unconsolidated hyaloclastic breccias that were deposited farther upslope along the margin of the basin (McPhie et al. 1993).

The various lithofacies of basaltic volcanic rocks in the Oak Mountain Formation are chemically similar to one another, indicating derivation from a single magma source. Table 1 shows the SiO_2 and MgO contents of the lithofacies. The different characteristics of the basaltic lithofacies are attributed to variations in the depositional environment, which ranged from a shallow to a deep submarine setting.

SUMMARY

The Ordovician volcanic stratigraphy of the Meductic Group in the Benton–Meductic area differs significantly from that of the Tetagouche Group in the Bathurst area. The sedimentary substrate and island-arc volcanic sequence in the former area are referred to as the Woodstock and Meductic groups, respectively.

The Woodstock Group includes interbedded quartzose sandstone and shale of the Baskahegan Lake Formation and overlying Early Ordovician silty mudstone and shale of the Bright Eye Brook Formation. The conformably overlying Meductic Group is divided into contrasting Early Ordovician volcanic assemblages of the Porten Road (mainly rhyolitic), Eel River (mainly andesitic), and Oak Mountain (mainly basaltic) formations; and Late Ordovician feldspathic wacke and shale of the Belle Lake Formation.

The emplacement of comagmatic rocks of the Gibson Pluton at 473 ± 1 Ma (Bevier 1990) suggests that this arc sequence is older than all but the basal part of the Tetagouche backarc succession in the northeastern Miramichi Terrane (Fig. 2, 3). The cessation of volcanic activity in the Meductic Group is interpreted to be related to northwestward migration of the subducting slab as a result of arc-rifting and opening of the Tetagouche backarc basin (van Staal 1987; van Staal et al. 1991).

Figure 8. Black shale with laminations and cleavage, Bright Eye Brook Formation. Laminations are parallel to the yellow pencil, and cleavage is parallel to the magnetic pencil. Magnetic pencil is 15 cm long. Location is Stop 2.

Figure 9. Angular volcanic fragments in andesitic breccia, Porten Road Formation. Hammer is 33 cm long.

Figure 11. Autobrecciated, pale pink porphyritic rhyolite of the Porten Road Formation, containing angular fragments and displaying a jigsaw texture. Lens cap is 5 cm across.

Figure 10. Massive porphyritic rhyolite containing conspicuous quartz phenocrysts, Porten Road Formation. Lens cap is 5 cm across. Exposure is along Eel River 700 m below Bright Eye Brook (Fig. 3).

Figure 12. Mafic fragment in porphyritic rhyolite, Porten Road Formation. Lens cap is 5 cm across.

Figure 13. Rhyolitic lapilli tuff with abundant felsic volcanic and sparse black shale fragments, Porten Road Formation. Coin is 23 mm across. Location is Stop 3.

Figure 14. Massive sulphide clasts in rhyolitic lapilli tuff, Porten Road Formation. Lens cap is 5 cm across. Location is Stop 3.

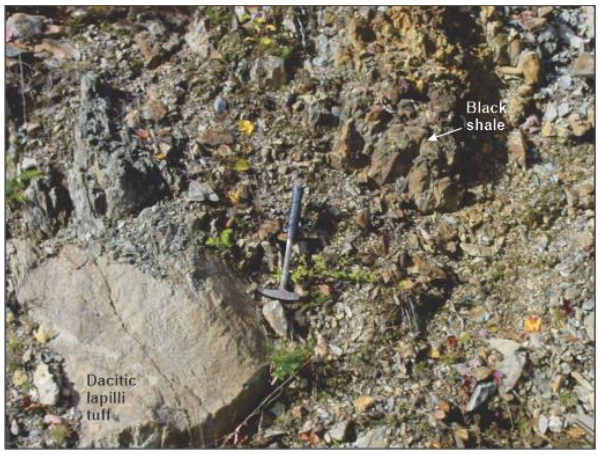

Figure 15. Dacitic lapilli tuff with incorporated block of black shale, Porten Road Formation. Hammer is 33 cm long.

Figure 16. Greyish green siltstone of the Eel River Formation, which overlies dacitic lapilli tuff of the Porten Road Formation (not shown) that is exposed a few metres to the north along this outcrop. Hammer is 33 cm long.

Figure 17. Maroon ferromanganiferous siltstone interlaminated with green mudstone (ash), Eel River Formation. Lens cap is 5 cm across. Location is southwest of Porten Settlement (Fig. 3).

Figure 19. Rhyolitic fragments (arrows), likely of the Porten Road Formation, in massive andesitic tuff of the Eel River Formation. Hammer is 33 cm long. Location is Stop 4.

Figure 18. Massive andesitic tuff containing abundant plagioclase crystals and lesser volcanic fragments, Eel River Formation. Coin is 23 mm across. Location is Stop 4.

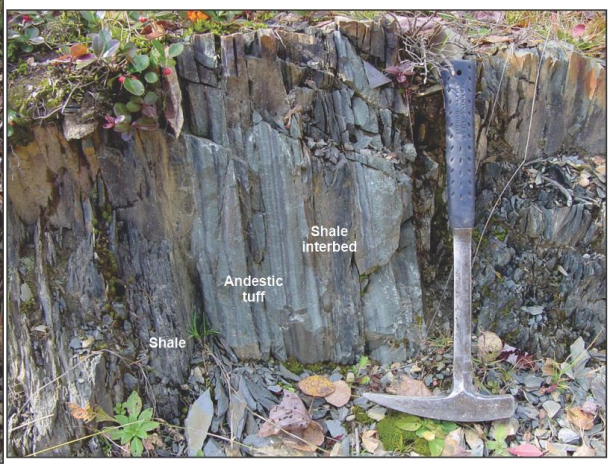

Figure 20. Bedded andesitic tuff overlain to the south (left) by dark grey shale, Eel River Formation. Hammer is 33 cm long. Location is Stop 4.

Figure 21. Tuff breccia of the Eel River Formation containing aphanitic felsic fragments of varied lengths (2–15 cm) and widths (1–5 cm). Lens cap is 5 cm across. Location is along Eel River southwest of Porten Settlement (Fig. 3).

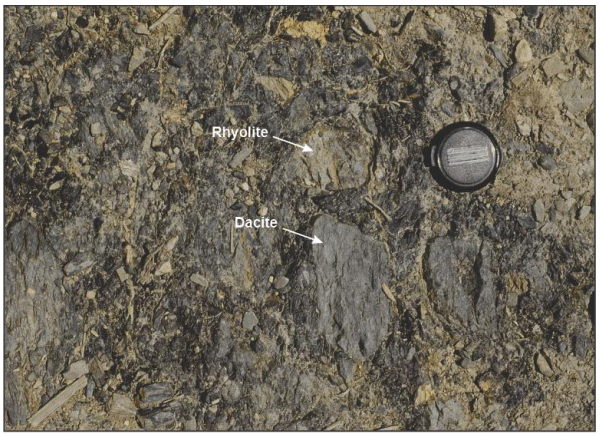

Figure 23. Volcanic clasts in dark grey mudstone, Eel River Formation. Clasts include pale pink, porphyritic rhyolite fragments, likely of the underlying Porten Road Formation; and light grey dacitic fragments, likely of the Eel River Formation. Lens cap is 5 cm across. Location is on Porten Road, 1.5 km north of Porten Settlement (Fig. 3).

Figure 22. Slump folds in bedded andesitic tuff, Eel River Formation. Beds generally are 25 cm thick and grade upward into a 5 cm thick laminated interval. Tops are to the southeast. Note truncation of slump folds by overlying beds (arrow). Lens cap is 5 cm across. Location is just southwest of Porten Settlement (Fig. 3).

Figure 24. Massive andesitic tuff containing sparse volcanic fragments at its base, Eel River Formation. Hammer is 33 cm long.

Figure 25. Bedded andesitic tuff that gradationally overlies massive tuff, Eel River Formation. Hammer is 33 cm long.

Figure 26. Bedded andesitic tuff and greyish maroon siltstone of the Eel River Formation, overlain by massive basalt of the Oak Mountain Formation. Northwest lies to the left of the hammer. Hammer is 33 cm long.

Figure 27. Basaltic breccia of the Oak Mountain Formation containing abundant, subrounded, mafic volcanic fragments ranging from 10 cm to 20 cm across. Lens cap is 5 cm across.

Figure 28. Pillow basalt of the Oak Mountain Formation, showing chert infillings (arrows). Hammer is 33 cm long.

Figure 29. Pillow basalt of the Oak Mountain Formation, showing large, open vesicles. Hammer is 33 cm long.

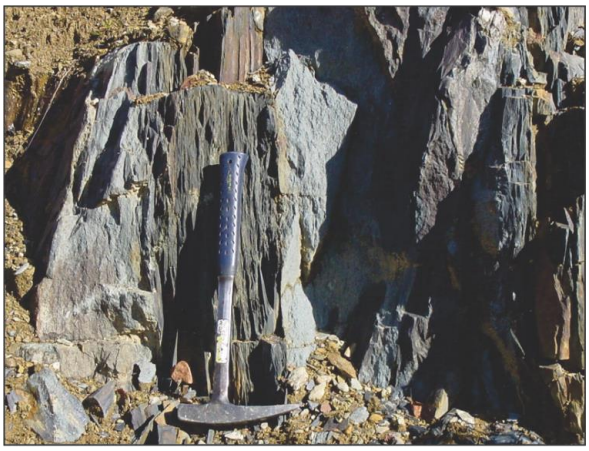

Figure 30. Bedded basaltic tuff (left and right of hammer) interstratified with dark grey siltstone (beneath hammer) of the Oak Mountain Formation. Hammer is 33 cm long. Location is Stop 5.

DRIVING AND WALKING LOG

MEETING POINT
Begin the field trip at the Meductic Irving convenience store, 307 Route 165 at 10:00 AM (AST). Food and washroom facilities are available at this location. Then proceed east along Route 165 for ?? km to Stop 1.

Mileage
0.0 From 307 Route 165, Irving convenience store, Meductic, turn left onto Route 165 (Temple Road)
1.6 Park on the south (right) side of the road.

9:45-10:05 20 min STOP 1A-Mn-bearing black shale, Porten Road Formation (E 618628, N 5094006 UTM Zone 19)

STOP 1A Walking Log: Proceed to the outcrop on the north side of the road.
STOP 1A Description: The Meductic Group in the area comprises the Porten Road Formation and the Eel River Formation. The Eel River Formation consists of intermediate flows, whereas the Porten Road Formation (this stop) consists of dark gray shale with minor interbedded felsic tuffaceous flows. The Porten Road Formation hosts dark manganiferous shales that vary in thickness. The thickest section lies just south of this location at the intersection between the Trans-Canada Highway #2 and Highway 122. reaching as thick as a kilometer. At this location, it has a thickness of about 700 m, and to the north near the St John River, it is approximately 300 m thick. Near Meductic village to the northwest of this location, reddish shales are also exposed. The Porten Road

Formation extends to the south and west as far as Benton for a distance of more than 15 km where they the beds are repeatedly folded and sliced into thinner beds (as narrow as 170 m thickness). The Porten Road Formation extends discontinuously north of the St John River as far as Taffy Lake, north of Millville. Bedding and foliation planes in these rocks are subparallel, striking 045-060°E and dipping at high angles toward the southeast, mostly to the northwest. Small-scale localized folds may be observed in this exposure. Mapping in this area by Gardiner and Venugopal (1990) reported the presence of manganiferous slates several hundred meters thick. Thirteen grab samples of dark shales were collected by Hennessy and Mossman (1996) just to the east of this exposure. Six of those samples contained elevated MnO values, some of which are believed to belong to the Porten Road Formation.

10:05 – 10:10 5 minute travel time to STOP 1B – V-bearing black shale, Bright Eye Brook Formation

Mileage
0.0 Continue heading east along Temple Road Drive 3.4 km to next road on the left
3.4 Turn left and proceed west.
6.8 Park on the right side of the road

10:10 – 10:25 15 minute STOP 1B – V-bearing black shale, Bright Eye Brook Formation (E 618982, N 5094388 UTM Zone 19)

STOP 1B Walking Log: Proceed to the outcrop
STOP 1B Description: The Baskahegan and Bright Eye Brook formations represent the Woodstock Group in the Meductic area. The former consists of gray shale and fine-grained sandstone and outcrops extensively both east and west of Meductic on Temple Road, on Main Street north of Meductic, near the Saint John River, and on the Trans-Canada Highway. Exposures of the Bright Eye Brook Formation are observed on Main Street near the Saint John River and consists mainly of shaley rocks. Sampling of these rocks along strike to the south by Hennessy and Mossman (1996) indicated that they are highly enriched in V (700-3000 ppm V) and Ba as well as moderately enriched in Nb, Th, Pb, Ti, and Cr.

10:25 – 10:55 30 minute travel time to STOP 2 - Black Shale, Bright Eye Brook Formation
Mileage
0.0 Leave Stop 1B and continue west along Main Street
2.2 Turn right onto Highway 165
5.4 Turn left onto Benton Road and proceed to Benton
13.8 Turn left and proceed through the covered bridge and continue along the Benton Road
16.7 Pull off to the right side of the road

10:55-11:10 15 min STOP 2 – Black Shale, Bright Eye Brook Formation (Fig. 8) – (E 608800, N 5090871 UTM Zone 19)

STOP 2 Walking Log: Proceed to the outcrop in the ditch on the right side of the road.
STOP 2 Description: Black shale on the west side of the road displays steeply dipping laminations (very thin bedding) that are cross-cut by a cleavage trending 030º and dipping 75º NW. Early Ordovician graptolites (GSC loc. 99359) have been recovered from black shale exposed along Eel River, a short distance downstream from the covered bridge in Benton (Fig. 3). The black shale overlies and therefore is younger than the Baskahegan Lake Formation, as indicated by graded bedding in quartzose sandstone beds of the latter formation.

11:10-11:12 2 minute travel time to STOP 3 – Rhyolitic lapilli tuff, Porten Road Formation

Mileage
0.0 Continue south along the Benton Road
5.4 Pull off to the right side of the road

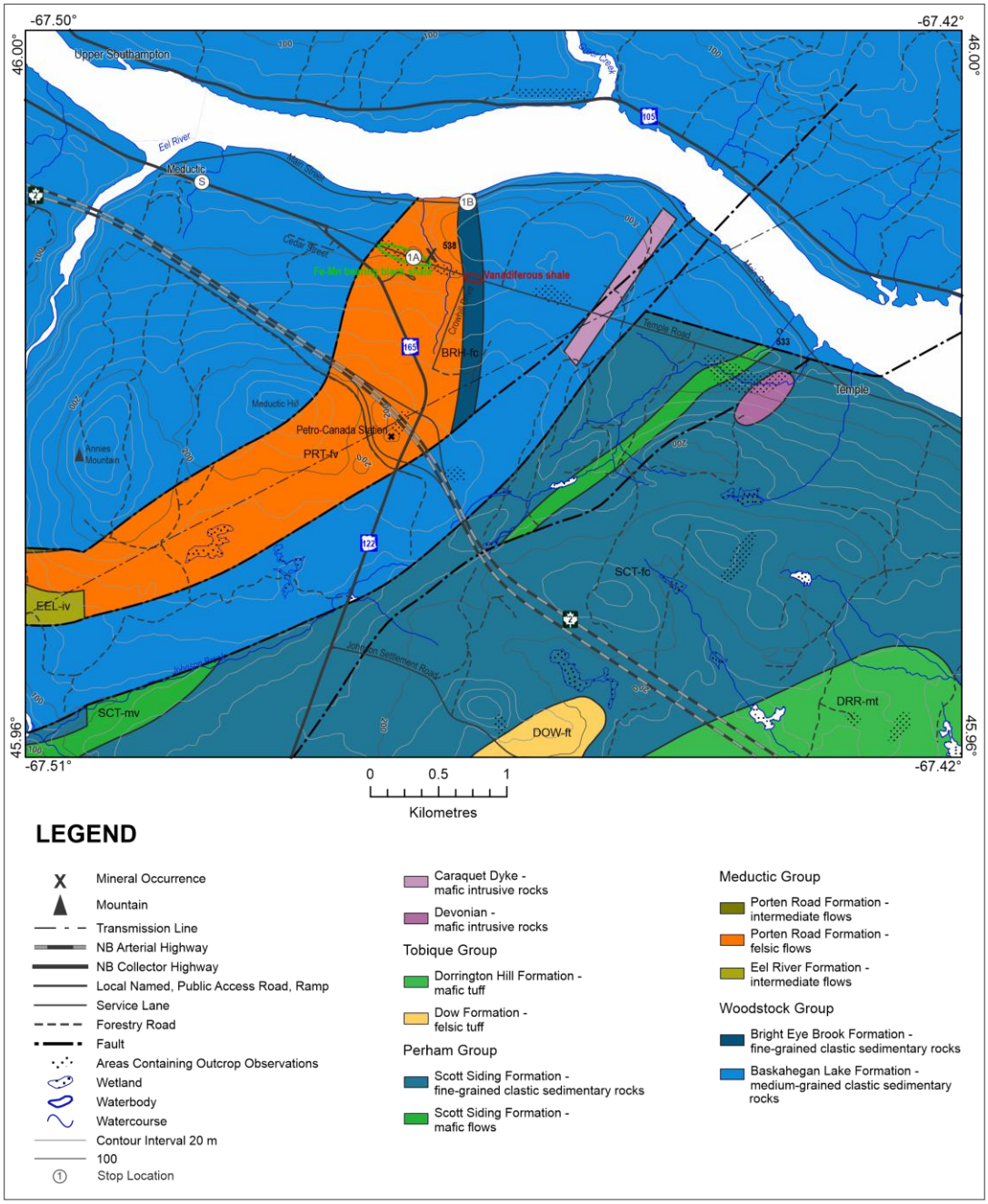

Figure 21. Geology of the Meductic area (New Brunswick Geological Survey, 2023).

11:12-11:37 15 minute STOP 3 - Rhyolitic lapilli tuff, Porten Road Formation (Fig. 13, 14) – (E 608951, N 5090381 UTM Zone 19)

STOP 3 Walking Log: Proceed to the outcrop in the ditch on the right side of the road.
STOP 3 Description: On the west side of the road, greyish pink rhyolitic lapilli tuff contains quartz crystals about 1 mm across and abundant felsic volcanic fragments that range from 1 cm to 15 cm across (Fig. 13). Sulphide clasts up to several centimetres long have been incorporated into the tuff (Fig. 14). These clasts were likely derived from stratiform massive sulphide mineralization that was deposited on the seafloor surrounding a hydrothermal vent proximal to an emerging felsic dome. The sulphide clasts would have become entrained in the pyroclastic flow during the eruptive event that produced the rhyolitic lapilli tuff.

11:37-11:39 2 minute travel time to Stop 4 – Massive and bedded andesitic tuff, Eel River Formation

Mileage
0.0 Proceed along the Benton Road
0.2 Pull off to the right side of the road

11:39-12:00 16 minute STOP 4 - Massive and bedded andesitic tuff, Eel River Formation (Fig. 18 to 20) – (E 609065, N 5089993 UTM Zone 19)

STOP 4 Walking Log: Proceed to the outcrop in the ditch on the right side of the road.
STOP 4 Description: On the west side of the road, massive, coarse-grained, greyish green andesitic tuff contains abundant plagioclase crystals ranging from 2 mm to 3 mm long and lesser andesitic volcanic fragments (Fig. 18). This massive tuff is interpreted to have been deposited as a large submarine pyroclastic flow. Scarce rhyolitic fragments in the massive tuff (Fig. 19) were likely derived from the underlying Porten Road Formation. About 5 m to the south, a sequence of bedded andesitic tuff grades southward from thin-bedded (3–4 cm), medium-grained tuff into laminated, fine-grained tuff overlain by 3 cm of dark grey shale (Fig. 20). The bedding trends 065º and dips 85º SE. These bedded tuffs are interpreted to have been derived from episodic eruptions of relatively small volumes of pyroclastic material that were deposited as submarine pyroclastic flows.

12:00-12:02 2 minute travel time to Stop 5 – Bedded basaltic tuff, Oak Mountain Formation

Mileage:
0.0 Proceed south along the Benton Road
0.2 Pull off to the right side of the road

12:02-12:17 15 minute STOP 5: Bedded basaltic tuff, Oak Mountain Formation (Fig. 30) – (E 609106, N 5089929 UTM Zone 19)

STOP 5 Walking Log: Proceed to the outcrop on the east side of the road.
STOP 5 Description: On the east side of the road, dark greyish green basaltic tuff beds, ranging from 0.5 m to 1 m thick, are interstratified with greyish maroon siltstone beds about 15 cm thick. The beds trend 055º and dip 75º NW. The basaltic tuff contains fragments (5–10 mm long) of porphyritic and aphyric basalt. These bedded tuffs were likely derived from reworking and transportation of hyaloclastic material eroded from basaltic lava flows that erupted farther upslope in the marine basin. These basaltic rocks form the uppermost part of the volcanic sequence in the Benton–Meductic area (Fig. 3, 4).

12:17-12:30 10 to 13 minute travel time & unloading to Stop 6 – Core display and lunch

Mileage:
0.0 Proceed south on the Benton Road.
0.4 Turn into the road on the left, turn around and head north on the Benton Road.
4.6 Turn right into the park near the Eel River covered bridge.

Driving and walking log continued on page 38.

PART II

CORE DISPLAY OF BASE METAL SULFIDE DEPOSITS OF THE MIDDLE ORDOVICIAN BATHURST MINING CAMP, NORTHERN NEW BRUNSWICK

James A. Walker
New Brunswick Geological Surveys Branch, 2574 Rt 180, South Tetagouche NB, E2A 7B8

THE BATHURST MINING CAMP (BMC)

The geology of the Bathurst Mining Camp, in particular the Tetagouche Group and the volcanogenic massive sulfide (VMS) deposits contained therein, have been the subject of countless scientific papers and reports, graduate thesis projects, mapping projects, field guides (e.g., McCutcheon and Lentz 1993; McCutcheon 1997; Sangster 1983; Walker 2014, 2022), and summary papers (Goodfellow 2007; van Staal et al 2003; Goodfellow and McCutcheon 2003; McCutcheon and Walker, 2019 etc.). The reader is referred to the NB Lexicon of stratigraphy (https://dnr-mrn.gnb.ca /Lexicon/ Lexicon/Lexicon_Search.aspx) for complete up-to-date descriptions and list of references for all of the stratigraphic units in the BMC. Also, the Economic Geology Monograph 11 (Goodfellow et al. 2003, and references therein), and the New Brunswick Minerals and Energy Division website https://www2.gnb.ca/content/gnb/en/departments/erd/ energy/content/minerals.html for a comprehensive listing of references via the Geoscience Publication and Mineral Reports of Work search tools.

Regional Geology

The rocks of the BMC are divided into three major tectono-stratigraphic packages (Figs. 1 and 2). At the base, Cambro-Ordovician clastic sedimentary rocks of the Miramichi Group were deposited as a fining-upward (basin-deepening sequence) on the stable Ganderia margin (van Staal et al. 2003). Middle- to Late Ordovician bimodal volcanic and related sedimentary rocks of the Bathurst Supergroup conformably to disconformably overlie the Miramichi Group and were erupted/deposited in the Tetagouche-Exploits back arc basin. This back arc basin formed in response to slab roll back induced rifting of the Popelogan Arc from the Ganderia margin in the earliest Middle Ordovician (van Staal et al. 2003).

The Bathurst Supergroup is divided into three groups that, from south to north, are: Sheephouse Brook, Tetagouche, and California Lake groups (Figs. 1 and 2; van Staal et al. 2002, 2003). These three groups are more-or-less coeval and were emplaced during the early stages of back-arc continental rifting. All three groups are at least locally conformable on the Miramichi Group but are always in tectonic contact with each other. Each of these three groups is dominated by early erupted felsic volcanic rocks that give way up-section to a second pulse of felsic volcanism (absent in California Lake Group) and thence mafic volcanic and sedimentary rocks. Minor diachrony in the ages of the felsic volcanic rocks (ca 470-465 Ma in the Tetagouche and Sheephouse Brook groups; Wilson and Kamo 2007), coupled with the ubiquitous overlying mafic volcanic rocks, is consistent with a propagating rift in an ensialic back-arc environment, with each of the three groups representing different eruptive centers (van Staal et al. 2003). In all three groups, the bulk of the VMS tonnage is associated with the first pulse of felsic volcanism, whereas second pulse felsic rocks (i.e., Flat Landing Brook Formation of the Tetagouche Group), host only a few small deposits (van Staal et al. 2003).

The Bathurst Supergroup is structurally overlain by mafic volcanic and related sedimentary rocks of the Fournier Supergroup. These rocks were deposited during the widening phase of the Tetagouche-Exploits back arc basin. Radiometric ages (Sullivan and van Staal 1996) show that the Fournier oceanic crust is slightly younger (ca. 460 Ma) than the oldest parts of Tetagouche, California Lake and Sheephouse Brook groups (ca. 470 Ma).

Late Ordovician closure of Iapetus and the Tetagouche-Exploits back arc basin via northwest directed subduction (van Staal 1987, 1994; van Staal et al. 2003) continued until final closure in the early Silurian (van Staal et al. 1990; 2003).

This led to accretion of BMC rocks onto the Laurentian margin and their incorporation into an accretionary prism (the Brunswick Subduction Complex of van Staal 1994), resulting in poly-phase deformation, mid- to upper-greenschist grade metamorphism, and assembly in a series of imbricate nappes (Fig. 2), i.e., California Lake and Tetagouche rocks were underplated to the oceanic part (Fournier Supergroup) of the accretionary wedge when the leading edge of the continental margin descended into the subduction zone (Fig. 3). The Tomogonops and Melanson Brook formations (Tetagouche Group), and the Middle River Formation (California Lake Group) formed from erosional detritus sourced from the Brunswick Subduction Complex and deposited on the down-going slab, i.e., syn-

tectonically, in a wedge-top basin during Late Ordovician-Early Silurian subduction of back arc lithosphere (Fig 3; Wilson et al. 2015).

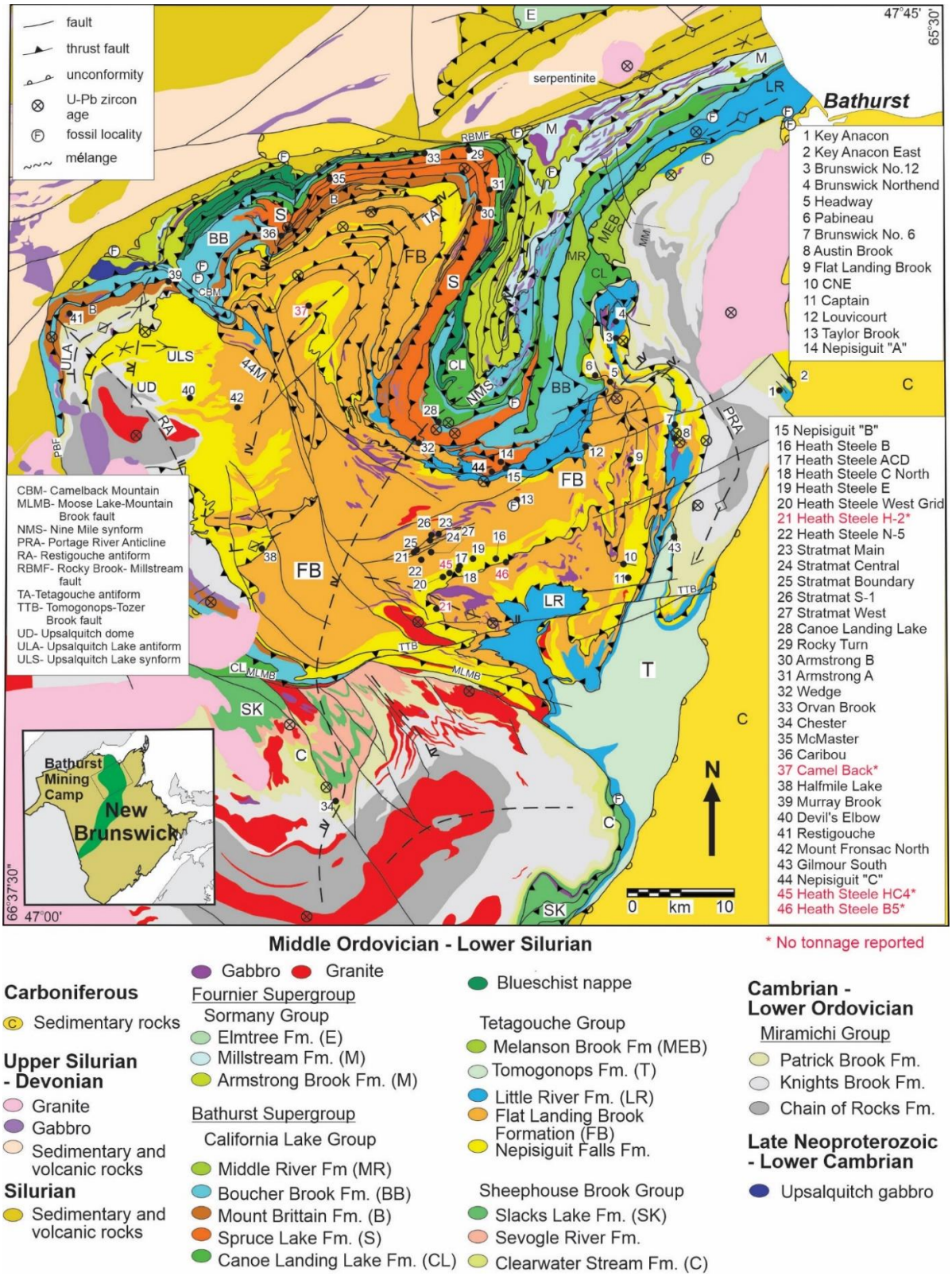

Figure 1. Geology and massive sulfide deposits of the Bathurst Mining Camp (modified from Walker 2022).

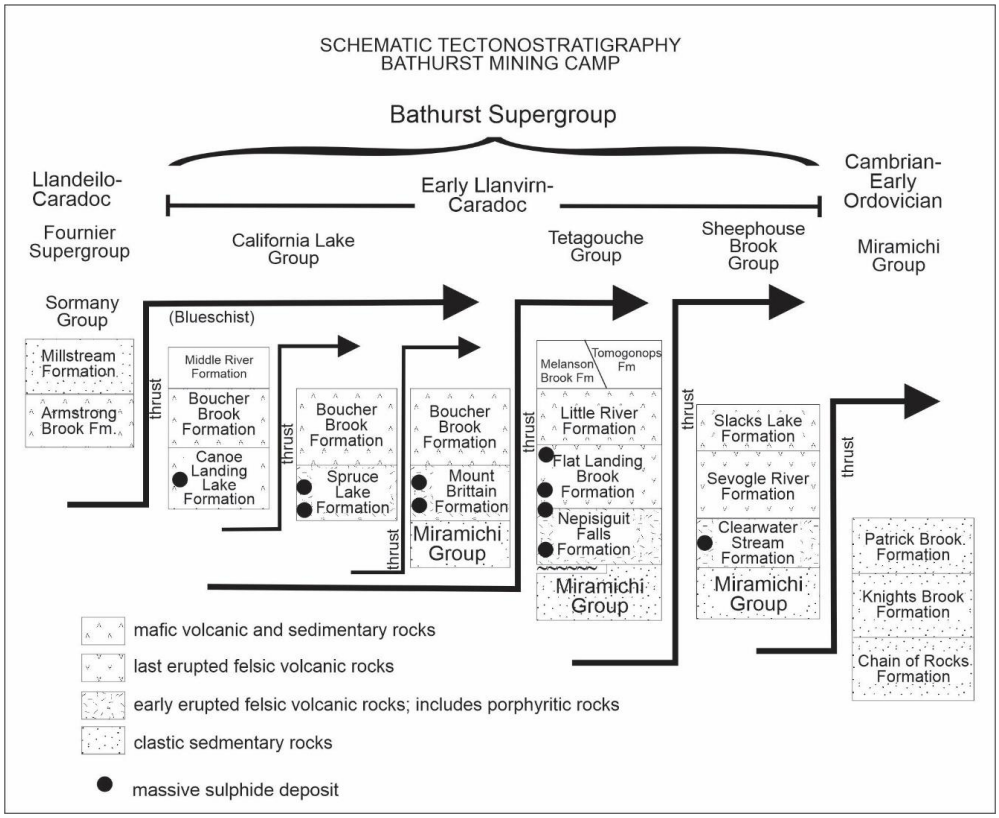

Figure 2. Tectono-stratigraphy of the major nappes in the BMC (modified from Walker 2022).

Structure and Metamorphism

Each of the three groups assigned to the Bathurst Supergroup are restricted to a major thrust nappe (or block) named for that Group (van Staal et al. 2003). The southernmost nappe (Sheephouse Brook Group) has undergone the highest grade of metamorphism, i.e., middle to upper greenschist, whereas the California Lake Group has undergone the lowest. Closure of the back-arc basin culminated with the obduction of trench-blueschist onto the former margin of the basin (van Staal et al. 1991). The time of ocean closure is constrained by the following: 1) Ar^{40}/Ar^{39} dating of phengites from the California Lake, Tetagouche and Sheephouse Brook blocks has yielded plateau ages ranging from 430 ± 4 Ma to 447 ± 6 Ma (van Staal et al. 2003), which are interpreted to date M1 deformation and metamorphic conditions (350-400ºC and 5.5-5.8 kbar; Currie et al. 2003); 2) the youngest rocks of the Tetagouche Group involved in thrusting are Late Ordovician i.e. Katian (van Staal 1994); and 3) the Fournier Supergroup is unconformably overlain by Early Silurian (Llandovery) conglomerates of the Quinn Point and Petit Rocher groups. Within this tectonic scenario, D_1 is subduction-related thrusting and occurred in the accretionary wedge prior to closure of the oceanic basin, whereas D_2 (upright isoclinal folding) is obduction-related and occurred when the accretionary wedge was thrust over the basin margin. Post-D_2 deformation includes a vertical shortening related to late Silurian-Early Devonian gravitational collapse of the orogen with recumbent folding (D3), and upright folding and associated axial planar cleavage associated with Early Devonian dextral oblique convergence and collision between Avalonia and Laurentia (D4).

Volcanogenic Massive Sulfide Deposits

The BMC contains 42 massive sulfide deposits with NI 43-101 compliant or historic resource estimates, along with 4 others significant sulfide accumulations without estimates. Collectively, these account for a pre-mining massive sulfide resource in excess of 0.5 B tonnes (McCutcheon and Walker 2019; Walker 2022). The massive sulfide deposits of the BMC are primarily tabular or sheet like stratiform masses of very fine-grained pyrite (85-95%) and subordinate zinc (sphalerite), lead (galena) and copper (chalcopyrite) sulfides. In addition, these deposits can contain significant amounts of Ag (up to 100 g/tonne), gold (typically 1 g/tonne), as well as trace amounts of Bi, Sn, Sb etc. These deposits formed at hydrothermal vent sites (commonly known as black smokers), on the sea floor (Fig. 4). Under reducing bottom water conditions, venting metal rich hydrothermal fluid (composed primarily of modified sea water that interacted with footwall rocks ± magmatic fluids) mix with sulphate rich seawater to form

metallic sulfides that precipitate from hydrothermal plumes, or from bottom hugging brines to accumulate as sulfide sheets on the seafloor. Sulfide dissolution and re-deposition occur within the growing sulfide mound due to changes in the physicochemical properties of the hydrothermal fluid with time. The upward migration of geotherms with the waxing of the system, referred to as zone-refining (Ohmoto 1996), is responsible for mineralogical zoning in VMS deposits (Fig. 4) and gives rise to Cu-rich stringer zones and vent complexes, bedded Zn-Pb rich sulfide and distal barren pyritic zones.

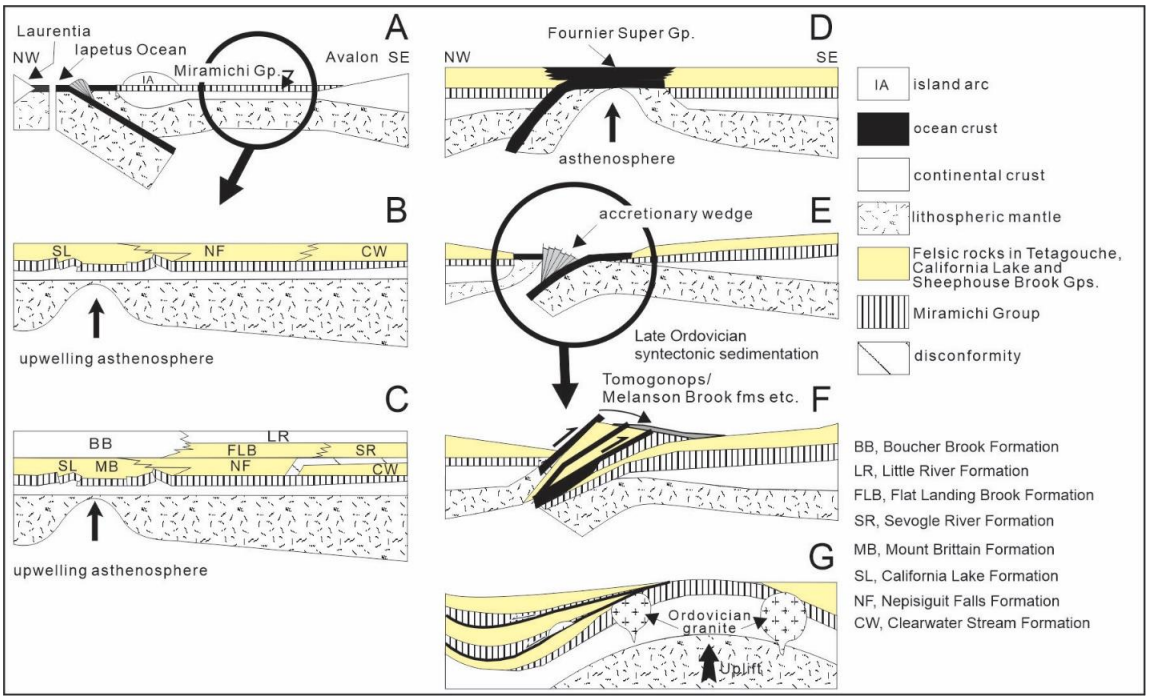

Figure 3. Middle Ordovician to Early Silurian Tectonic evolution of the BMC (modified from Walker 2022).

Massive sulfide bodies are commonly underlain by hydrothermally altered (chloritic to sericitic) footwall rocks (felsic volcanic and/or sedimentary rocks). Cross cutting stringer zone mineralization consisting of pyrite–pyrrhotite and chalcopyrite originally developed in the footwall but is commonly transposed into the massive sulfide lenses due to intense deformation in the BMC.

Algoma type iron-formation is common in deposits hosted by the Tetagouche Group in the eastern BMC where it can be traced for over 15 km along the Brunswick horizon; but is only locally developed in the western BMC. Algoma-type iron formation is not developed in the California Lake or Sheephouse Brook groups.

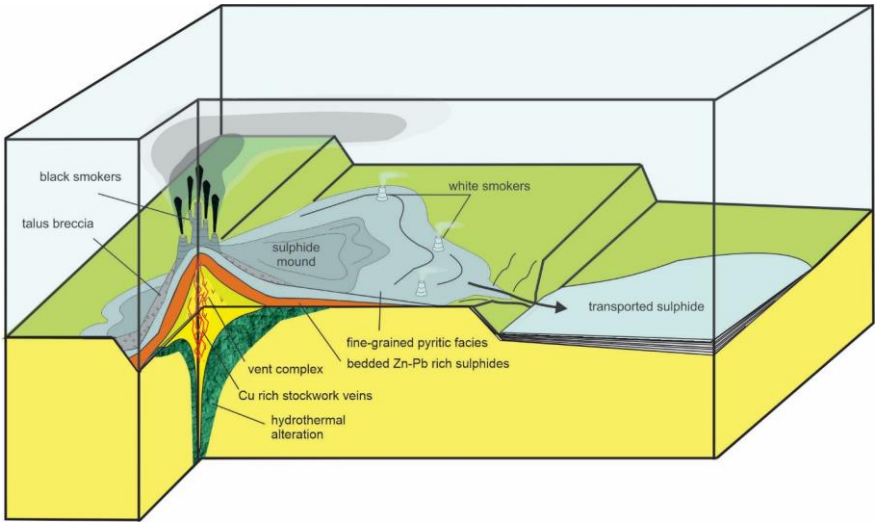

Figure 4. Idealized model of VMS system (modified from McCutcheon and Walker 2019).

BASE METAL SULFIDE MINERALIZATION FROM SEWELL BROOK; EARLY DEVONIAN VMS MINERALIZATION IN THE TOBIQUE-CHALEURS ZONE; NORTHERN NEW BRUNSWICK

James A. Walker
New Brunswick Geological Surveys Branch, 2574 Rt 180, South Tetagouche NB, E2A 7B8

Introduction

The bimodal volcanic-sedimentary succession of the Tobique-Chaleurs zone is interpreted to have formed in a transtensional tectonic setting due to oblique collision of Ganderia with Laurentia. Transpression was accomplished via movement along orogen parallel structure e.g., the Rocky Brook-Millstream (Fig. 1 inset) and Restigouche-Grand Pabos fault systems, which localized magmatic- volcanic activity and in-part controlled basin development. The Tobique-Chaleurs zone (TCZ) hosts a few base metal sulfides deposits; however, unlike the deposits in the BMC these are deposits primarily Zn >>> Pb rich (minor or no Cu) and pyrite-poor deposits that formed as subsurface replacements under oxidizing conditions and at water depths of 200 m or less.

The most significant deposit in the belt, in terms of tonnage, is the Nash Creek deposit located northwest of Bathurst (Walker 2010). In 2018, Callinex Mines Inc. reported an NI-43-101 compliant **Indicated mineral** resource totaling 13.6 Mt averaging 3.2% ZnEq. (2.7% Zn, 0.6% Pb and 17.8 g/t Ag) containing 963 million pounds of ZnEq. and an **Inferred mineral resource** totaling 5.9 Mt averaging 3.1% ZnEq. (2.7% Zn, 0.5% Pb and 14.0 g/t Ag) containing 407 million pounds of ZnEq. This deposit is hosted by bimodal volcanic (with rare flows of intermediate composition) and intercalated clastic and carbonate sedimentary rocks deposited in a shallow marine to nearshore emergent setting. Mineralization and stratigraphy appear to be controlled by a series of narrow second-order grabens adjacent the Black Point-Arleau Brook fault a major north-south striking normal fault that bounds the western limit of the Jacquet River half graben. Mineralization consists of sphalerite >> galena with very minor pyrite and marcasite and no Cu. This metal budget coupled with abundant open space and breccia fill textures, and the presence of framboids and marcasite suggest a low-temperature shallow replacement type hydrothermal volcanogenic massive sulfide (VMS) affinity.

The southern part of the Tobique-Chaleurs zone host several base metal sulfide ±Ag occurrences (Walker 2009), including: Shingle Gulch East (Walker 2005; Walker and Wilson 2013), Mount Costigan (Walker and Clark 2012), and Sewell Brook (Walker 2015) the highest-grade deposit in the Tobique-Chaleurs zone. This small (no tonnage estimate) but very high-grade system (has returned assays of up to 40% Zn. Sewell Brook is located east of Plaster rock (Fig. 1) and is the subject of this core display. Unlike most of the rest of the Tobique Group, the rocks hosting mineralization at Sewell Brook are all of intermediate composition, despite looking very much like an interlayered sequence of basalts and rhyolite at the macroscopic scale. This deposit was the subject of a New Brunswick Geological Surveys Branch report (Walker 2015); The following description is modified from that report.

Regional Geology

The TCZ is underlain by Lower Devonian bimodal volcanic and sedimentary rocks assigned to the Tobique Group (Davies 1977; Walker and McCutcheon 1995; Wilson 1990, 1992). In the study area, the Tobique Group is divided into the Costigan Mountain Formation, which overlies Cambro-Ordovician rocks of the Miramichi Zone along unconformable, intrusive and tectonic contacts, and the conformably overlying Wapske Formation (St. Peter, 1978; Fyffe and Pronk, 1985; Wilson, 1990, 1992). As originally defined, the Costigan Mountain and Wapske formations contain similar rock types, but differ in their relative proportions of sedimentary and volcanic material. As originally defined by St. Peter (1978), an isochronous contact between these two formations is inferred; however, later faunal evidence showed that they are only partly coeval and that the contact is at least locally diachronous (Han and Pickerill, 1994, and references therein).

The Costigan Mountain Formation is estimated to be on the order of 3000 m thick and contains a sequence of felsic volcanic rocks dominated by pink, light-grey or light-green massive to flow-layered, aphyric to sparsely feldspar-phyric rhyolite, ash-flow tuff, lapilli tuff and breccia interlayered with subordinate shale, siltstone, and quartzose to lithic sandstone (wacke), and minor mafic volcanic rocks (St. Peter, 1978). The overlying Wapske Formation is in gradational contact with the Costigan Mountain Formation and in the type-area consists of approximately 7900 m of locally pillowed mafic lavas, subordinate felsic volcanic and minor intermediate rocks interlayered with marine shale, siltstone, and quartzose to lithic sandstone or wacke (St. Peter 1978). However, to the north (including the Sewell Brook area) and extending to the northern limit of the Tobique Group, the Wapske Formation comprises large composite felsic-mafic volcanic edifices enveloped by sedimentary rocks (Fig. 1). According to Dostal et al. (1989) Wilson (1992) and Walker

and Wilson (2013), the felsic volcanic rocks of the Costigan Mountain and Wapske formations are dominantly rhyolites. Locally the rhyolites feature high Zr (commonly > 1000 ppm) and Zr/Ti, indicating a peralkaline composition. Intermediate compositions are not common in the Costigan Mountain Formation but locally constitute up to 20% of the volcanic rocks in the TCZ.

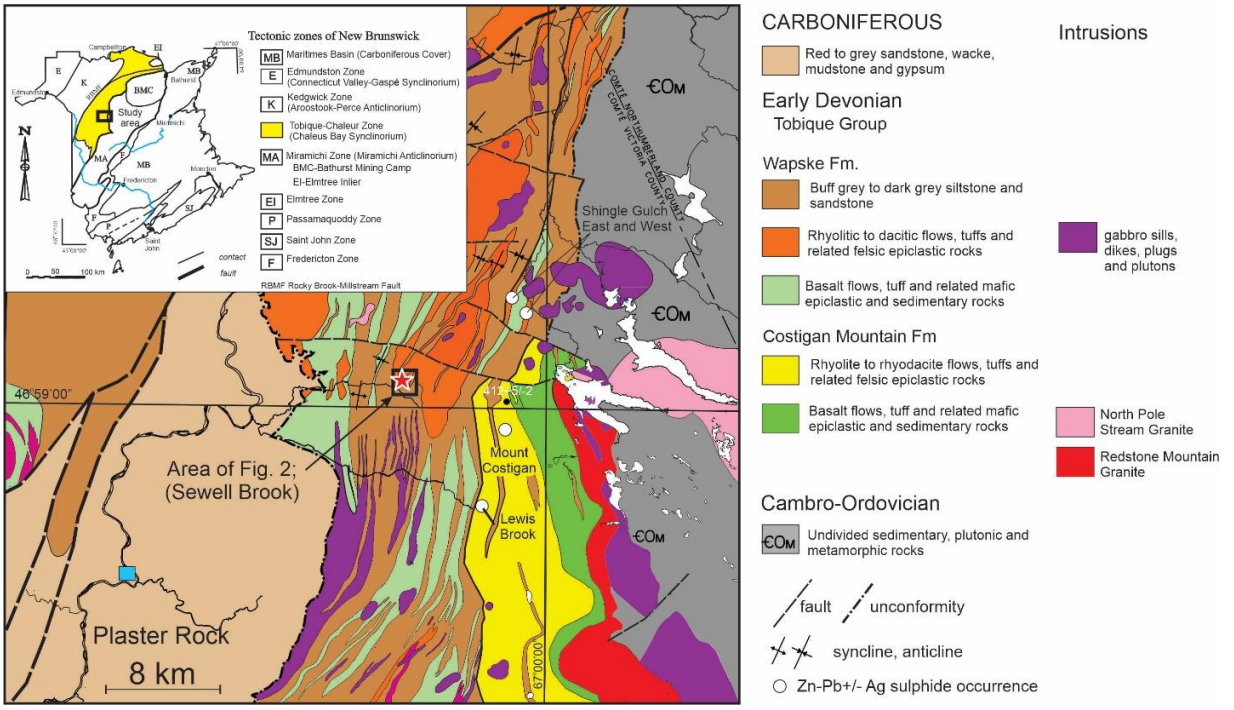

Fig 1. Location of Sewell Brook deposit (Walker, 2015).

Interlayered clastic sedimentary rocks are interpreted to reflect deposition below wave base in an outer shelf or upper slope setting in water depths of 200 m or more (Pickerill, 1986). To the northwest of the study area, Pickerill (1991) and Han and Pickerill (1994) identified trace fossils that are interpreted to have formed in a deep-water flysch environment. In contrast, the area northeast of Shingle Gulch (Fig. 1) contains scattered outcrops of quartz-pebble conglomerate indicating a much shallower to near-shore depositional environment. Collectively, paleo-environmental evidence is interpreted to reflect a deepening of the sedimentary basin from northeast to southwest, and possibly a marine transgression approximately coinciding with the Costigan Mountain-Wapske transition.

The Tobique Group in the southern TCZ is intruded by numerous small (surface area < 4 km^2) mafic and rare felsic plutons. One felsic pluton, the Redstone Mountain granite, sutures the contact between the TCZ and the Miramichi Anticlinorium east of Shingle Gulch (Fig 1).

Age control on the Tobique Group is based primarily on paleontological data that consistently yield Early Devonian ages. Two reliable radiometric ages are reported from the Tobique Group in this area. The first is a U–Pb (zircon) age of 412.5 ± 2.0 Ma, which was from a sub-volcanic felsic intrusion cutting rocks near the top of the Costigan Mountain Formation, approximately 16.5 km south of Shingle Gulch East (Fig. 1; Wilson and Kamo 2008). The second is a LA-ICPMS U-Pb zircon age of 420.7 Ma age (Lochkovian) obtained from the base of the Formation (Wilson pers. Comm.) and is consistent with a Pridoli (Latest Silurian) to Lochkovian age.

Overall, the TCZ is a northeast to locally east-northeast striking belt. Shallowly plunging fold axes are parallel or sub-parallel to the regional trend and may display reversals in plunge (Fig. 1). Despite the apparent folding in these rocks penetrative cleavage is absent to very weakly developed throughout the TCZ; however, penetrative fabric may be locally developed in proximity to faults. Numerous faults occur in the belt and are of two dominant orientations. The first group is oriented parallel to major fold axes and locally demarcates the margin of the belt, e.g., the Rocky-Brook−Millstream Fault (Fig. 1 inset). The second set of faults is oriented east west and is of dominantly dextral offset (Fig. 1).

Deposit Geology

Mineralization is not well exposed at Sewell Brook. Consequently, investigations and interpretation are based on the extensive inventory of reported diamond drill core and logs (Giggie 1991, 1992; Walker 1997, 1998; Burton 2009, 2010, 2012).

The volcanic rocks hosting the Sewell Brook deposit are dominated by fragmental facies (e.g., hyaloclastite breccia, micro-breccia, debris flow deposits, etc.) that are commonly less than 10 m thick (Figs 2 and 3). Fragmental rocks (hyaloclastite) are intercalated with tongues and lobes of massive, devitrified rhyodacite (TiO_2 > 0.5–1.5 wt %; avg ~0.9 wt % and Zr ≥ 500 ppm), and narrow intervals of sedimentary rock that commonly contain randomly distributed accidental fragments of volcanic rock. Dykes of rhyolite occur in very limited number and are unaffected by mineralization or deposit-related hydrothermal alteration. Fragmental volcanic units increase in thickness toward the north and east of the deposit (down section) and there is an increase in the proportion of massive volcanic flows to the north and the east (Figs. 3a and 3b). Collectively, these observations indicate that the Sewell Brook deposit formed on the margin of a submarine volcanic dome complex that was probably centred northeast of the deposit. Replacement style mineralization and associated alteration are developed in intercalated sedimentary units in proximity to volcanic units but only over relatively narrow widths.

The sulphide textures range from disseminated to stockwork veins to semi-massive zones; however, bedded, pyrite-rich stratiform sulphides that are typical of VMS systems and Fe-Si-rich Algoma-type exhalative sedimentary rocks are absent at Sewell Brook. Mineralization is dominated by sphalerite and subordinate galena, although a small chalcopyrite rich zone is present in which Cu ≥ (Zn + Pb). Pyrite is subordinate to sphalerite and galena throughout most of the deposit, although in some core intervals it is the dominant or only sulphide phase. With the exception of the rhyolite dykes, all the volcanic host rocks are affected by mass addition of K and mass loss of Na (Walker 2015). Deposit-related hydrothermal alteration is dominated by chlorite and subordinate sericite alteration in proximity to sulphides, whereas silicification and bleaching occurs in more distal parts of the system.

On the basis of sulphur isotopes in coexisting sphalerite-galena pairs, the temperature of formation of the deposit is approximately 310ºC. The relatively tight spread of $\delta^{34}S$ values for the various sulphide phases (3.9–12.6‰) is consistent with an Early Devonian seawater source for the sulphur. These data, together with the absence of bedded sulphides, support a submarine/subsurface replacement VMS model for the Sewell Brook deposit (Wilson 1992; Walker 2015).

Mileage

12:30-1:30 60 minute STOP 6: Eel River covered bridge, core display and lunch – (E 607829, N 5093479 UTM Zone 19)

STOP 6 Walking Log: Proceed to the drill core display set up in the park

STOP 6A Description: The drill core on display is not from one drill hole. Rather, it consists of selected boxes from several drill cores from three deposits, namely: Gilmour Brook South (Walker 2005); Halfmile Lake (Walker and McCutcheon 2011); Canoe Landing Lake (Walker and McDonald (1995) and from the Nepisiguit Brook area (see Fig 1 and poster). These cores provide examples of host rock types and sulfide mineralization typical of VMS deposits hosted by the Nepisiguit Falls Formation (Tetagouche Group). See "Tetagouche Group" on Fig. 2 for stratigraphic column. The Tetagouche Group is the most prolific group in the BMC in terms of massive sulfide endowment and host several significant past-producing mines, most notably: Brunswick #12 and #6, and Heath Steele ACD and B, as well as significant deposits at Halfmile Lakes, Key Anacon, and Gilmour Brook South.

1. Miramichi Group footwall sedimentary rocks from Gilmour Brook South deposit (DDH GS 99-28, box 180 790m)
2. First pulse felsic volcanic rocks quartz-feldspar crystal tuff (QFPorphyry) and altered equivalent quartz crystal tuff (QAS) from Nepisiguit Brook area (DDH STW 14-7 box 14 quartz feldspar crystal tuff, and DDH STW 14-7 box 105 quartz and quartz feldspar crystal tuff).
3. Pyrrhotite-chalcopyrite replacement mineralization from the base of the Halfmile Lake deposit (DDH HN 95-86A; 2 boxes 924-933 m).
4. Stratiform massive sulfides lens with infolded Algoma-type Fe formation from Halfmile Lake deep zone (DDH HN99-123; 3 boxes, 1173-1189 m).
5. Transported (debris flow) massive sulfides from Canoe Landing Lake deposit (DDH CL94-2 Box 56, 235.7-240 m).
6. Second pulse felsic volcanic rock, Flat Landing Brook Formation, from Gilmour Brook South (DDH GS-00-37B 788-791 m).
7. Little River Formation basalt; Gilmour Brook South; DDH GS-00-37B 615-620 m).
8. Tomogonops Formation syn-tectonic detritus from accretionary prism. From Gilmour Brook South; (DDH GS-00-37B Box 57- 226-231 m)

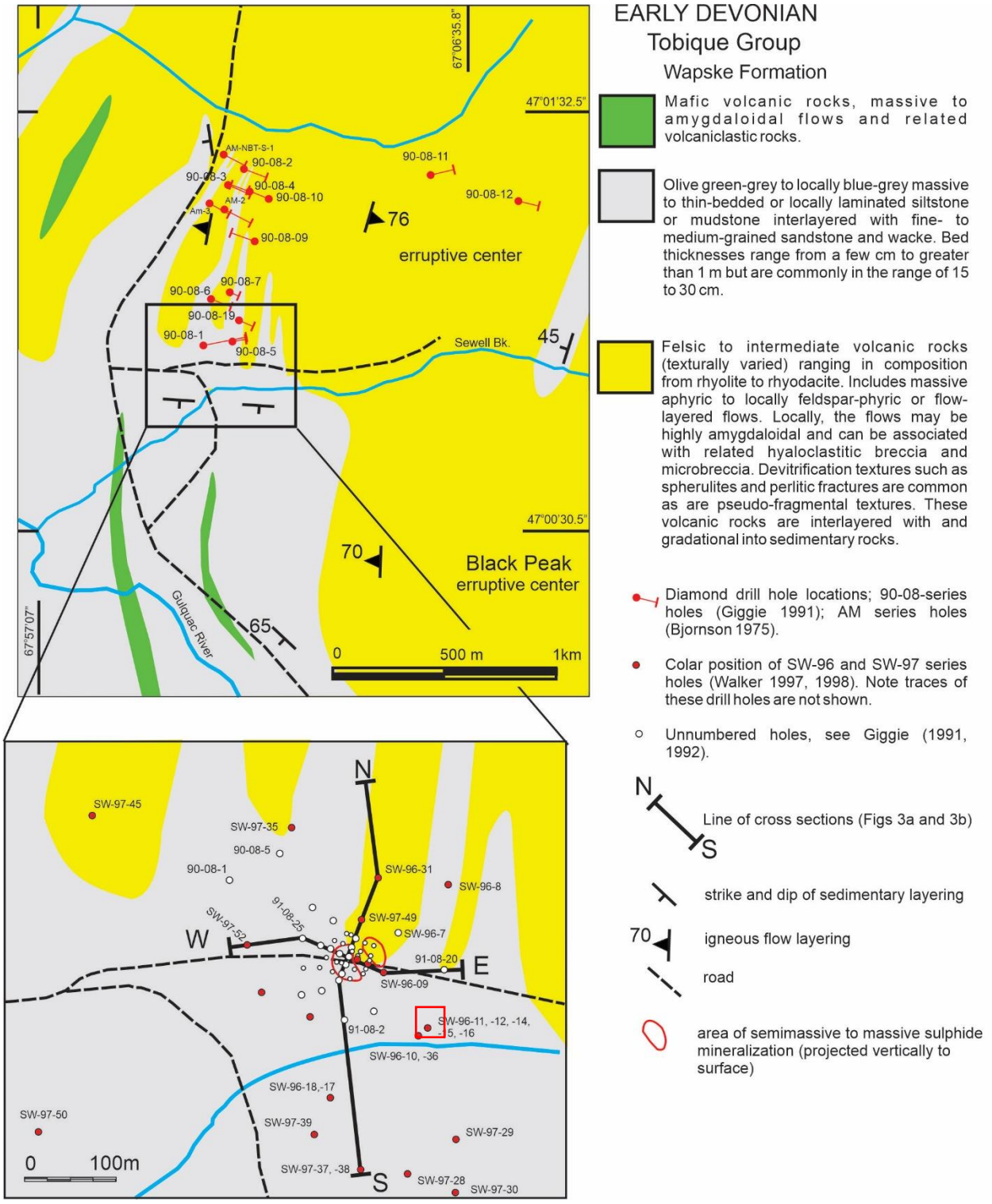

Fig. 2. Geology of the Sewell Brook deposit (Walker 2015). Area of Fig. is located on Fig. 1. N-S and E-W sections are presented in Figs. 3a and 3b. Core to be viewed is from DDH SW-96-12 (drilled toward 256º at a dip of -60º from horizontal) the interval on display is from 31-109 m. Red box highlights collar for SW96-12. See log for details.

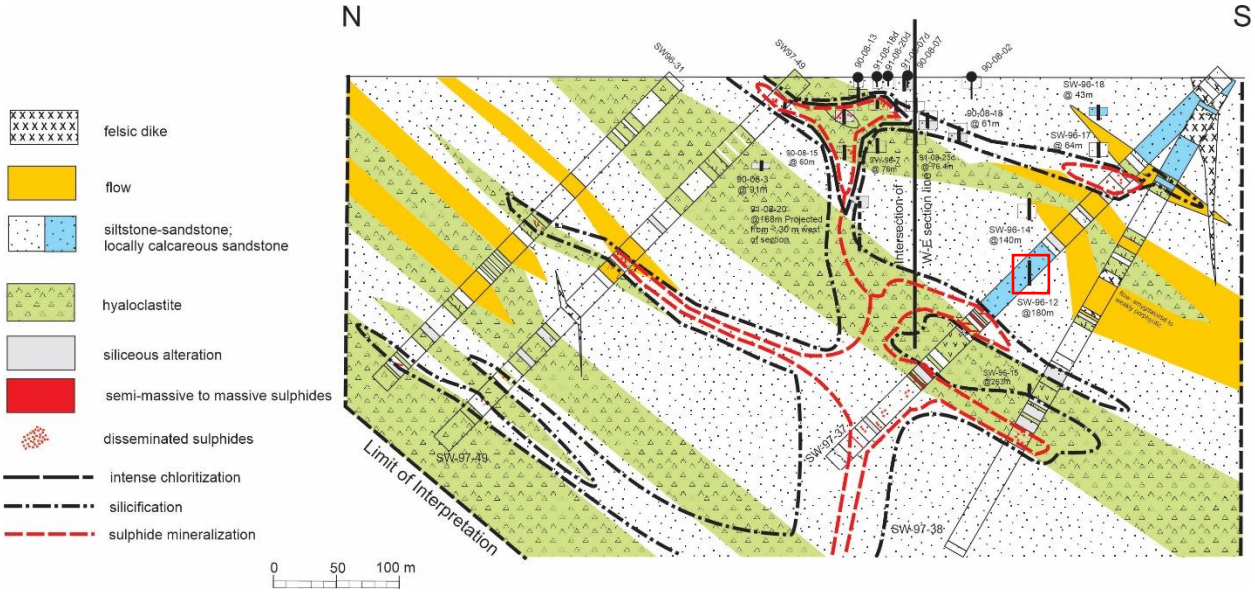

Fig 3a. N-S cross section through the Sewell Brook deposit with line of section is located on Fig. 2 (Walker 2015). Red box highlights area of intercept of DDH SW96-12 in this section.

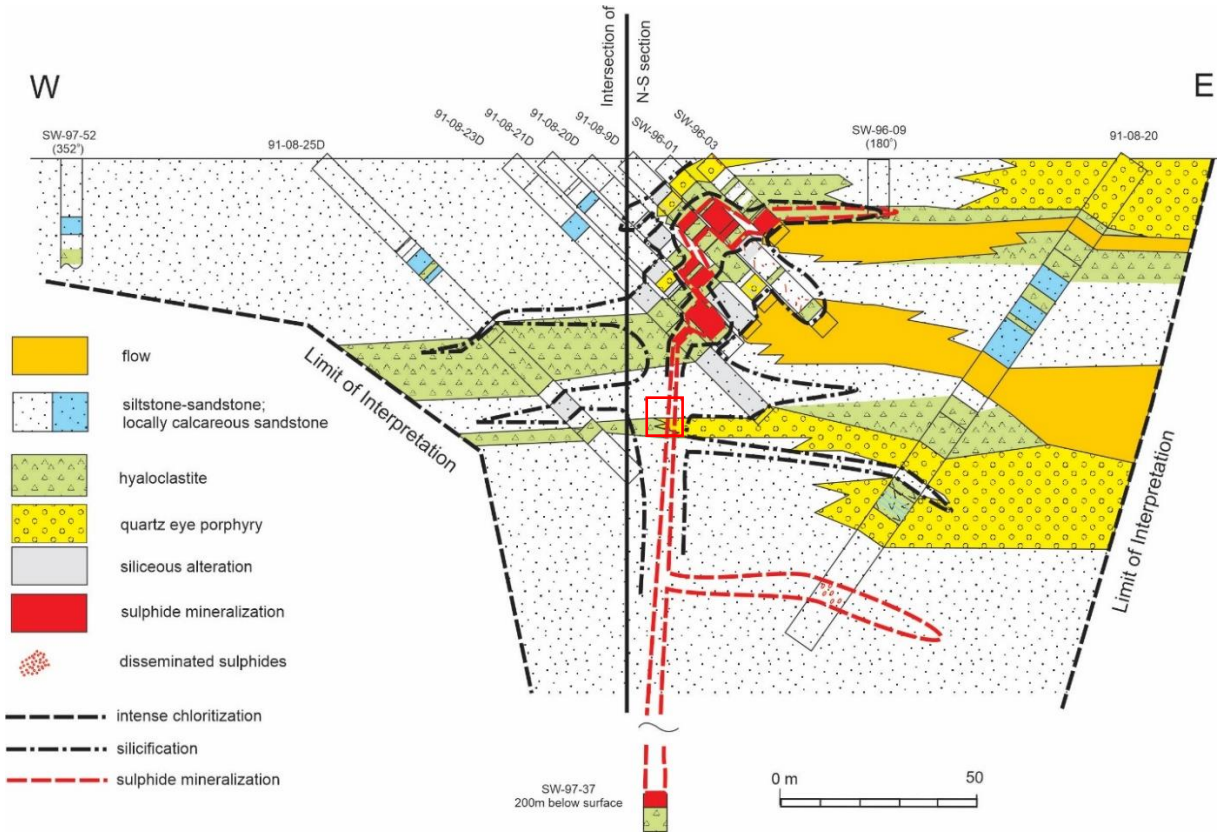

Fig 3b. West-East cross section through the Sewell Brook deposit, line of section is located on Fig. 2 (Walker 2015). Red square represents approximate position (projected up dip) of the mineralized drill core interval on display from drill core SW96-12

STOP 6B Description: The core display from Sewell Brook is from DDH SW-96-12 boxes 13-26 (31-109 m) and is typical of the syngenetic volcano-sedimentary hosted based metal sulfide mineralization of this deposit. The log for this drill core (reproduced below) is from Walker (1998). Note that log from 113.8m to 128.3 m (pg. 6) is missing.

CHAPLEAU RESOURCES LTD. HOLE NO.: SW96-12 PROPERTY: SEWELL BROOK

Commenced: 09/27/96	**Location:** Sewell Brook	**Hor. Comp:** ---	**Hole No.:** SW96-12
Completed: 10/01/96	**District:** ---	**Vert Comp.:** ---	**Length:** 201.14m
Co-Ordinates: 0+60S/0+90E	**Core Size:** NQ	**Logged By:** E.A. Brooks/K. Garnett	**Elevation:** ---
Longitude: ---	**Tests:** 100m, -59°; 268.5°	**Date:** 09/28/96	**Collar Dip:** -60°
	Latitude: ---	**Azimuth:** 256°	**Corr. Dip:** ---

METERS FROM	TO	DESCRIPTION	SAMPLE NO.	FROM	TO	AU ppb	AG ppm	PB ppm	ZN ppm	CU ppm
0	4.27	Casing - measuring from bottom of casing at 4.27m (0 is actually 4.27m downhole).								
4.27	25.7	MAFIC SEDIMENTS: Very fine grained, greenish in colour. Banded or layered at 30° to c/a. As with SW96-11 there is a distinct core angle of 30° with bedding. Some coarser layers contain disseminated py cubes along the contacts. Rock is generally quite soft and FeO stained along fracture surfaces. Some more porous zones are FeO-MnO stained due to apparent leaching and oxidation. Apparent graded bedding indicates tops as up-the-hole. Sharp lower contact at 30-35° to c/a.								
25.7	53.5	SILTSTONE (TUFFACEOUS INTERBEDS): Fine grained dark bluish grey siltstone with minor tuffaceous interbeds. 25.7-28.6m - blue-grey siltstone (35° to bedding) 29.5-29.75m - tuffaceous interbed 29.75-30.0m - siltstone 30.0-32.9m - tuff, minor sed interlayers, 35° to c/a. 32.9-49.6m - thick sedimentary interval. Blue-grey siltstone, soft sed. def. features common (load casts). Desiccation cracks - sub-aerial exposures at 44.1m. Bedding 35-40° to c/a. Blebs of py associated with turb layers (<0.5% py). Local, thin CaCO3 filled fractures crosscut bedding at 30° to c/a. Sharp lower contact at 35° to c/a. 49.6-53.5m - greenish tuffaceous seds. Core loss from 49.6-50.2m (60cm). 50.2-53.5m - tuffaceous seds (impermeable). Diffuse, graded bedding, olive green colour, tops up hole.								
53.5	57.5	STRONGLY SILICIFIED TUFFACEOUS SEDIMENT (TUFFACEOUS SILTSTONE?): Fine grained, grey, massive, hard aphanitic rhyolite. Layering at 50° to c/a. Occasional py stringers. Trace ZnS/PbS along fractures (<0.5%). Fragmental zone at 55.5-55.6m.	281646 281647	53.50 55.50	55.50 57.50	.50 0	5.83 7.88	510 2290	1970 7460	60 100

MINING RECORDER'S COPY
Fredericton, N. B.

475168

HOLE NO.: SW96-12 **PAGE: 2**

METERS FROM	TO	DESCRIPTION	SAMPLE NO.	FROM	TO	AU ppb	AG ppm	PB ppm	ZN ppm	CD ppm
		Broken lower contact. Stringer red brown Zns over last 10cm, trace PbS. Fragmented/brecciated upper contact over 3cm. PbS along laminations, parallel to bedding and along fractures.								
57.5	61.0	PYRITIC CHLORITIC FRAGMENTAL: Dark greenish grey fragmental with extensive CaCO3 veining at 10-30° to c/a. Interlayered cherty, rhyolite units from 57.7-57.9m, 58.8-59.2m. Contains 3-5% pyrite throughout except in rhyolitic units (layering 45° to c/a).	281648 281649	57.50 59.10	59.10 61.00	160 380	9.26 18.85	3590 14300	8800 33600	140 250
		58.8m - stringer and blebs of red-brown ZnS, trace PbS, parallel to c/a (5cm) (relict silicified bedding).								
		60.0-60.3m - stringer ZnS (3), trace PbS at 25-30° to c/a.								
		59.1-61.0m - zone with 10-15% py, trace - 2% ZnS/PbS. Sedimentary protolith suggested by silicified bedding from 58.7-59.1m. Relict silicified clasts in chlorite ± carbonate (calcite) matrix where most intensely altered.								
61.0	65.4	SILICIFIED TUFFACEOUS SEDIMENTS/SILTSTONE: Fractured and locally chloritized siliceous grey rhyolite. Occasional CaCO3 fracture fill. Flow banding local at 30° to c/a.								
		61.0-62.4m - contains trace - 1% ZnS/PbS as fracture fill. Fragmental, broken up core chips over last 50cm.	281650	61.00	62.40	90	10.63	7210	11500	990
		62.4-63.0m - chloritic, fragmental zone with friable core. 3-5% py, trace ZnS/PbS (sheared at top 10cm).	281651	62.40	63.00	80	6.86	6090	17300	170
		63.0-64.3m - grey rhyolite, local flow banding, silicified. Fractured with local CaCO3, chloritic, and trace PbS/ZnS fill. Silicified relict bedding.	281652	63.00	64.30	10	4.80	2660	4160	290
		64.3-65.4m - chloritized flow banded rhyolite (not fragmental) dark greenish grey, 2-3% py, trace ZnS, PbS along fractures. Broken lower contact (by fault). Strongest silicification associated with ZnS/PbS veinlets (ie 61.0-61.3m) - cut surface (63.0-64.3m). Veinlets rimmed by PbS with ZnS ± cpy in core. Relict evidence of soft sed. def. at 61.87m - siltstone(?)	281653	64.30	65.40	100	7.74	10500	22700	800
65.4	76.0	PYRITIC CHLORITIC FRAGMENTAL: Fault gouge over first 20cm with chlorite-rich chips of core.								
		65.4-67.2m - sheared interval - rounded siliceous clasts in a fragmental, chloritic - pyritic matrix. Local CaCO3 fractures. 8-10% py, 1% ZnS, trace PbS. Banded at 30° to c/a. First and last 20cm of this zone are fault gouged.	281654	65.40	67.20	120	15.43	19700	29200	1510

HOLE NO.: SW96-12 **PAGE: 3**

METERS FROM	TO	DESCRIPTION	SAMPLE NO.	FROM	TO	AU ppb	AG ppm	PB ppm	ZN ppm	CU ppm
		67.2-68.4m - siliceous zone with white siliceous fragments in a CaCO3 rich matrix with chloritic fragments. Trace blebs of red-brown ZnS and py.	281655	67.20	68.40	30	8.23	4390	10000	560
		68.4-70.6m - rounded, local siliceous fragments in a pyritic/chloritic matrix. Riddled with CaCO3 fracture fill at avg. 45° to c/a. Small, clay rich fault gouges at 69.2 and 70.2m. 8-10% py, trace ZnS. Sulphides at 30° to c/a. Pyritic replacement of relict silicified clasts evident at 68.9-69.0m.	281656	68.40	70.60	70	7.88	1010	2970	80
		70.6-76.0m - lower section of unit is intensely chloritized and pyritic. Remnant visible siliceous clasts (pyritized). Clasts and stringers of fine grained py (up to 10-15%). Local blebs (rounded) of red-brown ZnS, trace PbS. Locally faulted, with broken up fragments of core at: 71.2-72.2m; 73.5-73.5m. Sharp lower contact at 45° to c/a.	281657 281658 281659	70.60 72.60 74.60	72.60 74.60 76.00	120 310 80	10.63 6.17 9.60	1610 1240 2650	5460 10800 7160	120 170 170
76.0-80.9		FRAGMENTAL, SILICIFIED BRECCIA (INTENSELY SILICIFIED ZONE) - SILICIFIED BRECCIA: Fine grained, grey breccia with rounded light grey silicified fragments in a darker grey matrix. Local, interstitial sericite. Local blebs of red-brown ZnS. Up to 0.5% Pb + Zn (trace Pb). Lower contact broken, rounded off by drill bit. 70cm of core missing between this unit and top of massive sulphide zone as from 78.0-81.0m only measures 2.3m in core box and lower contact of rhyolite contains broken up pieces of core and top of massive sulphide zone is rounded off by drill (probable fault).	281660 281661	76.00 78.00	78.00 80.90	130 130	4.11 4.11	690 2050	7240 5760	260 200
80.9-86.1		MASSIVE SU[illegible]S (INTENSELY SILICIFIED, CHLORITIZED, PYRITIZED SEDS?): 80.9-8[illegible]m : [illegible]ritic, pyritic (10-20% py) host with local, rounded silice[illegible] (81.8-82.2m). Banded massive sulphides at 35-45° to c/a. Strin[illegible], f[illegible]rained light py (10-20%). Red-brown ZnS blebs, disseminated PbS an[illegible]py. [illegible]erall avg. 5-6% Pb + Zn, 0.5% Cu. 82.0-82.46m - fault zone.	281662 281663	80.90 81.70	81.70 82.60	0 350	60.00 32.22	106600 52100	203600 95300	13400 4180
		82.6-83.7m - 1.1m fault gouge (only 30cm in box therefore 80cm of missing core). Tiny chips of chloritic, pyritic core.	281664	82.60	83.70	180	19.88	33700	55700	4140
		83.7-86.1m - chlorite hosted massive sulphides. Weak banding/foliation at 35° to c/a. Chlorite host with local interstitial CaCO3. ZnS as spheroidal blebs. Disseminated and minor stringer py (10-20%). Disseminated PbS, cpy. Overall avg. 10% Pb + Zn + Cu (0.5% Cu). Last 30cm lower grade more host chlorite. Broken lower contact.	281665 281666 281667 281668	83.70 84.40 85.10 85.80	84.40 85.10 85.80 86.10	290 370 0 150	53.82 51.76 45.25 20.91	114000 95000 98900 30500	205200 205800 250800 136100	4360 5590 4030 4240
86.1-92.5		SILICEOUS SULPHIDE ZONE: Silicified, relict clasts/fragments - indeterminate unknown protolith. Fragmental, siliceous relict clasts of unknown protolith (suspect sediments) light to very light grey with local clasts of chlorite and interstitial sericite. Sulphides are interstitial around siliceous fragments with local massive to semi-massive zones. Contain local fractures filled with CaCO3 at 60-70° to c/a which crosscut sulphides and host rock.								

HOLE NO.: SW96-12 **PAGE: 4**

METERS FROM	TO	DESCRIPTION	SAMPLE NO.	FROM	TO	AU ppb	AG ppm	PB ppm	ZN ppm	CU ppm
		86.1-88.0m - interstitial sulphides in fragmental, siliceous host: =2-3% Pb + Zn, 0.25% Cu overall avg.	281669	86.10	87.00	10	8.23	12600	27000	1480
			281670	87.00	88.00	50	7.20	9300	26900	2120
		88.0-88.6m - higher concentration of sulphides, semi-massive from 88.4-88.5m. Overall avg: 5% Pb + Zn, 1% Cu.	281671	88.00	88.60	20	7.54	4150	61700	7950
		88.6-89.4m - locally semi massive (89.1-89.3m) with more visible cpy. =4% Pb + Zn, 1.25% Cu.	281672	88.60	89.40	0	7.20	1950	45900	9600
		89.4-89.7m - massive sulphides - 30% Pb + Zn + Cu (3% Cu).	281673	89.40	89.70	100	54.51	63900	316400	22000
		89.7-92.5m - stringer zone with stringers and blebs of red brown ZnS, minor stringer cpy, disseminated PbS. Stringers at random angles to c/a (around siliceous fragments. Avg. 1-3% Pb + Zn, 0.25% Cu (a bit higher in first sample section). Broken lower contact (rounded off by drill).	281674	89.70	90.30	40	7.54	2550	114800	5280
			281675	90.30	91.30	50	3.77	5340	21600	2300
			281676	91.30	91.90	60	11.66	24900	53300	890
			281677	91.90	92.50	10	7.20	15700	52900	1480
92.5-96.8		CHLORITE HOSTED SULPHIDE ZONE: 92.5-94.4m - massive sulphides in a chloritic matrix with local specks of CaCO3. ZnS as red brown spheroidal blebs surrounded by PbS. Local disseminated cpy and py. 20% Pb + Zn, 0.5% Cu overall avg. Fault gouge at 93.8m with 1cm of clay at 45° to c/a. Fault also at 93.5m at 50° to c/a. ZnS blebs (tear drops) within and/or rimmed by PbS. Locally masses of very fine grained py and possible clast fragment replacement.	281678	92.50	93.50	130	40.11	124700	308200	6050
			281679	93.50	94.40	160	19.54	51200	299600	4140
		94.4-95.1m - fragmental, siliceous zone with siliceous clasts in a chloritic pyritic matrix. Blebs of red brown ZnS both in fragments and matrix. Trace PbS, cpy. Avg. 2-3% Pb + Zn (<0.5% Cu).	281680	94.40	95.10	80	4.11	2450	49800	900
		95.1-96.8m - extremely chloritic zone with lenticular blebs of red brown ZnS aligned parallel to foliation at 30° to c/a. Fine grained, disseminated blebs and stringer py (10-20%) minor PbS, trace cpy. Overall avg. 4% Pb + Zn, <0.5% Cu. Sharp lower contact at 45° to c/a. Fault at 96.3-96.4m at 40°. Discrete fault planes at 96.5m, 96.12m at 30° to c/a.	281681	95.10	96.00	100	5.83	770	111900	2150
			281682	96.00	96.80	40	6.17	1620	88900	1850
96.8-102.0		FRAGMENTAL RHYOLITE (INTENSELY SILICIFIED ZONE - SILTSTONE(?) SEE 102.0-102.7m: (Same as from 76.0-80.9m.) Rounded, pale grey rhyolite fragments in a darker grey rhyolitic matrix. Local interstitial chlorite (esp. near upper contact) and CaCO3 (interstitial and fracture fill). Contains 2-3% py as fine grained disseminations blebs and minor stringers of red brown ZnS, trace PbS, cpy. Overall avg. 0.5% Pb + Zn, trace Cu. (May avg. a bit higher Zn over first sample section).	281683	96.80	98.80	30	3.09	1020	22900	190
			281684	98.80	100.30	70	2.74	380	15600	230
			281685	100.30	102.00	10	3.43	990	4450	1160
		98.9-99.0m - 10cm chlorite/pyrite zone with =5% ZnS. Fault zone.								
		99.8-100.0m - 20cm chlorite/py zone. Siltstone fragments evident from 101.0-102.0m. Sharp lower contact at 50° to c/a.								

HOLE NO.: SW96-12

METERS FROM	TO	DESCRIPTION	SAMPLE NO.	FROM	TO	AU ppb	AG ppm	PB ppm	ZN ppm	CU ppm
102.0	102.7	SILTSTONE: Massive, homogeneous, fine grained, silicified (hard) light grey siltstone. Bedding at 45° to c/a. Trace cpy in fracture at 102.45m, local chlorite filled fractures. Irregular lower contact ≈40-45° to c/a. Sheared at 102.16m - 45° - slickensides at ≈90° to long axis. Tops up hole - graded bedding load structures.	281686	102.00	102.70	20	1.71	70	1480	550
102.7	107.3	MAFIC/CHLORITIC FRAGMENTAL: With relict bedding at 103.1m (fragmental mixing zone mafics and seds). Mafics from below with in situ(?) sediments - both brecciated. Irregular shaped siltstone fragments in a chloritic mafic tuffaceous matrix. Grey/black mottled looking. Stringer sulphide zone with red brown ZnS stringers (random angles) dominating top section, py stringers near lower contact. Overall avg. 1-2% Pb + Zn (trace Pb), trace cpy. Local CaCO3 with stringers. 105.3-105.4m - large ZnS stringer with honey ZnS in center of stringer, disseminated PbS and cpy. Zoned ZnS red on margin, honey in core of stringer. 105.2-106.1m - siliceous, locally bleached zone. 106.4-107.3m - stringer py zone with 10-20% py. Weakly foliated near lower contact at 45° to c/a. Broken lower contact. Has appearance of mafic tuff breccia fragments rimmed by py in a py-rich matrix - Novagold/R. Wilson interpret as flow banded rhyolite fragmental also mafic tuff = devitrified rhyolite. May pass upward from mafic tuff below into overlying pyritic fragmental ± ZnS ± PbS. Complex, anastomosing py veinlets with local ZnS cores ± PbS.	281687 281688 281689 281690	102.70 104.30 105.20 106.40	104.30 105.20 106.40 107.30	10 40 0 80	5.14 4.80 9.94 12.00	2160 4530 27600 23200	58200 45000 67100 65700	1010 1140 1850 680
107.3	111.5	MAFIC TUFF: Fine grained bluish grey mafic tuff with devitrification texture throughout. Scattered stringers and fracture filling of py and red brown ZnS (local blebs also) at various angles to c/a. Local clasts and fracture fill of CaCO3. Tiny specks of chlorite occur throughout. Overall sulphide avg. ≈0.5% Zn, trace Pb and Cu (disseminated PbS and cpy). Hard, silicified for 1m at lower contact, sharp but broken lower contact. Looks to be ≈30° to c/a. Chlorite along contact with ZnS and py. Note: interpreted as devitrified rhyolite by R. Wilson. ZnS rimmed by PbS and py. Minor interstitial blebs of cpy. Py veinlets associated with darker (altered - chloritized) bands.	281691 281692 281693	107.30 109.20 110.40	109.20 110.40 111.50	60 20 50	3.77 4.46 5.14	5210 7390 8560	11800 14000 18400	350 740 1110
111.5	115.0	SILTSTONE: Fine grained, light grey, hard silicified siltstone. Bedding at 25° to c/a. Local CaCO3 in fractures with sulphides. 113.3m - 6cm wide ZnS stringer (red brown - 50% ZnS) trace PbS, py, cpy at 35° to c/a associated with brecciated, silicified siltstone fragments, stringer cored by ZnS and rimmed by PbS and py. Py ± PbS pervades veinlets extending into host silicified siltstone.	281694 281695 281696	111.50 113.00 113.50	113.00 113.50 115.00	20 10 10	5.14 18.17 2.40	6540 33300 780	15900 78400 1130	1120 2960 100

HOLE NO.: SW96-12 **PAGE: 7**

METERS FROM	TO	DESCRIPTION	SAMPLE NO.	FROM	TO	AU ppb	AG ppm	PB ppm	ZN ppm	CU ppm
		128.34-129.0m - ashey sediments, non-brecciated with 10-15% py.								
		129.0-129.85m - breccia zone in upper 0.2m balance of fragmental zone with sly increase chlorite. Py banding at 30-35° to c/a. as preferred orientation in breccia fragments.								
		131.0-135.8m - stockwork zone mainly hosted by chloritic fragmental with no sulphide zoning in quartz veins and veinlets, but throughout matrix of rock.								
		133.0-135.8m - 1-3% py only.								
135.8	153.0	MAFIC TUFF: with chloritic lapilli fragments. Fine grained, dark grey, weakly amygdaloidal with chlorite filling vesicles, trace to 2% py only locally in narrow 5mm to 1cm quartz-carb veinlets at 30° to c/a. Also very fine disseminations in siliceous matrix. "Ghost pyroclastic texture" due to alteration along fractures, possibly where coarser intervals are crosscut and subsequently altered. Coarser beds silicified at upper and lower contacts, 40° to c/a at 141.5m. Broken upper contact, sheared approximately 20-25° to c/a, slickenlines at 50° to long axis.	281720 281721 281722 281723	135.80 136.80 138.00 139.00	136.80 138.00 139.00 140.00	0 0 -- 20	3.09 2.40 ---- 3.43	150 60 -- 70	110 150 -- 170	10 0 -- 20
		138.0-140.0m - quartz-carb. veining with trace to 1% py.								
		140.6-140.7m - py filled stockwork veining with devitrification spotting. Passes downward (to 141.0m) to py rimmed, rounded lapilli.								
153.0	201.14	SILTSTONE: Upper contact to 156.6m - broken core (possible fault). Light grey, fine grained with calcitic fracture fillings. Core is friable with a recurrent breakage at 35-40° to c/a that implies a coarse cleavage. Calcite filled fractures 40-50° to c/a. Laminations defined by bedding disturbance (possibly slumping or turbulence) at 30-40° to c/a from 164.5-168.1m, 173.7-177.25m, 180.0-182.5m, 184.6-186.5m, 193.64-194.0m, 196.5-197.0m, 158.8-159.94m. Mini fault at 176.75-176.85 characterized by hardened gouge with 3mm long quartz crystals in mass with very small black crystals (barely visible with handlens) scattered throughout it. The mineral looks like hematite i.e black alaskan diamond. No visible graded bedding but the slumpage occurring between 158.8-159.94m has coarser clasts (angular, up to 2.5cm dia.) just above the clear, sharp lower contact (50° to c/a). Above the clasts the laminations are subparallel to c/a and less disturbed. At the top the laminations are at 40° to c/a and barely disturbed.								
		159.80m - shear zone with 0.5cm cataclastic zone at 159.80m.								
		164.5-168.1m - disrupted zone / incipient fault.								
201.14		END OF HOLE								

1:30-2:00 30 minute travel time to Stop 7 – Sharp Mountain

Mileage:
0.0 Proceed east on the Benton Road toward Route 165
8.5 Turn left onto Route 165 and proceed north until the intersection with Deakin Road and Route 585
27.8 Turn right onto Route 585 and cross the Saint John River
28.8 Turn left onto Route 105 and proceed north
29.0 Turn right onto Sharpe Street
29.2 Turn left onto Lewis Street
29.6 Turn left onto Second Avenue
29.9 Turn right onto Woodfield Drive
30.4 Turn left onto Hanover Street
30.6 Turn right and proceed to the Cul-de-Sac
30.9 Turn left and drive (or walk) ~375 m to the communication tower

2:10 – 2:55 45 minute STOP 7 – Sharpe Mountain and Connell Mountain Cu-Mo porphyry core display – (E 611926, N 5114823 UTM Zone 19)

Driving and walking log continued on page ??

REFERENCES

Bailey, L.W., 1901. On some geological correlations in New Brunswick. Royal Society of Canada, Transactions, Second Series, 1901-02, v. 7(4), p. 143–150.

Bevier, M.L., 1990. Preliminary U–Pb geochronologic results for igneous and metamorphic rocks, New Brunswick. *In* Project Summaries for 1989, Fourteenth Annual Review of Activities. *Edited by* S.A. Abbott. New Brunswick Department of Natural Resources and Energy; Minerals and Energy Division, Information Circular 89-2 (2nd edition), p. 208–212.

Burton, D., 2009. Report of work on the Sewell Brook property for Atlantic Zinc Exploration Inc. New Brunswick Department of Energy and Mines, Assessment Report # 476786.

Burton, D., 2010. Report of work on the Sewell Brook property for Atlantic Zinc Exploration Inc. New Brunswick Department of Energy and Mines, Assessment Report # 476919.

Burton, D., 2012. report of work on the Sewell Brook property for Atlantic Zinc Exploration Inc. New Brunswick Department of Energy and Mines, Assessment Report # 477188.

Cas, R.A.F., 1992. Submarine volcanism: eruptive style, products, and relevance to understanding the host-rock successions to volcanic-hosted massive sulfide deposits. Economic Geology, v. 89, p. 511–541.

Cole, R.B., and DeCelles, P.C., 1991. Subaerial to submarine transitions in early Miocene pyroclastic flow deposits, southern San Joaquin basin, California. Geological Society of America Bulletin, v. 103, p. 221–235.

Currie, K.L., van Staal, C.R., Peter, J.M. and Rogers N., 2003. Conditions of metamorphism on the main massive sulphide deposits and surrounding rocks in the Bathurst Mining Camp. Economic Geology Monograph 11, p. 65-78.

Davies, L., 1977. Geological map of northern New Brunswick. New Brunswick Department of Natural Resources and Energy, Minerals and Energy Division, Map-Plate NR3, 1:250 000 scale.

Dostal, J., Wilson, R.A. and Keppie, D., 1989. Geochemistry of Siluro-Devonian Tobique belt in northern and central New Brunswick (Canada). Canadian Journal of Earth Science, v. 26, pp. 1282-1296.

Fyffe, L.R., 1982. Geology of Woodstock NTS 21J. New Brunswick Department of Natural Resources and Energy; Minerals and Energy Division, Map NR-4.

Fyffe, L.R., 1999. Geology of the Eel River area (part of NTS 21G/13h), York and Carleton counties, New Brunswick. New Brunswick Department of Natural Resources and Energy; Minerals and Energy Division, Plate 99-30.

Fyffe, L.R., 2001. Stratigraphy and geochemistry of Ordovician volcanic rocks of the Eel River area, west-central New Brunswick. Atlantic Geology, v. 37, p. 81–101.

Fyffe, L.R., and Pickerill, R.K., 1993. Geochemistry of Upper Cambrian–Lower Ordovician black shale along a northeastern Appalachian transect. Geological Society of America Bulletin, v. 105, p. 897–910.

Fyffe, L. R. and Pronk, A. G., 1985. Bedrock and surficial geology - rock and till geochemistry in the Trousers Lake area, Victoria County, New Brunswick. Report of Investigations 20, Mineral Resources Division, New Brunswick Department of Natural Resources and Energy 74 p.

Fyffe, L.R., Forbes, W.H., and Riva. J., 1983. Graptolites from the Benton area of west-central New Brunswick and their regional significance. Maritime Sediments and Atlantic Geology, v. 19, p. 117–125.

Fyffe, L.R., McCutcheon, S.R., and Wilson, R.A., 1997. Miramichi–Tetagouche stratigraphic relationships, Bathurst Mining Camp, northern New Brunswick. *In* Current Research 1996. *Edited by* B.M.W. Carroll. New Brunswick Department of Natural Resources and Energy; Minerals and Energy Division, Mineral Resource Report 97-4.

Fyffe, L.R., Barr, S.M., Johnson, S.C., McLeod, M.J., McNicoll, V.J., Valverde-Vaquero, P., van Staal, C.R., and White, C.E., 2009. Detrital zircon ages from Neoproterozoic and early Paleozoic conglomerate and sandstone units of New Brunswick and coastal Maine: implications for the tectonic evolution of Ganderia. Atlantic Geology, v. 45, p. 110–144.

Fyffe, L.R., Johnson, S.C., and van Staal, C.R., 2011. A review of Proterozoic to early Paleozoic lithotectonic terranes in the northeastern Appalachian orogen of New Brunswick, Canada, and their tectonic evolution during Penobscot, Taconic, Salinic, and Acadian orogenesis. Atlantic Geology, v. 47, p. 211–248.

Giggie, K.V., 1991. Report of diamond drilling, geological and geophysical surveys, Sewell Brook claim group for NovaGold Resources Inc. New Brunswick Department of Energy and Mines, mineral assessment Report # 474026.

Giggie, K.V. ,1992. Report of diamond drilling, geological and geophysical surveys, Sewell Brook claim group for NovaGold Resources Inc. New Brunswick Department of Energy and Mines, Mineral assessment report # 474186.

Gill, J.B., 1981. Orogenic Andesites and Plate Tectonics. Springer-Verlag, Helderberg, Germany, 390 p.

Goodfellow, W.D., 2007. Metallogeny of the Bathurst Mining Camp, northern New Brunswick. *In* Goodfellow W.D. ed., Mineral Deposits of Canada: a synthesis of major deposit types, district metallogeny, the evolution of geological provinces and exploration methods: Geological Association of Canada, Mineral Deposits Division, Special Publication No. 5, p. 449-469.

Goodfellow, W. D. and McCutcheon, S. R., 2003. Geologic and genetic attributes of volcanic sediment-hosted massive sulfide deposits of the Bathurst Mining Camp, northern New Brunswick – a synthesis. Economic Geology Monograph 11, p. 245-301.

Goodfellow, W. D., McCutcheon, S. R. and Peter, J.M., 2003. Massive sulfide deposits of the Bathurst Mining Camp, New Brunswick, and northern Maine. *Edited by* W.D. Goodfellow, S.R. McCutcheon and J.M. Peter. Economic Geology Monograph, v. 11, p. 930.

Han, Y. and Pickerill, R.K., 1994. Palichnology of the Lower Devonian Wapske Formation, Perth-Andover-Mount Carleton region, northwestern New Brunswick, eastern Canada. Atlantic Geology, v. 30, pp. 217-245.

Hennessy, J.F., and Mossman, D.J., 1996. Geochemistry of Ordovician black shales at Meductic, southern Miramichi Highlands, New Brunswick. Atlantic Geology, v. 32, p. 233–245.

McClenaghan, S.H., Lentz, D.R., and Fyffe, L.R., 2006. Chemostratigraphy of volcanic rocks hosting massive sulphide clasts within the Meductic Group, west-central New Brunswick *In* Volcanic-Hosted Massive Sulphide Deposits and their Geological Settings in the Bathurst Mining Camp, New Brunswick. *Edited by* D.R. Lentz. Exploration and Mining Geology, Special Issue, v. 15, No. 3–4, p. 241–261.

McCutcheon, S.R., and Lentz, D.R., 1993. Guidebook to the Metallogeny of the Bathurst Mining Camp. Trip #4 of Bathurst '93: 3rd Annual Field conference, Geological Society of CIM, p. 159.

McCutcheon, S.R., Luff, W.M., and Boyle, R.W., 2003. The Bathurst Mining Camp, New Brunswick, Canada: history of discovery and evolution of geological models. *In* Massive Sulfide Deposits of the Bathurst Mining Camp, New Brunswick and Northern Maine. Edited by W.D. Goodfellow, S.R. McCutcheon, and J.M. Peter. Economic Geology, Monograph 11, p. 17–35.

McCutcheon, S. R., and Walker, J. A., 2019. Great Mining Camps of Canada 7. The Bathurst Mining Camp, New Brunswick, Part 1: Geology and Exploration History. *Geoscience Canada*, v. 46, No 3, p. 137-154.

McPhie, J., Doyle, M., and Allen, R., 1993. Volcanic textures: a guide to the interpretation of textures in volcanic rocks. Centre for Ore Deposit and Exploration Studies, University of Tasmania, Hobart, Australia, 196 p.

Neuman, R.B., 1984. Geology and paleobiology of islands in the Ordovician Iapetus Ocean: review and implications. Geological Society of America Bulletin, v. 95, p. 1188–1201.

Ohmoto, H., 1996. Formation of volcanogenic massive sulfide deposits: The Kuroko perspective. Ore Geology Reviews, 10 , p. 135–177.

Pickerill, R.K., 1986. Stratigraphy, sedimentology, and structural analysis of the geology of the Tobique Reserve lands with an economic assessment of its geologic resources. Unpublished report to the Department of Indian and Northern Affairs, Ottawa, Ontario, 61 p.

Pickerill, R.K., 1991. The trace fossil *Neonereites multiserialis* from the Devonian Wapske Formation, northwest New Brunswick. Atlantic Geology, v. 27, pp. 19–126.

Pickerill, R.K., and Fyffe, L.R., 1999. The stratigraphic significance of trace fossils from the Lower Paleozoic Baskahegan Lake Formation near Woodstock, west-central New Brunswick. Atlantic Geology, v. 35, p. 215–224.

St. Peter, C., 1978. Geology of head of Wapske River. Map area J-13, NTS 21 J/14. Map Report 78-1. Including map at 1 inch 1/4 mile scale. New Brunswick Department of Natural Resources and Energy, Minerals and Energy Division Map Plate 78-1.

Sullivan, R.W., and van Staal, C.R., 1996. Preliminary chronostratigraphy of the Tetagouche and Fournier groups in northern New Brunswick. *In* Radiogenic Age and Isotopic Studies: Report 9. Geological Survey of Canada, Current Research 1995-F, p. 43–56.

van Staal, C.R., 1987. Tectonic setting of the Tetagouche Group in northern New Brunswick: implications for plate tectonic models of the northern Appalachians. Canadian Journal of Earth Sciences, v. 24, p. 1329–1351.

van Staal, C.R., 1994. Brunswick subduction complex in the Canadian Appalachians: record of the Late Ordovician to Late Silurian collision between Laurentia and the Gander margin of Avalon. Tectonics, v. 13, p. 946-962.

van Staal, C.R., and Fyffe, L.R., 1991. Dunnage and Gander zones, New Brunswick: Canadian Appalachian Region. New Brunswick Department of Natural Resources and Energy; Mineral Resources, Geoscience Report 91-2, 39 p.

van Staal, C.R., and Fyffe L.R., 1995. Gander Zone–New Brunswick. *In* Geology of the Appalachian–Caledonian Orogen in Canada and Greenland. *Edited by* H. Williams. Geological Survey of Canada, Geology of Canada, No. 6, Chapter 3, p. 216–223.

van Staal, C.R., Winchester, J.A., and Bedard, J.H., 1991. Geochemical variations in Middle Ordovician volcanic rocks of the northern Miramichi Highlands and their tectonic significance. Canadian Journal of Earth Sciences, v. 28, p. 1031–1049.

van Staal, C.R., Ravenhurst, C.E., Winchester, J.A., Roddick, J.C., and Langton, J.P., 1990. Post-Taconic blueschist suture in the northern Appalachians of northern New Brunswick, Canada. Geology, v. 24, p. 1073-1077.

van Staal, C.R., Wilson, R.A., Rogers, N., Fyffe, L.R., Langton, J.P., McCutcheon, S.R., McNicoll, V., and Ravenhurst, C.E., 2003. Geology and tectonic history of the Bathurst Supergroup, Bathurst Mining Camp, and its relationships to coeval rocks in southwestern New Brunswick and adjacent Maine: a synthesis. *In* Massive Sulfide Deposits of the Bathurst Mining Camp, New Brunswick and Northern Maine. *Edited by* W.D. Goodfellow, S.R. McCutcheon, and J.M. Peter. Economic Geology, Monograph 11, p. 37–60.

Venugopal, D.V., 1978. Geology of Benton–Kirkland, Upper Eel River Bend, map area G-22 (21 G/13). New Brunswick Department of Natural Resources; Mineral Resources Branch, Map Report 78-3, 16 p.

Venugopal, D.V., 1979. Geology of Debec Junction–Gibson Millstream–Temperance Vale–Meductic region, map-areas G-21, H-21, I-21, and H-22 (Parts of 21 J/3, 21 J/4, 21 G/13, 21 G/14). New Brunswick

Walker, R.T., 1997. Report on diamond drilling on the Sewell Brook property for NovaGold Resources Inc. NTS 21 O/03E. New Brunswick Department of Energy and Mines, mineral assessment report # 474898.

Walker, R.T., 1998. Report on diamond drilling on the Sewell Brook property for NovaGold Resources Inc. NTS 21 O/03E. New Brunswick Department of Energy and Mines, mineral assessment report # 475168.

Wilson, R. A., 1990. Bedrock geology of the Riley Brook area, NTS 21 O/3E, part of 21 O/2W. New Brunswick Department of Natural Resources and Energy, Minerals and Energy Division, Map-Plate 90-162, 1:50 000 scale.

Walker, J.A., 2005. Petrogenesis and tectonic setting of Devonian volcanic and related rocks and their control on mineralization at the Shingle Gulch East Zn–Pb–Ag sulfide deposit, northwest New Brunswick. Unpublished Ph.D. thesis University of New Brunswick, New Brunswick, Canada, 430 p.

Walker, J.A., 2005. Gilmour Brook South base-metal occurrence, Bathurst Mining Camp, northern New Brunswick. In Geological Investigations in New Brunswick for 2004. *In* Martin, G. ed. New Brunswick Department of Natural Resources; Minerals Policy and Planning Division, Mineral Resource Report 2005-01, p. 127-166.

Walker, J.A., 2009. Early Devonian felsic volcanic rocks and associated Zn–Pb mineralization, Tobique–Chaleur Zone, New Brunswick, Canada. Extended abstract. *In* Lentz, D.R., Thorne, K.G., and Beal, K-L, (editors), Proceedings of the 24th IAGS, Fredericton, Canada, p. 535-538.

Walker, J.A., 2010. Stratigraphy and lithogeochemistry of Early Devonian volcano-sedimentary rocks hosting the Nash Creek Zn-Pb-Ag deposit, Northern New Brunswick. *In* Geological Investigations for 2009, *Edited b*y G.L. Martin. New Brunswick Department of Energy and Mines, Mineral Resources Report 2010-1, p. 52–97.

Walker J.A., 2014. Stratigraphic Setting of Base-Metal Deposits in the Bathurst Mining Camp (BMC), New Brunswick. Field trip A1 Guidebook. GAC/MAC annual meeting Fredericton, NB, 91 p.

Walker, J.A., 2015. The Sewell Brook Zn-Cu-Pb sulphide deposit, Northern New Brunswick: An example of Early Devonian sub-seafloor replacement mineralization New Brunswick Department of Energy and Mines; Geological Surveys Branch, Geoscience Report GR 2015-3, 62 p.

Walker J.A., 2022. Stratigraphic Setting of Base-Metal Deposits in the Bathurst Mining Camp (BMC), New Brunswick. Field trip B2 Guidebook. GAC/MAC annual meeting Halifax, NS, 103 p.

Walker, J.A. and Clark, D., 2012. The Mount Costigan Zn-Pb-Ag deposit, west central New Brunswick, Canada: Stratigraphic setting and evolution of felsic intrusion related mineralization. New Brunswick Dept. of Energy and Mines. Mineral Resources Report 2012-1 (CD ROM), 50 p.

Walker, J. A. and McCutcheon, S.R., 1995. Siluro-Devonian stratigraphy of the Chaleurs Bay Synclinorium, northern New Brunswick. *In* Current Research 1994. Compiled and Edited by S.A.A. Merlini. New Brunswick Department of Energy and Mines, Miscellaneous Report 18, p. 225-244.

Walker, J.A., and McCutcheon, S.R., 2011. A chemo-stratigraphic assessment of core from the discovery hole of the Halfmile Lake Deep VMS zone, Bathurst Mining Camp, north-eastern New Brunswick. *In* Geological Investigations For 2010, *Edited b*y G.L. Martin. New Brunswick Department of Natural Resources, Minerals, Policy, and Planning Division, Mineral Resources Report 2011-2, p. 1–49.

Walker, J. A. and McDonald, S.M., 1995. Preliminary investigation of the Canoe Landing Lake massive-sulphide deposit, NTS 21 O/08 E. *In* Langton, J.P. ed., Geoscience Research 1994. New Brunswick Department of Natural Resources, Minerals, Policy and Planning Division, Miscellaneous Report 15, p. 78-99

Walker, J.A**.** and Wilson, R.A., 2013. Stratigraphy and lithogeochemistry of bimodal volcanic rock and related intrusions of the Tobique Group at the Shingle Gulch East Zn-Pb-Ag Occurrence, west central New Brunswick Canada. New Brunswick Dept. of Energy and Mines; Geological Surveys, Mineral Resources Report 2013-2 (CD ROM), 52 p.

Wilson, R.A., 1992. Petrographic features of Siluro-Devonian felsic volcanic rocks in the Riley Brook area, Tobique Zone, New Brunswick: Implications for base metal mineralization at Sewell Brook. Atlantic Geology, v. 28, p. 115-135.

Wilson, R.A. and Kamo, S., 2007. Revised age of the Clearwater Stream Formation, and new structural observations near the Chester deposit, Bathurst Mining Camp, northeastern New Brunswick. *In* Geological Investigations in New Brunswick for 2006, *edited by* G.L. Martin. New Brunswick Department of Energy and Mines; Mineral Resource Report 2007-1, p. 1-20.

Wilson, R.A. and Kamo, S., 2008. New U–Pb ages from the Chaleurs and Dalhousie Groups: Implications for regional correlations and tectonic evolution of northern New Brunswick. *In* Geologic investigations in New Brunswick for 2007. Edited by G.L. Martin. New Brunswick Department of Natural Resources. Minerals, Policy and Planning Division, Mineral Resource Report 2008-1, p. 55–57.

Wilson, R.A., van Staal, C.R. and McClelland, W.C., 2015. Synaccretionary sedimentary and volcanic rocks in the Ordovician Tetagouche back arc basin, New Brunswick, Canada: evidence for a transition from foredeep to forearc basin sedimentation. American Journal of Science, 315, p. 958-1001.

Part III
Early Ordovician Connell Mountain Cu porphyries and Sharp Mountain diatreme, Woodstock, New Brunswick, Canada

David R Lentz and Fazilat Yousefi
Department of Earth Science, University of New Brunswick, Fredericton, NB Canada. Email: dlentz@unb.ca

Introduction

The Connell Mountain porphyry copper deposit is the largest of the known porphyry copper deposits in New Brunswick (Ruitenberg and Fyffe 1982, 1991), although quite small by global comparison. The geochemical anomalies associated with the copper deposit were delineated by Phelps-Dodge Corporation of Canada Ltd. in the late 1960s. During the period 1969 to 1974, Falconbridge Nickel Mines Ltd., Bethlehem Copper Corp., and United Siscoe Mines Ltd. carried out exploration, trenching, and drilling programs around Connell Mountain, and proved the existence of copper-rich zones. Slightly over one million tonnes of mineralization at 0.5% Cu was delineated (Lockhart 1970, 1976), included within a larger resource of 23 Mt of 0.18% Cu (Venugopal 1981). In 1998, Noranda Exploration Inc. carried out further exploration and drilling in the area (Moore 1998) to establish the controls on mineralization. A variety of mineralized occurrences have been noted in the Woodstock area (Fig. 1), predominantly concentrated around the Gibson–Bulls Creek intrusion(s). Thomas and Gleeson (1988) subdivided these mineral occurrences into porphyry copper, vein copper, fracture-filling copper, vein lead, vein gold, and vein barite deposits, based on the characteristics of their occurrences. There are seven copper occurrences known in the Connell Mountain area, mainly distributed in the north part of Gibson intrusive complex (Thomas and Gleeson 1988), probably reflecting the larger subvolcanic porphyry system at depth; most of these occurrences have less than 100 ppb gold, although epithermal precious metal occurrences occur throughout the region.

The most significant deposit is the Connell Mountain porphyry copper deposit that is hosted in a small cupola (500 m by 150 m), 1500 m north of the main Gibson pluton. Gold mineralization is present at Connell Mountain with up to 1300 ppb Au and 1.4% Cu noted in grab samples of an intensely altered quartz wacke (sample A143; see Thomas and Gleeson, 1988), although only 10% of the 43 samples analysed from Connell Mountain had greater than 100 ppb Au. Selenium (up to 52 ppm), Bi (up to 18 ppm), Co (up to 259 ppm), and Ag (up to 20 ppm) abundances are locally elevated in these samples. Molybdenum contents are universally low (< 50 ppm) throughout the Connell Mountain area (Thomas and Gleeson 1988), although one sample in this study yielded 289 ppm Mo (WK-98-1, 7.1 m). At the Bulls Creek occurrences (#9, 10, 11; Fig. 1), there is one copper-rich chip sample (0.5 m) with 1200 ppb Au in a gossaniferous sulfide-quartz-carbonate vein within the granodiorite (sample 017; Thomas and Gleeson, 1988), and several others with elevated Au contents. These samples have a notable As, W, and Bi association and occur within sulfide-rich veins and breccias within the metasedimentary rocks near the intrusion. The Upper Hampton (#32) and Saint John River (#33) epithermal gold occurrences are located within the main Gibson pluton (Fig. 1) near the outer contact with the metasedimentary rocks. At the Upper Hampton occurrence, Thomas and Gleeson (1988) documented in detail the quartz vein system. One of the vein sets consists mainly of pyrite and quartz, with up to 15% sulfide, and contains up to 0.4% Cu, 1.1% Pb, and 6.6 g/t Au (grab sample). Historical records also document samples grading 5.44% Cu and 0.05 oz/ton (1.7 g/t) Au at the Saint John River gold occurrence (R. Thomas written communication).

The main aim of this contribution is to provide a better understanding of the petrology and geochemical composition of the Gibson pluton (Fig. 2), related Connell Mountain porphyry and Sharp Mountain tuffisitic diatreme located just to the north, as well as ascertain the geochronologic constraints between intrusion and mineralization at Connell Mountain; ascertaining the controls on the porphyry Cu-related mineralization and spatially related Au and base-metal mineralization is also key. With this information, it will be easier to compare and contrast this older porphyry Cu-associated gold mineralization within the surrounding area, as well as with the epithermal gold mineralization at Poplar Mountain (Chi et al. 2008) located to the southwest, as well as the numerous other gold occurrences in the region (see McLeod and McCutcheon 2000).

Geologic Setting

The Connell Mountain Cu deposit occurs 5 km southeast of Woodstock, south-central New Brunswick, situated within the Miramichi zone. The Miramichi zone is bounded by the Woodstock Fault to the northwest and the Meductic Fault in southeast (Anderson 1968; Venugopal 1981; van Staal and Fyffe 1991). The middle Ordovician intrusive rocks and the cogenetic Meductic Group located to the southwest are interpreted as a remnant arc to the

Popelogan–Victoria arc to the north (Fyffe 2001; Wilson 2003; van Staal and Barr 2012). The local map area is dominated by a suite of Cambro-Ordovician metasedimentary rocks of the Woodstock Group (Fyffe 2001), which consists of quartz wackes, siltstones, and argillites (Fig. 1). These sedimentary rocks represent the passive margin of the peri-Gondwana Gander Terrane (van Staal and Fyffe 1991; van Staal and Barr 2012). Middle Ordovician arc-related volcano-sedimentary rocks of the Meductic Group (Fyffe 2001), Lower Devonian mafic flows and lapilli tuff, and interstratified red conglomerates, sandstones, and shale of the Carlisle Formation, and Mississippian rocks are dispersed locally in the southwest and northwest corner of the area.

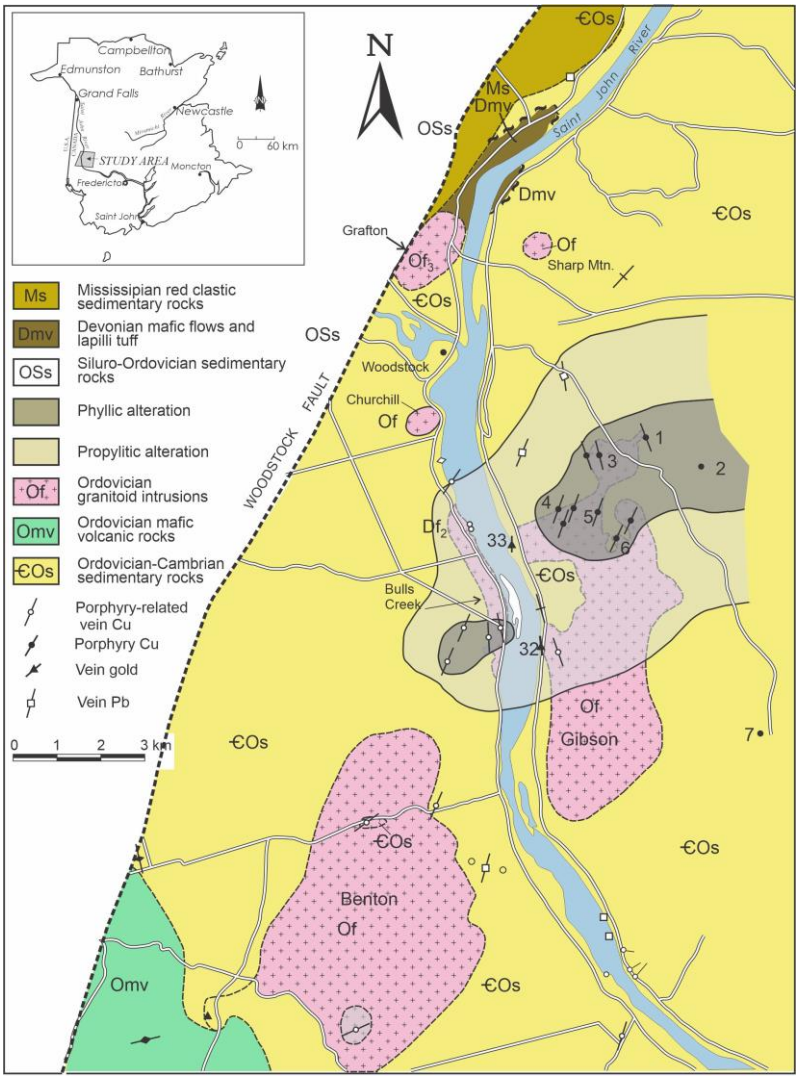

Fig. 1 Simplified geologic map of the Woodstock area, west-central New Brunswick (modified after Thomas and Gleeson 1988) with the locations of Cu and gold mineralization and the Connell Mountain porphyry copper deposit. Thomas and Gleeson (1988) Deposit numbers: (1) Connell Mountain Cu, (2) southeast Connell Mountain Cu, (3) Connell Brook Cu (Zn), (4) Moneith Farm Cu, (5) Smart Farm Cu (Au, Mo, Zn), (6) Upper North Hampton Cu (Mo), (7) Kilmarnock Settlement Cu, (32) Upper North Hampton Au (Pb, Cu, Zn), (33) Saint John River Gold (Cu, Pb).

The Gibson and Benton plutons (Fig. 1) are the two largest composite intrusions in the region, and were emplaced into the Cambro-Ordovician metasedimentary rocks of the Woodstock Group. A U-Pb zircon age of 473 ± 1 Ma was obtained from a roadside outcrop of the Gibson stock and a younger U-Pb titanite age (ca. 457 ± 1 Ma) (Bevier 1989), probably reflecting partial resetting during the Salinic orogeny. The Benton Granite was dated at 479 ± 7 Ma (Whalen et al. 1998). These two intrusions were ascribed to the Ordovician granite suite of the Miramichi subzone (Whalen 1993; Whalen et al. 1998). To the southwest, the volcanic sequence of the Ordovician Meductic Group (477–470 Ma; Fyffe 2001) is generally synvolcanic with these relatively high-level

plutons (Dostal 1989), although there are compositional differences within the Gibson intrusions. There are several small granitoid stocks to the northwest of the Gibson pluton, which were also intruded into Cambro-Ordovician metasedimentary rocks, but their relationship with Lower Devonian volcanic rocks in the area is uncertain. Mafic dikes (<50 m wide) of uncertain age are common throughout the Cambro–Ordovician metasedimentary sequence and within the Ordovician felsic intrusions.

Local geology

The porphyry copper deposit occurs along the north and western flanks of Connell Mountain; this hornblende-plagioclase porphyry stock discordantly intrudes the Cambro–Ordovician metasedimentary sequence, with copper mineralization predominately hosted in the porphyry near the contacts. Some late mafic dikes also occur in the area, but do not show any significant Cu or Mo mineralization, and are inferred to be post mineralization.

Woodstock Group metasedimentary rocks

The Cambro-Ordovician Woodstock Group metasedimentary rocks include three units: metamorphosed quartz wackes (quartzites), siltstones, and argillites (Fig. 1). van Staal (1994) noted that the Gander margin (Ganderia), an accretionary wedge, was formed from the Cambro-Ordovician Miramichi and Woodstock group sediments. The predeformational structure of these metasedimentary rocks, as well as their mineralogy and composition, seem to have affected the permeability of these units during the magmatic-hydrothermal mineralizing processes.

The mature quartz wackes are gray to greenish gray, usually containing more framework grains than matrix. The framework mainly comprises medium- to coarse-grained, subangular to subrounded quartz grains, with lesser feldspar grains and rock fragments (Fig. 2). The matrix is also composed of subangular quartz and feldspar, with sericite, chlorite, epidote, zircon, apatite, and pyrite ± pyrrhotite. There are abundant fractures many with quartz and quartz-sulfide veins in the brittle quartz wackes around the felsic intrusions (Fig. 2), but less so in the finer grained units.

The siltstones are fine grained, medium to dark gray, well layered, and are usually interbedded with argillaceous rocks. They mainly contain subangular to angular grains of quartz, feldspar, chlorite, sericite, and magnetite and pyrite ± pyrrhotite.

The argillaceous meta-sedimentary rocks are dark gray to black, very fine grained and typically massive without apparent bedding. The rocks are comprised of chlorite and sericite with minor quantities of silt-sized quartz and feldspar grains, locally. They are interbedded with siltstones. These units are several millimeters to several meters in thickness (Thomas and Gleeson 1988). Quartz wackes, siltstones, and argillites are interbedded with each other (cm to m scale), analogous to turbiditic Bouma sequences; they represent a passive margin sequence on the abyssal slope and rise. These very fine-grained units tend to be less fractured with mineralization-related veining.

Early Ordovician intrusions

The Early Ordovician Gibson intrusive complex is the main intrusion in the Woodstock area, although several smaller stocks (Churchill, Sharps Mountain, and Grafton) occur in the northern part of the region as well (Fig. 1) (see Thomas and Gleeson, 1988). The Gibson intrusive complex is subdivided into three phases: the main Gibson stock (16.5 km^2) on the east side of the Saint John River (Fig. 3); the Connell Mountain stock (0.1 km^2) to the northeast of the main Gibson pluton; and the Bulls Creek stock (1.2 km^2) on the west side of the Saint John River (Thomas and Gleeson 1988). Both the main Gibson intusion and Connell Mountain satellite stock host porphyry Cu mineralization, although the main Cu deposit is hosted by the Connell Mountain stock. The petrology and geochemical composition of the large plutons and other satellite stocks are examined as part of a larger regional examination of the exploration potential of the region. The

Intrusion petrography

The Connell Mountain stock consists of magnetite-bearing porphyritic tonalite to porphyritic granodiorite. Medium to dark gray tonalite (Fig. 4) is predominant in the Connell Mountain stock, and has a higher proportion of phenocrysts (50-60%) and a coarser groundmass (0.08-0.10 mm) relative to the Gibson intrusive complex. Phenocrysts include plagioclase, quartz, and hornblende (>>15%). Porphyritic light grey granodiorite has a lower proportion of phenocrysts (20–25%) and a finer grained groundmass (<0.04 mm). Although the types of phenocryst minerals in porphyritic granodiorite are similar to porphyritic tonalite, the proportion of ferromagnesian minerals (biotite ± hornblende) is lower. Both porphyritic tonalite and porphyritic granodiorite at

Connell Mountain show weak hydrothermal alteration (propylitic), but most of phenocrysts in the rocks are fresh and, where altered, their alteration products mainly occur as pseudomorphs of the original minerals.

The Sharps Mountain intrusive body is sizable as well and preliminary U-Pb zircon dating has confirmed a Middle Ordovician age. The area is almost entirely diatreme breccias of various facies (Figs. 5, 6, and 7) representing the volcanic pipe to a pyroclastic eruption. Intra-intrusion fragments (felsite) and host rock fragments are angular to rounded, as are the quartz and plagioclase phenoclasts. The weak alteration is differentially distributed in the fragments and the groundmass indicating the magmatic hydrothermal system was active during emplacement.

The main Gibson intrusion is greenish to pink in color, medium grained, equigranular, and of tonalitic composition. It contains 45% plagioclase, <5% K feldspar, 30% quartz, 20% hornblende, and trace pyrite and chalcopyrite. The Bulls Creek stock is a granodioritic intrusion, containing on average 40% plagioclase, 10% K feldspar, 35% quartz, and 15% hornblende, with an equigranular texture.

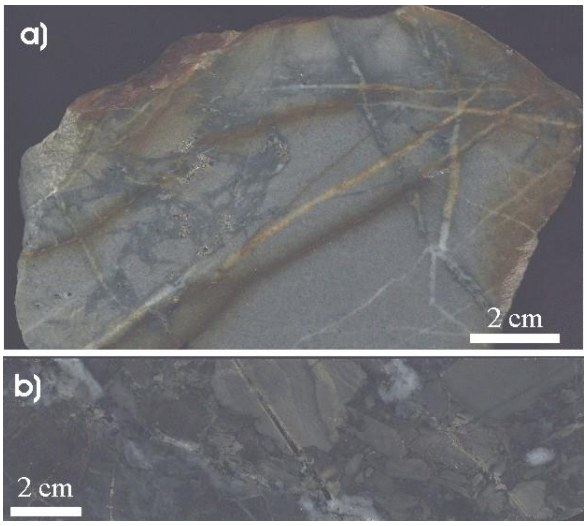

Fig. 2 Cambro-Ordovician quartz wacke (sample COs#2) (Woodstock Group). Photograph of pyrite-bearing quartz veins with alteration selvages, resembling a stockwork pseudobreccia network. These pyrite-bearing veins are cut by irregular barren quartz microveinlets. b) Photograph of metasedimentary quartz wacke (sample COs#2): Framework grains (70%) mainly consist medium- to coarse-grained, subangular to subrounded quartz grains, with lesser feldspar grains and rock fragments. The matrix (25%) is composed of sub-angular quartz and feldspar, with sericite and chlorite. Pyrite and opaques minerals (5%) occur in the matrix. Irregular fractures are filled by quartz and sulfide.

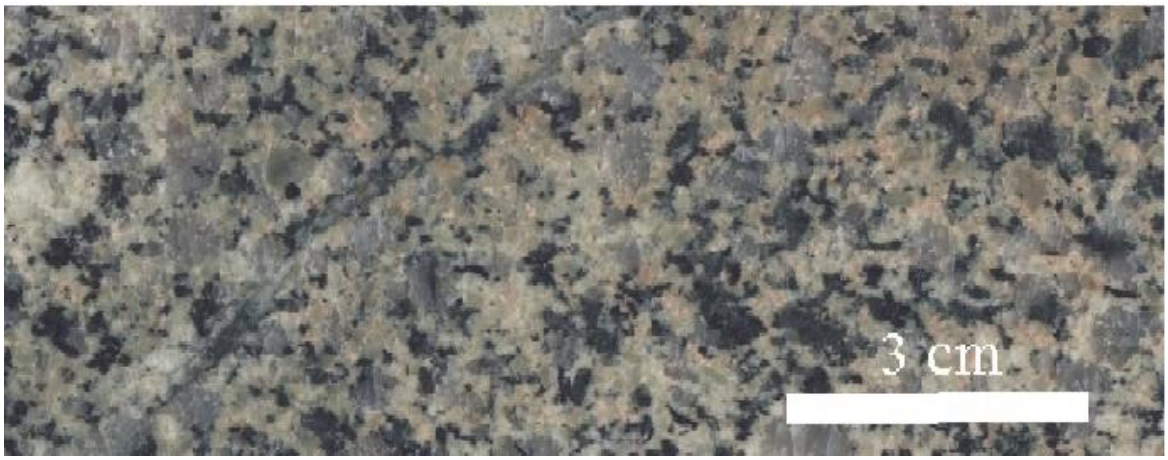

Fig. 3 Photograph of weakly altered, saussuritic medium-grained, equigranular, seriate-textured tonalite from the main phase of the Gibson stock; fractures are filled by quartz $\pm$ chlorite (sample WK-98-2, 318-319 m).

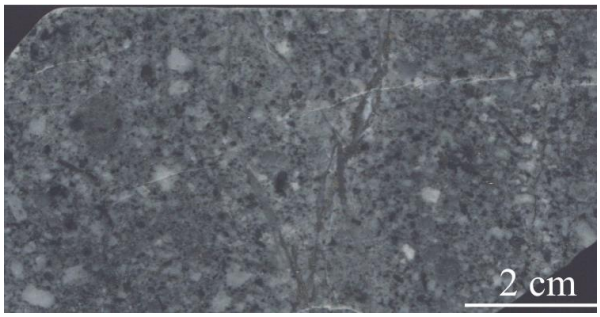

Fig. 4 Photograph of altered Connell Mountain hornblende-plagioclase-quartz porphyritic tonalite with quartz and feldspar phenocrysts and phenoclasts in a microcrystalline groundmass with 2% disseminated and veinlet pyrite and very minor quartz microveinlets. Rounded to subangular metasedimentary xenoliths (< 2 cm) occur in the sample (sample WK-98-1-120.8m).

Fig. 5 Photograph of the Sharp Mountain diatreme breccia with host rock and felsite fragments in a tuffisitic groundmass with weak phyllic alteration.

Fig. 6 Photograph of the Sharp Mountain diatreme breccia with mainly angular to rounded felsite fragments in a tuffisitic groundmass with weak phyllic alteration and local phenoclasts are visible.

Fig. 7 Photograph of a polished slab of the Sharp Mountain diatreme breccia with host rock and felsite fragments in a tuffisitic groundmass with weak phyllic alteration.

Connell Mountain porphyry copper deposit

Distribution of mineralization

The known mineralized zones in the Connell Mountain Cu deposit are located along the eastern contact of the Connell Mountain stock with two mineralized occurrences in the area; the main one is on the eastern side of the summit of Connell Mountain (see Figs. 1 and 8), and the others occurrences 3 to 6 are located to the west (Fig. 8). The stockwork Cu mineralization is continuous above the 0.1% Cu contour from drill core assays, but the mineralization becomes discontinuous beyond the central zone. At 362 to 363 m depth in drill hole WK 98-1, Cu assays up to 0.7% occur in quartz veins hosted in a fault. The Cu is predominately hosted in the altered porphyritic cupola, and to a lesser extent in metasedimentary rock near the contact (Figs. 8, 9). Minor supergene Cu enrichment (up to ~1.2 %) occurs in the two surface Cu showings, with weathering ranging from 3 to 10 meters depth (Thomas and Gleeson 1988).

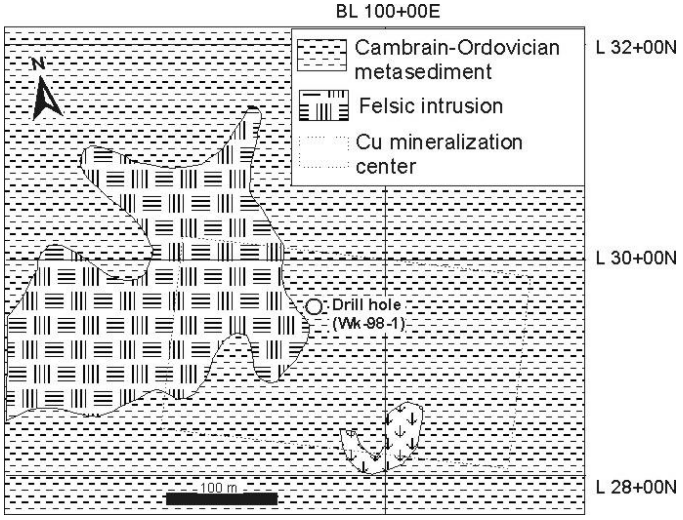

Fig. 8. Local geologic map of Connell Mountain porphyry copper deposit (modified from Moore 1998).

The principal ore mineral is chalcopyrite, which occurs together with pyrite and pyrrhotite. Small amounts of molybdenite and sphalerite occur locally. Secondary copper minerals include tenorite, malachite, and chalcocite occurring in an enriched weathered zone and (or) supergene zones, whereas the original hypogene sulfide content can constitute up to 5% of rock. Pyrite is more abundant than pyrrhotite in the deposit, but pyrrhotite is locally the main sulfide mineral in veins and disseminations, particularly in the host metasedimentary rocks. The sulfide grains vary from 0.03 to 0.5 mm in size, and are usually anhedral and disseminated within pervasively altered host rocks, although sulfide-chlorite-quartz veins are also evident. In porphyritic tonalite, sulfides usually replace the igneous hornblende-biotite assemblage in weak alteration zones, and also occur with chlorite, sericite, and prehnite in more intensely altered areas; alteration of Fe-bearing minerals, like primary hornblende-biotite, can lead to chalcopyrite and pyrite-pyrrhotite mineralization.

Alteration and Mineralization

Based on this and earlier studies, potassic alteration is not evident within the Connell Mountain porphyry copper deposit (see Thomas and Gleeson 1988) at least at this level of the system, which seems different from other porphyry deposits in the Appalachian Orogen (Hollister et al. 1974). Thomas and Gleeson (1988) recognized two different styles of alteration around the deposit: propylitic and phyllic; the deposit is located within the phyllic alteration zone (Fig. 1).

In this study, two different alteration zones, a weak propylitic and a stronger phyllic, were identified around the Connell Mountain copper deposit. In the weakly altered zone, sericite replaces plagioclase (although relic plagioclase is locally present), and hornblende is locally altered to chlorite. Fine-grained pyrite, pyrrhotite, and chalcopyrite is usually disseminated in altered ferromagnesian phases. In the more strongly altered phyllic zone, the alteration changes the rock from dark gray to light gray. All plagioclase is altered to fine-grained muscovite, and hornblende is altered to chlorite and prehnite; pyrite and pyrrhotite formed by sulfidation coincident with hydrolysis.

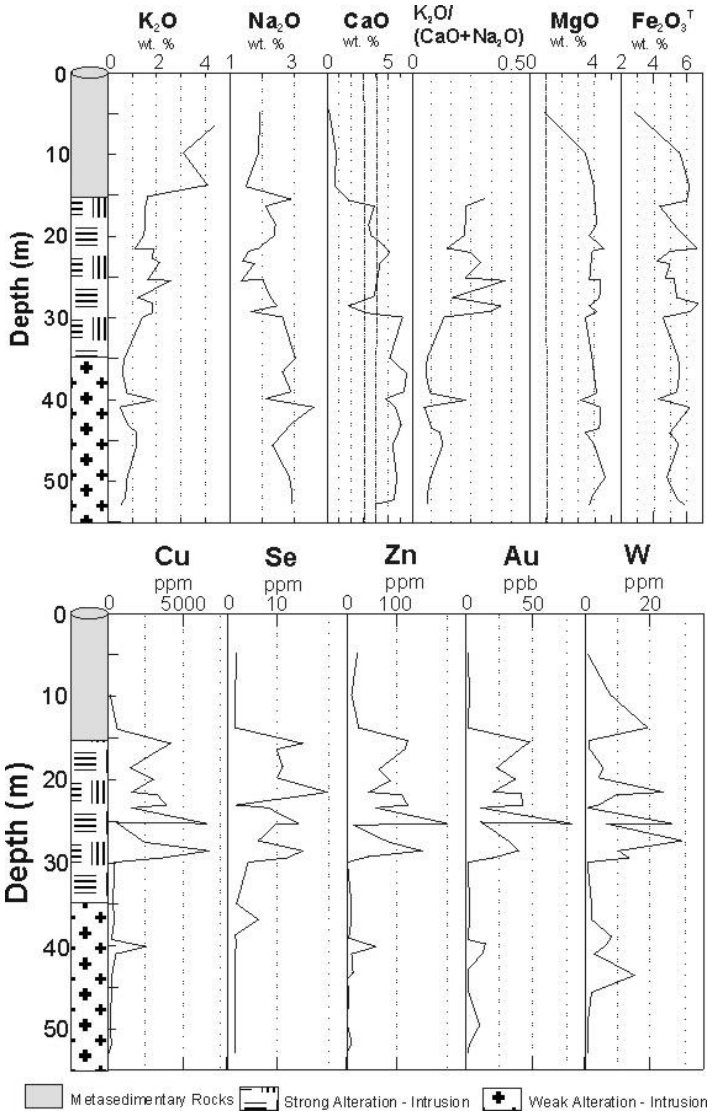

Fig. 8. Geochemical compositional profiles for DDH WK-98-1 in the Connell Mountain porphyry copper deposit: ***a***. Major element variations and ratios; ***b***. Ore-forming element variations.

During alteration, felsic intrusions reveal some changes in content of various major element contents. Figure 6a illustrates that the contents of Ca and Na decrease, the content of K increases, and the contents of Mg and Fe have no apparent change from the weak alteration zone to the strong alteration phyllic zone. Mineralizing elements exhibit changes during the alteration process, but mainly in the phyllic alteration zone; the Cu grades of interest are locally anomalous in Au (<2–77 ppb), As (<0.5–19.3 ppm), Sb (<0.1–3.5 ppm), Se (<3–20 ppm), Zn (<50–361 ppm), Mo (<1–289 ppm), and W (<1–29 ppm), although background values near detection limits are most common.

Geochronologic constraints

U-Pb Zircon Dating

Tonalite from a drill hole in the Cu mineralized porphyry system was sampled to ascertain the age of this particular stock relative to a previously determined preliminary date on coarse-grained granodiorite of the Gibson intrusion (473 ± 1 Ma, U-Pb zircon; Bevier 1989). The Connell Mountain tonalite sample is gray, fine to medium grained, porphyritic, and generally more evolved in composition relative to the Gibson pluton, and so warranted an additional age date. This sample contains abundant good to moderate quality zircons. Four multigrain zircon fractions were selected, based on cathodoluminescent features (zoning); these included large, elongate, euhedral

crystals with no inclusions (fractions A and D) and stubby prismatic grains with numerous inclusions (fractions B and C). All of the analyses plot along the Concordia, but are interpreted to contain minor inherited components of Pb due to slight discordant tangent probably associated with very minor zircon inheritance (Fig. 10). A linear regression of all four analyses has a lower intercept of 474.5 +1/-4 Ma (MSWD = 2.7), which is interpreted to be the crystallization age of the tonalite.

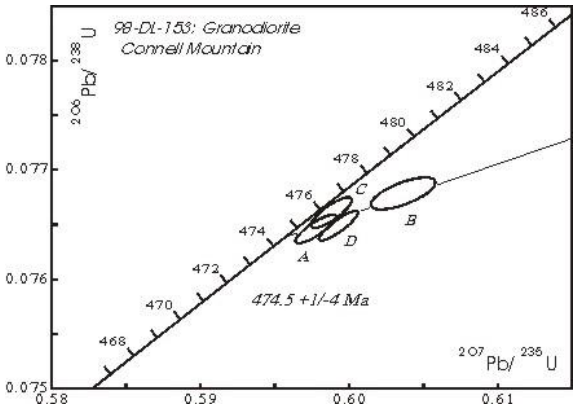

Fig. 10 U-Pb concordia plot for the Connell Mountian granodioritic porphyry, Woodstock, New Brunswick (sample 98-DL-153).

Discussion

There are numerous types and styles of granitoid-related mineralization in this part of the Appalachians (Ruitenberg and Fyffe 1991) that are associated with Ordovician to Devonian intrusions. Most intrusion-related mineralization, including the Poplar Mountain gold deposit to the west, are Devonian in age, associated with the Acadian orogeny (Chi et al. 2008). However, the Lower Ordovician ages of the Gibson intrusions reflect a pre-Acadian intrusive arc suite that rarely exhibits the deformation and metamorphic features (greenschist grade) associated with the main Salinic and Acadian orogenies. The distal turbiditic nature of the sedimentary sequence (Ganderia of the Appalachian Mountains) indicates that these primitive oxidized I-type magmas intruded into this submergent setting, although possibly intracontinental in nature; the associated Meductic volcanic sequence (Ordovician mafic volcanic rocks, Fig. 1) occurring immediately to the west is a submarine sequence. A protoarc to arc developed (Popelogan-Woodstock arc) on the rifted Ganderia (cf. Wilson 2003) located northwest of the Tetagouche-Exploits back arc (see Fig. 11), but is interpreted to have split to form the Woodstock remnant arc to the southwest.

Copper mineralization is mainly hosted in porphyritic tonalite at Connell Mountain, which is interpreted to be a high-level subvolcanic stock, analogous to the model presented by Sillitoe (2010), whereas the different phases of the Gibson pluton have coarser grained textures. The Connell Mountain stock contains two different phases: porphyritic fine-grained tonalite (high-level) and porphyritic coarse-grained granodiorite (deeper level). Based on the position of the stocks to the north of the larger Gibson intrusion and the Sharp Mountain tuffisitic diatreme, this observation is consistent with greater post-emplacement uplift (tilting) in the south, so the northern margin is generally more favorable for future exploration.

The volcanic vent-like nature of this stock, analogous to Sharp Mountain, supports a pressure-quench mechanism for the fine-grained groundmass within the upper part of the stock. The fragmental nature of some of the mineralized and altered intrusive breccias within the Connell Mountain stock indicates that episodic magmatic hydrothermal explosive activity was associated with the emplacement of the stock (see Burnham 1985). The focused intensity of alteration dominantly within the stock is consistent with multiple episodes of autometasomatic alteration like other high-level subvolcanic intrusive systems (Burnham and Ohmoto 1980), where replacement and vein-style mineralization is centered upon the source intrusion (see also Titley and Beane 1981). However, the present erosional level in the area precludes the associated volcanic rocks from being preserved (see Hollister et al. 1974). The development of Early Ordovician, volcanic massive sulfides in the Meductic volcanic rocks to the west (McClenaghan et al. 2006) is consistent with the interpretation of a deeper level of erosion in the Gibson pluton area. Like the Early to Middle Ordovician intrusions in the region described by Whalen et al. (1998), these plutons may represent subvolcanic intrusions to the arc-like volcanic rocks in this region.

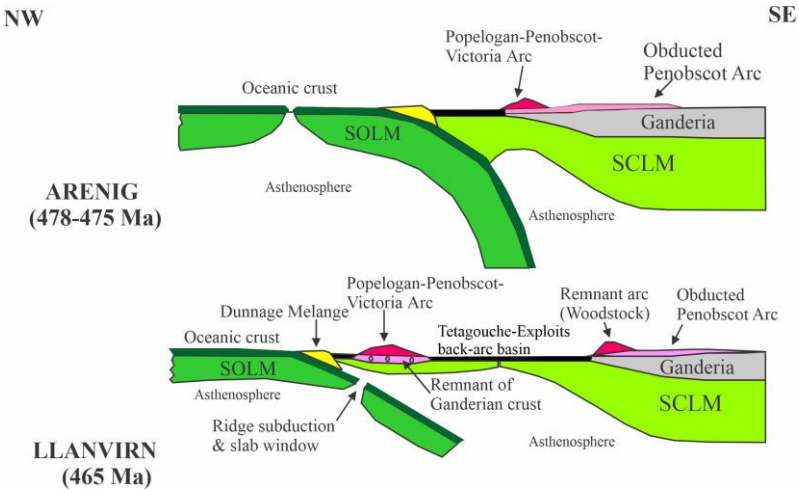

Fig. 11 Schematic model of the tectonic evolution of the Early to Middle Ordovician arc to back-arc in the northern Appalachians, modified after Wilson (2003) and Zagorevski et al. (2010). The timing of slab breakoff (slab failure and probable slab melting is uncertain, but pre-back-arc opening. SCLM - subcontinental lithospheric mantle; SOLM – suboceanic lithospheric mantle.

Based on the low Au abundances associated with the porphyry Cu mineralization at Connell Mountain (Thomas and Gleeson 1988; this study), there is lower gold potential associated with this specific porphyry system, although the epithermal systems do have significant gold. It may have been scrubbed during volatile saturation of these intrusions during emplacement and focused into syn-emplacement structures in the exocontact environment. In fact, the most significant gold occurrences are pyrite-quartz veins with a weak As-Bi-base-metal association that could form epithermal gold system if the intrusion-related mineralizing fluids were focused into a pre-existing structure. However, the age of gold mineralization relative to the various Ordovician intrusive episodes in the area is still uncertain. The lineament analysis presented by Thomas and Gleeson (1988) recognizes many post-emplacement structures around the Gibson pluton, although it is difficult to recognize the earliest syn-emplacement fault structures and the trends of the cupolas to this intrusion.

References

Anderson FD (1968) Woodstock, Milleville and Coldstream map areas, Carleton and York counties, New Brunswick. Geological Survey of Canada Memoir 353

Bevier ML (1989) Preliminary U-Pb geochronologic results for igneous and metamorphic rocks, New Brunswick, *in* Abbott, S.A., ed., Fourteenth Annual Review of Activities: New Brunswick Department of Natural Resources and Energy, Minerals and Energy Division, Information Circular 89-2:190-194

Burnham CW (1985) Energy release in subvolcanic environments: implications for breccia formation. Economic Geology 80:1515-1522

Burnham CW, Ohmoto H (1980) Late-stage processes of felsic magmatism. Mining Geology, Special Issue No. 8:1-11

Candela PA (1991) Felsic magmas, volatiles, and metallogenesis, *in* Whitney, J.A., and Naldrett, A.J., eds., Ore deposition associated with magmas. Reviews in Economic Geology 4:223-233

Chi G, Watters S, Davis WJ, Ni P, Castonguay S, Hoy D (2008) Geologic, geochemical, and geochronological constraints on the genesis of gold mineralization at Poplar Mountain, western New Brunswick, Canada. Exploration and Mining Geology 17(1-2):101-130

Dostal J (1989) Geochemistry of Ordovician volcanic rocks of the Tetagouche Group of southwestern New Brunswick. Atlantic Geology 25:199-209

Fyffe LR (2001) Stratigraphy and geochemistry of Ordovician volcanic rocks of the Eel River area, west-central New Brunswick. Atlantic Geology 37:81-101

Fyffe L, Barr SM, Bevier ML 1988. Origin and U-Pb geochronology of amphibolite-facies metamorphic rocks, Miramichi Highlands, New Brunswick. Canadian Journal of Earth Sciences 25:1674-1686

Gammons CH, Williams-Jones AE (1997) Chemical mobility of gold in the porphyry-epithermal environment. Economic Geology 92:45-59

Goodfellow WD, McCutcheon SR (2003) Geologic and genetic attributes of volcanic sediment-hosted massive sulfide deposits of the Bathurst Mining Camp, northern New Brunswick – a synthesis. Economic Geology Monograph 11:245-301

Hollister VF, Potter RR, Barker AL (1974) Porphyry-type deposits of the Appalachian Orogen. Economic Geology 69: 618-630

Lentz DR (1995) Preliminary evaluation of six in-house rock geochemical standards from the Bathurst Camp, New Brunswick, *in* Merlini SA ed. Current Research 1994: New Brunswick Department of Natural Resources and Energy, Minerals and Energy Division, Miscellaneous Report 18:81-89

Lentz DR (1998) Petrogenetic and geodynamic implications of extensional regimes in the Phanerozoic subduction zones and their relationship to VMS-forming systems. Ore Geology Reviews 12:289-327

Lentz DR, Goodfellow WD, Brooks E (1996) Chemostratigraphy and depositional environment of an Ordovician sedimentary section across the Miramichi-Tetagouche Group contact, northeastern New Brunswick. Atlantic Geology 32:101-122

Lockhart AW (1970) Woodstock claim group (21 J/4E): unpublished report for Falconbridge Nickel Mines Ltd., New Brunswick Department of Natural Resources and Energy, Mineral Resources, Assessment Files 470232 and 470233

Lockhart AW (1976) Geochemical prospecting of an Appalachian porphyry copper deposit, Woodstock, New Brunswick. Journal of Geochemical Exploration 6:13-33

Longerich HP (1995) Analysis of pressed powder pellets of geological samples using wavelength-dispersive x-ray fluorescence spectrometry. X-ray Spectrometry 24:123-136

Massawe RJ, Lentz DR (2020) Evaluation of crystallization and emplacement conditions of the McKenzie Gulch porphyry dykes using chemistry of rock-forming minerals: implications for mineralization potential. Ore Geology Reviews 116: p.103256.

McClenaghan SH, Lentz DR, Fyffe LR (2005) Chemostratigraphy of volcanic rocks hosting massive sulfide clasts within the Meductic Group, west-central New Brunswick. Exploration and Mining Geology 15:363-383

McLeod MJ, McCutcheon SR (2000) Gold environments in New Brunswick. New Brunswick Department of Natural Resources and Energy, Minerals and Energy Division, Map Plate 2000-8.

Moore C (1998) Assessment Report on the Connell Brook extension and Connell Mountain Claim groups. Noranda Inc. NBDNR Assessment File No. 475165, 17 p.

Roddick JC, Bevier ML (1995) U-Pb dating of granites with inherited zircon: conventional and ion microprobe results from two Paleozoic plutons, Canadian Appalachians. Chemical Geology 119:307-329

Ruitenberg AA, Fyffe LR (1982) Mineral deposits associated with the granitoid intrusions and subvolcanic stocks in New Brunswick and their relation to Appalachian tectonic evolution. Canadian Institute of Mining and Metallurgy Bulletin 75:83-97

Ruitenberg AA, Fyffe LR (1991) Characteristics and tectonic setting of granitoid-related mineral deposits in New Brunswick. New Brunswick Department of Natural Resources and Energy, Mineral Resources, Geoscience Report 91-1, 35 p.

Thomas RD, Gleeson CF (1987) Metallogeny of the Woodstock area: Geological Survey of Canada Paper 87-1A:489-498

Thomas RD, Gleeson CF (1988) Metallogeny of the Woodstock area. Geological Survey of Canada, Open File 1726, 128 p

van Staal CR (1994) Brunswick subduction complex in the Canadian Appalachians: record of the Late Ordovician to Late Silurian collision between Laurentia and the Gander margin of Avalon. Tectonics 13:946-962

van Staal CR, Barr SM (2012) Lithosphere structure and tectonic evolution of the Canadian Appalachians and Atlantic margin. Chapter 2, In Tectonic Styles in Canada: the Lithoprobe perspective. Edited by JA Percival, FA Cook, RM Clowes, Special Paper 49:41-95

van Staal CR, Fyffe LR (1991) Dunnage and Gander zones, New Brunswick: Canadian Appalachian Region. New Brunswick Department of Natural Resources and Energy, Mineral Resources, Geoscience Report 91-2, 39

Venugopal DV (1981) Geology of Hartland – Woodstock – Nortondale Region, Map areas H-19, H-20, I-20. New Brunswick Department of Natural Resources, MR 81-16.

Whalen JB, Rogers N, van Staal CR, Longstaffe FJ, Jenner GA, Winchester JA (1998) Geochemical and isotopic (Nd, O) data from Ordovician felsic plutonic and volcanic rocks of the Miramichi Highlands: petrogenetic and metallogenic implications for the Bathurst Mining Camp. Canadian Journal of Earth Sciences 35:237-252

Wilson RA (2003) Geochemistry and petrogenesis of Ordovician arc-related mafic volcanic rocks in the Popelogan Inlier, northern New Brunswick. Canadian Journal of Earth Sciences 40:1171-1189

Zagorevski A, van Staal CR, Rogers N, McNicoll VJ, Pollock J, Tollo RP, Bartholomew MJ, Hibbard JP, Karabinos PM (2010) Middle Cambrian to Ordovician arc-backarc development on the leading edge of Ganderia, Newfoundland Appalachians. Geological Society of America Memoirs 206:367-396.

INACTIVE AND RELICT ROCK GLACIERS OF THE DEBOULLIE LAKES ECOLOGICAL RESERVE, NORTHERN MAINE, USA

Aaron E. Putnam[1] and David E. Putnam[2]
[1]University of Maine, Department of Earth Sciences and Climate Change Institute, Orono, ME 04469
[2]University of Maine at Presque Isle, School of Science and Mathematics, Presque Isle, ME 04769

INTRODUCTION

Relict permafrost-related landforms, particularly permafrost-derived rock glaciers, have become important tools for deciphering the climatic manifestation of the abrupt climate changes of the last deglaciation (Kerschner, 1978; Sailer and Kerschner, 1999; Paasche *et al.*, 2007). At present, active rock glaciers are typically associated with rugged glacial and periglacial landscapes where the climate maintains air temperatures sufficiently low to sustain continuous permafrost (Wahrhaftig and Cox, 1959; Barsch, 1996; Humlum, 1998). Most active rock glaciers occur at sites where mean-annual air temperature (MAAT) is less than -4°C (Humlum, 1998; Paasche *et al.*, 2007). Therefore, inactive and relict (or 'fossil') rock glaciers can be used to reconstruct previous episodes when the MAAT was favorable for active rock-glacier growth. Rock-glacier-inferred MAAT can also complement summertime temperature proxy records, such as those based on glacier behavior and palaeosnowlines, to gauge the seasonality associated with past climate changes (Kerschner, 1978; Denton *et al.*, 2005).

The northeastern United States and adjacent Canada form the western boundary of the North Atlantic, and is an important region for tracking the spatial influence of late-glacial abrupt climate events that are thought to have originated from rapid changes in the North Atlantic thermohaline circulation (e.g., Broecker, 1998; Alley, 2000). Although much research has focused on the late-glacial history of relict rock glaciers in Europe, there is a paucity of recent information from the northeastern United States. In this study, we document previously unrecognized relict and inactive permafrost-derived rock glacier landforms in the remote Deboullie Lakes Ecological Reserve (DLER) of northern Maine, northeastern United States (Fig. 1). Several talus slopes located in the DLER have the characteristic lobate topography of landforms that are variably defined as 'protalus lobes' (White, 1976; Washburn, 1980; Harrison *et al.*, 2007), 'lobate rock glaciers,' (Wahrhaftig and Cox, 1959), 'talus glaciers' (Smith, 1973), 'talus-derived rock glaciers' (e.g., Kirkbride and Brazier, 1995; Brazier *et al.*, 1998; Ikeda and Matsuoka, 2002) and 'valley-wall rock glaciers' (e.g., Millar and Westfall, 2007). Over the course of four field expeditions conducted between 2004 and 2007, we conducted topographic surveys, temperature datalogger measurements, and geomorphic mapping to describe these landforms and determine possible linkages to present and past climate. In addition, a new radiocarbon-dated lacustrine record of sedimentation and organic content affords insight into the timing of deglaciation, the age of rock-glacier initiation, and the potential environmental conditions that may have accompanied rock-glacier formation. The rock glaciers of the northeastern United States and adjacent Canada offer important regional palaeoclimatic information, and together with European studies may afford a pan-Atlantic perspective on the seasonality of the abrupt climate changes that punctuated the last deglaciation.

PREVIOUS WORK

Nearly fifty years of discussions regarding rock-glacier classification based on origin and genesis, distribution, and climatic sensitivity have refined the general understanding of the geomorphic and climatic significance of rock glaciers (e.g., Wahrhaftig and Cox, 1959; Potter, 1972; Johnson, 1983; Hamilton and Whalley, 1995; Kirkbride and Brazier, 1995; Haeberli and Vonder Mühll, 1996; Brazier *et al.*, 1998; Clark *et al.*, 1998; Humlum, 1998; Steig *et al.*, 1998; Konrad *et al.*, 1999; Mitchell and Taylor, 2001; Janke and Frauenfelder, 2008; Millar and Westfall, 2007). As knowledge of periglacial landform-climate relationships progresses, rock glaciers are gaining increasing attention for their utility as recorders of past environmental changes (e.g., Kerschner, 1978; Konrad *et al.*, 1999; Humlum, 1998; Aoyama, 2006; Paasche *et al.*, 2007; Millar and Westfall, 2007). Some studies have used rock glaciers as a tool for reconstructing regional climate histories. For example, Birkeland (1982), Kirkbride and Brazier (1995), Ackert (1998), Aoyama (2004), and Paasche (2007), among others, showed that rock glaciers are (1) sensitive to climate changes, and (2) useful for deriving palaeoclimatic information.

Rock glacier descriptions in New England are few, and limited to relatively high-elevation regions. Goldthwait (1940; 1970) mapped a prominent 'block glacier' occupying the valley floor of King Ravine in the White Mountains of New Hampshire. Also in the White Mountains, Thompson (1999) suggested a rock-glacier origin for a tongue-like talus slope occurring along the north wall of Tuckerman's Ravine. A prominent tongue-shaped rock glacier

occupies the floor of North Basin, Mt. Katahdin, Maine (Thompson, 1961; Davis, 1989), but this feature has not yet been the subject of close investigation.

In addition, alpine permafrost and active permafrost-related landforms occur on the summits of Mt. Washington in the White Mountains of New Hampshire, Mt. Katahdin in Maine, and possibly other high alpine peaks in New England (Goldthwait, 1940; Thompson, 1962; Péwé, 1983; Walegur and Nelson, 2003; Nelson *et al.*, 2007). A number of investigators also reported rock glaciers and permafrost throughout the relatively low-elevation Chic Choc Mountains and coastal areas of the Gaspé Peninsula, Québec (Gray and Brown, 1979; Richard, *et al.*, 1997; Hétu and Gray, 2000a; Hétu and Gray, 2000b; Hétu *et al.*, 2003). For example, Hétu and Gray (2000b) identified at least eight relict talus-derived rock glaciers occurring in valleys along the north coast of the Gaspé Peninsula.

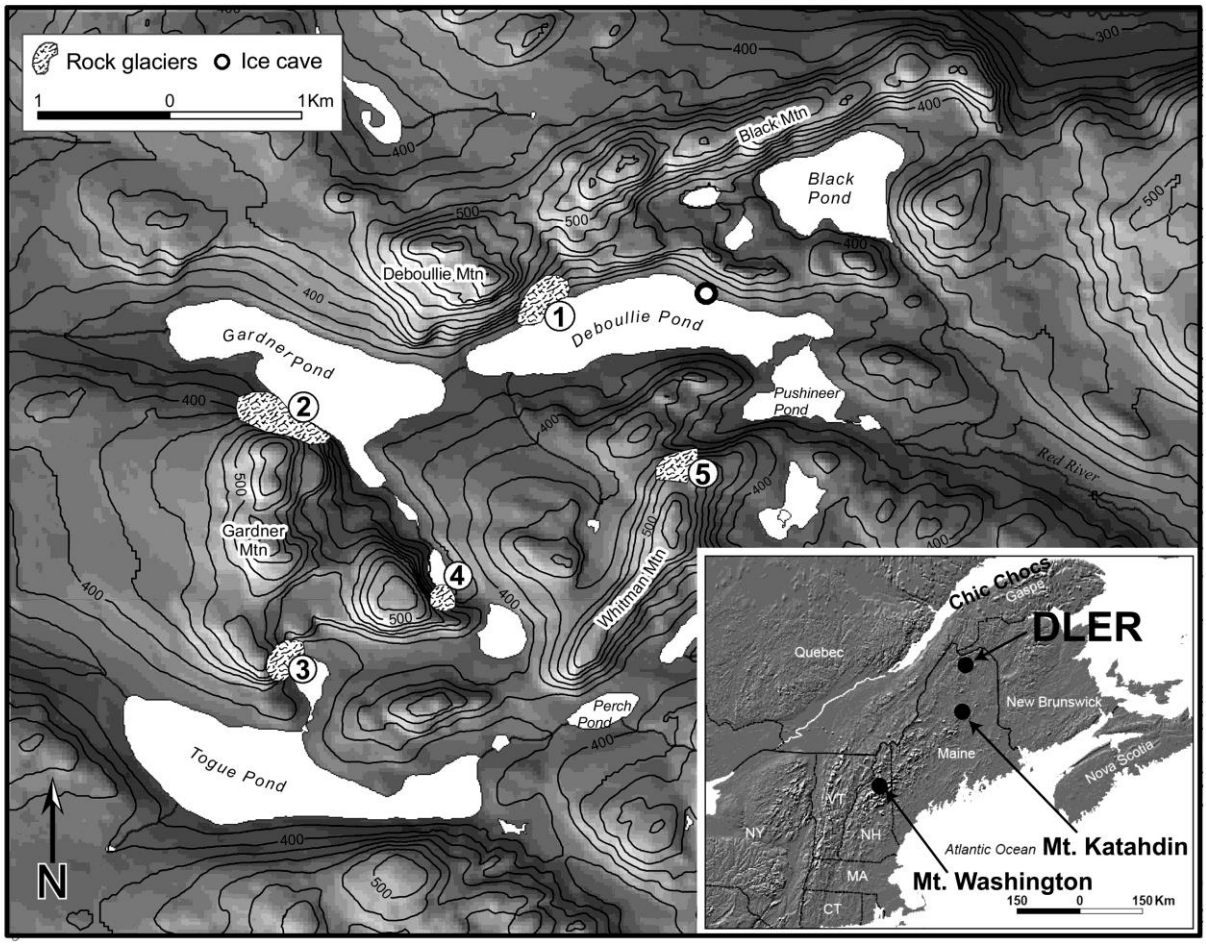

Figure 1. Map of the DLER study area. Stippled pattern indicates rock glaciers. Open dot shows ice cave. Circled numbers give the following rock glacier locations: 1) DPRG; 2) GPRG; 3) CPRG; 4) GalRG; 5) PPRG. Inset contains regional map with locations mentioned in the text.

STUDY AREA GEOLOGY AND ECOLOGY

The DLER is located in northern Maine between the Allagash and Fish River drainages (46°57'N, 68°53'W). Small, rugged mountains composed of quartzite and hornfels encircling the Deboullie syenite and granodiorite attain a maximum elevation of 599 m a.s.l. (Boone, 1958). Incipient cirques, paternoster lakes, U-shaped valleys with precipitous cliffs, and numerous large talus slopes give the area its name in the local Acadian French patois: *d'eboulis* – to tumble down.

The DLER supports a rare ecological assemblage that is typically associated with cold environments. The persistence of an isolated population of landlocked arctic char (*Salvelinus alpinus oquassa*), locally known as blueback trout, is attributed to the abnormally cold lake water, where summer deep-water temperatures range between 6 and 8°C (Bernatchez *et al.*, 2002; Wilkerson, 2007). Other rare boreal animal species found in the DLER

include the northern bog lemming (*Synaptomys borealis)*, and a freshwater amphipod (*Gammarus lacustris*). Several rare species of boreal plants occur in the DLER as well. For instance, the DLER is home to the only known Maine population of *Minuartia rubella* (Arctic Sandwort; Wilkerson, 2007).

At least five talus slopes in this region exhibit lobate rock-glacier characteristics as described by Wahrhaftig and Cox (1959), White (1976), Gordon and Ballantyne (2006), among others. We refer to these landforms as: 'Gardner Pond Rock Glacier' (GPRG), 'Crater Pond Rock Glacier' (CPRG), 'Deboullie Pond Rock Glacier' (DPRG), 'Galilee Pond Rock Glacier' (GalRG), and 'The Pushineer Pond Rock Glacier (PPRG). Figure 1 gives landform locations. This study focuses primarily on the three most prominent rock glaciers: GPRG, CPRG, and DPRG.

MODERN CLIMATE

Regional climate data recorded from the nearby Clayton Lake and Allagash weather stations between 1971 and 2000 give MAAT of 2.3°C and 2.2°C, respectively; mean summer temperatures of 15.8°C and 15.9°C, respectively; and mean winter temperatures of -13.2°C and -12.5°C, respectively (National Climatic Data Center, 2002). Mean annual precipitation (MAP) recorded between 1971 and 2000 is 903 mm/yr water equivalent (w.e.) and 912 mm/yr w.e. at the Allagash and Clayton Lake weather stations, respectively (National Climatic Data Center, 2002). The Allagash and Clayton Lake climate normals provide a close estimate for the climate of the Deboullie Lakes, where no permanent weather stations exist. These data reveal that central northern Maine experiences some of the coldest winter conditions in New England, and is affected by seasonality characteristic of a continental setting.

METHODS

Rock Glacier Classification

We used a field-based geomorphology approach to identify and describe several talus slopes with parabolic profiles in northern Maine, which we classify here as rock glaciers. The nomenclature of Wahrhaftig and Cox, (1959) as refined by more recent studies (e.g., Millar and Westfall, 2007), is used to classify rock-glacier activity and categorize these talus-derived rock glaciers (hereafter referred to as 'rock glaciers') as 'active,' 'inactive,' or 'relict' (see Table 1 for definitions). This classification is based on topographic data, observed distributions of persistent sub-surface ice, as well as vegetation and lichen cover (after Wahrhaftig and Cox, 1959; Ikeda and Matsuoka, 2002; Cannone and Gerdol, 2003).

Table 1. Rock glacier activity classification (adapted from Wahrhaftig and Cox, 1959; Cannone and Gerdol, 2003; Ikeda and Matsuoka, 2002; and Millar and Westfall, 2007).

Rock Glacier Activity	Description
Active	Embedded ice, active landform movement, oversteepened frontal slope, active clast sorting, no vegetation or lichens. Often associated with glaciers and persistent snowfields.
Inactive	Embedded ice, steep frontal slope, no landform movement, vegetation and lichen cover.
Relict (*Fossil)*	No embedded ice, no landform movement, 'deflated' appearance, vegetation cover.

Long Profile Survey

We used a traditional optical transit and metric stadia rod to measure longitudinal profiles of the DPRG, CPRG, and GPRG; and to classify rock glacier activity. Transects were from the top of each slope to the distal lobe where the rock glaciers intersect a lake shoreline. Subsurface temperature was measured at one-meter intervals along each profile. During the 2005 summer field season, we developed a high-resolution contour map of the GPRG surface using a total-station EDM to aid in geomorphic interpretation.

Temperature Dataloggers

To collect continuous temperature records, we placed three HOBO™ temperature dataloggers at different elevations along the longitudinal profile on the GPRG that recorded temperatures one-meter above and one-meter

below the rock-glacier surface. The subaerial probes were fastened to the top of wooden tripods, and the lower probes were suspended into the interstices between the large boulders of the GPRG surface. We left the subsurface temperature sensors uncovered by soil or rock so that we could gain an accurate assessment of the depth-to-surface air-temperature gradient. We programmed the instruments to collect data at 0.5-hr intervals for the summer/fall of 2004, and reduced the resolution to record once every hour over the fall/winter/spring of 2005/2006.

Lake Coring

Galilee Pond is the second highest pond in a paternoster chain located in the central DLER at an elevation of 348 m a.s.l (Fig. 1). Galilee Pond has an area of 0.03 km^2, a maximum depth of about nine meters, and occurs adjacent to a small rock glacier located beneath the steep, east-facing valley wall at its upper, southern end (GalRG; see Fig. 1). We used a modified Livingstone piston corer to extract a 7.92-m core from the sediments 8.4 m beneath the surface of Galilee Pond, for the purpose of determining a minimum age for deglaciation, and to provide a general constraint on the age of rock glacier formation. At the University of Maine palaeoecology laboratory, core-bottom sediments were sieved for organic macrofossils for radiocarbon dating, and loss-on-ignition (LOI) analyses were performed using the standard methods of Bengtsson and Enell (1986) and Heiri *et al.* (2001). We collected 2-cm^3 samples at 4-cm intervals in the lower 432 cm, and at 2-cm intervals in the upper portion of the core. Samples were dried overnight by oven, and combusted at 550°C. Percent LOI was determined from the ratio of the mass lost during combustion to the dry mass of the sample.

ROCK GLACIER MORPHOLOGY: RESULTS AND INTERPRETATIONS

Gardner Pond Rock Glacier

The GPRG is located beneath the northeast-facing cliff of Gardner Mountain, and has a parabolic slope that is comprised of large, tabular boulders between 0.5 and 2.0 m in length. At least three longitudinal furrows and three transverse lobes (see Figs. 2 and 3) characterize the slope surface. The largest lobe terminates at a steep slope ~11 m in height, is soil covered, and supports a thick 'spruce talus woodland', including *Picea mariana* (black spruce) and *Betula papyrifera* (paper birch) trees (Wilkerson, 2007). Pockets of ice were observed in boulder crevices during the late summer of each field season, and the July subsurface temperature profile, shown in Figure 2, reflects these observations. Mature vegetation indicates that the lobe is not actively advancing (Cannone and Gerdol, 2003), but the steep topography suggests that the rock glacier front is not significantly deflated. Post-depositional slumping has removed parts of the steep frontal slope. The resultant sections reveal that large, stacked angular boulders comprise the exposed portions of the rock glacier interior. Given the thick forest cover, parabolic topography, steep frontal slope and persistent sub-surface ice, we classify this lobe as 'inactive.'

A smaller concave lobe occurs above the larger, lower lobe (Fig. 3). The upper lobe terminates at a near-vertical slope ~3-m high. The slope is comprised of large boulders, and is covered by a 'Labrador Tea Talus Dwarf Shrubland' community consisting of ~30-cm thick 'cryophilic' floral mat containing numerous species of lichen (Wilkerson, 2007). Small, stunted *Picea mariana* (black spruce) are sparsely distributed on the lower lobe. We also observed persistent summer ice in the upper-lobe subsurface. For the same reasons given for the upper lobe, we consider this lobe inactive.

Finally, a forested terrace of talus boulders projects from the base of the GPRG lower lobe and terminates at the Gardner Pond shore where, underwater, the bouldery slope dips steeply toward the lake bottom. At its northern end, the GPRG overlies a diamicton interpreted to be a lodgement till that occurs as a thin drift throughout the DLER. The till is composed of rounded to subrounded cobbles and boulders of allocthonous lithologies. Similar outcrops of small, rounded, unsorted clasts outcrop at one location near the modern shoreline, indicating that the terminus of the rock glacier is roughly associated with the lakeshore. We interpret the lower rock glacier lobe as the oldest relict feature of the GPRG (Fig. 4).

Crater Pond Rock Glacier

The east-facing CPRG (Figure 2) has a parabolic form similar to that of GPRG. The most extensive lobe is a low-profile concave forested apron of talus-derived boulders lacking a steep frontal slope. Vegetation is classified as 'spruce talus woodland' (Wilkerson, 2007). As with the GPRG, this lower lobe overlies a diamicton comprised of allocthonous cobbles. No ice was observed during the 2004-2006 field seasons in this portion of CPRG. Therefore, we suggest that this deflated landform is a relict rock-glacier lobe.

The upper CPRG lobe occurs upslope of the lower lobe, and terminates in a steep front five meters in height. We observed persistent summer ice in the subsurface of the upper CPRG lobe, which is complemented by the July 2004 subsurface temperature profile (Fig. 2). A recent slump on the frontal slope has exposed the internal structure

of a small portion of the rock glacier. As with the GPRG, in this section the CPRG appears to be entirely clast supported, comprised almost exclusively of large, angular boulders. The upper lobe is in part forested, particularly on the steep frontal slope as well as on the upper talus. 'Labrador tea talus shrubland' covers the broad top surface of the lobe (Wilkerson, 2007). We classify the upper CPRG lobe as inactive on the basis of steep, lobate topography, the persistence of subsurface ice, and vegetated surfaces.

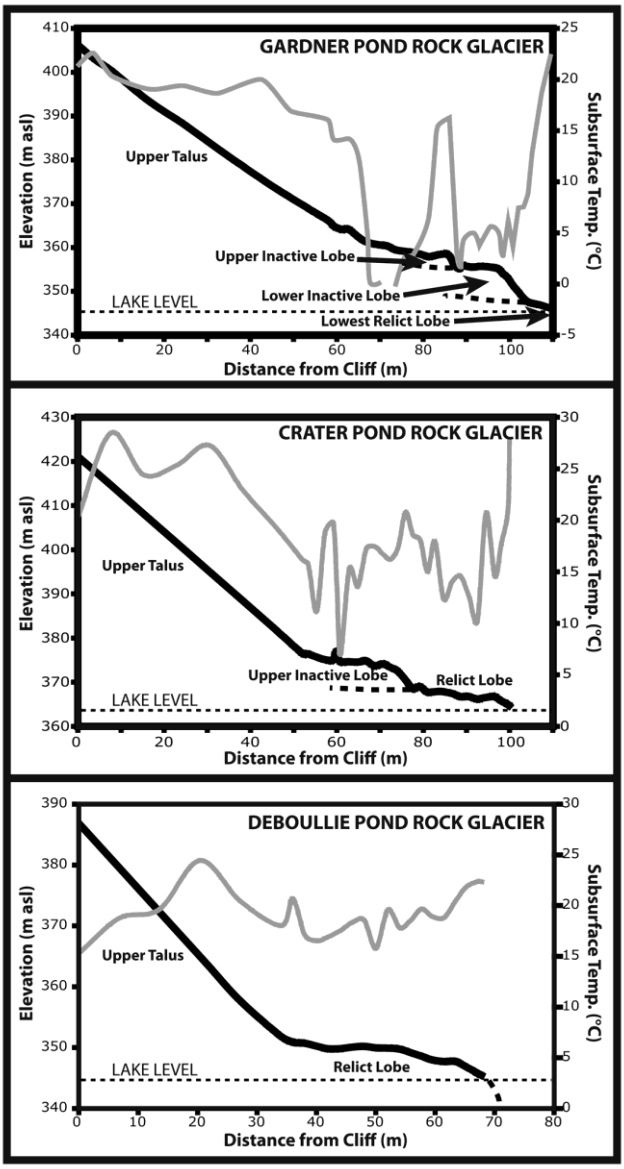

Figure 2. Longitudinal slope profiles of the GPRG (top panel), CPRG (middle panel), and DPRG (bottom panel). Black solid line represents slope surface, gray line gives July temperature profile along slope. Thick dotted black lines show inferred contacts between lobes, and thin, horizontal dotted lines indicate modern lake level.

Deboullie Pond Rock Glacier

The DPRG (Fig. 2) is comprised of large, unsorted tabular clasts about 1–2 m in diameter. The slope faces due south, and consists of one parabolic lobe that contains a more subdued frontal bulge with no obvious transverse ridges or furrows. The DPRG surface is mostly bare, with vegetation occurring only in a few small depressions. No visible ice could be found within the boulder interstices, and the July subsurface temperature profile does not show abnormally cool conditions (Fig. 2). We interpret the DPRG to be a 'relict' rock-glacier landform.

A man-made hole, known historically as the 'ice cave,' occurs in till at the foot of a forested lobate talus slope east of the DPRG. The ground subsurface at this site generally remains frozen throughout the summer, indicating that despite the relict form of the DPRG, perennial ice does occur sporadically in the south-facing slopes of the region.

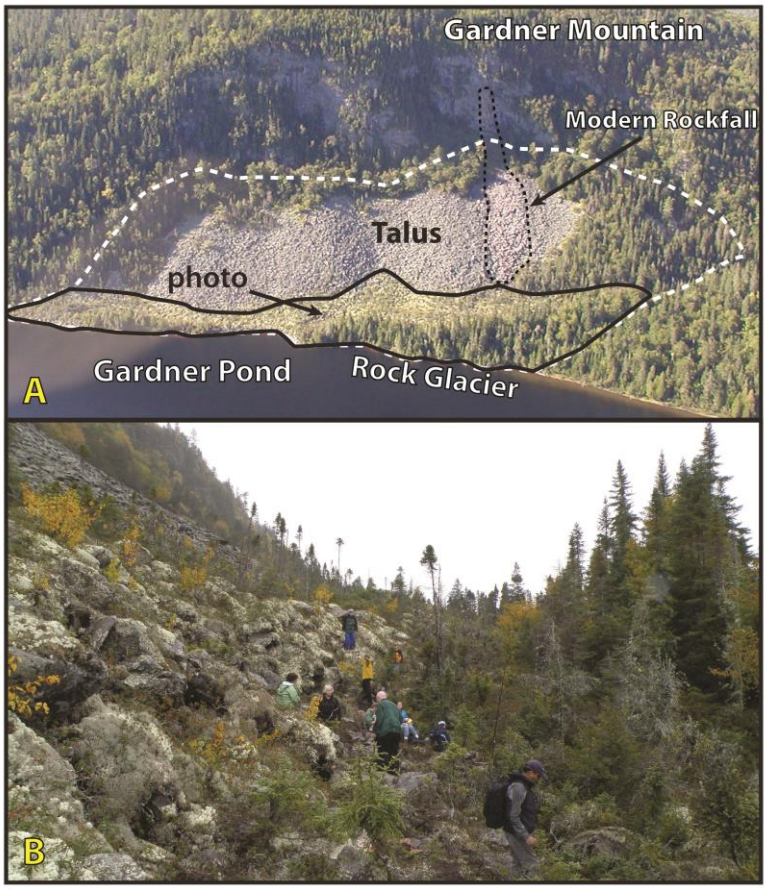

Figure 3. Panel A: oblique air photo taken south toward the GPRG. Dark line indicates rock glacier portion of slope; white, dashed-line outlines talus slope; black dashed line shows modern rockfall scar (cliff) and deposit (talus). Arrow indicates direction of photograph in panel B. Panel B is a photograph taken looking west along the frontal slope of the GPRG upper lobe. Note the steep slope angle, and the thick tundra-like vegetation cover. Members of the UMaine Climate Change

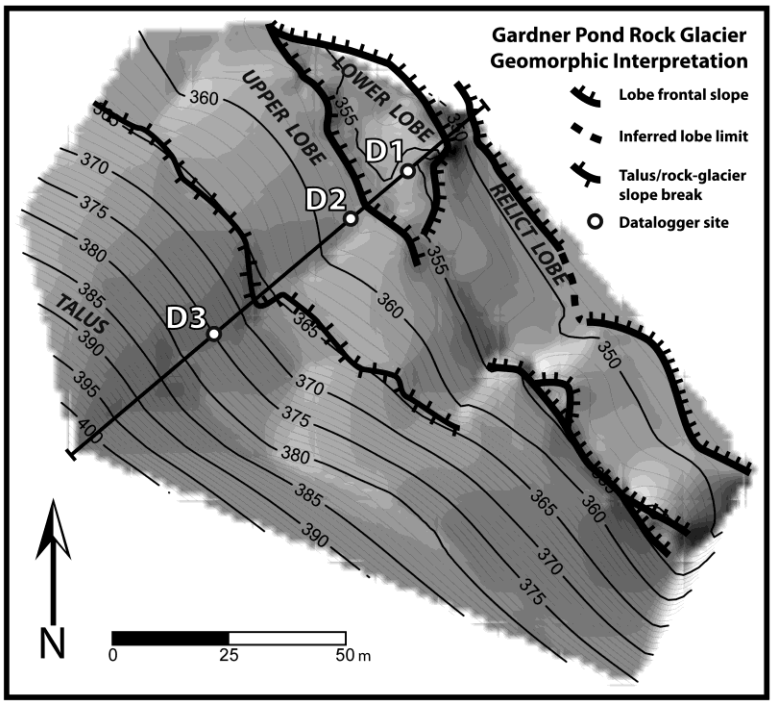

Figure 4. Geomorphic map of GPRG. Light contours are spaced at one-meter intervals, dark contours at five-meter intervals. Inset contains key to map symbols.

INTERPRETATIONS OF RELATIVE AGE AND GENESIS

The three described landforms exhibit distinct parabolic profiles that are classically associated with 'talus-derived' or 'valley-wall' rock glaciers, and these features consist of both relict and inactive lobes. We observed no distinct transverse ridges with well-defined hillside troughs, or clast sorting to indicate that these features formed as protalus (or pronival) ramparts (Gordon and Ballantyne, 2006). The inactive transverse lobes retain steep fronts indicating that ice may still exist beneath the surface. However, established vegetation communities suggest no recent rock-glacier activity (Cannone and Gerdol, 2003). In contrast, relict features are deflated, do not contain observable ice, and are forested on the distal surfaces of CPRG and GPRG. The DPRG is a conspicuous feature of the north shore of Deboullie Pond because it faces due south, is not vegetated, and consists of one deflated, yet extensive relict lobe.

The deflated form of the DPRG may be due to its southerly aspect, which exposes the landform to more direct solar radiation than GPRG or the CPRG, the latter two being situated beneath steep, northeast- and east-facing cliffs, respectively. The lack of vegetation may indicate relatively recent settling compared to the relict lobes of CPRG and GPRG. It is worth noting, however, that ice exists among the forested talus slopes that occur adjacent to the DPRG, and therefore may point to another reason for the deflated form of the rock glacier. Middle to late Holocene lake-level rise of northern Maine ponds has been by documented Dieffenbacher-Krall and Nurse (2006). In addition, young littoral features around Deboullie Pond indicate elevated lake level associated with a historical dam at the Pushineer Pond outlet (Wilkerson, 2007). Lake level changes, either climate-driven or anthropogenic, may thus explain the relict form of the DPRG, and perhaps the lower relict lobes of GPRG and CRPRG. With the exception of the DPRG, the other rock glaciers exhibit evidence for multiple advances based on the presence of multiple overlapping lobes.

Rock glacier advances occur when climate conditions are favorable for permafrost growth and creep (Haeberli and Vonder Mühll, 1996), as well as talus production resulting from freeze-thaw cycles in the overhead cliffs. Cooler climate and stronger seasonality enhance both of these processes. Vegetated cliff faces of the DLER indicate relative stability, with only one apparently recent rock-avalanche scar and deposit on the north end of the upper GPRG talus (Fig. 3). The fresh appearance of the recent rockfall deposit is a marked contrast to the nearby weathered lichen-covered talus. Distinct characteristics of ancient talus, such as weathering and lichen cover, indicate a low frequency of recent talus accumulation. Infrequent rockfall, taken together with the vegetated inactive and relict lobes of the various DLER rock glaciers, implies that the lobes represent earlier periods of climate conditions more favorable to rock-glacier development, including both temperature and debris supply. Due to the high shear stress required to deform coarse rock-ice mixtures, thick ice lenses are necessary to facilitate downslope creep of talus-derived rock glaciers (Whaley and Azizi, 2003; Harrison *et al.*, 2007). Present stability of the talus slopes implies that ice lenses are not sufficiently thick or actively accreting in the upper talus to facilitate downslope deformation. Therefore, frontal bulges of the inactive lobes of GPRG and CPRG indicate previous periods of downslope extension. The deflated, concave profile of the DPRG exhibits the result of the loss of internal ice. Overall, the DLER rock glaciers appear to be inactive or relict landforms formed during multiple episodes of prior growth.

TEMPERATURE DATALOGGERS: RESULTS AND INTERPRETATIONS

The temperature datalogger results for summer 2004 and winter 2005-06 are shown in Figure 5. Field observations suggest that as summer progresses, the visible ice, frozen among the surface interstices, gradually recedes into the depths of the rock glacier. Given that the subsurface temperature signatures for D1 and D2 show little resemblance to their respective above-surface counterparts (as well as the D3 signal), and display relatively cool or near-freezing temperatures throughout the summer, we assume that the subsurface temperature reflects the relative proximity of the sensor to the surface of the rock glacier ice.

Temperatures registered in the subsurface at sites D1 and D2 display a gradual rise throughout the summer of 2004, as well as in the late spring of 2006. In contrast, subsurface temperatures measured at D3 co-vary with above-surface temperatures throughout the year. We note that no ice has been observed in the interstices at the location of D3 in the upper talus. These results show that in portions of the slope that contained ice, subsurface temperatures rose slowly throughout the duration of the summer season, despite considerable variability in air temperature one-meter above the surface. During the late summer of 2004, the rising trend in rock-glacier subsurface temperature actually opposes the declining trend of above-surface temperature. From this we infer that warmth registered one-meter above the rock glacier is not apparent immediately below the surface. The extreme summer temperature-depth gradient is perhaps a result of the inefficient downward conduction of surface heat through the high-albedo granite

boulders forming the surface of the rock glacier, and through the spongy vegetation mat insulating the surface. This may also indicate the presence of deeper ice that may facilitate the persistence of ice so close to the rock-glacier surface during the summer. Thus, we interpret temperature data recorded by D1 and D2 to indicate the presence of permafrost in the GPRG.

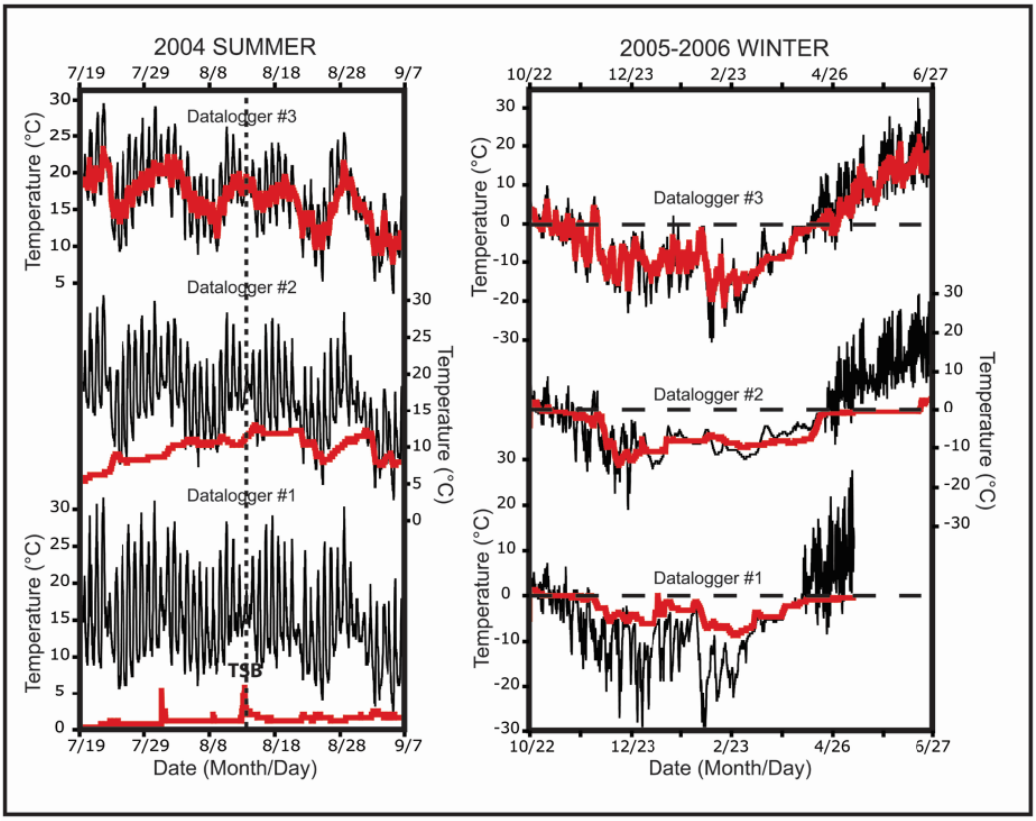

Figure 5. GPRG datalogger results for summer 2004 (left panel) and winter 2005-2006 (right panel). Thin, solid black lines show GPRG above-surface temperature; solid, red lines indicate subsurface temperatures. Vertical dashed line marks the date when the remnants of Tropical Storm Bonnie (TSB) reached northern Maine.

In contrast to the summer months, the colder above-surface temperature was matched by general cooling in the rock glacier subsurface at all datalogger locations during the winter. Thus, it appears that the GPRG subsurface is directly sensitive to cooling episodes, but seems to respond more slowly to warmth. Wintertime subsurface air sensitivity may be associated with the 'Balch' or 'chimney' effect: where winter convection in the upper talus draws cold air deep into the talus interstices, and supercools the base of the deposit (Delaloye and Lambiel, 2005). Thompson (1962) suggested that Balch ventilation may play an important role in the growth of subsurface ice in the King Ravine rock glacier of the White Mountains, and this may also be true for the DLER rock glaciers. Delaloye and Lambiel (2005) suggested that Balch ventilation, described as the 'chimney effect', might preserve relict permafrost bodies in the lower portions of relict and inactive rock-glacier landforms at or below the altitudinal limit of the discontinuous permafrost zone. We suspect this may be the mechanism allowing permafrost to persist in the CPRG and CPRG.

Finally, precipitation patterns appear to play a secondary role in elevating summer subsurface temperatures. The subsurface sensor of D1 registers a series of conspicuous peaks during the summer of 2004 that result in slightly elevated subsurface temperatures. These peaks correlate to thunderstorm events that occurred in northern Maine, as well as precipitation from the remnants of tropical storm Bonnie. The August 2004 'unusual weather phenomena storm data' (World Meterological Society, 2004) reported heavy rain, flooding, and mudslides as Tropical Storm Bonnie swept over northern Maine between Aug 13 and 14. This event was registered as an abrupt warming in the subsurface temperature of D1, perhaps related to rain percolating into the talus and rock-glacier interstices, and over the temperature sensor. However, D1 subsurface temperature returned to near-zero values following each event.

Though rainfall must play a role in the ablation of subsurface ice at D1, it is less noticeable against the overall warming trend registered in D2.

PALAEOTEMPERATURE RECONSTRUCTION

To estimate the MAAT favorable to initiate rock-glacier expansion in the DLER, we provide a simple conceptual model that uses the regional modern permafrost elevation to infer the climatic cooling necessary to initiate active rock-glacier growth (after Walegur and Nelson, 2003; Nelson *et al.*, 2007). The modern mountain permafrost-elevation gradient is constructed based on the known permafrost localities of Mt. Washington (e.g., Thompson, 1962; Péwe, 1983; Spear, 1989; Clark and Schmidlin, 1992) and the Gaspé Peninsula (Hétu and Gray, 2000b), as well as the geological and ecological indicators of active permafrost presence on the summit of Mt. Katahdin (Péwe, 1983; Walegur and Nelson, 2003; Fig. 6). The theoretical elevation of continuous permafrost at the latitude of the DLER was interpolated from the modern permafrost-elevation gradient, and from this we determined an elevation difference of ~900 m between the modern permafrost elevation and the toe of the GPRG. Assuming an adiabatic lapse rate of 6.5°C/km, we estimate that the DLER rock glaciers were formed at a time when MAAT was ~6.3°C cooler than present, yielding a palaeo-MAAT of about -4°C. Following the same procedure, the palaeo-MAAT difference was calculated using the King Ravine rock glacier in the White Mountains, New Hampshire, and the North Basin rock glacier of Mount Katahdin, Maine. The difference between the modern permafrost elevation and the toe of the King Ravine rock glacier is ~800 m, and indicates a MAAT temperature difference of ~5.3°C. The toe of the North Basin rock glacier occurs ~720 m below the modern permafrost elevation, indicating a ~4.7°C difference in MAAT. These temperature estimates range with respect to the adiabatic lapse rate used. For instance: 6.0°C/km (moist) = 8% warmer, 7.0°C = ~8% cooler, and 8.0°C/km (dry) = 23% colder.

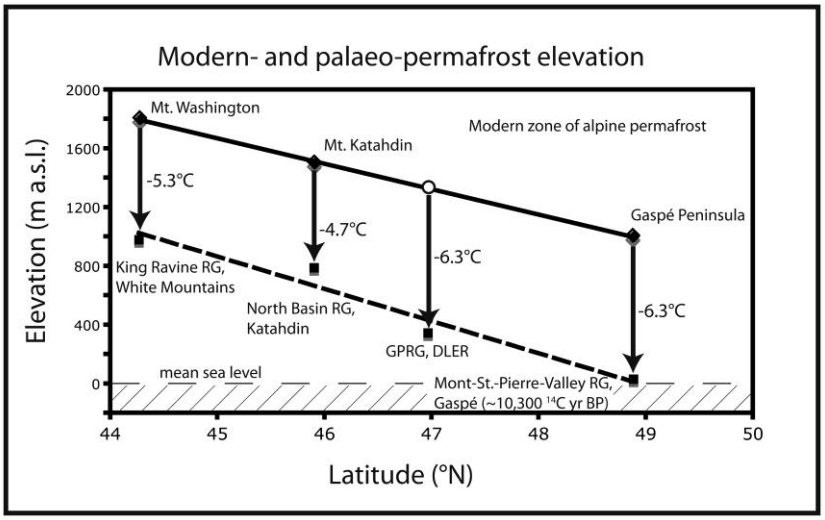

Figure 6. Diagram shows modern permafrost elevation trend with latitude as solid line, and reconstructed palaeo-permafrost gradient as dark dashed line. Filled diamonds represent regions of modern alpine permafrost occurrence, filled squares indicate rock glacier occurrence, the open circle represents the point interpolated from the modern permafrost trendline above DLER, and arrows show calculated MAAT changes inferred from modern vs. palaeo-permafrost elevation difference.

Our palaeotemperature estimates from the DLER and elsewhere in New England are very similar to values obtained by Hétu and Gray (2000b), who attributed relict rock glaciers occurring in the lowlands of the Gaspé Peninsula to a ~6°C lowering of MAAT. The observations of Hétu and Gray (2000b) together with the data from this study were used to calculate a palaeo-permafrost elevation gradient, shown in Figure 6. Since rock glacier length can be limited by debris input and moisture-availability for ice-lense growth, this trend probably reflects a minimum estimate for the lower elevation of continuous permafrost at the time the rock glaciers formed. This does not preclude the possibility that permafrost occurred at lower elevations, however the close agreement among the results from these four localities indicates that the rock glaciers of New England and maritime Canada may represent a close estimate for the former lower limit of continuous permafrost in the region.

This simple regional model should be considered a preliminary framework that requires future testing and refinement. Uncertainties involve topoclimatic effects that may complicate the relationship of permafrost distribution to regional climatic trends, as well as lapse-rate choice (Walegur and Nelson, 2003). Also, the interpreted palaeotemperature lowering for the New England rock glaciers slightly underestimates the palaeo-MAAT value calculated using the classification of Humlum (1998), who suggested that active rock glaciers are most common in environments with MAAT less than -6°C. Despite these caveats, our results reflect simple and consistent regional trends, and thus we hypothesize that the rock glaciers of New Hampshire, Maine, and the Gaspé Peninsula reached their maximum post-glacial extent at roughly the same time, during a period when MAAT was at least ~6°C cooler than today in New England and maritime Québec.

GALILEE POND SEDIMENT CORE: RESULTS AND IMPLICATIONS

The Galilee Pond core consists of three sedimentary units: 0.1 m of unconsolidated sand, gravel and pebbles at the very bottom, 1.4 m of blue-gray sandy clay and silt at the base, and 6.42 m of gyttja at the top (see Fig. 7). The bottom ten centimeters contain striated, rounded pebbles of the Seboomook formation and angular granules from the local granodiorite bedrock. We infer the basal unit to be till, probably continuous with the glacial drift that surrounds the pond. Two terrestrial plant macrofossil samples sieved from the basal sediments 76 cm and 49 cm above the base of the core returned basal AMS dates of 10,930 ± 40 and 11,320 ± 40 ^{14}C yrs BP, respectively (Table 2). Every four-centimeter sample from the lower 1.5 m of the core contained some plant material, although in most cases the total dry weight of the material was insufficient for AMS analysis. *Dryas* leaves and twigs occurred in all samples. *Betula* flowers appear 50-cm above the base of the core, and occur in each sample upwards into the gyttja.

Most basal ages of sediment cores recovered from northern Maine lakes have been obtained from plant macrofossils or bulk organics from gyttja overlying basal minerogenic sediments (e.g., Borns *et al.*, 2004; Dieffenbacher-Krall and Nurse, 2005). In this case, we collected plant macrofossils from within the mostly inorganic basal sediments, providing a closer minimum age for when the pond became free of overlying glacial ice. Radiocarbon dates indicate that the pond was deglaciated during the late Alleröd jnterstade, and plant macrofossils in the basal unit imply that a shrub-tundra environment persisted for much of the late glacial period in the region. We infer from these results that the northern Maine ice cap identified and discussed by Lowell (1985), Kite and Stuckenrath (1986), Lowell and Kite (1986), Lowell *et al.* (1990), Newman *et al.*, (1985), Borns *et al.* (2004), Pelletier and Robinson (2005), and Nurse *et al.* (2006), must have withdrawn from the DLER before the late-Allerød, with no evidence for Younger Dryas reoccupation (YD; 11,000 – 10,000 ^{14}C yrs BP; Mangerud *et al.*, 1974). This is consistent with the deglaciation isochrones of Borns *et al.* (2004) from central northern Maine, and with findings from the White Mountains and Mount Katahdin indicating pre-YD deglaciation (Davis, 1989; Davis, 1999).

The elevation of Galilee Pond, slow sedimentation rate (~0.07 cm/yr), and the continuous occurrence of plant macrofossils throughout the basal silty clay indicate a terragenous, non-glacial sediment source. This conclusion contrasts with previous assumptions that a similar basal clay unit found throughout northern Maine is glaciolacustrine in origin (i.e., Dieffenbacher-Krall and Nurse, 2006). Instead, we suspect that surface runoff may have gradually winnowed the relatively fresh till around the pond, transporting glacial silts and clays and contributing to the glaciogenic appearance of the blue-gray clay unit. Cryoturbation and eolian processes also may have augmented sediment supplied to Galilee Pond during the late-glacial period (Mott and Stea, 1993). Meltwater from the small GalRG could have contributed to the minerogenic basal sediments in the pond, however this explanation cannot account for the widespread occurrence of similar basal sediments in lakes throughout northern Maine (i.e., Borns *et al.*, 2004; Dieffenbacher-Krall and Nurse, 2006).

The stratigraphy and macrofossils of the relatively inorganic basal sediments indicate that a cold, possibly periglacial environment existed during late-glacial time, yielding climate conditions favorable for rock-glacier growth. Core stratigraphy and loss-on-ignition data show no indications that the climate reverted to similarly cold conditions at any time prior to deposition of the basal sediments, enhancing the probability that the DLER rock glaciers formed soon after the region was uncovered by ice at the end of the Pleistocene.

PALAEOCLIMATE IMPLICATIONS

For the reasons stated above, the late glacial was probably the most favorable period of any time throughout the post-glacial era for the growth of deep permafrost lenses required for rock-glacier development from the coarse talus slopes of New England and Atlantic Canada. Regional palaeoecological interpretations (e.g., Levesque *et al.*, 1993; 1997; Stea and Mott, 1999; Borns *et al.*, 2004; Dieffenbacher-Krall and Nurse, 2005), in addition to more distant ice

core analyses from Greenland (e.g., Alley, 2000) show that the late-glacial period was punctuated by the most recent severe cold events to occur in the North Atlantic region: the Killarney Oscillation (KO; 11,200 – 10,900 ^{14}C yrs BP; Levesque *et al.*, 1993), and the YD cold period (Levesque *et al.*, 1993; Levesque *et al.*, 1997; Borns *et al.*, 2004). In New England, proxy records of post-glacial climate show that the KO/YD oscillations bear the most outstanding signature of late-glacial cooling (Borns *et al.*, 2004), which is in accord with our stratigraphic and LOI record from Galilee Pond.

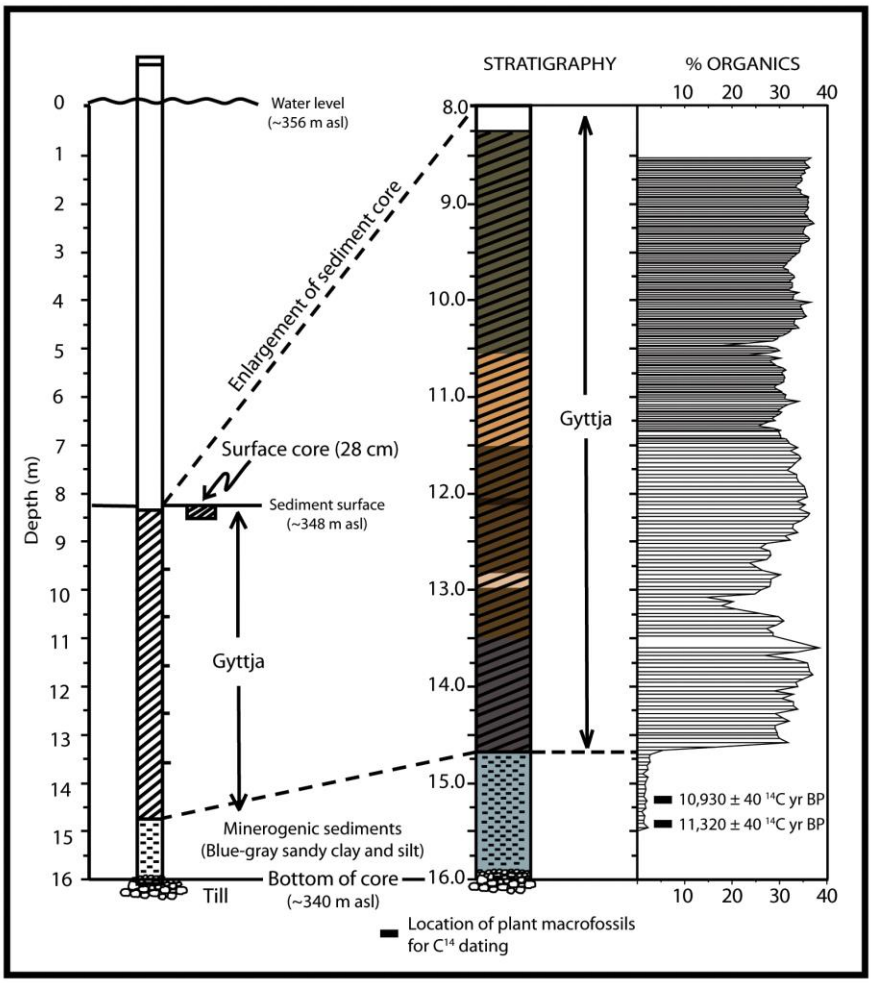

Figure 7. Galilee Pond core diagram. Left side of figure shows water column and sediment core, and the enlarged sediment stratigraphy is displayed in the middle. Different shades of gray reflect the relative color differences of the gyttja with depth. Diagonal lines indicate gyttja, and dot pattern is blue-gray sandy silt and clay. Percent organics inferred from loss-on-ignition analyses occur on right. Black squares signify depth of radiocarbon ages.

Table 2. Radiocarbon dates from the Galilee Pond basal sediments. 'NR' indicates that there was not sufficient mass for a $^{13}C/^{12}C$ ratio measurement, and thus the AMS laboratory reported none. A conventional radiocarbon age was derived from a $^{13}C/^{12}C$ ratio of a small aliquot of graphite that included laboratory and detector-induced fractionation, and therefore was not reported by Beta Analytic. This ratio corrects to the appropriate conventional radiocarbon age for sample GALM1516-12, however (D. Hood, personal communication, 2006).

Sample ID	Depth (cm)	Age (^{14}C yrs BP)	$\delta^{13}C$ (‰)	Sample Description	Laboratory ID
GALM1516-12	676	10,930 ± 40	-28.3	Herbaceous twigs, *Betula* flowers, and *Dryas* leaves	Beta-222924
GALM1543-40	703	11,320 ± 40	NR	One small herbaceous twig and several *Dryas* leaves	Beta-222923

Our analysis indicates that northern Maine was affected by a decrease in MAAT that led to the development of rock glaciers, but did not cause glaciers to readvance into the DLER. Additional supporting evidence for regional late-glacial rock-glacier growth comes from the Mont-St.-Pierre Valley, Gaspé. In this region, a wave-cut marine terrace that incised a now-relict rock glacier has been dated to 10,300 ^{14}C yrs BP (Hétu and Gray, 2000b), indicating that rock glacier expansion beyond glacier limits occurred during the YD on the Gaspé Peninsula. Kerschner (1978) presented a similar case, where he suggested that rock glaciers in the Austrian Alps expanded to lower elevations than local glaciers during the YD as a result of MAAT weighted towards colder, drier winters. Frauenfelder *et al.* (2007) presented a similar case for the Swiss Alps, showing that YD-age rock glaciers expanded to lower elevations than glacier equilibrium lines at that time, and YD-age rock-glacier expansion also occurred in the British Isles beyond the Loch Lomond moraine limits (Harrison *et al.*, 2007).

This situation is consistent with the findings of Denton *et al.* (2005), who proposed that MAATs during the YD, inferred from the isotopic composition of trapped gas in Greenland ice (e.g., Severinghaus and Brook, 1999), were most influenced by intensely cold winters that overwhelmed the summer temperature signal. They argued that intensely cold winters were a consequence of YD-weakening of the thermohaline circulation, which allowed winter sea ice to spread over the North Atlantic. During that time the extreme seasonality initiated periglacial processes across northern Europe, as well as on the eastern seaboard of North America, far from active glacial ice (e.g., Borns, 1965; Stea and Mott, 1998; Hétu and Gray, 2000b). Therefore, given the generally accepted link between rock glacier occurrence and MAAT, as well as our preliminary inferences about the dampened sensitivity of the DLER rock glaciers to summer temperature, we suggest that the expansion of the New England and maritime Canada rock glaciers occurred in response to the severe winter climate of the YD period, despite comparatively mild summers.

Finally, we consider the possibility that the DLER rock glaciers may have been completely free of ice, and hence relict, during the Middle Holocene when summers in New England were warmer (i.e., Sanger *et al.*, 2007), and that the modern ground ice observed in the DLER region represents the regrowth of permafrost during late-Holocene cooling. This hypothetical situation seems reasonable, though we have no data to confirm or deny the possibility. However, we offer the following speculation. Since rock glacier activity is apparently most sensitive to MAAT, it seems possible that the strong seasonality imposed by Earth's precessional cycle during the early and middle Holocene could have resulted in zero net effect on rock glacier activity. In this scenario, the impact of warmer summers on ground temperature would have been cancelled by equally cold winters. Developing a landform chronology using surface-exposure dating methods, more comprehensive lacustrine records, as well as chemical analyses of deep ice could help to inform our understanding, and develop reasonable hypotheses.

CONCLUSIONS

A series of talus landforms located in the Deboullie Lakes Ecological Reserve of northern Maine are classified as inactive and relict talus-derived rock glaciers on the basis of parabolic topographic profiles, and subsurface thermal characteristics. Inactive and relict lobes indicate past rock-glacier activity. Observations and temperature datalogger results of subsurface and above-surface conditions of the GPRG show that subsurface ice persists throughout the year in the lower portion of the slope. Subsurface temperature is largely decoupled from the magnitude of summer warmth in the lower, lobate portion of the landform, whereas during the winter, subsurface temperatures appear to respond more immediately to above-surface temperatures. This is particularly the case during periods of internal cooling, which may be related to Balch ventilation, and may be important for the preservation of subsurface ice in lower portions of the rock glaciers.

Using the published archive of modern alpine permafrost occurrence, we estimate that a MAAT depression of at least ~6°C is required to initiate active growth of the DLER rock glaciers. This estimate is consistent with the palaeotemperature depression derived from rock glaciers in Gaspésie, Québec (Hétu and Gray, 2000b), the King Ravine rock glacier in New Hampshire, and the North Basin rock glacier of Mount Katahdin. Finally, the radiocarbon-dated Galilee Pond sediments and organic content indicate that the DLER rock glaciers most likely formed during the late-glacial period. Similar to the case in Europe, rock-glacier activity in the absence of significant glacier readvance in the DLER implies that a severe wintertime climate characterized the late-glacial period in northern Maine.

ACKNOWLEDGEMENTS

We thank the Maine Department of Conservation, Bureau of Parks and Lands for access, logistical support, and aerial photography. John Helstrom's expertise in monitoring and maintaining dataloggers was invaluable. We thank Bert Pelletier for his EDM surveying expertise; Andrea Nurse for providing coring equipment and field expertise;

and Chunzeng Wang for his help drafting the figures. Karen Marysdaughter helped with LOI analyses. We are grateful for Mike Brophy's hospitality at Red River Camps, and for the use of his canoes. The wisdom, encouragement, and persistent support of Gary Boone, the late Dee Caldwell, Marvin Caldwell, and Bill Forbes precipitated many of the ideas presented in this study. Terry Hughes, Gordon Hamilton, Jorge Strelin, Roger Hooke, George Denton, Tom Weddle, Brenda Hall, and Tom Lowell contributed helpful insights. We thank Michael Kaplan for reviewing early drafts of this paper, and Jeffrey Munroe and Woody Thompson for providing constructive reviews that greatly improved the manuscript. Finally, we thank all of the hard-working students that assisted with fieldwork during each expedition.

REFERENCES

Ackert, R.P., Jr. 1998. A rock glacier/debris-covered glacier at Galena Creek, Absaroka Mountains, Wyoming. Geografiska Annaler 80A: 267-276.

Alley, R.B. 2000. The Younger Dryas cold interval as viewed from central Greenland. Quaternary Science Reviews 19: 213-226.

Aoyama, M. 2005. Rock glaciers in the northern Japanese Alps: palaeoenvironmental implications since the Late Glacial. Journal of Quaternary Science 20: 471-484.

Barsch, D. 1996. Rock Glaciers: Indicators for the Present and Former Goecology in High Mountain Environments. Springer: Berlin.

Bengtsson, L., Enell, M. 1986. Chemical analysis. In Handbook of Holocene Palaeoecology and Palaeohydrology, Berglund, BE (ed). John Wiley and Sons Ltd., Chichester, 423-451.

Bernatchez, L., Rhydderch, J.G., Kircheis, F.W. 2002. Microsatellite gene diversity analysis in landlocked arctic char from Maine. Transactions of the American Fisheries Society, 131: 1106-1118.

Birkeland, P.W. 1982. Subdivision of Holocene glacial deposits, Ben Ohau Range, New Zealand, using relative-dating methods. Geological Society of America Bulletin 93: 433-449.

Boone, G.E. 1958. The geology of the Fish River Lake-Deboullie area, northern Maine. Ph.D. Dissertation, Yale University, New Haven, Connecticut, 186 p.

Borns, H.W., Jr. 1965. Late glacial ice-wedge casts in northern Nova Scotia, Canada. Science 148: 1223-1226.

Borns, H.W., Jr., Doner, L.A., Dorion, C.C., Jacobson, G.L., Jr., Kaplan, M.R., Kreutz, K.J., Lowell, T.V., Thompson, W.B., Weddle, T.K. 2004. The deglaciation of Maine. In: Extent and Chronology of Glaciations, Vo.2: North America, Maine, Ehlers J., Gibbard P. (eds). INQUA commission on glaciation: Germany; 89-109.

Brazier, V., Kirkbride, M.P., Owens, I.F. 1998. The relationship between climate and rock glacier distribution in the Ben Ohau Range, New Zealand. Geografiska Annaler 80A: 193-207.

Broecker, W.S. 1998. Paleocean circulation during the last deglaciation: A bipolar seesaw? Paleoceanography 13: 119-121.

Cannone, N., Gerdol, R. 2003. Vegetation as an ecological indicator of surface instability in rock glaciers. Arctic, Antarctic, and Alpine Research 35: 384-390.

Clark, D.H., Steig, E.J., Potter, N., Jr., Gillespie, A.R. 1998. Genetic variability of rock glaciers. Geografiska Annaler 80A: 175-182.

Clark, G.M., Schmidlin, T.W. 1992. Alpine periglacial landforms of eastern North America: A review. Permafrost and Periglacial Processes 3: 225-230.

Davis, P.T. 1989. Late Quaternary glacial history of Mt. Katahdin and the nunatak hypothesis. Maine Geological Survey: Studies in Maine Geology 6: 119-134.

Davis, P.T. 1999. Cirques of the Presidential Range, New Hampshire, and surrounding alpine areas in the northeastern United States. Géographie physique et Quaternaire 53: 25-45.

Delaloye, R., Lambiel, C. 2005. Evidence of winter ascending air circulation throughout talus slopes and rock glaciers situated in the lower belt of alpine discontinuous permafrost (Swiss Alps). Norsk Geografisk Tidsskrift 59: 194-203.

Denton, G.H., Alley, R.B., Comer, G.C., Broecker, W.S. 2005. The role of seasonality in abrupt climate change. Quaternary Science Reviews 24: 1159-1182.

Dieffenbacher-Krall, A.C., Nurse, A.M. 2006. Late-glacial and Holocene record of lake levels of Matthews Pond and Whitehead Lake, Northern Maine, USA. Journal of Paleolimnology 34: 283-309.

Frauenfelder, R., Haeberli, W., Hoelzle, M., Maisch, M. 2007. Using relict rockglaciers in GIS-based modeling to reconstruct Younger Dryas permafrost distribution patterns in the Err-Julier area, Swiss Alps. Norsk Geografisk Tidsskrift 55: 195-202.

Gray, J.T., Brown, R.J.E. 1979. Permafrost presence and distribution in the Chic-Choc Mountains, Gaspésie, Québec. Géographie physique et Quaternaire 33: 299-316.

Goldthwait, R.P. 1940. Geology of the Presidential Range, Bulletin No.1, The New Hampshire Academy of Science: Hanover, New Hampshire; 1-43.

Goldthwait, R.P. 1970. Mountain glaciers of the Presidential Range in New Hampshire. Arctic and Alpine Research 2: 85-102.

Gordon, L.S., Ballantyne, C.K. 2006. 'Protalus ramparts' on Navajo Mountain, Utah: Reinterpretation as blockslope-sourced rock glaciers. Permafrost and Periglacial Processes 17: 179-187.

Haeberli, W., Vonder Mühll, D. 1996. On the characteristics and possible origin of ice in rock glacier permafrost. Zeitschrift für Geomorphologie 104: 43-57.

Hamilton, S.J., Whalley, W.B. 1995. Rock glacier nomenclature: a reassessment. Geomorphology 14: 73-80.

Harrison, S., Whalley, B., Anderson, E. 2008. Relict rock glaciers and protalus lobes in the British Isles: Implications for Late Pleistocene mountain geomorphology and palaeoclimate. Journal of Quaternary Science 23: 287-304. DOI: 10.1002/jqs.1148

Heiri, O., Lotter, A.F., Lemcke, G. 2001. Loss on ignition as a method for estimating organic and carbonate content in sediments: reproducibility and comparability of results. Journal of Paleolimnology 25: 101-110.

Hétu, B., Gray, J.T. 2000a. Les étapes de la déglaciation dans le nord de la Gaspésie (Québec): Les marges glaciaires des dryas ancien et recent. Géographie Physique et Quaternaire 54: 5-40.

Hétu, B., Gray, J.T. 2000b. Effects of environmental change on scree slope development throughout the postglacial period in the Chic-Choc Mountains in the northern Gaspé Peninsula, Québec. Geomorphology 32: 335-355.

Hétu, B., Gray, J.T., Gangloff, P., Archambault, B. 2003. Postglacial talus-derived rock glaciers in the Gaspé Peninsula, Québec (Canada). In Proceedings of the 8th International Conference on Permafrost, Phillips SM, Arenson LU (eds). International Permafrost Association, 8: 389-394.

Humlum, O. 1998. The climatic significance of rock glaciers. Permafrost and Periglacial Processes 9: 375-395.

Ikeda, A., Matsuoka, N. 2002. Degradation of talus-derived rock glaciers. Permafrost and Periglacial Processes 9: 375-395.

Janke, J., Frauenfelder, R. 2008. The relationship between rock glacier and contributing area parameters in the Front Range of Colorado. Journal of Quaternary Science 23: 153-163.

Johnson, P.G. 1983. Rock glaciers: a case for a change in nomenclature. Geografiska Annaler 65A: 27-34.

Kerschner, H. 1978. Paleoclimatic inferences from late Würm rock glaciers, eastern central Alps, western Tyrol, Austria. Arctic and Alpine Research 10: 635-644.

Kirkbride, M., Brazier, V. 1995. On the sensitivity of Holocene talus-derived rock glaciers to climate change in the Ben Ohau Range, New Zealand. Journal of Quaternary Science 10: 352-365.

Kite, J.S., Stuckenrath, R. 1986. Postglacial history of the upper St. John drainage basin. In Contributions to the Quaternary Geology of Northern Maine and Adjacent Canada, Kite JS and others (eds). Maine Geological Survey Bulletin 37: 113-128.

Konrad, S.K., Humphrey, N.F., Steig, E.J., Clark, D.H., Potter, N., Jr., Pfeffer, W.T. 1999. Rock glacier dynamics and paleoclimatic implications. Geology 27: 1057-1184.

Levesque, A.J., Mayle, F.E., Walker, I.R., Cwynar, L.C. 1993. A previously unrecognized late-glacial cold event in eastern North America. Nature 361: 623-626.

Levesque, A.J., Cwynar, LC., Walker, I.R. 1997. Exceptionally steep north-south gradients in lake temperatures during the last deglaciation. Nature 385: 423-426.

Lowell, T.V. 1985. Late Wisconsin ice-flow reversal and deglaciation, northwestern Maine. In Late Pleistocene history of northeastern New England and adjacent Québec, Borns HW Jr., LaSalle P, and Thompson WB (eds). Geological Society of America Special Paper 197: 59-70.

Lowell, T.V., Kite, J.S. 1986. Deglaciation of northwestern Maine. In Contributions to the Quaternary Geology of Northern Maine and Adjacent Canada, Kite JS and others (eds). Maine Geological Survey Bulletin 37: 113-128.

Lowell, T.V., Kite, J.S., Calkin, P.E., Halter, E.F. 1990. Analysis of small-scale erosional data and a sequence of late Pleistocene flow reversal, northern New England. Geological Society of America Bulletin 102: 74-85.

Mangerud, J., Andersen, S.T., Berglund, B.E., Donner, J.J. 1974. Quaternary stratigraphy of Norden, a proposal for terminology and classification. Boreas 3: 109-128.

Millar, C.I., Westfall, R.D. 2007. Rock glaciers and related periglacial landforms in the Sierra Nevada, CA, USA; Inventory, distribution, and climatic relationships. Quaternary International.

Mitchell, W.A., Taylor, P.J. 2001. Rock glaciers in the Northwestern Indian Himalaya. Glacial Geology and Geomorphology rp01: 1-26.

Mott, R.J., Stea, R.R. 1993. Late-glacial (Allerød/Younger Dryas) buried organic deposits, Nova Scotia, Canada. Quaternary Science Reviews 12: 645-657.

National Climatic Data Center/NESDIS/NOAA. 2002. Monthly station normals of temperature, precipitation, and heating and cooling degree days 1971-2000. Climatography of the United States 81

Nelson, K.J.P., Nelson, F.E., Walegur, M.T. 2007. Periglacial Appalachia: Palaeoclimatic significance of blockfield elevation gradients, eastern USA. Permafrost and Periglacial Processes 18: 61-73.

Newman, W.A., Genes, A.N., Brewer, T. 1985. Pleistocene geology of north-eastern Maine. In Late Pleistocene history of northeastern New England and adjacent Québec, Borns HW Jr., LaSalle P, and Thompson WB (eds). Geological Society of America Special Paper 197: 59-70.

Nurse, A.M., Borns, H.W., Hall, B.L., Dieffenbacher-Krall, A.C., Fastook, J.L. 2006. Geologic and paleoecologic evidence of ice-mass advance in northern Maine during the Younger Dryas cold reversal. Geological Society of America Abstracts with Programs 38: 236.

Paasche, Ø., Dahl, S.O., Løvlie, R., Nesje, A. 2007. Rockglacier activity during the Last Glacial-Interglacial transition and Holocene spring snowmelting. Quaternary Science Reviews. 26: 793-807.

Pelletier, B.G., Robinson, B.S. 2005. Tundra, ice and a Pleistocene cape on the Gulf of Maine: a case of paleoindian transhumance. Archaeology of Eastern North America 33: 163-176.

Péwé, T.L. 1983. Alpine permafrost in the contiguous United States: A review. Arctic and Alpine Research 15: 145-156.

Potter, N., Jr. 1972. Ice-cored rock glacier, Galena Creek, northern Absaroka Mountains, Wyoming. Geological Society of America Bulletin 83: 3025-3058.

Richard, P.J.H., Veillette, J., Larouche, A.C., Hétu, B., Gray, J.T., Gangloff, P. 1997. Chronologie de la déglaciation en Gaspésie: nouvelles données et implications. Géographie Physique et Quaternaire 51: 163-184.

Sailer, R., Kerschner, H. 1999. Equilibrium line altitudes and rockglaciers in the Ferwall-Group (western Tyrol, Austria) during the Younger Dryas cooling event. Annals of Glaciology 31: 275-280.

Sanger, D., Almquist, H., Dieffenbacher-Krall, A. 2007. Mid-Holocene cultural adaptations to central Maine. In Climate Change and Cultural Dynamics: A Global Perspectiveon Mid-Holocene Transitions, Anderson DG, Maasch KA, and Sandweiss DH (eds). Elsevier Inc., 435-456.

Severinghaus, J.P., Brook, E.J. 1999. Abrupt climate change at the end of the last glacial period inferred from trapped air in polar ice. Science 29: 930-934.

Smith, H.T.U. 1973. Photogeologic study of periglacial talus glaciers in northwestern Canada. Geografiska Annaler 55A: 69-84.

Spear, R.W. 1989. Late-Quaternary history of high-elevation vegetation in the White Mountains of New Hampshire. Ecological Monographs 59: 125-151.

Stea, R.R., Mott, R.J. 1998. Deglaciation of Nova Scotia: Stratigraphy and chronology of lake sediment cores and buried organic sections. Géographie Physique et Quaternaire 52 1-19.

Steig, E.J., Fitzpatrick, J.J., Jr., Potter, N., Jr., Clark, D.H. 1998. The geochemical record in rock glaciers. Geografiska Annaler 80A: 277-286.

Thompson, D.J. 1999. Talus fabric in Tuckerman Ravine, New Hampshire: Evidence for a tongue-shaped rock glacier. Géographie physique et Quaternaire 53: 47-57.

Thompson, W.F. 1961. The shape of New England mountains. Appalachia, Pt. III 27: 458-478.

Thompson, W.F. 1962. Preliminary notes on the nature and distribution of rock glaciers relative to true glaciers and other effects of climate on the ground in North America. International Association of Scientific Hydrology 58: 212-219.

Walegur, M.T., Nelson, F.E. Permafrost distribution in the Appalachian highlands, northeastern USA. In Proceedings of the 8th International Conference on Permafrost, Phillips M and others (eds). Lisse; Abingdon; A.A. Balkema 2: 1201-1206.

Washburn, A.L. 1980. Geocryology: A survey of periglacial processes and environments. Halsted Press:New York.

Wahrhaftig, C., Cox, A. 1959. Rock glaciers in the Alaska Range. Geological Society of America Bulletin 70: 383-436.

Whalley, B.W., Azizi, F. 2003. Rock glaciers and protalus landforms: Analogous forms and ice sources on Earth and Mars. Journal of Geophysical Research; Planets 108: 8032.

White, S.E. 1976. Rock glaciers and blockfields, review and new data. Quaternary Research 6: 77-97.

Wilkerson, B. 2007. Natural resource inventory of the northern Aroostook region: Deboullie. Bureau of Parks and Lands, Department of Conservation, Augusta, Maine.

World Meteorological Organization Storm Data and Unusual Weather Phenomena. 2004. http://findarticles.com/p/articles/mi_m0QRF/is_8_46/ai_n9481382 [August, 2004]

GEOLOGY OF THE MUNSUNGUN-WINTERVILLE BELT: THE WINTERVILLE INLIER AND THE PENNINGTON MOUNTAIN REE-Nb-Zr DEPOSIT

Chunzeng Wang
University of Maine at Presque Isle, Presque Isle, Maine 04769. chunzeng.wang@maine.edu

INTRODUCTION

The Munsungun–Winterville Belt (WMB) is a major early Paleozoic lithotectonic belt in the Northern Appalachians and characterized by widespread volcanic rocks. The belt includes two major inliers, the Munsungun inlier in the southwest and the Winterville inlier in the northeast, along with nine geologically similar but smaller inliers – the Portage Lake, Castle Hill, and York Ridge inliers in the north, and the much smaller ones in the headwaters of the East Branch Penobscot River and Aroostook River in the south (Fig. 1).

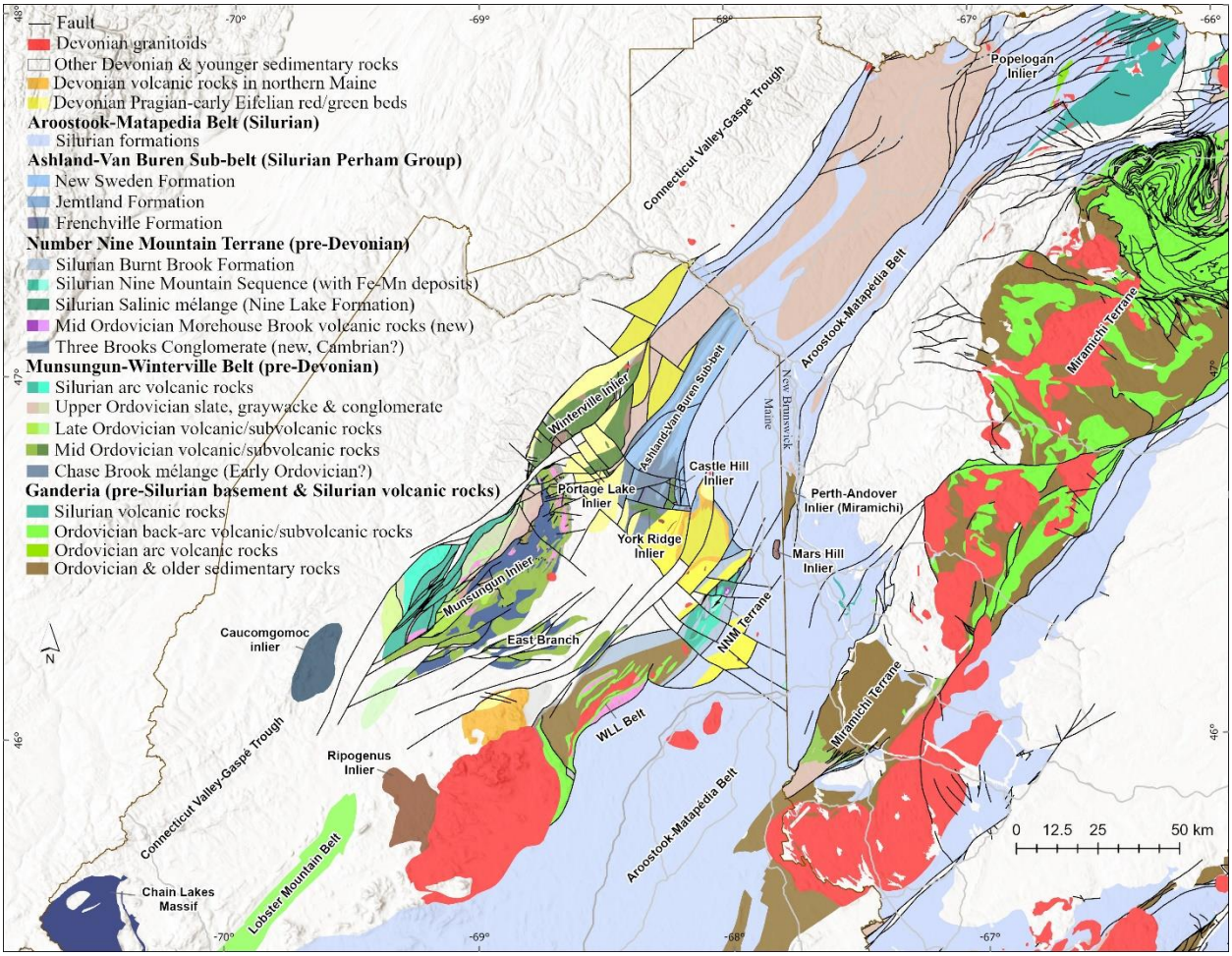

Figure 1. Simplified lithotectonic and regional geologic map of northern Maine and northern New Brunswick. Maine side is based on recent detailed and reconnaissance mapping. NNM Terrane – Number Nine Mountain Terrane. WLL Belt – Weeksboro-Lunksoos Lake Belt.

The pioneering, foundational mapping in the MWB was performed by Gary Boone who studied the area around Fish River Lake and Winterville, as well as the Deboullie syenite complex in the 1950's (Boone, 1958, 1970) and by Brad Hall who mapped the southwestern Munsungun inlier in the 1950–1960's (Hall, 1970). Supkow (1965) mapped the Spider Lake Formation in the Churchill and Spider Lake quadrangles and Horodyski (1968) conducted reconnaissance mapping in the area around Fish River Lake, Winterville, Greenlaw, and Mooseleuk Lake quadrangles. Exploration for base metals in the MWB peaked in the late 1970's and early 1980's with discovery of the Bald

Mountain volcanic massive sulfide (VMS) deposit and several occurrences including the Bull Hill VMS and "New Gold Prospect" at Chandler Mountain (Cummings, 1988) in the Munsungun inlier. In the late 1990's the U. S. Geological Survey (USGS) performed detailed studies of the Bald Mountain VMS deposit, focusing on its volcanic and tectonic settings, lithogeochemistry, geochronology, and metallogenesis (e.g., Ayuso and Schulz, 2003; Ayuso et al., 2003; Busby et al., 2003; Schulz and Ayuso, 2003; Slack et al., 2003).

The Winterville and Munsungun inliers are separated by a northeast-trending fault block of slate and sandstone of the Lower Devonian Seboomook Group (Fig. 1). The elongated Winterville inlier stretches northeastward from West Inlet to Square Lake. The inlier, as well as the Portage, York Ridge, and Castle Hill inliers, are dominated by volcanic rocks of the Ordovician Winterville Formation. Funding from the USGS STATEMAP Program and Maine Geological Survey (MGS) has supported detailed and reconnaissance mapping in the Winterville inlier starting in 2020, initially in the Big Machias, Fish River Lake, Carr Pond quadrangles. More reconnaissance mapping has since been conducted in the Winterville inlier and vicinity after discovery of non-foliated, plant fossil-rich green and red beds along the Fish River chain of lakes. These unique green and red beds were later named the St. Froid Lake Formation and determined to be of Early Devonian Emsian age based on brachiopods (Wang, 2022a, 2022b) and Emsian-early Eifelian based on recent palynological analyses.

Extensive mapping has also revealed that the Winterville inlier and vicinity, like the entire Munsungun-Winterville belt, has experienced significant faulting with considerable vertical and horizontal displacement, and that the faulting took place mostly during the Acadian and Neoacadian orogenies. Most of the faults strike southwest or northeast and are reverse-thrust faults with southeast-oriented reverse motion. These stacked, domino-style imbricate faults cut by later faults define the structural framework of northern Maine (Fig. 1). The topography of the Winterville Planation and Pennington Mountain is controlled by the imbricate fault system, with the upthrown Winterville volcanic rocks forming mountains and highlands and the downthrown St. Froid Lake red and green beds forming valleys and lowlands, giving drivers a roller-scooter riding experience on Rte-11.

During the exploration campaign for base and radioactive metals (Zn, Pb, Cu, U, Th, etc.) in the late 1970s and early 1980s, no significant mineral deposits were reported in the Pennington Mountain and Winterville Plantation areas except for several base and radioactive metal occurrences. Among the occurrences is the "Three Brooks radiometric anomaly" reported by General Crude Oil Company and included in an internal project report entitled "*Mineral Exploration in the Winterville Formation, Aroostook County, Maine*" (Ernest K. Lehmann & Associates, Inc. Report No. 7729) by Donald White and Edward Eisenbrey and dated in December 1977. The anomaly "corresponds to a small knob on the northeast slope of Pennington Mountain". The anomaly was discovered during an airborne radiometric survey and later inspected by bedrock mapping, a ground gamma-ray spectrometry survey, and even drilling of 17 holes, but only 6 holes successfully reached 24 feet in depth. According to the report, the exploration targeted base metals Cu, Zn, and Pb and radiometric elements U and Th even though the assays of three samples of drill cuttings from the sites "with the highest total gamma radiation", showed enrichment of zirconium (Zr, 1.2 wt.%), niobium (Nb, 0.23 wt.%), and several rare earth elements (La, Ce, Nd, and Y).

When the USGS Earth Mapping Resources Initiative (MRI) was launched in 2019 to improve our knowledge of the geologic framework in the United States and to identify areas that may have the potential to contain undiscovered critical mineral resources, the Munsungun-Winterville belt was recommended by MGS as a potential focus area. This initiative includes high-resolution airborne geophysical surveys (including magnetic and radiometric – eU, eTh, and K). In 2021, the Munsungun-Winterville belt was chosen for an airborne geophysical survey and the survey covered an area of 9,600 km^2. Later in 2021, the geophysical data was examined by Dr. Anjana Shah of the USGS and an abnormally high-eTh spot in the Pennington Mountain area was noticed. Wang carried out an initial two-day study of the site and collected ten samples that later were used for initial whole-rock geochemical and thin-section microscopic, microXRF, and microprobe analyses. A handheld radiation monitor (MAZUR PRM-9000) was used to measure radiation level at each sampling site. Two of the samples (along with other samples of volcanic rocks of the Winterville and Munsungun Lake formations) were sent to ALS Global for whole-rock geochemical analysis. Both samples showed extremely high contents of rare earth elements (REE), Y (yttrium), and other trace elements, such as Nb (niobium) and Zr (zirconium), confirming the existence of the Pennington Mountain REE-Nb-Zr occurrence. Petrographic and geochemical analyses of the Pennington Mountain samples indicated that they are trachyte, an igneous rock crystallized from alkali-rich magmas (i.e., high contents of potassium (K) and sodium (Na)). Trachyte generally occurs as lava flows, but occasionally occurs as shallow intrusive subvolcanic rocks.

Subsequent portable XRF (x-ray fluorescence) analysis of all the samples collected from the East Lobe of the Pennington Mountain trachyte, as well as microXRF and electron microprobe analyses were performed to learn more about the mineralized trachyte, its mineralogical composition and textures, identification of microcrystalline REE-Nb-Zr-bearing minerals, distribution pattern of the elements of interest, and characterization of mineralization (metallogenesis and paragenesis). Since spring 2022 more fieldwork and investigations have been performed to map,

sample, and delineate the extent of the Pennington Mountain trachyte and of the mineralization, including GPS-linked ground-based gamma-ray spectrometric survey of the airborne radiometrically anomalous region to enhance the understanding of the geologic distribution of the radiometric anomalies (Fig. 2). More samples were collected and analyzed for whole-rock geochemistry and microXRF analyses. Participants in field survey and investigations since spring 2022 include Anjana Shah, John Slack, Martin Yates, Robert Marvinney, Amber Whittaker, David Lentz, David Putnam, and Chunzeng Wang, with assistance of two undergraduate students Preston Bass and Liam Daniels.

Figure 2. GPS-linked ground-based gamma-ray spectrometry radiometric survey with Anjana Shah and Preston Bass on June 28, 2022 (a) and with Preston Bass and Liam Daniels on September 9, 2022 (b).

These preliminary efforts resulted in a research paper entitled "*A Recently Discovered Trachyte-hosted Rare Earth Element-Niobium-Zirconium Occurrence in Northern Maine, USA*" (Wang et al., 2023) published in the "express letter" format by the journal Economic Geology, online in November 2022 and in printed form in January 2023. (Please refer to the Economic Geology paper for data and information that are not included in this trip guide.)

Continued efforts have been made to perform geochronological analysis of the Pennington Mountain trachyte and the Winterville Formation at the University of New Brunswick (Canada) ICP-MS Laboratory by Dr. Christopher McFarlane. Two ages were obtained by zircon U-Pb analysis: 462.8 ± 1.4 Ma for the Pennington Mountain trachyte (a non-mineralized trachyte sample) and 459.5 ± 3.7 Ma for the Winterville Formation (a dacite sample from Hedgehog Mountain on Rte-11) in spring 2023.

REGIONAL GEOLOGY AND STRUCTURAL GEOLOGY

The Munsungun-Winterville Belt (MWB) is one of major early Paleozoic lithotectonic belts/terranes in the Northern Appalachians with origins as either peri-Gondwanan or peri-Laurentian fragments. For example, the Miramichi terrane and Weeksboro-Lunksoos Lake Belt (WWLB) are peri-Gondwanan and the Chain Lake Massif peri-Laurentian (Fig.1). The Lobster Mountain belt, Caucomgomoc inlier, and MWB have long been considered as part of the Ordovician Popelogan Arc of the leading edge of the Ganderia (peri-Gondwana). Silurian sedimentary strata, in particular the Silurian Aroostook-Matapedia Belt occur between the Miramichi and WLLB/MWB (Fig. 1).

The Winterville inlier is a northeast-trending tectonic terrane composed of volcanic rocks of the Ordovician Winterville Formation and slate and graywacke of the Ferguson Brook Formation (new) (Fig. 3). Its boundary with sedimentary rocks of the Lower Devonian Seboomook Group and St. Froid Lake Formation (Wang, 2022a, 2022b) is the West Inlet fault (Wang, 2021a), one of the longest faults in northern Maine. The Seboomook Group is the most widespread sedimentary formation in northern and northwestern Maine and a major component of the Connecticut Valley-Gaspe Basin, which is adjacent to Munsungun-Winterville Belt on the northwest. The St. Froid Lake Formation is a recently discovered, post-Acadian (Emsian-early Eifelian age) clastic sequence of red and green beds, widely distributed along the Fish River chain of lakes and in the Ashland area (Wang, 2022a, 2022b). The formation has been significantly displaced vertically by several northeast-striking longitudinal faults and horizontally by several northwest-striking transverse faults. These faults are considered to be Neoacadian in age. The north-northwestern part of the Winterville inlier is overlain unconformably by the Seboomook Group in the Fish River Lake and Island Pond areas as a result of late-stage Salinic orogenesis and by St. Froid Lake sedimentary rocks along the Red River valley and southern Eagle Lake as a result of the Acadian orogeny. The Fish River Lake fault (Wang, 2021a), a southeast-oriented reverse fault, has significantly and vertically displaced the Seboomook and St. Froid Lake formations, producing the most remarkable topographic feature in northern Maine – the Fishe River chain of lakes (including the Red River valley).

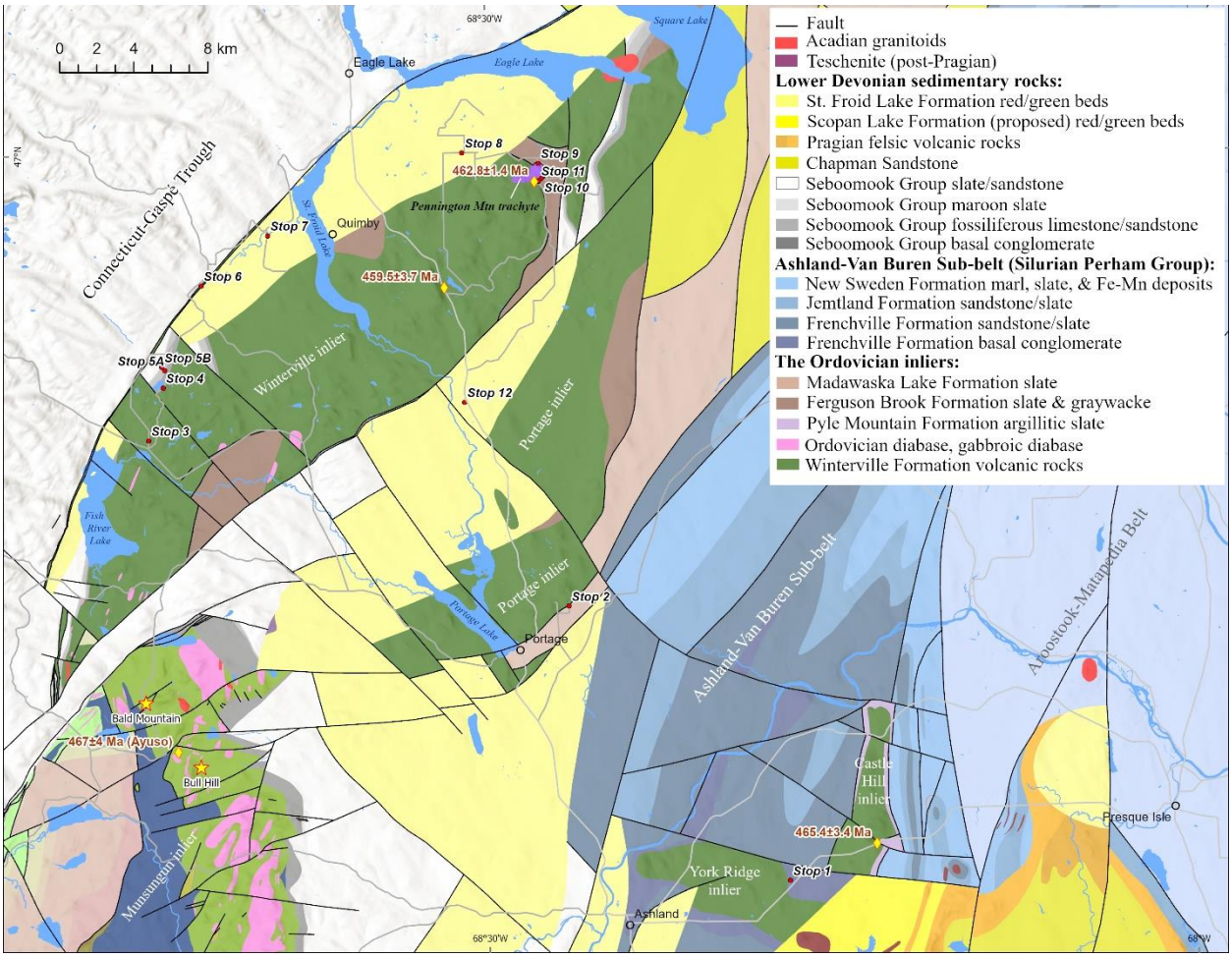

Figure 3. Geologic map of Winterville, Portage, York Ridge, and Castle Hill inliers and vicinity based on recent detailed and reconnaissance mapping, including locations of the stops to be made in this trip and zircon U-Pb ages and sample locations.

In the Pennington Mountain area, the Winterville Formation and Pennington Mountain trachyte are in fault contact with the Ferguson Brook Formation (Wang, 2022a, 2022b). The fault, here referred to as the Pennington Mountain fault, is a low-angle thrust fault with the Winterville volcanic rocks and Pennington Mountain trachyte as the overthrust hanging wall and the Ferguson Brook as the foot wall. Several Acadian faults occur within the northeast-striking Winterville fault block on the northeast side of Pennington Mountain, where they have displaced the unconformable contact between Seboomook sedimentary rocks and Winterville volcanic rocks. Two of these are named Middle Brook and Last Brook faults in this study.

Three smaller Ordovician inliers in the region are the Portage, York Ridge, and Castle Hill inliers. The Portage inlier, closest to the Winterville belt, is also composed of the Winterville and Ferguson Brook formations and used to be considered as part of the Winterville inlier. It is in fault contact with the Winterville inlier on the north side of the Goddard Valley by the West Inlet fault. To the southeast, it is in fault contact with the Upper Ordovician Madawaska Lake Formation along the Clayton Lake fault (Wang, 2021b); and its northwest is mostly unconformably overlain by St. Froid Lake Formation. The York Ridge inlier is unconformably overlain by the Silurian Frenchville Formation as a result of uplift in an early stage of the Salinic orogeny. The Castle Hill inlier is unconformably overlain by the Upper Ordovician Pyle Mountain Formation as a result of Taconic orogeny.

An extensive sequence of Silurian sedimentary rocks, collectively called the Perham Group or Perham Group sequence in this study occurs as a northeast-trending belt between Ashland and Van Buren (named the Ashland-Van Buren subbelt in this study). David Roy's mapping and study of the Silurian formations during 1960–1980 (Roy, 1970, 1976, 1987; Roy and Mencher, 1976) laid a solid foundation for future work. Based on recent and current mapping, the revised Perham Group sequence consists of, from bottom to top, the Frenchville (Boucot et al., 1964), Jemtland

(Roy and Mencher, 1976), and New Sweden (Roy and Mencher, 1976) formations, and the sequence or the sub-belt is in fault contact with the northeast-trending Carys Mills Formation to the southeast; the latter is a major component of the Aroostook-Matapedia Belt.

STRATIGRAPHY OF THE WINTERVILLE INLIER AND VICINITY

Stratified sedimentary and volcanic rocks in the Winterville inlier and vicinity include, from the oldest to the youngest, the Ordovician Winterville, Ferguson Brook, and Madawaska Lake formations, the Silurian Perham Group, and the Devonian Seboomook Group and St. Froid Lake Formation (Fig. 4).

Figure 4. Re-established stratigraphy of the Winterville inlier and vicinity.

Winterville Formation

The Winterville Formation (Boone, 1958, 1970; Mencher, 1963; Horodyski, 1968; Osberg et al., 1985) dominates the northeast-trending Winterville, Portage, York Ridge, and Castle Hill inliers. The formation consists predominantly of basalt with lesser amounts of pyroclastic rocks including volcanic breccia, lapillistone, and tuff, as well as minor rhyolite, dacite, trachyte, and a few subvolcanic diabase sills and stocks. Basalt commonly has vesicular and amygdaloidal textures in which vesicles are often filled by calcite, chlorite, zeolite, and quartz. Pillow basalt is common (Fig. 5). Agglomerate and hyaloclasite are less common. Basalt is aphyric, mostly microcrystalline, and composed predominantly of plagioclase feldspar and augite. Rhyolite and dacite are generally minor in the Winterville Formation, but increase in the Pennington Mountain area, for example, Hedgehog Mountain by Rte-11 is largely made of dacite. Most of the pyroclastic rocks are gray tuff. Tuff is locally foliated and laminated.

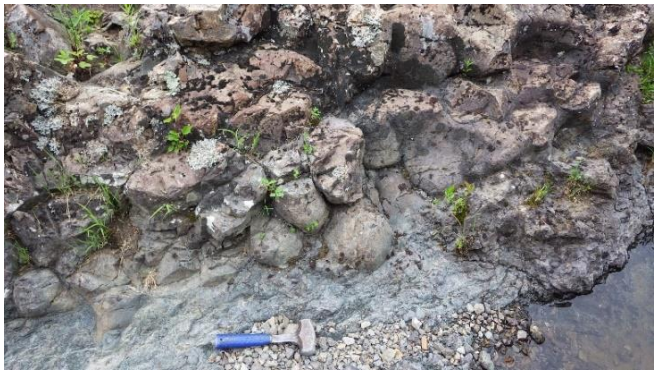

Figure 5. Pillow basalt of Winterville Formation at Fish River Falls by Round Pond.

Geochemically, most of the basalt samples show a transitional and calc-alkaline series (Fig. 6a). Their trace and REE spidergrams and distribution patterns (Fig. 6b, c) show a slope profile, with moderately elevated LREE (light rare earth elements), enriched LILE (large iron lithophile elements), and depleted Ta and Nb (dominantly). Tectonic discrimination diagrams such as La/10-Y/15-Nb/8 show “orogenic domains” or “late to orogenic intra-continental domains” (Fig. 6d). In general, geochemical characteristics of most of the basalt samples in the Winterville and Portage

inliers indicate an ensialic volcanic arc setting. The exceptions are basalt samples collected near the Pennington Mountain trachyte – see below for details.

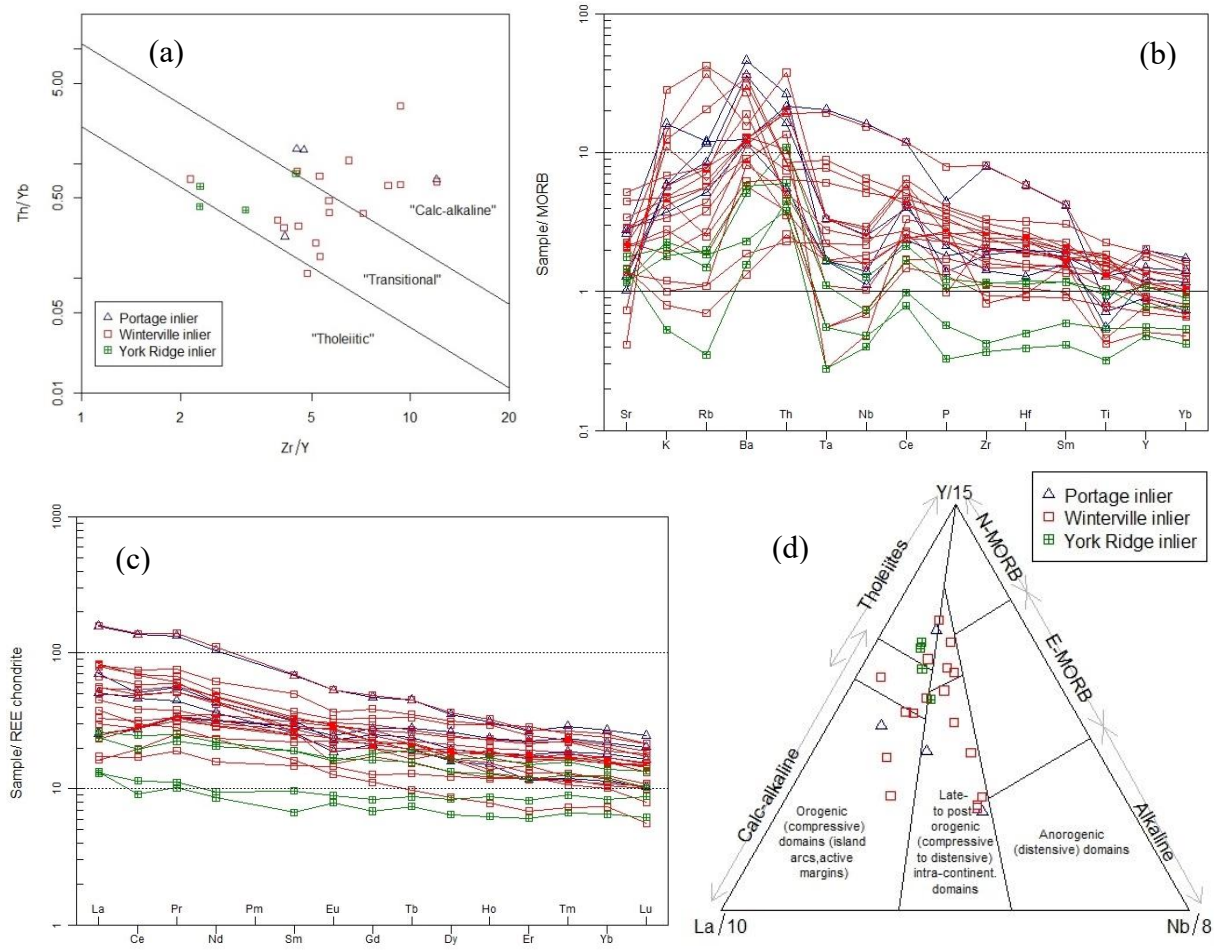

Figure 6. Geochemistry of the Winterville Formation basalt. (a) Zr/Y vs. Th/Yb diagram (Ross and Bedard, 2009); (b) MORB-normalized spider diagram (Pearce, 1983); (c) Chondrite-normalized REE pattern (Nakamura, 1974); (d) La/10–Y/15–Nb/8 tectonic discrimination diagram (Cabanis and Lecolle, 1989).

A Winterville Formation dacite sample collected from the Rte-11 roadcut on the east side of Hedgehog Mountain, was analyzed for zircon U-Pb dating at the University of New Brunswick ICP-MS Laboratory by Dr. Christopher McFarlane. The analysis yielded a $^{206}Pb/^{238}U$ weighted mean age of 459.5±3.7 Ma (MSWD = 0.62, n = 28) and a $^{207}Pb/^{235}U$–$^{206}Pb/^{238}U$ concordia age of 460.7±2.7 Ma (Fig. 7). Both ages are nearly identical and within error range. The results indicate a Middle Ordovician Darriwilian age for the Winterville Formation (more accurately for the Winterville volcanic rocks in the Hedgehog Mountain area). This geochronological work is the first ever performed in the Winterville inlier in northern Maine.

Another zircon U-Pb ICP-MS analysis was recently performed on a Winterville Formation trachyte sample collected from the Castle Hill inlier (at Rte-163 roadcut by Haystack) at Arizona LaserChron Center. It yielded a weighted mean age of 465.4±3.4 Ma (MSWD = 0.22, n =11) (Fig. 2). The discrepancy in ages of the volcanic rocks indicates that the volcanic rocks were emplaced during a span of at least five million years.

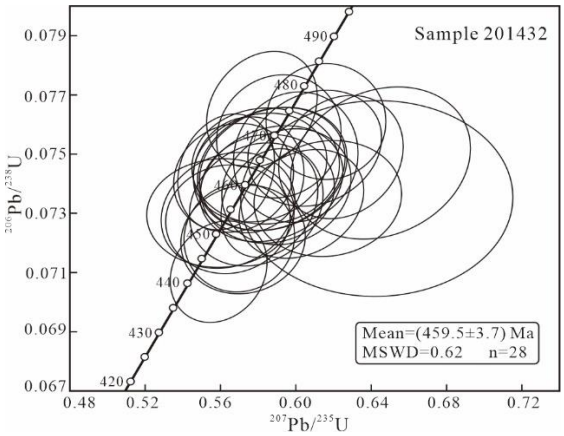

Figure 7. Zircon U-Pb concordia diagram of a dacite sample from Hedgehog Mountain of the Winterville inlier.

Ferguson Brook Formation

The Ferguson Brook Formation (Wang, 2022a, 2022b) forms part of the Winterville and Portage inliers. The formation is predominantly medium to thickly layered dark gray graywacke, dark gray, black pyritic slate, and minor intercalated conglomerate and black cherty siliceous mudstone (Fig. 8a, b). Some graywacke is turbiditic and characterized by horizontal lamination and cross ripples. The conglomerate, either pebble conglomerate or granule conglomerate, is poorly sorted, angular, and polymictic with mostly cherty tuff and basalt clasts that were probably derived from the volcanic rocks of the Winterville Formation. No fossils have been found in the formation. Based on the reported detrital zircon data from a similar formation in the Greenlaw Pond quadrangle in the Munsungun inlier in the southwest (Wang, 2021b), the Ferguson Brook Formation is considered Late Ordovician in age.

Figure 8. Ferguson Brook Formation. (a) Graywacke. (b) Dark gray, rusty slate.

Pyle Mountain Formation

The Pyle Mountain Formation (Roy, 1970, 1987) has been mapped only along the flanks of the Castile Hill inlier where it unconformably overlies the Mid Ordovician volcanic rocks of the inlier. First called "Pyle Mountain Argillite" (Boucot et al., 1964), it consists mostly of brown-weathering (greenish gray in fresh) silty argillaceous mudstone/slate with lesser medium-layered gray sandstone with only minor, intercalated thin-medium limestone, black cherty slate, and conglomerate. Its age was considered to be Ashgillian (Late Ordovician) based on study on fossils (reported by Boucot et al. (1964).

Madawaska Lake Formation

The Madawaska Lake Formation (Roy and Mencher, 1976) is a major sedimentary rock unit along the Fish River chain of lakes; it extends southwest to the Portage area and northeast for about 65 kilometers in Maine and across the St. John River into New Brunswick, Canada. The formation is dominated by interbedded slate and graywacke (Fig. 9a, b), with minor gray or brown quartzose sandstone and siltstone. Generally, the slate and graywacke are pyrite poor

with a little rusty appearance. The formation is in fault contact with several other formations. For example, in the area north of Beaver Brook valley and Portage, it is in fault contact with the Winterville Formation and Perham Group. Based on Roy and Mencher (1976), the Madawaska Lake Formation is possibly Upper Ordovician in age.

Figure 9. Madawaska Lake Formation. (a) Slate. (b) Graywacke.

Perham Group

The Perham Group was initially proposed by Roy and Mancher (1976) and later discontinued but is readapted and redefined in this study. It includes, from bottom to top, the comfortable Frenchville, Jemtland, and New Sweden formations of clastic and carbonate rocks. It is a Silurian series, referred to as the ***Perham Group sequence*** that extends southwestward to the Ashland-Castle Hill area and northeast across St. John River into New Brunswick, Canada. It is fault bounded with the Madawaska Lake Formation to the northwest and with the Carys Mills Formation of the Aroostook-Matapedia Belt to the southeast.

The Frenchville Formation (Boucot et al., 1964) includes a basal conglomerate unit and the rest, the major part of the formation consists of thin to thickly layered greenish or bluish gray quartzose or feldspathic sandstone with lesser gray slate. The basal conglomerate occurs mainly around Ashland, Frenchville, and southwest of Haystack and unconformably overlies the Ordovician York Ridge inlier. The unconformity represents the early stage of Salinic orogeny - equivalent to Salinic A in northern New Brunswick (Wilson and Kamo, 2012) and in Number Nine Mountain area (Wang and Madsen, trip B3). The Jemtland Formation (Roy and Mencher, 1976) is dominantly a well bedded package of thin to medium layered, graptolitic gray calcareous and micaceous siltstone and sandstone with relatively lesser gray and dark gray shale. Lamination is a common sedimentary structure of the formation and in places the formation shows Bouma sequence. A diagnostic feature of the formation is its orange or brownish tan color on weathered surfaces and well-developed leached weathering rind. The Jemtland Formation is known to be rich in *Monograptus* graptolite fossils of early Ludlow age (Berry, 1960, 1964). The New Sweden Formation (Roy and Mencher, 1976) generally consists of two successions, with the lower succession dominated by carbonate and occurring mostly as alternating thin marl (argillaceous limestone) and calcareous sandstone/siltstone/shale and the upper succession by green, maroon/red, or dark tan-colored slates with minor, intercalated thin argillaceous limestone. The green and maroon slate succession hosts manganese ironstone deposits/layers of the northern subdistrict of the Aroostook Manganese District.

Seboomook Group

The Seboomook Group (Perkins, 1925; Pollock, 1987) is the most widespread sedimentary rock formation in northern Maine, in the Connecticut Valley-Gaspé Basin. The Seboomook Group is lithologically divided into four conformable units, from bottom to top, the basal conglomerate, fossiliferous limestone and calcareous sandstone, maroon slate, and turbiditic sandstone and slate units, with the last one dominating the group. The bottom three units are informally called the “Trinity”. The Seboomook Group basal conglomerate unit unconformably overlies the Ordovician inliers and Silurian formations, including the Munsungun and Winterville inliers, as a result of the late stage of the Salinic orogeny - equivalent to Salinic C in northern New Brunswick (Wilson and Kamo, 2012) and in Number Nine Mountain area (Wang and Madsen, trip B3. However, as Figure 3 shows, the Paleozoic terranes in northern Maine have been significantly faulted and displaced by dominantly southwest-striking reverse-thrust faults, mainly during Acadian and Neoacadian orogeneses. In the Pennington Mountain area, the Seboomook Group occurs as part of two fault slivers/blocks (Fig. 3), along the Middle Brook and Last Brook valleys; within the slivers/blocks,

the Seboomook Group basal conglomerate unconformably overlies the volcanic rocks of the Winterville Formation, and contains significant components of basalt pebbles. The fossiliferous limestone and calcareous sandstone unit are rich in various marine invertebrate fossils, including corals, brachiopods, crinoids, stromatoporoids, bryozoan, etc. of the early Devonian (Helderberg) fauna. In the Fish River Lake area, the unconformity between the Seboomook basal conglomerate and the Winterville volcanic rocks remains intact although horizontally offset by several strike-slip faults (Fig. 3).

St. Froid Lake Formation

The St. Froid Lake Formation (Wang, 2022a, 2022b) consists of non-foliated, red, green, greenish gray, reddish-brown, and buff brown sandstone and shale/mudstone beds (Fig. 10a, b). It is distributed mostly along the Fish River chain of lakes and in the Ashland area as displaced fault blocks (Figs. 1 and 3) with a total area of nearly 500 km^2. The formation contains abundant terrestrial plant-fossil fragments of trimerophytes (most likely *Psilophyton* and *Pertica*) (Fig. 10c). All the plant material appears to have been transported and deposited in aqueous terrestrial or coastal settings. The formation was deposited during the Early Devonian Emsian time initially based on invertebrate fossils, particularly on brachiopods of mostly *Leptocoelia flabellites* (Fig. 10d), with a few *beachia* (terebratulid), *Atlanticocoelia,* and Acrospirifer *Hysteriolites sp*. (Wang, 2022a, 2022b). A most recent palynological analysis reported spores of *Ancyrospora kedoae, Ancyrospora sp., Apiculiretusispora brandtii, Apiculiretusispora gaspiensis, Apiculiretusispora minor, Apiculiretusispora plicata, Archaeozonotriletes chulus, Chelinospora sp., Dibolisporites abitibiensis, Dibolisporites wetteldorfensis, Dictyotriletes favosus, Emphanisporites annulatus, Latosporites sp.,* and *Gneudnaspora divellomedia* and confirmed the Emsian-early Eifelian age of the formation.

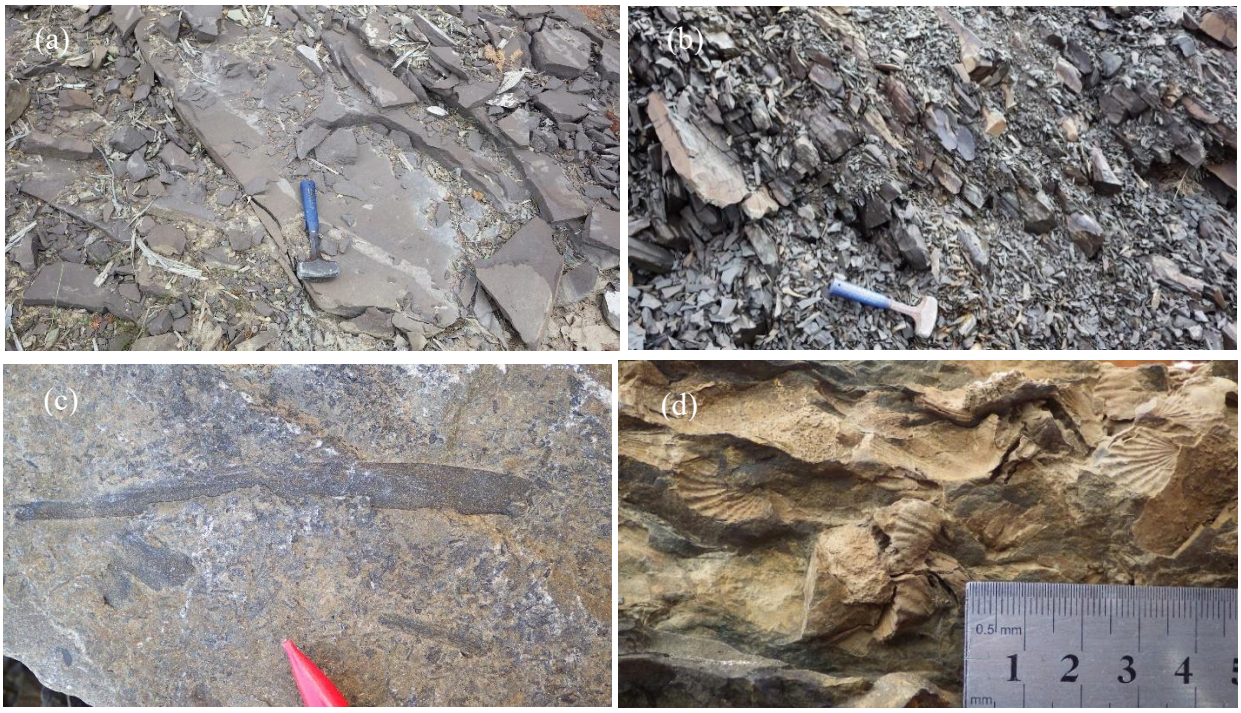

Figure 10. St. Froid Lake Formation. (a) Red sandstone. (b) Green mudstone and sandstone. (c) Fragments of plant fossils of mostly *Psilophyton* and *Pertica*. (d) Molds of brachiopods *Leptocoelia flabellites* and *Hysteriolites sp.*

THE PENNINGTON MOUNTAIN REE-Nb-Zr DEPOSIT

The Pennington Mountain trachyte: petrography, geochemistry, tectonic setting, and age

The Pennington Mountain trachyte occurs as an irregularly shaped stock (Figs. 3 and 11) that is in fault contact with graywacke and black slate of the Ferguson Brook Formation to the east. The fault, named Pennington Mountain Fault in this study is presented as a low-angle thrust fault. The currently delineated trachyte body has a minimum exposed area of 1.129 km^2. The trachyte is divided into the West Lobe and East Lobe (Fig. 11). The West Lobe is not

brecciated, nor mineralized. However, the East Lobe is thoroughly and pervasively brecciated and mineralized. The north-northwest-trending ridge (the no-name ridge referred to in this study) of the East Lobe is entirely and significantly mineralized based on the airborne radiometric survey performed in summer 2021 (Fig. 11; Shah, 2022), the ground radiometric survey performed in fall 2022 (Shah and Wang, 2022), and portable XRF (X-ray fluorescence spectrometer) and whole-rock geochemical analyses performed in 2022 and later in early 2023.

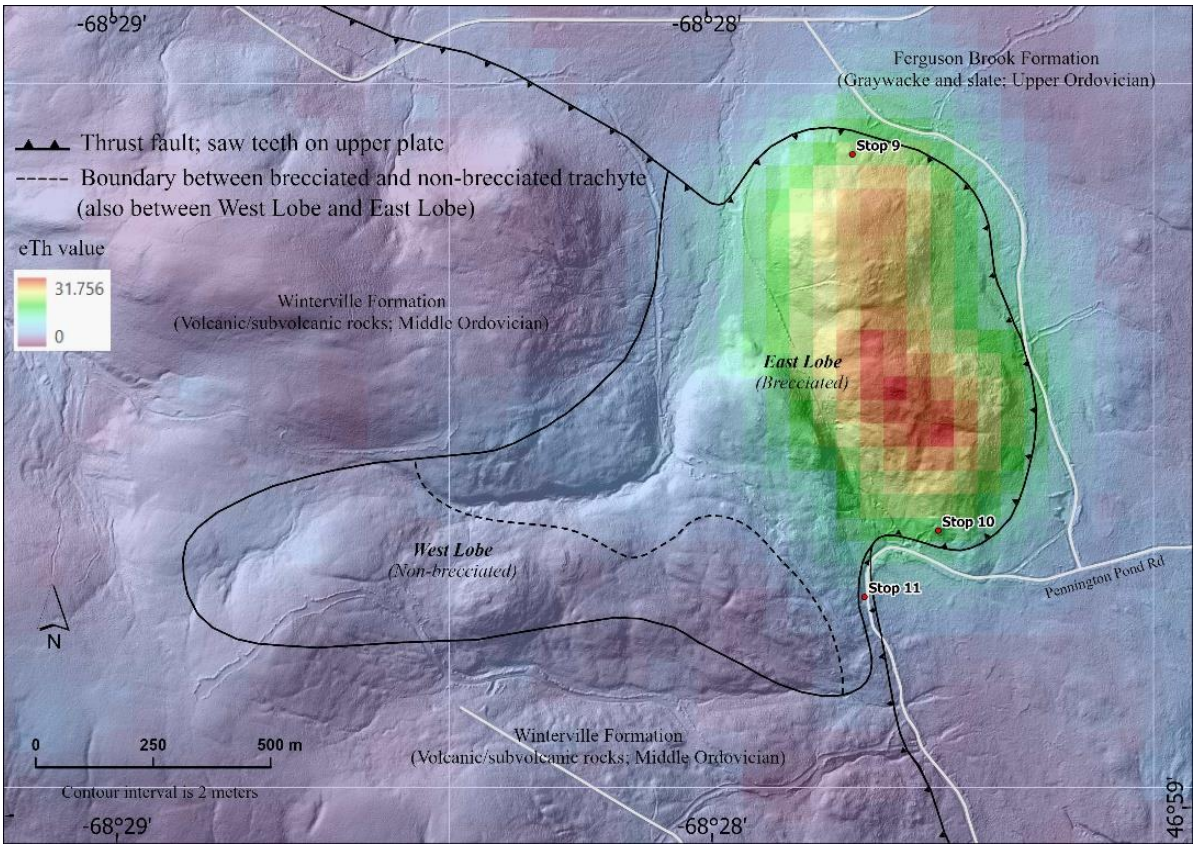

Figure 11. Geologic map of the Pennington Mountain trachyte.

Please note that the definitions for the East Lobe and West Lobe and how they are divided are different from the Economic Geology article (Wang et al., 2023). The redefinition here uses brecciation as the criterion: the East Lobe is brecciated, whereas the West Lobe is not. Wherever it is brecciated, it is also mineralized with REE-Nb-Zr mineralization, either significantly like the entire no-name ridge or weakly like the northwestern and western part of the East Lobe (or the rest of the East Lobe). The non-brecciated and non-mineralized West Lobe trachyte accounts for about one third of the Pennington Mountain trachyte body in terms of its surface exposure. Generally, the trachyte (including the mineralized component) is homogenously massive and microcrystalline. Part of the trachyte in the West Lobe is vesicular and amygdaloidal with dominating quartz-filled elongated amygdales (Fig. 12a, b), indicating that even if the trachyte is considered intrusive, it is very shallow and subvolcanic. Microscopically, the trachyte has a typical trachytic texture (Fig. 12b, c). Most of the trachyte also has a micro-porphyritic texture with euhedral perthite phenocrysts set in a microcrystalline matrix composed predominantly of potassium feldspar and subordinate albite (Fig. 11c, d). In general, alkali feldspar (perthite and some albite) accounts for about 95% of the trachyte, with the rest being ferromagnesian silicates (hornblende and biotite but now mostly altered into chlorite and iron oxides) and quartz.

Eighteen samples were collected from the trachyte body and analyzed for whole-rock geochemistry. Nearly all of them plot in the trachyte-trachydacite field in the TAS diagram (Fig. 13a) and in the calc-alkaline field in the Zr/Y vs. Th/Yb diagram (Fig. 13b). The MORB-normalized spider diagram (Fig. 13c) shows significant enrichment of U, Th, Nb, Ta, Zr, Hf, Ba, Rb, and Y, in particular in the strongly mineralized trachyte. The chondrite-normalized REE distribution patterns show slightly higher LREE than HREE with a significant negative Eu anomaly for most of the samples (Fig. 13d), which is typical for alkaline-peralkaline igneous rocks. Eu/Eu* values range from 0.139 to 0.626, but are mostly less than 0.2.

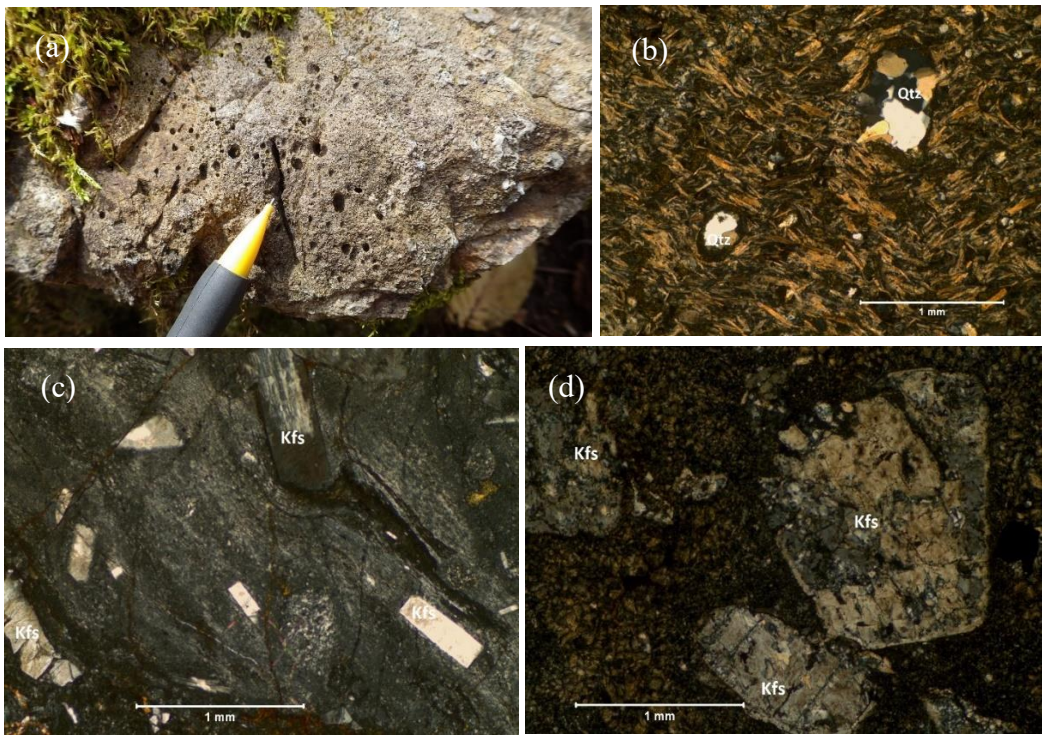

Figure 12. The Pennngton Mountain trachyte. (a) Trachye with vesicular texture. (b) Trachytic texture and quartz amygdales. (c) Trachytic and porphyritic textures with K-spar phenocrysts. (d) K-spar phenocrysts. (b), (c), and (d) under cross polarizing light. Kfs – potassium feldspar; Qtz – quartz.

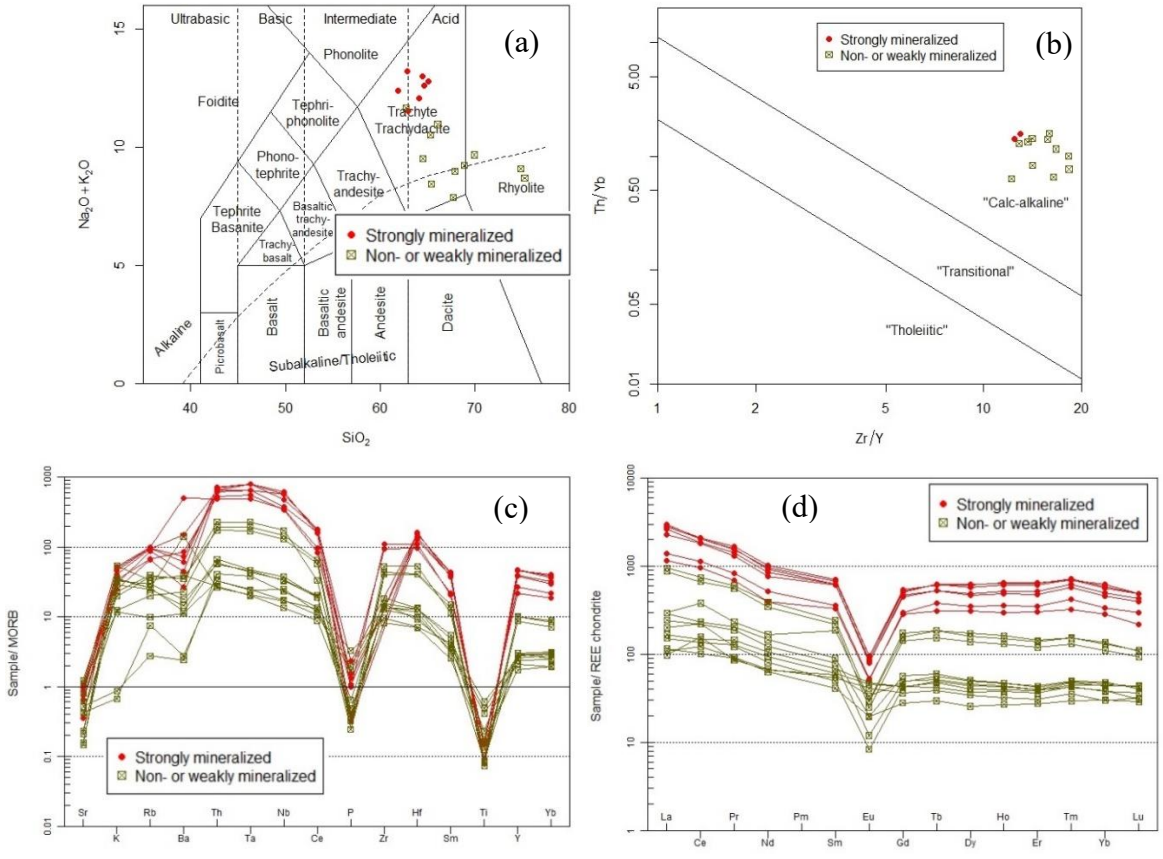

Figure 13. (a) TAS (SiO_2 vs. Na_2O+K_2O) classification diagram (LeBas et al., 1986). (b) Zr/Y vs. Th/Yb classification diagram (Ross and Bedard, 2009). (c) MORB-normalized spider diagram (Pearce, 1983). (d) Chondrite-normalized REE distribution pattern (Nakamura, 1974).

On Whalen's (1987) granitoid discrimination diagrams (Fig. 14), all the non- and weakly-mineralized trachyte samples plot in the A-type granitoid field, indicating that the Pennington Mountain trachyte was emplaced in an anorogenic setting. In the Y–Nb–Ce and Y–Nb–3GA ternary diagrams used for classification of A-type granitoids into A1 and A2 (Eby, 1992), the trachyte samples plot within or next to the A1-type field (Fig. 15). A1 type is generally related to OIB (ocean island basalt)-type enriched mantle source of anorogenic setting.

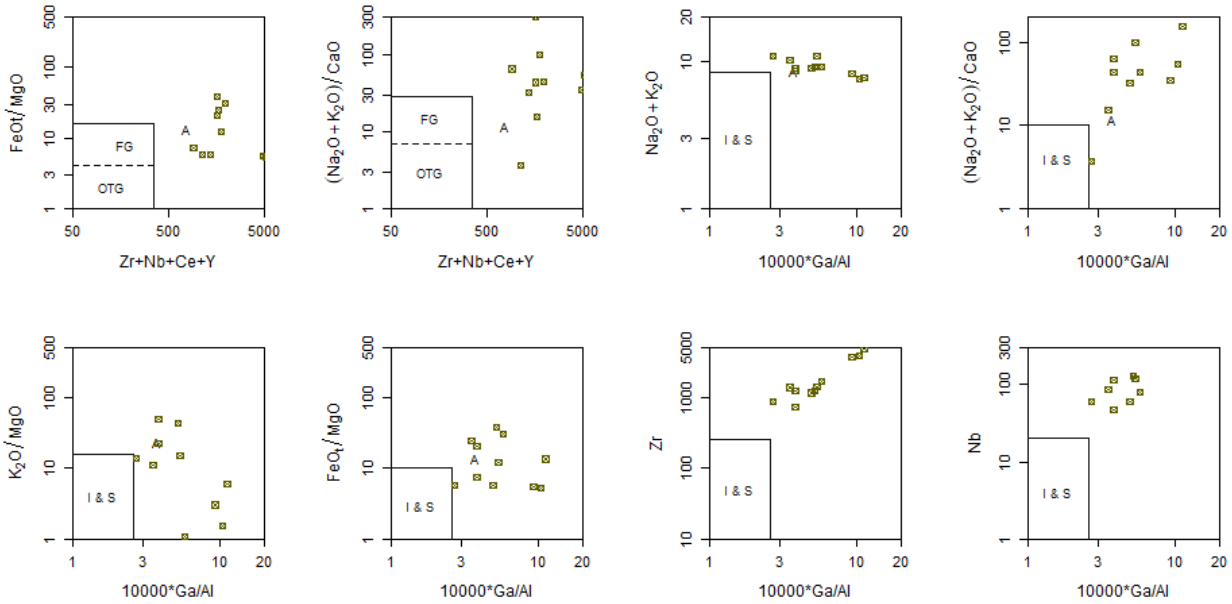

Figure 14. Granitoid discriminations diagrams of all kinds based on some discriminative major, trace, and rare earth elements (Whalen, et al., 1987). A – anorogenic. FG – fractionated I-type granitoids. I – product from an igneous or intracrustal source. OTG – unfractionated M-, I- and **S**-type. S – product of anatexis of metasedimentary of supracrustal protoliths.

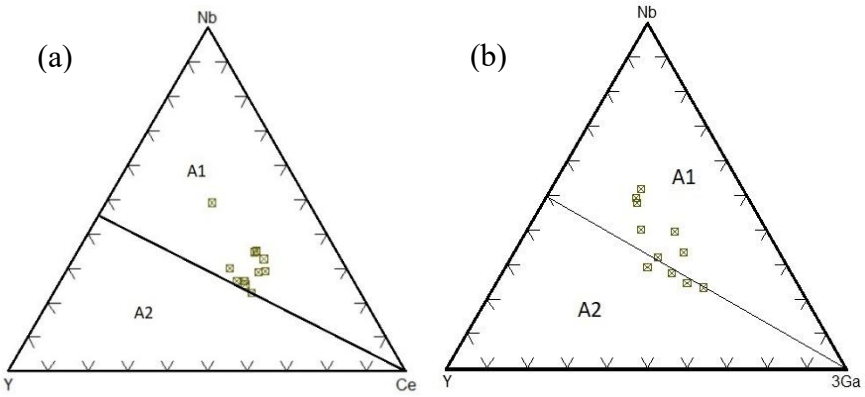

Figure 15. A1/A2 discrimination diagrams (Eby,1992). (a) Nb-Y-Ce; (b) Nb-Y-3 * Ga.

All the samples plot in the alkaline "anorogenic domains" (except one sample in the "late- to post-orogenic intra-continent domains") on the La/10–Y/15–Nb/8 diagram (Fig. 16a; Cabanis and Lecolle, 1989). On the Nb/Yb vs. Th/Yb diagram (Fig. 16b; Pearce, 2008), all the samples plot in the MORB-OIB array. In summary, based on geochemical characteristics and tectonic discriminations, the Pennington Mountain trachyte was emplaced in a non-orogenic setting.

Being the major component of the Winterville inlier, the Winterville Formation, however, is composed predominantly of orogenic volcanic rocks produced in an ensialic volcanic arc setting.

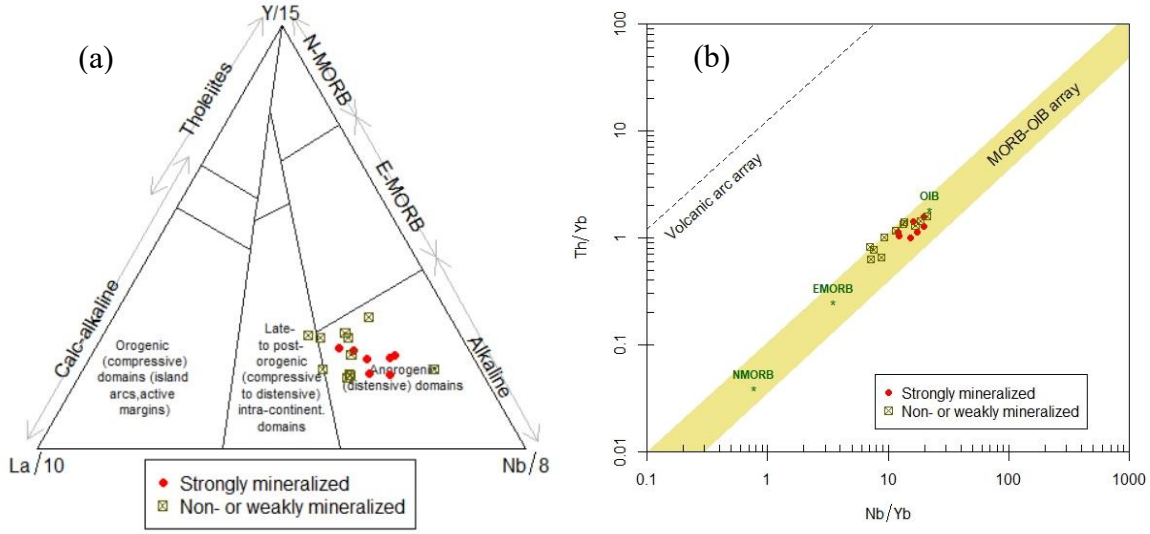

Figure 16. Tectonic setting discrimination diagrams: (a) La/10–Y/15–Nb/8 diagram (Cabanis and Lecolle, 1989). (b) Nb/Yb vs. Th/Yb diagram (Pearce, 2008) of the strongly mineralized and non- to weakly-mineralized trachyte. See the text for explanation. MORB – middle ocean ridge basalt; NMORB – normal MORB; EMORB – enriched MORB; OIB – ocean island basalt.

A non-mineralized trachyte collected from the West Lobe yielded nearly 40 igneous zircon crystals. On the Cl (cathodoluminescence) image (Fig. 17a), most of the zircon crystals are euhedral or sub-euhedral and prismatic. The zircon grains were analyzed by LA-ICP-MS at the ICP-MS Laboratory of the University of New Brunswick by Dr. Christopher McFarlane in spring 2023. Figure 17b shows the $^{207}Pb/^{235}U$ – $^{206}Pb/^{238}U$ concordia diagram with a U-Pb concordia age of 462.8±1.4 Ma, which is same as the weighted mean age from 28 zircon. This age is the emplacement age of the Pennington Mountain trachyte, also considered as the age of the REE-Nb-Zr mineralization event. It is within the error range with the age of the dacite (460.7±2.7 Ma) of the Winterville Formation.

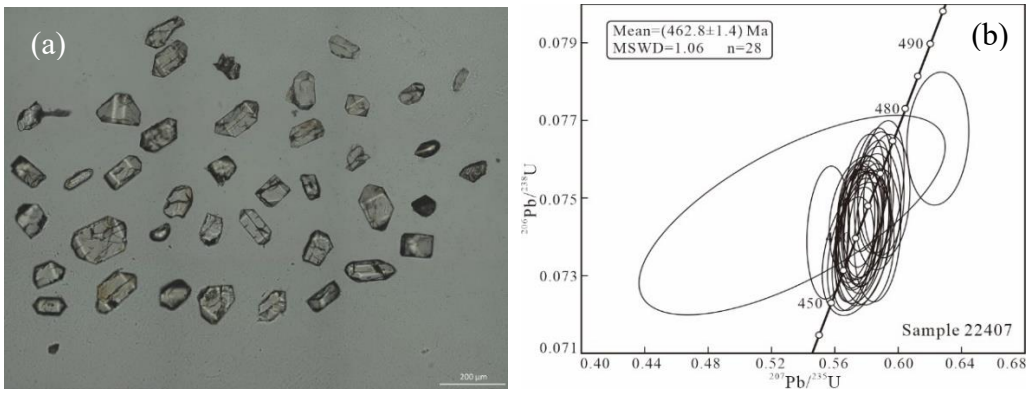

Figure 17. Zircon U-Pb dating of the Pennington Mountain trachyte. (a) CL image showing mostly euhedral-subhedral zircon crystals of igneous origin. (b) Concordia diagram and the weighted mean age of 28 analyses.

The Pennington Mountain REE-Nb-Zr deposit: texture, mineralogy, ore geochemistry, and metallogenesis

The East Lobe is characterized entirely by micro-breccia with pervasive fragmental textures (Fig. 18), and it is also entirely mineralized. Wherever it is fragmented, it is mineralized, although mineralization can be weak compared to the strongest mineralization along the entire no-name ridge. For the fragmented trachyte of the East Lobe, for both

strongly and weakly mineralized, most fragments range in size from 0.1 to at least 1 cm, with only a very small percentage up to 20 cm. Fresh, broken surfaces are generally in dark gray color (Fig. 18a). Some are pinkish brown (Fig. 18b) due to potassium alteration. Photomicrographs (e.g., Fig. 17c, d) show all kinds of fragmented trachyte and micro-porphyritic trachyte. Generally, pyrite is scarce in the trachyte. Only locally some mineralized trachyte may contain some pyrite.

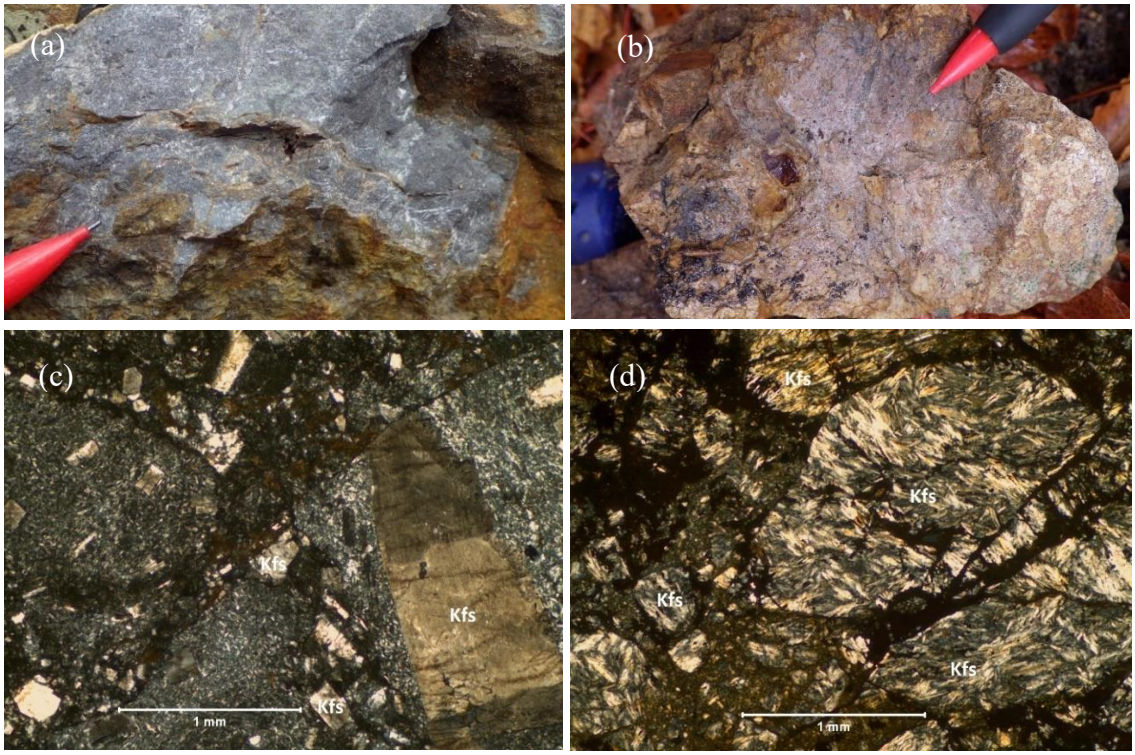

Figure 18. Fragmental and mineralized trachyte. (a) Fresh surfaces generally showing dark gray color and fragmental texture. (b) Some trachyte showing darker pinkish brown color due to alteration of potassium feldspar. (c) and (d) Photomicgraphs showing perthitic K-feldspar phenocrysts and mineralized groundmass (seams) of the fragments (in dark color). Cross-polarized light. Kfs – potassium feldspar.

Micro-XRF (or MicroXRF-EDS, µXRF-EDS) elemental scans of entire polished thin sections were performed at the University of New Brunswick by Dr. David Lentz and Fazilat Yousefi. The µXRF-EDS scans show distinctive fragmentation textures and element enrichments for La+Ce, Zr, and Nb (Fig. 19). High contents of La+Ce (Fig. 19a, b), Zr (Fig. 19c), and Nb (Fig. 19d) are mainly confined to the groundmass of the micro-breccia, with the fragments having only minor enrichments of these metals in veinlets and disseminations.

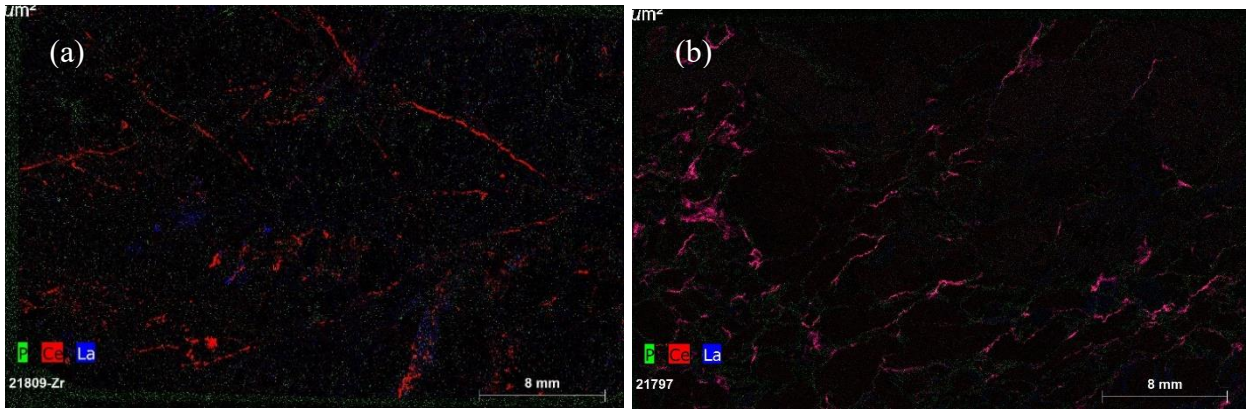

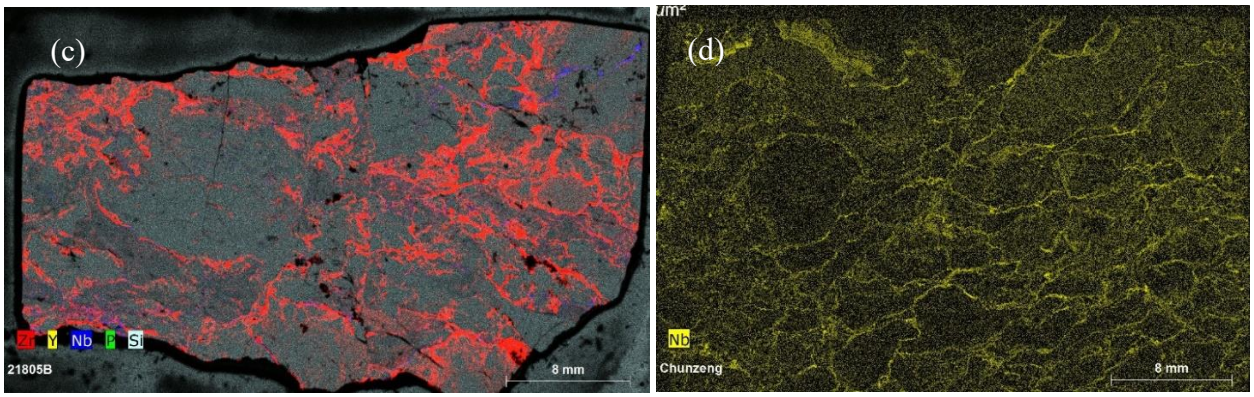

Figure 19. μXRF-EDS images of the selected elements Ce and/or La (a, b), Zr (c), and Nb (d). The images show extremely fine-grained REE-Nb-Zr-bearing minerals occurring mostly in seams, fractures, and groundmass of the fragmental trachyte.

Detailed observations and analysis of polished thin sections for mineral identification, in particular for identification of the ore-bearing minerals, were performed at the University of Maine Microprobe Laboratory by Drs. Martin Yates and John Slack (with Chunzeng Wang attending), by using EDS and WDS of an electron microprobe. Based on the microprobe analysis, abundant minerals in the groundmass of the trachyte micro-breccia are zirconium silicates and monazite (Fig. 20). Other REE- and Nb-bearing minerals include: bastnäsite, euxenite, and volumbite. Betafite and ilmenorutile are sparse to rare.

Field observations, petrographic microscopic, microXRF, and electron microprobe analyses (Fig. 20), as well as whole-rock geochemical data demonstrate that: (1) The East Lobe of the trachyte body is entirely brecciated or shattered (fragmented), and the trachyte fragments are generally less than one centimeter in diameter; (2) The fragmented East Lobe is entirely enriched with anomalously high REE+Y and trace elements, such as Nb and Zr, in particular the entire no-name ridge; (3) REE+Y, Nb, and Zr-bearing minerals (e.g., zirconium silicates, monazite, bastnäsite, and columbite) occur dominantly in the groundmass of the trachyte fragments as seams and veins, with only some (e.g., monazite) disseminated within the trachyte fragments. The significant brecciation or fragmentation was thus the precursor of the REE+Nb-Zr mineralization. Wherever it is brecciated/fragmented, it is mineralized. The metallogenesis of the trachyte with anomalously high enrichment of REE+Y and trace elements Nb and Zr must be related to the brecciation/fragmentation. (*Note: Because all the samples analyzed for this project were collected from the surface of the trachyte body, the word "entirely" or "entire" refer to the surface of the trachyte body and the no-name ridge.*)

The cause of the fragmentation remains to be fully understood. It is likely due to a near-surface explosion or crypto-explosion during emplacement of the trachyte magma. Small fragments are indicative of powerful crypto-explosion due to extremely high pressure during emplacement. As observed petrographically, the catastrophic fragmentation took place after the trachyte magma started to cool and crystalize because the alkali feldspar laths are broken or truncated by the fractures (Fig. 18c, d). The fractures provided space for precipitation and crystallization of the ore-bearing minerals (Fig. 20). As for the fragmentation process, considering the size of the fragments being mostly less than one centimeter in diameter and the huge volume of the fragmental East Lobe, the explosion that caused the fragmentation must be extremely catastrophic. Considering the fragmental East Lobe remains part of the entire trachyte as an integrated igneous body without capturing xenoliths of any country rocks, such as basalt, tuff, and rhyolite, the explosion must be strictly confined in the trachyte or localized in a closed system. The explosion or fragmentation produced a pervasive porous and permeable system of the trachyte, which could favor and facilitate penetrative infiltration and precipitation of REE+Y, Nb, and Zr-bearing minerals from REE+Y and Nb-Zr-rich fluids or solutions.

The fragmental trachyte could be caused by pressure-quenched, highly explosive subvolcanic event within a conduit or around a conduit as a result of degassing felsic magmas; in this case the fragmental trachyte can be formed as a tuffisite, a type of intrusive breccia, producing a giant trachytic tuffisite at Pennington Mountain. The volcanic-induced subsurface fragmentation could be subsequently followed or accompanied by precipitation of the REE+Y, Nb, and Zr-bearing minerals in the groundmass of the fragments and sintering. Therefore, the mineralization event could be considered as syn-volcanic.

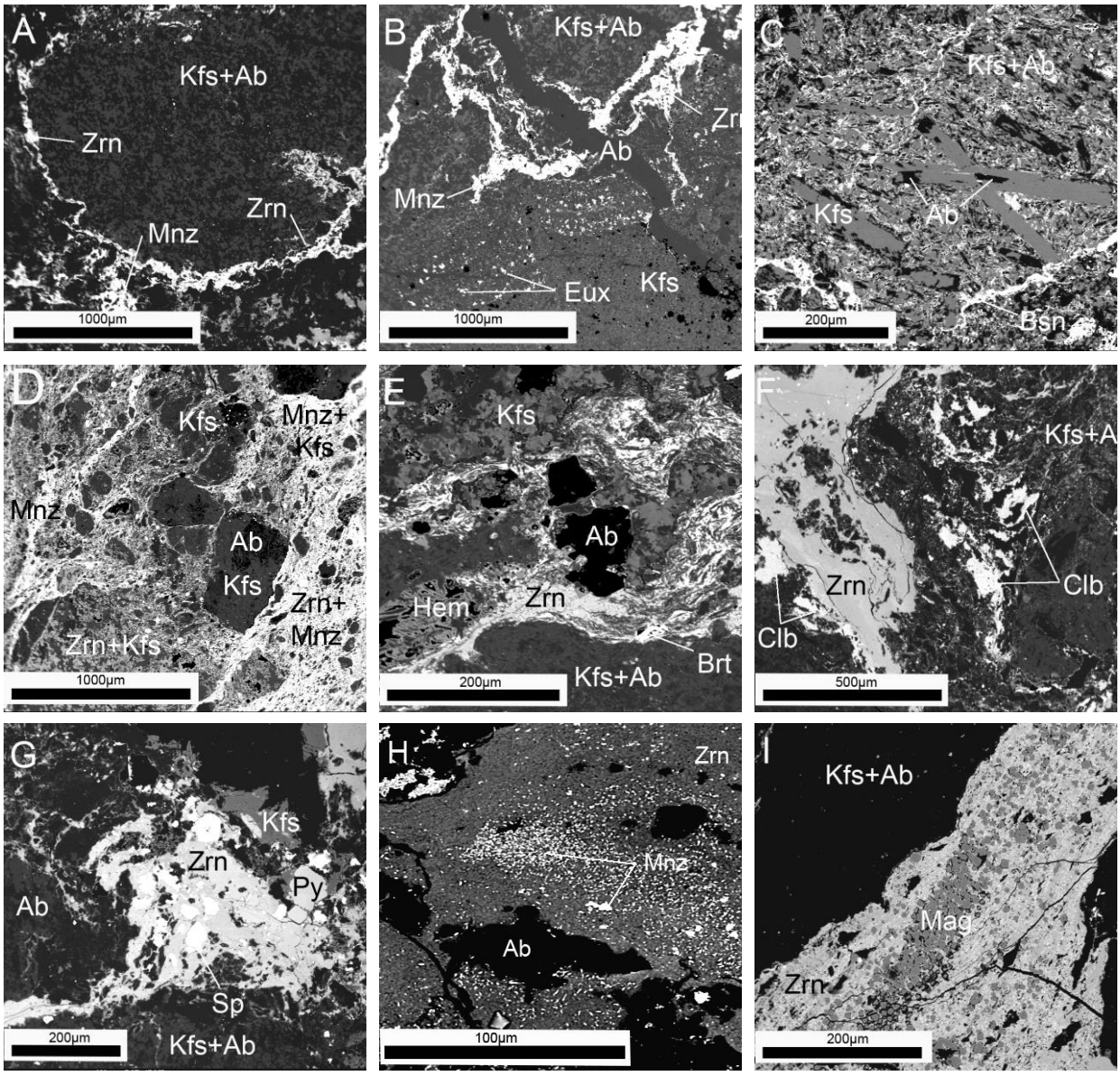

Figure 20. Backscattered electron images showing representative textures and minerals in the brecciated/fragmented, mineralized, and altered trachyte of the East Lobe. (A) A fragment of trachyte made of K-feldspar and albite is surrounded by a groundmass of zirconium silicates and minor monazite. (B) An albite vein truncates seams of zirconium silicates and monazite and a belt of disseminated euxenite. (C) Euhedral K-feldspar phenocrysts are partly replaced by albite and cut by bastnäsite veinlet. (D) Irregular network of seams and veinlets of zirconium silicates and monazite. (E) Seams of zirconium silicates with barite and secondary hematite. (F) Groundmass made of zirconium silicates and bright columbite. (G) Groundmass made of zirconium silicates intergrown with sphalerite; pyrite is secondary. (H) Disseminated monazite. (I) Aggregate of secondary euhedral magnetite crystals in zirconium silicate groundmass or seam. Abbreviations: Ab – albite; Brt – barite; Bsn – bastnäsite; Clb – columbite; Eux – euxenite; Hem – hematite; Kfs – K-feldspar; Mnz – monazite; Py – pyrite; Sp – sphalerite; Zrn – zircon or zirconium silicates.

Seven samples were collected from the strongly mineralized, no-name ridge of the East Lobe and six from the weakly mineralized western part of the East Lobe for whole-rock major, trace, and rare earth elemental analysis. The whole-rock geochemistry clearly demonstrates significantly enriched REE, Nb, and Zr in the brecciated East Lobe, in

particular the entire no-name ridge, where La, Ce, Pr, Dy, Er, Nb, Y, and Zr are respectively 16, 11.4, 10.8, 12.7, 14.2, 22, 16, and 10.5 times higher than the non-mineralized West Lobe.

Trace elements with the highest concentrations in the strongly mineralized East Lobe along the no-name ridge (seven samples in total) are Zr (ranging between 8410 ppm or 0.841wt.% and 13860 ppm or 1.386wt.% with an average of 11,766 ppm or 1.1766 wt.%) and Nb (ranging between 1200 ppm or 0.12 wt.% to 2160 ppm or 0.216 wt.% with an average of 1,656 ppm or 0.1656 wt.%). Both Zr and Nb contribute to the formation of the Pennington Mountain REE-Zr-Nb deposit.

Among LREEs in the strongly mineralized East Lobe along the no-name ridge, the average content of Ce is 1,479 ppm (824 – 1815 ppm), La is 763 ppm (383 – 981 ppm), and Nd is 489 ppm (252 – 640 ppm). Dy and Er are the most abundant HREEs on average, 167 ppm (106 – 213 ppm) and 114 ppm (68 – 147 ppm), respectively. The average Y content is 1,140 ppm, ranging from 649 ppm to 1415 ppm. Total REE+Y oxides average 5,613 ppm or 0.5613 wt.%.

Paragenesis of the Pennington Mountain trachyte REE-Nb-Zr mineralization: (1) Significant subsurface fragmentation of the highly pressurized trachytic magma produced trachytic micro-breccia or trachytic tuffisite, as a syn-volcanic event. (2) Immediate and rapid pervasive crystallization of REE-Nb-Zr-bearing minerals and other related minerals. This was the major stage of REE-Nb-Zr mineralization. (3) Filling of later, minor cross-cutting fractures by albite, bastnäsite, or barite. This stage was insignificant.

The decreased SiO_2 content from average 66.18% of the non-mineralized to average 59.37% of the strongly mineralized trachyte, rules out any post-emplacement silica-rich hydrothermal activity, for example, silicification, as observed through petrographic, and EDS and WDS electron microprobe analyses. CaO shows an apparent decrease from an average of 0.73% of the non-mineralized to an average of 0.09% of the mineralized trachyte, which rules out carbonation alteration. As a matter of fact, no calcite ($CaCO_3$) has been observed in the trachyte (except calcite amygdales in the non-mineralized trachyte), nor apatite ($Ca_5[PO_4]3(OH,F,Cl)$).

ACKNOWLEDGEMENTS

This trip guide is based on my recent and current USGS and MGS STATEMAP projects and on the Pennington Mountain collaborative project on the REE-Nb-Zr deposit. Dr. Gary Boone provided encouragement, guidance, and essential advice. Dr. Robert Marvinney has played a critical leadership role for the northern Maine projects since 2016. Anjana Shah, John Slack, David Lentz, Martin Yates, Amber Whittaker, Christopher McFarlane, and David Putnam have made significant contributions to the discovery and study of the Pennington Mountain trachyte and the REE-Nb-Zr deposit. Drs. Robert Gastaldo, Ian Glasspool, and Patricia Gensel help with identification of plant fossils and interpretation of the sedimentary facies of the St. Froid Lake Formation. Drs. Carlton Brett and Alex Bartholamew help with the identification of invertebrate fossils. Dr. Gil Machado helps with palynological analysis. Fieldwork for the Winterville inlier and Pennington Mountain projects has been assisted by UMPI students Eric Bradley (2020), Jesse Federico and Miranda Washinawatok (2021), Preston Bass and Liam Daniels (2022). I am always grateful to Amanda Barker for leading the early trips to North Maine Woods. Access and permissions granted by North Maine Woods Inc, Irving Woodlands, and Seven Islands are much appreciated.

ROAD LOG

Assembly time and location: Meet at the parking lot next to the soccer field/tennis court on UMPI campus. The departure time is 7:00 am ET. Other people may meet the group at Ashland One Stop at 7:30 am ET. Regular cars without sturdy tires are not recommended for the trip. Car-pooling is encouraged and appreciated. Bring whatever you plan to eat or drink. Wear warm clothes. Most stops are next to roads with only a couple require short and light hiking. While driving in the woods, pay attention to logging trucks. They have absolute right of way.

Cumulative milage	**Description**
0.0	Start logging from UMPI south entrance; make left turn to Main St (Rte-1).
0.7	Left turn to State St. after two traffic lights.
0.9	Left turn to Rte-163 toward Mapleton/Ashland at the five-street intersection. Keep on Rte-163.
15.0	Right turn to a logging road.
15.1	Stop by the borrow pit on the right side of the road.

Stop 1. Basal conglomerate of the Frenchville Formation and Salinic A unconformity: (554484, 5166185) This recently opened borrow pit exposes the basal conglomerate of the Silurian Frenchville Formation (Fig. 21). The conglomerate occurs as thick and massive beds with intercalated coarse lithic sandstone and mudstone layers. It is

poorly sorted, polymictic, and matrix supported. Most of the clasts at this site are vesicular basalts. The conglomerate contains fragments of marine invertebrate fossils of brachiopods, *favosites*, rugose corals, etc. The conglomerate lies unconformably on top of the basalt of the Ordovician Winterville formation around the York Ridge inlier (Fig. 2). The west side of the logging road is supposed to be the basalt if there were any outcrops. The unconformity represents the early stage of the Salinic orogeny, called Salinic A in northern New Brunswick (Wilson and Kamo, 2012) and in northern Maine in this study.

Figure 21. The borrow pit at Stop 1 shows thickly bedded conglomerate and intercalated sandstone and mudstone of the basal conglomerate unit of the Silurian Frenchville Formation.

Turn around and back to Rte-163

15.3 Right turn to Rte-163 toward Ashland.
21.4 Stop by ***Ashland One Stop*** parking lot to pick up more people. 10 minutes for gas, coffee, restroom, etc.
Turn either left or right onto Rte-11 toward Eagle Lake/Fort Kent.

21.7 Left turn and keep on Rte-11.
22.5 Right turn and keep on Rte-11 after the Aroostook River bridge.
29.9 Right turn to Beaver Brook Rd (active dirt logging road).
32.2 Left turn to a narrow dirt logging road (the first left turn on Beaver Brook Rd).
34.0 Right turn to another old logging road.
34.6 Stop by the borrow pit.

Stop 2. Reverse-thrust fault between Winterville basalt and Madawaska Lake slate: (542521, 5180973) This borrow pit shows excellent exposure of the Clayton Lake fault, one of the major faults in the northern Maine imbricate fault system. The basalt and slate in the fault are strongly brecciated. The fault is a southeast-directed reverse-thrust fault with the basalt of the Winterville Formation thrown over the slate and graywacke of the Madawaska Lake Formation (Fig. 22). The latter occurs as a fault sliver sandwiched between the Clayton Lake and Greenlaw Pond faults. Both faults are post-Acadian and likely Neoacadian.

Figure 22. Fault contact between Winterville basalt (upper left, rusty basalt) and Madawaska Lake slate (lower right, dark gray slate) at Stop 2. Viewer facing north. Eric Bagley (field assistant 2020) on the hanging wall basalt.

Turn around.
35.3 Left turn.
37.0 Right turn to Beaver Brook Rd at the end of the road.

39.4 Right turn to Rte-11 at the end of the road.
42.2 Left turn to West Rd (you are now downtown Portage Lake; you may see the lake on your right side.)
43.2 Left turn to Rocky Brook Rd (a major dirt logging road in this region. Watch for logging trucks).
47.5 ***Fish River gate***. Slow down, stop, and say hi to the gate staff. You are now in the North Maine Woods.
49.3 Right turn to Hewes Brook Rd at the big fork.
54.5 Left turn to Jacque Ouellet Rd at the big fork.
60.8 Right turn to Pinnacle Rd, right after passing the 6-mile sign.
61.1 Stop for pillow basalt.

Stop 3. Pillow basalt of the Winterville Formation: (519822, 5189868) This recent roadcut shows excellent pillow basalt of the Mid Ordovician Winterville Formation (Fig 23). Pillow basalt is a common feature in the formation. Another site with excellent pillow basalt is the Fish River Falls located southeast of Round Pond with access from both sides of the river; it is not far from Stop 3. Pillows form in a subaqueous environment, in particular when the eruption rate is low. What happens is the outer surface of a lobe would be quenched rapidly by water, but it is still hot and fluid inside the lobe and the lobe continues to inflate as lava continues to be supplied so that it forms a bulging, pillow-like lobe. The lobe then breaks off and new pillow-like lobes keep forming as the flow advances. Pillows commonly have a spherical or bulbous shape, generally show convex (rounded) upper surface and a keel projecting downward. The convex up surface and the keel help tell the top or bottom of a pillow. What is the top of the pillows at this stop? Pillows generally also have a chill margin and radial vesicles as shown at this stop (Fig.23b). Interstitial aragonite is common at this stop as well.

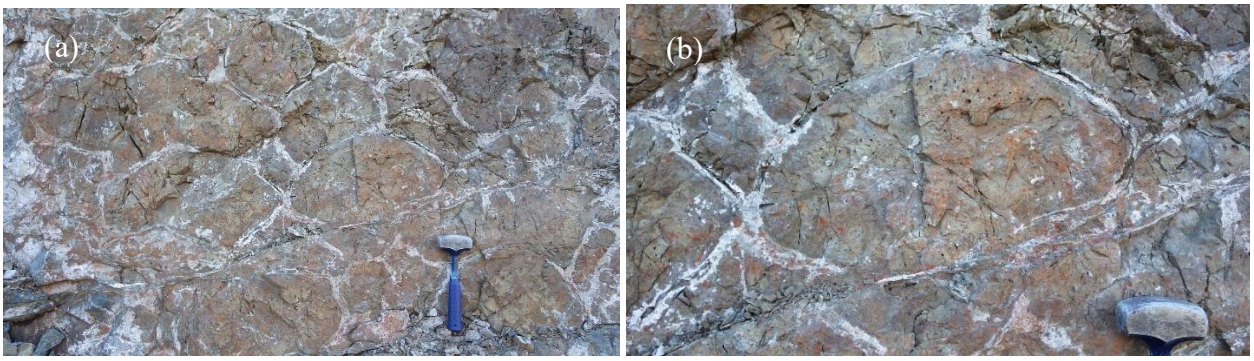

Figure 23. Pillow basalt of the Mid Ordovician Winterville Formation at Stop 3.

Continue on Pinnacle Rd.
64.6 Right turn to Horseshoe Pond Rd.
66.0 Stop for the outcrop on the left side of the road.

Stop 4. Basal conglomerate of the lower Devonian Seboomook Group: (520610, 5192728) The bottom succession of the Seboomook Group, informally called the "Trinity", includes basal conglomerate, fossiliferous limestone and calcareous sandstone, and maroon/red slate/siltstone. The unconformity between the group and the Winterville inlier, commonly presented as the basal conglomerate overlying the volcanic rocks of the inlier, is well preserved in the area around Island Pond and Fish River Lake even though it is offset by several northwest-striking strike-slip faults (Figs. 1, 2, & 25). The "Trinity" is well exposed in the Fish River Lake area, including the tiny islands on the lake. In the Island Pond area, however, only the basal conglomerate and fossiliferous limestone and calcareous sandstone units are exposed. Generally, the basal conglomerate is composed of clasts of mainly volcanic rocks, either dominated by tuff or by basalt, and characterized by red and/or green tuff pebbles (even red jasper pebbles). The basal conglomerate at Stop 4 is dominated by tuff pebbles and granules of light gray to dark gray colors (Fig. 24). A large ledge on the northeast side of the pond shows basal conglomerate dominated by basalt clasts (we will make a quick stop if time allows). We will visit Stops 5A and 5b for the fossiliferous limestone and calcareous sandstone.

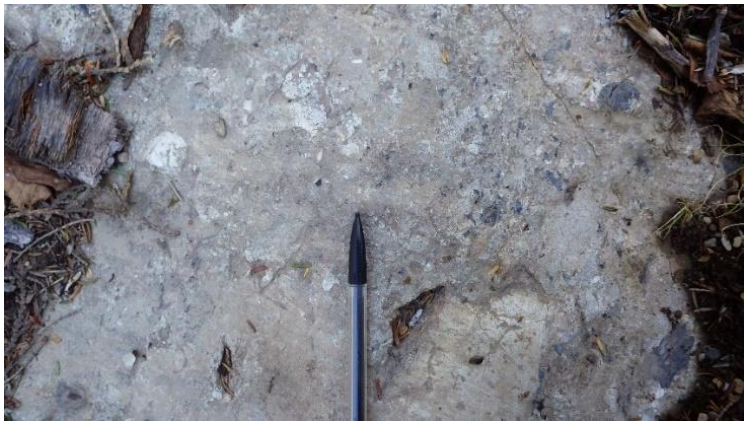

Figure 24. The basal conglomerate outcrop at Stop 4.

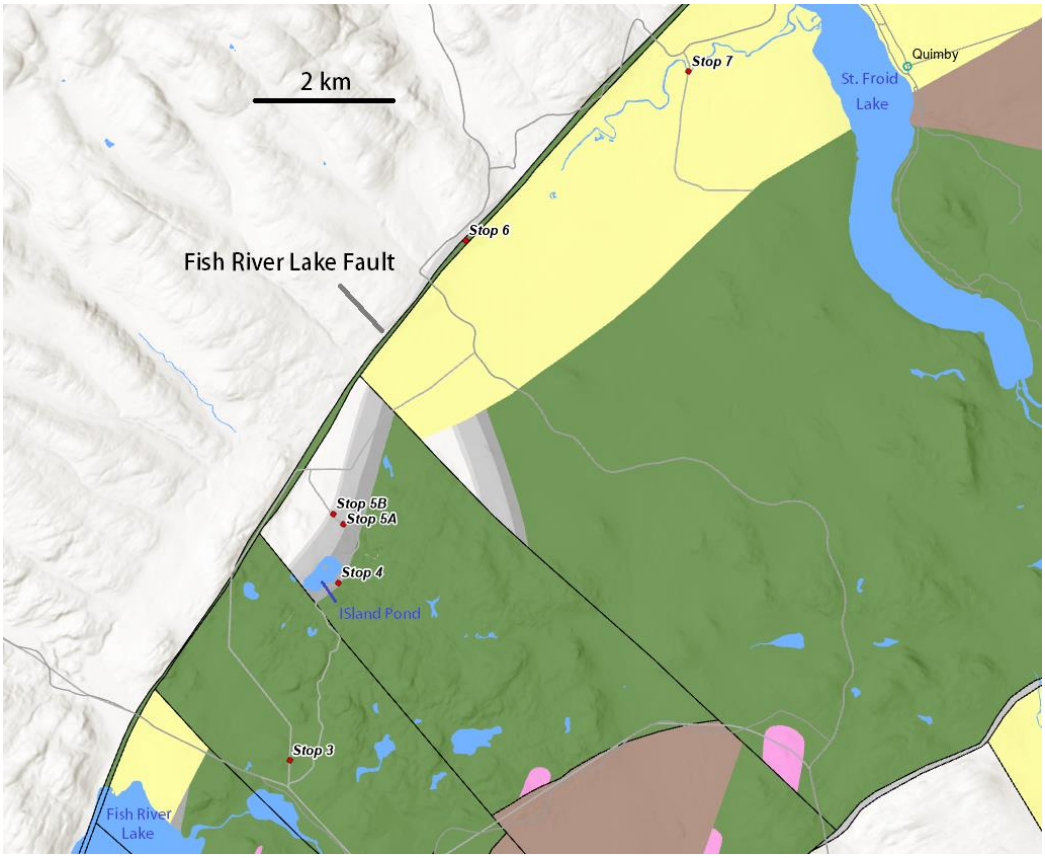

Figure 25. Local geologic map of the Island Pond and Red River valley area. See Figure 3 for legend.

Turn around.

66.8 Stop for fossiliferous limestone ledge on the left side. It is 35 meters (or 115 feet) from the road. Easy hike.

Stop 5A. Fossiliferous limestone of the "Trinity" (Fig. 25)**:** (520687, 5193662) It crops out on the road and also along a ledge on thesouth side of the road (Horseshoe Pond Rd), about 35 meters (or 115 feet) from the road. As always, this fossiliferous limestone is white or light gray and massive. It is a reef limestone and made of reef builders of dominantly stromatoporoids (a sponge) and *Thamnopora* (a tabulate coral). It may also contain minor fragments of *Favosites* (also a tabular coral), crinoids, brachiopods, etc. This fossiliferous limestone is widespread in northern Maine, north to Limestone Point on Square Lake, and southwest to at least the northeast side of Moosehead Lake. The Owen Brook limestone in East Branch Penobscot River is also this limestone.

Continue on Horseshoe Pond Rd.

67.0 Small borrow pit on the right side of the road.

Stop 5B. Fossiliferous calcareous sandstone of the "Trinity" (Fig. 25)**:** (520526, 5193833) This small pit shows the fossiliferous sandstone and slate of the "Trinity". The purple slate west side of the pit may be equivalent to the maroon slate/siltstone unit. The calcareous sandstone is weathered to be in orange color (Fig. 26c). Some brachiopods have been found at this pit, including *Atraypa* (Fig. 26d).

Figure 26. Fossiliferous limestone at Stop 5A (a and b) and calcareous sandstone at Stop 5B (c and d). (a) The white reef limestone; (b) Fragments of stromatoporoids, crinoids, etc. (c) Calcareous sandstone and slate weathered in orange. (d) A brachiopod (*Atrypa*?).

Continue on Horseshoe Pond Rd.

67.5 Right turn (bear right)

69.7 Left turn to Hewes Brook Rd at the end of the road. (And bear right!).

71.0 Stop for outcrop in the left side ditch.

Stop 6. The Fish River Lake fault, fault breccia, and basalt fault sliver (Fig. 25)**:** (522656, 5198227) What a view on top of this highland, the Seboomook highland! Looking down southeast-east is the Red River valley underlain by red and green beds of the Lower Devonian Emsian St. Froid Lake Formation. A red sandstone outcrop actually occurs about 200 meters (600 feet) down the road (on the southeast side) from this stop. Behind you is the Seboomook Group. In the ditch, on the west-northwest side of the road, is the Fish River Lake fault that separates the St. Froid Lake Formation from the Seboomook Group. The southwest-striking and southeast-directed Fish River Lake reverse fault is one of the longest and the most important faults in the northern Maine imbricate fault system. The Fish River Lake fault has created the longest and the most remarkable "fault scarp" in northern Maine; most of the Fish River chain of lakes and the Red River valley are controlled by this fault. Our driving after this stop and before reaching Rte-11 in Winterville Plantation is along the fault scarp, in other words, along the Fish River Lake fault.

A basalt fault sliver is sandwiched in the fault and the sliver extends off and on for at least 45 kilometers along with the length of the fault. The basalt is at this time considered to be part of the Winterville Formation. There also exists fault breccia with large fragments of crushed basalt and even fossiliferous limestone (Fig. 27).

Figure 27. Fault breccia with large fragments/breccias of fossiliferous limestone and vesicular basalt at Stop 6.

Continue on Hewes Brook Rd.

71.8 Right turn and stop at the remotely controlled gate (***Winterville gate***). Make a phone call in the booth and ask to lift the gate.

75.0 Right turn to Red River.

75.2 Stop after passing the bridge.

Stop 7. Red sandstone of St. Froid Lake Formation in Red River (Fig. 25)**:** (526245, 5200935) Red River gets its name from the red sandstone in which it flows. The Red River valley, in particular the riverbed is the lowest in elevation in this region. The St. Froid Lake Formation, as shown at this stop, is a homocline dipping toward northwest (Fig. 28a). In addition to red sandstone of various thickness, there are also intercalated red or purplish red mudstone and shale. The sandstone and mudstone contain plant fragments of trimerophytes – most likely *Psilophyton*, *Hostinella*, and *Pertica* (Fig. 28b).

Figure 28. Red River and the bridge at Stop 7. (a) The homocline of red sandstone and mudstone. Viewer facing southwest. Dave is looking for plant fossils. (b) Sandstone with fragments of plant fossils.

Turn around.

75.5 Right turn to the main road towards Winterville and Eagle Lake.

82.1 Right turn to Rte-11 at the end of the road.

89.1 Left turn to Pennington Pond Rd, a dirt logging road.

89.9 Left turn to Caron Rd. At the end of Caron Rd, make a right turn and continue on the only drivable road.

95.4 Stop by a small pit for St. Froid Lake Formation.

Stop 8. Red sandstone rich in plant fossils (St. Froid Lake Formation) (Fig. 2): (536738, 5205406) What a view! Looking northwest is the Red River valley (or Fish River valley); in the background is the upthrown Seboomook highland. On the southside of the logging road is a small pit with red sandstone and mudstone of St. Froid Lake Formation. As at the Red River stop (Stop 7), the beds also dip toward the northwest. Indeed, the entire St. Froid Lake Formation in this informally called "Red River basin" dips toward northwest, forming a single homocline. The sandstones are rich in fragments of plant fossils of trimerophytes – most likely *Psilophyton*, *Hostinella*, and *Pertica* (Fig. 29a, b), with less common *Protolepidodendron* (the earliest tree species) and *Taeniocrada* (Fig. 29c, d).

This is one of the best sites with better reserved plant fossils. We need to keep them in place for ongoing and future research. Thanks!

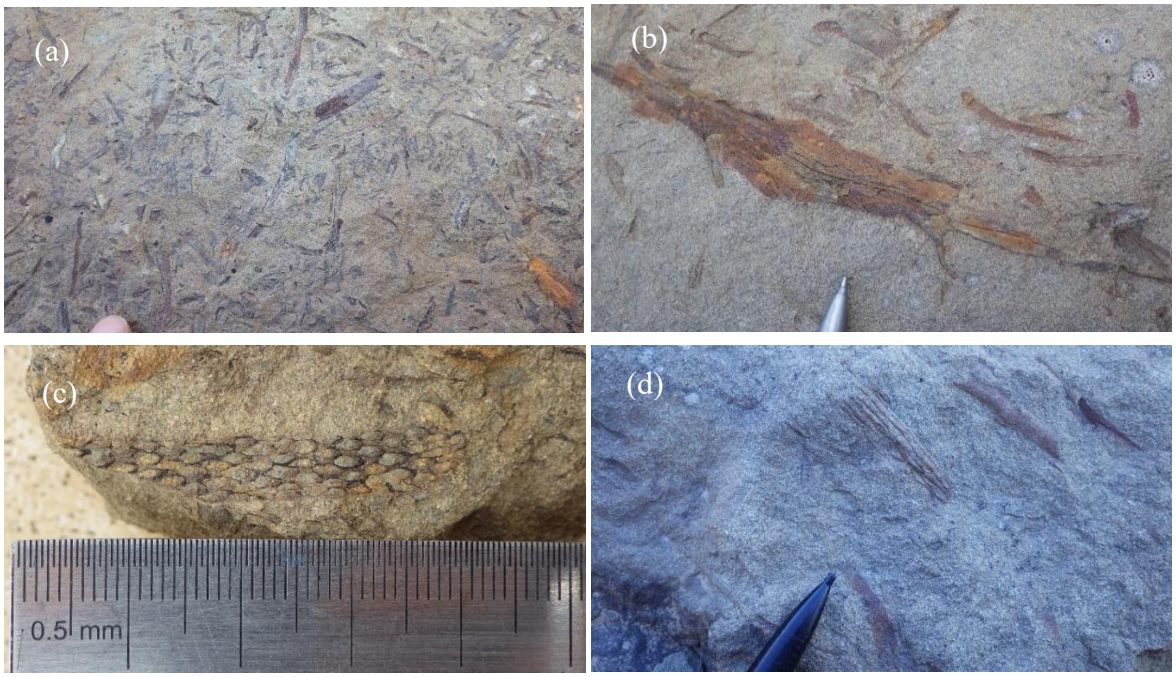

Figure 29. Plant fossils at Stop 8. (a) and (b) are fragments of likely *Psilophyton* and *Pertica.* (c) is a *Protolepidodendron* and (d) is a *Taeniocrada* (?) (the upper center).

Continue on the road straight forward and take the mostly used logging road toward Pennington Mountain.

98.3 Stop at the intersection with an overgrown logging road on the right side. We will hike on this overgrown but even road for about 150 meters (or 450 feet) before going uphill for about 90 meters (or 270 feet) to Stop 9.

Stop 9. The REE-Nb-Zr-mineralized trachyte with hydrothermal pyrite (East Lobe) (Fig. 11**):** (540858, 5204848) This is an excellent outcrop showing a special type of mineralized trachyte with abundance of pyrite. The trachyte is rusty due to oxidation of pyrite (Fig. 30). However, the Pennington Mountain trachyte, including the mineralized trachyte, generally lacks pyrite and the pyritiferous trachyte is the much less common type of the Pennington Mountain REE-Nb-Zr mineralization. Based on surface investigation over the entire mineralized trachyte body, probably only 2% may show pyritic trachyte like what you see at this stop. Pyrite is secondary, probably produced in localized hydrothermal alteration. The mineralized trachyte is dark gray or near black on fresh broken surfaces. It is massive, very fine grained, and homogenous; no minerals are visible with the naked eye.

Figure 30. Mineralized trachyte at Stop 9. (a) Visiting this outcrop on June 26, 2022. John Slack, Anjana Shah, Martin Yates, David Putnam, and Preston Bass. Photo taken by Wang. (b) The rusty, pyritic, mineralized trachyte.

Continue on the logging road.

100.0 Right turn to Pennington Pond Rd (old dirt logging road).

100.6 Stop for Stop 10.

Stop 10. The REE-Nb-Zr-mineralized trachyte without pyrite (East Lobe): (541041, 5204047) See Figure 11 for stop location. Before hiking 70 meters (or 210 feet) to a mineralized trachyte ledge located on the north side of the

road, let's quickly look at the black slate and graywacke of the Ferguson Brook Formation on the road. There are actually several borrow pits of various sizes dug in the formation along the road (Pennington Pond Road). The Pennington Mountain trachyte is likely in fault contact with the Ferguson Brook slate and graywacke and thrusted over the latter by the Pennington Mountain fault, a low-angle (lower than 5º) thrust fault named in this study.

Walk on a marked trail to the ledge on the north side of the road (Fig. 31). This ledge represents the main body or the major type of the REE-Nb-Zr mineralization of the Pennington Mountain trachyte without pyrite or with very few pyrite. Fresh, broken surfaces of the mineralized trachyte are dark gray or near black. It is again massive, very fine grained with a homogenous texture. Minerals are not visible with the naked eye.

Figure 31. (a) A visit to the ledge at Stop 10 on October 26, 2022. Chunzeng Wang, Robert Marvinney, and Amber Whittaker. Photo taken by Lauren Madsen. (b) Another visit to the ledge with David Lentz on August 16, 2023.

Continue on Pennington Pond Rd.

100.8 Stop for a small pit on the right side.

Stop 11. Basalt/pillow basalt next to the trachyte (Fig. 11**):** (540884, 5203906) The wall of the small pit is basalt and pillow basalt (Fig. 32a) of the Winterville Formation. It is only about 10–15 meters (or 30–45 feet) from the trachyte. The basalt is aphyric and fine gained. Part of it is vesicular and/or amygdaloidal with calcite amygdales (Fig. 32b). Whole-rock geochemical analysis of a sample collected from this basalt outcrop and another one from the northwest side of the trachyte body show calc-alkaline affinity; both are geochemically either "alkaline basalt" or "trachy-andesite". Their LREE are higher than HREE and their HREE are slightly higher than the trachyte. Geochemically both basalt samples are distinctively different from the basalt samples collected from other areas of the Winterville inlier, for example, they do not show any depletion in Ta and Nb. On tectonic discrimination diagrams (not posted here), they plot in "MORB-OIB array" or "oceanic islands" fields. It is highly likely that both the Pennington Mountain trachyte and the basalt around the trachyte were produced in a similar or same tectonic setting (non-orogenic or non-active arc), or even from the same source in the mantle.

At around this stop (or around the road – Pennington Pond Road) is the Pennington Mountain thrust fault that separates the basalt and trachyte from the Ferguson Brook black slate and graywacke to the east-southeast. The fault is about parallel to the road and located immediately on the west side of the road.

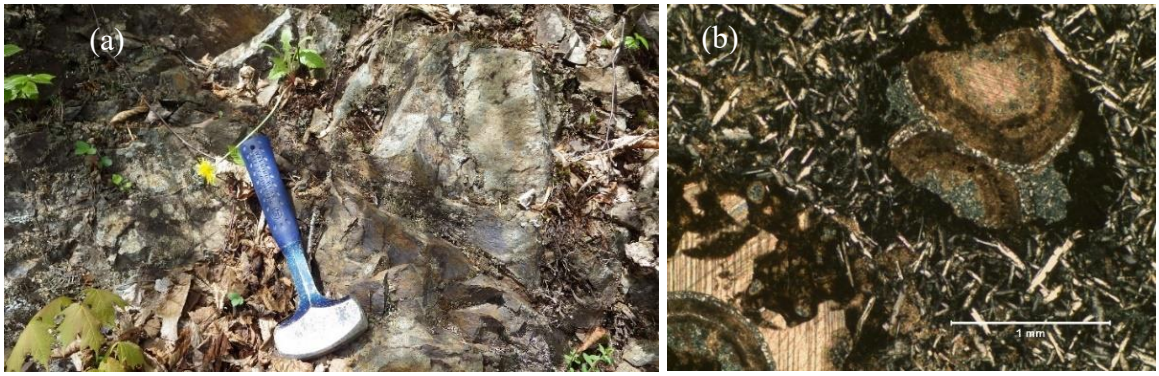

Figure 32. (a) Pillow basalt at Stop 11. (b) Amygdaloidal texture with calcite amygdales at Stop 11.

Continue on Pennington Pond Rd.

102.5 Left turn to another old logging road. Keep on the main, frequently used road that leads to Rte-11.

109.1 Left turn to Rte-11
110.2 Right turn to a dirt logging road named Nixon Siding Road.
110.4 Right turn to the big borrow pit for Stop 12.

Stop 12. Green beds of the St. Froid Lake Formation (Figs. 1 & 2): (536880, 5191959) This large borrow pit shows mostly the green beds of the St. Froid Lake Formation. The green beds are well bedded thin to medium-layered quartzofeldspathic micaceous sandstone, siltstone, and mudstone/shale (Fig. 33a); they are not foliated. They contain thin sandy and micaceous drapes of comminuted dark phytodebris (Fig. 33b) likely deposited in a coastal or nearshore setting. The phytodebris is, generally, ≤1 cm in length. All the plant material appears to be transported and deposited in aqueous terrestrial or coastal settings.

Figure 33. Green beds of St. Froid Lake formation at Stop 12. (a) The thin-medium-layered sandstone and shale. (b) Fragments of plant fossils.

Turn around and drive back to Rte-11.
110.6 Right turn to Rte-11. Keep on Rte-11 towards Ashland.
131.0 Ashland One Stop. Left turn to Rte-163 towards Mapleton and Presque Isle.
151.0 ***Back to Presque Isle***. Don't forget the banquet at UMPI Campus Center!

REFERENCES

Ayuso, R.A. and Schulz, K.J., 2003. Nd-Pb-Sr isotope geochemistry and origin of the Ordovician Bald Mountain and Mount Chase massive sulfide deposits, northern Maine. Economic Geology Monograph 11, p. 611–630.

Ayuso, R.A., Wooden, J.L., Foley, N.K., Slack, J.F., Sinha, A.K., and Persing, H., 2003. Pb isotope geochemistry and U–Pb zircon (SHRIMP–RG) ages of the Bald Mountain and Mount Chase massive sulfide deposits, northern Maine: Mantle and crustal contributions in the Ordovician. Economic Geology Monograph 11, p. 589–609.

Berry, W. B. N., 1964. Early Ludlow graptolites from the Presque Isle quadrangle, Maine: Journal of Paleontology, v. 38, p. 587–599.

Berry, W. B. N., 1960. Early Ludlow graptolites from the Ashland area, Maine: Journal of Paleontology, v. 34, p. 1158–1163.

Boone, G.M., 1958. The Geology of the Fish River Lake–Deboullie Area, Northern Maine: Ph.D. thesis, Yale University, 186 p.

Boone, G.M., 1970. The Fish River Lake Formation and its environments of deposition: in Shorter Contributions to Maine Geology: Maine Geological Survey, Bulletin 23, p. 27–41.

Busby, C.J., Kessel, L., Schulz, K.J., Foose, M.P., and Slack, J.F., 2003. Volcanic setting of the Ordovician Bald Mountain massive sulfide deposit, northern Maine. Economic Geology Monograph 11, p. 219–244.

Boucot, A.J., Field, M.T., Fletcher, R., Forbes, W.H., Naylor, R.S., and Pavlides, L., 1964. Reconnaissance bedrock geology of the Presque Isle quadrangle, Maine: Maine Geological Survey, Bulletin 15, No. 2, 123 p.

Cabanis, B. and Lecolle, M., 1989, Le diagramme La/10 – Y/15 – Nb/8: Un outil pour la discrimination des series volcaniques et en evidence des mélange et/ot de vontamination crustale. Comptes Rendus de l'Académie des Sciences, Série II, 309, p. 2023–2029.

Cummings, J.S., 1988. Geochemical detection of volcanogenic massive sulphides in humid-temperate terrain (using surficial methods): Bangor, Maine, J.S. Cummings, Inc., 298 p.

Eby, G.N., *1992*. Chemical subdivision of the *A-type* granitoids: Petrogenetic and tectonic implications: Geology, v. 20, p. 641–644.

Hall, B., 1970. Stratigraphy of the southern end of the Munsungun anticlinorium, Maine. *Maine* Geological Survey Bulletin 22, 63 p.

Horodyski, R.J., 1968. Bedrock geology of portions of Fish River Lake, Winterville, Greenlaw, and Mooseleuk Lake quadrangles, Aroostook County, Maine. M.S. thesis, Cambridge, Massachusetts, Massachusetts Institute of Technology, 192 p.

LeBas, M.J., LeMaitre, R.W., Streckeisen, A., and Zanettin, B., 1986. A Chemical Classification of Volcanic Rocks Based on the Total Alkali-Silica Diagram: Journal of Petrology, v. 23, no. 3, p. 745–750.

Mencher, E., 1963. Annual report on work accomplished during 1963 under NSF grant GP-1547 "Geology of Northern Aroostook County, Maine and its Bearing on the Development of the Northern Appalachian" (unpublished report).

Nakamura, N., 1974. Determination of REE, Ba, Mg, Na and K in carbonaceous and ordinary chondrites: Geochimica et Cosmochimica Acta, 38, p. 757–775.

Osberg, P.H., Hussey, A.M., II, and Boone, G.M. (editors), 1985. Bedrock geologic map of Maine: Maine Geological Survey.

Pearce, J.A., 2008. Geochemical fingerprinting of oceanic basalts with applications to ophiolite classification and the search for Archean oceanic crust: Lithos 100, p.14–48

Pearce, J.A., Harris, N.B.W., and Tindle, A.G., 1984. Trace element discrimination diagrams for the tectonic interpretation of granitic rocks: Journal of Petrology 25(4), p. 956–983.

Pearce, J. A., 1983. Role of sub-continental lithosphere in magma genesis at destructive plate margins, in Continental Basalts and Mantle Xenoliths, edited by C. J. Hawkesworth and M. J. Norry, p. 230–249, Shiva, Nantwich, UK.

Perkins, E.H. and Smith, E.S.C., 1925. Contributions to the geology of Maine, No. 1: A geological section from the Kennebec River to Penobscot Bay: American Journal of Science, 5th series, v. 9, no. 51, p. 204–228.

Pollock, S.G., 1987. The Lower Devonian slate problem of western and northern Maine revisited: Northeastern Geology, v.9, no. 1, p. 37–50.

Ross, P.S. and Bédard, J.H., 2009. Magmatic Affinity of Modern and Ancient Subalkaline Volcanic Rocks Determined from Trace-Element Discriminant Diagrams: Canadian Journal of Earth Sciences, 46, p. 823–839.

Roy, D.C., 1987. Geologic Map of the Caribou and Northern Presque Isle 15' Quadrangle, Maine: Maine Geological Survey, Open-File No. 87-2, 44 p.

Roy, D.C. and Mencher, E., 1976, Ordovician and Silurian stratigraphy of northeastern Aroostook County, Maine: Geol. Soc. Amer., Memoir 148, p. 25–52.

Roy, D. C., 1970. The Silurian of Northeastern Aroostook County, Maine, (Ph.D. thesis): Massachusetts Institute of Technology, 482 p.

Roy, D.C., and Mencher, E., 1976. Ordovician and Silurian stratigraphy of northeastern Aroostook County, Maine: Geol. Soc. Amer., Memoir 148, p. 25–52.

Schulz, K. J. and Ayuso, R. A., 2003. Lithogeochemistry and paleotectonic setting of the Bald Mountain massive sulfide deposit, northern Maine. Economic Geology Monograph 11, p. 79–109.

Shah, A.K., 2022. Airborne magnetic and radiometric survey, Munsungun region in northern Maine, 2021: U.S. Geological Survey data release, https://doi.org/10.5066/P97VUIJS.

Shah, A.K., and Wang, C., 2022. Ground-based gamma spectrometry data collected in northern Maine (Version 2.0, September 2022): U.S. Geological Survey data release, https://doi.org/10.5066/P9WFQ30O.

Slack, J.F., Foose, M.P., Flohr, M.J.K., Scully, M.V., and Belkin, H.E., 2003. Exhalative and subsea-floor replacement processes in the formation of Bald Mountain massive sulfide deposit, northern Maine. Economic Geology Monograph 11, p. 513–547.

Supkow, D.J., 1965. Stratigraphy and structure of the Spider Lake Formation, Churchill and Spider Lake quadrangles, Maine. M.S. thesis, Orono, University of Maine, 118 p.

Wang, Chunzeng, Slack, John, Shah, Anjana, Yates, Martin, Lentz, David, Whittaker, Amber, and Marvinney, Robert, 2023. A Recently Discovered Trachyte-Hosted Rare Earth Element-Niobium-Zirconium Occurrence in Northern Maine, USA: Economic Geology, Vol. 118, No. 1, p. 1–13.

Wang, C., 2022a. Bedrock Geology of the Fish River Lake Quadrangle, Maine: Maine Geological Survey, Open-File Map 22-5, scale 1:24,000.

Wang, C., 2022b. Bedrock geology of the Carr Pond quadrangle, Maine: Maine Geological Survey, Open-File Map 22-6, scale 1:24,000.

Wang, C., 2021a. Bedrock geology of the Big Machias Lake quadrangle, Maine: Maine Geological Survey Open-File No. 21-12, scale 1:24,000.

Wang, C., 2021b. Bedrock geology of the Greenlaw Pond quadrangle, Maine: Maine Geological Survey Open-File No. 21-2, scale 1:24,000.

Whalen, J.B., Currie, K.L., Chappell, B.W. 1987. A-type granites: geochemical characteristics, discrimination and petrogenesis: Contributions to Mineralogy and Petrology, vol. 95, p. 407–419.

Wilson, R.A., and Kamo, S.L., 2012. The Salinic Orogeny in northern New Brunswick: geochronological constraints and implications for Silurian stratigraphic nomenclature. Canadian Journal of Earth Sciences, 49, p. 222–238.

GEOLOGY OF THE MUNSUNGUN-WINTERVILLE BELT: THE WINTERVILLE INLIER AND THE PENNINGTON MOUNTAIN REE-Nb-Zr DEPOSIT

Chunzeng Wang
University of Maine at Presque Isle, Presque Isle, Maine 04769. chunzeng.wang@maine.edu

INTRODUCTION

The Munsungun–Winterville Belt (WMB) is a major early Paleozoic lithotectonic belt in the Northern Appalachians and characterized by widespread volcanic rocks. The belt includes two major inliers, the Munsungun inlier in the southwest and the Winterville inlier in the northeast, along with nine geologically similar but smaller inliers – the Portage Lake, Castle Hill, and York Ridge inliers in the north, and the much smaller ones in the headwaters of the East Branch Penobscot River and Aroostook River in the south (Fig. 1).

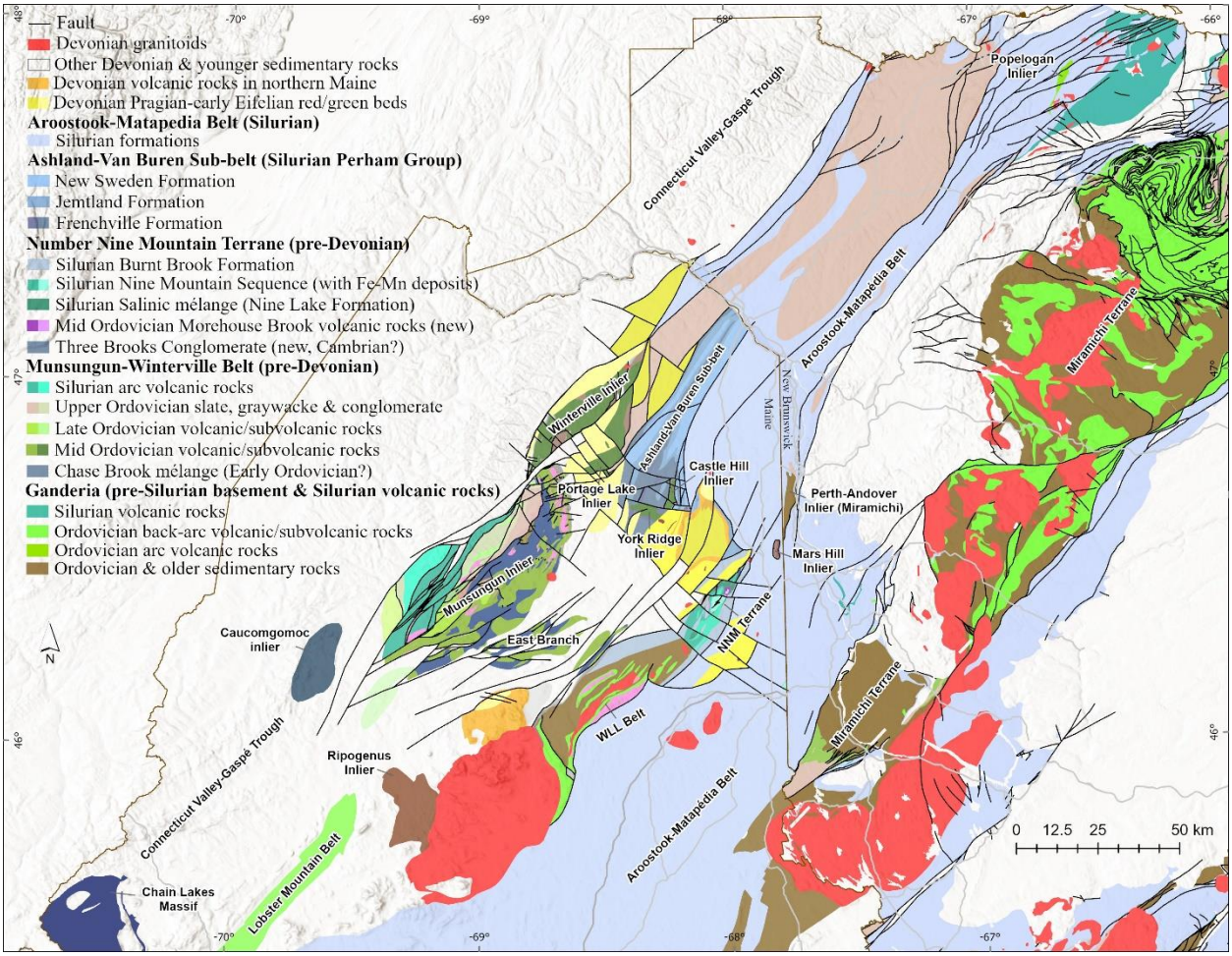

Figure 1. Simplified lithotectonic and regional geologic map of northern Maine and northern New Brunswick. Maine side is based on recent detailed and reconnaissance mapping. NNM Terrane – Number Nine Mountain Terrane. WLL Belt – Weeksboro-Lunksoos Lake Belt.

The pioneering, foundational mapping in the MWB was performed by Gary Boone who studied the area around Fish River Lake and Winterville, as well as the Deboullie syenite complex in the 1950's (Boone, 1958, 1970) and by Brad Hall who mapped the southwestern Munsungun inlier in the 1950–1960's (Hall, 1970). Supkow (1965) mapped the Spider Lake Formation in the Churchill and Spider Lake quadrangles and Horodyski (1968) conducted reconnaissance mapping in the area around Fish River Lake, Winterville, Greenlaw, and Mooseleuk Lake quadrangles. Exploration for base metals in the MWB peaked in the late 1970's and early 1980's with discovery of the Bald

Mountain volcanic massive sulfide (VMS) deposit and several occurrences including the Bull Hill VMS and "New Gold Prospect" at Chandler Mountain (Cummings, 1988) in the Munsungun inlier. In the late 1990's the U. S. Geological Survey (USGS) performed detailed studies of the Bald Mountain VMS deposit, focusing on its volcanic and tectonic settings, lithogeochemistry, geochronology, and metallogenesis (e.g., Ayuso and Schulz, 2003; Ayuso et al., 2003; Busby et al., 2003; Schulz and Ayuso, 2003; Slack et al., 2003).

The Winterville and Munsungun inliers are separated by a northeast-trending fault block of slate and sandstone of the Lower Devonian Seboomook Group (Fig. 1). The elongated Winterville inlier stretches northeastward from West Inlet to Square Lake. The inlier, as well as the Portage, York Ridge, and Castle Hill inliers, are dominated by volcanic rocks of the Ordovician Winterville Formation. Funding from the USGS STATEMAP Program and Maine Geological Survey (MGS) has supported detailed and reconnaissance mapping in the Winterville inlier starting in 2020, initially in the Big Machias, Fish River Lake, Carr Pond quadrangles. More reconnaissance mapping has since been conducted in the Winterville inlier and vicinity after discovery of non-foliated, plant fossil-rich green and red beds along the Fish River chain of lakes. These unique green and red beds were later named the St. Froid Lake Formation and determined to be of Early Devonian Emsian age based on brachiopods (Wang, 2022a, 2022b) and Emsian-early Eifelian based on recent palynological analyses.

Extensive mapping has also revealed that the Winterville inlier and vicinity, like the entire Munsungun-Winterville belt, has experienced significant faulting with considerable vertical and horizontal displacement, and that the faulting took place mostly during the Acadian and Neoacadian orogenies. Most of the faults strike southwest or northeast and are reverse-thrust faults with southeast-oriented reverse motion. These stacked, domino-style imbricate faults cut by later faults define the structural framework of northern Maine (Fig. 1). The topography of the Winterville Planation and Pennington Mountain is controlled by the imbricate fault system, with the upthrown Winterville volcanic rocks forming mountains and highlands and the downthrown St. Froid Lake red and green beds forming valleys and lowlands, giving drivers a roller-scooter riding experience on Rte-11.

During the exploration campaign for base and radioactive metals (Zn, Pb, Cu, U, Th, etc.) in the late 1970s and early 1980s, no significant mineral deposits were reported in the Pennington Mountain and Winterville Plantation areas except for several base and radioactive metal occurrences. Among the occurrences is the "Three Brooks radiometric anomaly" reported by General Crude Oil Company and included in an internal project report entitled "*Mineral Exploration in the Winterville Formation, Aroostook County, Maine*" (Ernest K. Lehmann & Associates, Inc. Report No. 7729) by Donald White and Edward Eisenbrey and dated in December 1977. The anomaly "corresponds to a small knob on the northeast slope of Pennington Mountain". The anomaly was discovered during an airborne radiometric survey and later inspected by bedrock mapping, a ground gamma-ray spectrometry survey, and even drilling of 17 holes, but only 6 holes successfully reached 24 feet in depth. According to the report, the exploration targeted base metals Cu, Zn, and Pb and radiometric elements U and Th even though the assays of three samples of drill cuttings from the sites "with the highest total gamma radiation", showed enrichment of zirconium (Zr, 1.2 wt.%), niobium (Nb, 0.23 wt.%), and several rare earth elements (La, Ce, Nd, and Y).

When the USGS Earth Mapping Resources Initiative (MRI) was launched in 2019 to improve our knowledge of the geologic framework in the United States and to identify areas that may have the potential to contain undiscovered critical mineral resources, the Munsungun-Winterville belt was recommended by MGS as a potential focus area. This initiative includes high-resolution airborne geophysical surveys (including magnetic and radiometric – eU, eTh, and K). In 2021, the Munsungun-Winterville belt was chosen for an airborne geophysical survey and the survey covered an area of 9,600 km^2. Later in 2021, the geophysical data was examined by Dr. Anjana Shah of the USGS and an abnormally high-eTh spot in the Pennington Mountain area was noticed. Wang carried out an initial two-day study of the site and collected ten samples that later were used for initial whole-rock geochemical and thin-section microscopic, microXRF, and microprobe analyses. A handheld radiation monitor (MAZUR PRM-9000) was used to measure radiation level at each sampling site. Two of the samples (along with other samples of volcanic rocks of the Winterville and Munsungun Lake formations) were sent to ALS Global for whole-rock geochemical analysis. Both samples showed extremely high contents of rare earth elements (REE), Y (yttrium), and other trace elements, such as Nb (niobium) and Zr (zirconium), confirming the existence of the Pennington Mountain REE-Nb-Zr occurrence. Petrographic and geochemical analyses of the Pennington Mountain samples indicated that they are trachyte, an igneous rock crystallized from alkali-rich magmas (i.e., high contents of potassium (K) and sodium (Na)). Trachyte generally occurs as lava flows, but occasionally occurs as shallow intrusive subvolcanic rocks.

Subsequent portable XRF (x-ray fluorescence) analysis of all the samples collected from the East Lobe of the Pennington Mountain trachyte, as well as microXRF and electron microprobe analyses were performed to learn more about the mineralized trachyte, its mineralogical composition and textures, identification of microcrystalline REE-Nb-Zr-bearing minerals, distribution pattern of the elements of interest, and characterization of mineralization (metallogenesis and paragenesis). Since spring 2022 more fieldwork and investigations have been performed to map,

sample, and delineate the extent of the Pennington Mountain trachyte and of the mineralization, including GPS-linked ground-based gamma-ray spectrometric survey of the airborne radiometrically anomalous region to enhance the understanding of the geologic distribution of the radiometric anomalies (Fig. 2). More samples were collected and analyzed for whole-rock geochemistry and microXRF analyses. Participants in field survey and investigations since spring 2022 include Anjana Shah, John Slack, Martin Yates, Robert Marvinney, Amber Whittaker, David Lentz, David Putnam, and Chunzeng Wang, with assistance of two undergraduate students Preston Bass and Liam Daniels.

Figure 2. GPS-linked ground-based gamma-ray spectrometry radiometric survey with Anjana Shah and Preston Bass on June 28, 2022 (a) and with Preston Bass and Liam Daniels on September 9, 2022 (b).

These preliminary efforts resulted in a research paper entitled "*A Recently Discovered Trachyte-hosted Rare Earth Element-Niobium-Zirconium Occurrence in Northern Maine, USA*" (Wang et al., 2023) published in the "express letter" format by the journal Economic Geology, online in November 2022 and in printed form in January 2023. (Please refer to the Economic Geology paper for data and information that are not included in this trip guide.)

Continued efforts have been made to perform geochronological analysis of the Pennington Mountain trachyte and the Winterville Formation at the University of New Brunswick (Canada) ICP-MS Laboratory by Dr. Christopher McFarlane. Two ages were obtained by zircon U-Pb analysis: 462.8 ± 1.4 Ma for the Pennington Mountain trachyte (a non-mineralized trachyte sample) and 459.5 ± 3.7 Ma for the Winterville Formation (a dacite sample from Hedgehog Mountain on Rte-11) in spring 2023.

REGIONAL GEOLOGY AND STRUCTURAL GEOLOGY

The Munsungun-Winterville Belt (MWB) is one of major early Paleozoic lithotectonic belts/terranes in the Northern Appalachians with origins as either peri-Gondwanan or peri-Laurentian fragments. For example, the Miramichi terrane and Weeksboro-Lunksoos Lake Belt (WWLB) are peri-Gondwanan and the Chain Lake Massif peri-Laurentian (Fig.1). The Lobster Mountain belt, Caucomgomoc inlier, and MWB have long been considered as part of the Ordovician Popelogan Arc of the leading edge of the Ganderia (peri-Gondwana). Silurian sedimentary strata, in particular the Silurian Aroostook-Matapedia Belt occur between the Miramichi and WLLB/MWB (Fig. 1).

The Winterville inlier is a northeast-trending tectonic terrane composed of volcanic rocks of the Ordovician Winterville Formation and slate and graywacke of the Ferguson Brook Formation (new) (Fig. 3). Its boundary with sedimentary rocks of the Lower Devonian Seboomook Group and St. Froid Lake Formation (Wang, 2022a, 2022b) is the West Inlet fault (Wang, 2021a), one of the longest faults in northern Maine. The Seboomook Group is the most widespread sedimentary formation in northern and northwestern Maine and a major component of the Connecticut Valley-Gaspe Basin, which is adjacent to Munsungun-Winterville Belt on the northwest. The St. Froid Lake Formation is a recently discovered, post-Acadian (Emsian-early Eifelian age) clastic sequence of red and green beds, widely distributed along the Fish River chain of lakes and in the Ashland area (Wang, 2022a, 2022b). The formation has been significantly displaced vertically by several northeast-striking longitudinal faults and horizontally by several northwest-striking transverse faults. These faults are considered to be Neoacadian in age. The north-northwestern part of the Winterville inlier is overlain unconformably by the Seboomook Group in the Fish River Lake and Island Pond areas as a result of late-stage Salinic orogenesis and by St. Froid Lake sedimentary rocks along the Red River valley and southern Eagle Lake as a result of the Acadian orogeny. The Fish River Lake fault (Wang, 2021a), a southeast-oriented reverse fault, has significantly and vertically displaced the Seboomook and St. Froid Lake formations, producing the most remarkable topographic feature in northern Maine – the Fishe River chain of lakes (including the Red River valley).

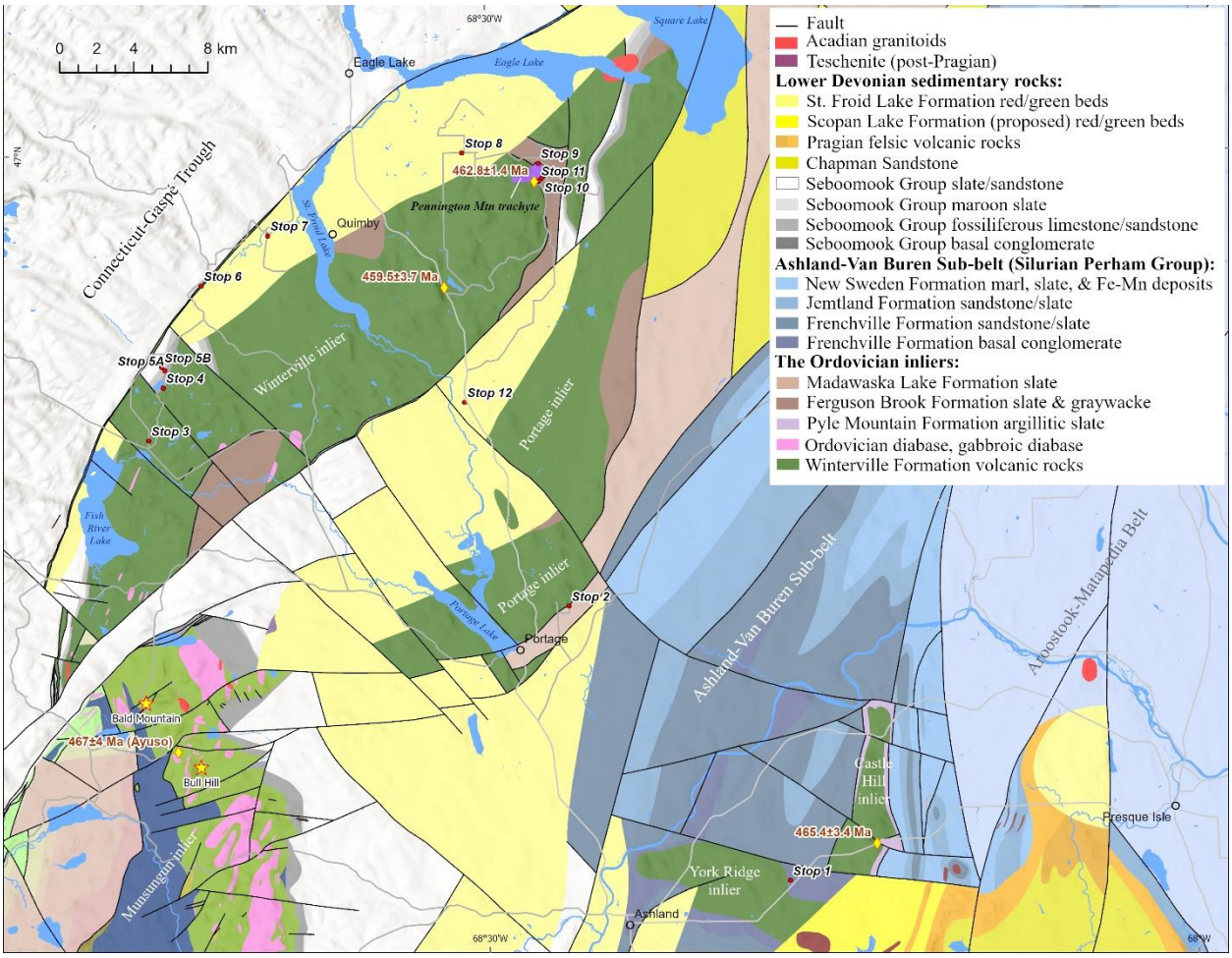

Figure 3. Geologic map of Winterville, Portage, York Ridge, and Castle Hill inliers and vicinity based on recent detailed and reconnaissance mapping, including locations of the stops to be made in this trip and zircon U-Pb ages and sample locations.

In the Pennington Mountain area, the Winterville Formation and Pennington Mountain trachyte are in fault contact with the Ferguson Brook Formation (Wang, 2022a, 2022b). The fault, here referred to as the Pennington Mountain fault, is a low-angle thrust fault with the Winterville volcanic rocks and Pennington Mountain trachyte as the overthrust hanging wall and the Ferguson Brook as the foot wall. Several Acadian faults occur within the northeast-striking Winterville fault block on the northeast side of Pennington Mountain, where they have displaced the unconformable contact between Seboomook sedimentary rocks and Winterville volcanic rocks. Two of these are named Middle Brook and Last Brook faults in this study.

Three smaller Ordovician inliers in the region are the Portage, York Ridge, and Castle Hill inliers. The Portage inlier, closest to the Winterville belt, is also composed of the Winterville and Ferguson Brook formations and used to be considered as part of the Winterville inlier. It is in fault contact with the Winterville inlier on the north side of the Goddard Valley by the West Inlet fault. To the southeast, it is in fault contact with the Upper Ordovician Madawaska Lake Formation along the Clayton Lake fault (Wang, 2021b); and its northwest is mostly unconformably overlain by St. Froid Lake Formation. The York Ridge inlier is unconformably overlain by the Silurian Frenchville Formation as a result of uplift in an early stage of the Salinic orogeny. The Castle Hill inlier is unconformably overlain by the Upper Ordovician Pyle Mountain Formation as a result of Taconic orogeny.

An extensive sequence of Silurian sedimentary rocks, collectively called the Perham Group or Perham Group sequence in this study occurs as a northeast-trending belt between Ashland and Van Buren (named the Ashland-Van Buren subbelt in this study). David Roy's mapping and study of the Silurian formations during 1960–1980 (Roy, 1970, 1976, 1987; Roy and Mencher, 1976) laid a solid foundation for future work. Based on recent and current mapping, the revised Perham Group sequence consists of, from bottom to top, the Frenchville (Boucot et al., 1964), Jemtland

(Roy and Mencher, 1976), and New Sweden (Roy and Mencher, 1976) formations, and the sequence or the sub-belt is in fault contact with the northeast-trending Carys Mills Formation to the southeast; the latter is a major component of the Aroostook-Matapedia Belt.

STRATIGRAPHY OF THE WINTERVILLE INLIER AND VICINITY

Stratified sedimentary and volcanic rocks in the Winterville inlier and vicinity include, from the oldest to the youngest, the Ordovician Winterville, Ferguson Brook, and Madawaska Lake formations, the Silurian Perham Group, and the Devonian Seboomook Group and St. Froid Lake Formation (Fig. 4).

Figure 4. Re-established stratigraphy of the Winterville inlier and vicinity.

Winterville Formation

The Winterville Formation (Boone, 1958, 1970; Mencher, 1963; Horodyski, 1968; Osberg et al., 1985) dominates the northeast-trending Winterville, Portage, York Ridge, and Castle Hill inliers. The formation consists predominantly of basalt with lesser amounts of pyroclastic rocks including volcanic breccia, lapillistone, and tuff, as well as minor rhyolite, dacite, trachyte, and a few subvolcanic diabase sills and stocks. Basalt commonly has vesicular and amygdaloidal textures in which vesicles are often filled by calcite, chlorite, zeolite, and quartz. Pillow basalt is common (Fig. 5). Agglomerate and hyaloclasite are less common. Basalt is aphyric, mostly microcrystalline, and composed predominantly of plagioclase feldspar and augite. Rhyolite and dacite are generally minor in the Winterville Formation, but increase in the Pennington Mountain area, for example, Hedgehog Mountain by Rte-11 is largely made of dacite. Most of the pyroclastic rocks are gray tuff. Tuff is locally foliated and laminated.

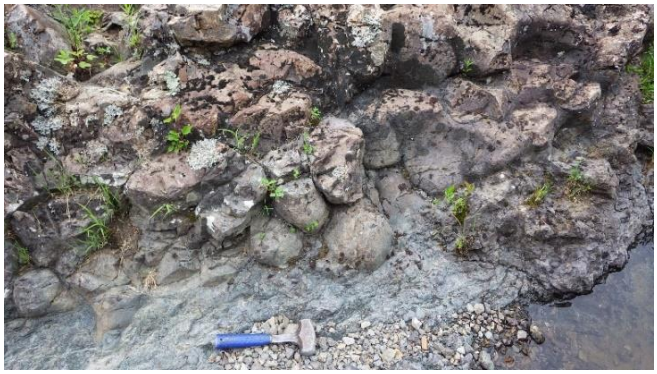

Figure 5. Pillow basalt of Winterville Formation at Fish River Falls by Round Pond.

Geochemically, most of the basalt samples show a transitional and calc-alkaline series (Fig. 6a). Their trace and REE spidergrams and distribution patterns (Fig. 6b, c) show a slope profile, with moderately elevated LREE (light rare earth elements), enriched LILE (large iron lithophile elements), and depleted Ta and Nb (dominantly). Tectonic discrimination diagrams such as La/10-Y/15-Nb/8 show “orogenic domains” or “late to orogenic intra-continental domains” (Fig. 6d). In general, geochemical characteristics of most of the basalt samples in the Winterville and Portage

inliers indicate an ensialic volcanic arc setting. The exceptions are basalt samples collected near the Pennington Mountain trachyte – see below for details.

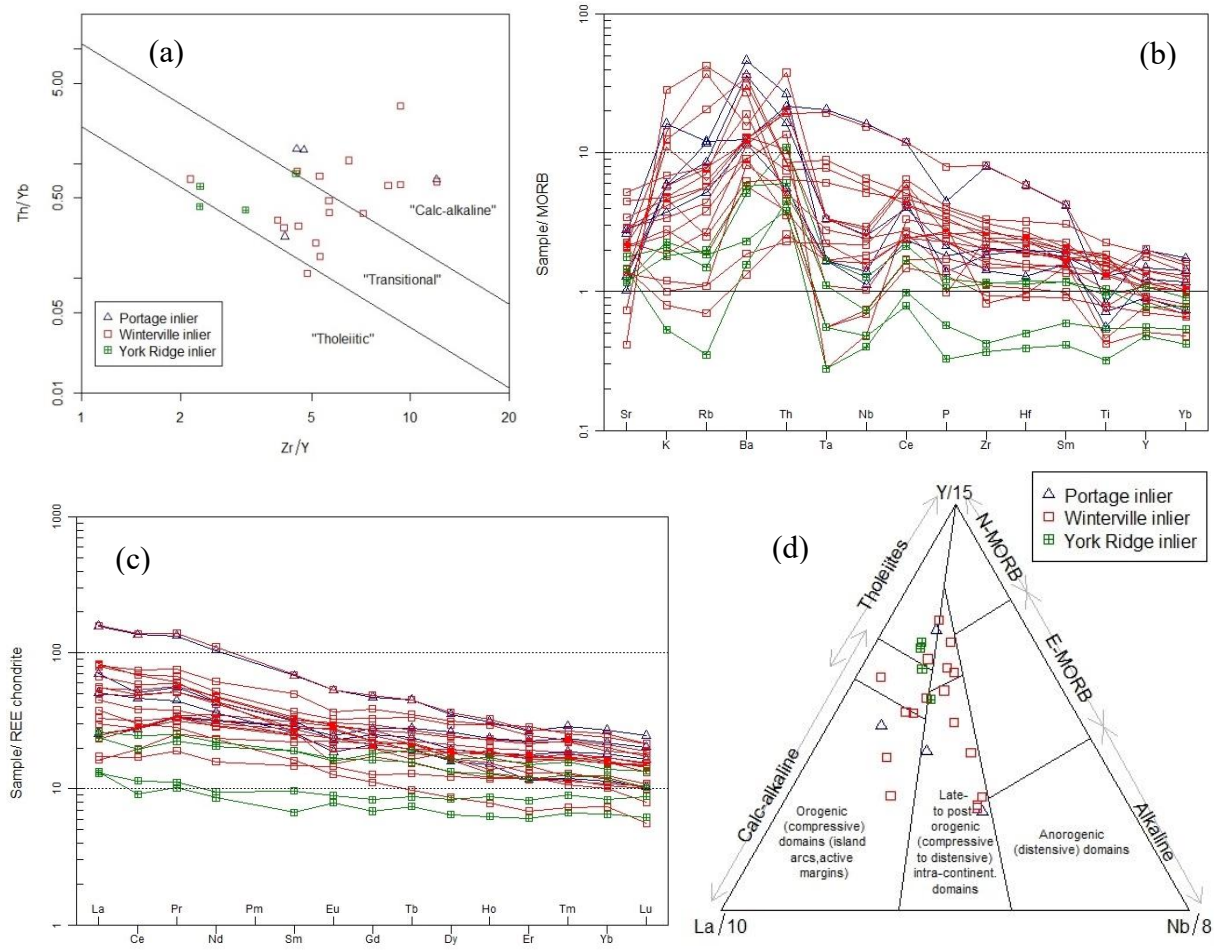

Figure 6. Geochemistry of the Winterville Formation basalt. (a) Zr/Y vs. Th/Yb diagram (Ross and Bedard, 2009); (b) MORB-normalized spider diagram (Pearce, 1983); (c) Chondrite-normalized REE pattern (Nakamura, 1974); (d) La/10–Y/15–Nb/8 tectonic discrimination diagram (Cabanis and Lecolle, 1989).

A Winterville Formation dacite sample collected from the Rte-11 roadcut on the east side of Hedgehog Mountain, was analyzed for zircon U-Pb dating at the University of New Brunswick ICP-MS Laboratory by Dr. Christopher McFarlane. The analysis yielded a $^{206}Pb/^{238}U$ weighted mean age of 459.5±3.7 Ma (MSWD = 0.62, n = 28) and a $^{207}Pb/^{235}U$–$^{206}Pb/^{238}U$ concordia age of 460.7±2.7 Ma (Fig. 7). Both ages are nearly identical and within error range. The results indicate a Middle Ordovician Darriwilian age for the Winterville Formation (more accurately for the Winterville volcanic rocks in the Hedgehog Mountain area). This geochronological work is the first ever performed in the Winterville inlier in northern Maine.

Another zircon U-Pb ICP-MS analysis was recently performed on a Winterville Formation trachyte sample collected from the Castle Hill inlier (at Rte-163 roadcut by Haystack) at Arizona LaserChron Center. It yielded a weighted mean age of 465.4±3.4 Ma (MSWD = 0.22, n =11) (Fig. 2). The discrepancy in ages of the volcanic rocks indicates that the volcanic rocks were emplaced during a span of at least five million years.

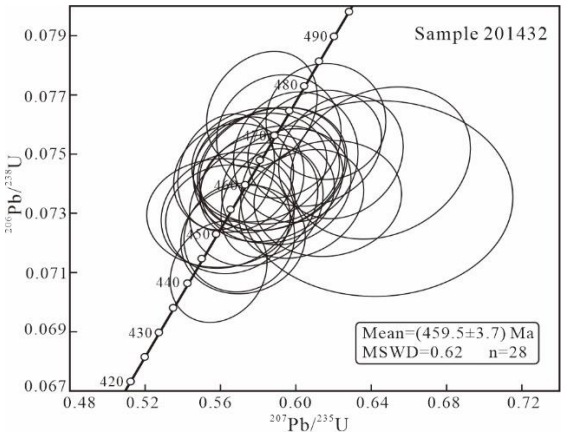

Figure 7. Zircon U-Pb concordia diagram of a dacite sample from Hedgehog Mountain of the Winterville inlier.

Ferguson Brook Formation

The Ferguson Brook Formation (Wang, 2022a, 2022b) forms part of the Winterville and Portage inliers. The formation is predominantly medium to thickly layered dark gray graywacke, dark gray, black pyritic slate, and minor intercalated conglomerate and black cherty siliceous mudstone (Fig. 8a, b). Some graywacke is turbiditic and characterized by horizontal lamination and cross ripples. The conglomerate, either pebble conglomerate or granule conglomerate, is poorly sorted, angular, and polymictic with mostly cherty tuff and basalt clasts that were probably derived from the volcanic rocks of the Winterville Formation. No fossils have been found in the formation. Based on the reported detrital zircon data from a similar formation in the Greenlaw Pond quadrangle in the Munsungun inlier in the southwest (Wang, 2021b), the Ferguson Brook Formation is considered Late Ordovician in age.

Figure 8. Ferguson Brook Formation. (a) Graywacke. (b) Dark gray, rusty slate.

Pyle Mountain Formation

The Pyle Mountain Formation (Roy, 1970, 1987) has been mapped only along the flanks of the Castile Hill inlier where it unconformably overlies the Mid Ordovician volcanic rocks of the inlier. First called "Pyle Mountain Argillite" (Boucot et al., 1964), it consists mostly of brown-weathering (greenish gray in fresh) silty argillaceous mudstone/slate with lesser medium-layered gray sandstone with only minor, intercalated thin-medium limestone, black cherty slate, and conglomerate. Its age was considered to be Ashgillian (Late Ordovician) based on study on fossils (reported by Boucot et al. (1964).

Madawaska Lake Formation

The Madawaska Lake Formation (Roy and Mencher, 1976) is a major sedimentary rock unit along the Fish River chain of lakes; it extends southwest to the Portage area and northeast for about 65 kilometers in Maine and across the St. John River into New Brunswick, Canada. The formation is dominated by interbedded slate and graywacke (Fig. 9a, b), with minor gray or brown quartzose sandstone and siltstone. Generally, the slate and graywacke are pyrite poor

with a little rusty appearance. The formation is in fault contact with several other formations. For example, in the area north of Beaver Brook valley and Portage, it is in fault contact with the Winterville Formation and Perham Group. Based on Roy and Mencher (1976), the Madawaska Lake Formation is possibly Upper Ordovician in age.

Figure 9. Madawaska Lake Formation. (a) Slate. (b) Graywacke.

Perham Group

The Perham Group was initially proposed by Roy and Mancher (1976) and later discontinued but is readapted and redefined in this study. It includes, from bottom to top, the comfortable Frenchville, Jemtland, and New Sweden formations of clastic and carbonate rocks. It is a Silurian series, referred to as the ***Perham Group sequence*** that extends southwestward to the Ashland-Castle Hill area and northeast across St. John River into New Brunswick, Canada. It is fault bounded with the Madawaska Lake Formation to the northwest and with the Carys Mills Formation of the Aroostook-Matapedia Belt to the southeast.

The Frenchville Formation (Boucot et al., 1964) includes a basal conglomerate unit and the rest, the major part of the formation consists of thin to thickly layered greenish or bluish gray quartzose or feldspathic sandstone with lesser gray slate. The basal conglomerate occurs mainly around Ashland, Frenchville, and southwest of Haystack and unconformably overlies the Ordovician York Ridge inlier. The unconformity represents the early stage of Salinic orogeny - equivalent to Salinic A in northern New Brunswick (Wilson and Kamo, 2012) and in Number Nine Mountain area (Wang and Madsen, trip B3). The Jemtland Formation (Roy and Mencher, 1976) is dominantly a well bedded package of thin to medium layered, graptolitic gray calcareous and micaceous siltstone and sandstone with relatively lesser gray and dark gray shale. Lamination is a common sedimentary structure of the formation and in places the formation shows Bouma sequence. A diagnostic feature of the formation is its orange or brownish tan color on weathered surfaces and well-developed leached weathering rind. The Jemtland Formation is known to be rich in *Monograptus* graptolite fossils of early Ludlow age (Berry, 1960, 1964). The New Sweden Formation (Roy and Mencher, 1976) generally consists of two successions, with the lower succession dominated by carbonate and occurring mostly as alternating thin marl (argillaceous limestone) and calcareous sandstone/siltstone/shale and the upper succession by green, maroon/red, or dark tan-colored slates with minor, intercalated thin argillaceous limestone. The green and maroon slate succession hosts manganese ironstone deposits/layers of the northern subdistrict of the Aroostook Manganese District.

Seboomook Group

The Seboomook Group (Perkins, 1925; Pollock, 1987) is the most widespread sedimentary rock formation in northern Maine, in the Connecticut Valley-Gaspé Basin. The Seboomook Group is lithologically divided into four conformable units, from bottom to top, the basal conglomerate, fossiliferous limestone and calcareous sandstone, maroon slate, and turbiditic sandstone and slate units, with the last one dominating the group. The bottom three units are informally called the “Trinity”. The Seboomook Group basal conglomerate unit unconformably overlies the Ordovician inliers and Silurian formations, including the Munsungun and Winterville inliers, as a result of the late stage of the Salinic orogeny - equivalent to Salinic C in northern New Brunswick (Wilson and Kamo, 2012) and in Number Nine Mountain area (Wang and Madsen, trip B3. However, as Figure 3 shows, the Paleozoic terranes in northern Maine have been significantly faulted and displaced by dominantly southwest-striking reverse-thrust faults, mainly during Acadian and Neoacadian orogeneses. In the Pennington Mountain area, the Seboomook Group occurs as part of two fault slivers/blocks (Fig. 3), along the Middle Brook and Last Brook valleys; within the slivers/blocks,

the Seboomook Group basal conglomerate unconformably overlies the volcanic rocks of the Winterville Formation, and contains significant components of basalt pebbles. The fossiliferous limestone and calcareous sandstone unit are rich in various marine invertebrate fossils, including corals, brachiopods, crinoids, stromatoporoids, bryozoan, etc. of the early Devonian (Helderberg) fauna. In the Fish River Lake area, the unconformity between the Seboomook basal conglomerate and the Winterville volcanic rocks remains intact although horizontally offset by several strike-slip faults (Fig. 3).

St. Froid Lake Formation

The St. Froid Lake Formation (Wang, 2022a, 2022b) consists of non-foliated, red, green, greenish gray, reddish-brown, and buff brown sandstone and shale/mudstone beds (Fig. 10a, b). It is distributed mostly along the Fish River chain of lakes and in the Ashland area as displaced fault blocks (Figs. 1 and 3) with a total area of nearly 500 km^2. The formation contains abundant terrestrial plant-fossil fragments of trimerophytes (most likely *Psilophyton* and *Pertica*) (Fig. 10c). All the plant material appears to have been transported and deposited in aqueous terrestrial or coastal settings. The formation was deposited during the Early Devonian Emsian time initially based on invertebrate fossils, particularly on brachiopods of mostly *Leptocoelia flabellites* (Fig. 10d), with a few *beachia* (terebratulid), *Atlanticocoelia,* and Acrospirifer *Hysteriolites sp*. (Wang, 2022a, 2022b). A most recent palynological analysis reported spores of *Ancyrospora kedoae, Ancyrospora sp., Apiculiretusispora brandtii, Apiculiretusispora gaspiensis, Apiculiretusispora minor, Apiculiretusispora plicata, Archaeozonotriletes chulus, Chelinospora sp., Dibolisporites abitibiensis, Dibolisporites wetteldorfensis, Dictyotriletes favosus, Emphanisporites annulatus, Latosporites sp.,* and *Gneudnaspora divellomedia* and confirmed the Emsian-early Eifelian age of the formation.

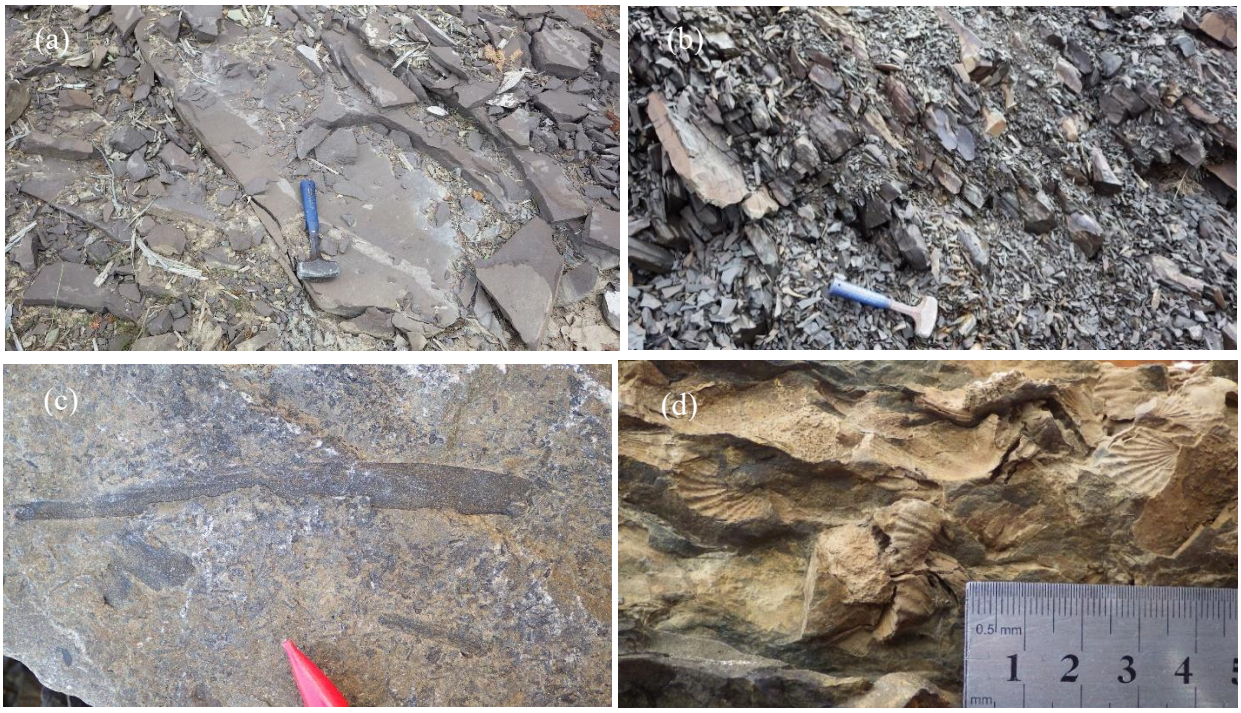

Figure 10. St. Froid Lake Formation. (a) Red sandstone. (b) Green mudstone and sandstone. (c) Fragments of plant fossils of mostly *Psilophyton* and *Pertica*. (d) Molds of brachiopods *Leptocoelia flabellites* and *Hysteriolites sp.*

THE PENNINGTON MOUNTAIN REE-Nb-Zr DEPOSIT

The Pennington Mountain trachyte: petrography, geochemistry, tectonic setting, and age

The Pennington Mountain trachyte occurs as an irregularly shaped stock (Figs. 3 and 11) that is in fault contact with graywacke and black slate of the Ferguson Brook Formation to the east. The fault, named Pennington Mountain Fault in this study is presented as a low-angle thrust fault. The currently delineated trachyte body has a minimum exposed area of 1.129 km^2. The trachyte is divided into the West Lobe and East Lobe (Fig. 11). The West Lobe is not

brecciated, nor mineralized. However, the East Lobe is thoroughly and pervasively brecciated and mineralized. The north-northwest-trending ridge (the no-name ridge referred to in this study) of the East Lobe is entirely and significantly mineralized based on the airborne radiometric survey performed in summer 2021 (Fig. 11; Shah, 2022), the ground radiometric survey performed in fall 2022 (Shah and Wang, 2022), and portable XRF (X-ray fluorescence spectrometer) and whole-rock geochemical analyses performed in 2022 and later in early 2023.

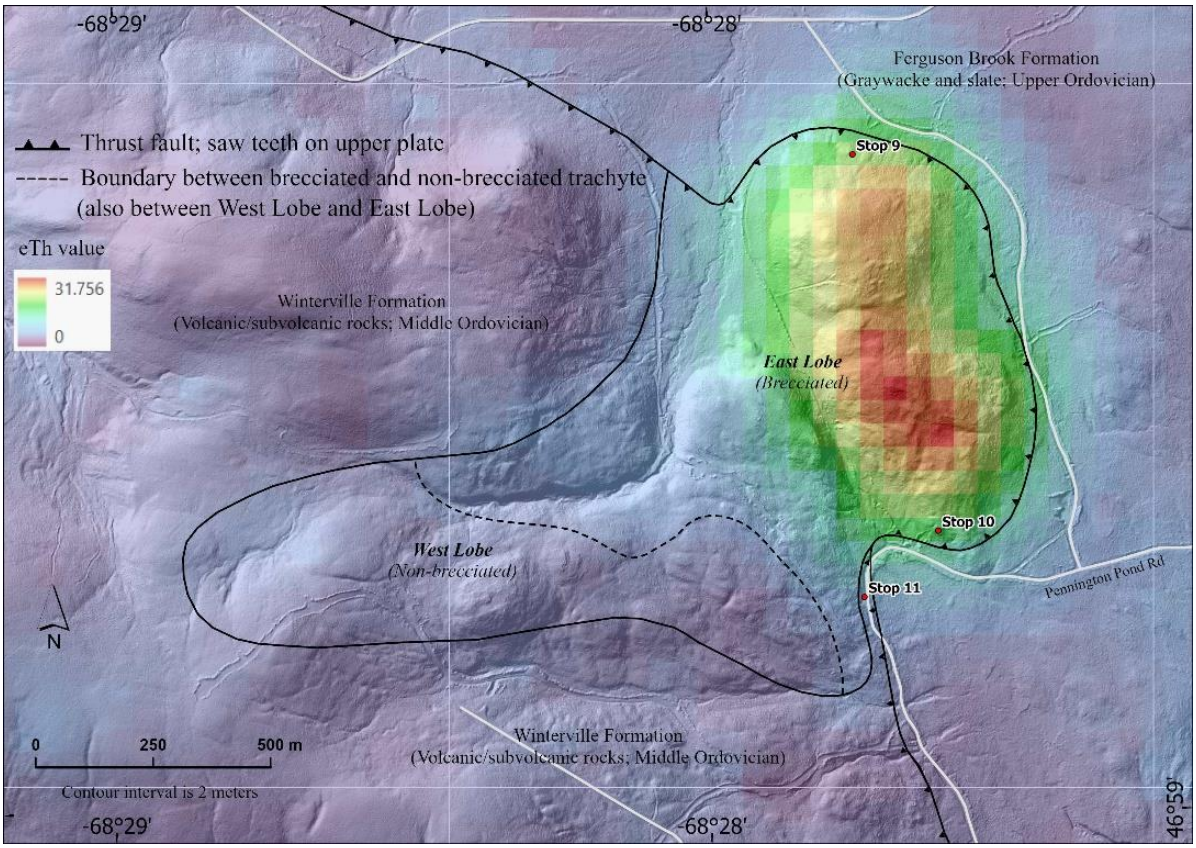

Figure 11. Geologic map of the Pennington Mountain trachyte.

Please note that the definitions for the East Lobe and West Lobe and how they are divided are different from the Economic Geology article (Wang et al., 2023). The redefinition here uses brecciation as the criterion: the East Lobe is brecciated, whereas the West Lobe is not. Wherever it is brecciated, it is also mineralized with REE-Nb-Zr mineralization, either significantly like the entire no-name ridge or weakly like the northwestern and western part of the East Lobe (or the rest of the East Lobe). The non-brecciated and non-mineralized West Lobe trachyte accounts for about one third of the Pennington Mountain trachyte body in terms of its surface exposure. Generally, the trachyte (including the mineralized component) is homogenously massive and microcrystalline. Part of the trachyte in the West Lobe is vesicular and amygdaloidal with dominating quartz-filled elongated amygdales (Fig. 12a, b), indicating that even if the trachyte is considered intrusive, it is very shallow and subvolcanic. Microscopically, the trachyte has a typical trachytic texture (Fig. 12b, c). Most of the trachyte also has a micro-porphyritic texture with euhedral perthite phenocrysts set in a microcrystalline matrix composed predominantly of potassium feldspar and subordinate albite (Fig. 11c, d). In general, alkali feldspar (perthite and some albite) accounts for about 95% of the trachyte, with the rest being ferromagnesian silicates (hornblende and biotite but now mostly altered into chlorite and iron oxides) and quartz.

Eighteen samples were collected from the trachyte body and analyzed for whole-rock geochemistry. Nearly all of them plot in the trachyte-trachydacite field in the TAS diagram (Fig. 13a) and in the calc-alkaline field in the Zr/Y vs. Th/Yb diagram (Fig. 13b). The MORB-normalized spider diagram (Fig. 13c) shows significant enrichment of U, Th, Nb, Ta, Zr, Hf, Ba, Rb, and Y, in particular in the strongly mineralized trachyte. The chondrite-normalized REE distribution patterns show slightly higher LREE than HREE with a significant negative Eu anomaly for most of the samples (Fig. 13d), which is typical for alkaline-peralkaline igneous rocks. Eu/Eu* values range from 0.139 to 0.626, but are mostly less than 0.2.

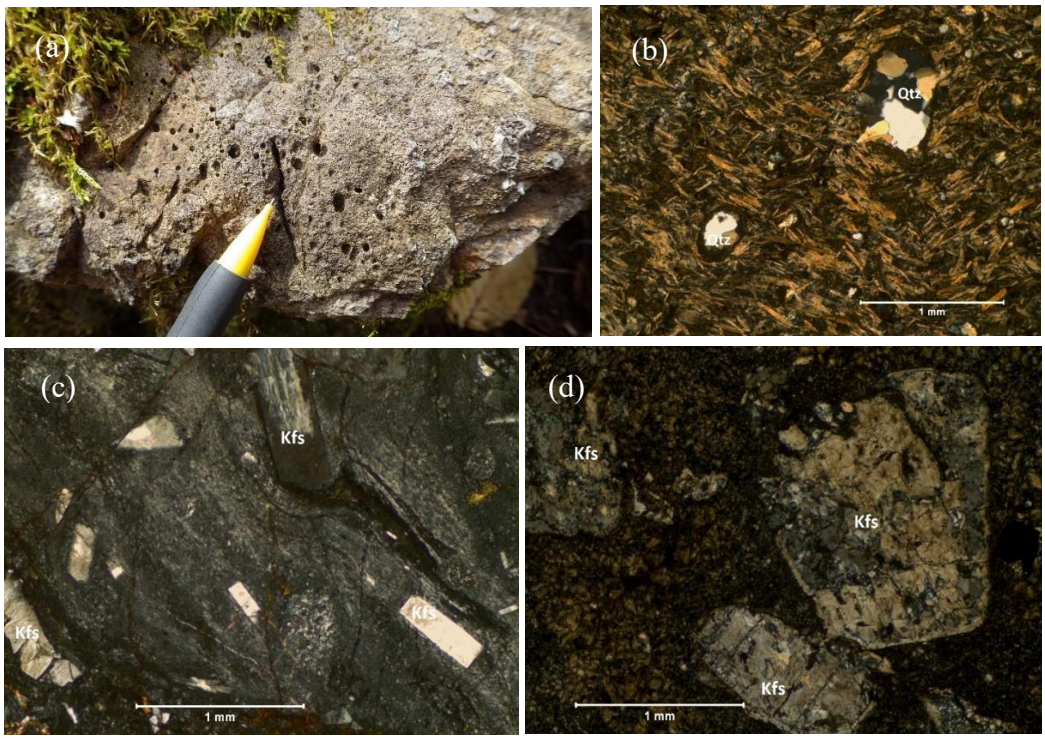

Figure 12. The Pennngton Mountain trachyte. (a) Trachye with vesicular texture. (b) Trachytic texture and quartz amygdales. (c) Trachytic and porphyritic textures with K-spar phenocrysts. (d) K-spar phenocrysts. (b), (c), and (d) under cross polarizing light. Kfs – potassium feldspar; Qtz – quartz.

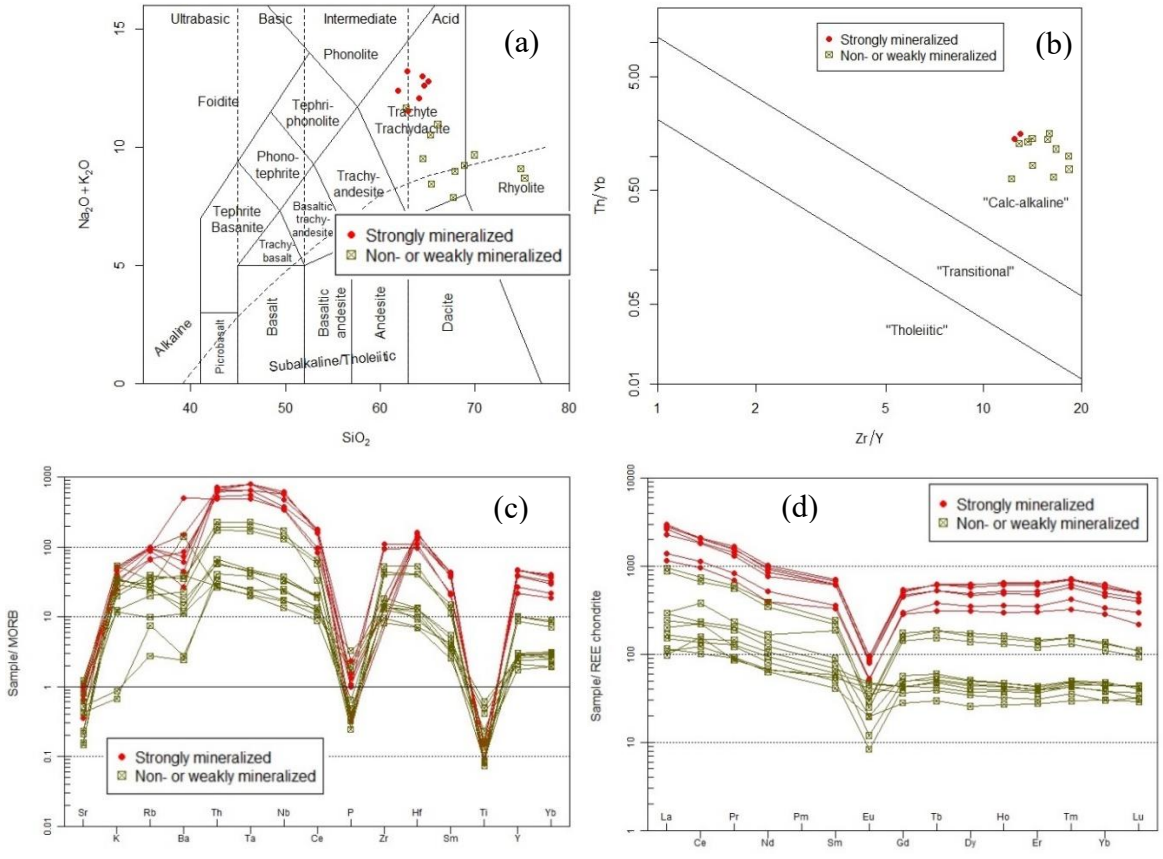

Figure 13. (a) TAS (SiO_2 vs. Na_2O+K_2O) classification diagram (LeBas et al., 1986). (b) Zr/Y vs. Th/Yb classification diagram (Ross and Bedard, 2009). (c) MORB-normalized spider diagram (Pearce, 1983). (d) Chondrite-normalized REE distribution pattern (Nakamura, 1974).

On Whalen's (1987) granitoid discrimination diagrams (Fig. 14), all the non- and weakly-mineralized trachyte samples plot in the A-type granitoid field, indicating that the Pennington Mountain trachyte was emplaced in an anorogenic setting. In the Y–Nb–Ce and Y–Nb–3GA ternary diagrams used for classification of A-type granitoids into A1 and A2 (Eby, 1992), the trachyte samples plot within or next to the A1-type field (Fig. 15). A1 type is generally related to OIB (ocean island basalt)-type enriched mantle source of anorogenic setting.

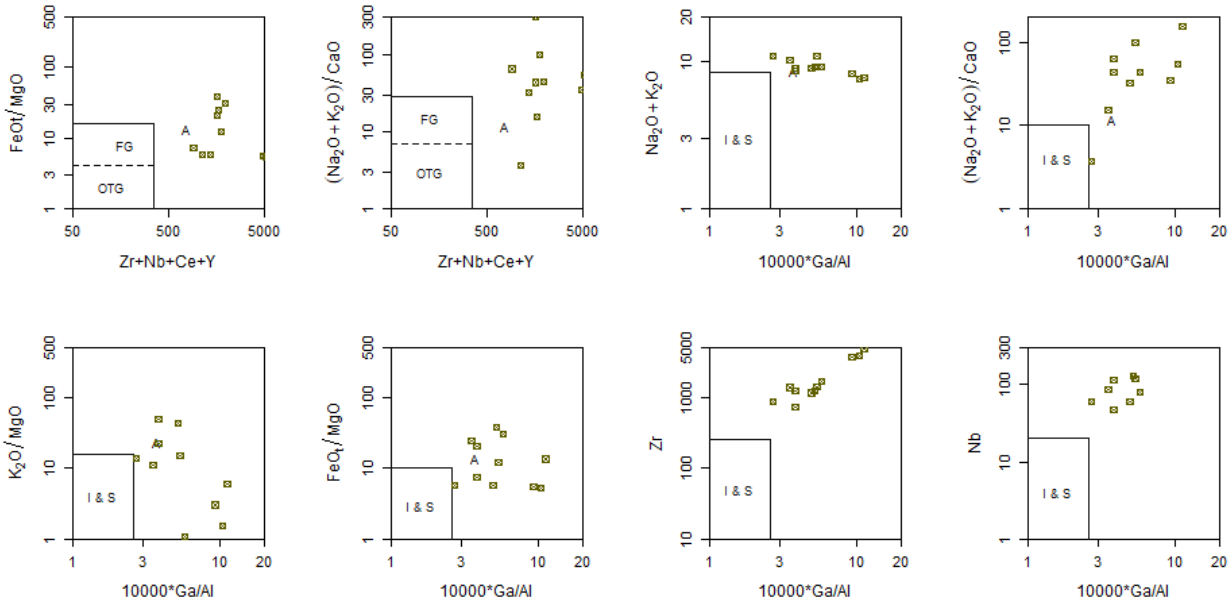

Figure 14. Granitoid discriminations diagrams of all kinds based on some discriminative major, trace, and rare earth elements (Whalen, et al., 1987). A – anorogenic. FG – fractionated I-type granitoids. I – product from an igneous or intracrustal source. OTG – unfractionated M-, I- and **S**-type. S – product of anatexis of metasedimentary of supracrustal protoliths.

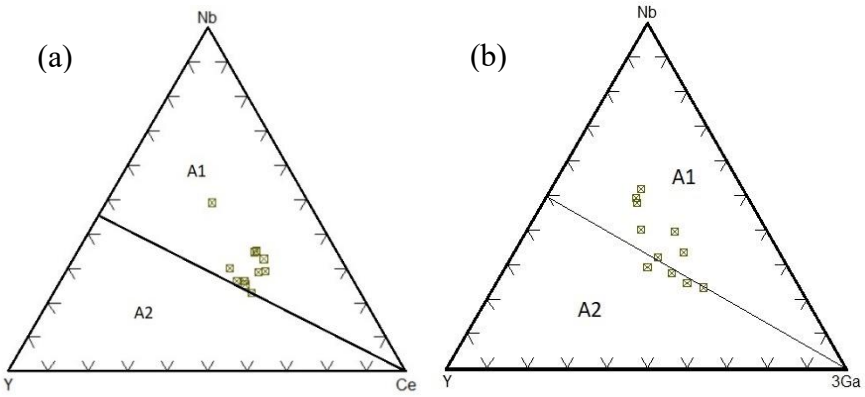

Figure 15. A1/A2 discrimination diagrams (Eby,1992). (a) Nb-Y-Ce; (b) Nb-Y-3 * Ga.

All the samples plot in the alkaline "anorogenic domains" (except one sample in the "late- to post-orogenic intra-continent domains") on the La/10–Y/15–Nb/8 diagram (Fig. 16a; Cabanis and Lecolle, 1989). On the Nb/Yb vs. Th/Yb diagram (Fig. 16b; Pearce, 2008), all the samples plot in the MORB-OIB array. In summary, based on geochemical characteristics and tectonic discriminations, the Pennington Mountain trachyte was emplaced in a non-orogenic setting.

Being the major component of the Winterville inlier, the Winterville Formation, however, is composed predominantly of orogenic volcanic rocks produced in an ensialic volcanic arc setting.

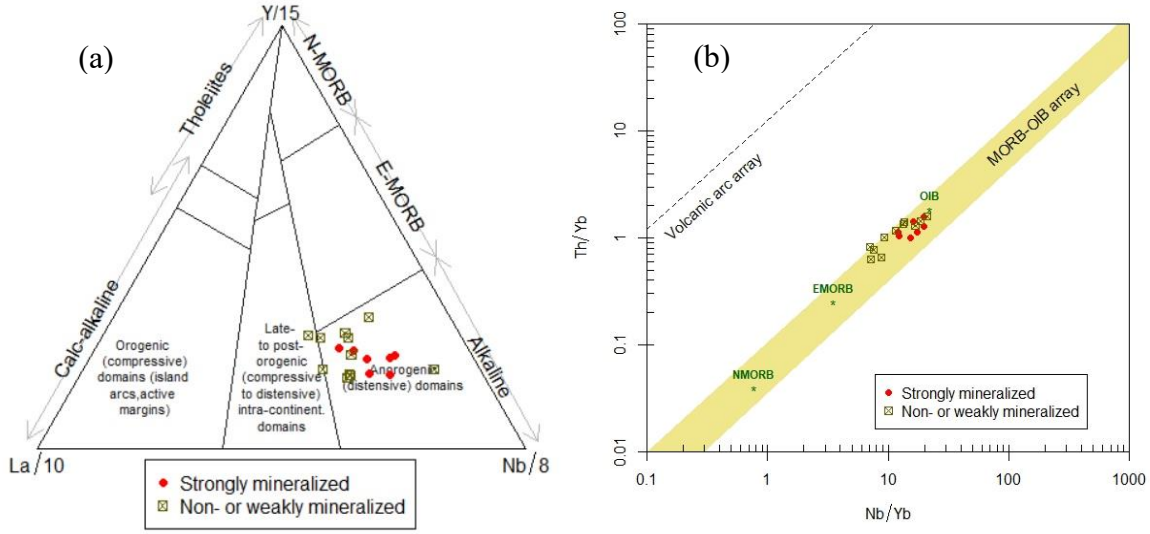

Figure 16. Tectonic setting discrimination diagrams: (a) La/10–Y/15–Nb/8 diagram (Cabanis and Lecolle, 1989). (b) Nb/Yb vs. Th/Yb diagram (Pearce, 2008) of the strongly mineralized and non- to weakly-mineralized trachyte. See the text for explanation. MORB – middle ocean ridge basalt; NMORB – normal MORB; EMORB – enriched MORB; OIB – ocean island basalt.

A non-mineralized trachyte collected from the West Lobe yielded nearly 40 igneous zircon crystals. On the Cl (cathodoluminescence) image (Fig. 17a), most of the zircon crystals are euhedral or sub-euhedral and prismatic. The zircon grains were analyzed by LA-ICP-MS at the ICP-MS Laboratory of the University of New Brunswick by Dr. Christopher McFarlane in spring 2023. Figure 17b shows the $^{207}Pb/^{235}U$ – $^{206}Pb/^{238}U$ concordia diagram with a U-Pb concordia age of 462.8±1.4 Ma, which is same as the weighted mean age from 28 zircon. This age is the emplacement age of the Pennington Mountain trachyte, also considered as the age of the REE-Nb-Zr mineralization event. It is within the error range with the age of the dacite (460.7±2.7 Ma) of the Winterville Formation.

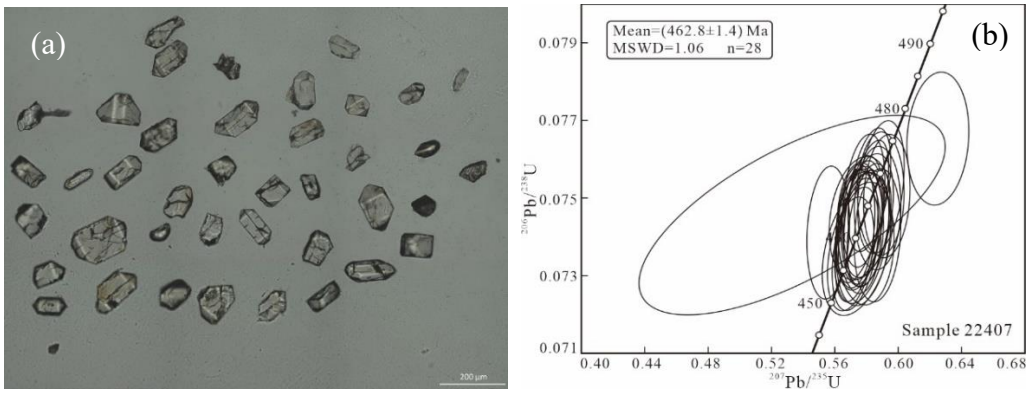

Figure 17. Zircon U-Pb dating of the Pennington Mountain trachyte. (a) CL image showing mostly euhedral-subhedral zircon crystals of igneous origin. (b) Concordia diagram and the weighted mean age of 28 analyses.

The Pennington Mountain REE-Nb-Zr deposit: texture, mineralogy, ore geochemistry, and metallogenesis

The East Lobe is characterized entirely by micro-breccia with pervasive fragmental textures (Fig. 18), and it is also entirely mineralized. Wherever it is fragmented, it is mineralized, although mineralization can be weak compared to the strongest mineralization along the entire no-name ridge. For the fragmented trachyte of the East Lobe, for both

strongly and weakly mineralized, most fragments range in size from 0.1 to at least 1 cm, with only a very small percentage up to 20 cm. Fresh, broken surfaces are generally in dark gray color (Fig. 18a). Some are pinkish brown (Fig. 18b) due to potassium alteration. Photomicrographs (e.g., Fig. 17c, d) show all kinds of fragmented trachyte and micro-porphyritic trachyte. Generally, pyrite is scarce in the trachyte. Only locally some mineralized trachyte may contain some pyrite.

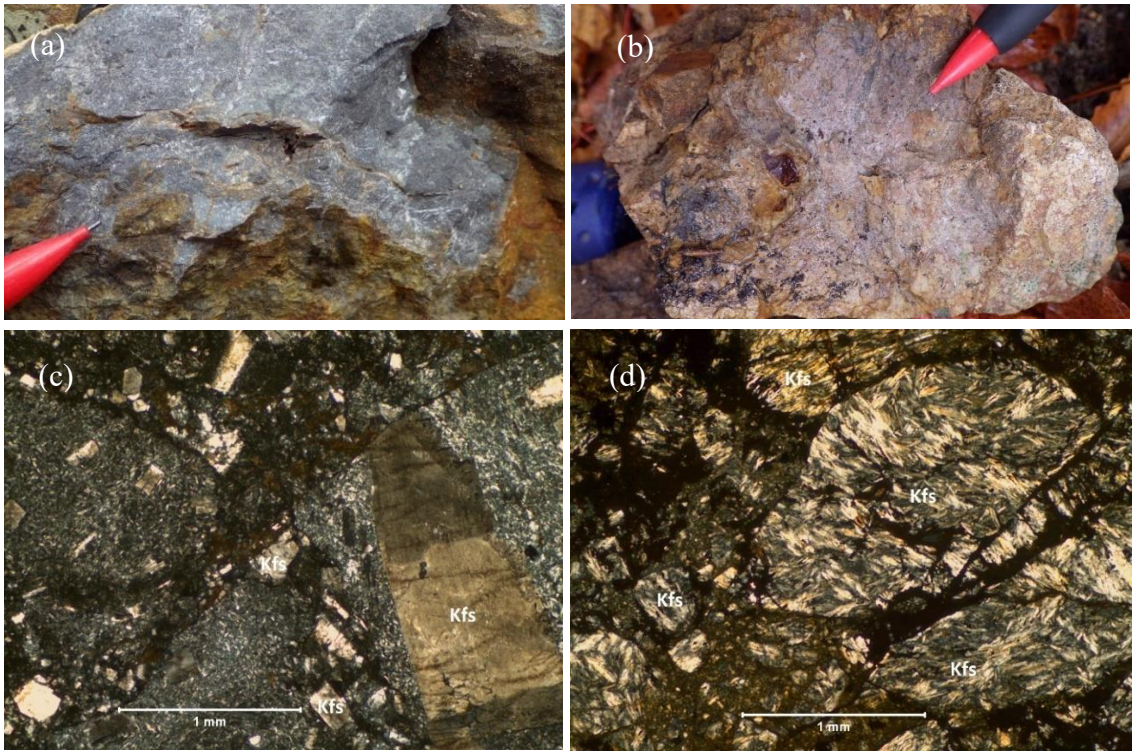

Figure 18. Fragmental and mineralized trachyte. (a) Fresh surfaces generally showing dark gray color and fragmental texture. (b) Some trachyte showing darker pinkish brown color due to alteration of potassium feldspar. (c) and (d) Photomicgraphs showing perthitic K-feldspar phenocrysts and mineralized groundmass (seams) of the fragments (in dark color). Cross-polarized light. Kfs – potassium feldspar.

Micro-XRF (or MicroXRF-EDS, µXRF-EDS) elemental scans of entire polished thin sections were performed at the University of New Brunswick by Dr. David Lentz and Fazilat Yousefi. The µXRF-EDS scans show distinctive fragmentation textures and element enrichments for La+Ce, Zr, and Nb (Fig. 19). High contents of La+Ce (Fig. 19a, b), Zr (Fig. 19c), and Nb (Fig. 19d) are mainly confined to the groundmass of the micro-breccia, with the fragments having only minor enrichments of these metals in veinlets and disseminations.

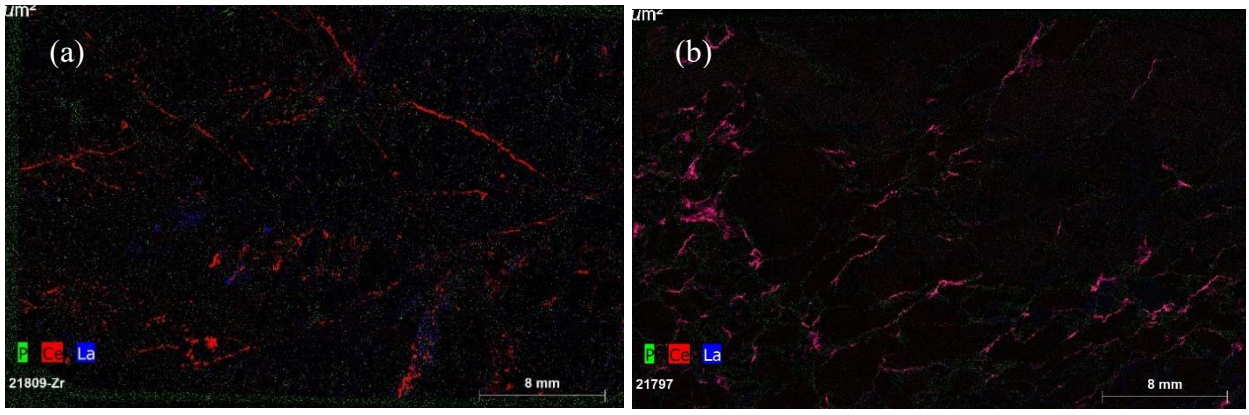

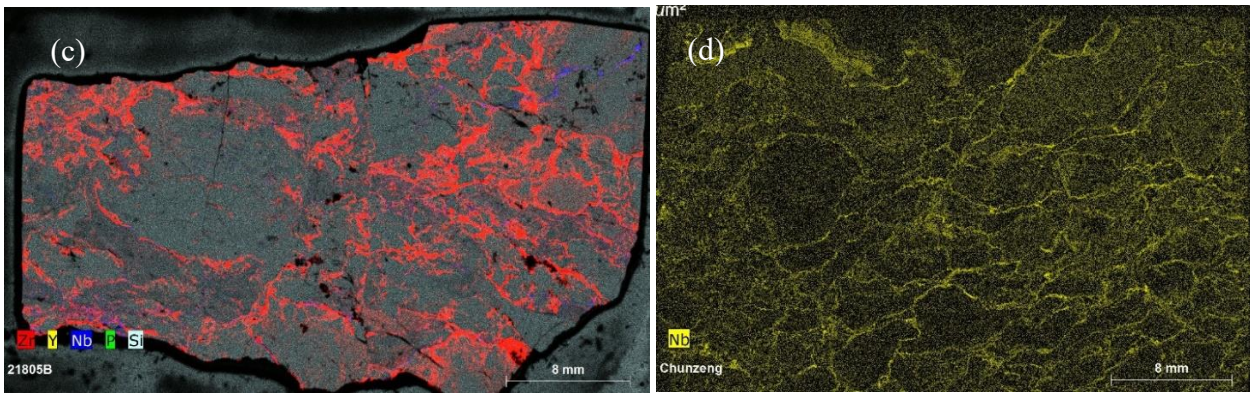

Figure 19. μXRF-EDS images of the selected elements Ce and/or La (a, b), Zr (c), and Nb (d). The images show extremely fine-grained REE-Nb-Zr-bearing minerals occurring mostly in seams, fractures, and groundmass of the fragmental trachyte.

Detailed observations and analysis of polished thin sections for mineral identification, in particular for identification of the ore-bearing minerals, were performed at the University of Maine Microprobe Laboratory by Drs. Martin Yates and John Slack (with Chunzeng Wang attending), by using EDS and WDS of an electron microprobe. Based on the microprobe analysis, abundant minerals in the groundmass of the trachyte micro-breccia are zirconium silicates and monazite (Fig. 20). Other REE- and Nb-bearing minerals include: bastnäsite, euxenite, and volumbite. Betafite and ilmenorutile are sparse to rare.

Field observations, petrographic microscopic, microXRF, and electron microprobe analyses (Fig. 20), as well as whole-rock geochemical data demonstrate that: (1) The East Lobe of the trachyte body is entirely brecciated or shattered (fragmented), and the trachyte fragments are generally less than one centimeter in diameter; (2) The fragmented East Lobe is entirely enriched with anomalously high REE+Y and trace elements, such as Nb and Zr, in particular the entire no-name ridge; (3) REE+Y, Nb, and Zr-bearing minerals (e.g., zirconium silicates, monazite, bastnäsite, and columbite) occur dominantly in the groundmass of the trachyte fragments as seams and veins, with only some (e.g., monazite) disseminated within the trachyte fragments. The significant brecciation or fragmentation was thus the precursor of the REE+Nb-Zr mineralization. Wherever it is brecciated/fragmented, it is mineralized. The metallogenesis of the trachyte with anomalously high enrichment of REE+Y and trace elements Nb and Zr must be related to the brecciation/fragmentation. (*Note: Because all the samples analyzed for this project were collected from the surface of the trachyte body, the word "entirely" or "entire" refer to the surface of the trachyte body and the no-name ridge.*)

The cause of the fragmentation remains to be fully understood. It is likely due to a near-surface explosion or crypto-explosion during emplacement of the trachyte magma. Small fragments are indicative of powerful crypto-explosion due to extremely high pressure during emplacement. As observed petrographically, the catastrophic fragmentation took place after the trachyte magma started to cool and crystalize because the alkali feldspar laths are broken or truncated by the fractures (Fig. 18c, d). The fractures provided space for precipitation and crystallization of the ore-bearing minerals (Fig. 20). As for the fragmentation process, considering the size of the fragments being mostly less than one centimeter in diameter and the huge volume of the fragmental East Lobe, the explosion that caused the fragmentation must be extremely catastrophic. Considering the fragmental East Lobe remains part of the entire trachyte as an integrated igneous body without capturing xenoliths of any country rocks, such as basalt, tuff, and rhyolite, the explosion must be strictly confined in the trachyte or localized in a closed system. The explosion or fragmentation produced a pervasive porous and permeable system of the trachyte, which could favor and facilitate penetrative infiltration and precipitation of REE+Y, Nb, and Zr-bearing minerals from REE+Y and Nb-Zr-rich fluids or solutions.

The fragmental trachyte could be caused by pressure-quenched, highly explosive subvolcanic event within a conduit or around a conduit as a result of degassing felsic magmas; in this case the fragmental trachyte can be formed as a tuffisite, a type of intrusive breccia, producing a giant trachytic tuffisite at Pennington Mountain. The volcanic-induced subsurface fragmentation could be subsequently followed or accompanied by precipitation of the REE+Y, Nb, and Zr-bearing minerals in the groundmass of the fragments and sintering. Therefore, the mineralization event could be considered as syn-volcanic.

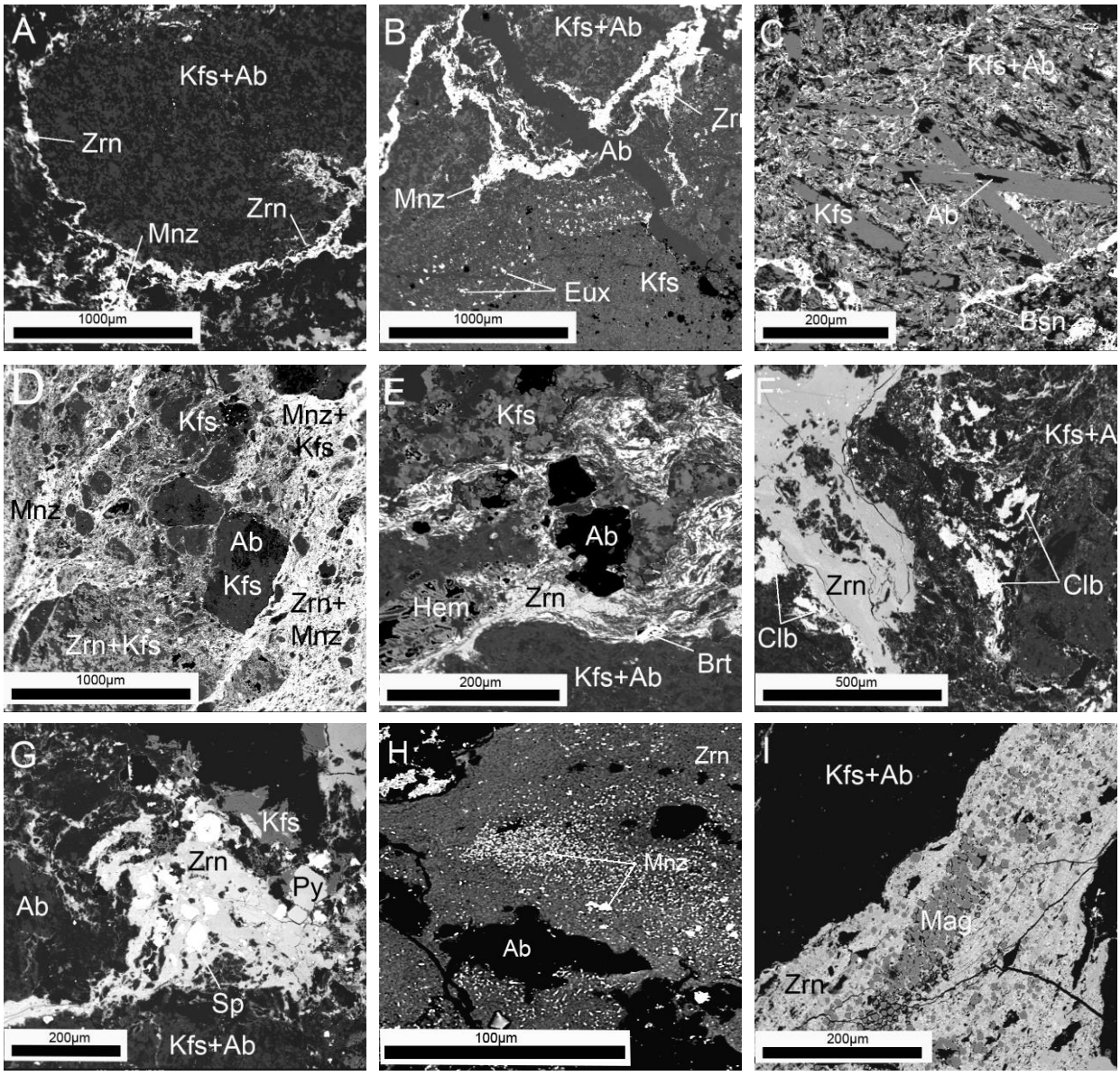

Figure 20. Backscattered electron images showing representative textures and minerals in the brecciated/fragmented, mineralized, and altered trachyte of the East Lobe. (A) A fragment of trachyte made of K-feldspar and albite is surrounded by a groundmass of zirconium silicates and minor monazite. (B) An albite vein truncates seams of zirconium silicates and monazite and a belt of disseminated euxenite. (C) Euhedral K-feldspar phenocrysts are partly replaced by albite and cut by bastnäsite veinlet. (D) Irregular network of seams and veinlets of zirconium silicates and monazite. (E) Seams of zirconium silicates with barite and secondary hematite. (F) Groundmass made of zirconium silicates and bright columbite. (G) Groundmass made of zirconium silicates intergrown with sphalerite; pyrite is secondary. (H) Disseminated monazite. (I) Aggregate of secondary euhedral magnetite crystals in zirconium silicate groundmass or seam. Abbreviations: Ab – albite; Brt – barite; Bsn – bastnäsite; Clb – columbite; Eux – euxenite; Hem – hematite; Kfs – K-feldspar; Mnz – monazite; Py – pyrite; Sp – sphalerite; Zrn – zircon or zirconium silicates.

Seven samples were collected from the strongly mineralized, no-name ridge of the East Lobe and six from the weakly mineralized western part of the East Lobe for whole-rock major, trace, and rare earth elemental analysis. The whole-rock geochemistry clearly demonstrates significantly enriched REE, Nb, and Zr in the brecciated East Lobe, in

particular the entire no-name ridge, where La, Ce, Pr, Dy, Er, Nb, Y, and Zr are respectively 16, 11.4, 10.8, 12.7, 14.2, 22, 16, and 10.5 times higher than the non-mineralized West Lobe.

Trace elements with the highest concentrations in the strongly mineralized East Lobe along the no-name ridge (seven samples in total) are Zr (ranging between 8410 ppm or 0.841wt.% and 13860 ppm or 1.386wt.% with an average of 11,766 ppm or 1.1766 wt.%) and Nb (ranging between 1200 ppm or 0.12 wt.% to 2160 ppm or 0.216 wt.% with an average of 1,656 ppm or 0.1656 wt.%). Both Zr and Nb contribute to the formation of the Pennington Mountain REE-Zr-Nb deposit.

Among LREEs in the strongly mineralized East Lobe along the no-name ridge, the average content of Ce is 1,479 ppm (824 – 1815 ppm), La is 763 ppm (383 – 981 ppm), and Nd is 489 ppm (252 – 640 ppm). Dy and Er are the most abundant HREEs on average, 167 ppm (106 – 213 ppm) and 114 ppm (68 – 147 ppm), respectively. The average Y content is 1,140 ppm, ranging from 649 ppm to 1415 ppm. Total REE+Y oxides average 5,613 ppm or 0.5613 wt.%.

Paragenesis of the Pennington Mountain trachyte REE-Nb-Zr mineralization: (1) Significant subsurface fragmentation of the highly pressurized trachytic magma produced trachytic micro-breccia or trachytic tuffisite, as a syn-volcanic event. (2) Immediate and rapid pervasive crystallization of REE-Nb-Zr-bearing minerals and other related minerals. This was the major stage of REE-Nb-Zr mineralization. (3) Filling of later, minor cross-cutting fractures by albite, bastnäsite, or barite. This stage was insignificant.

The decreased SiO_2 content from average 66.18% of the non-mineralized to average 59.37% of the strongly mineralized trachyte, rules out any post-emplacement silica-rich hydrothermal activity, for example, silicification, as observed through petrographic, and EDS and WDS electron microprobe analyses. CaO shows an apparent decrease from an average of 0.73% of the non-mineralized to an average of 0.09% of the mineralized trachyte, which rules out carbonation alteration. As a matter of fact, no calcite ($CaCO_3$) has been observed in the trachyte (except calcite amygdales in the non-mineralized trachyte), nor apatite ($Ca_5[PO_4]3(OH,F,Cl)$).

ACKNOWLEDGEMENTS

This trip guide is based on my recent and current USGS and MGS STATEMAP projects and on the Pennington Mountain collaborative project on the REE-Nb-Zr deposit. Dr. Gary Boone provided encouragement, guidance, and essential advice. Dr. Robert Marvinney has played a critical leadership role for the northern Maine projects since 2016. Anjana Shah, John Slack, David Lentz, Martin Yates, Amber Whittaker, Christopher McFarlane, and David Putnam have made significant contributions to the discovery and study of the Pennington Mountain trachyte and the REE-Nb-Zr deposit. Drs. Robert Gastaldo, Ian Glasspool, and Patricia Gensel help with identification of plant fossils and interpretation of the sedimentary facies of the St. Froid Lake Formation. Drs. Carlton Brett and Alex Bartholamew help with the identification of invertebrate fossils. Dr. Gil Machado helps with palynological analysis. Fieldwork for the Winterville inlier and Pennington Mountain projects has been assisted by UMPI students Eric Bradley (2020), Jesse Federico and Miranda Washinawatok (2021), Preston Bass and Liam Daniels (2022). I am always grateful to Amanda Barker for leading the early trips to North Maine Woods. Access and permissions granted by North Maine Woods Inc, Irving Woodlands, and Seven Islands are much appreciated.

ROAD LOG

Assembly time and location: Meet at the parking lot next to the soccer field/tennis court on UMPI campus. The departure time is 7:00 am ET. Other people may meet the group at Ashland One Stop at 7:30 am ET. Regular cars without sturdy tires are not recommended for the trip. Car-pooling is encouraged and appreciated. Bring whatever you plan to eat or drink. Wear warm clothes. Most stops are next to roads with only a couple require short and light hiking. While driving in the woods, pay attention to logging trucks. They have absolute right of way.

Cumulative milage	**Description**
0.0	Start logging from UMPI south entrance; make left turn to Main St (Rte-1).
0.7	Left turn to State St. after two traffic lights.
0.9	Left turn to Rte-163 toward Mapleton/Ashland at the five-street intersection. Keep on Rte-163.
15.0	Right turn to a logging road.
15.1	Stop by the borrow pit on the right side of the road.

Stop 1. Basal conglomerate of the Frenchville Formation and Salinic A unconformity: (554484, 5166185) This recently opened borrow pit exposes the basal conglomerate of the Silurian Frenchville Formation (Fig. 21). The conglomerate occurs as thick and massive beds with intercalated coarse lithic sandstone and mudstone layers. It is

poorly sorted, polymictic, and matrix supported. Most of the clasts at this site are vesicular basalts. The conglomerate contains fragments of marine invertebrate fossils of brachiopods, *favosites*, rugose corals, etc. The conglomerate lies unconformably on top of the basalt of the Ordovician Winterville formation around the York Ridge inlier (Fig. 2). The west side of the logging road is supposed to be the basalt if there were any outcrops. The unconformity represents the early stage of the Salinic orogeny, called Salinic A in northern New Brunswick (Wilson and Kamo, 2012) and in northern Maine in this study.

Figure 21. The borrow pit at Stop 1 shows thickly bedded conglomerate and intercalated sandstone and mudstone of the basal conglomerate unit of the Silurian Frenchville Formation.

Turn around and back to Rte-163

15.3 Right turn to Rte-163 toward Ashland.
21.4 Stop by ***Ashland One Stop*** parking lot to pick up more people. 10 minutes for gas, coffee, restroom, etc.
Turn either left or right onto Rte-11 toward Eagle Lake/Fort Kent.

21.7 Left turn and keep on Rte-11.
22.5 Right turn and keep on Rte-11 after the Aroostook River bridge.
29.9 Right turn to Beaver Brook Rd (active dirt logging road).
32.2 Left turn to a narrow dirt logging road (the first left turn on Beaver Brook Rd).
34.0 Right turn to another old logging road.
34.6 Stop by the borrow pit.

Stop 2. Reverse-thrust fault between Winterville basalt and Madawaska Lake slate: (542521, 5180973) This borrow pit shows excellent exposure of the Clayton Lake fault, one of the major faults in the northern Maine imbricate fault system. The basalt and slate in the fault are strongly brecciated. The fault is a southeast-directed reverse-thrust fault with the basalt of the Winterville Formation thrown over the slate and graywacke of the Madawaska Lake Formation (Fig. 22). The latter occurs as a fault sliver sandwiched between the Clayton Lake and Greenlaw Pond faults. Both faults are post-Acadian and likely Neoacadian.

Figure 22. Fault contact between Winterville basalt (upper left, rusty basalt) and Madawaska Lake slate (lower right, dark gray slate) at Stop 2. Viewer facing north. Eric Bagley (field assistant 2020) on the hanging wall basalt.

Turn around.
35.3 Left turn.
37.0 Right turn to Beaver Brook Rd at the end of the road.

39.4 Right turn to Rte-11 at the end of the road.
42.2 Left turn to West Rd (you are now downtown Portage Lake; you may see the lake on your right side.)
43.2 Left turn to Rocky Brook Rd (a major dirt logging road in this region. Watch for logging trucks).
47.5 ***Fish River gate***. Slow down, stop, and say hi to the gate staff. You are now in the North Maine Woods.
49.3 Right turn to Hewes Brook Rd at the big fork.
54.5 Left turn to Jacque Ouellet Rd at the big fork.
60.8 Right turn to Pinnacle Rd, right after passing the 6-mile sign.
61.1 Stop for pillow basalt.

Stop 3. Pillow basalt of the Winterville Formation: (519822, 5189868) This recent roadcut shows excellent pillow basalt of the Mid Ordovician Winterville Formation (Fig 23). Pillow basalt is a common feature in the formation. Another site with excellent pillow basalt is the Fish River Falls located southeast of Round Pond with access from both sides of the river; it is not far from Stop 3. Pillows form in a subaqueous environment, in particular when the eruption rate is low. What happens is the outer surface of a lobe would be quenched rapidly by water, but it is still hot and fluid inside the lobe and the lobe continues to inflate as lava continues to be supplied so that it forms a bulging, pillow-like lobe. The lobe then breaks off and new pillow-like lobes keep forming as the flow advances. Pillows commonly have a spherical or bulbous shape, generally show convex (rounded) upper surface and a keel projecting downward. The convex up surface and the keel help tell the top or bottom of a pillow. What is the top of the pillows at this stop? Pillows generally also have a chill margin and radial vesicles as shown at this stop (Fig.23b). Interstitial aragonite is common at this stop as well.

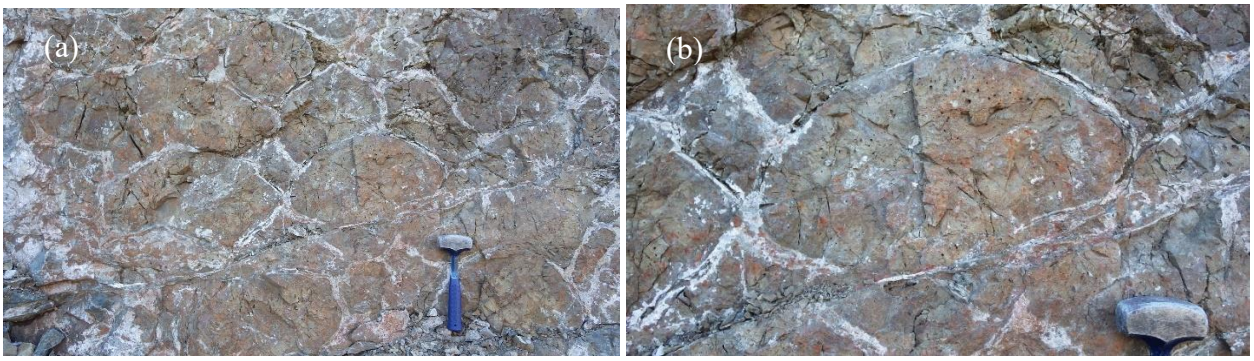

Figure 23. Pillow basalt of the Mid Ordovician Winterville Formation at Stop 3.

Continue on Pinnacle Rd.
64.6 Right turn to Horseshoe Pond Rd.
66.0 Stop for the outcrop on the left side of the road.

Stop 4. Basal conglomerate of the lower Devonian Seboomook Group: (520610, 5192728) The bottom succession of the Seboomook Group, informally called the "Trinity", includes basal conglomerate, fossiliferous limestone and calcareous sandstone, and maroon/red slate/siltstone. The unconformity between the group and the Winterville inlier, commonly presented as the basal conglomerate overlying the volcanic rocks of the inlier, is well preserved in the area around Island Pond and Fish River Lake even though it is offset by several northwest-striking strike-slip faults (Figs. 1, 2, & 25). The "Trinity" is well exposed in the Fish River Lake area, including the tiny islands on the lake. In the Island Pond area, however, only the basal conglomerate and fossiliferous limestone and calcareous sandstone units are exposed. Generally, the basal conglomerate is composed of clasts of mainly volcanic rocks, either dominated by tuff or by basalt, and characterized by red and/or green tuff pebbles (even red jasper pebbles). The basal conglomerate at Stop 4 is dominated by tuff pebbles and granules of light gray to dark gray colors (Fig. 24). A large ledge on the northeast side of the pond shows basal conglomerate dominated by basalt clasts (we will make a quick stop if time allows). We will visit Stops 5A and 5b for the fossiliferous limestone and calcareous sandstone.

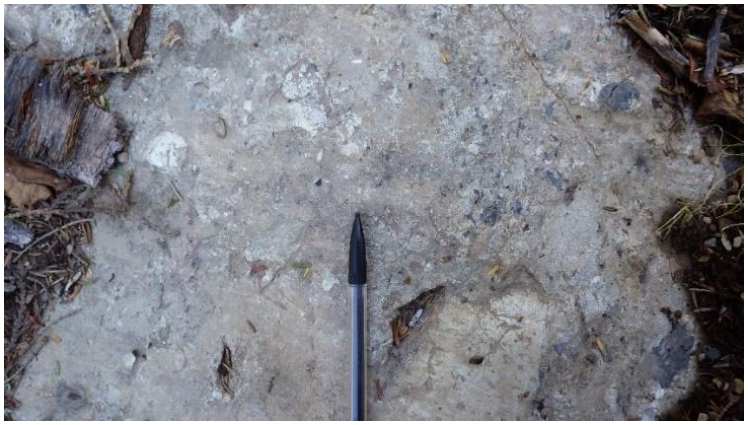

Figure 24. The basal conglomerate outcrop at Stop 4.

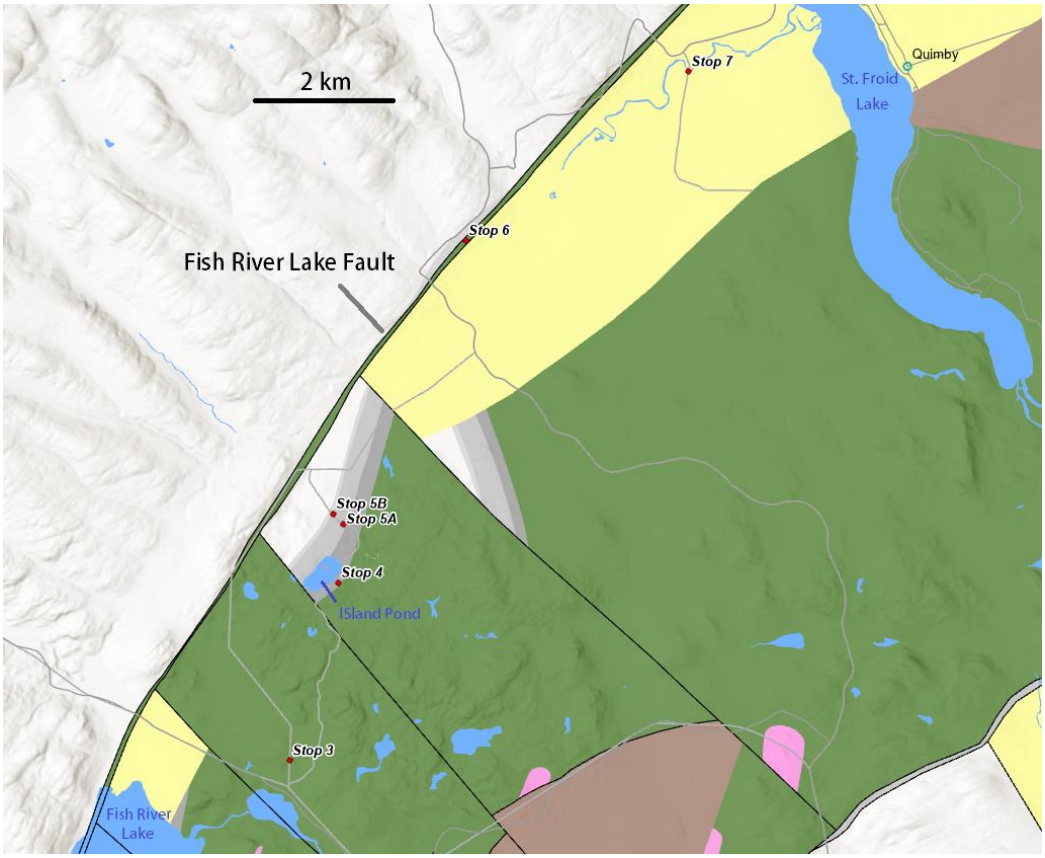

Figure 25. Local geologic map of the Island Pond and Red River valley area. See Figure 3 for legend.

Turn around.

66.8 Stop for fossiliferous limestone ledge on the left side. It is 35 meters (or 115 feet) from the road. Easy hike.

Stop 5A. Fossiliferous limestone of the "Trinity" (Fig. 25)**:** (520687, 5193662) It crops out on the road and also along a ledge on thesouth side of the road (Horseshoe Pond Rd), about 35 meters (or 115 feet) from the road. As always, this fossiliferous limestone is white or light gray and massive. It is a reef limestone and made of reef builders of dominantly stromatoporoids (a sponge) and *Thamnopora* (a tabulate coral). It may also contain minor fragments of *Favosites* (also a tabular coral), crinoids, brachiopods, etc. This fossiliferous limestone is widespread in northern Maine, north to Limestone Point on Square Lake, and southwest to at least the northeast side of Moosehead Lake. The Owen Brook limestone in East Branch Penobscot River is also this limestone.

Continue on Horseshoe Pond Rd.

67.0 Small borrow pit on the right side of the road.

Stop 5B. Fossiliferous calcareous sandstone of the "Trinity" (Fig. 25)**:** (520526, 5193833) This small pit shows the fossiliferous sandstone and slate of the "Trinity". The purple slate west side of the pit may be equivalent to the maroon slate/siltstone unit. The calcareous sandstone is weathered to be in orange color (Fig. 26c). Some brachiopods have been found at this pit, including *Atraypa* (Fig. 26d).

Figure 26. Fossiliferous limestone at Stop 5A (a and b) and calcareous sandstone at Stop 5B (c and d). (a) The white reef limestone; (b) Fragments of stromatoporoids, crinoids, etc. (c) Calcareous sandstone and slate weathered in orange. (d) A brachiopod (*Atrypa*?).

Continue on Horseshoe Pond Rd.

67.5 Right turn (bear right)

69.7 Left turn to Hewes Brook Rd at the end of the road. (And bear right!).

71.0 Stop for outcrop in the left side ditch.

Stop 6. The Fish River Lake fault, fault breccia, and basalt fault sliver (Fig. 25)**:** (522656, 5198227) What a view on top of this highland, the Seboomook highland! Looking down southeast-east is the Red River valley underlain by red and green beds of the Lower Devonian Emsian St. Froid Lake Formation. A red sandstone outcrop actually occurs about 200 meters (600 feet) down the road (on the southeast side) from this stop. Behind you is the Seboomook Group. In the ditch, on the west-northwest side of the road, is the Fish River Lake fault that separates the St. Froid Lake Formation from the Seboomook Group. The southwest-striking and southeast-directed Fish River Lake reverse fault is one of the longest and the most important faults in the northern Maine imbricate fault system. The Fish River Lake fault has created the longest and the most remarkable "fault scarp" in northern Maine; most of the Fish River chain of lakes and the Red River valley are controlled by this fault. Our driving after this stop and before reaching Rte-11 in Winterville Plantation is along the fault scarp, in other words, along the Fish River Lake fault.

A basalt fault sliver is sandwiched in the fault and the sliver extends off and on for at least 45 kilometers along with the length of the fault. The basalt is at this time considered to be part of the Winterville Formation. There also exists fault breccia with large fragments of crushed basalt and even fossiliferous limestone (Fig. 27).

Figure 27. Fault breccia with large fragments/breccias of fossiliferous limestone and vesicular basalt at Stop 6.

Continue on Hewes Brook Rd.

71.8 Right turn and stop at the remotely controlled gate (***Winterville gate***). Make a phone call in the booth and ask to lift the gate.

75.0 Right turn to Red River.

75.2 Stop after passing the bridge.

Stop 7. Red sandstone of St. Froid Lake Formation in Red River (Fig. 25)**:** (526245, 5200935) Red River gets its name from the red sandstone in which it flows. The Red River valley, in particular the riverbed is the lowest in elevation in this region. The St. Froid Lake Formation, as shown at this stop, is a homocline dipping toward northwest (Fig. 28a). In addition to red sandstone of various thickness, there are also intercalated red or purplish red mudstone and shale. The sandstone and mudstone contain plant fragments of trimerophytes – most likely *Psilophyton*, *Hostinella*, and *Pertica* (Fig. 28b).

Figure 28. Red River and the bridge at Stop 7. (a) The homocline of red sandstone and mudstone. Viewer facing southwest. Dave is looking for plant fossils. (b) Sandstone with fragments of plant fossils.

Turn around.

75.5 Right turn to the main road towards Winterville and Eagle Lake.

82.1 Right turn to Rte-11 at the end of the road.

89.1 Left turn to Pennington Pond Rd, a dirt logging road.

89.9 Left turn to Caron Rd. At the end of Caron Rd, make a right turn and continue on the only drivable road.

95.4 Stop by a small pit for St. Froid Lake Formation.

Stop 8. Red sandstone rich in plant fossils (St. Froid Lake Formation) (Fig. 2): (536738, 5205406) What a view! Looking northwest is the Red River valley (or Fish River valley); in the background is the upthrown Seboomook highland. On the southside of the logging road is a small pit with red sandstone and mudstone of St. Froid Lake Formation. As at the Red River stop (Stop 7), the beds also dip toward the northwest. Indeed, the entire St. Froid Lake Formation in this informally called "Red River basin" dips toward northwest, forming a single homocline. The sandstones are rich in fragments of plant fossils of trimerophytes – most likely *Psilophyton*, *Hostinella*, and *Pertica* (Fig. 29a, b), with less common *Protolepidodendron* (the earliest tree species) and *Taeniocrada* (Fig. 29c, d).

This is one of the best sites with better reserved plant fossils. We need to keep them in place for ongoing and future research. Thanks!

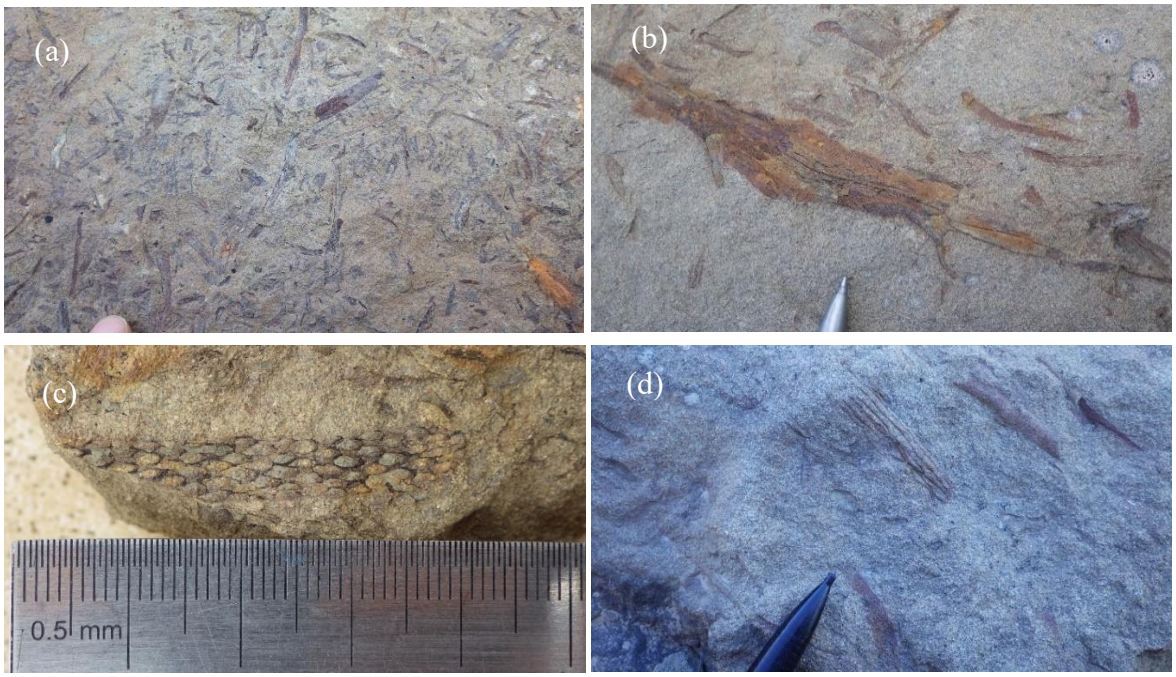

Figure 29. Plant fossils at Stop 8. (a) and (b) are fragments of likely *Psilophyton* and *Pertica.* (c) is a *Protolepidodendron* and (d) is a *Taeniocrada* (?) (the upper center).

Continue on the road straight forward and take the mostly used logging road toward Pennington Mountain.

98.3 Stop at the intersection with an overgrown logging road on the right side. We will hike on this overgrown but even road for about 150 meters (or 450 feet) before going uphill for about 90 meters (or 270 feet) to Stop 9.

Stop 9. The REE-Nb-Zr-mineralized trachyte with hydrothermal pyrite (East Lobe) (Fig. 11**):** (540858, 5204848) This is an excellent outcrop showing a special type of mineralized trachyte with abundance of pyrite. The trachyte is rusty due to oxidation of pyrite (Fig. 30). However, the Pennington Mountain trachyte, including the mineralized trachyte, generally lacks pyrite and the pyritiferous trachyte is the much less common type of the Pennington Mountain REE-Nb-Zr mineralization. Based on surface investigation over the entire mineralized trachyte body, probably only 2% may show pyritic trachyte like what you see at this stop. Pyrite is secondary, probably produced in localized hydrothermal alteration. The mineralized trachyte is dark gray or near black on fresh broken surfaces. It is massive, very fine grained, and homogenous; no minerals are visible with the naked eye.

Figure 30. Mineralized trachyte at Stop 9. (a) Visiting this outcrop on June 26, 2022. John Slack, Anjana Shah, Martin Yates, David Putnam, and Preston Bass. Photo taken by Wang. (b) The rusty, pyritic, mineralized trachyte.

Continue on the logging road.

100.0 Right turn to Pennington Pond Rd (old dirt logging road).

100.6 Stop for Stop 10.

Stop 10. The REE-Nb-Zr-mineralized trachyte without pyrite (East Lobe): (541041, 5204047) See Figure 11 for stop location. Before hiking 70 meters (or 210 feet) to a mineralized trachyte ledge located on the north side of the

road, let's quickly look at the black slate and graywacke of the Ferguson Brook Formation on the road. There are actually several borrow pits of various sizes dug in the formation along the road (Pennington Pond Road). The Pennington Mountain trachyte is likely in fault contact with the Ferguson Brook slate and graywacke and thrusted over the latter by the Pennington Mountain fault, a low-angle (lower than 5º) thrust fault named in this study.

Walk on a marked trail to the ledge on the north side of the road (Fig. 31). This ledge represents the main body or the major type of the REE-Nb-Zr mineralization of the Pennington Mountain trachyte without pyrite or with very few pyrite. Fresh, broken surfaces of the mineralized trachyte are dark gray or near black. It is again massive, very fine grained with a homogenous texture. Minerals are not visible with the naked eye.

Figure 31. (a) A visit to the ledge at Stop 10 on October 26, 2022. Chunzeng Wang, Robert Marvinney, and Amber Whittaker. Photo taken by Lauren Madsen. (b) Another visit to the ledge with David Lentz on August 16, 2023.

Continue on Pennington Pond Rd.

100.8 Stop for a small pit on the right side.

Stop 11. Basalt/pillow basalt next to the trachyte (Fig. 11**):** (540884, 5203906) The wall of the small pit is basalt and pillow basalt (Fig. 32a) of the Winterville Formation. It is only about 10–15 meters (or 30–45 feet) from the trachyte. The basalt is aphyric and fine gained. Part of it is vesicular and/or amygdaloidal with calcite amygdales (Fig. 32b). Whole-rock geochemical analysis of a sample collected from this basalt outcrop and another one from the northwest side of the trachyte body show calc-alkaline affinity; both are geochemically either "alkaline basalt" or "trachy-andesite". Their LREE are higher than HREE and their HREE are slightly higher than the trachyte. Geochemically both basalt samples are distinctively different from the basalt samples collected from other areas of the Winterville inlier, for example, they do not show any depletion in Ta and Nb. On tectonic discrimination diagrams (not posted here), they plot in "MORB-OIB array" or "oceanic islands" fields. It is highly likely that both the Pennington Mountain trachyte and the basalt around the trachyte were produced in a similar or same tectonic setting (non-orogenic or non-active arc), or even from the same source in the mantle.

At around this stop (or around the road – Pennington Pond Road) is the Pennington Mountain thrust fault that separates the basalt and trachyte from the Ferguson Brook black slate and graywacke to the east-southeast. The fault is about parallel to the road and located immediately on the west side of the road.

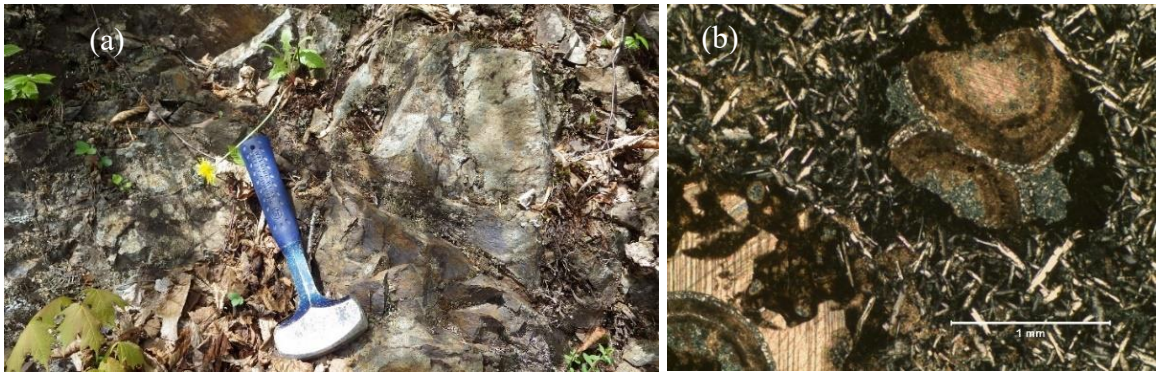

Figure 32. (a) Pillow basalt at Stop 11. (b) Amygdaloidal texture with calcite amygdales at Stop 11.

Continue on Pennington Pond Rd.

102.5 Left turn to another old logging road. Keep on the main, frequently used road that leads to Rte-11.

109.1 Left turn to Rte-11
110.2 Right turn to a dirt logging road named Nixon Siding Road.
110.4 Right turn to the big borrow pit for Stop 12.

Stop 12. Green beds of the St. Froid Lake Formation (Figs. 1 & 2): (536880, 5191959) This large borrow pit shows mostly the green beds of the St. Froid Lake Formation. The green beds are well bedded thin to medium-layered quartzofeldspathic micaceous sandstone, siltstone, and mudstone/shale (Fig. 33a); they are not foliated. They contain thin sandy and micaceous drapes of comminuted dark phytodebris (Fig. 33b) likely deposited in a coastal or nearshore setting. The phytodebris is, generally, ≤1 cm in length. All the plant material appears to be transported and deposited in aqueous terrestrial or coastal settings.

Figure 33. Green beds of St. Froid Lake formation at Stop 12. (a) The thin-medium-layered sandstone and shale. (b) Fragments of plant fossils.

Turn around and drive back to Rte-11.
110.6 Right turn to Rte-11. Keep on Rte-11 towards Ashland.
131.0 Ashland One Stop. Left turn to Rte-163 towards Mapleton and Presque Isle.
151.0 ***Back to Presque Isle***. Don't forget the banquet at UMPI Campus Center!

REFERENCES

Ayuso, R.A. and Schulz, K.J., 2003. Nd-Pb-Sr isotope geochemistry and origin of the Ordovician Bald Mountain and Mount Chase massive sulfide deposits, northern Maine. Economic Geology Monograph 11, p. 611–630.

Ayuso, R.A., Wooden, J.L., Foley, N.K., Slack, J.F., Sinha, A.K., and Persing, H., 2003. Pb isotope geochemistry and U–Pb zircon (SHRIMP–RG) ages of the Bald Mountain and Mount Chase massive sulfide deposits, northern Maine: Mantle and crustal contributions in the Ordovician. Economic Geology Monograph 11, p. 589–609.

Berry, W. B. N., 1964. Early Ludlow graptolites from the Presque Isle quadrangle, Maine: Journal of Paleontology, v. 38, p. 587–599.

Berry, W. B. N., 1960. Early Ludlow graptolites from the Ashland area, Maine: Journal of Paleontology, v. 34, p. 1158–1163.

Boone, G.M., 1958. The Geology of the Fish River Lake–Deboullie Area, Northern Maine: Ph.D. thesis, Yale University, 186 p.

Boone, G.M., 1970. The Fish River Lake Formation and its environments of deposition: in Shorter Contributions to Maine Geology: Maine Geological Survey, Bulletin 23, p. 27–41.

Busby, C.J., Kessel, L., Schulz, K.J., Foose, M.P., and Slack, J.F., 2003. Volcanic setting of the Ordovician Bald Mountain massive sulfide deposit, northern Maine. Economic Geology Monograph 11, p. 219–244.

Boucot, A.J., Field, M.T., Fletcher, R., Forbes, W.H., Naylor, R.S., and Pavlides, L., 1964. Reconnaissance bedrock geology of the Presque Isle quadrangle, Maine: Maine Geological Survey, Bulletin 15, No. 2, 123 p.

Cabanis, B. and Lecolle, M., 1989, Le diagramme La/10 – Y/15 – Nb/8: Un outil pour la discrimination des series volcaniques et en evidence des mélange et/ot de vontamination crustale. Comptes Rendus de l'Académie des Sciences, Série II, 309, p. 2023–2029.

Cummings, J.S., 1988. Geochemical detection of volcanogenic massive sulphides in humid-temperate terrain (using surficial methods): Bangor, Maine, J.S. Cummings, Inc., 298 p.

Eby, G.N., *1992*. Chemical subdivision of the *A-type* granitoids: Petrogenetic and tectonic implications: Geology, v. 20, p. 641–644.

Hall, B., 1970. Stratigraphy of the southern end of the Munsungun anticlinorium, Maine. *Maine* Geological Survey Bulletin 22, 63 p.

Horodyski, R.J., 1968. Bedrock geology of portions of Fish River Lake, Winterville, Greenlaw, and Mooseleuk Lake quadrangles, Aroostook County, Maine. M.S. thesis, Cambridge, Massachusetts, Massachusetts Institute of Technology, 192 p.

LeBas, M.J., LeMaitre, R.W., Streckeisen, A., and Zanettin, B., 1986. A Chemical Classification of Volcanic Rocks Based on the Total Alkali-Silica Diagram: Journal of Petrology, v. 23, no. 3, p. 745–750.

Mencher, E., 1963. Annual report on work accomplished during 1963 under NSF grant GP-1547 "Geology of Northern Aroostook County, Maine and its Bearing on the Development of the Northern Appalachian" (unpublished report).

Nakamura, N., 1974. Determination of REE, Ba, Mg, Na and K in carbonaceous and ordinary chondrites: Geochimica et Cosmochimica Acta, 38, p. 757–775.

Osberg, P.H., Hussey, A.M., II, and Boone, G.M. (editors), 1985. Bedrock geologic map of Maine: Maine Geological Survey.

Pearce, J.A., 2008. Geochemical fingerprinting of oceanic basalts with applications to ophiolite classification and the search for Archean oceanic crust: Lithos 100, p.14–48

Pearce, J.A., Harris, N.B.W., and Tindle, A.G., 1984. Trace element discrimination diagrams for the tectonic interpretation of granitic rocks: Journal of Petrology 25(4), p. 956–983.

Pearce, J. A., 1983. Role of sub-continental lithosphere in magma genesis at destructive plate margins, in Continental Basalts and Mantle Xenoliths, edited by C. J. Hawkesworth and M. J. Norry, p. 230–249, Shiva, Nantwich, UK.

Perkins, E.H. and Smith, E.S.C., 1925. Contributions to the geology of Maine, No. 1: A geological section from the Kennebec River to Penobscot Bay: American Journal of Science, 5th series, v. 9, no. 51, p. 204–228.

Pollock, S.G., 1987. The Lower Devonian slate problem of western and northern Maine revisited: Northeastern Geology, v.9, no. 1, p. 37–50.

Ross, P.S. and Bédard, J.H., 2009. Magmatic Affinity of Modern and Ancient Subalkaline Volcanic Rocks Determined from Trace-Element Discriminant Diagrams: Canadian Journal of Earth Sciences, 46, p. 823–839.

Roy, D.C., 1987. Geologic Map of the Caribou and Northern Presque Isle 15' Quadrangle, Maine: Maine Geological Survey, Open-File No. 87-2, 44 p.

Roy, D.C. and Mencher, E., 1976, Ordovician and Silurian stratigraphy of northeastern Aroostook County, Maine: Geol. Soc. Amer., Memoir 148, p. 25–52.

Roy, D. C., 1970. The Silurian of Northeastern Aroostook County, Maine, (Ph.D. thesis): Massachusetts Institute of Technology, 482 p.

Roy, D.C., and Mencher, E., 1976. Ordovician and Silurian stratigraphy of northeastern Aroostook County, Maine: Geol. Soc. Amer., Memoir 148, p. 25–52.

Schulz, K. J. and Ayuso, R. A., 2003. Lithogeochemistry and paleotectonic setting of the Bald Mountain massive sulfide deposit, northern Maine. Economic Geology Monograph 11, p. 79–109.

Shah, A.K., 2022. Airborne magnetic and radiometric survey, Munsungun region in northern Maine, 2021: U.S. Geological Survey data release, https://doi.org/10.5066/P97VUIJS.

Shah, A.K., and Wang, C., 2022. Ground-based gamma spectrometry data collected in northern Maine (Version 2.0, September 2022): U.S. Geological Survey data release, https://doi.org/10.5066/P9WFQ30O.

Slack, J.F., Foose, M.P., Flohr, M.J.K., Scully, M.V., and Belkin, H.E., 2003. Exhalative and subsea-floor replacement processes in the formation of Bald Mountain massive sulfide deposit, northern Maine. Economic Geology Monograph 11, p. 513–547.

Supkow, D.J., 1965. Stratigraphy and structure of the Spider Lake Formation, Churchill and Spider Lake quadrangles, Maine. M.S. thesis, Orono, University of Maine, 118 p.

Wang, Chunzeng, Slack, John, Shah, Anjana, Yates, Martin, Lentz, David, Whittaker, Amber, and Marvinney, Robert, 2023. A Recently Discovered Trachyte-Hosted Rare Earth Element-Niobium-Zirconium Occurrence in Northern Maine, USA: Economic Geology, Vol. 118, No. 1, p. 1–13.

Wang, C., 2022a. Bedrock Geology of the Fish River Lake Quadrangle, Maine: Maine Geological Survey, Open-File Map 22-5, scale 1:24,000.

Wang, C., 2022b. Bedrock geology of the Carr Pond quadrangle, Maine: Maine Geological Survey, Open-File Map 22-6, scale 1:24,000.

Wang, C., 2021a. Bedrock geology of the Big Machias Lake quadrangle, Maine: Maine Geological Survey Open-File No. 21-12, scale 1:24,000.

Wang, C., 2021b. Bedrock geology of the Greenlaw Pond quadrangle, Maine: Maine Geological Survey Open-File No. 21-2, scale 1:24,000.

Whalen, J.B., Currie, K.L., Chappell, B.W. 1987. A-type granites: geochemical characteristics, discrimination and petrogenesis: Contributions to Mineralogy and Petrology, vol. 95, p. 407–419.

Wilson, R.A., and Kamo, S.L., 2012. The Salinic Orogeny in northern New Brunswick: geochronological constraints and implications for Silurian stratigraphic nomenclature. Canadian Journal of Earth Sciences, 49, p. 222–238.

GEOLOGY OF THE SOUTH BRANCH PONDS AND NORTH TRAVELER MOUNTAIN AREA, BAXTER STATE PARK, MAINE

Robert A. Johnston[1] and Lindsay J. Theis[2]
[1]Maine Geological Survey (retired; rajohnston73@gmail.com)
[2]Maine Geological Survey (lindsay.theis@maine.gov)
17 Elkins Lane 93 SHS Augusta, ME 04333

INTRODUCTION

This guide has been updated and adapted from the field trip of the same name that was part of NEIGC 2013 (Johnston and Weddle, 2013), and was based on *A Guide to the Geology of Baxter State Park* (Rankin and Caldwell, 2010). Since 2013, LiDAR topographic imagery was made available for the Baxter State Park region, so improved maps that highlight the field trip area's geomorphology have been produced for this guide (Fig. 1). (However, it is important to note that while Rankin and Caldwell (2010) did not have the benefit of LiDAR, their maps were produced at a smaller scale (1:100,000) where delineating more detailed features may not have been appropriate. Understanding the proper minimum mapping unit size (MMU) at various scales is important in geologic mapping!) This field trip is a moderate day hike to observe bedrock and glacial features in the South Branch Ponds and North Traveler Mountain area of Baxter State Park, Maine, a place described as 'scenic and geologically interesting' by Rankin and Caldwell (2010). Stops on the trip include outcrops of Traveler Rhyolite, views of a glacially sculpted landscape from the North Traveler ridgeline, the Howe Brook landform, and glacial potholes along Howe Brook. ***Use of rock hammers and specimen collecting is strictly prohibited in the park.***

GENERAL GEOLOGY

The South Branch Ponds and Traveler Mountain area of Baxter State Park is dominated by volcanic Traveler Rhyolite exposures. This unit covers an area approximately six by ten miles (10 by 16 kilometers) across the northern part of Baxter State Park and is estimated to be about 10,500 feet (3,200 meters) thick (Rankin and Hon, 1987). This porphyritic, extrusive volcanic rock varies in color from dark green to bluish-gray (unweathered) and exhibits conchoidal fracturing when broken. Columnar jointing is the Traveler Rhyolite's most notable feature, with many examples to observe during the trip. The effects of glaciation on local geomorphology can be viewed from the North Traveler ridgeline, including glacially plucked cliffs and the U-shaped South Branch Ponds Valley - hikers may traverse this entire valley via the Pogy Notch Trail from South Branch Pond Campground to Russell Pond (Kish, 2012). Glacially streamlined topography with a northwest to southeast trend reveals the dominant former ice flow direction. Several glacial meltwater channels are present south of the Park Tote Road near its intersection with the South Branch Pond Campground Road (Fig. 1). The Howe Brook landform is a prominent Holocene feature that separated a larger water body into Upper and Lower South Branch Ponds (Fig. 1). The South Branch Ponds and North Traveler Mountain area is a complex landscape that exposes some of Maine's most interesting geology. The underlying bedrock, glacial features, post-glacial erosion and deposition, and modern fluvial processes all combine to tell a compelling story.

BEDROCK GEOLOGY

The Traveler Rhyolite is an isolated deposit along the Piscataquis volcanic belt - a contemporaneous and lithologically similar series of volcanic rocks that were likely part of an ancient volcanic island-arc system and extend about one hundred miles (160 kilometers) across northwestern Maine (Rankin, 1968; Hon, 1980). Rocks of the Piscataquis belt are felsic, mostly rhyolites, and underlie some of Maine's highest mountains due to their resistance to erosion. It has been claimed that Traveler Mountain (3,550 feet/1,082 meters) is the tallest mountain composed of volcanic rock east of the Mississippi River.

The Traveler Rhyolite formed when a volcano erupted in close proximity to the ocean – a setting which is known because marine fossils from the underlying Matagamon Sandstone are incorporated into the base of the rhyolite. Fossils from the Matagamon Sandstone indicate an early Devonian age, and zircon ages (407 Ma) from the Traveler Rhyolite agree, showing that these formations were deposited in a relatively short span of time (Rankin and Tucker, 1995). Explosive volcanic eruptions produced clouds of froth (a liquid magma and gas mix

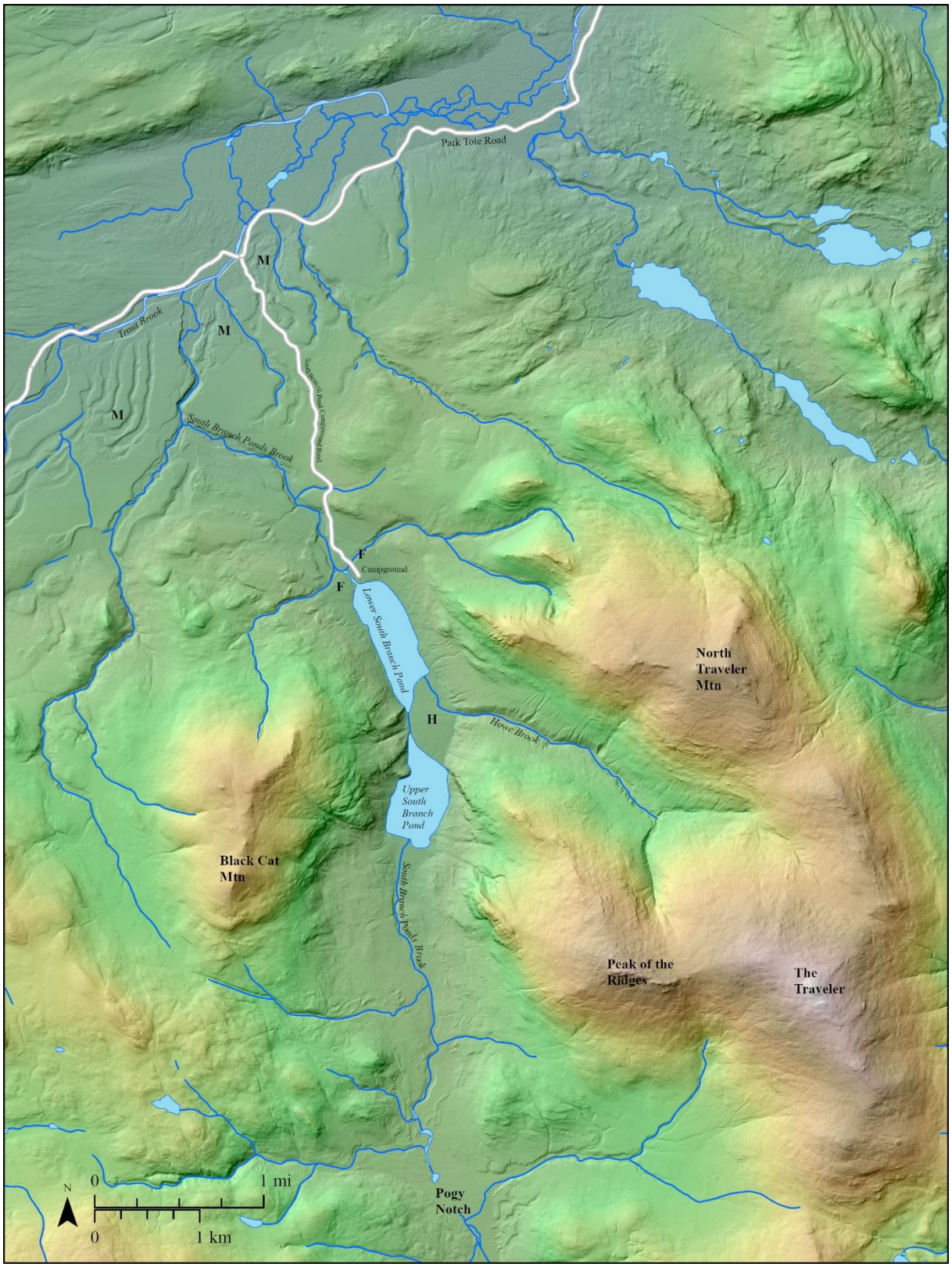

Figure 1: Overview map of the field trip area (2017 MEGIS 1-meter lidar DEM color ramp with hillshade; hotter colors = higher elevations); M = meltwater channel areas; H = Howe Brook landform; F = alluvial fans at South Branch Campground. Map: Maine Geological Survey.

that cools to form pumice), spewing ash into the atmosphere and hot ash flows that surged down the volcano slopes. The ash flows retained enough heat when they were deposited downslope that the particles fused together to form welded tuff. Pumice fragments in the ash flows were compacted by the weight of subsequent overlying flows, creating a planar structure in the Traveler Rhyolite known as compaction foliation (Fig. 2). Welded tuff layers of varying thickness can be seen in numerous exposures along the North Traveler Trail, forming terraces along the mountainsides. After deposition, the bedrock in this area was warped into a broad, north plunging anticline with an axis along the South Branch Ponds Valley, so the once level layers of welded tuff are tilted (Fig. 3).

Figure 2: An example of Traveler Rhyolite (Black Cat Member). Flattened pumice (tan areas) highlights the compaction foliation of this welded tuff. Phenocrysts appear as white specks. Photo modified from Rankin and Caldwell (2010).

Figure 3: Northeast dipping ash flow layers along the North Traveler Trail. Photo: Maine Geological Survey/Lindsay Theis.

Rankin (1980) divided the Traveler Rhyolite into two main members based on their phenocryst compositions. The Pogy Member is the approximately 3,000 foot (900 meter) thick, moderately compacted basal member. This member contains about 15% phenocrysts, which are roughly one-third quartz and two-thirds plagioclase feldspar. Outcrops of the Pogy Member are best viewed on the shore of Matagamon Lake or along the Park Tote Road just west of the Matagamon Gate and therefore, we will not be able to view this member on the trip. The Black Cat Member (Fig. 2) overlies the Pogy Member and is about 7,000 feet (2,100 meters) thick.

It is highly compacted and contains about 10% phenocrysts, which are approximately 75% plagioclase feldspar and 20% pyroxene. Rotated phenocrysts may be visible in the field and indicate that the ash flow was still moving downslope as it cooled. Rankin (1968) concluded that the basal Pogy Member erupted from the cooler, more gas and water-rich upper part of the magma chamber, while the overlying Black Cat Member followed from the deeper, hotter, and less gas and water-rich portion of the chamber.

Columnar jointing in the Traveler Rhyolite is one of the most notable features found in the South Branch Ponds and Traveler Mountain area (Fig. 4). These joints form during rapid cooling of tabular igneous deposits, developing perpendicular to the bounding cooling surfaces. The columns typically have four to eight sides and vary in length and diameter from inches or centimeters to tens of feet or meters. Compaction foliation is usually perpendicular to the columns' long axes, indicating that the flows were deposited on a relatively level surface and subsequent tectonic activity did not cause significant internal deformation. Since the Traveler Rhyolite was formed by a series of ash flows, one wonders how much time elapsed between the eruptions and flows. We will consider this question as we look at the bounding surfaces of the ash flows along the North Traveler Trail.

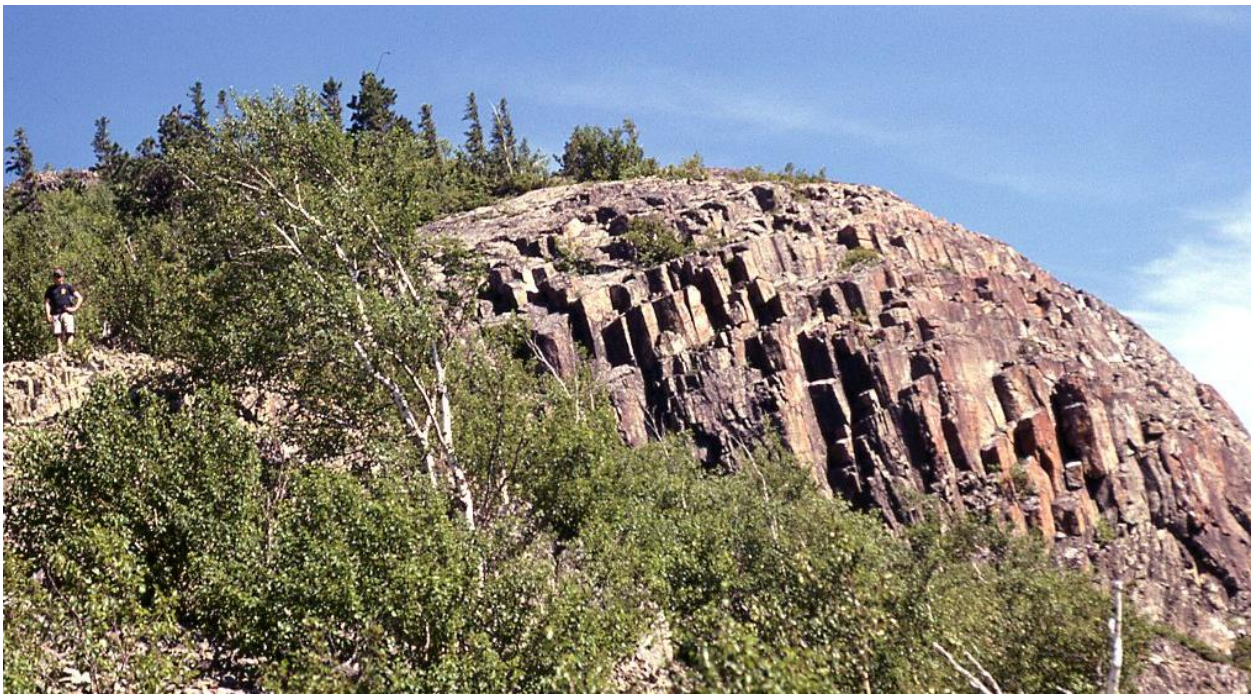

Figure 4: Columnar joints on North Traveler Mountain. Photo: Maine Geological Survey/Joe Kelley.

Other significant bedrock geology in the South Branch Ponds area includes outcrops of the fossiliferous Trout Brook Formation along South Branch Ponds Brook, in which the Maine state fossil (*Pertica quadrifaria*) may be found. While it is unlikely that there will be time to visit these outcrops on this trip, participants staying in the park before or after are encouraged to visit if water conditions are safe (especially given this year's wet weather). A guided traverse for this location is provided in Rankin and Caldwell (2010). ***Please remember that fossil and rock collecting in the park is strictly prohibited.***

GLACIAL GEOLOGY

The effects of glacial processes can be observed in several areas of Baxter State Park's northern region. Most researchers agree that even the tallest mountains in the area, such as Katahdin and Traveler, were covered by glacial ice at some point during the last Ice Age, but the timing and manner of glaciation and deglaciation is still being investigated (Davis, 1989; Davis et al., 2015). A basal radiocarbon age from Upper South Branch provides a minimum estimate of ice-free conditions in the South Branch Ponds Valley by about 12,890 calendar years before present (Anderson et al., 1986). More recent cosmogenic exposure ages from the Katahdin area estimate ice-free conditions by about 15,000–16,000 years ago (Davis et al., 2015).

The U-shaped valley that now contains Upper and Lower South Branch Pond was carved when glacial ice took advantage of a weaker, more erodible bedrock zone. The valley is best viewed from an overlook on The Ledges Trail north of South Branch Pond Campground, but we will also have a nice view from the North Traveler ridgeline. As continental glacial ice flowed over the entire region, it streamlined and smoothed up-ice (typically northwest) slopes and plucked bedrock from down-ice aspects (typically southeast) to form steep slopes - Black Cat Mountain is an excellent example of this morphology (Fig. 1). Glacial till was deposited on the hillsides, ranging from compact lodgement till (a.k.a. hardpan) that was smeared onto up-ice slopes, to more typical stony diamictons elsewhere. As the ice retreated, glacial meltwater flowed along, or subglacially very near the ice margin, eroding many deep channels in glacial till. Glacial meltwater channels are often difficult to spot under Maine's thick forest cover, but the series of channels around the confluence of Trout Brook and South Branch Ponds Brook are so remarkable that they were recognized on air photos long before LiDAR (Fig. 1). These channels may be occupied by modern streams but are often swampy or eerily strewn with moss-covered cobbles and boulders that provide evidence of former meltwater flow. Lowland areas may be occupied by glaciofluvial deposits such as outwash and eskers, but we will not encounter any examples on this trip.

The Howe Brook landform is a fan-shaped deposit that separates what was once one large lake into Upper and Lower South Branch Ponds (Fig. 5). It has been described as a delta (Caldwell, 1966), a debris flow or landslide deposit (Rankin and Hon, 1987; Caldwell, 1990), and as a landform of 'uncertain origin' (Rankin and Caldwell, 2010). Debate over whether the landform was created by fluvial, mass wasting processes, or both seems to have stemmed from the coarse sediments found in the deposit (Fig. 6) – did Howe Brook have the power to move these or were they transported by a debris flow? LiDAR topographic imagery reveals that the first theory was closest. The Howe Brook Valley and its tributaries are distinctly V-shaped and have been carved by fluvial processes. Evidence of significant mass wasting in the form of craters and bowl-shaped depressions is lacking. It is likely that the Howe Brook landform began to develop in early post-glacial times when the unstable, sparsely vegetated landscape would have yielded more sediment that was deposited first as a subaqueous fan into one lake that filled the South Branch Ponds Valley. Over time, the subaqueous fan may have built up into a delta (and some may argue that it should still be designated as a delta since it is built into a water body), but it now has the distinctly sloping, dry surface of an alluvial fan, especially in comparison to the delta where South Branch Ponds Brook enters Upper South Branch Pond from the more subdued topography of Pogy Notch (Fig. 1). Eventually, the landform extended across the valley, splitting one large lake into Upper and Lower South Branch Ponds. Large alluvial fans are very common in Maine where steep mountainside streams meet valley floors or lakes – there are many nice examples in Baxter State Park, including the area on which South Branch Pond Campground is located (Fig. 1). It is interesting to consider the history of this area and the many paths Howe Brook has taken as we traverse the landform. The precipitation/flood magnitudes required to move stony sediments to the fan and the speed at which the fan was built are unknown.

Figure 5: Southwest view from the North Traveler Mountain Trail. The Howe Brook landform fills photo center, separating Upper and Lower South Branch Ponds. Photo: Maine Geological Survey/Lindsay Theis.

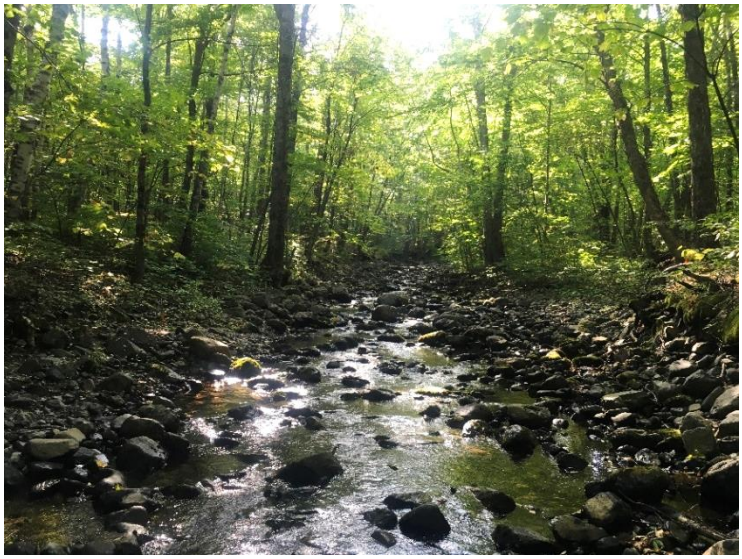

Figure 6: Coarse bedload in Howe Brook where it traverses the landform. Photo: Maine Geological Survey/Lindsay Theis.

Walking along the Howe Brook Trail, one will encounter many potholes scoured into the Howe Brook streambed consisting of Traveler Rhyolite (Black Cat Member; Fig. 7). The Howe Brook drainage path was likely initiated by subglacial meltwater flow, so these deep, smooth-sided, rounded holes were scoured by sediment-laden water flowing under great hydraulic pressure, similar to the well-known Screw Auger Falls in western Maine's Grafton Notch State Park. Modern stream processes continue this erosive process but at a much slower rate. Some of the potholes in Howe Brook are reported to be over 20 feet (6 meters) deep.

Figure 7: Pothole in Howe Brook. Note the gravel at the bottom – how does this continue the potholing process? Photo: Maine Geological Survey/Joe Kelley.

In addition to modern stream processes, evidence of mass wasting abounds in Baxter State Park. Avalanches, landslides, and rock fall scars stripe the various mountainsides. LiDAR topographic imagery has also revealed many more subtle landslides at lower elevations (Maine Geological Survey, 2020).

ROAD AND TRAIL LOGS

Start time and location: Saturday, October 7, 9 AM at the South Branch Pond Campground lakeside shelter (507699E, 5106027N UTM). Field trip parking will be in the day-use lot at the campground entrance. ***Provisions (including potable water) are not available at the campground*** – please bring enough food and water for the day, along with clothing and footwear appropriate for fall hiking. Day use fee is $16 for non-residents and may be purchased ahead of entry (see Baxter State Park website for details). ***Use of rock hammers and specimen collecting is strictly prohibited in the park.***

Directions to the Matagamon Gatehouse (north entrance to Baxter State Park):

From the south (Bangor and southern Maine area): Travel on I-95 to Exit 264; turn west (left) on ME Route 158 which shortly joins ME Route 11 north. Bear right on ME Route 11 and travel 9 miles north to Patten. Just north of Patten village, leave ME Route 11, turning left on ME Route 159 (Shin Pond Road). Continue 26 miles on this road to the Matagamon Gatehouse.
From the north (Presque Isle and Ashland area): From Presque Isle, take ME Route 163 to Ashland (for 20 miles). Turn left onto ME Route 11 at Ashland One Stop. Continue 42.5 miles south on ME Route 11 before making a right turn onto Owlsboro Road. In 4.6 miles, turn right onto ME Route 159 (Shin Pond Road). Continue 19.4 miles on this road to the Matagamon Gatehouse.

Road Mileage to South Branch Pond Campground from Matagamon Gate:
0.0 Matagamon Gate. Follow Park Tote Road west.
2.6 Pass Trout Brook Farm Campground on right (group campsite).
7.3 Turn left onto South Branch Pond Campground Road before crossing over Trout Brook bridge.
9.0 Arrive at South Branch Pond Campground day-use parking lot. Lakeside shelter is straight ahead past the Ranger Cabin.

Trail Mileage for North Traveler Ridgeline:
NOTE: This trail is short but steep with many cliff areas and loose rocks. Please go slow and use caution!
0.0 Trail log is from the east end of South Branch Pond Campground (Fig. 8). Follow the Pogy Notch Trail 0.1 miles to North Traveler Mountain trailhead. See Baxter State Park (2012) for trail details.
0.5 Break out of forested talus area onto open ledges and continue steep ascent along edge of ridge.

STOP 1: EXPOSURE OF TRAVELER RHYOLITE, BLACK CAT MEMBER
Thin beds of welded-ash flows can be seen in several outcrops. Can you identify the different layers? In what direction are they dipping? Look for flattened pumice and compaction foliation. Use a hand lens to observe phenocrysts. Columnar joints are exposed on the nearby cliffs. Stop to observe the area of deformed columns identified as megabreccia by Rankin and Caldwell (2010) – do you agree? Views of the U-shaped valley and Howe Brook landform are prominent.

0.8 After going along the edge of steep cliffs, bear left around a rocky knob with a large cairn.

STOP 2: GLACIAL EROSION
Glacial ice flowed over the mountain, plucking bedrock and steepening the southern, down-ice side of the ridge.

1.1 Reach the crest of North Traveler Ridge at knob. ***It is unlikely that we will have time to hike past this ridgeline and we will return to the campground for lunch after exploring this area and taking in the views.***

Trail Mileage for Howe Brook:
0.0 Trail log is from the east end of South Branch Pond Campground (Fig. 8). The Howe Brook Trail is described in Kish (2012) as a moderate hike with little elevation change along a mountain brook with chutes and potholes. Follow the Pogy Notch Trail and pass the North Traveler Mountain trailhead at 0.1 miles.
1.0 Junction of Pogy Notch and Howe Brook Trails. Howe Brook Trail turns east to climb along the streambed of Howe Brook.

STOP 3: HOWE BROOK LANDFORM
Explore the landform area (Fig. 9). Do you notice any possible former paths of Howe Brook?

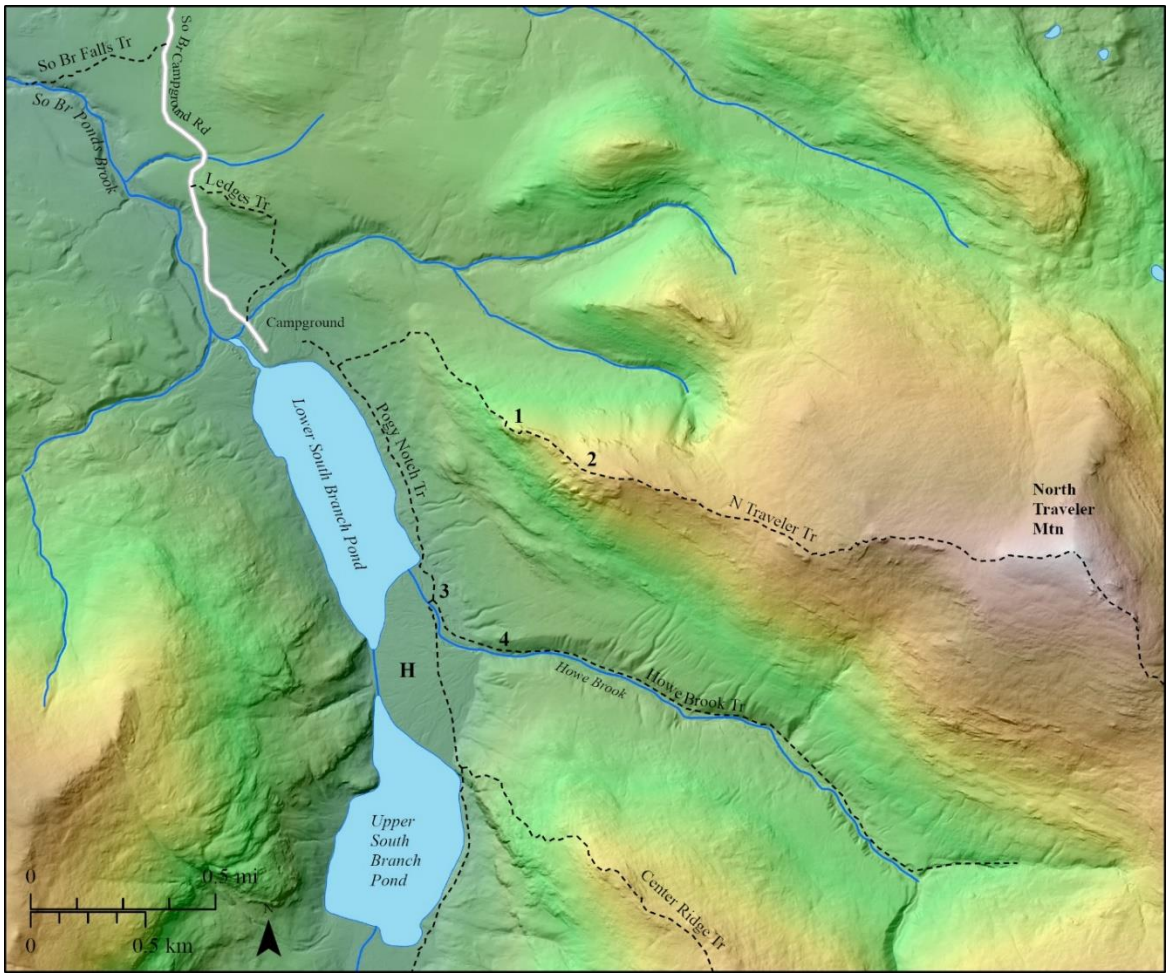

Figure 8: Detailed map of the field trip area (2017 MEGIS 1-meter LiDAR DEM color ramp with hillshade; hotter colors = higher elevations). Dashed black lines = hiking trails; H = Howe Brook landform; bold numbers = approximate stop locations. Map: Maine Geological Survey.

1.2 First falls area along Howe Brook.

STOP 4: POTHOLES ALONG HOWE BROOK

A series of chutes and potholes are encountered as you climb along Howe Brook. How were the chutes and potholes initiated? How and when is the modern Howe Brook continuing the work of glacial meltwater flow? As you ascend the valley, think about possible sources for large angular blocks in the stream that refute the debris flow theory. The stream valley is often restricted – how would this affect water velocity and sediment transport during flood events? It is a two-mile hike east from the junction of the Pogy Notch and Howe Brook Trails to the waterfall at the terminus of the Howe Brook Trail – for the sake of time, we will explore the first three sets of falls before returning to the campground.

END OF TRIP

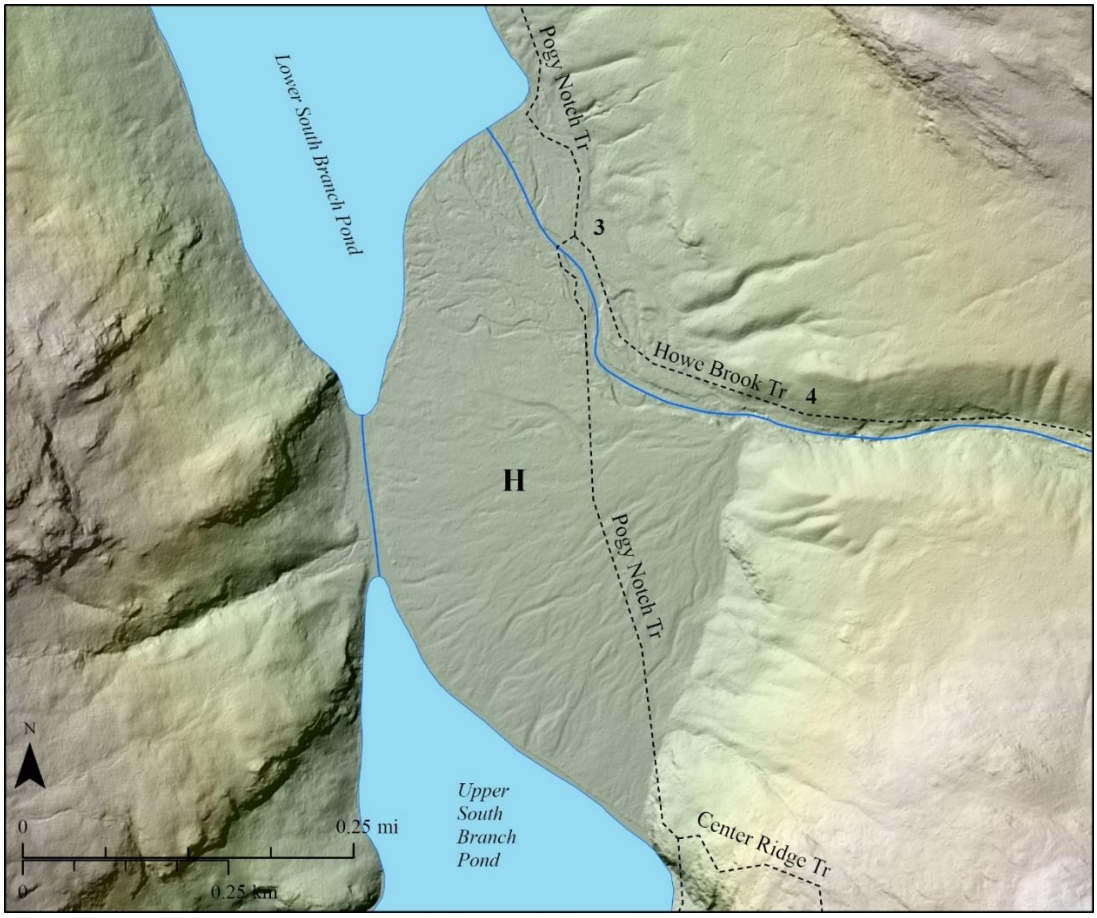

Figure 9: Detailed map of the Howe Brook landform area showing distributary channels (2017 MEGIS 1-meter LiDAR DEM color ramp with hillshade; hotter colors = higher elevations). Dashed black lines = hiking trails; H = Howe Brook landform; bold numbers = approximate stop locations. Map: Maine Geological Survey.

REFERENCES

Anderson, R.S., Davis, R.B., Miller, N.G., and Stuckenrath, R., 1986, History of late- and post-glacial vegetation and disturbance around Upper South Branch Pond, northern Maine: Canadian Journal of Botany, v. 64, no. 9, p. 1977–1986.

Baxter State Park, 2012, Katahdin, A Guide to Baxter State Park, 7th Edition: Baxter Park Authority, 220 p.

Caldwell, D.W., 1966. Pleistocene and surficial geology between Togue Pond and South Branch Pond, *in* Caldwell, D.W., ed., Field Trips in the Mt. Katahdin Region, Guidebook for the 58th New England Intercollegiate Geological Conference, p. 51–61.

Caldwell, D.W., 1990. The geomorphology and sedimentology of the northern portion of Baxter State Park and vicinity, *in* Fieldtrip Guide for the Summer Meeting of the Geological Society of Maine (July 28-29, 1990): Geological Society of Maine, 7 p.

Davis, P.T., 1989. Quaternary glacial history of Mt. Katahdin and the nunatak hypothesis, *in* Tucker, R.D. and Marvinney, R.G., eds., Studies in Maine Geology, vol. 6, Quaternary Geology: Maine Geological Survey, Augusta, Maine, p. 119–134.

Davis, P.T., Bierman, P.R., Corbett, L.B., and Finkel, R.C., Cosmogenic exposure age evidence for rapid Laurentide deglaciation of the Katahdin area, west-central Maine, USA, 16 to 15 ka: Quaternary Science Reviews, v. 116, p. 95–105.

Hon, R., 1980. Geology and petrology of igneous bodies within the Katahdin pluton, *in* Roy, D.C. and Naylor, R.S., eds., Geology of Northeastern Maine and Neighboring New Brunswick, Guidebook for 72nd New England Intercollegiate Geological Conference, p. 65–79.

Johnston, R.A., and Weddle, T.K., 2013, Geology of the South Branch Pond and North Traveler Mountain Area, Baxter State Park, Maine, *in* Hanson, L.S., ed., Guidebook for Field Trips in North-central Maine, New England Intercollegiate Geological Conference, 105th annual meeting, Millinocket, Maine, p. 16–22.

Kish, C. M., 2012, Maine Mountain Guide: Appalachian Mountain Club. 402 p.

Maine Geological Survey, 2020, Maine Inland Landslides – Points (available at https://mgs-maine.opendata.arcgis.com/datasets/maine-inland-landslides-points/explore).

Rankin, D.W., and Caldwell, D.W., 2010. A Guide to the Geology of Baxter State Park and Katahdin: Maine Geological Survey, Bulletin 43, 80 p., 2 maps.

Rankin, D.W., 1968, Volcanism related to tectonism in the Piscataquis volcanic belt, an island arc of Early Devonian age in north-central Maine, *in* Zen, E., White, W. A., Hadley, J.B., and Thompson, J.B., Jr., eds., Studies in Appalachian geology: Northern and maritime: New York, Interscience Publishers, p. 355–369.

Rankin, D. W., and Hon, R., 1987, Traveler Rhyolite and the overlying Trout Valley Formation and the Katahdin pluton: A record of basin sedimentation and Acadian magmatism, north-central Maine, *in* Roy, D. C., ed., Northeastern Section of the Geological Society of America, Centennial Field Guide, v. 5, p. 293–301.

Rankin, D.W., and Tucker, R.D., 1995, U-Pb age of the Katahdin-Traveler Igneous Suite, Maine, local age of the Acadian orogeny, and thickness of the Taconian crust: Geological Society of America Abstracts with Programs, v. 27, no. 6, p. A224–A225.

GEOCHEMISTRY OF MAFIC MAGMATISM AND STRUCTURAL RELATIONSHIPS IN MÉLANGE OF THE CAUCOMGOMOC LAKE INLIER, NORTHERN MAINE

Adam Schoonmaker
Department of Geology, Utica University 1600 Burrstone Road, Utica, NY 13502. adschoon@utica.edu

INTRODUCTION

This trip repeats some of the stops conducted during an NEIGC trip in 2013 (B6) but includes new geochemical data, structural data, and addresses the implications of these for the tectonic history of the Caucomgomoc Lake inlier.

The Caucomgomoc Lake inlier is made up of four probable Cambrian to Ordovician metasedimentary and metavolcanic formations including mélange (Fig. 1). Beyond early reconnaissance studies, they were first mapped in detail by Raabe (1977) and more thoroughly studied, formally named, and mapped by Pollock (1982, 1983, 1985a, 1985b, 1989). They generally form north-south striking units, in part separated by faults, and generally dip steeply to the west. In structural order, from east to west (bottom to top), they include the Loon Stream, Caucomgomoc Lake, Hurd Mountain, and Avery Brook formations that are probably reshuffled by thrusting (Pollock, 1989). These pre-Silurian units are bounded on all sides by younger sedimentary units of the Seboomook, Allagash Lake, Northeast Carry, Ironbound Mountain, and Frontenac formations.

While no fossil or isotopic ages have been determined for the pre-Silurian units, they have been correlated, based on lithologic similarity, with rocks in other northern Maine inliers, including the Lobster Mountain, Weeksboro-Lunksoos, Munsungun, and the Chesuncook Dome (Boone et al., 1984, Pollock, 1989; Boone et al., 1989; Fig. 2). Pollock (1989) correlated the Avery Brook and Caucomgomoc Lake formations with the Jim Pond Formation, the Hurd Mountain Formation with the Hurricane Mountain Formation and part of the Dead River Formation, and the Loon Stream Formation with part of the Dead River Formation (Fig. 3). The Caucomgomoc Lake inlier is the northwestern-most of the Cambro-Ordovician inliers in Maine.

The Hurd Mountain mélange of Pollock (1989) is composed of a disrupted part of the Hurd Mountain Formation and the Avery Brook Formation. It is correlated with the Hurricane Mountain mélange and Chase Brook Formation (Boone et al., 1989) and has been proposed to represent a segment of the suture between Gander terrane to the southeast and Boundary Mountain terrane to the northwest (Boone et al., 1989; Pollock, 1989). The Caucomgomoc Lake inlier lies somewhat off-strike from the other Maine inliers (Fig. 2), but shares much lithologic similarity and deformation style with those inliers, so a direct connection may occur beneath the intervening Devonian cover rocks. Alternately, Pollock (1989) suggested that the off-axis position might represent a stepping-back of an east-dipping subducting slab from a trench position in which the Hurricane Mountain Formation formed, to one in which the Hurd Mountain and Chase Brook mélanges were formed separately.

This field trip focuses on the mélange of the Hurd Mountain and Avery Brook formations (Hurd Mountain mélange), although a brief visit to the younger Allagash Lake will be made. Specifically, the trip will examine the evidence for a mélange interpretation for the Hurd Mountain and Avery Brook formations; the evidence for syntectonic emplacement of metabasalts and metagabbros in the Hurd Mountain Formation; and discuss the geochemical compositions of the Avery Brook greenschist and mafic igneous blocks in the Hurd Mountain Formation, and structural evolution of the Caucomgomoc Lake inlier.

STRATIGRAPHY

The stratigraphy is described in structural order from lowest to highest, not necessarily in chronological order, and is based on descriptions by Pollock (1985, 1989) and supplemented by observations of the author.

Loon Stream Formation

The Loon Stream Formation is divided into lower metasedimentary and upper mélange/olistostromal parts. The lower metasedimentary part is dominantly green/gray/red slate, phyllite and metasiltstone with local buff-weathering tuffaceous laminae and minor metawacke. The upper part was interpreted by Pollock (1989) as either an olistostromal unit or mélange and is composed of a slate matrix with inclusions similar to rocks of the lower part, with the exception of rare metarhyolite in the mélange. If the upper part is mélange, then the upper contact of the Loon Stream Formation is likely to be a thrust contact with the base of the Caucomgomoc Lake Formation. If olistostromal, then the structurally

higher Caucomgomoc Lake Formation may be conformable over the Loon Stream Formation. In this case, it would be younger than the Loon Stream Formation in contradiction to the interpretation in Figure 3.

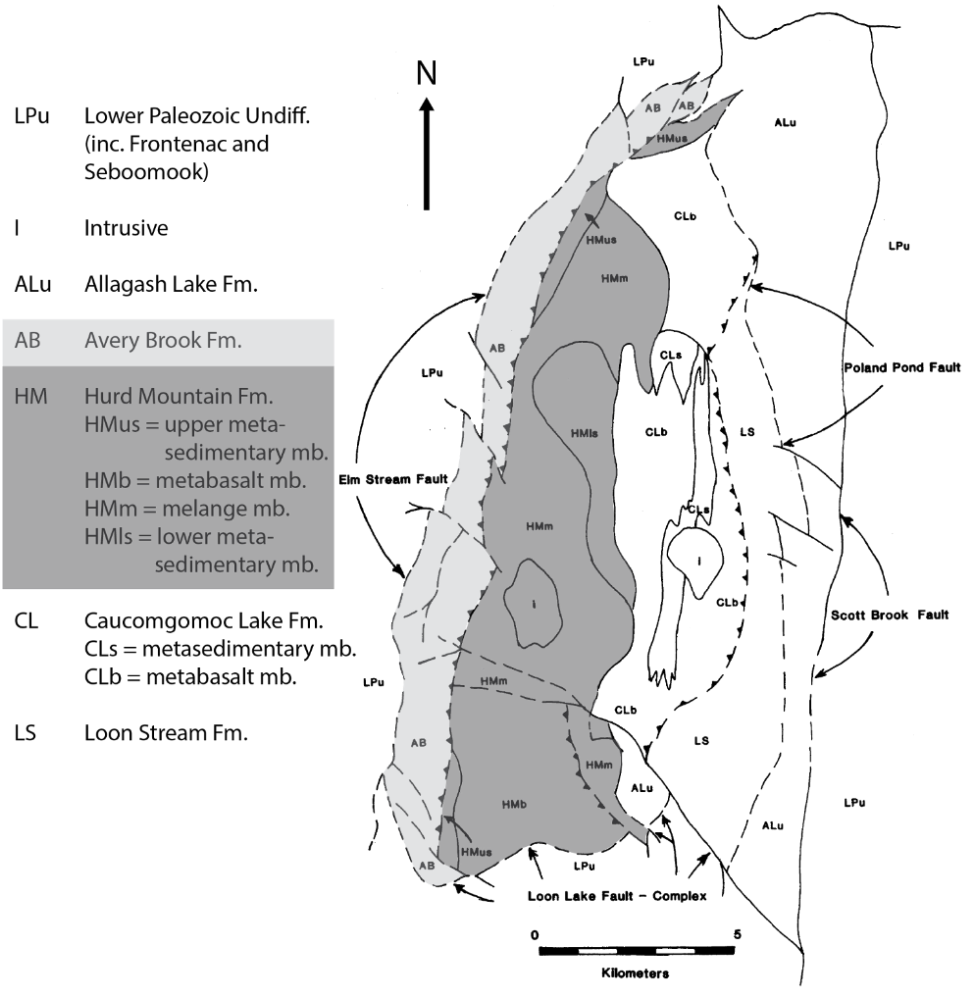

Figure 1. Geologic map of the Caucomgomoc Lake area (modified from Pollock, 1989).

Caucomgomoc Lake Formation

The Caucomogomoc Lake Formation is dominantly metabasalt with some quartz and feldspar metawacke members that contain interbeds of slate and phyllite. The metawacke horizons contain minor olistostromal sections with inclusions of metawacke and metabasalt. The metabasalts are green/gray pillowed basalts with some agglomerates and tuffs.

Hurd Mountain Formation

The Hurd Mountain Formation is a slate-phyllite-meta-quartz arenite-metawacke mélange with numerous blocks and inclusions. Pollock (1989) assigned these rocks to a trench/slope depositional environment that underwent deformation in an active accretionary prism. It contains a thick, internal metabasalt section and a lower non-mélange section of interbedded metasandstone and metabasalt. The metabasalts are phyric and aphyric pillowed greenstone and agglomerates. The mélange section is dominantly a pervasively sheared and disrupted phyllite with meta-arenite horizons, and contains numerous blocks and inclusions of metasandstone, meta-limestone, metabasalt, and metagabbro/diabase. Blocks range in size from centimeter-scale inclusions up to several meters in size. Metadiabase and metabasalt intrusions occur in the mélange matrix, some also intruding metagabbro blocks. The Avery Brook Formation is in fault contact with, and above the Hurd Mountain Formation that Pollock (1989) inferred as a thrust. Collectively, the mélange part of the Hurd Mountain Formation and the Avery Brook Formation are the Hurd Mountain mélange (Pollock, 1989).

Avery Brook Formation

The Avery Brook Formation is a thick (+1000 m) slab of greenschist composed of chlorite-plagioclase-epidote greenschist. The greenschists are strongly deformed with a well-developed schistose foliation. Pillows are evident in some outcrops where flattening has not completely obliterated them, and epidote is ubiquitous. Although the Avery Brook is included with the Hurd Mountain Formation in the Hurd Mountain mélange, the metabasalts of the Avery Brook Formation differ from Pollock's (1989) lower metabasalt slab and with knockers and intrusions in the Hurd Mountain Formation in the intensity of their deformation. Volcanic structures are common in the Hurd Mountain but uncommon in the Avery Brook and epidotization is ubiquitous in the Avery Brook. If the Avery Brook greenschists are part of a lower, fault-separated unit (as indicated in Fig. 3), then they are possibly deformed equivalents to the Caucomgomoc Lake metabasalts or the metabasalt section of the Hurd Mountain Formation.

Intrusive Rocks

Two intrusive stocks, approximately 2 km across occur in the Hurd Mountain and Caucomgomoc Lake formations (Fig. 1). Pollock (1989) reported evidence of differentiation and they range in composition from metagabbro/pyroxenite to hornblende monzodiorite. Typically, the mafic minerals are mostly recrystallized to chlorite. They cut contacts of members in the Caucomogomoc Lake Formation, but are also weakly deformed and interpreted to be late syntectonic intrusions (Pollock, 1989).

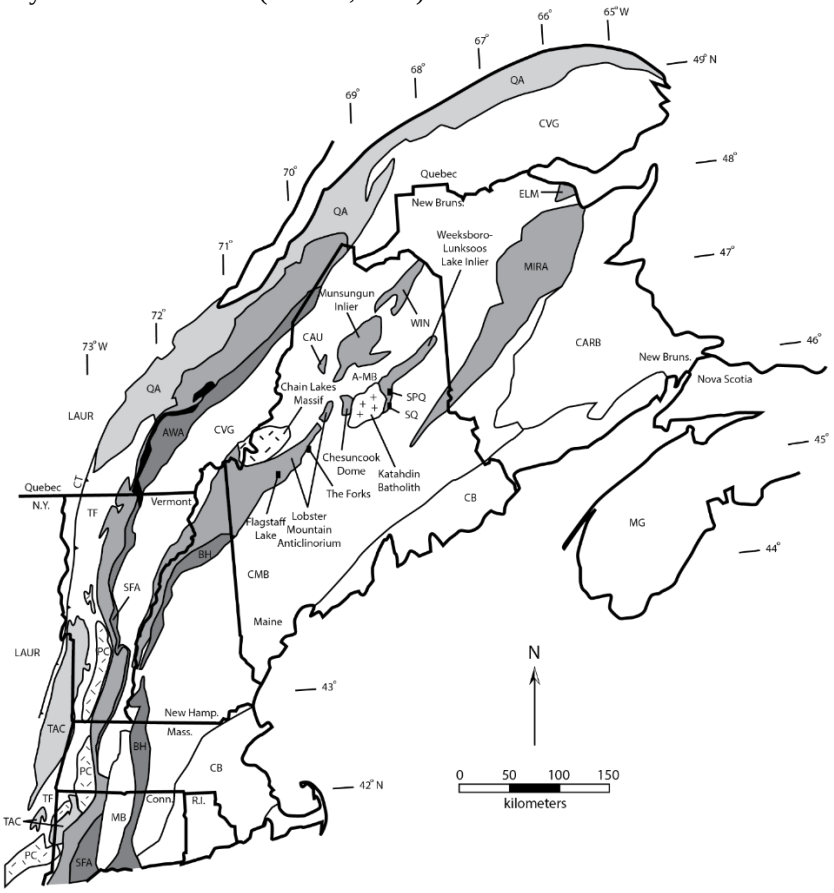

Figure 2. Generalized geology of the northern Appalachians. Pre-Late Ordovician units are shaded. LAUR=autochthonous Laurentian margin, QA=Quebec Allochthons, TAC=Taconic Allochthons, TF=transported Laurentian margin and basin deposits, PC=Precambrian massifs, SFA-AWA=Shelburne Falls arc, Ascot-Weedon arc, and related oceanic rocks, including ophiolitic fragments (black), MB=Mesozoic basin, CVG=Connecticut Valley Gaspe Synclinorium, BH=Bronson Hill Arc, CAU=Caucomgomoc inlier, A-MB=Aroostook-Matapedia belt, SPQ=Shin Pond quadrangle, SQ=Stacyville quadrangle, WIN=Winterville inlier, MIRA=Miramichi Highlands, CMB=Central Maine belt, ELM=Elmtree-Belledune inlier, CARB=Carboniferous cover rocks, CB=Coastal belt, MEG=Meguma terrane. Adapted from Williams (1978), Osberg et al. (1985), Robinson et al. (1998), and Schoonmaker et al. (2011).

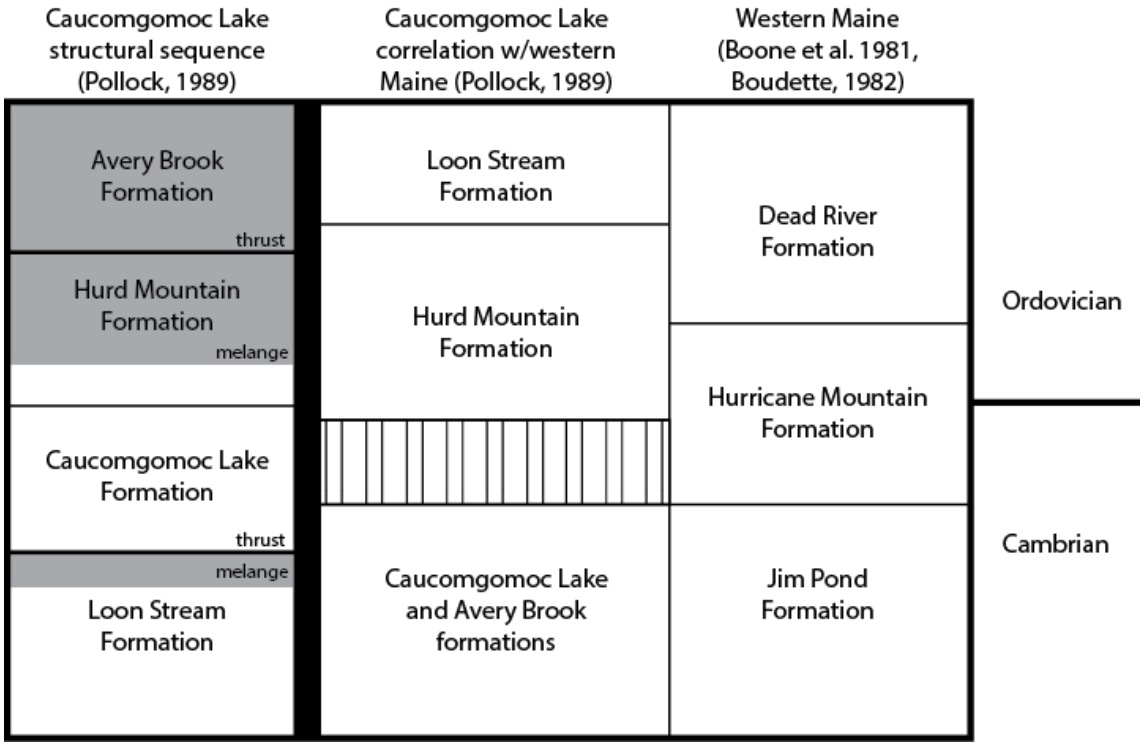

Figure 3. Pollock's (1989) correlation of pre-Silurian Caucomgomoc Lake inlier units with those of western Maine, relative to the current structural order. Shaded areas are mélange: upper shaded area = Hurd Mountain mélange, lower shaded area = Loon Stream mélange. Olistostromes in Caucomgomoc Lake Formation not illustrated.

GEOCHEMISTRY OF VOLCANIC AND INTRUSIVE ROCKS

Major, trace, and rare earth element (REE) concentrations of seven samples of Avery Brook greenschists, 13 samples of metabasalt/metagabbro blocks in the Hurd Mountain Formation, and three intrusives were determined by XRF and ICP-MS. Because all of the rocks analyzed have been exposed to greenschist grade metamorphism (typical metamorphic assemblages include chlorite-plagioclase-epidote-actinolite-clinozoisite; pumpellyite was also reported by Pollock, 1989), only the immobile trace elements and REE are discussed here. In thin-section, remnant igneous plagioclase, pyroxene, and olivine are present in both Hurd Mountain inclusions and Avery Brook greenschists, although they are better preserved in the Hurd Mountain inclusions. All samples, except the intrusives, plot as basalts on the classification diagram of Winchester and Floyd (1977; Fig. 4).

Chondrite- and MORB-normalized diagrams of Hurd Mountain and Avery Brook samples are shown in Figure 5 and it is evident that the Hurd Mountain and Avery Brook samples are quite similar. Both show moderately enriched, flat patterns with a slight enrichment in LREEs on the chondrite-normalized diagrams and resemble E-MORB. On the MORB-normalized diagram, patterns also show a slight negative slope, but are enriched in Th, La, and Ce relative to Ta and Nb, creating a negative Nb anomaly typical of samples from volcanic arcs.

On tectonic diagrams where arc and MORB/EMORB fields overlap, most samples plot in the overlap fields (Fig. 6). However, on tectonic diagrams that discriminate between arc and MORB environments, conflicting interpretations of arc (Fig. 7b and 7c) and MORB (Fig. 7a and 7d) can be made. This conflict is also seen for other Cambrian-Ordovician basalts from the other inliers of northern Maine, including the Dry Way Volcanics, Bean Brook Gabbro of the Chesuncook Dome, Lobster Mountain Volcanics of the Lobster Mountain Anticlinorium, Munsungun Lake and Bluffer Pond Formations of the Munsungun inlier and Stacyville Volcanics of the Weeksboro-Lunksoos Belt. For the Chesuncook Dome rocks, this is explained by ridge subduction (Schoonmaker and Kidd, 2006).

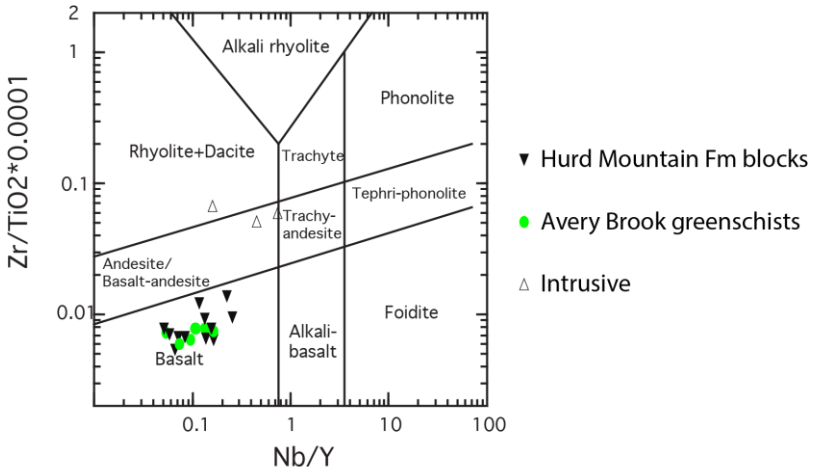

Figure 4. Rock classification diagram of Winchester and Floyd (1977) using immobile Zr/Ti vs. Nb/Y.

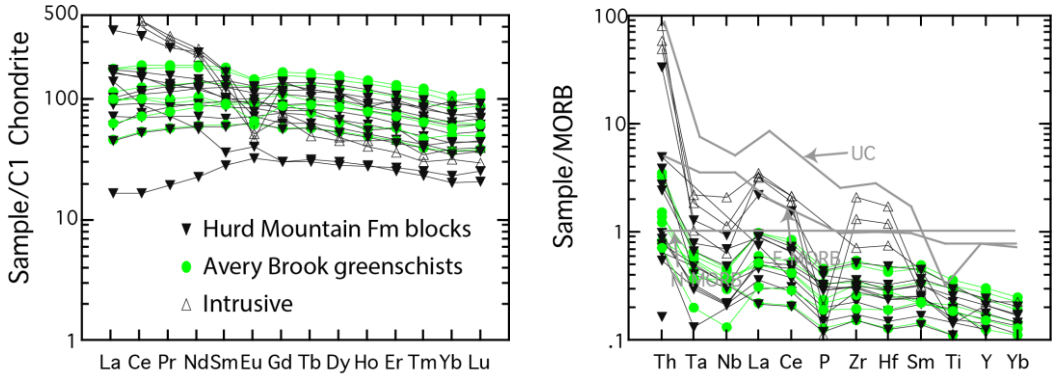

Figure 5. Chondrite- and MORB-normalized diagrams for metabasalt and metagabbro inclusions in Hurd Mountain Formation and Avery Brook greenschists. UC = upper crustal composition (McLennan, 2001), N-MORB = normal, depleted mantle-derived mid-ocean ridge basalt composition (Sun and McDonough, 1989), E-MORB = enriched mid-ocean ridge basalt (Sun and McDonough, 1989). Normalization values from Sun and McDonough (1989).

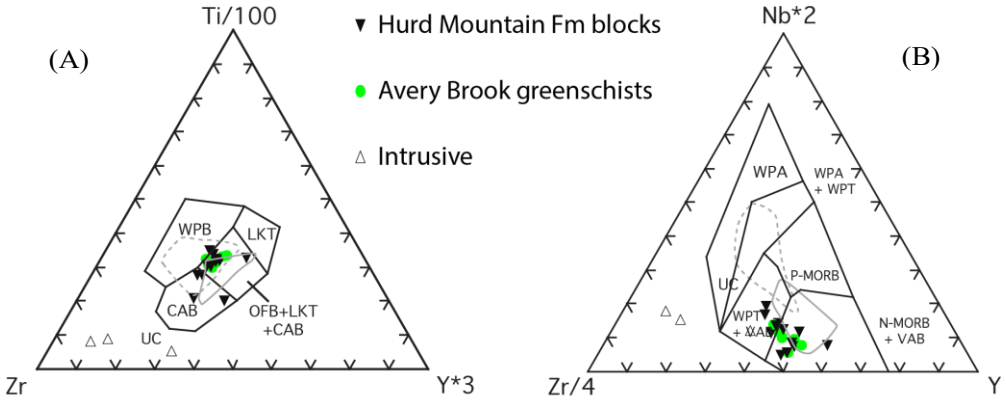

Figure 6**.** A) Ti-Zr-Y diagram of Pearce and Cann (1973). WPB = within plate basalts (oceanic and continental), OFB = ocean floor basalts, LKT = low-K tholeiites, CAB = calc-alkaline basalts. B) Nb-Zr-Y diagram of Meschede (1986). WPA = within-plate alkaline basalts, WPT = within-plate tholeiites, P-MORB = plume-influenced mid-ocean ridge basalt, N-MORB = normal, mid-ocean ridge basalt, VAB = volcanic arc basalt. CC = average upper continental crust composition from McLennan (2001). Solid gray line = Chile Ridge and Chile margin basalts (Klein and Karsten, 1995).

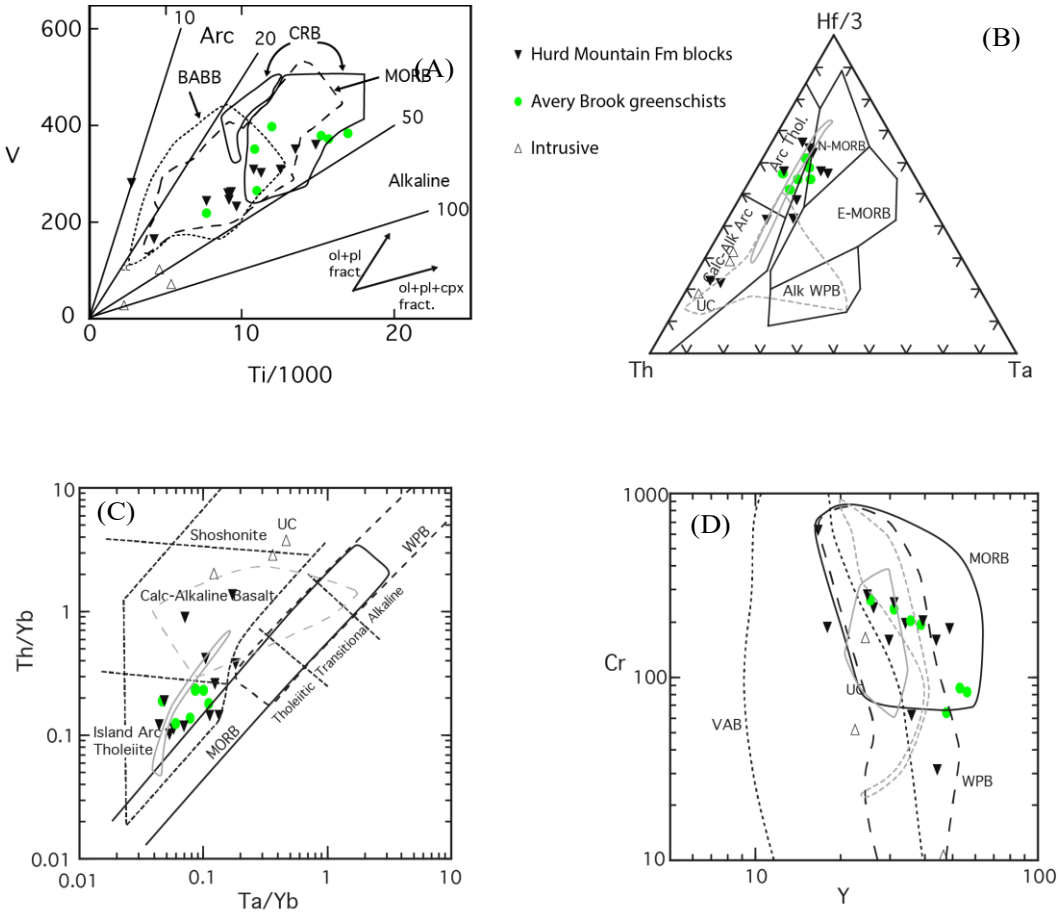

Figure 7. A) Ti-V diagram of Shervais (1982). ARC = volcanic arc basalt, MORB = mid-ocean ridge basalt, ALK WPB = alkaline within-plate basalt, BABB = back-arc basin basalt field, CRB = Columbia River flood basalt field. B) Th-Hf-Ta diagram of Wood (1980). Calc-Alk Arc = calc-alkaline volcanic arc basalt, Arc Thol = volcanic arc tholeiite, N-MORB = normal, depleted mid-ocean ridge basalt, E-MORB/WPT = enriched mid-ocean ridge basalt and within-plate tholeiite, Alk WPB = alkaline within-plate basalt. The two arc subfields are collectively referred to as the "destructive margin and differentiates" field, separated by the dashed line. C) Th/Yb-Ta/Yb diagram of Pearce (1982). MORB = mid-ocean ridge basalt, WPB = within-plate basalt, TH = tholeiitic basalts, ALK = alkaline basalts, TR = transitional basalts, IAT = island arc tholeiite field, CAB = calc-alkaline basalt field, SHO = shoshonitic basalt field. D) Cr-Y diagram of Pearce (1982), VAB = volcanic arc basalt, MORB = mid-ocean ridge basalt, WPB = within-plate basalt. CC = average upper continental crust composition from McLennan 2001. Solid gray line = Chile Ridge and Chile margin basalts (Klein and Karsten, 1995).

STRUCTURAL RELATIONSHIPS

The dominant structure seen in outcrops within the field area is a penetrative cleavage that locally includes compositional banding. In the greenschists of the Avery Brook Formation, this also includes flattened pillows and stretched plagioclase and epidote amydules. In the Hurd Mountain Formation, it is typically a slaty to phyllonitic cleavage and in some cases is mylonitic. Some arenaceous horizons are interpreted to be metamorphosed sandy beds and are parallel to the foliation. Foliation orientations are shown in Figure 8. Overall, foliations dip moderately to steeply to the west. Mineral lineations are often present on cleavage surface and plunge to the west (Fig. 8).

Pollock (1989) interpreted the strong deformation pattern in the Avery Brook Formation and parts of the Hurd Mountain Formation as mélange. Abundant exotic blocks (knockers) within the Hurd Mountain Formation support this conclusion. They include basalt and diabase, gabbro, and, in at least one case, limestone. Often, cleavage in the Hurd Mountain slates and phyllites wraps around blocks and, in some cases, there is a foliation present in the margins of the blocks. In many locations within the area mapped as Hurd Mountain, outcrop-scale whalebacks and oblate

outcrops of gabbro occur that are interpreted to be erosionally resistant knockers surrounded by the erosionally weak Hurd Mountain slates (under soil cover). Additionally, while many occurrences of gabbro occur as knockers in the Hurd Mountain schists, some outcrops show undeformed diabase and gabbro intruding the schists. Geochemically, these are similar to the knockers and suggests that intrusion of mafic rocks was broadly contemporaneous with deformation of the mélange.

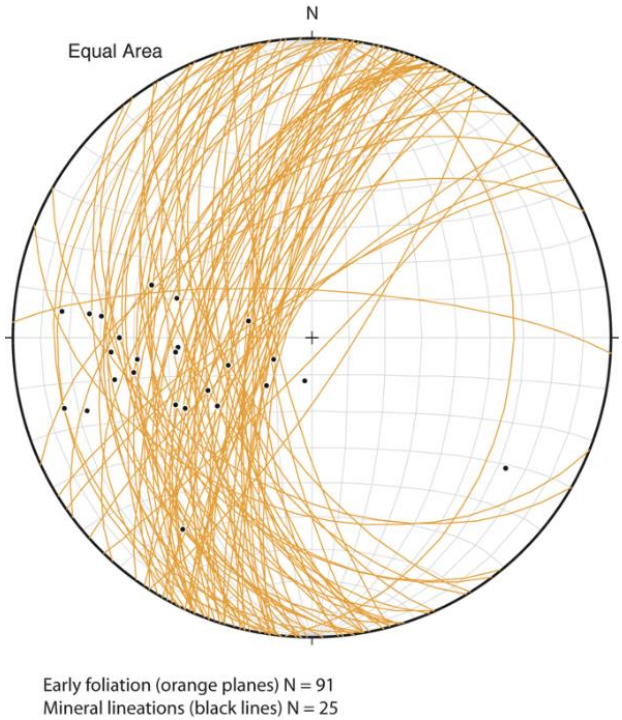

Figure 8. Orientation of slaty cleavage and compositional banding in Hurd Mountain and Avery Brook formations. Black dots represent mineral lineations in the plane of foliation. Shear sense indicators are present in the mylonites of the Hurd Mountain and Avery Brook Formations; mesoscopic shear sense indicators were measured in the field in addition to 25 oriented thin-sections that were analyzed by Frisa and Schoonmaker (2022). Mesoscopic shear sense indicators in the Avery Brook are typically sigma-type asymmetric porphyroclasts (often epidote amygdules). In the Hurd Mountain mylonites microscopic sigma-type porphyroclasts, C-S fabrics, asymmetrical folds, and mica fish are present. Shear sense is consistently down-dip of the penetrative cleavage and is normal (west-side down).

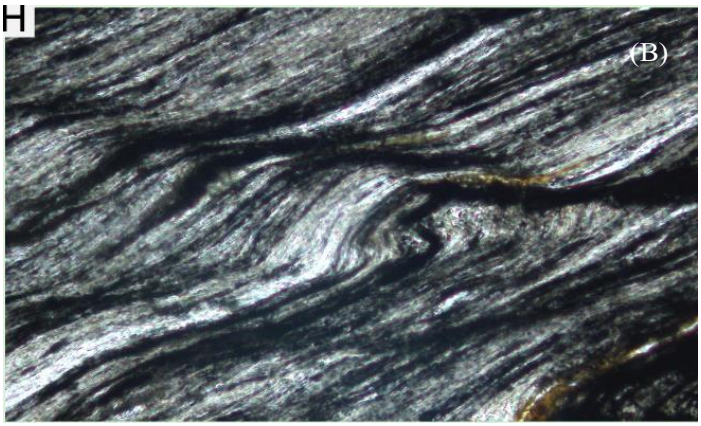

Figure 9. A) sigma-type porphyroclast in the Avery Brook Formation (looking north). B) C-S fabric in Hurd Mountain mylonite (looking south).

Also present are younger, presumably Acadian, open-to-tight folds that deform the penetrative cleavage and compositional banding (Fig. 10). These folds resemble those seen in the turbidites of the surrounding Seboomook Formation. These folds indicate that several tens of degrees of rotation of older structures, like the cleavage and foliation in the Hurd Mountain and Avery Brook formations, may have occurred.

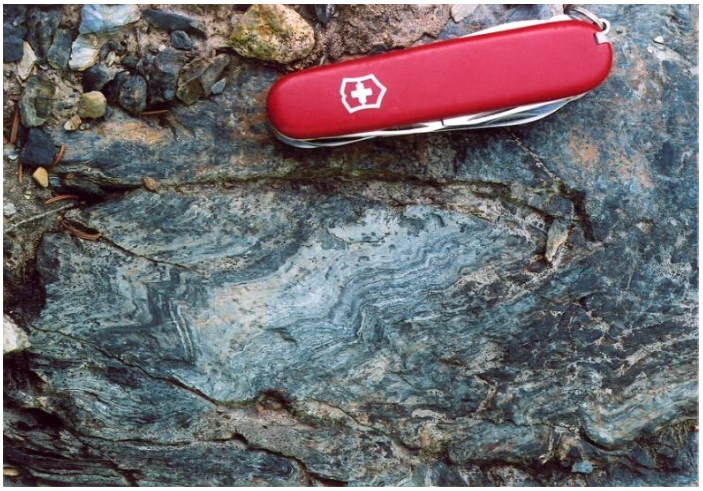

Figure 10. Acadian folds in Hurd Mountain slate.

DISCUSSION

Overall, these rocks show good geochemical similarity with those of the other northern Maine inliers, including the Chesuncook Lake area where Cambro-Ordovician volcanics and gabbro (Bean Brook Gabbro) have been interpreted to be the result of ridge subduction (Schoonmaker and Kidd, 2006). During ridge subduction, MORB-like mafic volcanism and plutonism occurs within an actively deforming accretionary prism, resulting in both intrusive and fault contact relations between the volcanic/plutonic rocks and the deforming trench and slope deposits. The magmatic rocks have typical MORB chemistries, but show evidence of contamination by arc fluids (Klein and Karsten, 1995) resulting in conflicting tectonic interpretations on standard tectonic discrimination diagrams. As a means of comparison, the field outlined by the gray solid line in Figures 6a, 6b, 7b, 7c, and 7d represents selected Chile Ridge and Chile Margin basalts that are related to modern ridge subduction in South America. The Caucomgomoc Lake samples have similar chemical compositions to those rocks suggesting that hypothesis may be also applicable here.

Schoonmaker and Kidd (2006) suggest an alternative hypothesis: that these rocks formed in a backarc basin. Backarc basin basalts typically show chemical compositions that vary between arc and MORB, as these do. In the tectonic discrimination diagrams shown in Figure 7, backarc basin basalts plot in overlap fields with MORB and/or

volcanic arcs. The tectonic diagrams in Figure 11 discriminate between basalts from MORB, arc, and backarc basins. Here, both the Avery Brook and Hurd Mountain inclusions plot in the backarc basin fields. However, because it can be demonstrated that the Hurd Mountain inclusions intruded into an actively deforming mélange, subsequent collapse of such a backarc basin would be probable.

Tentatively, two possible tectonic models involving subduction polarity previously proposed may explain the evidence from the Caucomgomoc Lake inlier. Boone et al. (1989) and Pollock (1989) proposed that mélange formation occurred above an east-dipping subduction zone, consistent with the model of van Staal et al. (2016). Schoonmaker and Kidd (2006, 2013) described a west-dipping subduction system during ridge subduction for the Chesuncook Lake area. The two possible settings (ridge subduction or backarc basin creation and collapse) are evaluated below in the context of subduction polarity.

Given the primary evidence from the Caucomgomoc Lake inlier (mélange formation with contemporaneous mafic intrusions), it seems most likely that the Hurd Mountain and Avery Brook mafic rocks formed during ridge subduction. This would allow mafic magmatism with both MORB and arc chemical characteristics to be intruded into an actively deforming fore-arc accretionary prism. Subduction polarity is irrelevant in this case and could occur in either direction. One wrinkle occurs in the off-axis position (to the northwest of strike) of the Caucomgomoc Lake inlier relative to the other northern Maine inliers. Pollock (1989) suggested that two consecutive subduction systems could have been involved, where the initial subduction associated with the Hurricane Mountain mélange stepped back, forming a second, off-axis subduction system associated with the Hurd Mountain mélange. If the syn-deformational intrusions within the mélange are the result of ridge subduction, then this would need to occur in both systems (Caucomgomoc Lake and Chesuncook Lake).

In a west-dipping subduction system, a backarc basin model for the Caucomgomoc Lake rocks is possible. If the Hurricane Mountain Anticlinorium and Chesuncook Dome represent the locus of arc activity to the southeast, then the Caucomgomoc Lake inlier (and possibly the Chase Brook mélange as well) is located in a backarc position. According to this hypothesis, backarc rifting resulted in the formation of the volcanic and metasedimentary rocks of the Caucomgomoc Lake inlier, but was quickly followed by collapse and disruption of backarc sediments and volcanics of the Hurd Mountain and Avery Brook formations. This also would suggest that arc rocks lie buried beneath the Devonian cover rocks between the Caucomgomoc Lake and Lobster Mountain inliers. In an east-dipping model, the position of the Caucomgomoc Lake inlier places it well towards a fore-arc rather than a backarc position, so if the model of van Staal et al. (2016) is accepted, then it is hard to assign a back-arc setting for these rocks.

If we consider the orientation of foliations developed during mélange formation we might discard a west-dipping subduction model. Currently, foliations in the mélange are moderately, to steeply west-dipping, with a normal sense of shear. If later Acadian folding had rotated these rocks, they might have originated in an east-dipping position and the sense of shear would then be reverse (east-over-west). This model is consistent with that of van Staal et al. (2016) and a ridge subduction explanation best explains the mélange of the Caucomgomoc Lake inlier.

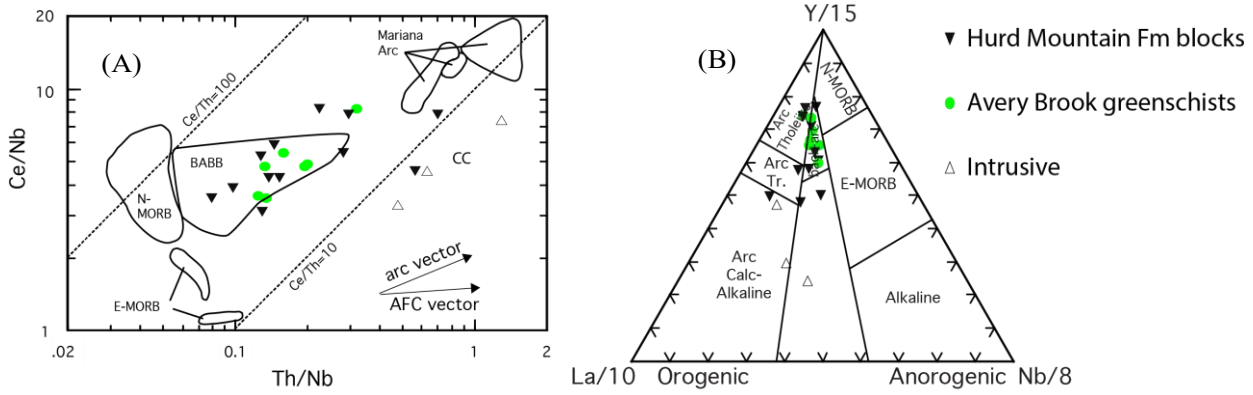

Figure 11. A) Ce/Nb vs. Th/Nb diagram of Saunders and others (1988). N-MORB = depleted mid-ocean ridge basalt field, E-MORB = enriched mid-ocean ridge basalt field, BABB = back-arc basin basalt field. CC = average upper continental crust composition (from McLennan, 2001). B) Y-La-Nb diagrams of Cabanis and Lecolle (1988). Anorogenic mantle array basalts plot on the right-hand side and volcanic arc and calc-alkaline basalts plots along left. Backarc basin basalts (BABB) plot in small intermediate field between orogenic and anorogenic fields.

ROAD LOG

IMPORTANT: *This trip is about 175 miles in length and will take participants deep into the Maine North Woods along potentially muddy and rough dirt roads. If logging operations are not occurring in the area, few to no other persons will be encountered if assistance is needed. No services, including cell service, are available in the Caucomgomoc Lake area. Vehicle fuel tanks MUST be full before starting. It is strongly advised that more than one spare tire, tire plugs, tire pump, and tire jacks be included in vehicles. Towing chains/straps and "come-along" (hand cable puller) are also recommended. Food for the day should be purchased in advance, although potable water and a primitive restroom are available at Caucomgomoc Lake campground. Many roads in the North Maine Woods are unmarked, and there are many side-tracks that can be confusing. A good map of northern Maine is strongly suggested (Maine Atlas and Gazetteer, for example) and a GPS unit is critical if participants become separated.*

Once on the Golden Road, and everywhere in the Maine North Woods, PULL OVER AS FAR TO THE RIGHT AS YOU CAN WHEN APPROACHED BY LOGGING TRUCKS. You will be on private timber company-owned roads and logging trucks have the right-of-way. They will typically drive down the center of the road at relatively high speed and you are expected to move out of their way! Particular care should be exercised when approaching blind turns.

Stop locations are shown in Figure 12.

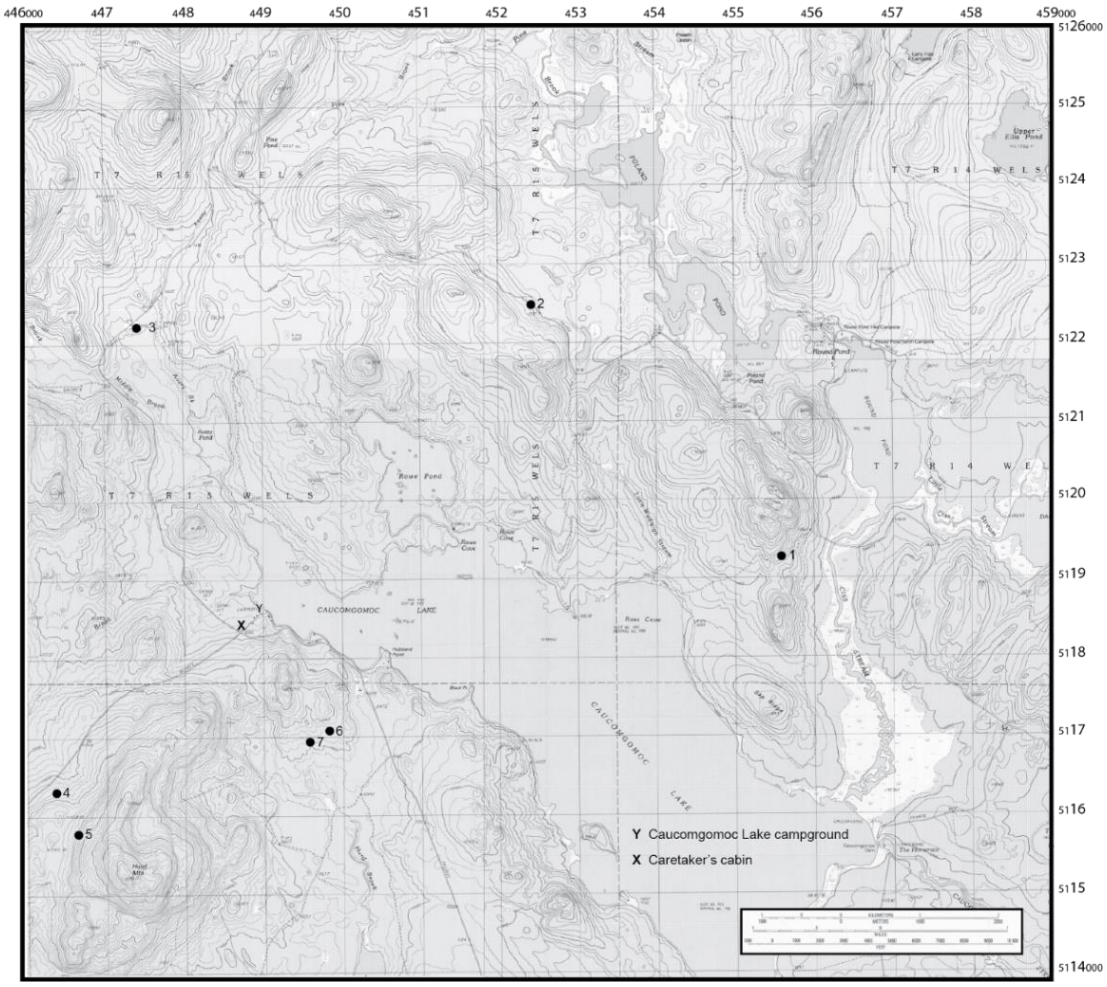

Figure 12. Stop location map. Parts of Caucomgomoc Lake West, Caucomgomoc Lake East, Wadleigh Pond, and Allagash Lake USGS 7.5' quadrangles shown (UTM coordinates, NAD83 datum).

Meeting time and place: 7:00 am, Sunday October 9 at the Ashland One Stop, intersection of Presque Isle Road (Rt. 163) and Main St (Rt. 11), Ashland, ME. Gasoline and food are available. It is strongly recommended to fill or top off gas tanks here. Depart 7:30 am.

Mileage		
Cum.	**Incr.**	
0.0	0.0	Turn left onto Main St (Rt. 11) and proceed to intersection with Frenchville Rd/Station St.
0.3	0.3	Turn left onto Station St (Rt. 11).
1.1	0.8	Turn left onto Garfield Rd after passing the bridge.
1.7	0.6	Turn right onto American Realty Rd that soon becomes a dirt road, a major logging road in NMW.
6.5	4.8	Stop at ***Six Mile Gate*** (North Maine Woods checkpoint).
6.6	0.1	Continue past the gate and bear left onto Pinkham Road
53.1	46.5	Turn left onto Telos Road.
63.6	10.5	Turn right on Umbazookus Road.
66.7	3.1	Road turns into Longley Stream Road – continue straight.
69.9	3.2	Turn right at Y-intersection onto Grand Marche Road
77.9	8.0	Stay right on Grande Marche/Shallow Lake Road
80.3	2.4	Turn left onto Ledge Road.
82.7	2.4	Take right at Y-intersection to stay on Ledge Road (not Old Ledge Road).
91.6	8.9	Continue past Guy Allen Road on right (19T 456087 E, 5120290 N) – road becomes single lane. If trucks are present, be prepared to back out.
92.0	0.4	Take right at Y-intersection.
92.4	0.4	Pull over at active road metal quarry on right.

STOP 1. ALLAGASH LAKE FORMATION (19T 455607 E, 5119190 N): This pit exposes what Pollock (1989) mapped as the Allagash Lake Formation. Here, it is fine-grained green and red slate, and a massive forest-green greenstone is in apparent conformable contact with the slate near the entrance on the right. Near the contact with the greenstone is a folded, arenaceous, graded bed. The slate here bears a strong similarity to the Frost Pond Shale in the Chesuncook Dome and contains greenstones similar to the West Branch Volcanics of earliest Devonian age.

Return back the way we came to the intersection with Guy Allen Road.

93.2	0.8	Turn left on Guy Allen Road.
96.2	3.0	Pull over at active road metal quarry on left.

STOP 2. BLOCKS IN HURD MOUNTAIN FORMATION (19T 452412 E, 5122531 N): In 2013, logging companies began actively mining this pit for road metal. The material used is the highly foliated slate/phyllite of the mélange section of the Hurd Mountain Formation. Within the quarry and along its walls, several blocks of metasedimentary beds and metabasalts may be found in the phyllite, depending on recent excavations. The block illustrated in Figure 13 is no longer present, but new ones may be exposed. These blocks illustrate the mélange-like nature of the Hurd Mountain Formation. Also, in 2013, a pavement near the road exposed a block of limestone that no longer is present.

Figure 13. Metabasalt block in the Hurd Mountain Formation (unfortunately, block has since been removed by mining activity). Block is the lozenge-shaped mass in the center of the photo and directly above the dark mass of phyllite behind the hammer handle. The contact between the phyllite and the bottom of the block is about 1' above the end of the hammer handle.

Continue west on Guy Allen Road.

99.2	3.0	Turn left onto Caucomgomoc Road (19T 448339 E, 5124240 N).
101.5	1.3	Turn left into an old quarry.

STOP 3. AVERY BROOK FORMATION (19T 447367 E, 5121305 N): In this gravel pit, a large lobate block of Avery Brook-like greenschist is present. It is not clear if this is part of the main mass of the Avery Brook that makes up the prominent ridge on the other side of the road, or is a block in the Hurd Mountain mélange. The strong degree of deformation and epidote growth is identical to other outcrops of Avery Brook although the block appearance of this exposure in the quarry is characteristic of other metagabbro blocks in the Hurd Mountain mélange.

Facing the large exposed face of the outcrop, along the left side (NW) a prominent epidote knot deformed into a sigma-type asymmetric porphyroclast can be found indicating west-side down (normal) sense of motion (Figure 14). Other, similar type shear sense indicators can be found in the Avery Brook Formation. Unlike the Hurd Mountain shear sense indicators, these are usually unequivocal and all indicate a west-side-down (normal) sense of shear.

Figure 14. Sigma-type asymmetric porphyroclast developed from epidote knot. Porphyroclast is approximately the same size as hammer head and occurs directly adjacent to the rock fragment directly underneath the hammer head. Foliation dips to the west and view is to the north. Foliation orientation: 17°, 83° W.

Continue south on Caucomgomoc Road.

104.4	2.9	Turn left at intersection with Russell Mountain Road (old caretaker cabin on corner, 19T 448753 E, 5118353 N). *NOTE: This is the only practical source of potable water on this trip.*
104.6	0.2	Caucomgomoc Lake Campground. LUNCH BREAK.
104.8	0.2	Return to Caucomgomoc Road. Continue straight through intersection onto Russell Mountain Road.
106.7	1.9	Top of rise, park at woods track on left. Walk up woods track (east).
	0.1	Large outcrop on right side of track.

STOP 4. PILLOW LAVAS OF THE AVERY BROOK FORMATION (19T 446322 E, 5116288 N): This outcrop displays a typical example of the Avery Brook Formation (Figure 15), a deformed chlorite-epidote-plagioclase schist that is ~1000 m thick. Epidote knots and veins are characteristic of the Avery Brook greenschists. Veins often create a skeletal framework through the rock. Careful examination of the outcrop reveals numerous pillow lavas flattened parallel to the dominant compositional foliation [N08E, 81W]. Pollock (1985) reported a sedimentary member containing metabasalt clasts that occurs along the eastern margin of the main greenschist belt, but within the belt only monotonous pillowed greenschists and greenstones have been observed.

Although there is no direct age determined for the Avery Brook, its structural position relative to the Hurd Mountain rocks directly to the east may provide clues to its relative age. Its position as the apparent down-dropped

block west of the west-dipping, metasedimentary rocks of the probably Cambrian to Ordovician-aged Loon Lake, Caucomgomoc Lake, and Hurd Mountain formations would indicate it may be younger than those units. Similarly, if the current west dip of the fault separating it from the Hurd Mountain has been rotated by younger deformation, then it becomes the lower block beneath overthrust Hurd Mountain rocks, again indicating that it is younger than those rocks. Pollock (1985) inferred that a west-dipping thrust between the Avery Brook and Hurd Mountain formation (Fig. 1) would suggest it is older.

There is no throw determination for the fault contact with the Hurd Mountain Formation to the east and the similarity in geochemistry of these rocks with the metabasalts and metagabbro blocks in the Hurd Mountain mélange suggests they are likely related and of broadly similar ages.

Figure 15. Deformed Avery Brook greenschists. Visible veins are epidote. Photo courtesy W. Kidd.

Continue east up woods track.

0.5 Large outcrop on the left scraped by lumber road building equipment.

STOP 5. HURD MOUNTAIN FORMATION (19T 446645 E, 5115784 N): Pollock (1985; 1989) described the western part of the Hurd Mountain Formation as mélange (along with the Avery Brook Fm). Typically, it is composed of dark gray slate or phyllite with thin siliceous zones. A strong cleavage and compositional bands are present, often with rusty weathering along cleavage surfaces. Siliceous bands occur, some the result of metamorphic recrystallization, but some of the thicker horizons (> few cm) were probably arenaceous beds. Pollock (1989) interpreted these rocks to be trench slope deposits incorporated into an accretionary prism. Some of the thicker arenaceous beds probably represent the coarser deposits (turbidites) occurring on the trench slope. The mélange contains numerous disrupted blocks of metabasalt, metadiabase, metagabbro, and thick-bedded sedimentary rocks. Blocks of magmatic rocks in the Hurd Mountain mélange differ from Avery Brook greenschists in two important ways: 1) Hurd Mountain metagabbros and diabase are usually only lightly deformed or undeformed (although locally, a strong shearing foliation can be observed), while Avery Brook greenschists show strong evidence of shear, shortening, and dynamic metamorphic recrystallization throughout, and 2) development of epidote knots and veins is characteristic of Avery Brook greenschists and is much less well-developed in Hurd Mountain blocks. Typically, gabbro blocks occur as more resistant lobate whalebacks in the softer metasediments. Metagabbros and metadiabase occur in both intrusive and sheared contact with the mélange indicating syn-deformational intrusion with some intrusion occurring during the later stages of deformation. In the lower part of this outcrop (NW end of scraped outcrop) diabase veins can be seen intruding highly foliated mélange and coarser metagabbro (Fig.16).

Diabase from this outcrop was sampled and its geochemical analysis is included in the geochemistry discussion above. The chemical composition of these blocks is similar to that of rocks from the Avery Brook Formation and other gabbro blocks within the Hurd Mountain Fm. This suggests that they may have been formed during the same tectonic event, and may be broadly coeval.

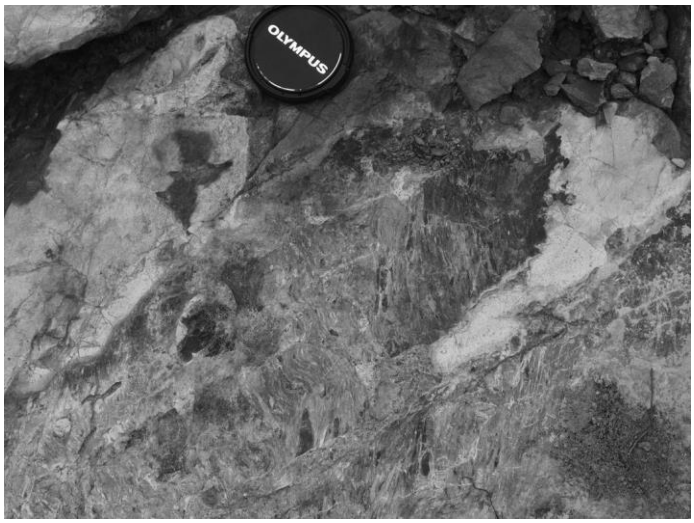

Figure 16. Diabase (light colored; upper left and right) intruding highly foliated dark gray phyllites of Hurd Mountain mélange (center and lower). Photo courtesy W. Kidd.

	0.6	Return back down woods track to vehicles. Turn around and return to intersection with Caucomgomoc Road.
108.6	1.9	Turn right onto Caucomgomoc Road.
109.8	1.2	Turn right onto truck trail (old yellow gate in the bushes on left). Continue along track.
110.4	0.6	Outcrops on the right in ditch.

STOP 6. MYLONITE IN THE HURD MOUNTAIN FORMATION (19T 449895 E, 5117104 N): All the Cambrian-Ordovician(?) units in the area are strongly deformed with a penetrative foliation and overlain by less deformed Seboomook, or Seboomook-like slates and turbiditic meta-arenites that do not contain the penetrative foliation, although a spaced cleavage is seen in the younger rocks. The penetrative cleavage is mylonitic in places (Figure 17 and 18). Macroscopic shear sense indicators in the Hurd Mountain Formation include asymmetric porphyroclasts, asymmetrical folds, and shear bands but are equivocal and have counter senses. However, a microscopic shear-sense analysis by a former student (Timothy Frisa), using oriented thin-sections, has found that they are the same as those seen in the Avery Brook Fm, that is, down-to-the-west (normal sense).

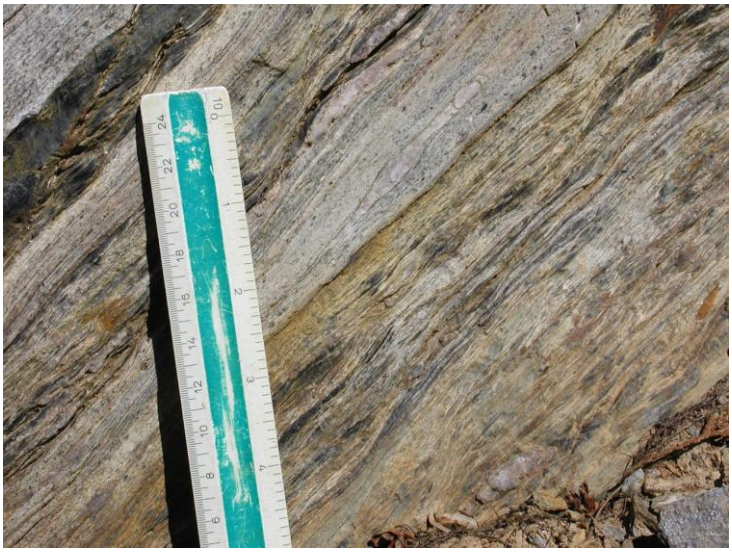

Figure 17. Mylonite in the Hurd Mountain Formation. View to the north.

Figure 18. Shearing in the Avery Brook Formation.

Continue forward (west) along track.

110.5 0.1 Park in log landing. Outcrop to the northwest.

STOP 7. PROBABLE ACADIAN FOLDS IN PRIMARY FOLIATION OF HURD MOUNTAIN INCLUSION (19T 449565 E, 5116987 N): This outcrop displays good, probably Acadian folding of the dominant foliation in a greenschist block within the Hurd Mountain mélange. These folds resemble other folds found throughout the field area and in graded beds of the Devonian Seboomook Formation found northeast of Caucomgomoc Lake (Bichrest and Schoonmaker, 2011). These younger folds suggest that the foliation orientation seen throughout the field area may have undergone some rotation. The dominant foliation that dips steeply to the west, with normal sense, down-to-the west shear sense indicators may have been rotated from an earlier, east-dipping orientation with reverse-sense, up-to-the-west shear sense. If this is the case then it is consistent with the interpretation of the Hurricane Mountain mélange of Boone et. al. (1989).

111.2 0.7 Turn around and return to Caucomgomoc Road.

From here, participants can turn left onto Caucomgomoc Road and return the way we came to Ashland. Or, turn right onto Caucomgomoc Road to exit at Millinocket or Greenville (closest for those concerned about gasoline). To do that, continue to Ragmuff Road (8.9 miles) and turn right onto Ragmuff Road and go 14.0 miles to the Golden Road. Then, turn left and go 11.8 miles to the Caribou gate. Then go 5.8 miles to the intersection with Greenville Road. Participants can either continue on the Golden Road to Millinocket (~36 miles), or take Greenville Road to Kokadjo (gasoline available, ~15 miles) and then on to Greenville (another ~18 miles).

End of Road Log.

REFERENCES

Bichrest, T. and Schoonmaker, A., 2011, A structural transect of the Seboomook Formation, Caucomgomoc Lake, northwestern Maine: Geological Society of America Program with Abstracts, v. 43, p. 148-149.

Boone, G.M., Boudette, E.L., and Moench, 1981, Geologic outline map of pre-Silurian stratigraphic units north-central Maine to northern New Hampshire: Geological Society of America Program with Abstracts, v. 13, p. 123.

Boone, G.M., Boudette, E.L., Hall, B.A., and Pollock, S.G., 1984, Correlation and tectonic significance of pre middle Ordovician rocks of northwestern Maine: Geological Society of America Program with Abstracts, v. 16, p. 4.

Boone, G.M., Doty, D.T., and Heizler, M.T., 1989, Hurricane Mountain Formation mélange: Description and tectonic significance of a Penobscottian accretionary complex, in Tucker, R.D., and Marvinney, R.G., eds., Studies in Maine geology, Volume 2: Structure and stratigraphy: Augusta, Maine Geological Survey, p. 33–83.

Bunyon, E. and Schoonmaker, A., Geochemical Study of Likely Cambrian or Orodovician Age Rocks of the Avery Brook Formation and an Unnamed Tonalite Near Caucomgomoc Lake, Northern Maine, Geological Society of America Northeastern Section Meeting, v. 51, p. 54-3.

Cabanis, B. and Lecolle, M., Le diagramme La/10-Y/15-Nb/8; un outil pour la discrimination des series volcaniques et la mise en evidence des processus de mélange et/ou de contamination crustale: Comptes Rendus de l'Academie des Sciences, Serie 2, Mecanique, Physique, Chimie, Sciences de l'Univers, Sciences de la Terre, 1989, Vol. 309, Issue 20, pp. 2023-2029.

Frisa, T. and Schoonmaker, A., 2022, shear sense micro-analysis of mélange in the Caucomgomoc Inlier, northern Maine, Geological Society of America Northeastern Section Meeting, v 54, p.

Klein, E.M. and Karsten, J.L., 1995, Ocean-ridge basalts with convergent-margin affinities from the Chile ridge: Nature, v. 374, p. 52-57.

McClennan, S.M., 2001, Relationships between the trace element composition of sedimentary rocks and upper Continental crust: Geochemistry Geophysics Geosystems, v. 2, paper no. 2000GC000109, 24 p.

Meschede, M. 1986, A method of discriminating between different types of mid-ocean ridge basalts and continental tholeiites with the Nb-Zr-Y diagrams: Chemical Geology, v. 56, p. 207-218.

Pearce, J.A. and Cann, J.R., 1973, Tectonic setting of basic volcanic rocks determined using trace element analyses: Earth and Planetary Science Letters, v. 19, p. 290-300.

Pearce, J.A., 1982, Trace element characteristics of lavas from destructive plate boundaries, *in*, R.S. Thorpe, editor, Andesites: John Wiley and Sons, New York, p. 525-548.

Plows, D.R. and Schoonmaker, A., 2013, Petrography, field relations and geochemical analysis of Ordovician metamorphosed mafic igneous rocks of the Caucomgomoc lake inlier, northern Maine: Geological Society of America Program with Abstracts, v. 45, p. 59.

Pollock, S.G., 1982, Stratigraphy of the Caucomgomoc Lake area northern Maine: Example of an obducted ophiolite-mélange complex: Geological Society of America Program with Abstracts, v. 14, p. 73.

Pollock, S.G., 1983, Ophiolite and Mélange Terrain Caucomgomoc Lake area, northwestern Maine: in Caldwell, D.W. and Hanson, L.S. [eds], New England Intercollegiate Geological Conference Guidebook for the Greenville-Millinocket regions, north central Maine, p. 175-189.

Pollock, S.G., 1985a, Bedrock geology of the Caucomgomoc Lake area, Maine: Maine Geological Survey Open-File Report 85-85, Scale 1:62,500.

Pollock, S.G., 1985b, Ophiolitic mélange, Caucomgomoc Lake are, northern ME: Geological Society of America Program with Abstracts, v. 17, p. 692.

Pollock, S.G., 1989, Mélanges and olistostromes associated with ophiolitic metabasalts and their significance in Cambro-Ordovician forearc accretion in the northern Appalachians, in Horton, J.W., Jr. and Rast, N. [eds], Mélanges and Olistostromes of the U.S. Appalachians, Geological Society of America Special Paper 228, p. 43-64.

Raabe, J.A., 1977, Bedrock geology of the Allagash Lake-Caucomgomoc Lake map area, west central Maine: [M.Sc. thesis] Boston University, Boston, MA, 171 p.

Saunders, A.D., Norry, M.J., and Tarney, J., 1988, Origin of MORB and chemically-depleted mantle reservoirs; trace element constraints, *in* Menzies, M., editor, Oceanic and continental lithosphere; similarities and differences: Journal of Petrology Special Volume 1988, p. 415-445.

Shervais, J.W., 1982, Ti-V plots and the petrogenesis of modern and ophiolitic lavas: Earth and Planetary Science Letters, v. 59, p. 101-118.

Sun, S.s. and Mcdonough, W.F., 1989, Chemical and isotopic systematics of oceanic basalts: implications for mantle composition and processes; in Magmatism in the Ocean Basins, A.D. Saunders and M.J. Norry (eds): Geological Society Special Publication, London, no. 42, p. 313-345.

Van Staal, C.R., Wilson, R.A., Kamo, S.L., McClelland, W.C., and McNicoll, V., 2016, Evolution of the Early to Middle Ordovician Popelogan arc in New Brunswick, Canada, and adjacent Maine, USA: Record of arc-trench migration phases of rifting: Geological Society of America Bulletin, v. 128, p. 122-146.

Winchester, J.A. and Floyd, P.A., 1977, Geochemical discrimination of different magma series and their differentiation products using immobile elements: Chemical Geology, v. 20, p. 325-343.

Wood, D.A., 1980, The application of a Th-Hf-Ta diagram to problems of tectonomagmatic classification and to establishing the nature of crustal contamination of basaltic lavas of the British Tertiary Volcanic Province: Earth and Planetary Science Letters, v. 50, p. 11-30.

A REVIEW OF ROBERT B. NEUMAN'S CLASSIC FOSSIL LOCALITY ON SUGARLOAF MOUNTAIN, SHIN POND AREA, MAINE

Robert G. Marvinney
Readfield, Maine, 04355. rgmarvinney@gmail.com

INTRODUCTION

This trip will investigate the fossiliferous Shin Brook Formation of Early Ordovician age in excellent exposures on the south end of Sugarloaf Mountain, just west of Shin Pond, Maine. This is the classic locality discovered by Robert B. Neuman (1920-2013) through his mapping in the 1950s and 1960s of the Shin Pond and Stacyville quadrangles that led to his early adoption of plate tectonic theory. Here, Neuman recognized a brachiopod fauna in volcanic tuffs and tuffaceous sediments that was more closely aligned with the "Celtic" fauna of the British Isles than with North American fauna of the same age, and thus supported the concept of an intervening Ordovician ocean – the Iapetus. This fauna, together with the unconformity between the Shin Brook Formation and the underlying Cambrian Grand Pitch Formation, form much of the basis for the Penobscottian orogeny as defined by Neuman.

THE GEOLOGY CONTEXT

Sugarloaf Mountain and the surrounding landscape are underlain by some of the oldest rocks in Maine, spanning portions of the Cambrian and Ordovician periods of geologic time (540-470 million years ago) (Figure 1). The oldest formation in this area is the Grand Pitch Formation, which is mostly gray, green, and red slate and siltstone (Neuman, 1967). Trace fossils of burrows produced by the worm-like organism *Oldhamia* set the age of this formation as latest Precambrian to Cambrian.

Resting unconformably on the Grand Pitch Formation is the Shin Brook Formation, a mixture of volcanic ash, sandstone, and breccia. At Sugarloaf Mountain, the Shin Brook is exposed in a doubly plunging syncline that extends from its terminus at Sugarloaf northeastward to beyond Roberts Mountain. Neuman (1967) discovered fossils in the formation that set its age as Early to Middle Ordovician (485-470 million years ago). He identified fossils at eight localities, with the largest number and greatest variety coming from localities on Sugarloaf (Figure 2 shows the locality that is the subject of this field trip). The fossils include six species of brachiopods, including *Platytoechia boucoti* (Figure 3), *Orthambonites robustus*, *Productorthis mainensis*, *Tritoehia* sp., and *Platystrophia* sp, and several trilobite species (Neuman, 1964).

The capstone on Sugarloaf is a massive, dark green metadiabase (Figure 4) of Ordovician age exposed in the core of the syncline. Weathered surfaces are brown, and are dotted by white plagioclase phenocrysts and pitted where calcite fillings of amygdules have weathered out. Some joints are filled by narrow veins of epidote. The metadiabase forms the prominent cliffs on the west side of the mountain, and the magma that formed this rock probably intruded as a sill parallel to the layering in the Shin Brook Formation, rather than cutting across it.

SIGNIFICANCE

Penobscottian orogeny: The Grand Pitch Formation has suffered several episodes of folding, while the younger Shin Pond Formation has been subjected to only one period of folding. Thus, the contact between these formations represents an erosional period between folding of the older rocks and subsequent deposition of the younger rocks in flat-lying fashion above - the classic occurrence of an unconformity. Neuman and Rankin (1966) coined the term Penobscot disturbance for the event that folded the older rocks, representing the collision of islands within the ancestral Atlantic Ocean, Iapetus, during the Late Cambrian period. These were violent times, as volcanoes formed on the assembled islands, spewing forth huge clouds of volcanic ash into the shallow sea. Tenaciously clinging to the edges of these volcanic islands was a rich assemblage of marine life.

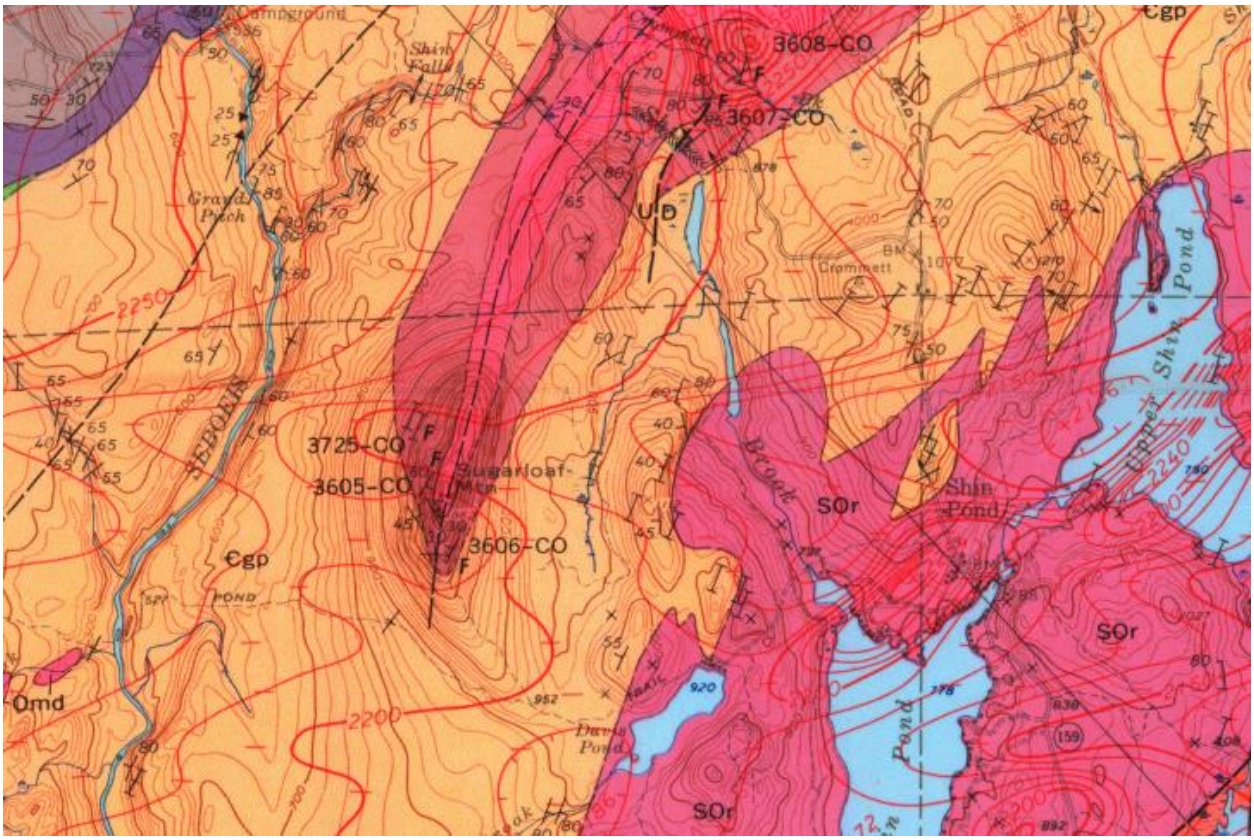

Figure 1. A portion of the geologic map of the Shin Pond quadrangle (Neuman, 1967). Sugarloaf Mountain is left center. Beige areas are the Cambrian Grand Pitch Formation (Cgp). The fossiliferous Shin Brook Formation (Osb) is in dark red and the metadiabase (Omd) is in brighter red. SOr is the Rockabema quartz diorite. Aeromagnetic contours are shown as red lines. The fossil locality, the objective of this trip, is labeled 3606-CO.
Figure 2. Left: Photograph of a fossil-bearing outcrop on Sugarloaf Mountain taken by Neuman's field assistant,

John Duane, in 1957 and presented as Figure 3 in Neuman (1964). The underside of the overhanging ledge exposes a dense fossil bed primarily composed of brachiopod fragments. This fossil locality is labeled 3606-CO on the geologic map (Figure 1), and fossil locality "A" on the map in Figure 2 of Neuman's 1987 field guide. Right: Image of the same outcrop taken in 2012 (Bill Duffy, photographer).

Figure 3. Left: Impressions of the brachiopod *Platytoechia boucoti* in a hand sample. The well-preserved fossil at left center is about 1 cm across. Right: Close-up of broken and complete brachiopod impressions from the ledge in Figure 2.

Figure 4. View to the north from just below the summit of Sugarloaf. The rock in the foreground is dark, grayish-green metadiabase of probable Ordovician age.

Ordovician paleogeography and tectonics: Neuman recognized that the assemblage of fossils in the Shin Brook Formation was unlike the North American fauna of that time period, and more like the fauna of Ireland (the Celtic fauna) (Figure 5). Neuman (1984) posited that the subduction that consumed the Iapetus Ocean, progressively narrowing its width to eventual closure, rafted mid-ocean volcanic islands to the eastern margin of Laurentia. Subsequent opening of the modern Atlantic Ocean distributed rocks containing fossils of the Celtic fauna on both sides of the ocean.

Following this brief introduction and the Road Log is a reprint of Neuman's 1987 GSA Centennial Field Guide on the Shin Brook Formation. Although the 1987 field guide does not focus directly on the Sugarloaf Mountain area, it presents a thorough discussion in Neuman's own words of the significance of the Shin Brook Formation and its fossils to the understanding of Ordovician paleogeography and the tectonic history of North America.

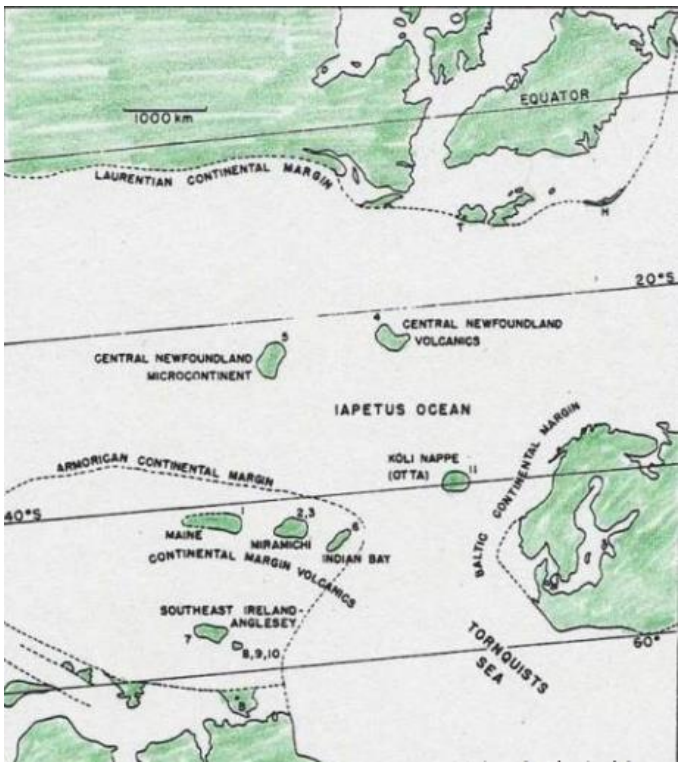

Figure 5. Neuman's (1984) reconstruction of the distribution of islands with Celtic fauna in the Iapetus Ocean during the early Ordovician period. North America (Laurentia) is at the top and Europe is at the bottom. Islands with Celtic fauna are labeled with numbers.

ROAD LOG

Assembly point: Intersection of Rte-11 and Rte-159, Patten, Maine, Patten Recreation Area parking lot. 10:00 AM. **From Presque Isle*:*** Take Rte-163 towards Mapleton/Ashland for 20 miles. Make a left turn onto Rte-11 at Ashland One Stop. Continue south on ME Rte-11 for 49 miles to Patten. Stop at the intersection with Rte-159 – park in the Patten Recreation Area parking lot on the left. Trip mileage starts here.

0.0	Take Rte-159 (Shin Pond Rd) toward Shin Pond from the intersection of Rte-11 and Rte-159 in Patten.
5.7	Turn left (west) onto Grondin Road. The remainder of the trip will be on dirt logging roads.
11.6	Bear left at fork.
12.3	Pass straight through the four-way intersection. Note the prominent southern end of Sugarloaf Mountain dead ahead.
12.9	Turn left at the four-way intersection.
13.0	Park at trailhead on right.

Hiking directions: It is about half mile hike to the top of Sugarloaf from the trailhead. When the trail steepens significantly at about the 1600-foot level, you should see a large rock on the right side by the trail (Figure 6). Leave the trail and walk along contour to the east until you see the prominent ledges shown in Figure 2.

IMPORTANT NOTE! This is a unique natural exposure that has been used for detailed geologic study and for teaching students. While photographs are encouraged, there is no reason or excuse for breaking or damaging these rocks and fossils. There are plenty of broken rocks below the ledge from which you may sample. Please take care of this special place.

Figure 6. When you encounter these boulders along the trail, leave the trail and walk along contour to the right (east) for about 75 meters (225 feet) to reach the ledges shown in Figure 2.

Continue up the trail for another ~ 500 meters (1500 feet) to the top of Sugarloaf Mountain. On a clear day, the hiker will be rewarded with views of Katahdin, the Travelers, and Mt. Chase.
Retrace the hiking route back down the mountain and the driving route back to Patten.

REFERENCES

Neuman, Robert B., 1964, Fossils in Ordovician tuffs, northeastern Maine, with a section on Trilobita by H.B. Whittington: U. S. Geological Survey, Bulletin 1181-E, p. E1-E38.

Neuman, Robert B., 1967, Bedrock geology of the Shin Pond and Stacyville quadrangles, Penobscot County, Maine: U. S. Geological Survey, Professional Paper 524-I, p. I1-I37, scale 1:62,500.

Neuman, Robert B., 1984, Geology and paleobiology of islands in the Ordovician Iapetus Ocean; review and implications: Geological Society of America, Bulletin, v. 95, no. 10, p. 1188–1201.

Neuman, Robert B., 1987, Type section of the Early Ordovician Shin Brook Formation and evidence of the Penobscot orogeny, northern Penobscot County, Maine, *in* Roy, David C. (editor), Northeastern section of the Geological Society of America: Geological Society of America, Centennial Field Guide, v. 5, p. 307–309.

Neuman, Robert B., and Rankin, Douglas W., 1966, Bedrock geology of the Shin Pond region: in Caldwell, D. W. (editor), Guidebook for Field Trips in the Mount Katahdin Region, Maine: 58th New England Intercollegiate Geological Conference, p. 8–17.

Type section of the Early Ordovician Shin Brook Formation and evidence of the Penobscot orogeny, northern Penobscot County, Maine

***Robert B. Neuman,** Department of Paleobiology, E-501 National Museum of Natural History, Smithsonian Institution, Washington, D.C. 20560*

LOCATION

The type section of the Early Ordovician Shin Brook Formation is along Shin Brook near Crommet Spring, about 11 mi (18 km) northwest of Patten and 100 mi (161 km) north of Bangor. It is accessible from the east via I-95 from the Island Falls or Sherman exists; through Patten and the Shin Ponds on Maine 159 (Fig. 1); or from the west about 12 mi (19 km) east of the Mattagamon gate of Baxter State Park.

From Crommet Spring walk approximately 2,300 ft (700 m) WNW (downhill) along the graveled hauling road to the bridge across Shin Brook; east of the bridge the Grand Pitch Formation is exposed in and adjacent to the roadbed. The section is measured northwestward (downstream) from the bridge.

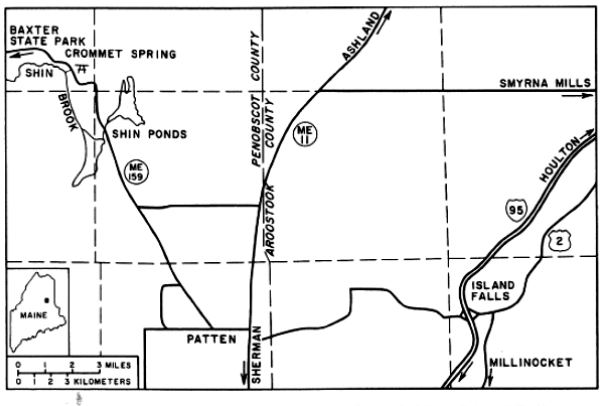

Figure 1. Access to Crommet Spring from I-95 at Island Falls.

SIGNIFICANCE

Tuffs and tuffaceous sedimentary rocks of the Early Ordovician Shin Brook Formation are underlain by pelite and quartzitic sandstone of the Cambrian(?) Grand Pitch Formation. The Shin Brook Formation in this area (Fig. 2) is unique in the State of Maine. Brachiopods, trilobites, and other fossils from several exposures are characteristic of assemblages that lived around islands in the Early Ordovician Iapetus Ocean. The Grand Pitch Formation, one of several largely unfossiliferous units of altered shale and quartzite that occupy the cores of anticlines in Maine and beyond (Boone and others, 1984), is assigned a Cambrian(?) age based on the occurrence of the trace fossil *Oldhamia smithi* Ruedemann (1942) in red shale 10 mi (16 km) SW of Crommet Spring (Smith, 1928).

The lithic contrasts between the Grand Pitch and Shin Brook formations are accompanied by contrasts in their structural styles. The former, here and elsewhere, contains evidence of multiple deformation, while the latter was deformed only once, presumably by Acadian events of Devonian age. Quartzite clasts in conglomerate at the base of the Shin Brook Formation confirm that this contact is an important unconformity, the result of the Penobscot orogeny, an event named from exposures in this vicinity where its age is constrained by these fossiliferous formations.

SITE INFORMATION

The route from Patten into Baxter State Park through Mattagamon gate traverses several of Maine's important geologic features (Neuman, 1967; Neuman and Rankin *in* Roy and Naylor, 1980). Silurian rocks of the northwestern margin of the Kearsarge–Central Maine synclinorium (Osberg and others, 1985) crop out between Patten and the Shin Ponds. Northwest of the Shin Ponds the route crosses the Weeksboro–Lunksoos Lake anticlinorium, one of several anticlinal structures of northern Maine in which pre-Silurian rocks are exposed. Silurian and Lower Devonian rocks on the northwest flank of this structure are encountered on this route north and west of the Seboeis River.

Preservation of the Shin Brook Formation in a shallow syncline in the central part of the Weeksboro–Lunksoos Lake anticlinorium permits insights into the geologic history of the region not available elsewhere. Evidence of multiple deformation of the rocks of the Grand Pitch Formation and of but one deformation of the rocks of the Shin Brook at this site and at other places in the region have led to the acceptance of the post-Cambrian–pre-Early Ordovician Penobscot orogeny here; and other criteria (Drake, 1987) have led to the identification of effects of this event over a much larger area.

The rocks and fossils of the Shin Brook Formation are of special interest. The Early Ordovician age of the formation, determined from its fossils, establishes it as the oldest volcanogenic unit in the region. The occurrence of welded tuff at one place on Sugarloaf Mountain, where it is overlain by richly fossiliferous tuff (Locality A of Fig. 2), suggests subaerial volcanism—a volcanic island. That this and other islands in the ancient Iapetus

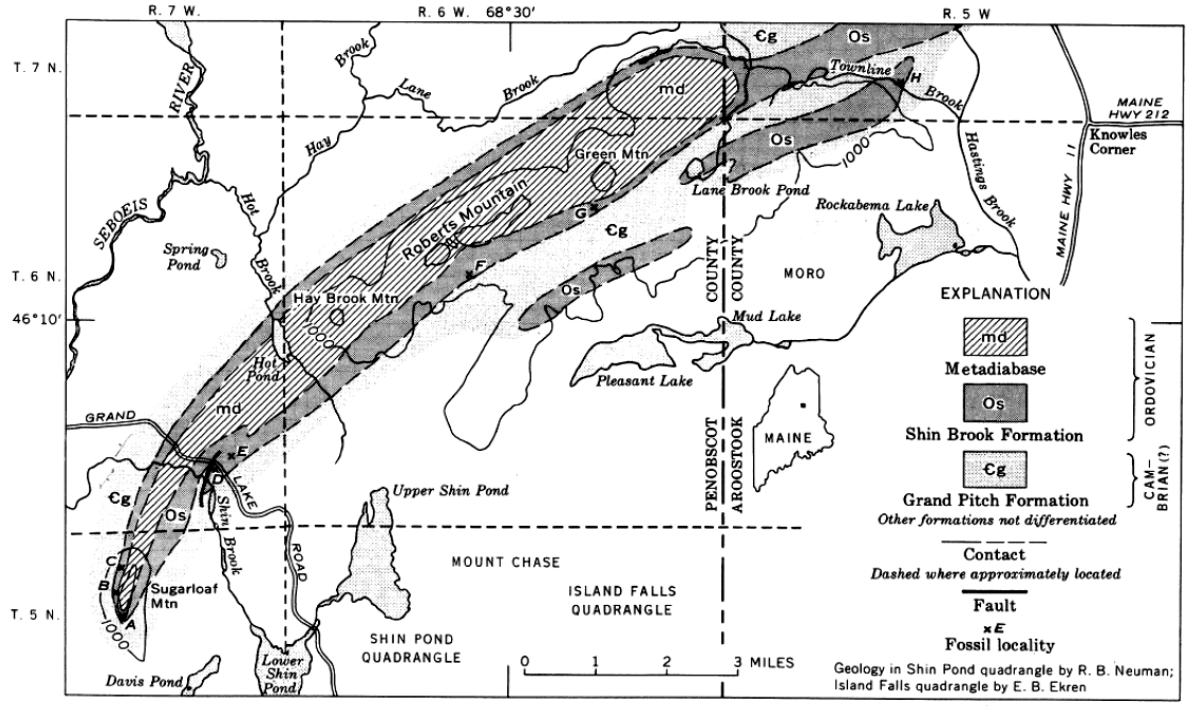

Figure 2. Map showing distribution of Shin Brook Formation (from Neuman, 1964). For more comprehensive geologic maps see the Shin Pond (Neuman, 1967) and Island Falls (Ekren and Frischknecht, 1967) quadrangles.

Ocean lay far seaward of the North American continental margin was inferred from these fossils and those from similar rocks in New Brunswick and Newfoundland (Neuman, 1984).

Identifiable fossils were found at several places in the outcrop belt of the Shin Brook Formation, but none have been found in the exposures along Shin Brook. Fossils nearest the brook were found in a small ledge SW of the road, about 0.75 mi (1.2 km) NW of Crommet Spring (Locality D of Fig. 2), but this ledge was covered by road construction shortly after it was discovered.

No dated rocks are known to overlie the Shin Brook Formation. The metadiabase that occupies the trough of the syncline (Figs. 2 and 3) is probably a sill, the roof of which has been eroded away.

MEASURED SECTION OF SHIN BROOK FORMATION, ADAPTED FROM NEUMAN (1964); SEE FIGURE 3

Shin Brook Formation: 902 ft (280 m) measured **Thickness**

19. Tuffaceous sandstone and siltstone in graded layers 3.2 to 12 in (8 to 30 cm) thick, with coarse-grained sandstone in their basal parts and finely laminated siltstone at their tops; siltstone more abundant than sandstone; unit includes two layers of crystal tuff, 6 and 12 in (15 and 30 cm) thick, respectively ..... 35 ft (11 m)
18. Crystal tuff, greenish-gray; crystals are green altered plagioclase ..... 10 ft (3 m)
17. Covered ..... 3 ft (1 m)
16. Tuffaceous sandstone, grit, and conglomerate; finer grained part is well laminated, part not laminated includes fragments of porphyritic and nonporphyritic fine-grained igneous rock; ledge in streambed has distorted bedding structures that suggest deformation prior to lithification; base concealed ..... 7 ft (2 m)
15. Tuffaceous sandstone, fine- to medium-grained, calcareous, strongly sheared with weathered pits that may have been concentrations of fragmentary fossils deformed beyond recognition ..... 18 ft (5 m)
14. Covered ..... 70 ft (21 m)
13. Crystal tuff, greenish-gray, with scattered angular cognate rock fragments 0.4 to 6 in (1 to 15 cm) average diameter; crystals of both matrix and fragments are green altered plagioclase; lacks primary layering; quartz veins abundant ..... 20 ft (6 m)
12. Covered ..... 375 ft (114 m)
11. Crystal tuff; light-green altered plagioclase crystals in a darker aphanitic matrix; fractured ..... 45 ft (29 m)
10. Covered ..... 95 ft (29 m)
9. Tuff, fine-grained, light greenish-gray; abundant, carbonate; strongly sheared, no bedding

preserved ..... 30 ft (9 m)
8. Covered ..... 30 ft (10 m)
7. Volcanic conglomerate; granules of aphanitic volcanic rock and dark slate, strongly sheared; bedding obliterated ..... 50 ft (15 m)
6. Tuffaceous sandstone, gray, medium- and fine-grained; abundant carbonate; bedding obliterated by strong shearing ..... 20 ft (6 m)
5. Covered ..... 30 ft (9 m)
4. Volcanic granule conglomerate and coarse-grained sandstone; light-gray, strongly sheared ..... 25 ft (8 m)
3. Sandstone and conglomerate; conglomerate beds 8 to 10 in (20 to 25 cm) thick, sandstone somewhat thinner; volcanic rocks and fine-grained quartzite clasts in conglomerate angular to subrounded, maximum 1.6 in (4 cm) average diameter ..... 35 ft (11 m)
2. Phyllite, light-gray, probably tuffaceous ..... 2 ft (0.6 m)
1. Slate, dark-gray, with abundant small (0.25 to 0.5 mm) rhombic white grains (altered plagioclase?) ..... 2 ft (0.6 m)

Grand Pitch Formation: approximately 200 ft (61 m) exposed in streambank and roadbed. Gray slate and lesser amounts of gray quartzite and dark-gray feldspathic quartzite in thin, discontinuous beds, some tightly folded.

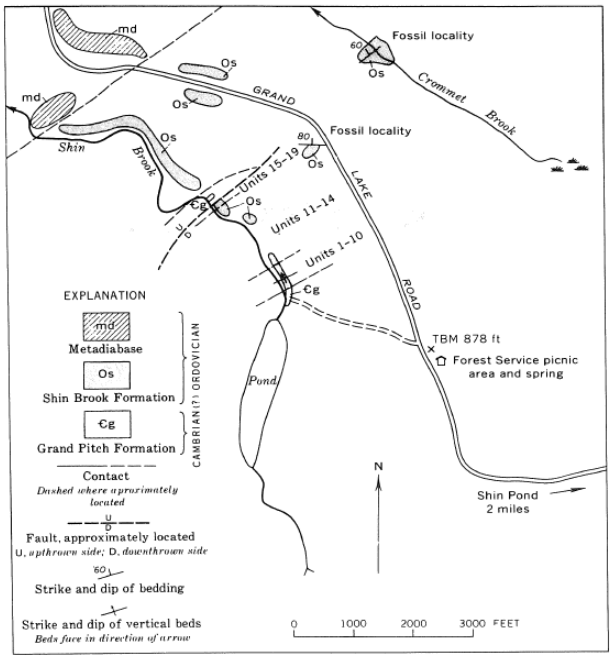

Figure 3. Geologic sketch map of the type section of the Shin Brook Formation; units 1–19 described in text. Outlined areas indicate outcrops (from Neuman, 1964).

REFERENCES CITED

Boone, G. M., Boudette, E. L., Hall, B. A., and Pollock, S. G., 1984, Correlation and tectonic significance of pre-Middle Ordovician rocks of northwestern Maine: Geological Society of America Abstracts with Programs, v. 16, p. 4.

Drake, A. A., Jr., 1987, The Taconic Orogen: *in* Hatcher, R. D., Jr., Viele, G. W. and Thomas, W. A., The Appalachian and Ouachita regions: Geological Society of America, The Geology of North America, v. F2 (in press).

Ekren, E. B., and Frischknecht, F. C., 1967, Geological-geophysical investigations of bedrock in the Island Falls Quadrangle, Aroostook and Penobscot counties, Maine: U.S. Geological Survey Professional Paper 527, 36 p.

Neuman, R. B., 1964, Fossils in Ordovician tuffs, northeastern Maine, with a section on Trilobita by H. B. Whittington: U.S. Geological Survey Bulletin 1181-E, p. E1–E38.

—— , 1967, Bedrock of the Shin Pond and Stacyville Quadrangles, Penobscot County, Maine: U.S. Geological Survey Professional Paper 524-1, 1-37.

—— , 1984, Geology and paleobiology of islands in the Ordovician Iapetus Ocean; Review and implications: Geological Society of America Bulletin, v. 95, p. 1188–1201.

Osberg, P. H., Hussey, A. M. II, and Boone, G. M., eds., 1985, Bedrock Geologic Map of Maine: Maine Geological Survey, scale 1:500,000.

Roy, D. C., and Naylor, R. S., 1980, The geology of northeastern Maine and neighboring New Brunswick: New England Intercollegiate Geological Conference, 72nd, Presque Isle, Maine, Guidebook, Chestnut Hill, Massachusetts, Boston College Press, 296 p.

Ruedemann, R., 1942, *Oldhamia* and the Rensselaer Grit problem: New York State Museum Bulletin 327, p. 5–18.

Smith, E.S.C., 1928, The Cambrian in northern Maine: American Journal of Science, 5th series, v. 15, p. 484–486.

THE AROOSTOOK MANGANESE DISTRICT, SILURIAN FORMATIONS, NUMBER NINE MOUNTAIN TERRANE, AND THE MAPLE-HOVEY MANGANESE DEPOSIT

Chunzeng Wang[1] and Lauren Madsen[2]
[1]University of Maine at Presque Isle, Presque Isle, Maine 04769. chunzeng.wang@maine.edu
[2]University of Maine, Orono, Maine 04469. lauren.madsen@maine.edu

INTRODUCTION

Even as the 12th most abundant element in the Earth's crust, manganese is one of the ***most critical minerals*** for the United States, Canada, and other industrialized countries. Manganese has superior desulfurizing, deoxidizing, and alloying properties, and is primarily used as an essential component in steelmaking for which there is no substitute (Cannon, 2017). But there is increasing demand for high purity manganese in the battery metal market as part of an effort to reduce carbon emissions and decrease dependence on fossil fuels worldwide. However, the United States and Canada are entirely dependent on imports of manganese. The combination of total import reliance, the essential uses in our ever transforming industrialized society, and the potential for supply disruptions because of the limited sources of the ore makes manganese a critical mineral that compels the United States and Canada to evaluate their existing manganese resources and build a foundation for future exploration.

Manganese ironstone deposits have been known in Aroostook County, Maine for more than 180 years since Jackson (1837) first reported a "Red Hematite Iron" occurrence in a farm between Washburn and Castle Hill, later named "Haines deposit" (Miller, 1947). The reputed "***Aroostook Manganese District***" stretches from New Sweden to the Houlton-Hodgdon area for nearly 110 km. Miller (1947) divided the Aroostook Manganese District into northern, central, and southern subdistricts (Fig. 1). Deposits in the northern subdistrict occur within the Silurian New Sweden Formation (Roy and Mencher, 1976). The best example is the Dudley deposit in Castle Hill in which 26 holes were drilled and 17 trenches dug between 1941 and 1943. The Silurian Maple Mountain Formation hosts the Maple-Hovey manganese ironstone deposits in the Number Nine Mountain, in the central subdistrict (Pavlides, 1964). The deposits in the southern subdistrict occur in the Silurian Smyrna Mills Formation (Pavlides and Berry, 1966), along strike with the manganese deposits of the Woodstock area, New Brunswick, Canada (the "Woodstock District" in Fig.1). The last campaign of exploration for manganese ironstone deposits, and the largest historically, were conducted at the Maple-Hovey manganese ironstone deposit 70 years ago (1949–1951) by the U. S. Bureau of Mines (USBM) (Eilersten, 1952) with 61 boreholes drilled and about 105 trenches dug. Kilgore and Thomas (1982) later re-examined the exploration data and reported 260 million metric tons of ore (averaging 8.87% Mn, of which 121 million tons averaged 11.16% Mn) with approximately 23.1 million metric tons of manganese. The Maple-Hovey deposit is ***the largest manganese deposit*** with the greatest manganese reserve in the United States.

This trip guide is based on our USGS Earth MRI (Mapping Resources Initiative) project "*Geologic mapping of manganese-bearing deposits in Aroostook County, Maine*" that was launched in 2022 to better understand the geologic setting and mineralization of the deposits in the central and northern subdistricts. The project includes detailed 1:24,000-scale bedrock mapping and geochemical, geochronological, and bio-stratigraphical characterization of the manganese ironstone deposits and surrounding sedimentary and volcanic rocks of the Number Nine Lake, Mapleton, and Presque Isle quadrangles. The project focuses mostly on the Silurian formations that host manganese ironstone deposits.

Based on our study, there are three distinctive Silurian sequences: the ***Perham Group sequence*** that constitutes the Silurian Ashland-Van Buren sub-belt identified in our study and that hosts the manganese ironstone deposits in the northern subdistrict, the ***Nine Mountain sequence*** that hosts the manganese ironstone deposits in the central subdistrict of the Number Nine Mountain terrane, and the ***Carys Mills sequence*** that hosts the manganese ironstone deposits in the Aroostook-Matapedia basin/belt in the southern subdistrict. The ***Perham Group sequence*** includes, from the oldest to the youngest, the conformable Frenchville, Jemtland, and New Sweden formations of dominantly sedimentary rocks with minor pyroclastic rocks. The ***Nine Mountain sequence*** is the major component of the Number Nine Mountain Cambro-Ordovician-Silurian terrane (henceforth the Number Nine Mountain terrane), a newly recognized independent terrane that had previously been considered part of the Weeksboro-Lunksoos Lake Belt.

This trip will focus on the Silurian formations of the Perham Group sequence in the northern subdistrict and the Nine Mountain sequence in the central subdistrict, with a brief look at older rocks in the Number Nine Mountain terrane. Stops will include visits to major Ordovician-Silurian formations and representative manganese ironstone deposits – the Dudley deposit hosted by the New Sweden Formation in the northern subdistrict and the Maple-Hovey deposits hosted by the Maple Mountain Formation in the central subdistrict.

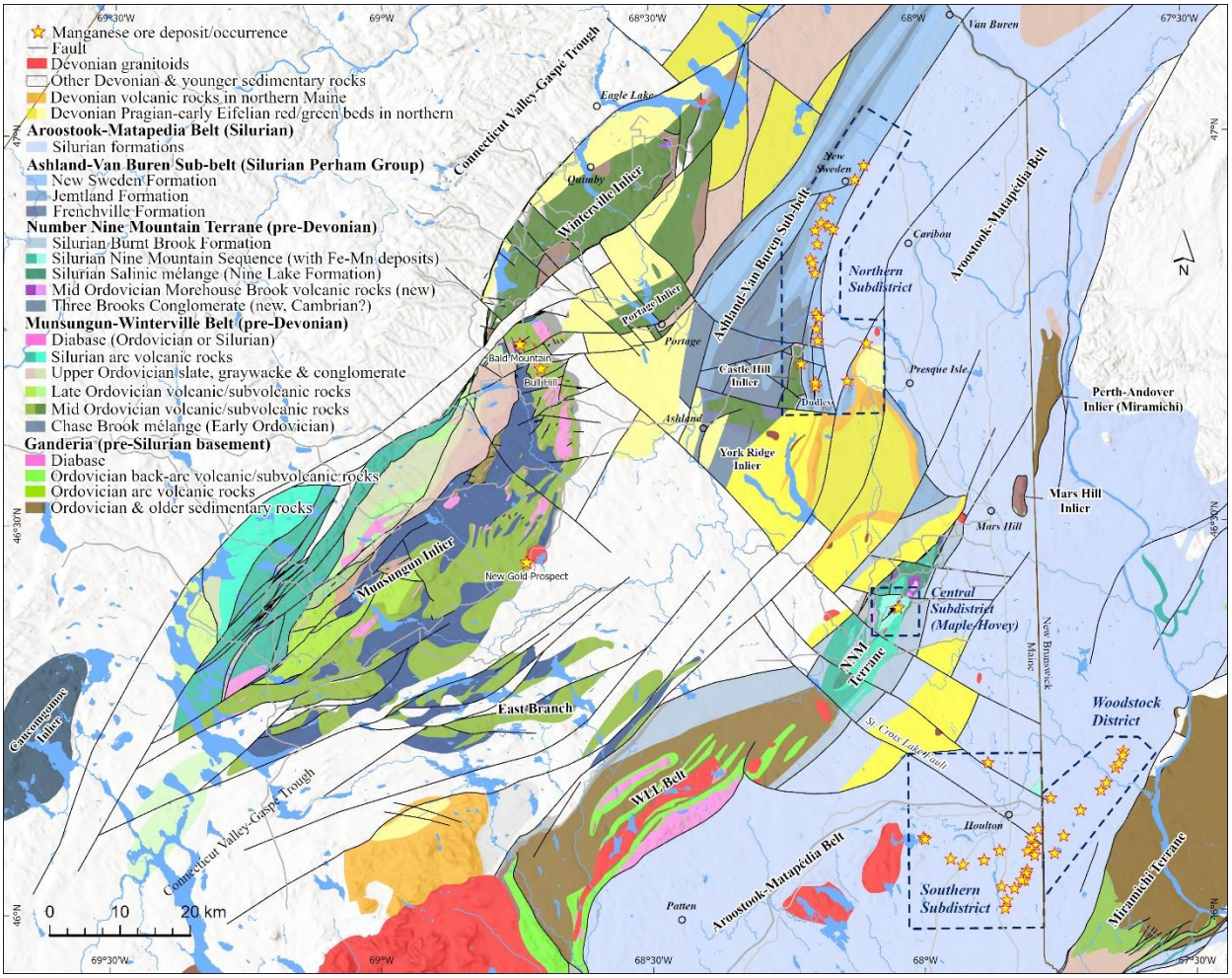

Figure 1. Simplified regional geologic map of northern Maine showing major lithotectonic belts and subdistricts of the Aroostook Manganese District. WLL Belt – Weeksboro-Lunksoos Lake Belt. NNM Terrane – Number Nine Mountain Terrane. Manganese deposits/occurrences based on Miller (1947).

REGIONAL GEOLOGY

Major lithotectonic belts and terrane in northern Maine include, from the west to east, the Connecticut Valley-Gaspé Trough, the Munsungun-Winterville Belt, the Weeksboro-Lunksoos Lake Belt, the Number Nine Mountain terrane, the Mars Hill inlier, the Aroostook-Matapédia Basin, and the Miramichi terrane (Fig. 1). The following is a brief description for each lithotectonic belt or terrane except for the Number Nine Mountain terrane that will be covered in detail in a separate section.

The Connecticut Valley*-Gaspé *Trough is the most extensive Mid-Late Paleozoic sedimentary belt in Maine – it extends southwestward to southwestern New England, and northeastward to the eastern Gaspé peninsula. In northern Maine, the belt is composed predominantly of clastic and turbiditic sedimentary rocks and minor limestone of the Devonian Lochkovian Seboomook Group (Perkins and Smith, 1925; Pollock, 1987). These sedimentary rocks were substantially folded and foliated during the Acadian orogeny.

The Munsungun-Winterville Belt consists of multiple inliers. In addition to the largest Munsungun and Winterville inliers, other smaller ones include Portage Lake, York Ridge, Castle Hill, and the inliers in the headwaters of the East Branch Penobscot River and Aroostook River (Fig. 1). The Munsungun inlier and the smaller inliers in the headwaters are characterized by a mélange basement of the Chase Brook Formation. Reported by Wang et al., (2022a), a geochronological work of detrital zircons from the mélange showed an age spectrum typical for Laurentia and peri-Laurentia terranes, indicating that the Munsungun-Winterville Belt is likely a peri-Laurentia terrane. The mélange is unconformably overlain by Middle to early Late Ordovician (470–448 Ma) volcanic rocks generated mainly in arc setting, for example, the Munsungun Lake, Bluffer Pond, Ragged Mountain, and Ingalls Brook Road formations in

the Munsungun inlier (Wang et al., 2022a, b; Wang, 2021; 2022a, b). The Munsungun-Winterville Belt also contains several Upper Ordovician sedimentary formations, including the Chase Lake, Blind Brook, Rowe Lake, and Ferguson Brook formations in the Munsungun inlier and the Ferguson Brook Formation in the Winterville inlier. The Winterville inlier is in fault contact with the Upper Ordovician Madawaska Lake Formation of slate and sandstone. Several southwest-striking fault slivers composed of Silurian Ludlow-aged volcanic rocks of the Spider Lake Formation (Hall, 1970) and a recently named Churchill Ridge Formation (Wang, 2023b) occur to the west and southwest of the Ordovician volcanic belts. Their ages were recently confirmed by two zircon U-Pb ages of 424 Ma and 427 Ma (Pollock, 2023) for the Spider Lake Formation and of 425 Ma (Wang, 2023b) for the Churchill Ridge Formation. The Silurian volcanic rocks were generated in arc setting based on whole-rock geochemical data, dominated by basalt, and considered to be related to the prolonged Silurian Salinic orogenesis (Wang et al., 22b).

The Weeksboro-Lunksoos Lake Belt (WLLB) is a Cambro-Ordovician lithotectonic belt composed predominantly of sedimentary rocks of the Grand Pitch Formation (Newman, 1962) and volcanic-volcanogenic rocks and minor basalt and rhyolite flows of bimodal association of the Shin Brook Formation (Newman and Whittington, 1964; McCormick, 2021). The Grand Pitch Formation consists of well-bedded but folded and foliated quartzose and quartzofeldspathic sandstones and slates, similar to the Cambrian Baskahegan Lake Formation of the Woodstock Group in the Miramichi Terrane in southwestern New Brunswick and eastern Maine. A Grand Pitch sandstone sample yielded 210 detrital zircon grains for LA-ICP-MS U-Pb analyses. Their ages (Fig. 2) exhibit a Gondwanan spectrum with the largest peak at 626 Ma, in addition to peaks at 807 Ma, 1022 Ma, 1191 Ma, 1532 Ma, 1869 Ma, and 2015 Ma. The youngest zircon grains of 528–550 Ma demonstrate a maximum Cambrian age for the Grand Pitch Formation. The Grand Pitch is unconformably overlain by the Shin Brook Formation. The unconformity was identified as "Penobscot disturbance" first by Newman (1967) and later known as the Penobscot orogeny. Recent dating of a crystal tuff sample from the footwall and a rhyolite sample from the much higher stratigraphic level at the Pickett Mountain volcanic massive sulfide deposit hosted by the Shin Brook Formation yielded 484.6 ± 2.7 Ma and 481.1 ± 3.4 Ma ages, respectively (McCormick, 2021). Geochemical analysis based on a large quantity of whole-rock geochemical data confirmed the back-arc setting of the Shin Brook Formation (McCormick, 2021). Another formation of volcanic rocks in the WLLB occurs along the Deasy Mountain–Hunt Mountain–Whetstone Mountain ridge on the west side of the East Branch Penobscot River; it was called "Ordovician volcanic rocks (greenstone)" by Newman (1974) or "Stacyville volcanics" by Wellensiek et al., (1990). It is conformable with the "Haskell Rock Conglomerate" of Upper Ordovician age (Rankin, 1961; Newman and Rankin, 1980).

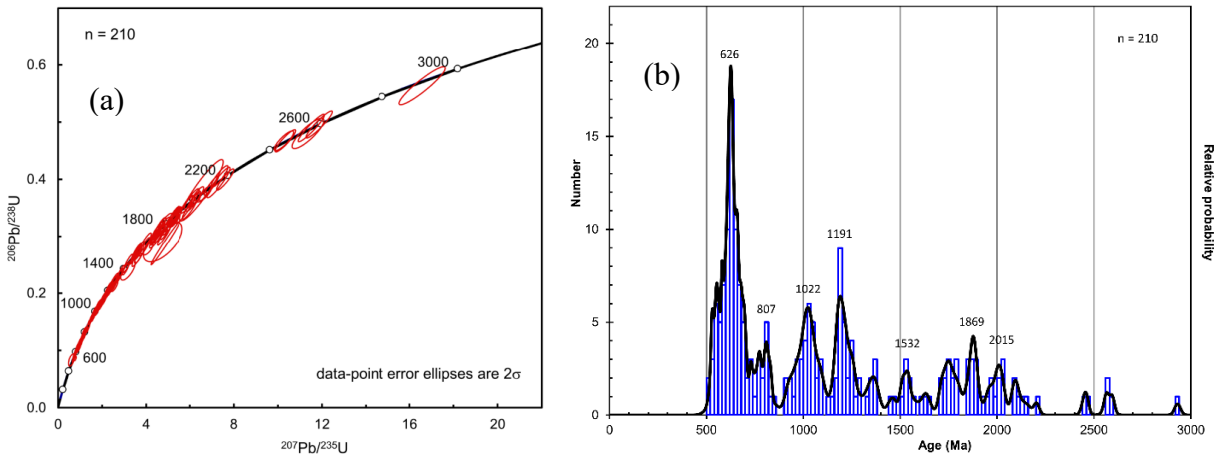

Figure 2. Concordia (a) and relative age-probability (b) diagrams of the detrital zircon grains from the Grand Pitch Formation.

The Mars Hill inlier is a newly recognized early Paleozoic inlier. The small inlier is dominated by the "Mars Hill Conglomerate" (Williams and Gregory, 1900) or "Mars Hill Formation" (Lacombe, 1988). Conformably overlying the voluminous, polymictic, and poorly sorted conglomerate is a sequence of basalt and tuff found only on the southwestern flank of the Mars Hill Mountain. The conformity between the conglomerate and volcanic rocks is comparable to the Ordovician Stacyville volcanic rocks and Haskell Rock Conglomerate in southwestern WLLB. The Mars Hill inlier is in fault contact with and overlain by the Silurian Chandler Ridge and Carys Mills formations. No radiometric dating has ever been performed for the Mars Hill inlier, but a speculated Late Ordovician age is based on a few fossil fragments (Lacombe, 1988).

The Aroostook-Matapédia Basin/Belt (AMB) is mostly a Silurian basin and is the northeastern extension of the Central Maine Belt. In northern Maine, south of Mars Hill, the AMB includes the Chandler Ridge (Pavlides, 1966), Carys Mills (Pavlides, 1966), Smyrna Mills (Pavlides and Berry, 1966), Allsbury (Ekren and Frischknecht, 1967), and Madrid formations (Osberg et al., 1968). North of Mars Hill, the AMB includes the Chandler Ridge, Carys Mills (dominant), and Spragueville formations. Other Silurian formations, e.g., Frenchville (Boucot et al., 1964), Jemtland (Roy and Mencher, 1976), and New Sweden (Roy and Mencher, 1976) formations that occur in a belt containing Ashland, New Sweden, Stockholm, and Van Buren, have long been considered as part of the AMB. However, our study shows that they form an independent sequence (referred to the Perham Group sequence) and constitute an independent, fault-bounded terrane, referred to the ***Ashland-Van Buren sub-belt***. Both sequences/belts are in fault contact. The Silurian formations in both belts were substantially folded and foliated during the Acadian orogeny.

The Chandler Ridge Formation is composed predominantly of thin-medium-layered gray sandstone and gray slate. The Carys Mills Formation makes up at least 80% of the Carys Mills sequence. In our revised definition, the Carys Mills Formation is strictly carbonate, including only the thin to thick (mostly thin-medium) layered micrite, argillaceous micrite, and limy slate/mudstone, well-known as "ribbon limestone". In the past, the sandstone and slate unit in the AMB was mapped as part of the Carys Mills Formation (or a lower member of the Carys Mills Formation in the Washburn-New Sweden area). Instead, they belong to the Chandler Ridge Formation and occur in cores of anticlines surrounded by the Carys Mills. The Spragueville Formation is composed of laminated calcareous silty mudstone and argillaceous micrite of generally 1–15 cm thick, usually weathered to a buff or greenish gray or orange color characterized by bioturbation of burrowing organisms. The Spragueville Formation occurs in cores of synclines only in Presque Isle because only this area exposes the complete Carys Mills sequence.

The Miramichi terrane is the most extensive Cambrian-Ordovician terrane in the Maine and New Brunswick Appalachian orogen, extending ~400 km from northern New Brunswick to east-central Maine (Ludman, 2023; Ludman and Whittaker, 2023), and comprises northeastern and central components in New Brunswick, and a southwestern component in Maine (Fyffe et al., 2023; Ludman and Whittaker, 2023). The oldest rocks in all three components are lithologically similar and temporally equivalent to the Grand Pitch Formation: the Cambrian to Lower Ordovician Miramichi Group (northeastern), Woodstock Group (central), and the Baskahegan Lake Formation (southwestern). In the central segment, the Woodstock Group is overlain by the Ordovician calc-alkaline arc volcanic rocks of the Meductic Group. In the northeastern segment, however, the Miramichi Group is overlain by Middle Ordovician Tetagouche back-arc volcanic rocks. Because it is on strike with the Perth-Andover inlier of the Woodstock Group in New Brunswick (Fig. 1) and shares the same pre-volcanic basement, the WLLB is probably associated with the Miramichi terrane, separated from it today by Aroostook-Matapedia cover strata. The bimodal Shin Brook volcanic sequence appears to represent a back-arc rifting event older than that of the Tetagouche basin. Thus, the WLLB, the Perth-Andover inlier, the Mars Hill inlier, and the Miramichi terrane were parts of the peri-Gondwanan Ganderia micro-continent, unlike the MWB.

The Pragian-Eifelin green/red beds: In addition to the Lower Devonian, post-Seboomook clastic sedimentary rocks of the Chapman Sandstone (Williams and Gregory, 1900; Pragian age based on our palynology study) in the Chapman Basin, the Mapleton Sandstone/Formation in Mapleton (Williams and Gregory, 1900; Early to Middle Eifelian age based on McGregor (1992)), and the Trout Valley Formation (Dorf and Rankin, 1962; Andrews et al., 1977; Late Emsian to Early Eifelian age by McGregor (1992)) in northern Baxter State Park, recently, a widespread Lower Devonian, post-Seboomook (i.e., post-Lochkovian), red and green clastic formation was discovered in northern Maine, first reported along the Fish River chain of lakes and in the Ashland area (Wang et al., 2020), and later named as St. Froid Lake Formation (Wang, 2022a, b). Brachiopods and palynological analysis in our study demonstrate an Emsian-early Eifelian age for the formation. Another formation of dominantly green beds with minor red beds was also recently discovered in the region. Palynological analysis confirms the age of the formation to be Pragian, slightly older than the St. Froid Lake Formation. It has been named the Scopan Lake Formation in our study.

All the terranes, belts, and formations, from the oldest (Cambrian) to the youngest (Devonian Emsian) in northern Maine have been significantly faulted and displaced starting from Late Ordovician, as shown in Figure 1, mostly by southwest-northeast-striking reverse-thrust faults of multiple generations. The most significant were the post-Acadian, Neoacadian, southeast-directed reverse-thrust faulting event that produced a domino-style, imbricate fault system in northern Maine, called the "Northern Maine imbricate fault system" in our study.

THE ASHLAND-VAN BUREN SUB-BELT, PERHAM GROUP SEQUNCE, AND THE MANGANESE-IRON DEPOSITS

In the past, the Silurian sedimentary rocks along the stretch from Ashland, through Perham, New Sweden, Stockholm, to Van Buren were mapped as various formations, including Frenchville, New Sweden, Jemtland, and

Fogelin Hill formations and attributed to the Aroostook-Matapedia Basin/Belt. Based on our study, first, the Fogelin Hill Formation is not a separate formation but is equivalent to the New Sweden Formation and the name should be dropped, second, these Silurian sedimentary rocks occur as a conformable and transgressive sequence of, from the oldest to the youngest, Frenchville, Jemtland, and New Sweden formations. We propose to reuse the name Perham Group for this sequence of three formations. The Perham Group constitutes the ***Ashland-Van Burent sub-belt*** that is separated from the Carys Mills sequence of the Aroostook-Matapedia Belt on the east by a fault (Fig. 3). It is likely that the Perham Group used to be the western part of the original, much wider Aroostook-Matapedia Basin and the Perham Group was unconformably deposited on the Ordovician inliers, but later displaced and split from the Aroostook-Matapedia Belt (of the Carys Mills sequence). In other words, it is a sub-belt of the original Aroostook-Matapedia Basin. The Perham Group sequence is tightly folded with the axes of the folds striking south or north or northeast. The folds are plunging to either north-northeast or south-southwest, with some doubly plunging. The folds have been faulted mostly by southwest-striking reverse faults with moderate to substantial horizontal and/or vertical displacement. These longitudinal faults were later displaced by several northwest- or southeast-striking transverse faults (Fig. 3).

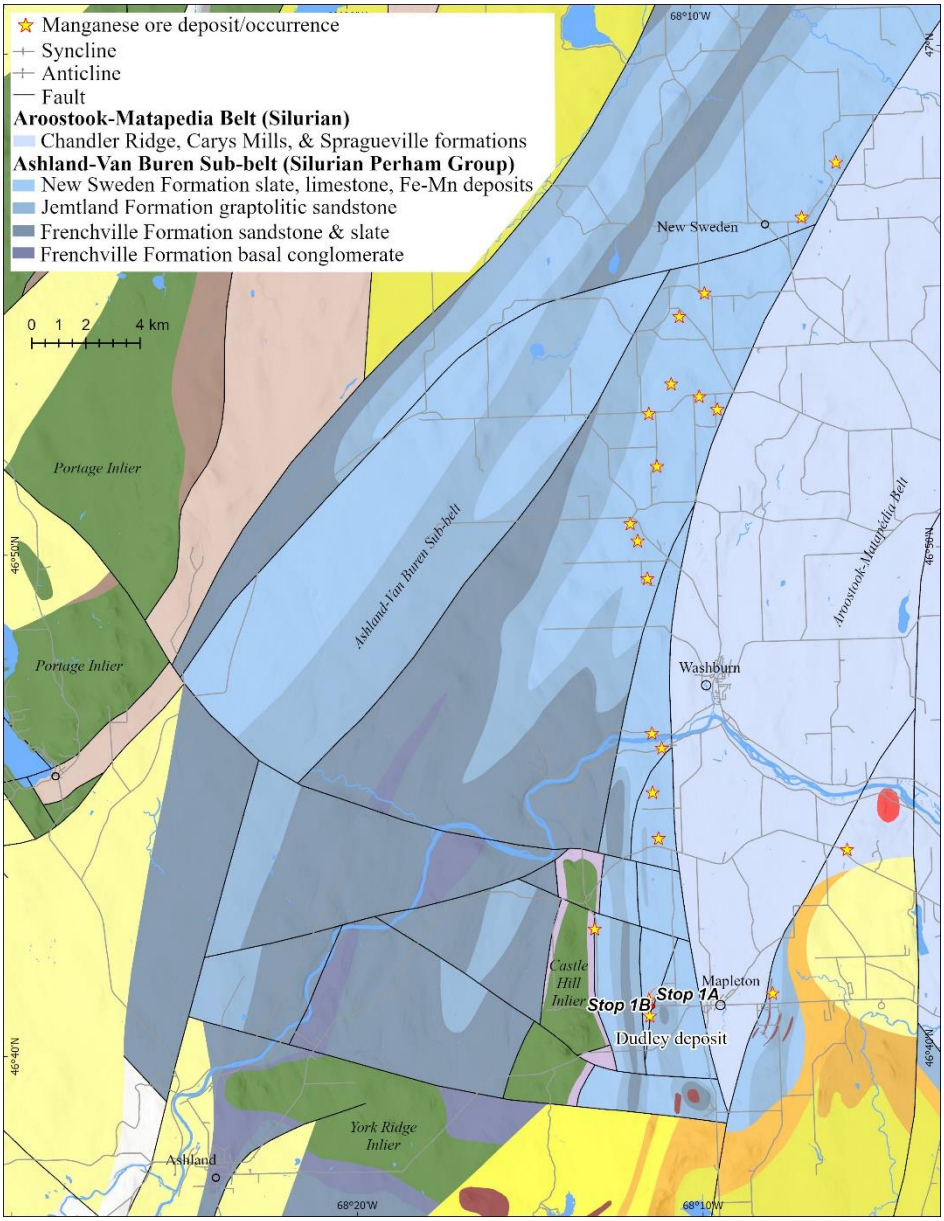

Figure 3. Simplified geologic map of the southern-central Ashland-Van Buren sub-belt and the Aroostook-Matapedia Belt in the Ashland-Castle Hill-New Sweden area.

The Perham Group

Frenchville Formation: The Frenchville Formation (Boucot et al., 1964) includes a basal conglomerate unit (Fig. 4a, b) and is dominated by thin to thickly layered greenish or bluish gray quartzose and feldspathic sandstone with lesser gray slate (Fig. 4c, d). Part of the sandstone can be calcareous and locally contain brachiopods, bryozoans, and other marine invertebrates. The basal conglomerate unconformably overlies the Middle Ordovician Winterville Formation volcanic rocks. Clasts in the conglomerate are predominantly basalt but there are subordinate amounts of other lithic clasts, including tuff, quartz, sandstone, etc. The conglomerate also commonly contains fragments of brachiopods, corals, crinoids, etc. The unconformity represents the early stage of the Salinic orogeny (Salinic A). A sample of sandstone and granule conglomerate collected from the basal conglomerate in Ashland yielded 300 detrital zircon grains and produced a characteristic Laurentian age spectrum, with the younger grains clustered at around 449 Ma (Fig. 5), indicating that the Frenchville Formation is Silurian in age, and was derived from composite Laurentia. The fossils reported by Roy (1970, 1987) from the Frenchville Formation suggested an age range from Early Llandoverian to Earliest Ludlovian (Ludlow). Because the Frenchville Formation conformably underlies the Ludlow Jemtland Formation, it is most probably Wenlock.

Figure 4. Frenchville Formation. (a) Basal conglomerate with primarily basalt clasts. (b) Basal conglomerate with polymictic clasts. (c) Thin sandstone and siltstone. (d) Medium-thick sandstone and Bouma sequence of turbidites.

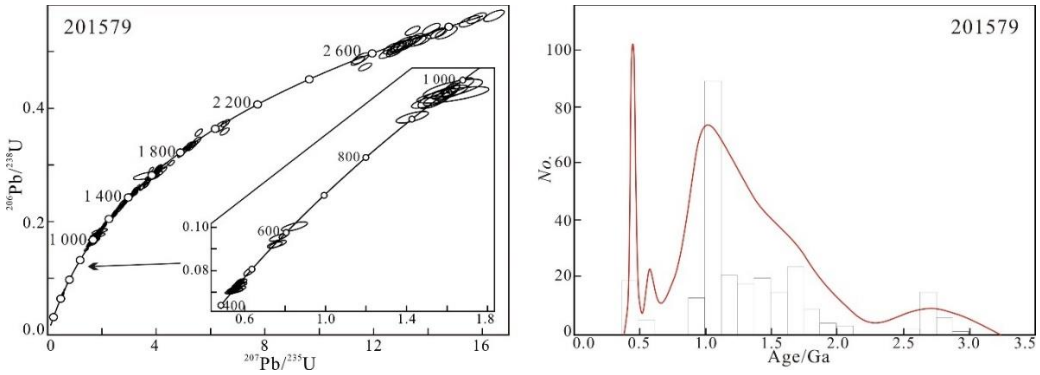

Figure 5. Age spectrum and distribution histogram of detrital zircon grains of the Frenchville Formation conglomerate. Analysis was performed by the Arizona LaserChron Center.

Jemtland Formation: The Jemtland Formation (Roy and Mencher, 1976) is primarily a well bedded package of graptolitic thin to medium layered gray calcareous and micaceous siltstone and sandstone with subordinate gray and dark gray shale. Lamination is common throughout the formation and Bouma sequences are abundant locally. A diagnostic feature of the formation is its orange or brownish tan color on weathered surfaces (Fig. 6a) and well-developed leached weathering rind. The formation is known to be rich in *monograptus* graptolite. Berry (1960, 1964) reported early Ludlow graptolites. Roy (1970) reported an extensive graptolite collection in the region identified by Berry as the early Ludlow age. Figure 6b shows a common monograptid *Saetograptus* aged Ludlow identified by David Loydell. In addition to the monograptids, the formation also contains crinoids, brachiopods, cephalopods, and gastropods, as well as burrows and tracks. A layer of gray coarse tuff and lapillistone about 18 meters thick occurs as an interval within the sandstone, siltstone, and slate in western New Sweden township along the west limb of the Stockholm Mountain syncline. Roy (1970) named this horizon "Aquagene Tuff Member". A sample of the tuff will be analyzed for zircon U-Pb dating.

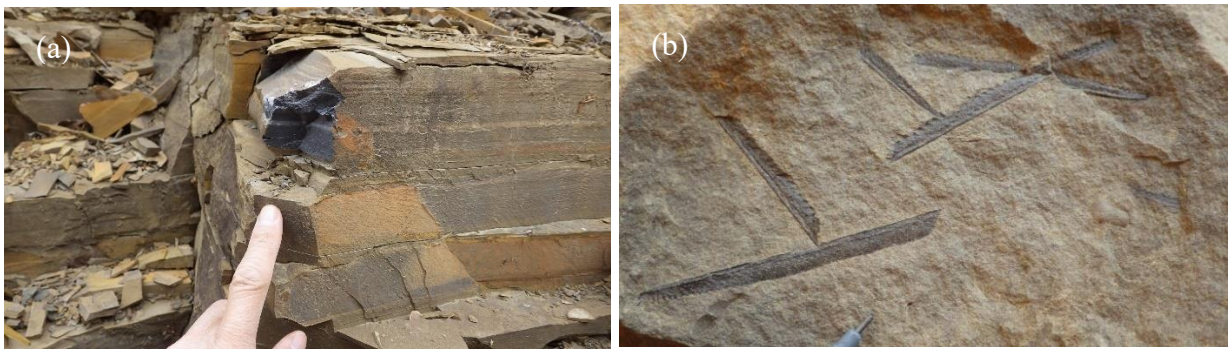

Figure 6. Jemtland Formation. (a) Thin to medium layered gray sandstone: before weathered and after weathered. (b) *Saetograptus* fossils identified by Dr. David Loydell.

New Sweden Formation: The New Sweden Formation (Roy and Mencher, 1976) generally consists of two successions, the lower succession dominated by carbonate (Fig. 7a, b) and comprising alternating thin marl (argillaceous limestone) and calcareous sandstone/siltstone/shale (Fig. 7b), and the upper succession characterized by carbonate-poor green and/or maroon/red slate (Fig. 7d). The formation begins with a layer of massive and fragmental limestone or limestone breccia of about 10-15 meters thick (Fig. 7a). The thin marl layers in the lower succession contain fossils of brachiopods, crinoids, rugose corals, bryozoans, etc. (Fig. 7c). The manganese ironstone deposits are hosted within the upper green and maroon/red slate succession. Along the northwestern flank of the Ashland-Van Buren sub-belt, however, due to an interpreted facies change, the New Sweden Formation is dominated by green and maroon slate and occurs in the cores of the Stockholm Mountain syncline and the unnamed syncline southeast of Beaver Brook Road where it had been mapped as "Fogelin Hill Formation" (Roy, 1970). Macrofossils broadly constrain the age of the New Sweden Formation, between Llandoverian to Ludlovian times, based on Roy (1970, 1987). Our initial attempt to use conodonts failed because none was found in the limestone samples. Because the New Sweden Formation conformably overlies the early Ludlovian (Gorstian) Jemtland Formation, the New Sweden is either late Ludlow (Ludfordian) or Pridoli. Roy (1970) reported fossils of Pridoli from the "Fogelin Hill Formation", supporting this proposal.

Figure 7. New Sweden Formation. (a) The massive limestone at the bottom of the formation. (b) The alternating thin layers of marl (argillaceous limestone) and calcareous siltstone/slate. (c) Fragments of all types of fossils. (d) The green and maroon/red slate.

The Fe-Mn deposits

The Fe-Mn deposits occur in the middle-lower level of the New Sweden Formation. Based on our mapping, there are several Fe-Mn (i.e., manganiferous ironstone) layers, but most of the known occurrences are of the same major layer. The Fe-Mn layers may occur either as continuous strata extending up to several hundred meters or as lenses. The Fe-Mn deposits generally occur as two stratified forms within the red and/or green/dark green slate succession: laminated to thin layers of Fe-dominated hematite, and alternating layers of laminated and/or banded Fe-rich hematite and Mn-bearing minerals. All the minerals, including hematite are microcrystalline. When fresh, Mn-mineral laminae or bands are pink or light gray, but they are generally oxidized and covered with a black film of Mn oxides, signifying higher Mn content. Some horizons have high magnetic susceptibility due to the content of magnetite. Pyrite is locally disseminated within the rock but is also concentrated in thin seams.

The Fe-Mn deposits are exposed well in several pits along the Ashland-Van Buren sub-belt. Examples include the Dudley and Ryn pits in Castle Hill and the Anderson pit in New Sweden. The largest and best example is the Dudley deposit next to Dudley Road in Castle Hill. It is located on the west limb of an anticline at a north-south-trending ridge. For convenience, we refer to the ridge as the Radio Tower Ridge. The top of the ridge exposes Frenchville Formation sandstone in the farm fields. The anticline is a doubly plunging anticline. The flanks (limbs) of the anticline are Jemtland and New Sweden formations. The west limb of the anticline is overturned and the beds dip east. A north-northeast-striking reverse fault, named the Dudley Farm Fault in this study, has moderately displaced the Frenchville and Jemtland formations. The deposit is well exposed in two pits, the north pit and south pit. We will visit the south pit that is generally called the Dudley pit.

Extensive work on ore geochemistry by portable-XRF and whole-rock XRF and ICP-MS analytical methods and on ore mineralogy by microXRF and microprobe analytical methods are underway when this trip guide is being written. As a result, this guide can only provide a description of the geology and lithology of the deposit and the orebodies – Stop 1B for the information.

THE NUMBER NINE MOUNTAIN TERRANE AND THE MAPLE MOUNTAIN SEQUENCE

The Number Nine Mountain terrane is a newly recognized lithotectonic terrane with unique composition and history. It is composed predominantly of several distinctive pre-Devonian sedimentary and volcanic rock formations and is fault bounded with the Silurian Aroostook-Matapédia Belt to the southeast and with the younger, Devonian sedimentary rocks to the northwest. The terrane is on strike with the northeast-trending Cambrian-Ordovician WLLB to the southwest (Fig. 1) and in the past, was considered part of the WLLB. However, they are different stratigraphically and are separated by a northwest-striking fault along the St. Croix Lake–St. Croix Stream valley, named the St. Croix Lake Fault in our study (Fig. 1). The stratigraphy of the Number Nine Mountain terrane is shown in Figure 9. The informally named basalt Cambrian (?) Three Brooks Conglomerate and overlying Middle Ordovician Morehouse Brook Formation are newly identified but the younger units have been described previously: the Silurian Nine Lake (Pavlides, 1964), Spruce Top (Pavlides and Milton, 1962), Dunn Brook (Pavlides, 1964), Maple Mountain (Pavlides, 1964), and Burnt Brook (Pavlides, 1966) formations (Figs. 8, 9). The Spruce Top, Dunn Brook, and Maple Mountain formations are conformable with the Maple Mountain Formation hosting the Maple-Hovey Fe-Mn deposit and are referred to here as the “Nine Mountain sequence”. The younger Devonian sedimentary and volcanic rocks

occur on the north and south sides of the Number Nine Mountain terrane: the Seboomook Group (sedimentary), Scopan Lake Formation (new; sedimentary), Hedgehog Formation (volcanic), Chapman Formation/Sandstone (sedimentary), and Mapleton Sandstone (sedimentary).

The Cambro (?)-Ordovician Formations

Three Brooks Conglomerate/Sandstone (new)

This informally named unit is exposed in an area of about 1.25 km^2 at the northeastern terminus of Nineteen Mountain ridge and on the southeast side of Three Brooks, in the E Plantation township. It consists dominantly of massive pebble conglomerate and minor pebbly sandstone and coarse lithic sandstone. The conglomerate and sandstone are commonly thick bedded and massive. The conglomerate is poorly sorted, matrix supported, and polymictic but dominated by pebbles and cobbles of gray tuff (Fig. 10). Other lithic clasts include rhyolite, black chert, quartz, granite, and red jasper. The sandstone beds are massive; the sandstone itself is coarse grained with mostly lithic fragments of tuff and lesser amounts of quartz. The dominance of volcanic clasts in both conglomerate and sandstone suggests a location close to a volcanic source.

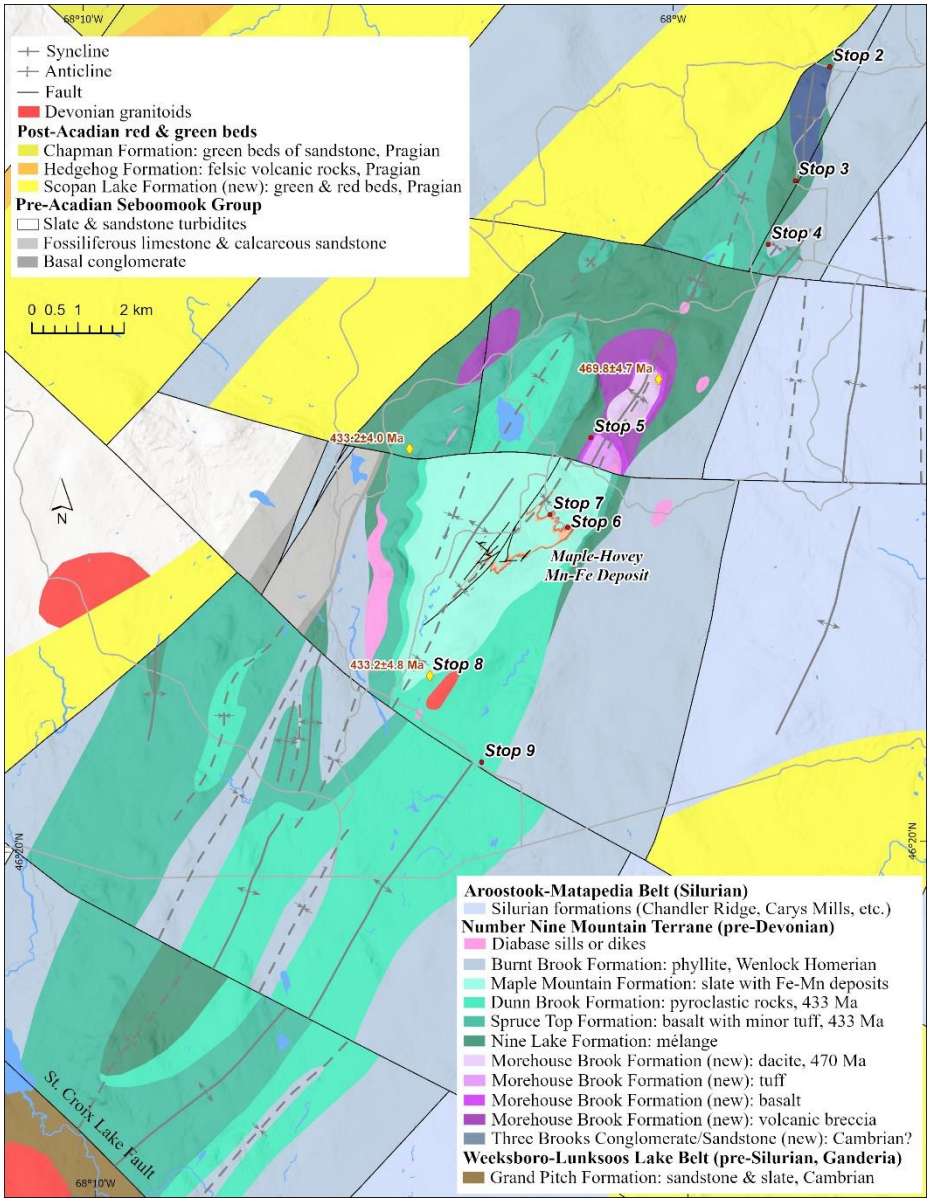

Figure 8. Geologic map of the Number Nine Mountain terrane and vicinity with stops.

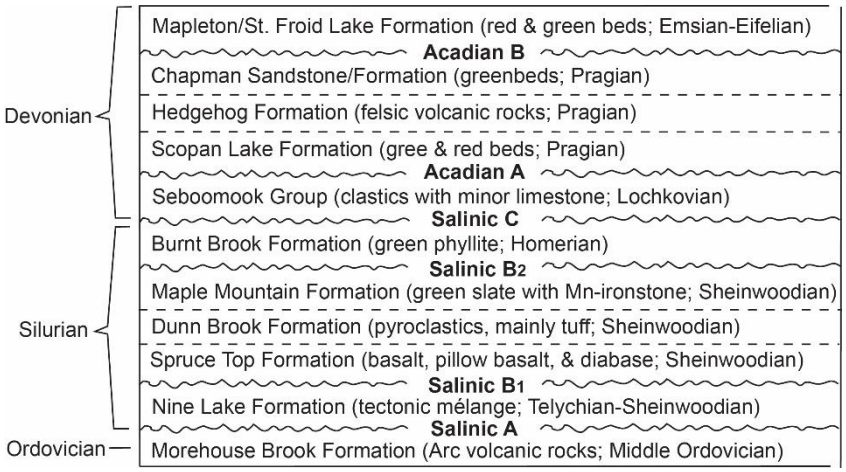

Figure 9. Simplified stratigraphic column showing interpreted stratigraphy of the Number Nine Mountain terrane and vicinity and orogenic events. Wavy lines mark unconformities. Dashed lines indicate conformable contact.

Figure 10. Three Brooks Conglomerate/Sandstone. (a) Preston Bass (left, undergraduate field assistant) and Lauren Madsen (right, graduate student) at a conglomerate outcrop. (b) The poorly sorted pebble conglomerate.

A sandstone sample was collected for detrital zircon U-Pb geochronological analysis at the University of Maine MAGIC Laboratory (Laser Ablation ICP-MS). After separation, 277 zircon grains were suitable for U-Pb dating. The detrital age spectrum reveals distinct peaks at 2730 Ma, 2479 Ma, 1675 Ma, 1349 Ma, 1078 Ma, and one grain at 565 Ma (Fig. 11). These peaks are typical for Laurentian terranes, indicating a peri-Laurentian affinity for the Number Nine Mountain Terrane.

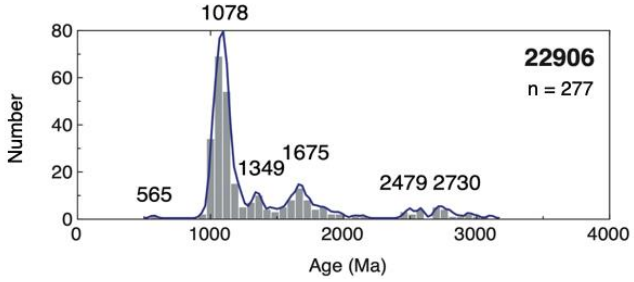

Figure 11. Detrital zircon spectrum and distribution histogram of the Three Brooks Conglomerate/Sandstone.

Morehouse Brook Formation (new)

The Morehouse Brook Formation consists of four volcanic-subvolcanic rock units, from the oldest to the youngest, the foliated volcanic breccia, basalt, tuff, and dacite units (Fig. 8). The first three appear to be conformable while the dacite (the "Morehouse Brook dacite") has a sub-discordant intrusive contact with the three older units and is interpreted to be a sub-volcanic lopolith. The volcanic breccia is composed of blocks or fragments of vesicular basalt, basalt, rhyolite, pumice, and tuff (Fig. 12a). These vary in size but are generally between 3 cm and 15 cm in diameter

with a few up to boulder size. The finer grained breccias and lapillistone are locally strongly foliated (Fig. 12b). The basalt is predominantly vesicular and amygdaloidal, is not foliated, and is locally pillowed. The tuff unit includes dominantly fine-grained gray crystal tuff with plagioclase microphenocrysts, coarser tuff with small endogenous blocks of tuff and tuffaceous breccia (Fig. 12c), most of which is foliated. The Morehouse Brook dacite is massive and porphyritic with euhedral-subhedral plagioclase phenocrysts (up to 50% of the rock; Fig. 12d) set in a fine-grained matrix of essentially small plagioclase feldspar laths and minor augite or hornblende and quartz.

Lithogeochemical analyses of four tuff and five dacite samples from the formation show peraluminous, calc-alkaline affinity with a few being transitional (Fig. 13a). Both tuff and dacite samples are characterized by depletion in high field strength elements P, Ti, Ta, and Nb and enrichmet in large ion lithophile elemets Rb, K, Ba, and Th on the MORB-normalized spidergram (Fig. 13b), typical of a subduction signature. The samples also show slope profile and negative Eu anomalies (Fig. 13c), with an avarage Eu/Eu* value of 0.748 (ranging from 0.379 to 1.021). On the La/Yb vs. Nb/La diagram, most of the samples plot in the "continental arcs" field (Fig. 13d).

A dacite sample yielded a LA-ICP-MS U-Pb zircon $^{207}Pb/^{235}U$–$^{206}Pb/^{238}U$ concordia age of 468.9 ± 1.8 Ma (Fig. 14a) and a weighted mean $^{206}Pb/^{238}U$ age of 469.8 ± 4.7 Ma (Fig. 14b). The Number Nine Mountain terrane therefore represents an active continental arc setting during the Middle Ordovician time.

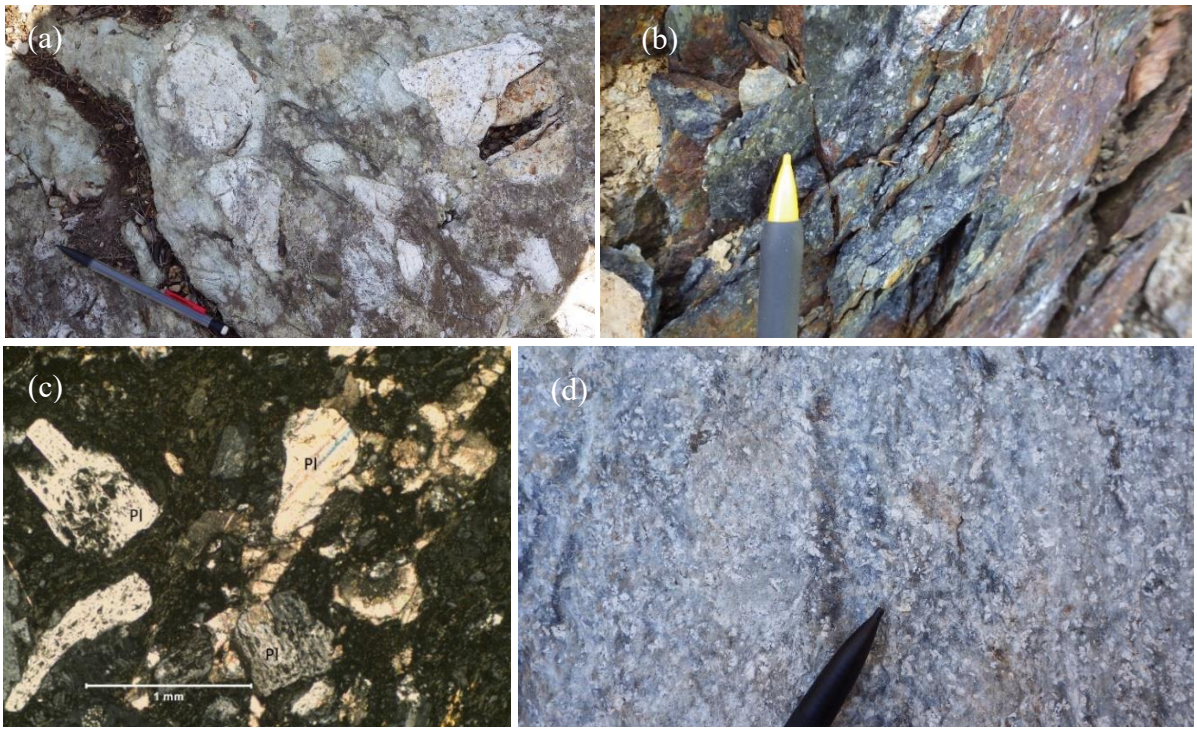

Figure 12. Morehouse Brook Formation. (a) Blocks and fragments of dominantly felsic tuff, rhyolite, and pumice. (b) Substantially foliated volcanic breccia or lapillistone made of smaller fragments of tuff and/or basalt. (c) Photomicrograph showing foliated coarse crystal tuff dominated mostly by feldspar fragments and minor lithic fragments. Cross-polarized light. Pl – plagioclase feldspar. (d) Outcrop photo of the Morehouse Brook dacite showing ~50% vol. of plagioclase feldspar phenocrysts.

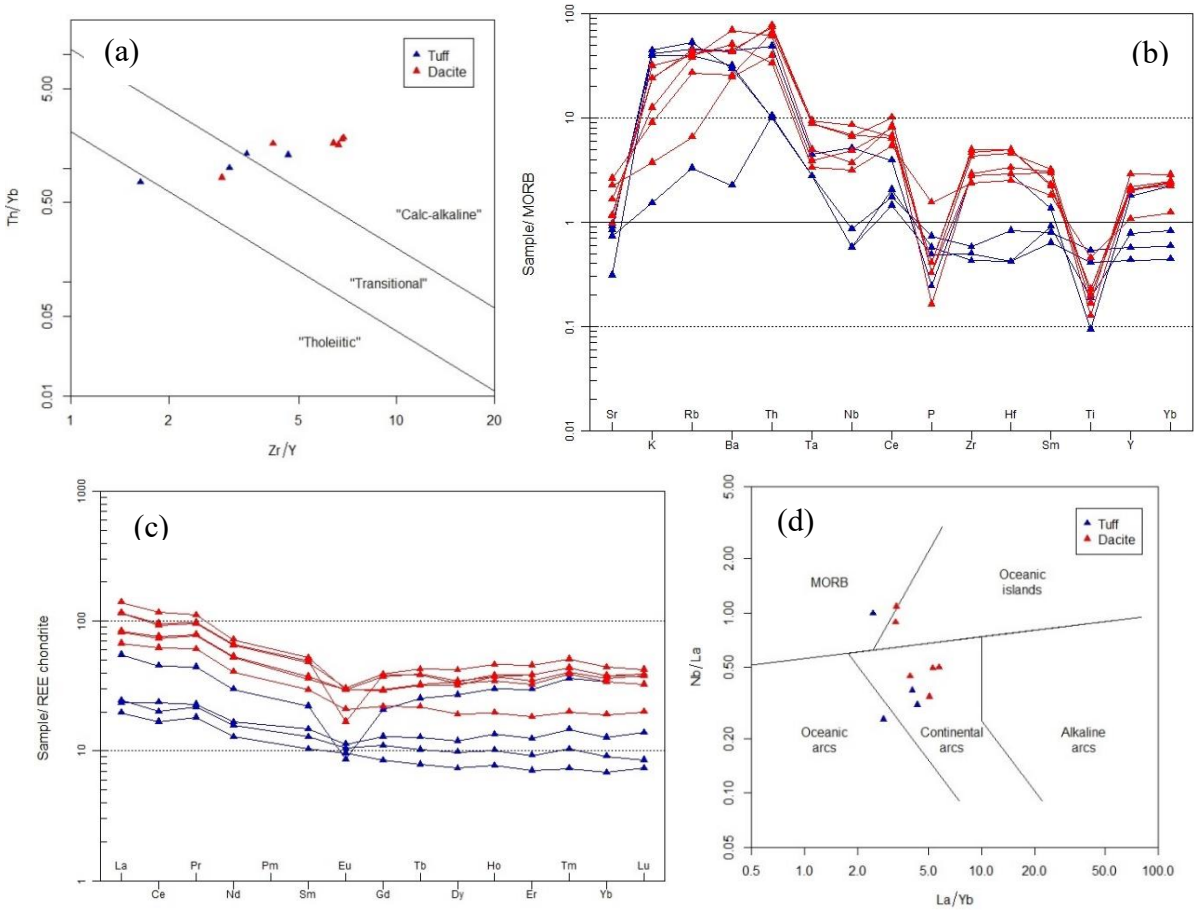

Figure 13. Classification and discrimination diagrams for the Morehouse Brook dacite and tuff. (a) Zr/Y vs. Th/Yb diagram (Ross and Bedard, 2009). (b) MORB-normalized spidergram (Pearce, 1983). (c) Chondrite-normalized REE pattern (Nakamura, 1974). (d) La/Yb vs. Nb/La diagram (Hollocher et al., 2012).

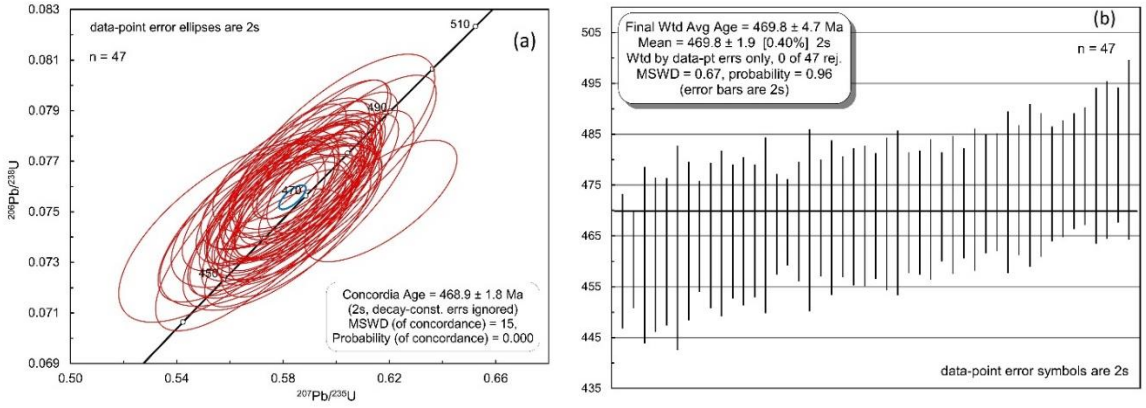

Figure 14. (a) Zircon $^{207}Pb/^{235}U$–$^{206}Pb/^{238}U$ concordia diagram of the Morehouse Brook dacite. (b) Weighted mean $^{206}Pb/^{238}U$ age diagram of 47 analyses giving an age of 469.8 ± 4.7 Ma for the Morehouse Brook dacite.

The Silurian Formations

Nine Lake Formation

The Nine Lake Formation (Pavlides, 1964) has been redefined to be predominantly mélange. The mélange was mistaken as conglomerate in the past. The mélange is widespread within the northeast-trending Number Nine

Mountain terrane in the region between St. Croix Lake in the southwest and E Plantation in the northeast. The formation also includes some sizable portions of well-bedded, medium-thin-layered gray or green sandstone, slate, and phyllite that may occur as giant blocks of the mélange package. The formation unconformably overlies the Middle Ordovician Morehouse Brook Formation but underlies the younger, Silurian and Devonian sedimentary and volcanic formations (Figs. 8 and 9). The mélange is characterized by various sizes (up to a meter in diameter, but mostly between 5 cm and 20 cm) of exotic and native (endogenic) angular fragments and blocks of sedimentary rocks such as sandstone, slate, cherty mudstone, and quartzite, with minor dolomite and limestone (Fig. 15). The mélange is pervasively foliated with anastomosing foliation, particularly where the blocks and fragments are small (Fig. 15b). The matrix of the mélange is generally dark slate, but exhibits rusty weathering in places where it is pyritic. The mélange also contains rare pyrite concretion balls or nodules, as large or as long as 15 cm.

Figure 15. Nine Lake mélange. (a) Least foliated. (b) Foliated.

A sample from a sandstone block in the mélange yielded 258 detrital zircons, most of which cluster at 435 Ma on the age-probability diagram (Fig. 16), with only a few older ones of 558 Ma, 616 Ma, 1009.9 Ma, and 1377 Ma. Many younger ones range from 435 Ma to 421 Ma. The results indicate a limited sediment source and deposition in a small, restricted basin. The age range 435–421 Ma for the younger zircon grains would normally suggest the upper limit of the sedimentation age – in this case, it would be from Wenlock to Pridoli. However, the mélange is unconformably overlain by the stratified volcanic rocks of the Spruce Top and Dunn Brook formations both of which are dated at 433 Ma, which suggests that the Nine Lake mélange should be slightly older.

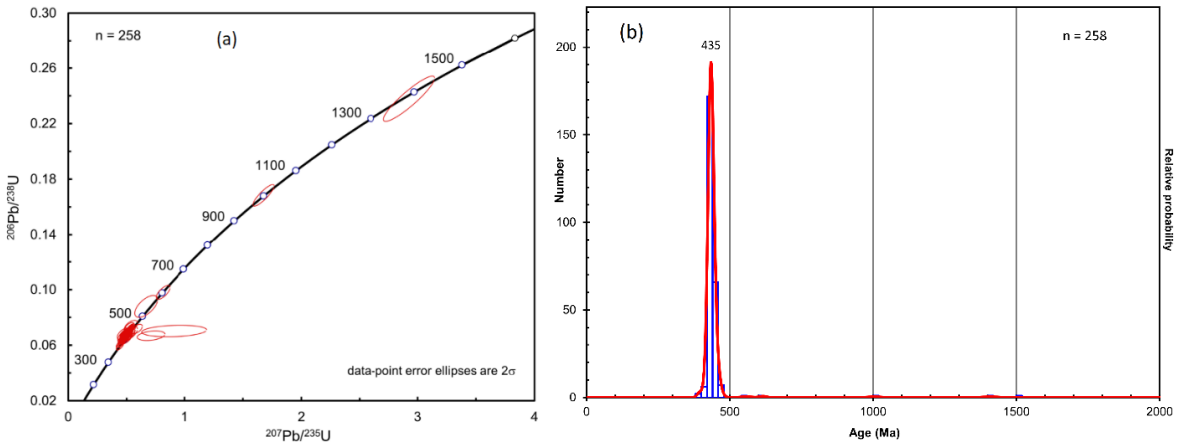

Figure 16. Detrital zircon age data of the Nine Lake mélange. (a) U-Pb concordia diagram showing a single-cluster spectrum. (b) Age-probability diagram showing only one peak at around 435 Ma.

The Nine Mountain Sequence

The Nine Mountain sequence includes three conformable formations: Spruce Top, Dunn Brook, and Maple Mountain formations. The Maple-Hovey Fe-Mn deposit is hosted by the Maple Mountain Formation, making the Nine Mountain sequence of economic importance.

Spruce Top Formation: Initially named "Spruce Top greenstone" (Pavlides and Milton, 1962), the formation is composed predominantly of basalt with minor andesite and dacite, as well as several subvolcanic diabase sills

interlayered within the basalt, for example, a large diabase sill along the Meduxnekeag Mountain ridge. Basalt is commonly vesicular and amygdaloidal with amygdales of quartz, calcite, chlorite, and epidote. Some basalts are featureless, while others occur as pillows (Fig. 17a), hyaloclastite, or agglomerate. Basalt can be phyric with plagioclase phenocrysts. Some basalt flows show spectacular spherulitic textures caused by devitrification (Fig. 17b). Dacite is porphyritic or slightly porphyritic with mostly plagioclase feldspar phenocrysts in fine-grained matrix (Fig. 17c); Other phenocrysts include augite and corroded quartz (Fig. 17c). Thin layers of foliated, laminated gray coarse tuff and lapillistone occur within the basalt flows at Saddleback Mountain and Meduxnekeag Mountain (Fig. 17d). The formation unconformably overlies the mélange of the Nine Lake Formation and the volcanic rocks of the Morehouse Brook Formation.

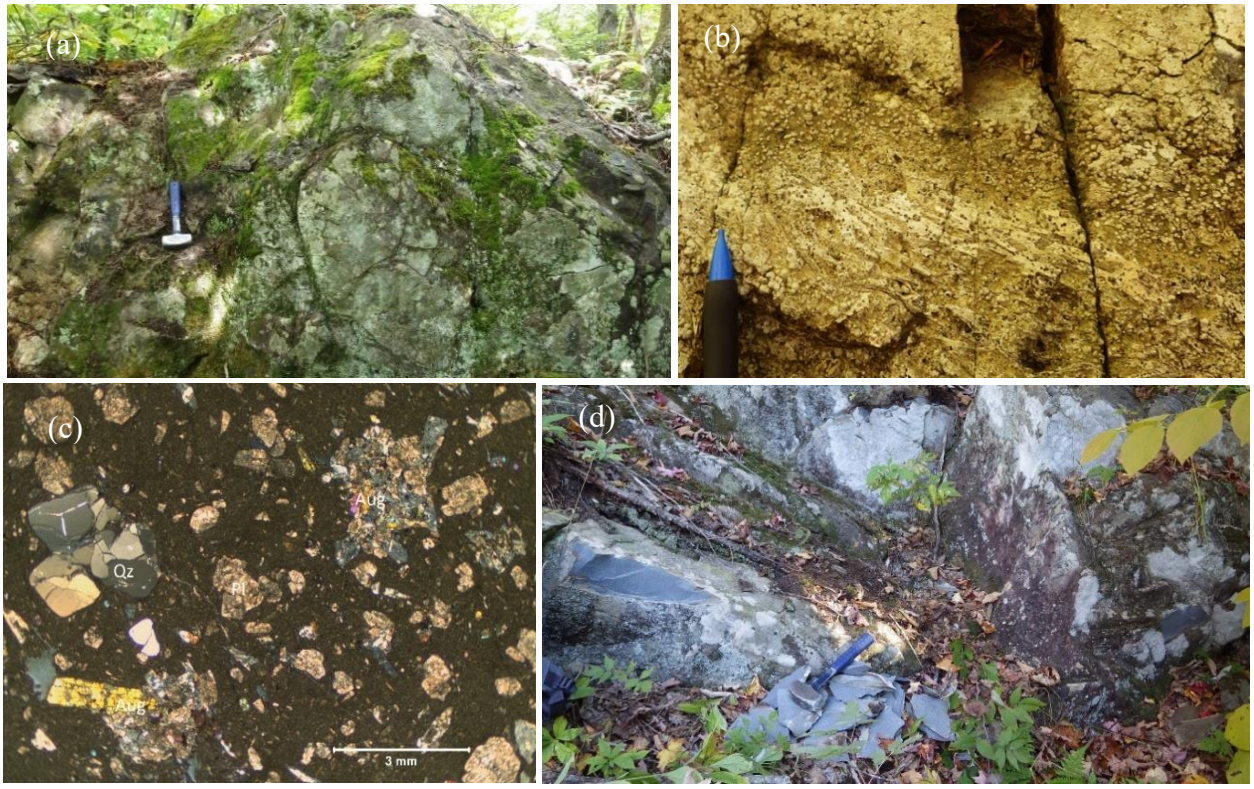

Figure 17. Spruce Top Formation. (a) Pillow basalt. (b) Spherulitic basalt caused by devitrification. (c) Photomicrograph showing typical porphyritic texture of dacite with plagioclase, corroded quartz, and augite phenocrysts. (d) Laminated gray fine tuff sandwiched in the Spruce Top basalt.

Geochemical analyses of twelve Spruce Top volcanic rocks plot in transitional to calc-alkaline fields (Fig. 18a). The dominantly basaltic volcanic rocks are substantially enriched in LILE elements Rb, Ba, and K, and are depleted in HFSE elements Nb, Ta, P, and Ti, as well as enrichment of Th on the primitive-mantle-normalized and MORB-normalized spidergram (Fig. 18b). The chondrite normalized REE patterns (Fig. 18c) demonstrate relative enrichment of LREE over HREE. All of these are typical subduction signatures. The chondrite normalized REE patterns also show negative Eu anomalies from seven samples. The average Eu/Eu* value is 0.783, indicating a moderate negative Eu anomaly for the volcanic rocks. On the Nb/Yb vs. Th/Yb discrimination diagram (Fig. 18d), all the samples fall in the "volcanic arc array". In summary, the calc-alkaline basalt-dominating volcanic rocks of the Spruce Top Formation were products of oceanic subduction along a continental arc.

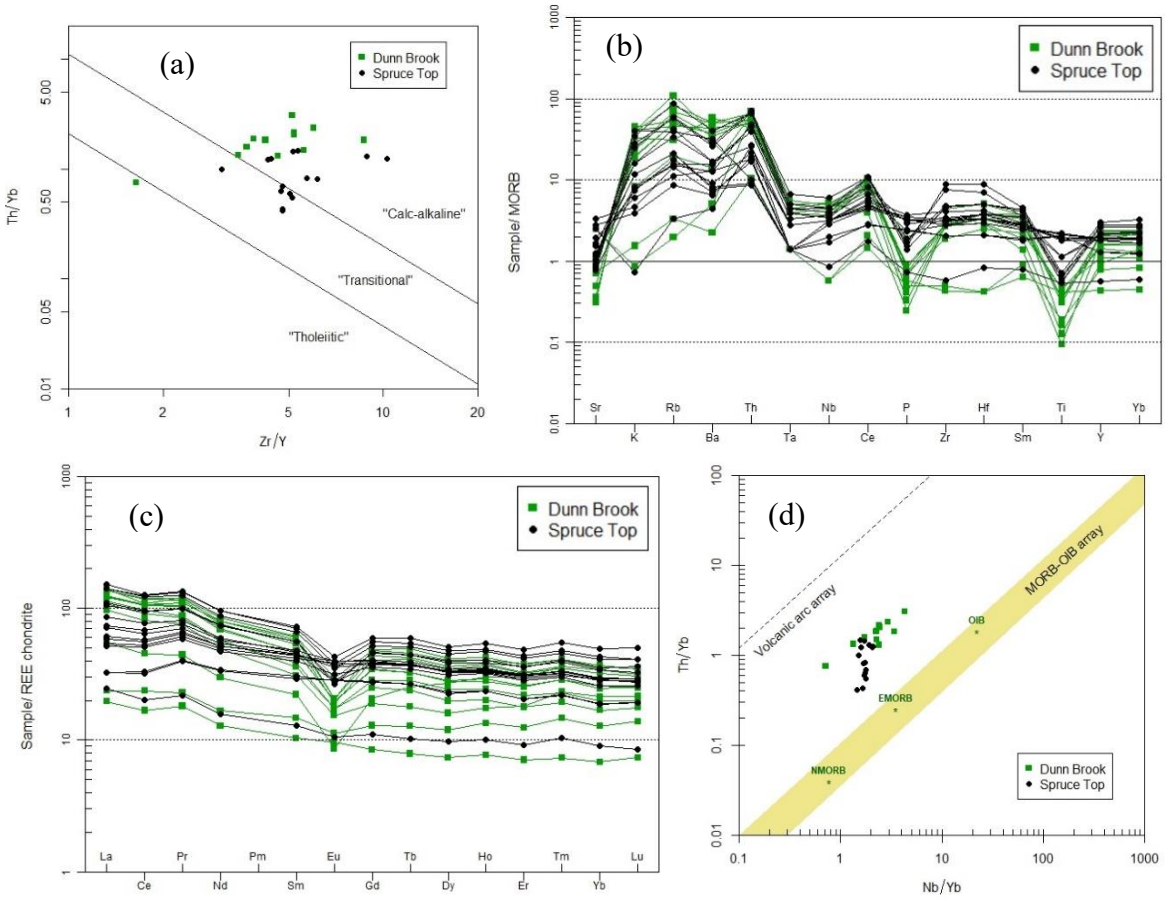

Figure 18. Geochemistry and tectonic discrimination of the Spruce Top and Dunn Brook formations. (a) Zr/Y vs. Th/Yb diagram (Ross and Bedard, 2009). (b) MORB-normalized spidergram (Pearce, 1983). (c) Chondrite-normalized REE pattern (Nakamura, 1974). (d) Nb/Yb vs. Th/Yb diagram (Pearce, 2008).

A coarse gray tuff yielded a $^{207}Pb/^{235}U$–$^{206}Pb/^{238}U$ concordia age of 432.2 ± 2.5 Ma and a weighted mean $^{206}Pb/^{238}U$ age of 433.2 ± 4.0 Ma (Fig. 19). A few zircon crystals contain cores between 1000–1300 Ma that are most likely inherited from initial Grenvillian zircons. Spruce Top arc volcanism thus took place in mid-Silurian time – the beginning of the Sheinwoodian Stage (Wenlockian).

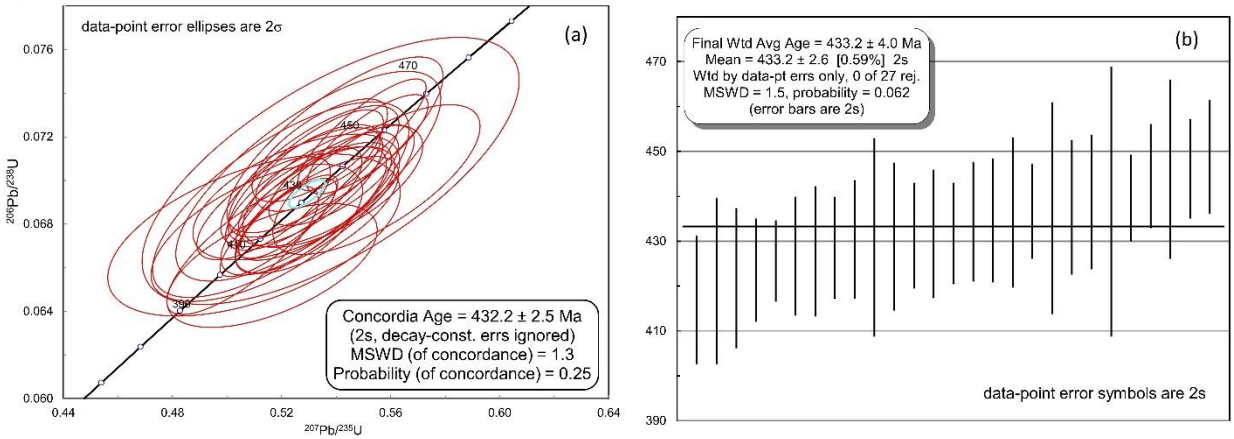

Figure 19. Concordia and weighted mean ages of zircon crystals from the Spruce Top Formation. (a) U-Pb concordia diagram. (b) Weighted mean age.

Dunn Brook Formation: The Dunn Brook Formation (Pavlides, 1964, 1974) has been redefined to include only pyroclastic rocks of dominantly gray tuff and lesser volcanic breccia and lapillistone. The pyroclastic volcanic rocks are well bedded, varying from laminated to thickly layered. The volcanic breccia is made mainly of light-colored felsic tuff with lapillistone blocks that generally range between 7 cm and 15 cm in diameter (Fig. 20a). The tuff is either fine or coarse grained and most of it is felsic crystal tuff (Fig. 20b), with only very minor lithic tuff. Mafic tuff is also generally minor except for a large exposure of mafic crystal tuff with abundant augite crystals (Fig. 20b) along an unnamed ridge south of Hovey Mountain and north of North Meduxnekeag Branch. All the pyroclastics are typically pervasively foliated. The formation conformably overlies the basalts of the Spruce Top Formation and underlies the fine clastic sedimentary rocks of the Maple Mountain Formation.

Nine Dunn Brook tuff samples show similar geochemical characteristics to the Spruce Top basalt-andesite-dacite samples. They plot in the andesite–rhyodacite/dacite-rhyolite fields, but dominantly in the rhyodacite/dacite field in the Nb/Y vs. Zr/TiO_2 diagram (not shown here). All but one of the tuff samples are peraluminous and calc-alkaline (Fig. 18a). The primitive-mantle-normalized and MORB-normalized trace elemental spidergrams show significant depletion in P and Ti and moderate depletion in Ta and Nb of the HFSE, and strong enrichment in K, Rb, and Ba of the LILE (Fig. 18b). The chondrite-normalized REE patterns (Fig. 18c) indicate enrichment of LREE relative to HREE. The chondrite normalized REE patterns also show very strong negative Eu anomalies for all the analyses (except for one sample). The average Eu/Eu* value is 0.492, indicating significant negative Eu anomalies for the Dunn Brook tuff. Like the basalt-dominant Spruce Top Formation, the notable depletion of Ta, Nb, P, and Ti, enrichment of K, Rb, Ba, and Th, and elevated LREE relative to HREE with a very strong Eu negative anomaly are typical of subduction signatures. On the Nb/Yb vs. Th/Yb discrimination diagram, all the samples fall in the "volcanic arc array" (Fig. 18d). Thus, the calc-alkaline felsic tuff was product of oceanic subduction along a continental arc.

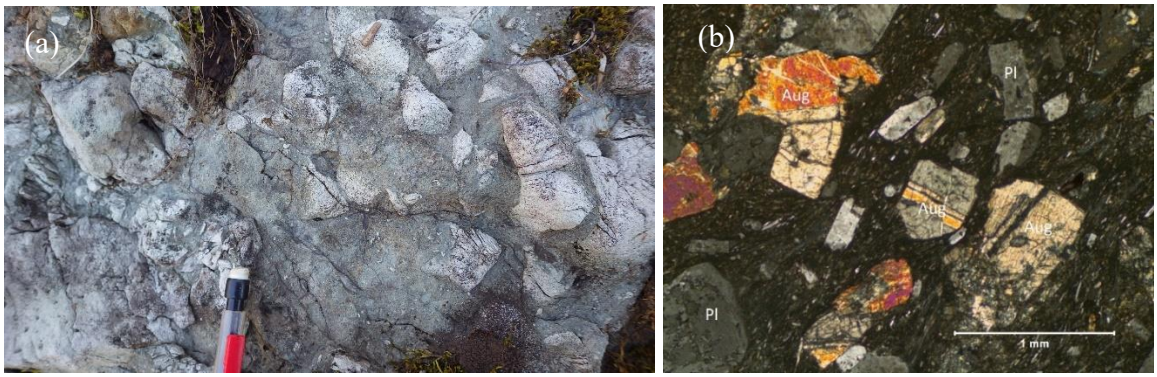

Figure 20. Pyroclastic rocks of the Dunn Brook Formation. (a) Volcanic breccia with mostly light gray felsic tuff blocks. (b) Photomicrograph showing foliated coarse mafic crystal tuff composed of augite and plagioclase feldspar fragments. Cross polarized light. Aug – augite; Pl – plagioclase feldspar.

A gray coarse tuff sample from the Dunn Brook next to its conformable contact with the Maple Mountain formations yielded a weighted mean $^{206}Pb/^{238}U$ age of 433.2 ± 4.8 Ma (Fig. 21) that is the same as the weighted mean age of the underlying Spruce Top Formation. A dozen zircon crystals contain inherited cores around 1000–1300 Ma, again suggesting Grenvillian inheritance, with a couple at 2600–2800 Ma and several at around 450–490 Ma. The 433 Ma age indicates that the Dunn Brook arc volcanism took place in the beginning of the Sheinwoodian Stage of the Silurian – Wenlock time, about in the middle of the Silurian, as indicated by the age of the immediately underlying, conformable Spruce Top Formation. It was likely that the northwest-dipping (current coordinates) Salinic subduction with the Tetagouche back-arc oceanic basin subducting underneath the composite Laurentia, resulted in the Spruce Top and Dunn Brook arc volcanism. The Silurian arc volcanic rocks distributed in the southwestern Munsungun inlier are 424–427 Ma and are also considered as products of the Salinic Brunswick Subduction (Wang, 2023b). The age data suggests that the subduction zone migrated towards the west (current coordinates) in a trench advance mode with slab rollover.

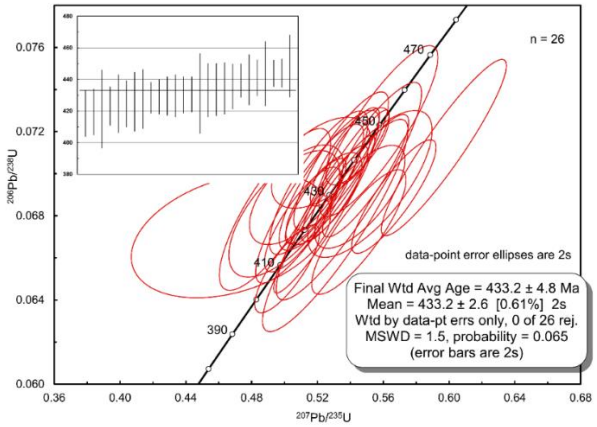

Figure 21. Zircon U-Pb concordia and weighted mean age of the Dunn Brook tuff.

Maple Mountain Formation: The Maple Mountain Formation (Pavlides, 1964) has been redefined to consists predominantly of green and gray-green slate with minor intercalated thinly layered gray calcareous siltstone, limy mudstone, and slate at lower levels of the formation. The formation is conformable with the underlying gray tuff layers of the Dunn Brook Formation. The parent rocks of the dominant green slate are thin to medium-layered, either calcareous or non-calcareous, micaceous mudstone, silty mudstone, and siltstone. Microscopically, the green slate is composed mostly of small muscovite flakes and chlorite, with chlorite causing the green color. The formation is limited to the Maple-Hovey basin and has not been found in any other place (Fig. 8). Fe-Mn layers in the middle-upper level across Maple and Hovey mountains form the "Maple-Hovey manganese deposit".

Burnt Brook Formation

The Burnt Brook Formation (Pavlides, 1966, 1973) has been also redefined and it consists predominantly of green and grayish green (or rarely pinkish green and gray) phyllite with rare intercalated polymictic, matrix-supported conglomerate layers and sparse fossiliferous limestone nodules or thin marl layers. The formation is widespread in the Number Nine Mountain area, along the southeast and northwest flanks of the Number Nine Mountain terrane and the Weeksboro-Lunksoos Lake Belt (Fig. 8). The green phyllite (Fig. 22a) is characteristically non-calcareous. Its parent rocks were fine-grained clastic sedimentary rocks of interlayered mudstone (dominating) and sandstone/siltstone of deep-water turbidites. The thickness of the mudstone and sandstone/siltstone beds generally varies from 1 cm to 20 cm (laminated to medium layered). Again, the abundance of chlorite (Fig. 22b) causes the phyllite to be green.

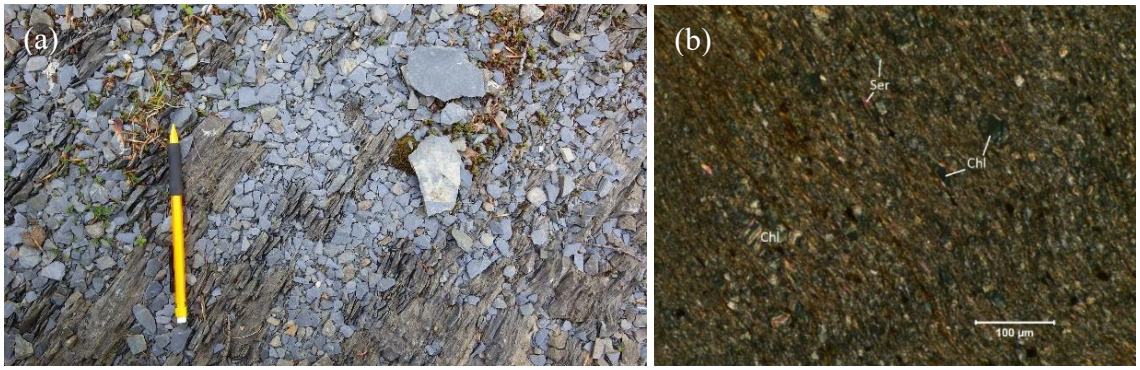

Figure 22. Burnt Brook Formation. (a) Typical green phyllite. (b) Photomicrograph showing sericite and chlorite in crenulated green phyllite. Chlorite is present as larger flakes. Cross polarized light. Chl – chlorite; Ser – sericite.

The calcareous sandstone and siltstone contain crinoid fragments, bryozoans (*Cryptostomes*), rugose corals (*Blothrophyllumv sp.*), *Favosites*, bivalves (*Paleoneilo sp.*), and dendroid graptolite. A sample of fossiliferous limestone was collected for conodonts and microfossils, processed at the University of Évora, Portugal, and yielded abundant *Ozarkodina bohemica*. The presence of *Ozarkodina bohemica*, the index species of the *Ozarkodina bohemica* biozone, indicates a Wenlock Homerian age/stage (of Middle to Late Silurian) (Fig. 23).

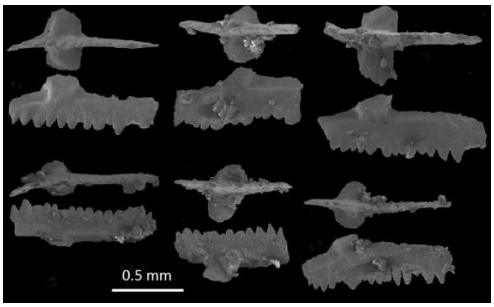

Figure 23. *Ozarkodina bohemica* from the Burnt Brook Formation.

LA-ICP-MS U-Pb ages of 283 detrital zircons are shown on the U-Pb concordia (Fig. 24a) and relative age-probability diagrams (Fig. 24b). Both diagrams show a Laurentia spectrum with a robust Grenvillian peak at 1052 Ma and an addition of an early Late Ordovician thermal peak at 455 Ma (which is also the youngest age peak), demonstrating that the sediments of the Burnt Brook Formation were sourced from composite Laurentia.

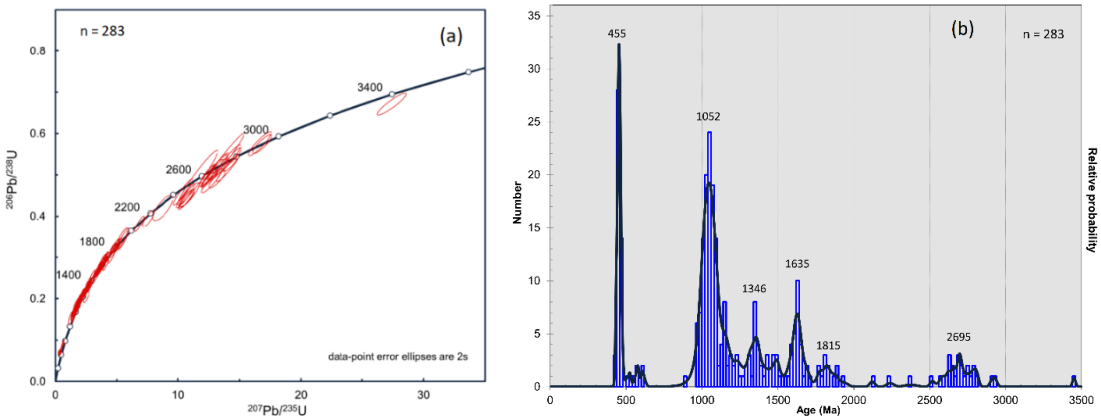

Figure 24. Zircon U-Pb concordia age spectrum (a) and age-probability diagram (b) of the detrital zircon grains from the Burnt Brook Formation.

Geologic and tectonic history of the Number Nine Mountain terrane

Unconformities reveal seven hiatuses within the stratigraphy of the Number Nine Mountain terrane and associated peripherals (Fig. 9), each representing separate orogenic events: the hiatus between the Middle Ordovician Morehouse Brook Formation and the possible Cambrian Three Brooks Conglomerate/Sandstone, the hiatus between the Mid Silurian Nine Lake and Morehouse Brook formations, the hiatus between the Spruce Top and Nine Lake formations, the hiatus between the Burnt Brook and Maple Mountain formations, the hiatus between the Seboomook Group and Burnt Brook Formation, the hiatus between the Scopan Lake Formation and Seboomook Group, and the hiatus between the Mapleton Sandstone and Chapman Sandstone/Formation. The earliest hiatus was probably caused by the Taconic orogeny along the Laurentian margin. The second hiatus is interpreted to represent the first phase of the Salinic orogeny (Salinic A), the second and third to Salinic B, and the fourth to Salinic C, as reported in northern New Brunswick by Wilson and Kamo (2012). The fifth ("Acadian A" in our study) corresponds to the early and main phase of the Acadian orogeny, and the sixth ("Acadian B" in our study) to the later and weak phase of the Acadian orogeny.

The Laurentian spectrum of the Three Brooks Conglomerate/Sandstone indicates its affinity to the Laurentian continent. Any sedimentary formation deposited after the accretion of peri-Gondwanan Ganderia to the peri-Laurentian margin since Middle Ordovician could contain detrital zircons with Laurentian signature – this is true for all the post-Middle Ordovician formations of northern Maine that we have dated. However, every detrital zircon study we have done also shows Middle Ordovician and/or Silurian zircons. Therefore, the likelihood of the Three Brooks Conglomerate/Sandstone being older than Ordovician is very high. Nevertheless, it is remotely possible that a post-Middle Ordovician formation may not contain any Ordovician and/or Silurian zircon. To be cautious, we use "possibly" for the Three Brooks Conglomerate/Sandstone to be peri-Laurentia before more work to be done.

The Middle Ordovician (470 Ma) Morehouse Brook calc-alkaline volcanic rocks erupted in a continental arc setting probably along a peri-Laurentia terrane margin. The formation is unconformably overlain by the Middle Silurian Nine Lake Formation mélange. In addition to absence of any Upper Ordovician sedimentary rocks, the unconformity (Salinic A) also indicates a lack of any Lower Silurian sedimentary or volcanic rocks in the terrane due to the relatively long hiatus. It is suggested that during the Salinic A phase, the NNM terrane and vicinity went through significant uplifting during the early stage of the Salinic orogeny.

The unconformably overlying 433 Ma, Middle Silurian Spruce Top and Dunn Brook calc-alkaline volcanic rocks erupted in a continental arc setting, suggesting a short episode of volcanism due to Salinic subduction. Compared to the tectonic history of northern New Brunswick, it is suggested that this arc volcanism was resulted from the northwest-west-dipping subduction of the Tetagouche back-arc basin, called the New Brunswick Subduction during Salinic B (Wilson and Kamo, 2012). The 433 Ma age of the Spruce Top-Dunn Brook volcanic rocks are near coeval to the Nine Lake mélange, suggesting that the mélange was accreted to the arc immediately prior to the volcanism, forming an unconformity, called Salinic B1 in our study. The Spruce Top and Dunn Brook volcanic rocks could be correlated with Quinn Point and Pointe Rochette volcanic rocks in northern New Brunswick where the volcanic rocks are considered as important evidence for the Early-Middle Silurian Salinic subduction (Wilson, 2008).

No ***Salinic mélange*** had been reported in New England or New Brunswick before our study. Now we believe we have found it in the Number Nine Mountain terrane – it is the Nine Lake mélange.

The Fe-Mn-bearing fine clastic rocks of the Maple Mountain Formation which conformably overly the Dunn Brook volcanic rocks were likely deposited in a constricted foredeep along the Salinic arc after the 433 Ma volcanism halted in the Number Nine Mountain area. The Salinic subduction culminated with rapid closing of the Tetagouche back-arc basin and collision of the back-arc basin with the composite Laurentia during the early Homerian (Silurian – Wenlock), at around 430 Ma. The area was uplifted but the uplifting did not last long before another marine transgression deposited the widespread turbidites of the Burnt Brook Formation along the Number Nine Mountain terrane and the Weeksboro-Lunksoos Lake belt (both belts were amalgamated and became part of composite Laurentia after Popelogan arc accretion). The Burnt Brook sediments were sourced from composite Laurentia as indicated by its detrital zircon age spectrum. The unconformity (Salinic B2 in our study) represents the end of the significant Salinic orogenesis (subduction, volcanism, collision, and uplifting).

The Homerian Burnt Brook Formation is unconformably overlain by Lower Devonian sedimentary rocks, such as the Lochkovian Seboomook Group and Pragian Scopan Lake Formation. The short hiatus between the Seboomook and the Burnt Brook indicates another short period of uplifting, followed quickly by another marine transgression – forming the Devonian sea on the foreland. The unconformity is called Salinic C; it marks the end of the Silurian Salinic orogeny. Northern Maine then stepped into the Acadian phase. The Salinic orogenesis did not produce significant deformation structures, likely only faults, without any penetrative foliation.

The Early Acadian orogeny associated with subduction and collision of the Avalon terrane was significant throughout Maine, including this study area. It produced tight folds, large-scale reverse-thrust faults, and penetrative foliation and affected all the pre-Acadian formations in Maine. Examples are the northeast- and southwest-plunging anticline and synclines, including the Maple-Hovey composite syncline that hosts the Maple-Hovey Fe-Mn deposit.

The Number Nine Mountain terrane and the vicinity were significantly faulted and displaced mostly during the Neoacadian orogenesis, producing a number of fault blocks that characterize the structural pattern of the Number Nine Mountain region.

THE MAPLE-HOVEY MANGANESE IRONSTONE DEPOSITS

Fe-Mn deposits are generally characterized by interbedded iron-bearing minerals (dominantly hematite) and manganese-bearing minerals (e.g., Mn-carbonate rhodochrosite, rhodonite, braunite, pyrolusite, and manganite), which indicates that the Fe-Mn deposits were precipitated in seawater enriched in both iron and manganese elements, but that they were differentiated from each other at the site of precipitation, likely by change in oceanic water oxidation state or acidity (Cannon et al., 2017). The solubility of manganese and iron is enhanced in anoxic water, and such water may deliver these elements to sites of nucleation and precipitation of manganese and iron oxides and/or carbonates by coastal upwelling onto continental margins. This mechanism for Fe-Mn metallogenesis originally proposed by Petránek (1991), is favored by almost all recent interpretations of Fe-Mn deposits.

Geology of the Maple-Hovey Fe-Mn Deposit

The Spruce Top, Dunn Brook, and Maple Mountain formations of the Nine Mountain sequence that hosts the Fe-Mn deposits have been folded into a composite syncline, named the Maple-Hovey composite syncline (Fig. 25). The

composite syncline consists of three major sub-folds, including the sub-syncline along the Hovey and Maple mountains where the Fe-Mn deposit exists. This sub-syncline is well revealed by 105 trenches and 61 boreholes made in 1949–1951, and by limited outcrops at both mountains. The axial plane of the sub-syncline dips to the northwest at 60–70º. The sub-syncline shows a complicated folding style with numerous second-order folds of various sizes as shown by the folded layers of Fe-Mn minerals. The sub-syncline is faulted and displaced by the northwest-dipping Hovey Mountain reverse fault.

The Fe-Mn deposits are presented as sedimentary manganese-bearing ironstone layers or lenses within the green slate of the Maple Mountain Formation. The Fe-Mn orebodies vary in composition from almost pure manganese layers to almost pure iron layers but generally represent a mixture of both in variable concentrations. Based on our study and Eilertsen (1952) and Pavlides and Milton (1962), the Fe-Mn deposit occurs in two forms: the stratiform manganiferous hematitic ironstone layers that constitute the main deposit of the Maple-Hovey Fe-Mn deposit – the "*main deposit*", and the magnetic manganiferous siliceous carbonate lenses – the "*magnetic carbonate lenses*". Both lie in the upper part of the Maple Mountain Formation but at different levels, with the main deposit slightly higher than the magnetic carbonate lenses. The main deposit includes all the major Fe-Mn orebodies.

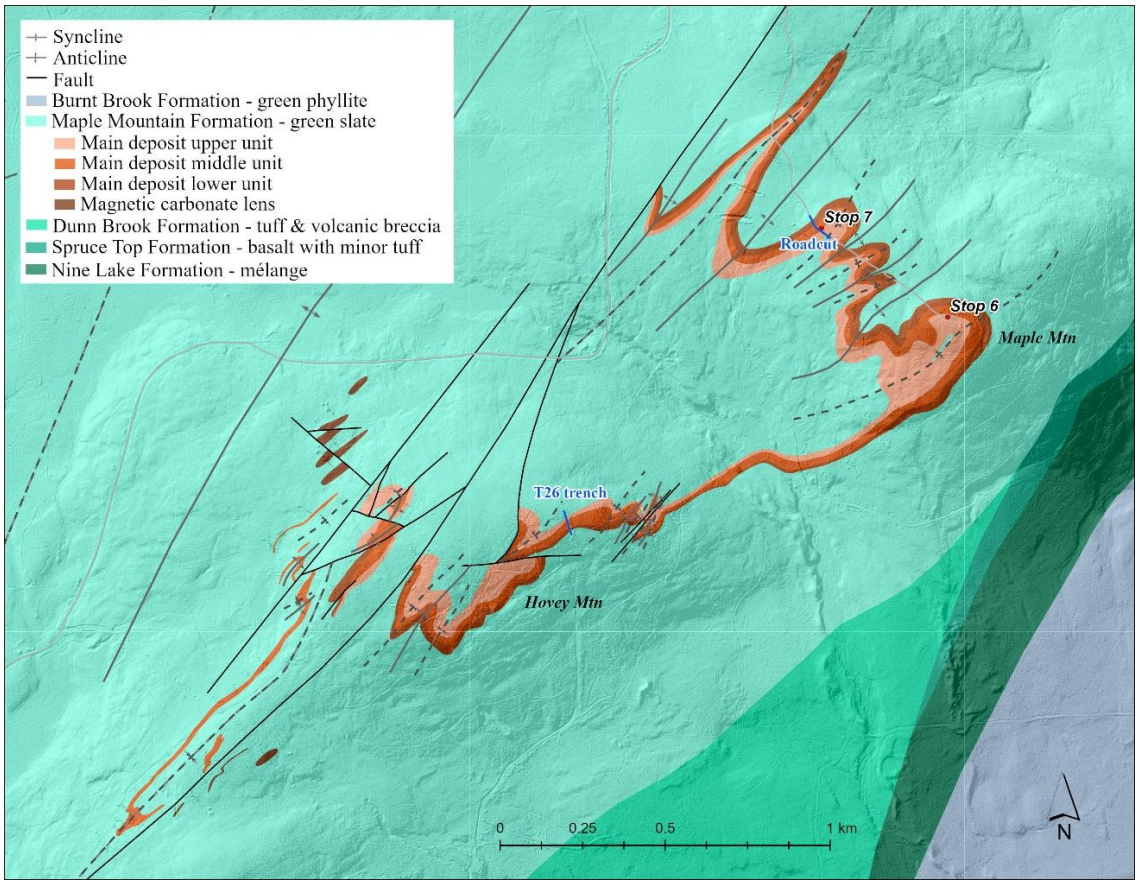

Figure 25. Geologic map of the Maple-Hovey Fe-Mn deposit based on Eilertsen (1952) and Pavlides and Milton (1962) and our mapping.

The Main Deposit

The main deposit is divided into lower, middle, and upper units, first proposed by Eilertsen (1952) and Pavlides and Milton (1962). These three units can be clearly viewed along the new roadcut at Maple Mountain and detailed description of each unit at the roadcut are included at road log Stop 7.

The lower manganiferous unit: In general, the lower unit consists predominantly of dark green, pyritic slate/silty slate with interbedded manganiferous hematitic ironstone, hematitic slate, and green slate, with an average thickness of 17 m (Pavlides and Milton, 1962). It is 21-m thick at the Maple Mountain new roadcut cross section and only 5-m thick at trench T26 at Hovey Mountain. The lower part of the unit is characterized by thin layers of spheric pyrite aggregates and disseminated pyrite in rusty dark green slate. The dark green slate contains a higher amount of

disseminated green chlorite. The upper part shows increased maroon manganiferous banded hematitic ironstone with distinctively alternating, equal amounts of medium-thin layers of dark green slate and maroon manganiferous banded hematitic ironstone or hematitic slate.

The middle manganiferous unit: In general, the middle unit is almost entirely composed of banded or laminated manganiferous hematitic ironstone and constitutes the major manganiferous orebody of the deposit (Fig. 26). The thickness of the middle unit varies, for example, it is about 29 m at the Maple Mountain new roadcut cross section, and 32 m at the old trench T26. Based on Pavlides and Milton (1962), the average thickness is 17 m. Part of the middle manganiferous unit at Hovey Mountain is strongly magnetic due to abundant metamorphic magnetite. Magnetite occurs either in bands/laminae or as disseminated (Fig. 27a), but is more commonly found in Fe-poor, silicate-and-Mn-rich laminae, for example, spessartine-rich laminae (Fig. 27b).

Figure 26. The middle manganiferous unit at trench T26 at Hovey Mountain is dominated by banded or laminated manganiferous hematitic ironstone. Black filmed due to manganese oxides from weathering.

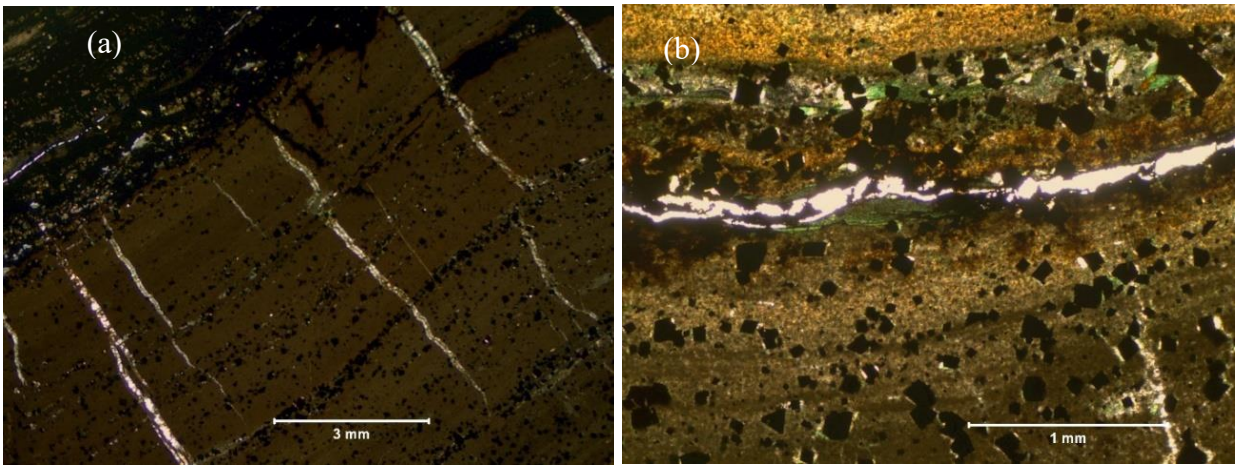

Figure 27. The magnetic middle manganiferous unit at Hovey Mountain. (a) Magnetite (opaque) occurs in laminae/bands. (b) Disseminated euhedral magnetite in spessartine laminae. Cross-polarized light.

The upper manganiferous unit: In general, the upper unit is composed predominantly of earthy red to bright red hematitic slate and silty slate, purple slate, and intercalated dark green pyritic slate, light green slate, with much lesser amount of intercalated banded manganiferous hematitic ironstone. The unit is characterized by the bright red hematitic slate/siltstone. Layers of banded manganiferous hematitic ironstone are generally restricted to the lower half of the unit. At the old trench T26, the upper unit is only about 3-m thick and almost entirely red hematitic slate and silty slate.

Based on Pavlides and Milton (1962), the average thickness is 10 m. Near the bottom of the unit there are thin (4–5 cm), laminated layer(s) of pyrite.

The Magnetic Siliceous Carbonate Lenses

The magnetic siliceous carbonate lenses at Hovey Mountain are stratigraphically below the level of the main deposit. The lenses are composed of irregularly interbedded, thinly layered, green and dark green pyritic chloritic slate/mudstone and dark green to almost black laminated manganiferous siliceous carbonates, with notably very minor amount of hematite component. The lenses are characterized by abundant metamorphic magnetite, and therefore are called *magnetic siliceous carbonate lenses*. Magnetite is disseminated ubiquitously throughout the lenses and largely concentrated and accumulated in thin laminae. Rhodochrosite (Ca-Mn-carbonate) is a major Mn-bearing mineral. Other minor or sparse Mn minerals include spessartine, rhodonite, and stilpnomelane. Chlorite is a major mineral and is disseminated throughout the lenses. Pyrite occurs as disseminated single grains and in clusters, and pyrite may also occur in layers intercalated in the dark green slate/siltstone. This magnetic type is characterized by interbedded magnetite-rich and Ca-Mn-carbonate-rich laminae, with generally more volume of the magnetite-rich laminae than that of the Ca-Mn-carbonate-rich laminae (Fig. 28a, b). Like the main deposit type, the magnetic type also includes some intercalated laminae of apatite.

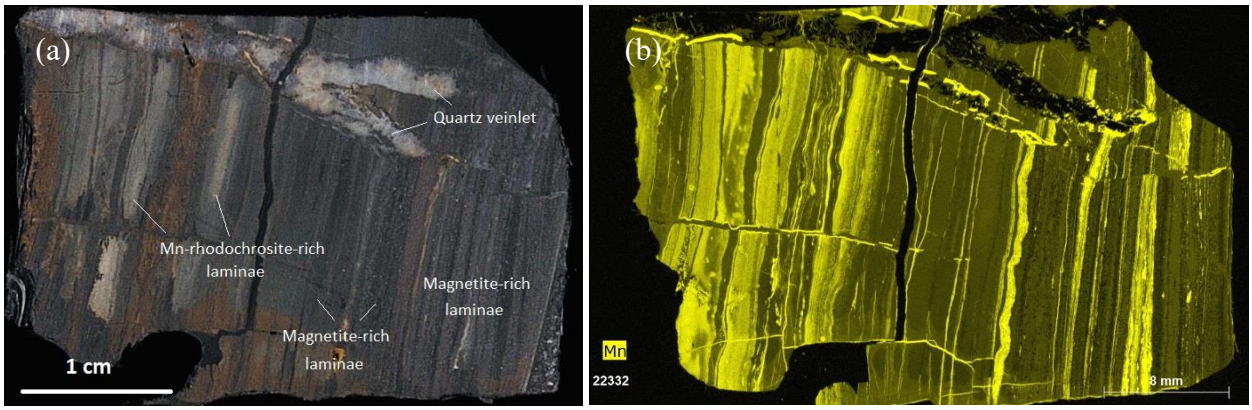

Figure 28. The magnetic siliceous carbonate lens-type Fe-Mn ore at Hovey Mountain. (a) A photographed slab; (b) A microXRF scan of the same slab.

Mineralogic composition of the Fe-Mn bands/laminae

The Fe-Mn deposit is characterized by alternating laminae or bands of varying color and composition (Fig. 29a). The dark red or very dark red (almost black) laminae are composed mainly of iron oxides (hematite, >70%), with other minerals being mostly quartz and sericite. The light red or light maroon laminae are composed mainly of rhodochrosite, with apatite and sericite and other minerals such as rhodonite, albite, and spessartine. The light gray or pinkish white Mn-rich laminae are composed mainly of apatite (Fig. 29c) with some rhodochrosite and minor rhodonite, potassium feldspar, albite, and are nearly completely free of iron oxides (Fig. 29 b, c, d, e, f). The light gray or white apatite-rich laminae generally account for 15–35% of freshly cut slabs. Spessartine is common in Mn laminae and may account for up to 70% of the Mn-rich laminae. Rhodonite is disseminated in Mn layers in primary form.

The thickness of a lamina varies from less than half a mm to 3 cm, but most ranges 1–10 mm, and commonly pinch and swell. Laminae are generally parallel but often are contorted or folded at microscopic to outcrop scale (Fig. 30), mostly as second-order structures. Laminae could be slightly crenulated due to the regional Acadian compressional deformation.

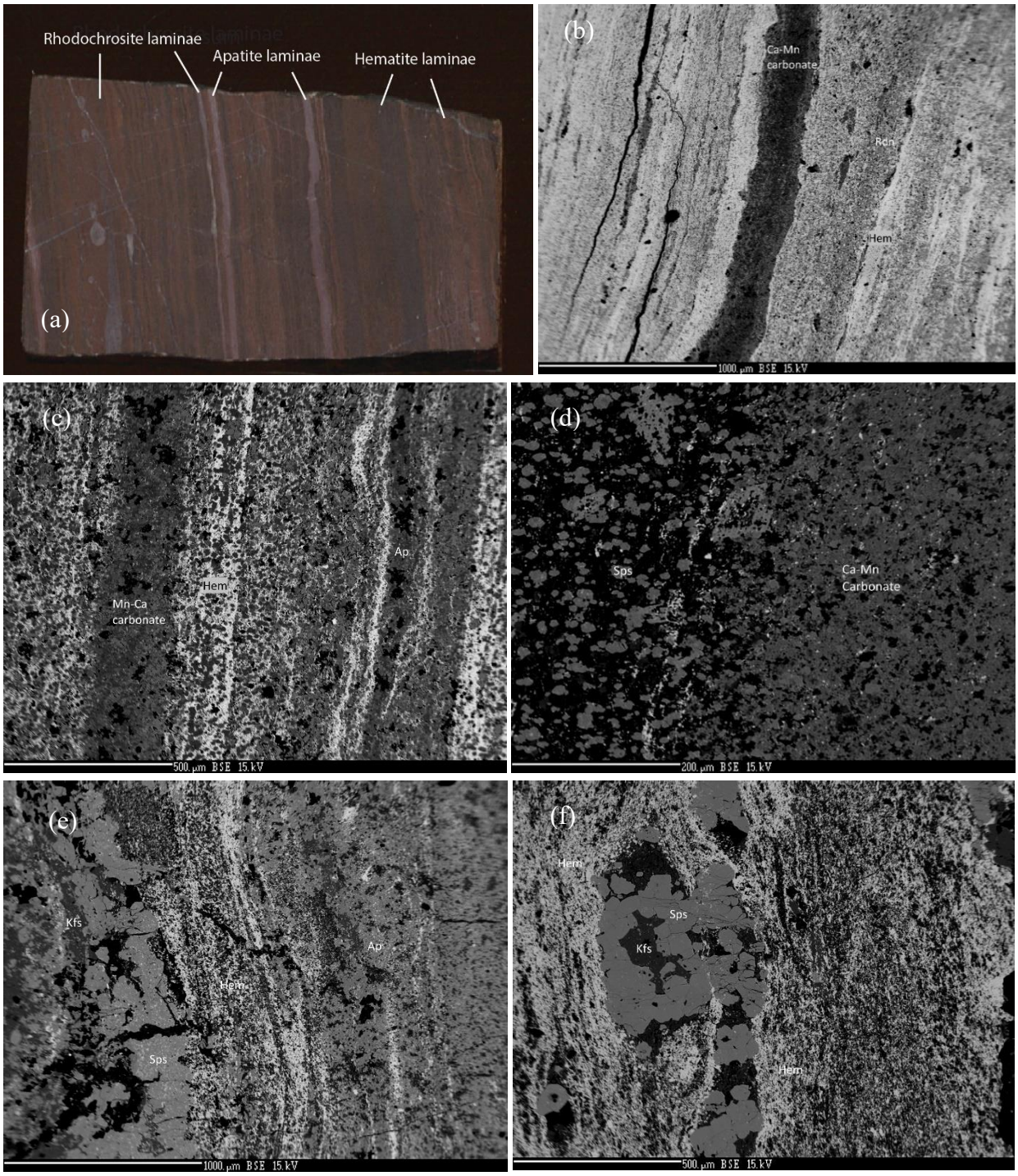

Figure 29. BSE images of the Fe-Mn laminae. (a) Hand specimen showing alternating laminae of varying color and composition, typical of the Fe-Mn deposit. (b) Rhodochrosite lamina intercalated in hematitic laminae with varying amounts of hematite and other minor, disseminated minerals quartz, sericite, and rhodonite. (c) Alternating hematite-rich and rhodochrosite-rich laminae, with apatite laminae. (d) Close-up of a rhodochrosite-rich lamina (right) and a spessartine-rich lamina (left). (e) Laminae with varying amounts of hematite and an interlayered lamina rich in spessartine and potassium feldspar. (f) A lens of spessartine and potassium feldspar lamina within hematitic laminae. Ap – apatite; Hem – hematite; Kfs – potassium feldspar; Rdn – rhodonite; Sps – spessartine.

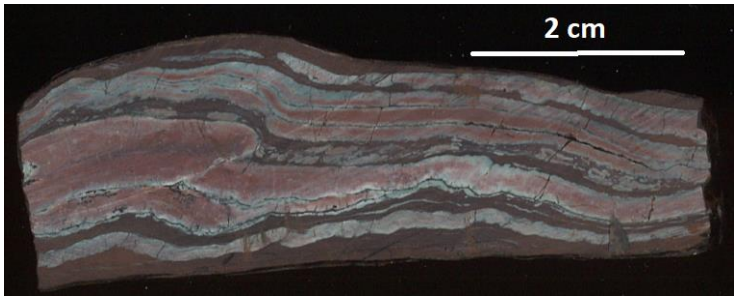

Figure 30. A cut slab showing boudinage and pinch-and-swell of alternating Mn-rich (lighter color) and Fe-rich (darker color) laminae.

Geochemistry of the Maple-Hovey Fe-Mn Deposits

Forty-four samples were systematically collected from the Maple Mountain new roadcut and the old trench T26 for whole-rock geochemical analyses at SGS Laboratories. The data are grouped into seven lithological types of the main deposit: from the least mineralized to the most mineralized, these are tuffite, green slate, green siltstone, dark green slate, dark green siltstone (with higher amounts of chlorite and pyrite), maroon hematitic siltstone, and Fe-Mn laminae. Generally, Fe and Mn are elevated in each lithological type, even including the green and dark green slate and siltstone. The dark green slate and siltstone have the highest Total S (average 0.496%, compared to 0.00975% in green slate/siltstone and <0.005% in both Fe-Mn laminae and maroon hematitic siltstone), due to the presence of pyrite. The Total C is low in green slate/siltstone (average 0.018%) and maroon hematitic siltstone (average 0.0204%) but much higher in dark green slate/siltstone (average 2.420%, the highest) and Fe-Mn laminae (average 1.1619%). The latter contains rhodochrosite. Apatite in dark green slate/siltstone, primarily in Fe-Mn laminae is consistent with the higher content of P_2O_5 (average 2.06–1.57%).

With all the lithological types considered for the deposit, on the PAAS (Post-Archean Australian Shale, Taylor and McLennan, 1985)-normalized spidergram (Fig. 31a), MnO is much elevated in each lithological type, Fe_2O_3 is generally also elevated, though not as much as MnO. SiO_2 is slightly lowered, in particular in the Fe-Mn laminae, Al_2O_3, K_2O, and TiO_2 are also lowered, in particular in the Fe-Mn laminae, CaO is generally elevated in the Fe-Mn laminae but lowered in green and dark green slate/siltstone and maroon hematitic siltstone, and P_2O_5 is remarkably elevated in much of the Fe-Mn laminae but lowered in green and dark green slate/siltstone and some maroon hematitic siltstone. On the PAAS-normalized trace elemental spidergram (Fig. 31b), As (arsenic) is remarkably elevated, and Co is elevated in Fe-Mn laminae, maroon hematitic siltstone, and dark green slate/siltstone. Co is considered predominantly hydrogenous in origin (Crerar et al., 1980) and has an exceptional crystal field preference for adsorption by tetravalent Mn oxides (Burns, 1976). The PAAS-normalized REE patterns (Fig. 31c) are generally convex-upward shaped, with relatively enriched MREE (middle rare earth elements) and positive Ce anomalies. The chondrite-normalized REE patterns (Fig. 31d) show more enriched LREE than HREE with apparent negative Eu anomalies and positive Ce anomalies in all the seven lithological types. Both diagrams show that most of the analyses share the same or similar REE patterns with the exception of only a couple of dark green slate/siltstone samples.

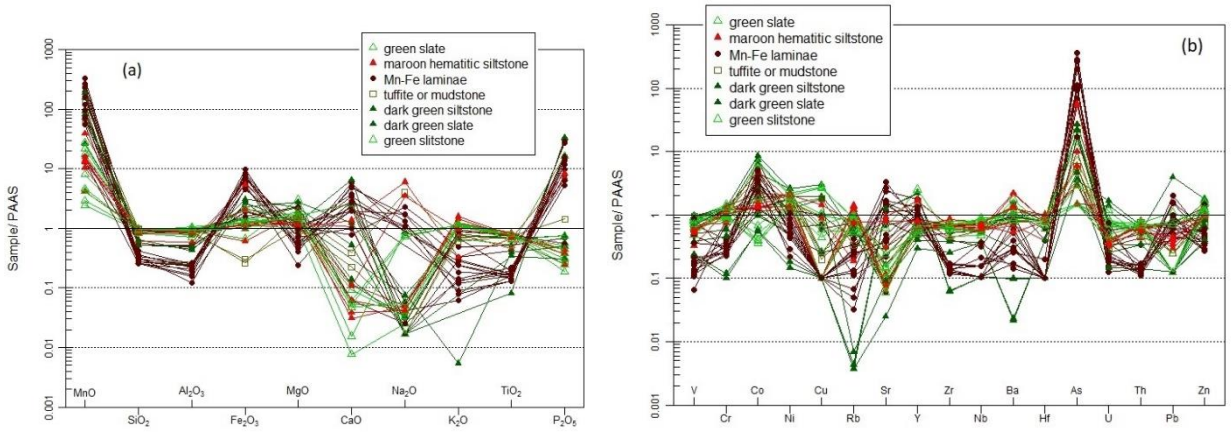

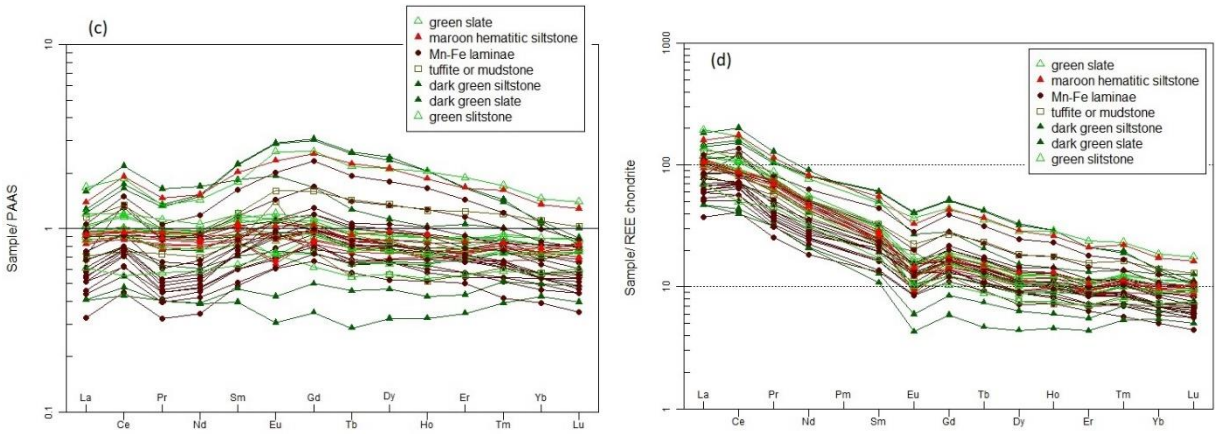

Figure 31. PAAS-normalized major elemental (a), trace (b), and REE (c) spidergrams and patterns, as well as chondrite-normalized REE patterns (c) (Nakamura, 1974) of the Maple-Hovey Fe-Mn deposit. PAAS values are from Taylor and McLennan (1985).

The Fe-Mn laminae have an average of 14.5% MnO (1.46–36.6%) and 39.82% Fe_2O_3 (11.47–70.34%). The maroon hematitic siltstones have an average of 1.68% MnO (0.45–4.28%) and 11.95% Fe_2O_3 (4.41–14.86%). After conversions of Mn and Fe oxides to Mn and Fe elements, the maroon hematitic siltstones have an average Fe content of 8.36% (ranging 3.08–27.35%) and average Mn content of only 1.30% (ranging 0.34–3.31%) with an average Mn/Fe ratio of 0.156. The Fe-Mn laminae have an average Fe content of 27.85% (ranging 8.02–49.2%) and average Mn content of 11.23% (ranging 1.13–28.35%) with an average Mn/Fe ratio of 0.403. The average Mn/Fe ratio of the Fe-Mn lamina samples at the Hovey Mountain trench T26 is 1.125, six times higher than that at the Maple Mountain new roadcut cross-section (average 0.187). For the Fe-Mn laminae (which is the major Mn ore), the Maple Mountain new roadcut cross-section has higher Fe content than the old trench T26 at Hovey Mountain (average 34.26% versus average 21.44%) but lower Mn content than the old trench T26 at Hovey Mountain (average 5.38% vs. average 17.07%, about three times different). See Figure 25 for locations of the old trench T26 and the new roadcut.

Origin and Paragenesis of the Maple-Hovey Manganese Deposit

Origin of the Maple-Hovey Fe-Mn deposit

Marine sedimentary Fe-Mn deposits are commonly subdivided into three major genetic types: hydrothermal, hydrogenetic/hydrogenous, and diagenetic (Halback, 1981; Fleet, 1983; Takematsu et al., 1989; Bau et al., 1996; Usui and Terashima, 1997). In the hydrothermal type, Fe and Mn (oxyhydr)oxides are precipitated from marine medium- to low-temperature hydrothermal fluids when mixed with cold seawater after being derived from seafloor vents as a result of igneous activities, for example, along mid-ocean-ridges. In the hydrogenetic/hydrogenous type, Fe–Mn (oxyhydr)oxides are precipitated from seawater as initially colloidal particles within the water column. In the diagenetic type, Fe–Mn (oxyhydr)oxides form diagenetic nodules from metal ions in sub-oxic porewaters either within the soft sediment or at the sediment-water interface. The last type is much less common than the first two types.

Geochemical characteristics of some major and trace elements, as well as contents and distribution patterns of REE, are the main discriminators used to identify and distinguish different genetic types of marine sedimentary Fe-Mn deposits. In general, as shown in Figure 32a, the PAAS-normalized REY patterns of the different genetic types of marine sedimentary Fe-Mn deposits differ considerably. For the two most common types: (1) The hydrogenetic (or hydrogenous) type shows more enriched REE with an almost flat distribution pattern and moderately enriched MREE (convex-upward) and distinctive positive anomalies for redox-sensitive Ce and negative anomalies for redox-insensitive Y. (2) The hydrothermal type displays depleted REE with a left-inclined distribution pattern and even more depleted LREE, as well as significant negative Ce and positive Y anomalies. The PAAS-normalized REY patterns for all the lithological types (Figs. 31c, d) match the pattern for the hydrogenetic (or hydrogenous) type very well, indicating that the Maple-Hovey Fe-Mn deposit is hydrogenetic (or hydrogenous) in origin.

This determination is supported by several other popular discrimination diagrams using major and trace elements. For example, on the Ni-Zn-Co ternary diagram, nearly all the samples of the seven lithological types plot in the field of "hydrogeneous-detrital" field (Fig. 32b). On the Fe_2O_3-Al_2O_3-MnO ternary diagram for green and dark green slate/siltstone samples, nearly all the green slate/siltstone plot in the non-hydrothermal field and other fields of non-

hydrothermal (Fig. 32c). On the Ni-Zn-Co ternary diagram for the mineralized maroon hematitic siltstone and Fe-Mn laminae, all but one Fe-Mn laminae sample plot in the hydrogenous field (Fig. 32d).

Paragenesis of the Fe-Mn mineralization

Five paragenetic stages of manganese mineralization are recognized at the Maple-Hovey Fe-Mn deposit: (1) sedimentary-diagenetic mineralization stage, (2) early hydrothermal state, (3) metamorphic stage, (4) late hydrothermal stage, and (5) supergenetic oxidation stage (i.e., supergene stage). The primary interbedded hematite and Ca-Mn-carbonate bands and laminae were precipitated during the first, sedimentary-diagenetic stage. The metamorphic stage was associated with the regional Acadian orogenesis; the deposit and its hosting Maple Mountain Formation experienced not only folding and foliation development, but also lower greenschist facies metamorphism at low pressure and relatively low temperature for a sericite-chlorite-quartz assemblage (300–350ºC) as indicated by the Conodont Alteration Index of 4–5 for the conodonts from the Burnt Brook Formation. In addition to new silicate minerals sericite (major), chlorite (major), albite (major), and quartz produced in the green slate/siltstone, other minerals, in particular the Mn-bearing minerals spessartine (major), magnetite (major), stilpnomelane (sparse), and pyrophanite (sparse) were produced in the Mn-rich dark green slate/siltstone and Mn-rich laminae/bands of the Fe-Mn deposit. In short, significant changes were made to the deposit during the metamorphic stage. Veinlets produced during the early hydrothermal stage are pervasive throughout the deposit but are relatively insignificant with little contribution to the formation of the Fe-Mn deposit; some present with replacement texture following the Fe-Mn laminae and the late-stage hydrothermal present as dominantly quartz veins. The supergenetic oxidation stage was essentially insignificant in the deposit; it basically did not make any visible change to the deposit except producing a thin black film of manganese oxides on surface of Mn-rich bands and laminae at the deposit. No measurable iron gossan was produced by the process.

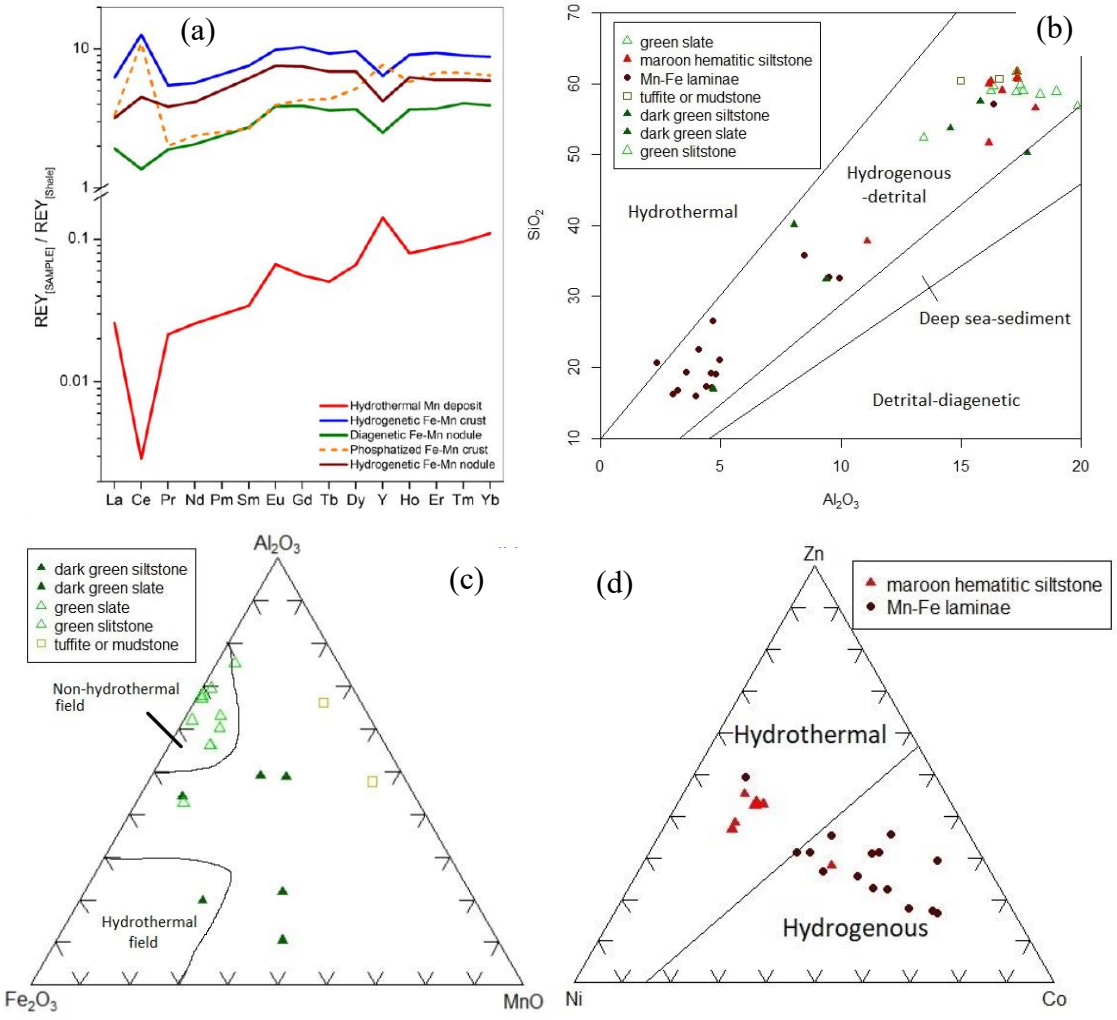

Figure 32. (a) Examples of typical PAAS-normalized REY patterns for marine hydrothermal, hydrogenetic/hydrogenous, diagenetic, and phosphatized Fe-Mn deposits (Bau et al., 2014). (b), (c), and (d) are discrimination diagrams based on major and trace elements: (a) Al_2O_3 vs. SiO_2 binary diagram (Toth 1980); (b) Fe_2O_3-Al_2O_3-MnO ternary diagram (Boström 1973); (c) Ni-Zn-Co ternary diagram (Hein et al. 1997).

Road Log

Assembly time and location: Meet at the parking lot next to the soccer field/tennis court on the UMPI campus. The departure time is 7:00 am ET. The first part of the trip is in the Castle Hill area, west of Presque Isle, on paved roads. We will carpool for the second part of the trip in the Number Nine Mountain area, and regular cars not going to the woods will park in the Bridgewater town office parking lot (or the First Baptist Church parking lot by Rte-1). We will return to the parking lots by ~3 pm and will disassemble from there. Bring whatever you plan to eat and drink. Most of the Number Nine Mountain area have reception. All the stops are next to roads.

Cumulative mileage	**Description**
0.0	Start logging from UMPI south entrance; make left turn to Main St. (Rte-1).
0.7	Left turn to State St. after two traffic lights.
0.9	Left turn to Rte-163 toward Mapleton/Ashland at the five-street intersection. Bear left and keep on Rte-163.
8.5	Right turn to Dudley Rd.
9.4	Stop on the road for Stop 1A.

Stop 1A. Jemtland sandstone and New Sweden limestone (561958, 5170115): The outcrops are in the ditch north side of the road, west of the driveway. We will start with two outcrops of the Jemtland thin-medium layered, laminated gray calcareous micaceous sandstone/siltstone that is weathered to orange or tan color (Fig. 33a). If time allows, you may find a piece of graptolite. Walking 42 meters (or 138 feet) downhill from the second Jemtland outcrop across a fault (Dudley Farm Fault) and the boundary between both formations is a limestone outcrop (actually two; Fig. 33b). The limestone contains fossil brachiopods, e.g., *Atrypa.* The limestone is the bottom of the New Sweden Formation. The beds at these outcrops dip to the east but are ***overturned*** – as indicated by graded bedding in the Jemtland sandstone. We are on the overturned west limb of the Radio Tower ridge anticline (Fig. 34).

Figure 33. At Stop 1A: (a) Jemtland Formation laminated sandstone. (b) New Sweden Formation limestone.

Continue on Dudley Rd.

9.5	Left turn onto a dirt road leading to Dudley pit (south pit).
9.7	Dudley pit for Stop 1B.

Stop 1B. The Dudley Fe-Mn deposit at Dudley pit (south pit) (561838, 5169717): The Dudley deposit is the largest and best-known Fe-Mn deposit in the northern subdistrict. Miller (1947) estimated that, based on the exploration work, the orebody is 4,600-foot long (1,400 m) and extends to depths of "several hundred feet without marked change in width or attitude". In the deepest hole drilled, the continuity of the orebody reaches a depth of more than 640 feet (195 m). The orebody is widest in the northern part (north side of Dudley Road) (Fig. 34). Of all the deposits of the northern subdistrict, the Dudley deposit contains the highest-grade ore, and its estimated manganese metallic tonnage (indicated) is 934,000 metric tons (5% cut-off) or 619,000 metric tons (10% cutoff) (Miller, 1947).

The deposit is located on the overturned west limb of the Radio Tower ledge anticline (Fig. 34). It is well exposed in two borrow pits, one on the north side of Dudley Rd (north pit) and the other on the south side (south pit); the south

pit offers a more complete exposure of the ore zone. In the south pit, we will walk westward from the massive limestone (or limestone breccia) at the bottom of the New Sweden Formation across the entire Fe-Mn zone and stop at a green slate outcrop. The east side of the massive limestone is supposed to be Jemtland Formation sandstone and slate but there are no outcrops of Jemtland but rather floats of the graptolitic sandstone and slate around the boundary. The lower part of the New Sweden Formation is significantly and vertically displaced by the northeast-striking Dudley Farm reverse fault that is clearly shown along the rim of the pit (Fig. 35). The fault dips to 260º at a dip angle of 80º. Due to the displacement, the Fe-Mn zone is almost in direct contact with the limestone.

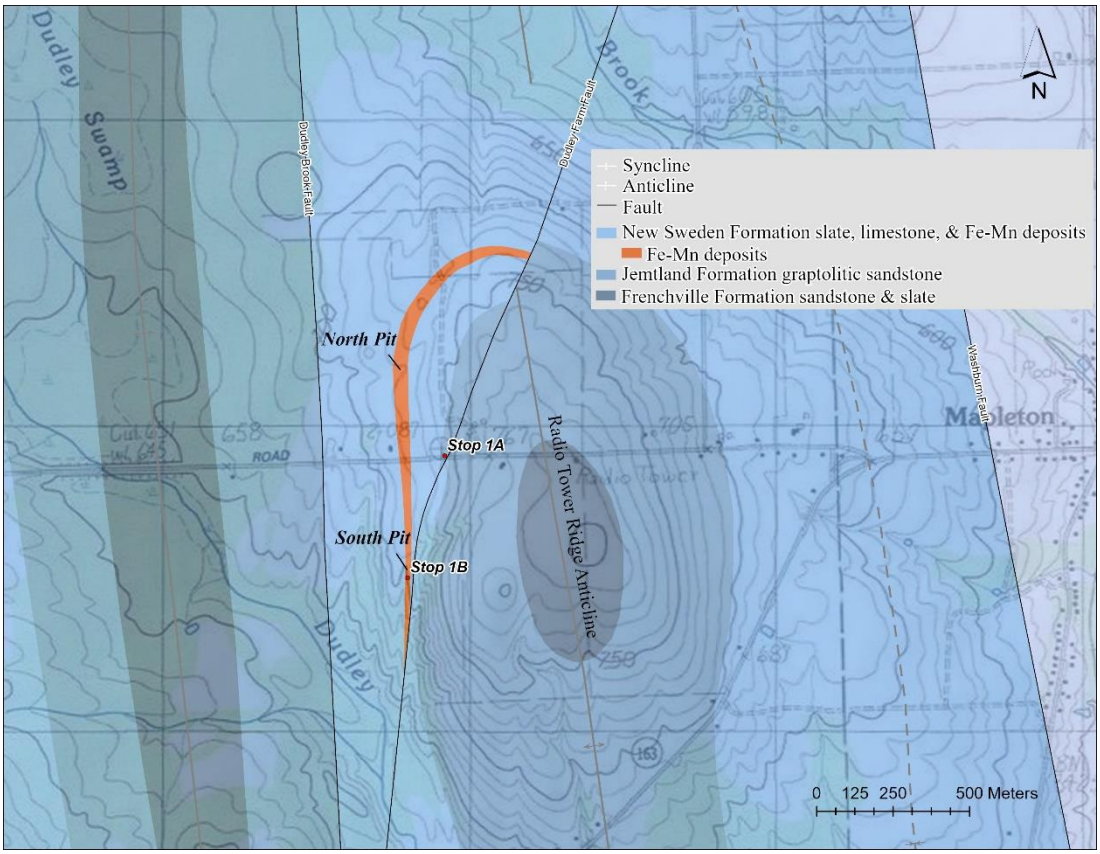

Figure 34. Geological map of the area around Dudley pit, Castle Hill.

The deposit begins with green slate (of about 5-m thick) and then alternating green slate and red hematitic siltstone/slate (of about 6 m together; Fig. 36a), before increasing layers of dark red hematitic siltstone/slate and black-filmed hematitic siltstone/slate (Fig. 36b). The black film indicates higher Mn content, indicating Mn oxides produced by supergenetic oxidation. The Fe-Mn ore zone with extensive laminae of high-Fe hematite and Mn-carbonates and silicates (Fig. 36c) is about 20-m thick. Above the Fe-Mn layers is dark green pyritic slate and then light green slate. The hematite and Fe-Mn laminae and bands display manganese nodules at a size ranging from 2 mm up to 2 cm but mostly at around 0.5–1 cm in diameter (Fig. 36d). Nearly all the nodules or spherules are flattened due to compressive deformation during the Acadian shortening. Hydrothermal veins are scarce and small (normally thinner than 0.5 cm). Most contain quartz, with some of them containing barite or Mn-minerals such as rhodochrosite or rhodonite, but they are scarce (Fig. 36c).

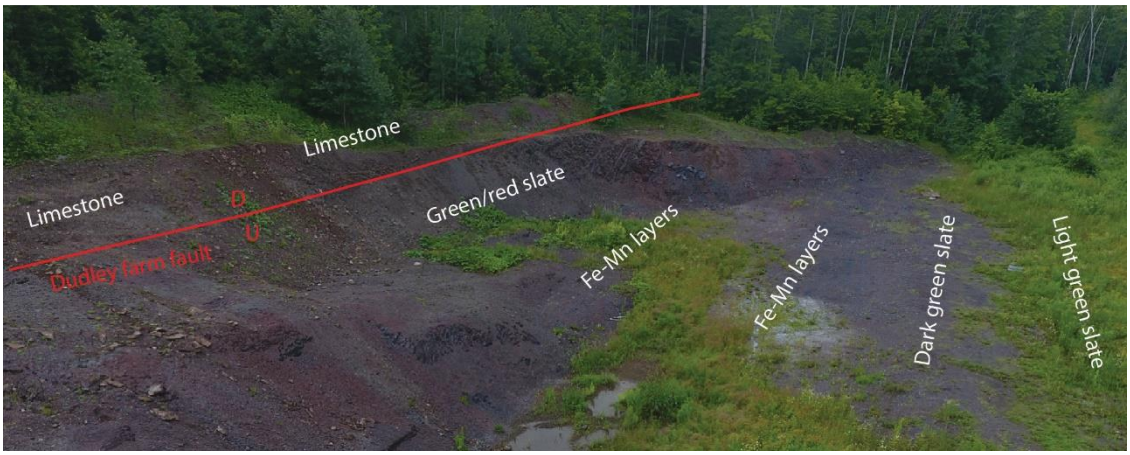

Figure 35. Birdseye view of the Dudley pit (south pit) from a drone. Facing south. U – upthrown, D – downthrown.

Figure 36. Fe-Mn deposit at the Dudley pit. (a) Alternating green and red hematitic siltstone/slate. Dr. Martin Yates measuring magnetic susceptibility. (b) Black filmed Fe-Mn laminae. (c) Fe-Mn laminae cut by a replacement-type quartz veinlet. (c) Manganese nodules.

Turn around and go back to Dudley Rd.

10.0 Right turn onto Dudley Rd.
10.9 Left turn onto Rte-163 towards Mapleton/Presque Isle.
18.5 Right turn to State St. at the five-street intersection. Bear right.
18.7 Right turn to Main St. (US Rte-1) and continue on Rte-1.
40.0 Right turn to Bootfoot Rd after passing the church in Bridgewater, bear left and stay on Bootfoot Rd.
40.1 Right turn to the town office parking lot. ***Regroup and carpool for the Number Nine Mtn trip***.

From the town office parking lot or the church parking lot, turn left back to Rte-1 northbound.

43.9 Left turn to Kinney Rd.
46.3 Right turn to Warren Rd. Bear left and keep on this road.
47.2 Bear left on Warrant Rd and continue on the road – it changes to E Plantation Rd in 0.1 mile.
48.5 Park on the road for outcrops on the south side of the road.

Stop 2. The Nine Lake mélange, Three Brooks conglomerate/sandstone, and the unconformity (Salinic A) (580129, 5148436): *The mélange* – The outcrop in the ditch on the south side of the road is the mélange of the Nine

Lake Formation. The mélange contains blocks mostly of sandstone and laminated sandstone up to 15 cm long at the outcrop. It is foliated (Fig. 37a). ***The conglomerate/sandstone*** –Three Brooks conglomerate and sandstone (minor) unit is dominated by pebble conglomerate that is massive, poorly sorted, matrix supported, and polymictic with clasts of light gray tuff, rhyolite, black chert, quartz, granite, and red jasper (Fig. 10). Interbedded in the conglomerate, the sandstone is generally coarse, lithic, quartzose, also poorly sorted. ***The unconformity*** – Exposed after digging and moss peeling, the outcrop (Fig. 37b) shows a perfect unconformity with the mélange overlying the conglomerate and sandstone, indicating the latter is older than the early Middle Silurian mélange. The unconformity may represent Salinic A.

Figure 37. (a) Nine Lake mélange. (b) The unconformity – the mélange (right) unconformably overlying the conglomerate/sandstone (left).

Turn around.
48.7 Right turn to an old dirt logging road.
50.0 Park by the pit for Stop 3.

Stop 3. Nine Lake mélange (579387, 5145970): The stop is shown in Figure 8. This pit shows excellent exposure of the Nine Lake mélange. Blocks of various sizes (up to 1 m in diameter) include quartzite, limestone, chert, sandstone, etc. (Fig. 38a). The mélange matrix is foliated, pyritic in this pit and even contains pyrite aggregates (Fig. 38b). Is this tectonic mélange or olistostromal mélange? The Nine Lake Formation is Silurian 433 Ma and slightly older than and unconformably overlain by the Nine Mountain sequence (Spruce Top, Dunn Brook, and Maple Mountain formations). No Salinic mélange had been reported in Maine or New Brunswick before our project. So, have we found the Salinic tectonic mélange?

Figure 38. Nine Lake mélange at Stop 3. (a) A limestone block up to 1 m in diameter. (b) Pyrite aggregates.

Continue on the old dirt logging road and bear right and keep on the frequently traveled road.
51.9 Right turn to # 9 Rd, a major dirt road in this area.
52.4 Bear right at the fork.
52.9 Right turn to E Plantation Rd, another major dirt road in the area.
53.4 Right turn to an old logging road. (It is overgrown but the road foundation is solid)
53.6 Right turn to another old logging road that leads to a borrow pit.
53.7 Stop at the borrow pit for Stop 4.

Stop 4. Unconformity between Burnt Brook and Spruce Top formations (578801, 5144583): This pit shows an excellent exposure of the unconformity/disconformity (Fig. 39a) between the Burnt Brook (Silurian Homerian, 427–430 Ma) and Spruce Top (433Ma) formations in addition to the pillow basalt (Fig. 39b) of the Spruce Top Formation.

The unconformity represents Salinic B2 in the Number Nine Mountain terrane. Pillow basalt is not a common feature for the Spruce Top Formation, but it is exposed at several locations.

Figure 39. (a) Unconformity at Stop 4. Lauren stands right on the Burnt Brook slate side; most of the pit wall is Spruce Top pillow basalt. Viewer facing northwest. (b) The Spruce Top pillow basalt.

Turn around at the pit.
53.8 Left turn.
53.9 Left turn to E Plantation Rd.
54.5 Right turn to # 9 Rd.
58.3 Left turn (the road is still # 9 Rd) towards Number Nine Lake. Look right for the small but populated lake.
60.1 Left turn to an old logging road.
60.6 Park on the road for Stop 5. We will walk on a skidder trail for about 50 meters to the outcrop.

Stop 5. Volcanic breccia of the Morehouse Brook Formation (574956, 5140393): The Morehouse Brook Formation is a Mid Ordovician volcanic formation consisting of volcanic breccia, tuff, basalt, and dacite. It would be nice to see the large Morehouse Brook dacite but we would have to take a two-hour trip on another road (Hanington Rd) east of Number Nine Mountain. This outcrop shows excellent foliated volcanic breccia of the formation in which the blocks are mostly dark gray and gray cherty fine tuff (Fig. 40).

Figure 40. Volcanic breccia of the Morehouse Brook Formation at Stop 5.

Turn around.
61.2 Left turn to the main road (still # 9 Rd).
61.5 Turn right or bear right at the fork onto Hovey Mtn Rd.
61.8 Left turn toward Maple Mtn.
62.7 Summit of Maple Mtn for Stop 6 and ***it is lunch time!***

Stop 6. The Maple-Hovey Fe-Mn deposit at the summit of Maple Mountain (574450, 5138452): While having lunch, walk around and check out excellent outcrops of the Fe-Mn ores around the summit. The summit is underlain by a southwest-plunging second-order syncline of the Maple-Hovey composite syncline of the main deposit Fe-Mn layers (Figs. 8 and 25). The ditch on the north side of the road shows probably a third-order fold (Fig. 41).

Figure 41. Third-order folds of the Fe-Mn layers at Stop 6, the summit of Maple Mountain.

Turn around.

63.0 Stop for the roadcut cross section of the Fe-Mn deposit.

Stop 7: The Maple Mountain roadcut Fe-Mn deposit cross-section (574060, 5138714): The road leading to the summit of Maple Mountain was newly rebuilt in fall 2021 and uncovered the main Maple-Hovey Fe-Mn deposit. This stop will examine the entire exposure of the deposit from the footwall to the hanging wall. Because the deposit is hosted in the green slate of the Maple Mountain Formation, the footwall and hanging wall are green slate. The best exposure is a limb of a southwest-plunging syncline at Stop 7. See Figures 8 and 25 for the location and Figure 42 for the cross-section for details. The following is a brief description of the cross-section. As previously introduced, the main deposit is divided into three units: the lower manganiferous unit, the middle manganiferous unit, and the upper manganiferous unit.

Figure 42. Generalized cross section at Stop 7 showing the lower, middle, and upper manganiferous units.

The lower manganiferous unit is about 21 meters thick. The lower part of the unit is green and dark green slate (Fig. 43a) and is characterized by thin layers of spherical pyrite aggregates (Fig. 43b) and disseminated pyrite in rusty dark green slate. The increased amount of disseminated green chlorite and pyrite have contributed to the darkened color of the green slate. Only a few thin layers of maroon manganiferous banded hematitic ironstone are present in the lower part of the unit. The upper part shows increased maroon manganiferous banded hematitic ironstone (Fig. 43c) with distinctively alternating, equal numbers of medium-thin layers of dark green slate and maroon manganiferous banded hematitic ironstone or hematitic slate toward the top of the lower unit (Fig. 43d). The lower unit also shows 1–2 thin layers of white or greenish buff, creamy, and cherty rock that is probably a tuffite.

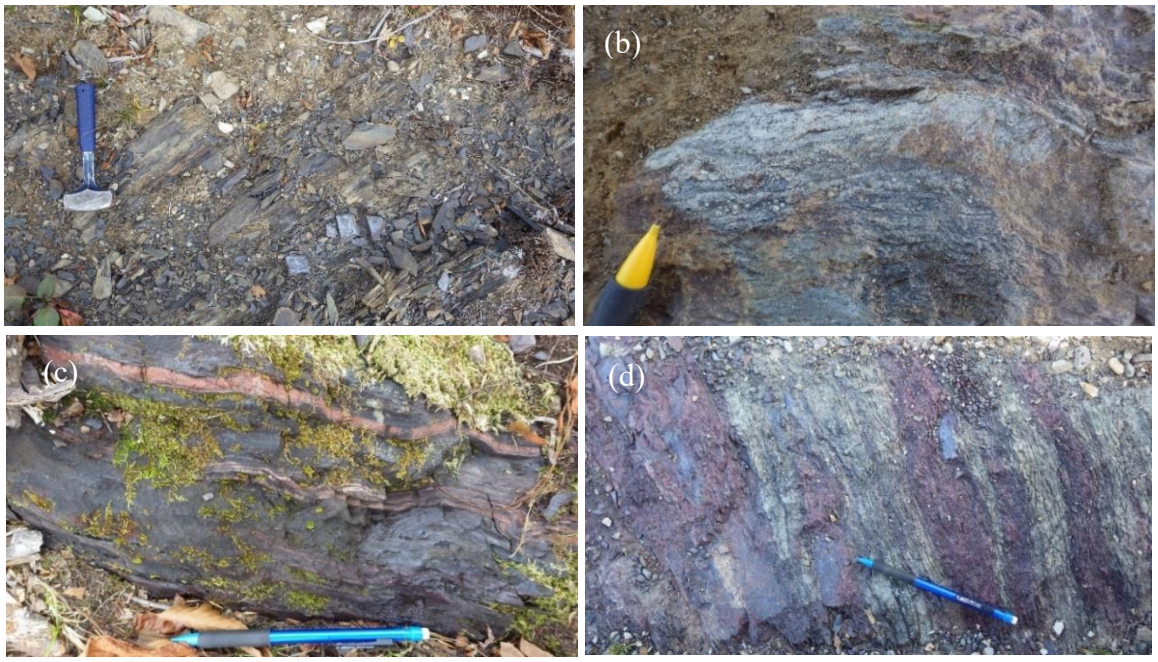

Figure 43. The lower manganiferous unit of the main deposit. (a) Dark green pyritic slate/silty slate near the bottom of the lower unit. (b) Thin layers of pyrite in the lower part of the lower unit. (c) Fe-Mn laminae in the upper part of the lower unit. (d) Alternating layers of maroon manganiferous hematitic slate and dark green slate.

The middle manganiferous unit is almost entirely composed of medium-thinly layered, banded or laminated manganiferous hematitic ironstone (Fig. 44) and constitutes the major manganiferous orebodies of the Maple-Hovey deposit. Exposed Mn-oxide-rich ironstone layers are normally covered by a black film of manganese oxides as a result of surficial chemical weathering process. Rhodochrosite-rich layers may preserve their reddish color. In the middle part of the unit, there are several interbedded layers of dark green silty slate, with the thickest at 2 m and also including at least two thin layers (1–5 cm) of creamy tuffite. The middle unit is about 29 m thick.

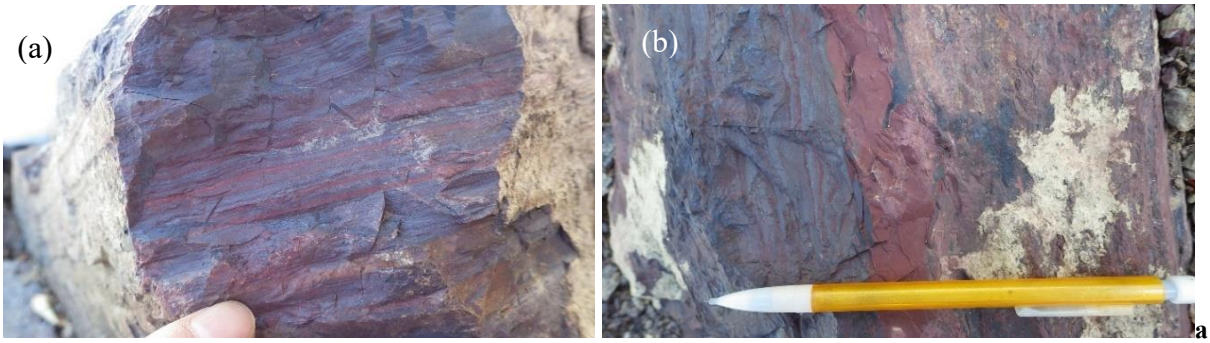

Figure 44. The middle manganiferous unit. (a) Fresh exposure of the typical laminated Fe-Mn ore. (b) Transition from more Mn-rich (left) to more Fe-rich layers (right).

The upper manganiferous unit begins with nearly 8 meters of dominantly dark to light red/maroon hematitic silty slate, and then about 7 meters of alternating medium layers of maroon and purple hematitic silty slate and dark green silty slate (Fig. 45). Near the bottom of the upper unit there are thin (4–5 cm), laminated layer(s) of pyrite and also thin horizon(s) of possibly felsic volcanic tuffite. In general, the upper unit is composed predominantly of earthy red to bright red hematitic slate/silty slate, purple slate, and intercalated dark green pyritic slate, light green slate, with lesser amount of intercalated banded manganiferous hematitic ironstone restricted to the lower half of the unit. The unit is characterized by the bright red hematitic slate/siltstone.

Figure 45. Typical alternating thin-medium layers of maroon and light green slate or siltstone of the upper unit.

Continue downhill on the road.
63.6 Left turn to Hovey Mtn Rd.
68.0 Left turn to another logging road.
68.6 Bear left.
68.7 Left turn to another old logging road.
69.2 Left turn to another old logging road.
69.3 Park on the road for Stop 8.

Stop 8. Conformable contact between the Dunn Brook tuff and Maple Mountain slate (571453, 5135228): This excellent outcrop shows the conformable gradational change from the laminated to thick layered, gray coarse and fine crystal tuff (Fig. 46a, c) of the Dunn Brook Formation to the gray, greenish gray, and green micaceous siltstone and silty mudstone/slate (Fig. 46d) of the Maple Mountain Formation. Only about 25 meters away from the conformable contact there is rusty laminated marl or limy mudstone layer intercalated in the green slate (Fig. 46b). The limy mudstone is weathered in rusty brown color (Fig. 46b). It is supposed to contain microfossils like conodonts.

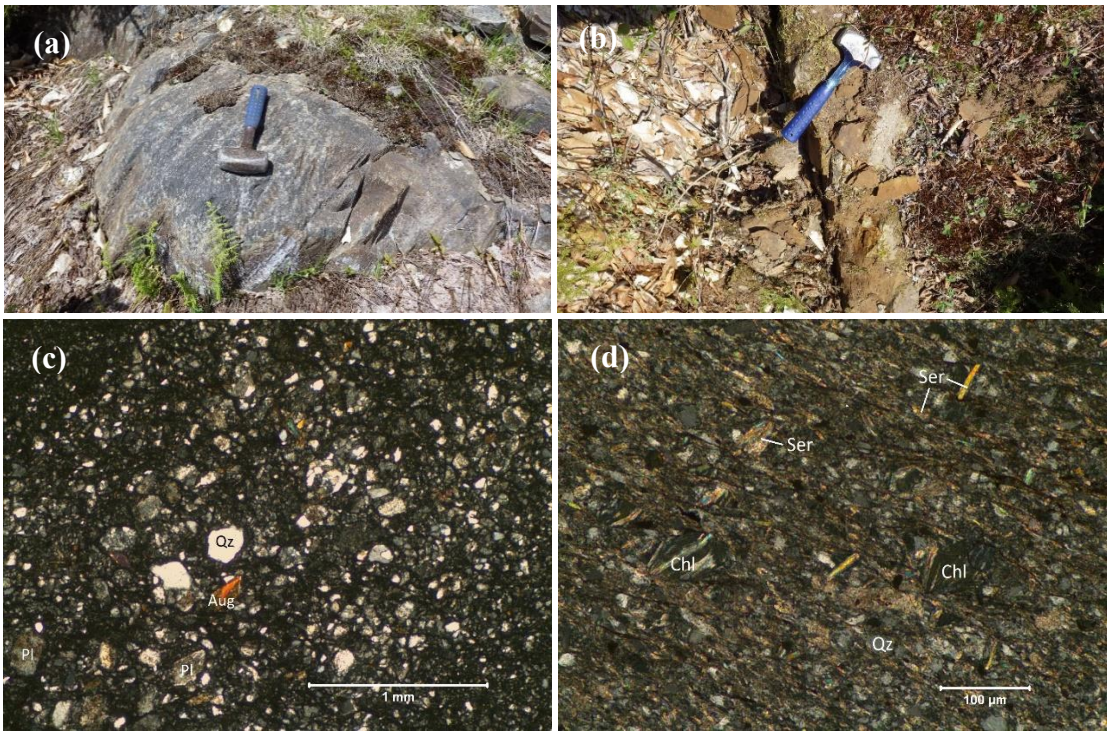

Figure 46. Conformable contact between Dunn Brook and Maple Mountain formations at Stop 8. (a) The gray tuff near the contact. Viewer facing north. (b) The rusty calcareous limy mudstone 25 m from the contact. (c)

Photomicrograph of the crystal tuff next to the contact. (d) Photomicrograph of the green slate next to the contact. Cross polarized light. Aug – augite; Chl – chlorite; Pl – plagioclase; Ser – sericite; Qz – quartz.

Turn around.
69.6 Right turn.
70.0 Right turn.
70.2 Left turn to the main logging road.
71.3 Left turn to an old logging road.
71.4 Park for Stop 9.

Stop 9. Volcanic breccia of the Dunn Brook Formation (572582, 5133355): This outcrop/roadcut on a recently rebuilt logging road shows an excellent exposure of the volcanic breccia of Dunn Brook pyroclastic rocks (Fig. 47a, b). The blocks, up to 25-30 cm long, are mostly coarse crystal tuff and lapillistone. The matrix itself is coarse, lapillus, and largely crystal (e.g., fragments of mostly plagioclase feldspar with minor quartz). The breccia is foliated.

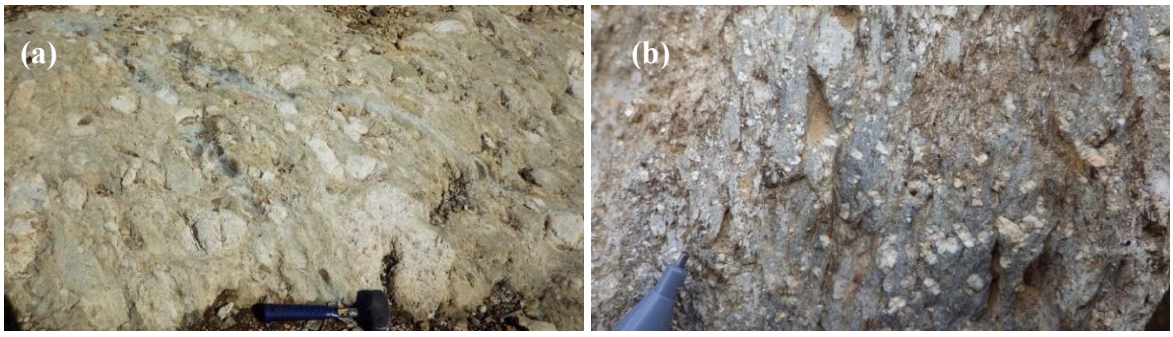

Figure 47. Volcanic breccia of the Dunn Brook Formation at Stop 9.

Turn around.
71.5 Left turn to the main logging road.
73.0 Left turn to St. Croix Rd, a straight, major logging road.
80.0 Right turn to an asphalt road, named West Rd. Continue on the zigzag road till Rte-1.
83.8 Left turn to Rte-1 towards Bridgewater.
89.5 Left turn to Bootfoot Rd to the Bridgewater town office parking lot or to the church parking lot.

End of the road log.

ACKNOWLEDGEMENTS

The trip guide is based on our work for the U.S. Geological Survey Earth Mapping Resources Initiative (MRI)-funded project entitled "*Geologic mapping of manganese-bearing deposits in Aroostook County, Maine*" (Earth MRI G22AC00594; 2022–2025). The project is managed, overseen, and advised by Amber Whittaker of the Maine Geological Survey and advised by former State Geologist Dr. Robert Marvinney. Dr. Martin Yates provided consultation and assisted with microprobe analysis at the University of Maine Microprobe Lab. Dr. David Lentz provided consultation and assisted microXRF analysis at the University of New Brunswick. Dr. Alicia-Cruz-Uribe aided with zircon U-Pb analysis at the University of Maine MAGIC Lab. Dr. Carlton Brett helped identify the marine invertebrate fossils. Special thanks to Dr. Allan Ludman, Dr. John Slack, Brian Way, and David Putnam for advice, discussions, and assistance in the field. Gil Machado and Gonçalo Silvério provided services on palynological and conodont analyses. Special thanks to field assistants Ethan Albair (2023), Preston Bass (2022), and Liam Daniels (2022). Permissions from Irving Woodlands and Gardner Companies are appreciated.

REFERENCES

Andrews, H.N., Kasper, A.E., Forbes, W.H., Gensel, P.G., and Chaloner, W.G., 1977, Early Devonian flora of the Trout Valley Formation of northern Maine: Review of Palaeobotany and Palynology, v. 23, p. 255–285.

Bau, M., Schmidt, K., Koschinsky, A., Hein, J., Kuhn, T., Usui, A., 2014, Discriminating between different genetic types of marine ferro-manganese crusts and nodules based on rare earth elements and yttrium. Chemical Geology, 381, p. 1–9.

Bau, M. and Dulski, P., 1996, Distribution of yttrium and rare-earth elements in the Penge and Kuruman iron-formations, Transvaal Supergroup, South Africa. Precambrian Research. 79 (1–2), p. 37–55.

Berry, W. B. N., 1964, Early Ludlow graptolites from the Presque Isle quadrangle, Maine: Journal of Paleontology, v. 38, p. 587–599.

Berry, W. B. N., 1960, Early Ludlow graptolites from the Ashland area, Maine: Journal of Paleontology, v. 34, p. 1158–1163.

Boström, K., 1973, The origin and fate of ferromanganoan active ridge sediments. Stockholm Contributions in Geology, 27, p. 149-243.

Boucot, A.J., Field, M.T., Fletcher, R., Forbes, W.H., Naylor, R.S., and Pavlides, L., 1964, Reconnaissance bedrock geology of the Presque Isle Quadrangle, Maine. Maine Geological Survey, Quadrangle Mapping Series No. 2. 123 p.

Burns, R. G., 1976, The uptake of cobalt into ferromanganese nodules, soils, and synthetic manganese (IV) oxides. Geochimica et Cosmochimica Acta, v. 40, p. 95–102.

Cabanis, B. and Lecolle, M., 1989, Le diagramme La/10 – Y/15 – Nb/8: Un outil pour la discrimination des series volcaniques et en evidence des mélange et/ot de vontamination crustale. Comptes Rendus de l'Académie des Sciences, Série II, 309, p. 2023-2029.

Cannon, W.F., Kimball, B.E., and Corathers, L.A., 2017, Manganese, chap. L of Schulz, K.J., DeYoung, J.H., Jr., Seal, R.R., II, and Bradley, D.C., eds., Critical mineral resources of the United States—Economic and environmental geology and prospects for future supply: U.S. Geological Survey Professional Paper 1802, p. L1– L28.

Crerar, D.A., Cormick, R.K., and Barnes, H.L., 1980, Geochemistry of manganese: An overview, *in* Varentsov, I.M. and Grasselly, G., eds., Geology and geochemistry of manganese: Budapest, Hungarian Academy of Science., v. 1., p. 293–334.

Dorf, E. and Rankin, D.W., 1962, Early Devonian plants from the Traveler Mountain area, Maine: Journal of Paleontology, v. 36, p. 999–1004.

Eilertsen, N.A., 1952, Maple Mountain-Hovey Mountain manganese project, central district, Aroostook County, Maine: U. S. Bureau of Mines, Report of Investigations 4921, 118 p.

Ekren, E.B. and Frischknecht, F.C., 1967, Geological-geophysical investigations of bedrock in the Island Falls quadrangle, Aroostook and Penobscot counties, Maine: Geological Survey Professional Paper 527. 36 p.

Fleet, A.J., 1983, Hydrothermal and hydrogenous ferromanganese deposits: Do they form a continuum? The rare earth element evidence, *in* Rona, P.A., Boström, K., Laubier, L., Smith, K.L. (eds), Hydrothermal Process at Seafloor Spreading Centers: New York, Plenum Press, p. 535-555.

Fyffe, L., van Staal, C., Wilson, R., and Johnson, S., 2023a, An overview of Early Paleozoic arc systems in New Brunswick, Canada, and eastern Maine, USA. Atlantic Geoscience 59, p. 1–28.

Fyffe, L., Ludman, A., and McFarlane, C., 2023b. Composition, age and tectonic significance of the Benton granite, Eel River area, west-central New Brunswick, Canada. Atlantic Geosciences v. 59, p. 87–108

Gehrels, G.E., Valencia, V., Ruiz, J., 2008, Enhanced precision, accuracy, efficiency, and spatial resolution of U-Pb ages by laser ablation–multicollector–inductively coupled plasma–mass spectrometry: Geochemistry, Geophysics, Geosystems, v. 9, Q03017, doi:10.1029/2007GC001805.

Hall, B., 1970, Stratigraphy of the southern end of the Munsungun anticlinorium, Maine. *Maine* Geological Survey Bulletin 22, 63 p.

Hein, J.R., Koschinsky, A., Halbach, P., Manheim, F.T., Bau, M., Kang, J-K., Lubick, N, 1997, Iron and manganese oxide mineralization in the Pacific. In: Nicholson K, Hein JR, Bühn B, Desgupta S (eds) Manganese mineralization: geochemistry and mineralogy of terrestrial and marine deposits. Geol Soci Special Publication, p. 123–138.

Hollocher, K., Robinson, P., Walsh, E., and Roberts, D., 2012, Geochemistry of amphibolite-facies volcanics and gabbros of the Støren Nappe in extensions west and southwest of Trondheim, Western Gneiss Region, Norway: a key to correlations and paleotectonic settings. American Journal of Science, 312, p.357-416.

Jackson, C.T., 1837, Second Report on the Geology of the State of Maine, p. 127–128.

Kilgore, C.C., and Thomas, P.R., 1982, Manganese availability–Domestic: U.S. Bureau of Mines Information Circular 8889, 14 p.

Lacombe, P., 1988, Stratigraphic, Structural, and Magnetic Investigations of the Mars Hill Area, Aroostook County, Maine: Unpublished Master thesis, Boston College.

Ludman, A., 2023, Bedrock geology of the Greenfield quadrangle, Maine: Maine Geological Survey, Open-File Report 23-1, 31 p. report and color map, scale 1:24,000.

Ludman, A., and Whittaker, A., 2023, Termination of the Ganderian Cambrian–Ordovician Miramichi terrane in east-central Maine, northern Appalachian orogen, USA. Atlantic Geosciences v. 59, 123-146.

Ludwig, K.R., 2008, Isoplot 3.60. Berkeley Geochronology Center, Special Publication No. 4, 77 p.

Machado, G. and Flores, D., 2015, An effective method for the observation and documentation of highly matured palynomorphs using reflected light microscopy. Palynology, 39 (3): p. 345–349.

McCormick, M., 2021, Geology and lithogeochemistry of the Pickett Mountain volcanogenic massive sulfide deposit, northern Maine. Unpublished Master's thesis, University of Maine at Orono, Maine, USA, 204 p.

Meschede, M., 1986, A method of discriminating between different types of mid-ocean ridge basalts and continental tholeiites with the Nb-Zr-Y diagram. Chem. Geol., 56, p. 207−218.

Miller, R.J., 1947, Manganese deposits of Aroostook County, Maine: Maine Geological Survey Bulletin, 4, 77 p.

Nakamura, N., 1974, Determination of REE, Ba, Mg, Na and K in carbonaceous and ordinary chondrites. Geochimica et Cosmochimica Acta, 38, p. 757–775.

Neuman, R.B., 1962, The Grand Pitch Formation; new name for the Grand Falls Formation (Cambrian?) in northeastern Maine: American Journal of Science, v. 260, no. 10, p. 794–797.

Neuman, R.B., 1967, Bedrock geology of the Shin Pond and Stacyville quadrangles, Penobscot County, Maine: Geological Survey Professional Paper 524-1.

Neuman, R.B., and Whittington, H. B., 1964, Fossils in Ordovician tuffs, northeastern Maine; U. S. Geological Survey, Bulletin 1181-E, p. E1–E38.

Neuman, R.B. and Rankin, D.W., 1980, Bedrock geology of the Shin Pond-Traveler Mountain region: in Roy, David C., and Naylor, Richard S. (editors), A guidebook to the geology of northeastern Maine and neighboring New Brunswick: New England Intercollegiate Geological Conference, 72nd Annual Meeting, Presque Isle, Maine, p. 86–97.

Osberg, P. H., Moench, R. H., and Warner, J., 1968, Stratigraphy of the Merrimack Synclinorium in western Maine: in E. Zen and others (eds.), Studies in Appalachian Geology – Northern and Maritime: New York, Interscience, p. 241–253.

Osberg, P.H., Hussey, A.M., II, and Boone, G.M. (editors), 1985, Bedrock geologic map of Maine: Maine Geological Survey.

Petránek, J., 1991, Ordovician oolitic ironstones and their source of iron. Bulletin of the Geological Survey of Prague. v. 66, no. 6, p. 321–327.

Pavlides, L. and Milton, C., 1962, Geology and manganese deposits of the Maple and Hovey Mountains area, Aroostook County, Maine: U.S. Geological Survey Professional Paper 362, 116 p.

Pavlides, L., 1964, The Hovey Group of northeastern Maine: Contributions to Stratigraphy, U.S. Geological Survey Bulletin 1194-B. p. B1–B6.

Pavlides, L., 1966, Meduxnekeag Group and Spragueville Formation of Aroostook County, northeast Maine: Contributions to Stratigraphy, U.S. Geological Survey Bulletin 1194-B. p. B1–B6. p. A52–A57.

Pavlides, L. and Berry, W.B.N., 1966. Graptolite-bearing Silurian rocks of the Houlton-Smyrna Mills area, Aroostook County, Maine. Geological Survey Research 1966: U.S. Geological Survey Professional Paper, 550-B, p. B51–B61.

Pavlides, L., 1973, Geologic map of the Howe Brook quadrangle, Aroostook County, Maine: U.S. Geological Survey Geologic Quadrangle Map GQ-1094, scale 1:24,000.

Pearce, J.A., 2008, Geochemical fingerprinting of oceanic basalts with applications to ophiolite classification and the search for Archean oceanic crust. Lithos 100, p.14–48

Pearce, J. A., 1983, Role of sub-continental lithosphere in magma genesis at destructive plate margins, in Continental Basalts and Mantle Xenoliths, edited by C. J. Hawkesworth and M. J. Norry, p. 230–249, Shiva, Nantwich, UK.

Perkins, E.H. and Smith, E.S.C., 1925, Contributions to the geology of Maine, No. 1: A geological section from the Kennebec River to Penobscot Bay: American Journal of Science, 5th series, v. 9, no. 51, p. 204–228.

Pollock, S.G., 1987, The Lower Devonian slate problem of western and northern Maine revisited: Northeastern Geology, v. 9, no. 1, p. 37-50.

Pollock, S.G., 2023, Bedrock Geology of the Fifth Musquacook Lake Quadrangle, Maine: Maine Geological Survey, Open-File Map, scale 1:24,000.

Rankin, D.W., 1961, Bedrock geology of the Traveler-Katahdin area, Maine. Unpublished Ph.D. thesis, Harvard University, Cambridge, Mass., 317 p., 4 plates.

Ross, P.S. and Bédard, J.H., 2009, Magmatic Affinity of Modern and Ancient Subalkaline Volcanic Rocks Determined from Trace-Element Discriminant Diagrams. Canadian Journal of Earth Sciences, 46, p. 823-839.

Roy, D.C., 1987, Geologic Map of the Caribou and Northern Presque Isle 15' Quadrangle, Maine: Maine Geological Survey, Open-File No. 87-2, 44 p.

Roy, D.C. and Mencher, E., 1976, Ordovician and Silurian stratigraphy of northeastern Aroostook County, Maine: Geol. Soc. Amer., Memoir 148, p. 25–52.

Roy, D. C., 1970, The Silurian of Northeastern Aroostook County, Maine, (Ph.D. thesis): Massachusetts Institute of Technology, 482 p.

Sun, S.S. and McDonough, W.F., 1989, Chemical and isotopic systematics of oceanic basalts: implications for mantle composition and processes. In: Saunders, A.D., Norry, M.J. (Eds.), Magmatism in the Ocean Basins. Geological Society, London, Special Publications 42, pp. 313–345.

Stacey, J.S., and Kramers, J.D., 1975, Approximation of terrestrial lead isotope evolution by a two-stage model: Earth and Planetary Science Letters, v. 26, p. 207–221.

Takematsu, N., Sato, Y., Okabe, S., 1989, Factors controlling the chemical composition of marine manganese nodules and crusts: a review and synthesis. Mar. Chem. 26 (1), p. 41–56.

Taylor, S.R. and McLeannan, S.M., 1985, The Continental Crust: Its Composition and Evolution. Blackwell, Oxford, 312 pp.

Toth, J.R., 1980, Deposition of submarine crusts rich in manganese and iron. Geological Society of America Bulletin, 91, p. 44–54

Usui, A., Terashima, S., 1997, Deposition of hydrogenetic and hydrothermal manganese minerals in the Ogasawara (Bonin) Arc Area, Northwest Pacific. Marine Georesources & Geotechnolology, 15 (2), p. 127–154.

Wang, C., 2021, Bedrock Geology of the Big Machias Lake Quadrangle, Maine: Maine Geological Survey, Open-File Map 21-3, scale 1:24,000.

Wang, C., 2022a, Bedrock Geology of the Fish River Lake Quadrangle, Maine: Maine Geological Survey, Open-File Map 22-5, scale 1:24,000.

Wang, C., 2022b, Bedrock Geology of the Carr Pond Quadrangle, Maine: Maine Geological Survey, Open-File Map 22-6, scale 1:24,000.

Wang, C., 2023, Bedrock Geology of the Northern Half of the Chase Lake Quadrangle, Maine: Maine Geological Survey, Geologic Map 23-X.

Wang, C., Marvinney, R., Putnam, D., Bagley, E., and Belair, S., 2020, The newly discovered, giant Fish River post-Acadian rift system in the Northern Appalachian Mountains of Northern Maine. Geological Society of America Abstracts with Programs, Vol. 52.

Wang, C., Marvinney, R., Whittaker, A., and Putnam, D., 2022a, The Munsungun-Winterville Belt of Northern Maine: An Ordovician volcanic arc developed on a Laurentia massif: Geological Association of Canada-Mineralogical Association of Canada, Volume of Abstracts, v. 45, p. 220.

Wang, C., Marvinney, R., Whittaker, A., Pollock, S., and Putnam, D., 2022b. Advances in understanding the complex and protracted tectonic and deformational history of the Munsungun-Winterville Belt in the Maine Appalachians. Geological Society of America Abstracts with Programs, v.54, no.3.

Wellensiek, M.R., van der Pluijm, B.A., Van der Voo, R., and Johnson, R.J.E., 1990, Tectonic history of the Lunksoos composite terrane in the Maine Appalachians: Tectonics, v. 9, p. 719–734.

Williams, H.S. and Gregory, H. E., 1900, Contributions to the Geology of Maine: U. S. Geological Survey Bull. 165, 212 p.

Wilson, R.A., and Kamo, S.L., 2012, The Salinic Orogeny in northern New Brunswick: geochronological constraints and implications for Silurian stratigraphic nomenclature. Canadian Journal of Earth Sciences, 49, p. 222–238.

Wilson, R.A., van Staal, C.R., and Kamo, S., 2008, Lower Silurian subduction-related volcanic rocks in the Chaleurs Group, northern New Brunswick, Canada. Canadian Journal of Earth Sciences, 45, p. 981–998.

DEVONIAN-AGED MINERALIZATION TYPES IN SOUTHWESTERN NEW BRUNSWICK

David R Lentz [1], Kathleen Thorne [2], Fazilat Yousefi [1], Niyayesh Khorshidi[1], Alan Cardenas-Vera[1], Moya MacDonald[1],
[1] Department of Earth Sciences, University of New Brunswick, Fredericton, NB E3B 5A3 Canada. dlentz@unb.ca
[2]Geological Surveys Branch, New Brunswick Department of Natural Resources and Energy Development, P.O. Box 6000, Fredericton, NB E3B 5H1 Canada

DESCRIPTION

This trip will examine the various types and styles of mineralization related to Devonian magmatism related to the multiphase middle Devonian Pokiok Batholith in south-central New Brunswick. The Lake George antimony mine (closed due to low Sb prices and considered as an abandoned mine site, so wear protective footwear) was found in the late 1800's and was the largest antimony deposit in North America until it was closed in 1998; presently it is a legacy site managed by the province of New Brunswick with a tailing impoundment that is being studied for reclamation - reprocessing purposes. The drill core on the site has been studied for the earlier contact metasomatic W-Mo-Au mineralization, the associated Hawkshaw granodiorite intrusions at depth, the porphyry and lamprophyre dikes, and the late Sb-Au fault-filled vein that was mined; these are mostly hosted in the folded Silurian Fredericton Trough metasedimentary rocks. We will also see drill core from the Golden Ridge epithermal gold deposit from near Poplar Mountain that is similar in age, based on Ar-Ar dating. Afterwards we will visit a small pegmatite-aplite dike (allandale granite) that intrudes the Hawkshaw Granite (roadside) that is known to be associated with Be-Mo-W mineralization in the region. We will also visit a part of the Magagudavic Fault zone (highway on ramp) that hosts the Pokiok South Au occurrence and will see some drill core from the drilling about 15 years ago.

Assembly time and location: 9:30 am (Atlantic time, or 8:30 am Eastern time) at the Petro-Canada gas station & Denny's in Prince William (45.873581, -66.985576). Use Exit 253 from the TransCanada Highway (#2). Americans going to the trip need to have their passport ready.

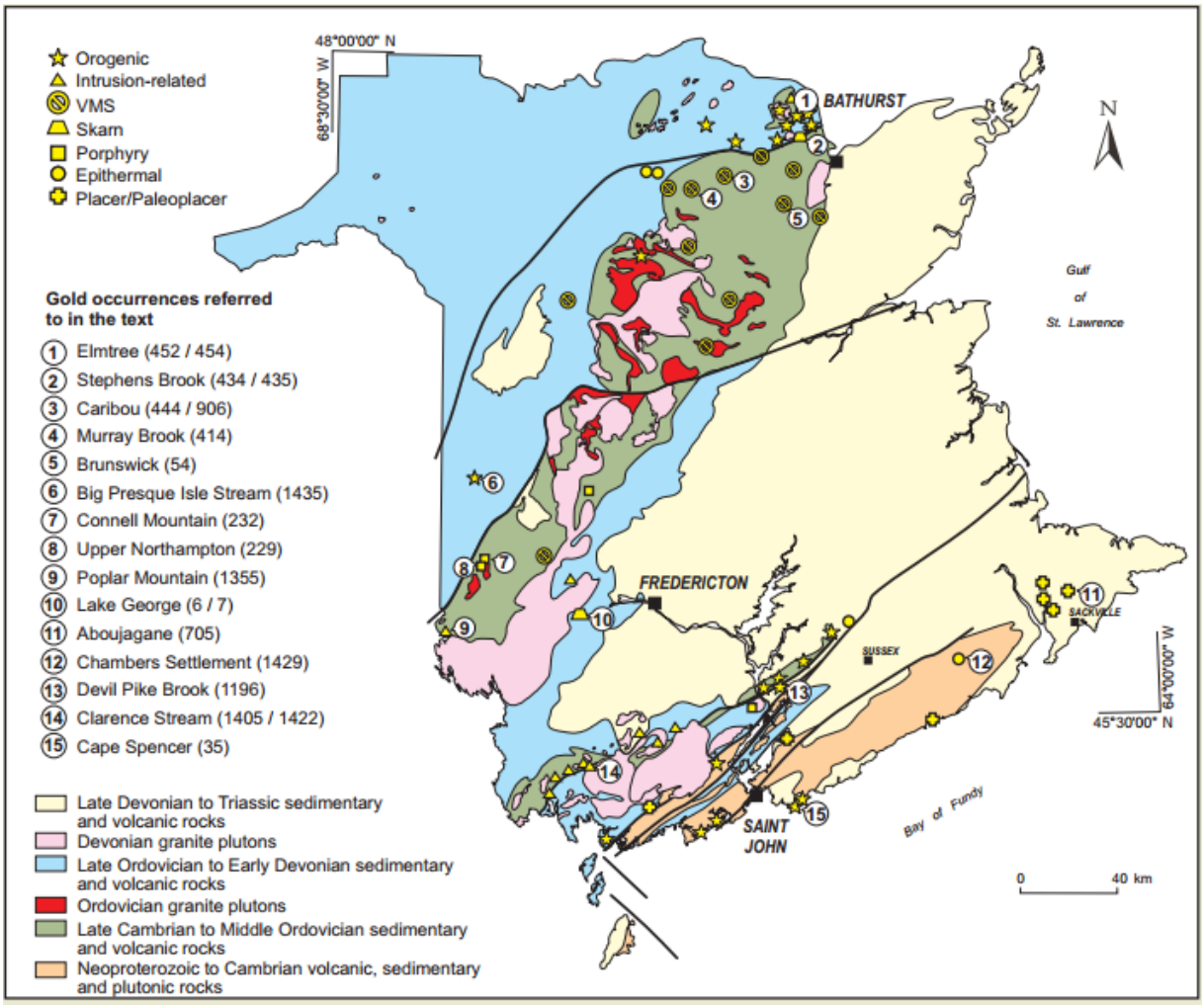

New Brunswick Geological map showing the locations of the various types of gold deposits throughout New Brunswick (from NB DEM 2011). Note Devonian Granites in light pink.

Reference

McLeod, M.J., Hoy, D., Thorne, K.G. 2008. History, Tectonic Setting, and Models for Intrusion-related Gold Deposits in Southwestern New Brunswick, Canada: Examples from the Clarence Stream Area. Explor. Min. Geol. 17, 1–12.

Part I

Field trip to Lake George Antimony Mine, Central New Brunswick

David R Lentz, Fazilat Yousefi, Niyayesh Khorshidi
Department of Earth Science, University of New Brunswick, Fredericton, NB E3B 5A3

Antimony

Antimony is a silvery-white critical metalloid, located in Group 15 of the periodic table, mostly found in the environment in companion with other elements like arsenic and bismuth. Low-temperature magmatic hydrothermal fluids circulating at shallow depths is the most favorable system for the formation of antimony deposits. It is widely used in numerous fields, including production of semiconductors, antimony alloys for acid batteries, printing; antimony oxides for glass, ceramics, polyethylene terephthalate (PET) plastics, textiles, pigments, flame retardants, brake pads, etc. It is a key component flame retardant in children's clothing (Figure 1).

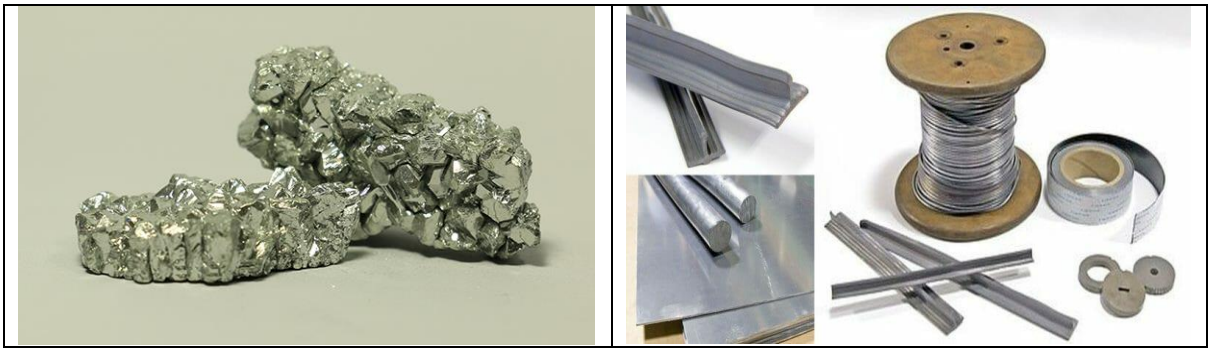

https://www2.gnb.ca/content/gnb/en/departments/erd/energy/content/minerals/content/FactSheets.html

Deposit Geology and Production History

The Lake George antimony mine is located approximately 30 km west of Fredericton in west-central New Brunswick (Fig. 2, Caron 1996; Lentz et al. 2020), and was once North America's largest producer of antimony (stibnite, Sb_2S_3) until it closed in 1998, due to low Sb prices. In addition to the late fault-filled stibnite-quartz vein cutting folded Siluro-Devonian metasedimentary rocks and intrusions (Figs. 3, 4, 5) (Scratch et al. 1984); the area surrounding the Lake George Sb vein contains earlier W (tungsten, as scheelite), Mo (molybdenum, as molybdenite) (Seal et al. 1988), and Au (native gold) stockwork mineralization around the top of the Hawkshaw granodioritic intrusion (U-Pb zircon 419.6±3.0 Ma); however, these commodities were never the focus of the original development (Lentz et al., 2020). The relative ages of rocks, and mineralization systems are documented in detail by Lentz et al. (2020).

Antimony was first discovered in the Lake George area during road construction in 1863; since then, the area has seen sporadic exploration and mining activity. The Lake George Mining and Smelting company was formed in 1876 to operate the Hibbard mine. In 1869, the first shaft was sunk on the property followed by the construction of a mill and smelter by the Hibbard Antimony Company in 1880. Between 1863 and 1969, three shafts were sunk on the Hibbard, Adams, and Lawrence showings. Between 1972 and 1981, 34,417 tonnes of concentrate grading 65–66% Sb was produced at the Lake George Mine. Prior to 1984, approximately 0.85 Mt of ore grading approximately 4.15% antimony was mined from several deposits. APOCAN operated the mine until it closed in 1998, and it was returned to the Crown in 2021 including the tailings.

Presently, Lake George has a resource (NI 43-101 compliant 2014 technical report by MRB & Associates): Indicated – 153,147 tonnes grading 3.73% Sb and Inferred – 718,046 tonnes grading 2.61% Sb at a cut-off grade of 1.5% Sb (Bourgoin 2014).

The Lake George region is now being examined from a multidisciplinary perspective to distill the important features suitable to enhance gold exploration and has been recently explored for gold around the mine property (Morrissy 1991; Lentz et al. 2003). Tailings and tailings pond research and hydrogeological research, cooperatively between the New Brunswick Department of Natural Resources and Energy Development and the University of New Brunswick, is beginning at this site, and it will be discussed during the trip.

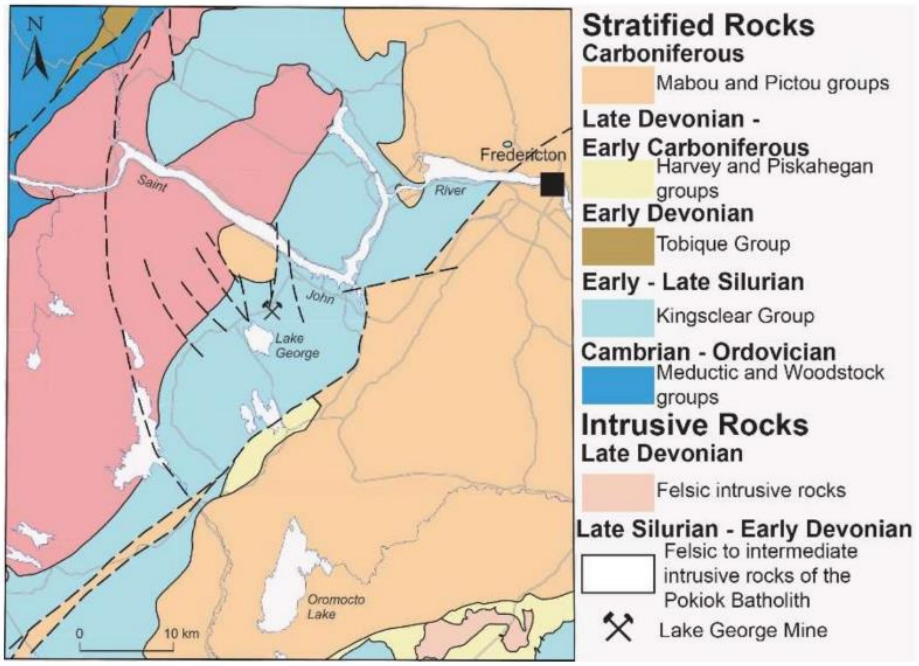

Fig. 2. Geological map of the Lake George area and surrounding region in central New Brunswick (from Lentz et al. 2020).

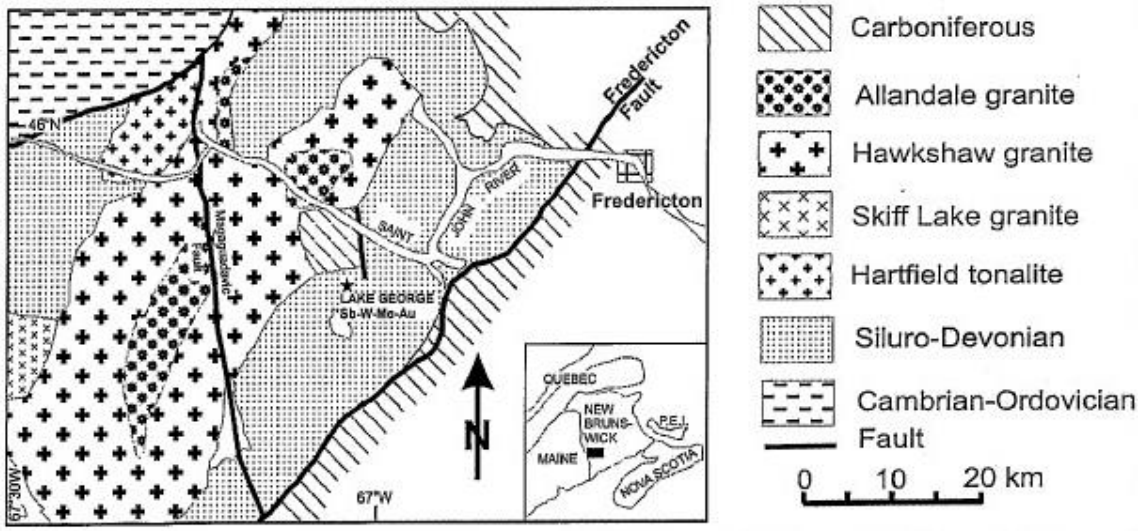

Fig. 3. Location and general geology of the Lake George antimony mine, New Brunswick (modified after Seal et al., 1998).

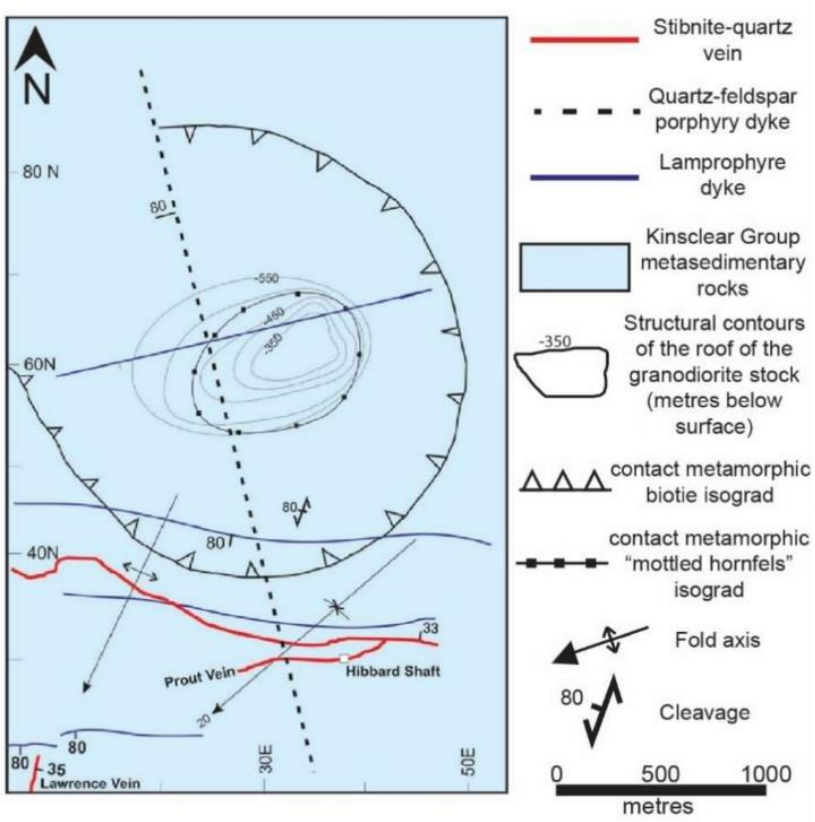

Fig. 4. Geological map of the Lake George mine, illustrating the granodiorite stock contoured at depth, the quartz–feldspar porphyry dyke, the lamprophyre dykes, and vein systems in the area (modified after Seal et al. 1988).

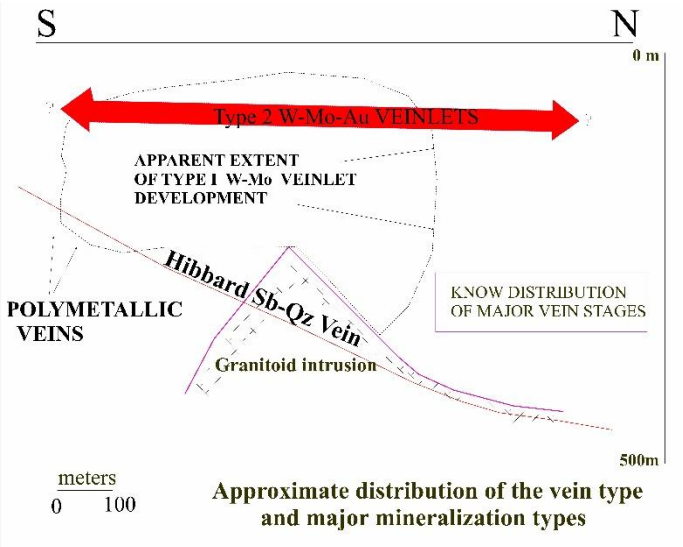

Fig. 5. Cross section through the Lake George Antimony deposit illustrating the earlier stage W-Mo-Au stockwork veins and the large Hibbard gold-bearing Sb-quartz vein and the Lake George granodiorite cupola that is related to the Hawkshaw Granite of the Pokiok Batholith to the north (modified from Seal et al. 1988).

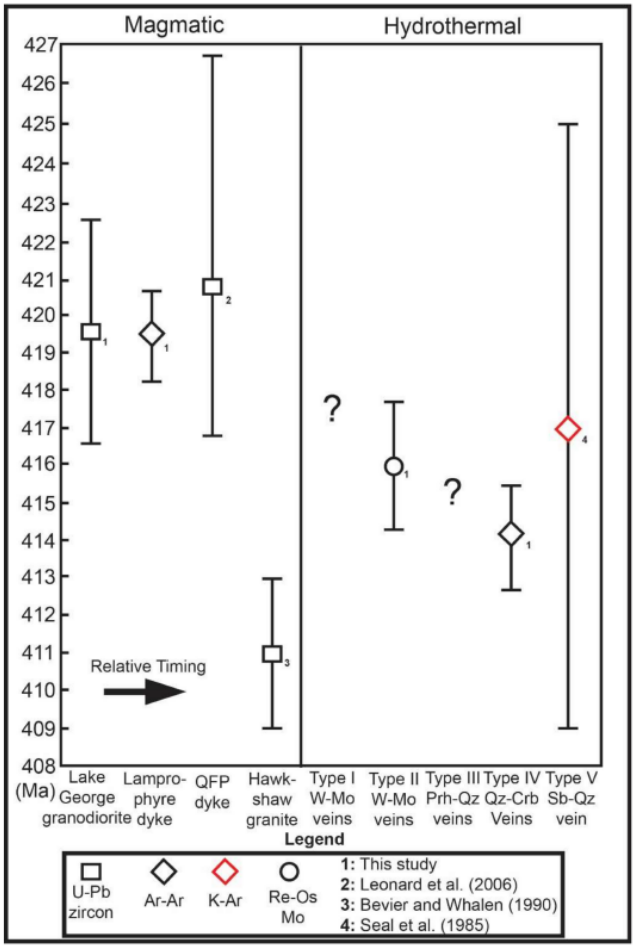

Fig. 6. Schematic representation comparing the dates obtained from this study and others (see Lentz et al. 2020) of the various magmatic–hydrothermal events at the Lake George mine. The events are ordered from left to right by previously identified cross-cutting relationships and labeled with the age of the most recent geochronological methods used to date them. The errors associated with the dates reported are all 2 sigma.

References

Bourgoin, M. 2014. Lake George Antimony Project, Province of New Brunswick; National Instrument 43-101 Technical Report; MRB and Associates Geological Consultants: Val-d'Or, QC, Canada, p. 68.

Caron, A. 1996. Geology of the Pokiok Batholith Aureole, with Emphasis on the Lake George Mine, York County, New Brunswick; Geoscience Report 94-2; New Brunswick Department of Natural Resources and Energy, Minerals and Energy Division: Fredericton, NB, Canada, 91 p.

Lentz, C., Thorne, K., McFarlane, C.R., Archibald, D.A. 2020. U-Pb, Ar-Ar, and Re-Os Geochronological Constraints on Multiple Magmatic–Hydrothermal Episodes at the Lake George Mine, Central New Brunswick. *Minerals 10*(6), 566.

Lentz, D.R. 2003. Multi-Element Instrumental Neutron Activation Analysis of Drill Core from the Lake George Mine, York County, New Brunswick; Open File 2003-1; New Brunswick Department of Natural Resources and Energy, Minerals Policy and Planning Division: Fredericton, NB, Canada, 22 p.

Morrissy, C.J. 1991. Gold Assessment at the Lake George Mine, York County, New Brunswick; Open File Report 91-1; New Brunswick Department of Natural Resources and Energy, Mineral Resources: Fredericton, NB, Canada, 22 p.

Scratch, R.B., Watson, G.P., Kerrich, R., Hutchinson, R.W. 1984. Fracture-controlled antimony-quartz mineralization, Lake George Deposit, New Brunswick; mineralogy, geochemistry, alteration, and hydrothermal regimes. Econ. Geol. 79, 1159–1186.

Seal, R., Clark, A., Morrissy, C.1988. Lake George, southwestern New Brunswick: A Silurian, multi-stage, polymetallic (Sb-W-Mo Au-base metal) hydrothermal center. In Recent Advances in the Geology of Granite-Related-Mineral Deposits; Canadian Institute of Mining and Metallurgy: Montréal, QC, Canada, Volume 39, pp. 252–264.

Part II

Devonian-aged Golden Ridge Epithermal Gold Deposit, New Brunswick, Canada

Alan Cardenas-Vera[1], Moya MacDonald[1], David R Lentz[1], Kathleen G Thorne[2]
[1] Department of Earth Sciences, University of New Brunswick, Fredericton, NB E3B 5A3 Canada. dlentz@unb.ca
[2]Geological Surveys Branch, New Brunswick Department of Natural Resources and Energy Development, P.O. Box 6000, Fredericton, NB E3B 5H1 Canada

** Excerpted from the paper published in Minerals 2023 (free on line).*

The Golden Ridge gold deposit (Figs. 1, 2), formerly known as Poplar Mountain, was initially discovered in the 1990s when a series of Au-Ag-As-Hg-Sb-enriched till geochemistry samples collected by the New Brunswick Department of Natural Resources and Energy was further investigated given their anomalous contents. Gold mineralization is principally associated with arsenopyrite and to a lesser degree with pyrite, stibnite, and sphalerite. As no visible gold has been observed, it is thought that gold is contained in arsenopyrite as an ionic substitution or as submicron-sized inclusions. The classification of the Golden Ridge mineralization is still debated. It has been regarded as a low sulphidation epithermal deposit, based on the presence of quartz-cemented breccia, locally cockscomb textures, with a Au-As-Sb association and the low contents of Cu. Nonetheless, it was later argued that considering the proximity of the Early Devonian Pokiok Batholith and available geochronological data indicating mineralization was coeval with the age of the batholith, the ore-forming fluid had originated from a granitic intrusion. Moreover, due to the presence of a deep-seated granitic intrusion below the Middle Ordovician Poplar Mountain volcanic complex indicated by regional magnetic data and the CO_2-rich composition of the ore-forming fluid, mineralization was considered to be mesothermal granite intrusion related. At Golden Ridge, both arsenopyrite and pyrite are the main auriferous phases forming the quartz-sericite assemblage (Fig. 3) and therefore can provide insights related to the ore-forming processes, including information about the evolution in gold deposition (Fig. 4). However, mineral chemistry studies of these sulphides and their trace elements have not been previously documented at Golden Ridge, and the relationship between Au and other trace elements is still poorly understood. Therefore, in this contribution, geochemical vectors to gold mineralization are ascertained by evaluating the bulk rock chemistry of sericitized host rocks from low-grade to high-grade drill core samples. The paragenetic sequence of the mineralization (Fig. 4), mineralogical texture of pyrite and arsenopyrite, and their *in situ* chemical composition via LA-ICP-MS spot analyses are comprehensively investigated in order to determine the mineralization process and their implications on the mechanism of gold saturation. This study complements the earlier studies of Chi and Watters (2002) and Chi et al. (2008) who focused on detailed petrographic work based on field and drill core observations followed by geochemical analysis of the different rock units, U-Pb and ^{40}Ar-^{39}Ar geochronology that attempted to constrain the age of the mineralization, and fluid inclusion and carbon and oxygen isotope analyses to characterize the mineralizing fluids. The significance of this study, which includes drill core material not studied previously, is the analysis of new bulk geochemical data and trace element compositions of arsenopyrite and pyrite that will enhance and reevaluate the paragenetic relationship between gold mineralization and sulphides to better understand this mineralizing system.

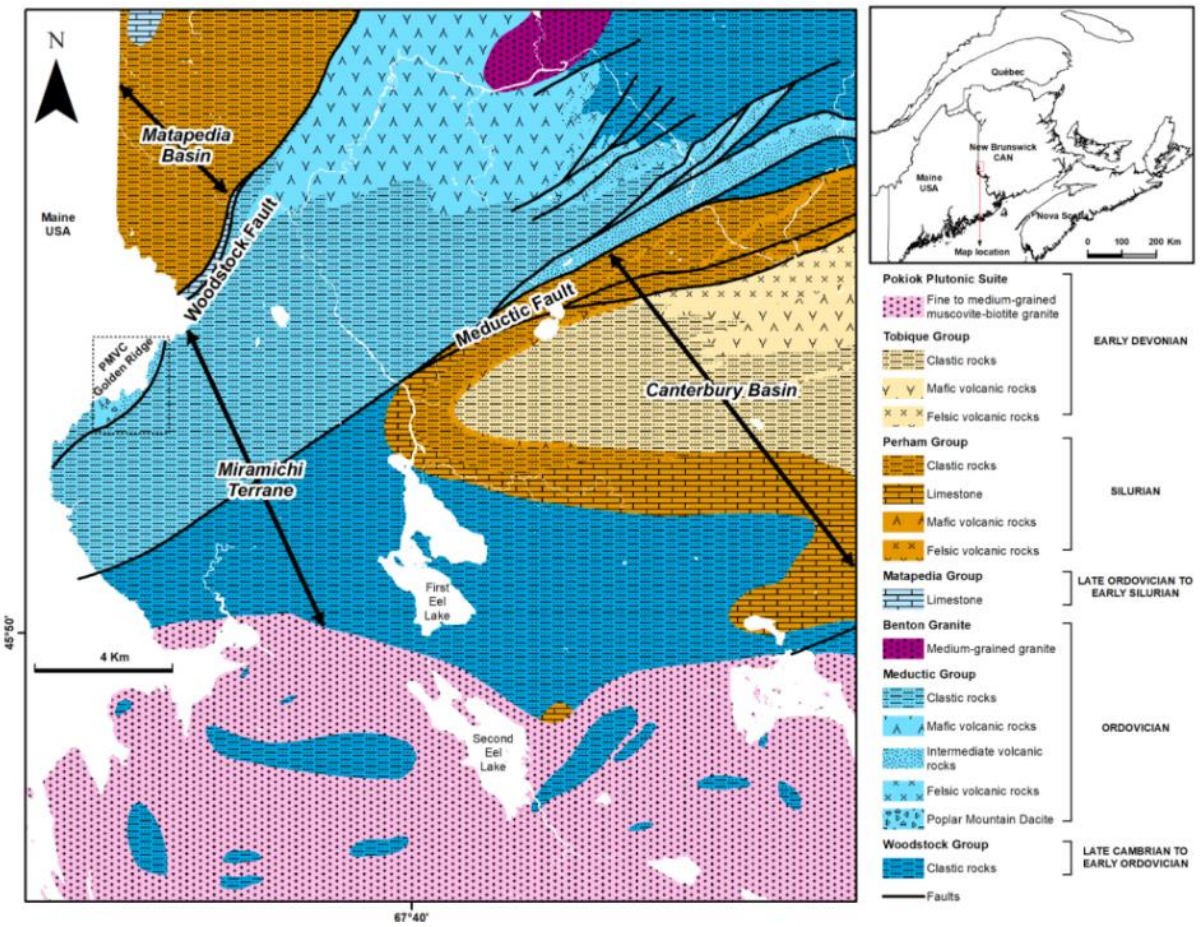

Fig. 1 Regional geological map of southwestern New Brunswick, showing the location of the Poplar Mountain volcanic complex (PMVC). Modified from Chi and Watters (2002) and Chi et al. (2008).

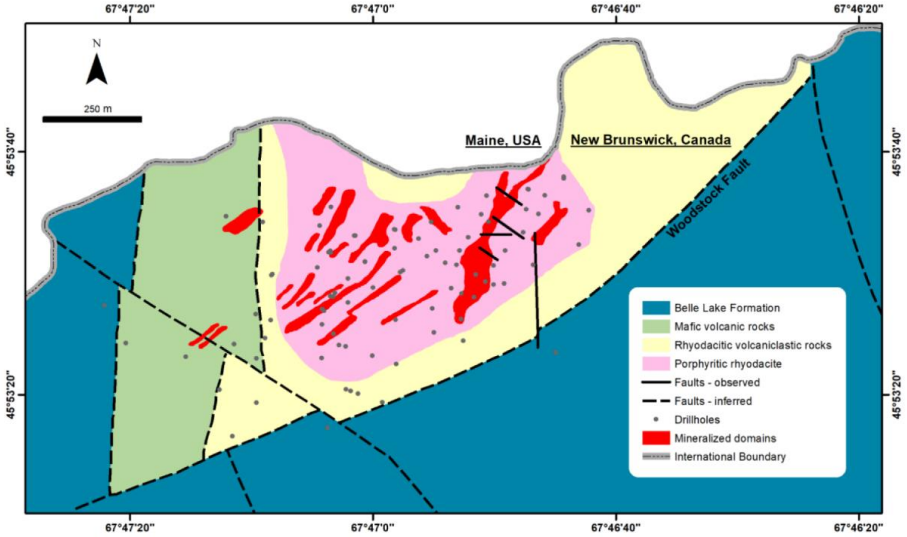

Fig. 2 Local geologic map of the Golden Ridge area (Poplar Mountain). Modified from Chi et al. (2008) and Hilchey and Webster (2011). (See inset in Fig. 1).

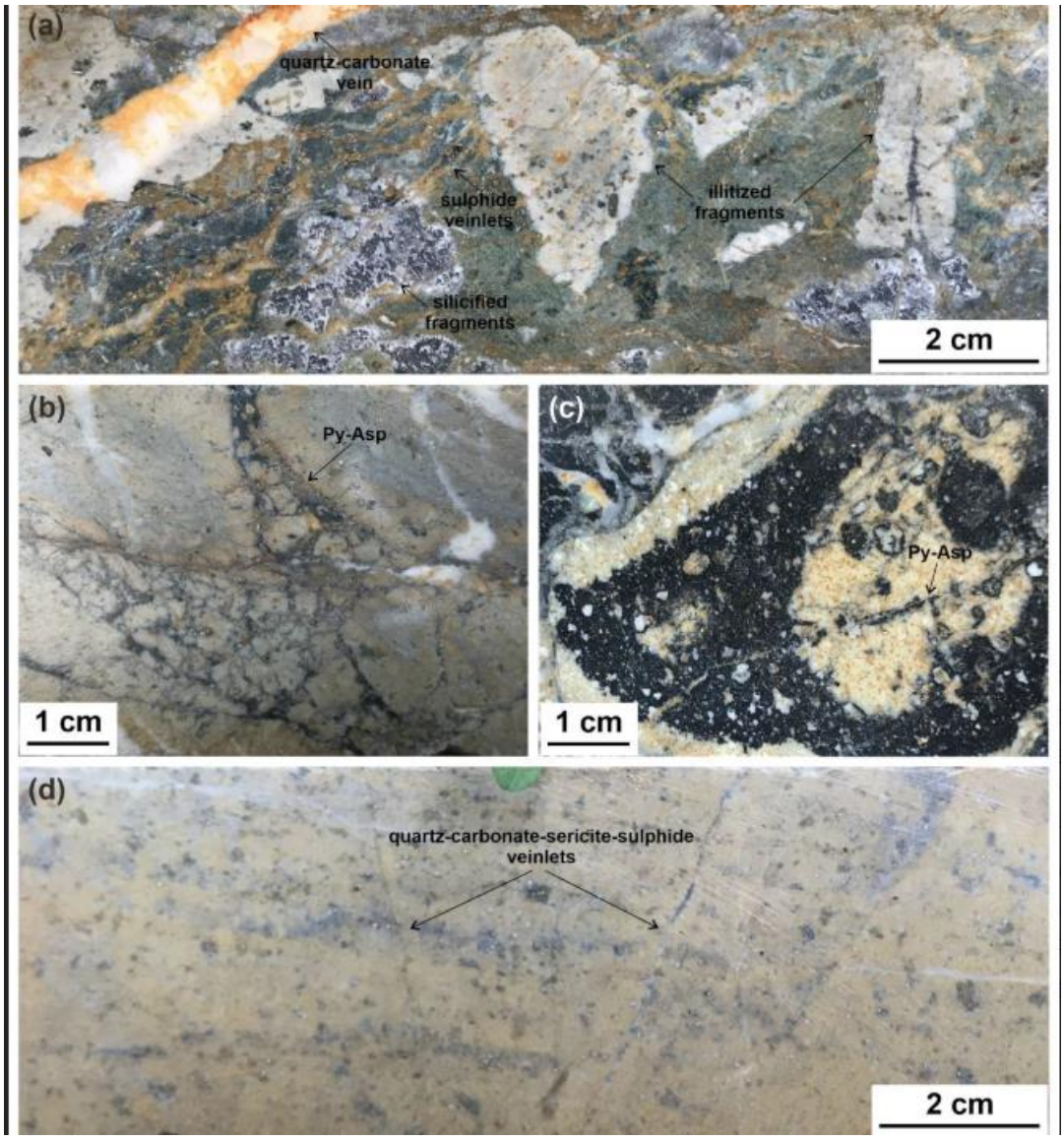

Fig. 3 Heterolithic brecciated and altered rhyodacitic volcaniclastic unit. The fragments are locally altered to chlorite-illite-carbonate (beige) and others are silicified (dark grey). A later quartzcarbonate vein crosscuts the breccia and a set of sulphide veinlets, locally oxidized, crosscut the breccia fragments (sample from drillhole GR1164A, 0.723 g/t Au). (b) Pyrite-arsenopyrite aggregates in quartz-cemented breccia cutting the sericite-illite altered porphyritic rhyodacite (sample from drill hole GR1168, 0.905 g/t Au). (c) Brecciated quartz-feldspar porphyritic rhyodacite with sericiteillite altered fragments and disseminated ultrafine pyrobitumen (black). Pyrite-arsenopyrite in mm thick veinlets crosscut fragments (sample from drillhole GR1168, 4.740 g/t Au). (d) Sericite-illite altered porphyritic rhyodacite with fractures filled by thin quartz-carbonate-sericite-sulphide veinlets (sample from GR1053, 4.410 g/t Au). Py: Pyrite; Asp: Arsenopyrite (see Cardenas-Vera et al. 2023).

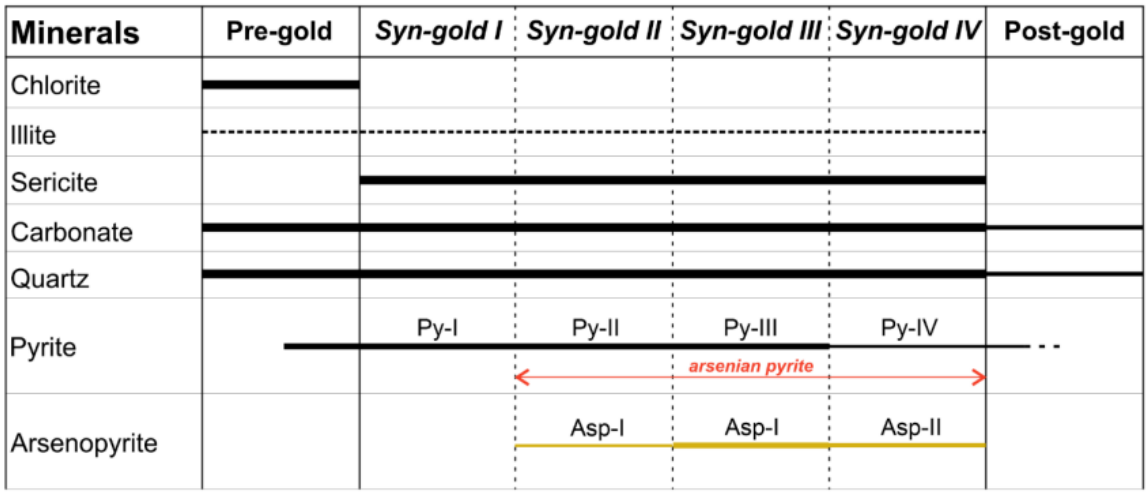

Fig. 4 Paragenetic mineral sequence for the Golden Ridge gold deposit. Modified from Chi and Watters (2002). The relative abundance of each mineral is represented by increasing line thickness.

References

Cardenas-Vera, A., MacDonald, M., Lentz, D.R., Thorne, K.G. 2023. Trace Element Characteristics of Pyrite and Arsenopyrite from the Golden Ridge Gold Deposit, New Brunswick, Canada: Implications for Ore Genesis. *Minerals 13*(7), 954.

Chi, G., Watters, S.E. 2002. Preliminary Geological and Petrographic Study of the Poplar Mountain Au Occurrence, Southwestern New Brunswick; Current Research 2002-D6; Geological Survey of Canada: Ottawa, ON, Canada, 11 p.

Chi, G., Watters, S., Davis, W.J., Ni, P., Castonguay, S., Hoy, D. 2008. Geologic, Geochemical, and Geochronological Constraints on the Genesis of Gold Mineralization at Poplar Mountain, Western New Brunswick, Canada. Explor. Min. Geol. 17, 101–130.

Hilchey, A., Webster, P. 2011. Technical Report on Mineral Resource Estimate for Portage Minerals Inc. and Freewest Resources Canada Inc: Mercator Geological Services; Golden Ridge Property: York County, NB, Canada, 81 p.

This Stop will be examining available drill core from the Golden Ridge deposit that is laid out at Lake George for this visit.

PART III

Gold-Silver Mineralization in Epithermal Quartz Veins along the Magaguadavic Fault Zone, Pokiok Batholith, Southwestern New Brunswick

Laurin Branscombe

**This contribution is from Branscombe (2015)*

The regional-scale Magaguadavic Fault that hosts the gold and silver mineralization generally strikes north and extends for approximately 65 km, transecting the Pokiok Batholith (see Whalen 1993) and locally marking the boundary between the Hawkshaw and Allandale granites within the central part of the batholith (Figs 1, 2). The Pokiok Batholith, located approximately 45 km west of Fredericton, intrudes sedimentary rocks of the Silurian Burtts Corner Formation (Kingsclear Group) to the east and the Cambro-Ordovician Baskahegan Lake Formation (Woodstock Group) to the west. The batholith comprises two predominant intrusive phases: the Allandale and Hawkshaw granites. The multi-phase Hawkshaw Granite consists of fine- to medium-grained, pink biotite granite and minor muscovite-biotite granite and has previously been dated by U-Pb zircon methods at 411 ± 1 Ma. The younger grey Allandale Granite, which was previously dated using U-Pb zircon methods at 402 ± 1 Ma, is composed of fine-grained, muscovite-biotite granite; these granites are no cogenetic and the Allandale maybe controlled by these late faults. The Allandalle Granite (and pegmatite and aplites) is spatially and temporally linked to W, Mo, and Be mineralization in the Zealand area to the northeast (see Fig. 1).

Along the northerly-trending Magaguadavic Fault, base-metal-bearing Au-Ag mineralization associated with extensive quartz veining, enveloped by pyrite-sericite-chlorite alteration (Beauchamp 2012). Native Au has been identified within the comb-quartz veins by StrikePoint Gold Inc. during their trenching and drilling program conducted in 2012 (Figs 3, 4). Reject materials from selected samples were reanalyzed using Au-Fire Assay –Metallix Screen-500g and Aqua Regia ICP-MS techniques and yielded higher Au and Ag grades overall. The study of drill core, then polished thin sections and polished slabs of samples collected from the six drill holes, the alteration and mineralization within and surrounding the quartz veins shows that there is no visible Au present, but assays returned high Au values of up to 3460 ppb. The nature of the quartz vein mineralization is characteristic of veins formed in a low-sulfidation epithermal environment. Geochronological analyses were conducted to determine the timing of mineralization and hydrothermal activity of the fault zone. The Ar^{40}/Ar^{39} geochronology returned a date of 389 Ma, which indicates the cooling through the closure temperature and gives an idea of timing of one event of hydrothermal activity that has gone through the Magaguadavic Fault zone.

Stop 2 will be at Dumfies at the Pokiok exit (231) of the TransCanada Highway (#2) (45.948437, -67.251777) we will walk down the exit ramp looking at epidote-chlorite-sericite-pyrite assemblages with slickensides on a splay of Magaguadavic Fault. Then we will look at selected drill core from this Pokiok gold occurrence occurrence.

From the Lake George minesite parking
Turn left onto NB-635 E
Proceed 5.8 km

Turn left to merge onto Trans-Canada Hwy/NB-2 W toward Edmundston
Proceed for 22.2 km

Take exit 231 toward NB-102 N
For 350 m

Turn left onto NB-102 N
Proceed to parking area 350 m

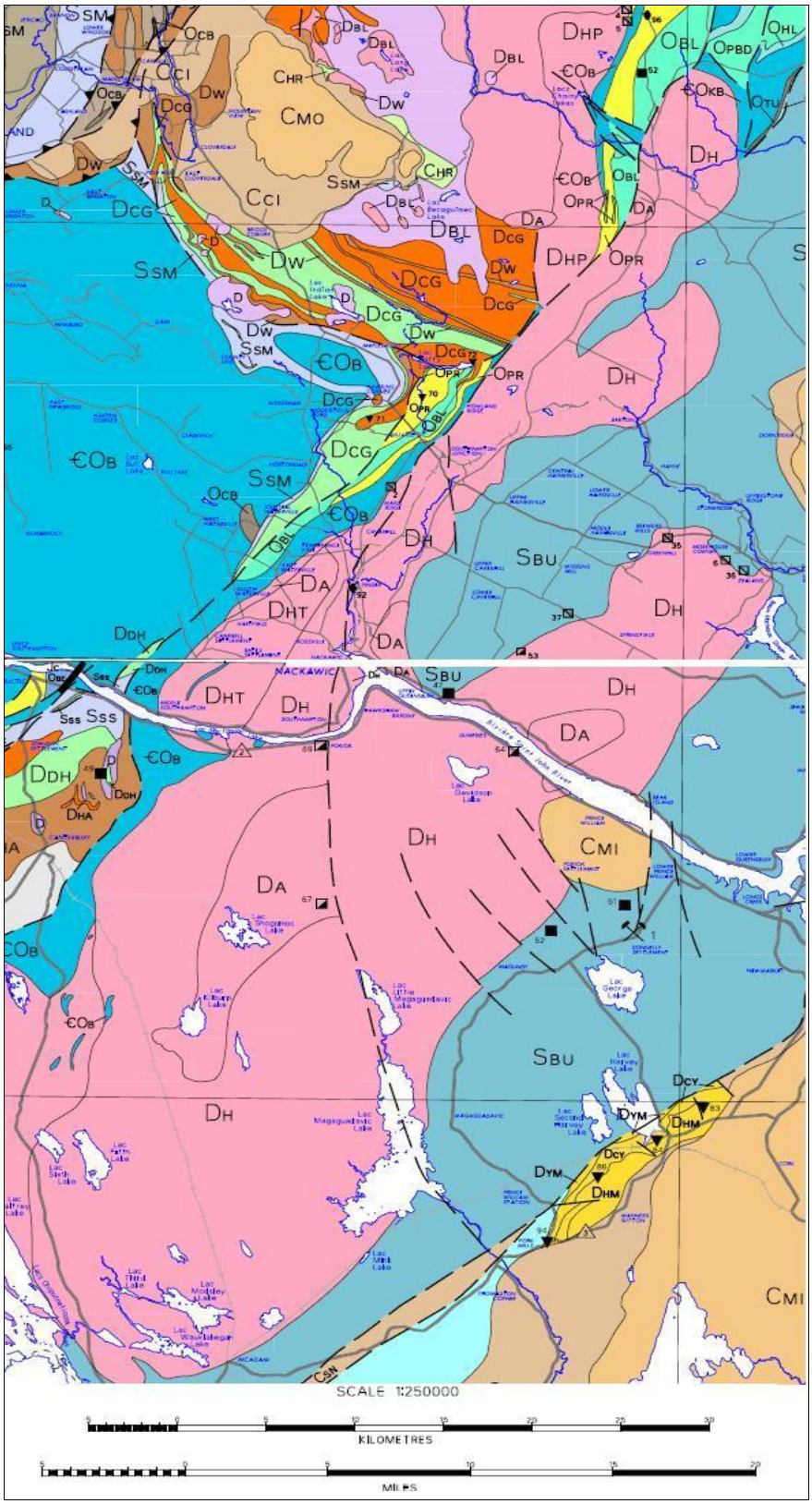

Fig. 1 Regional-scale geological map of southwestern New Brunswick including major fault zones; Compilation of map sheets NR 4 & 5 (from Smith and Fyffe 2006).

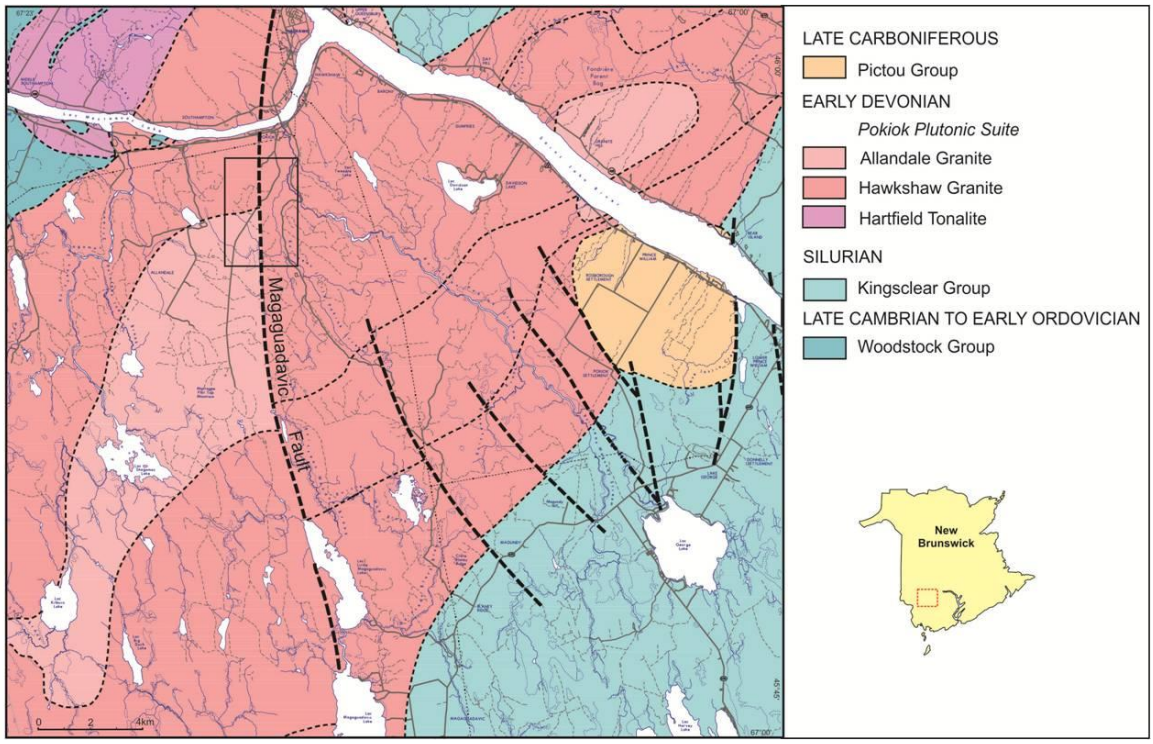

Fig. 2 Local-scale geological map showing the central part of the Pokiok Batholith, highlighting the Magaguadavic Fault Zone that transects both Middle Devonian Hawkshaw and Allandale granites. Outlined area represents project location (modified after Smith and Fyffe 2006; NB DEM 2014).

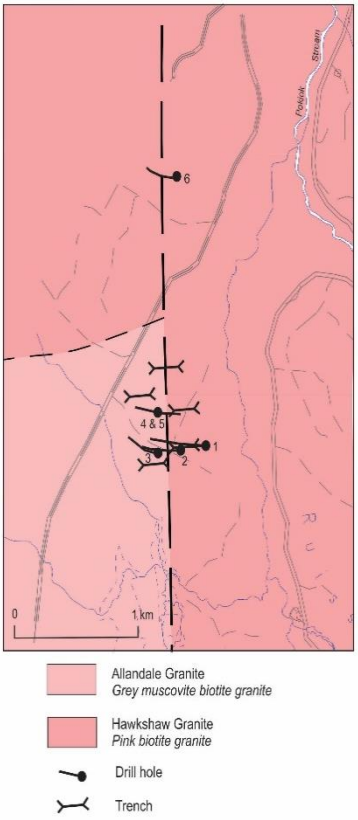

Fig. 3 Plan map of trench and drill hole locations in the Pokiok project area (modified from Beauchamp 2012). The Magaguadavic Fault location has been inferred using the airborne vertical gradient magnetic map done by the Geological Survey of Canada (GSC) for the New Brunswick Department of Energy and Mines (NB DEM). Drill holes were predominantly drilled to the west and mainly intersected Hawkshaw granite.

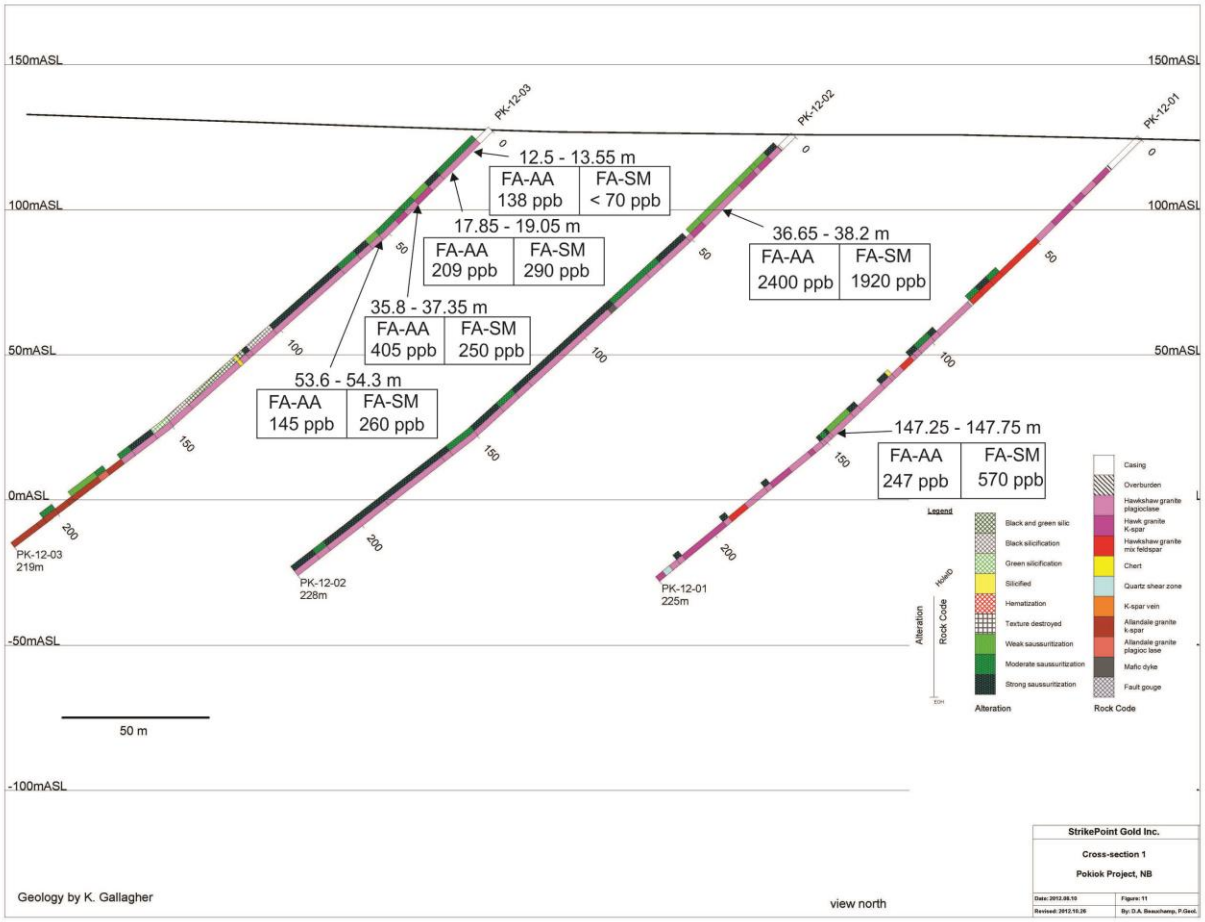

Fig. 4 Composite cross-section of drill holes PK-12-01, PK-12-02 and PK-12-03 from Strikepoint Gold Inc.'s 2012 exploration program. The right side of the drill hole column denotes the rock type encountered during drilling and the left side indicates the type of alteration. Drill holes were logged by Kandy Gallagher (Beauchamp 2012).

References

Beauchamp, D.A. 2012. Pokiok Project. Assessment Report for Strikepoint Gold Inc. New Brunswick, pp. 1-213 and 1-86.

Branscombe, L. 2015.Genesis of Gold-Silver Mineralization in Epithermal Quartz Veins along the Magaguadavic Fault Zone in the Pokiok Batholith, southwestern New Brunswick. Unpublished BSc thesis, University of New Brunswick, Fredericton, NB, 81 p.

Smith, E.A. and Fyffe, L.R. 2006. Bedrock geology of central New Brunswick (NTS 21 J). New Brunswick Department of Natural Resources, Minerals, Policy and Planning Division. Plate NR-4 (Second Edition).

Whalen, J.B. (1993) Geology, petrology and geochemistry of Appalachian granites in New Brunswick and Gaspesie, Quebec. Geological Survey of Canada, Bulletin 463, 124 p.

VERY-LOW-GRADE METAMORPHIC TRENDS IN THE AROOSTOOK-MATAPEDIA BELT OF NORTHEASTERN MAINE USING GRAPTOLITE AND VITRINITE REFLECTANCE, AND OTHER INDICATORS

MaryAnn Love Malinconico
Department of Geology and Environmental Geosciences, Lafayette College
Easton, PA 18042. lovem@lafayette.edu

INTRODUCTION AND BACKGROUND

Since 1970, various diagenetic to very-low-grade metamorphic indicators have been used to describe the level of metamorphism and its trend in the sub-greenschist area of northeastern Maine. Very-low-grade prehnite-pumpellyite assemblages were first described from Ordovician and Devonian volcanic rocks of the Munsungun inlier near Big Machias Lake (Coombs et al., 1970). However, the seminal regional study using prehnite-pumpellyite mineral assemblages from intermediate and mafic volcanic rocks in the Winterville inlier east into Silurian greywackes and conglomerates of the Aroostook-Matapedia basin was by Dorothy Richter and David Roy (1974, 1976) who included the Coombs et al. (1970) data, to the southwest, on their map. Richter and Roy found that level of metamorphism increased from prehnite-analcime subfacies in the northwest along the western limb of the Winterville inlier (adjacent to the Fish River chain of lakes) southeast through prehnite-pumpellyite subfacies and then pumpellyite-epidote-actinolite subfacies around Portage and Ashland (see Fig. 2). Jeffrey Walker (1989) examined chlorite polytypes (changes in silicate-hydroxide layer stacking patterns) across the region but found no variation.

Conodont alteration indices (CAI; Epstein et al., 1977) by Anita (Epstein) Harris of the United States Geological Survey (USGS) published in various quadrangle maps (Pavlides, 1978), papers (Slack et al., 1997; Bradley et al., 2000; Foose et al., 2003), and unpublished reports show a similar increase to the prehnite-pumpellyite metamorphic trend from northwest to east-southeast (see Fig. 2). This trend continues just across the eastern border with New Brunswick (Nowlan and Barnes, 1987). Conodont elements, whose color darkens with increasing diagenesis/metamorphism, are the teeth from an extinct (Cambrian-Triassic) marine worm-like vertebrate. The change in color is due to both temperature and duration at maximum temperature. For example, for a CAI of 1.5, the temperature range is 50˚C- 90˚C with associated durations of 500 million to 1 million years, respectively. That is, a heating time of 1 million years at 90˚C will produce the same CAI as heating for 500 million years at 50˚C (Epstein et al., 1977). CAI is a qualitative method in which the color of the conodont element is compared to standardized color charts and assigned a number from 1 to 8 (Epstein et al., 1977; Rejebian et al., 1987).

The reflectance of vitrinite (coalified fossil wood) and graptolites (Paleozoic marine colonial hemi-chordates with a carbonaceous exoskelton) (Fig. 1) are organic petrologic indicators of level of diagenesis and very-low-grade metamorphism, also called “thermal maturity”. The reflectance, like reflectivity of opaque minerals, is the quantitative measurement of the percent (%) of incident light reflected from the polished surface of the sample. However, organic petrography is done under oil immersion: a meniscus of immersion oil connects the sample surface and the microscope objective, so that incident and reflected light travels through that medium. Oil immersion increases the contrast between the different coal macerals (organic components like spores, wood, charcoal), but decreases the percent of light reflected relative to reflectance “in air”. Vitrinite reflectance has been used for over 60 years (Burgess, 1977) on 1) coals for identification of rank (i.e., bituminous vs. anthracite) and determination of industrial reactivity, and 2) on dispersed vitrinite in organic-bearing sedimentary rocks for basin thermal history analysis (level of diagenesis and very-low-grade metamorphism) and petroleum exploration (an indicator if organic matter has been heated enough to produce oil or gas). Like conodonts, vitrinite reflectance evolution is due to both temperature and time (Sweeney and Burnham, 1990).

However, vitrinite does not commonly exist in rocks that precede the flourishing of land plants in the Devonian. Since the mid-1970’s, graptolite reflectance has been used as a maturation indicator in lower Paleozoic marine rocks both for oil and gas exploration and for very-low-grade metamorphic studies in mountain belts. However, the correlation of graptolite reflectance (GR) to vitrinite reflectance (VR) is problematic because graptolites and vitrinite rarely occur in the same rocks. Correlation of GR to VR uses intermediaries such as CAI or Rock-Eval pyrolysis Tmax that may commonly co-exist with both vitrinite and graptolites, but not all the correlations consistently agree with each other (Luo et al., 2020: see Fig. 13). In addition, individual studies are usually also restricted to a specific region (e.g., Saudi Arabia, China, eastern Europe, western Canada). Nevertheless, graptolite reflectance, especially when combined with other metamorphic data, is a valuable indicator of the degree and trend of very-low-grade

metamorphism in Lower Paleozoic rocks. A detailed discussion of graptolite reflectance, correlation among graptolite reflectance studies and various indicators, plus relevant references is in Malinconico (2016).

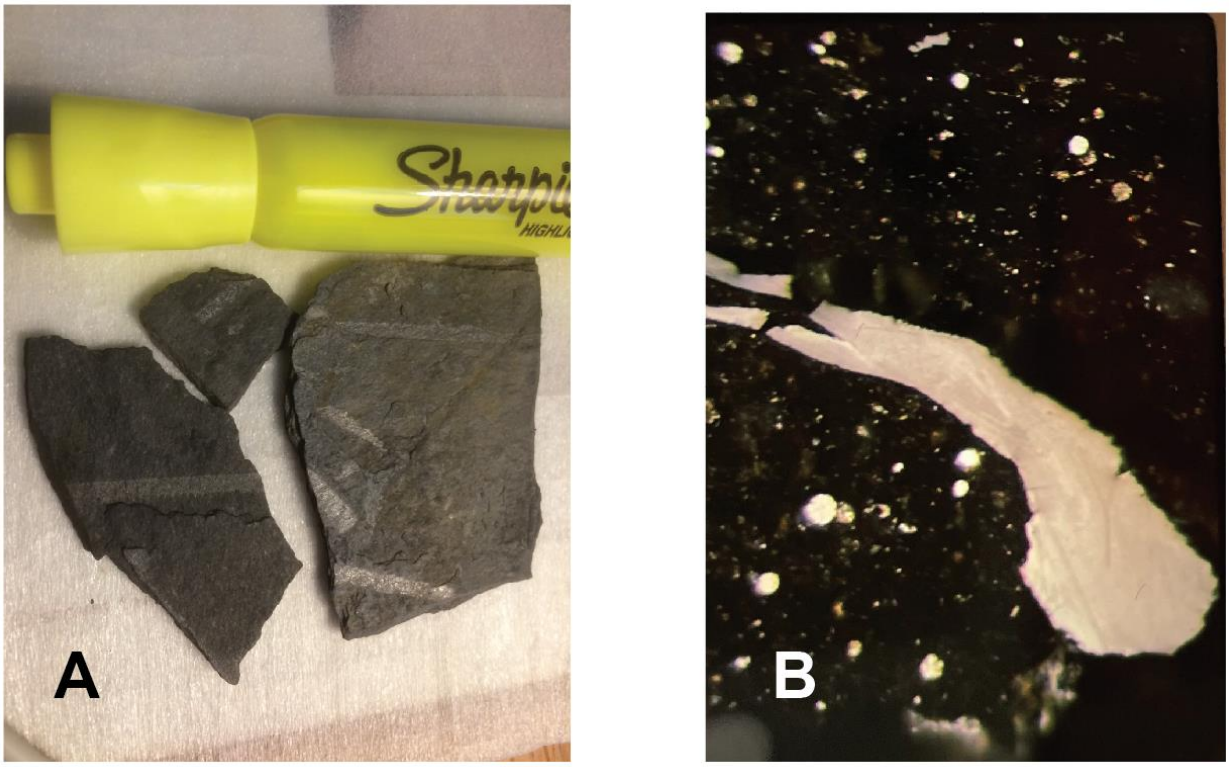

Figure 1. (A) Silurian graptolites, Lawler Ridge, I-95, north of Millinocket, Maine (mean maximum reflectance 10.6%). (B) Graptolite, photomicrograph, reflected light, oil immersion, 500X. Upper Ordovician Pyle Mountain Formation, Castle Hill, Maine (mean maximum reflectance 4.2%).

In 1988, I decided that the very-low-grade metamorphic, plus fossiliferous, lower Paleozoic strata of northeastern Maine would be an ideal location to test using graptolite reflectance in the northern Appalachians after a conversation with my former graduate-school classmate, Jeff Walker, during his dissertation on chlorite polytypes in northeastern Maine, mentioned above. Preliminary results were published in Malinconico (1992, 1993). Preparing all data for publication, with updated tectonometamorphic interpretation, based in new mapping (Wang et al., 2020; Wang, 2022; Wang et al., 2022b; pers. comm.) is currently underway (Malinconico, 2022).

METHODS

Most of the graptolite samples used in this study are those collected by David Roy, Boston College (Roy, 1970), William Forbes, University of Maine at Presque Isle (Boucot, 1964), and other workers during thirty years of field mapping in northeastern Maine (~1960–1990) and taxonomically identified by William B.N. Berry, University of California, Berkeley (Roy, 1970; Berry, 1964); Berry donated those samples through this author to the Maine Geological Survey in 1989. Other graptolite samples were 1) collected by this author in the field; 2) donated by William Forbes, University of Maine at Presque Isle (UMPI), including two from the Nylander Collection, Caribou, Maine; 3) donated by the New York State Museum (NYSM) (two samples), courtesy of Ed Landing; 4) donated by the Smithsonian through Robert Neuman to the Maine Survey (Colby locality). Plant samples for vitrinite reflectance were 1) recently collected by Chunzeng Wang (UMPI); 2) donated by Andrew Kasper, Rutgers University (Newark); and 3) included in the graptolite collection from W.B.N. Berry.

Graptolite reflectance (GR) was measured in oil immersion in plane polarized light at 546 nm on microscopes at Southern Illinois University (SIU), and the University of Kentucky. Vitrinite reflectance (VR) was similarly measured at SIU and the USGS in Reston, Virginia. Several to 100 reflectance points, if possible, are measured, and a mean and standard deviation calculated. All reflectance data was collected by the author.

Vitrinite acts like a uniaxial to biaxial negative material with anisotropy increasing with increasing rank or reflectance. Graptolite exoskeleton is also biaxial negative but very anisotropic at high rank, so it has been frequently reported as "maximum" reflectance in the very-low-grade metamorphic studies of mountain belts. Maximum reflectance is measured by rotating the microscope stage until the maximum reflectance of the target particle is identified. In vitrinite, the maximum reflectance usually occurs parallel to bedding. For dispersed vitrinite in sedimentary rocks, "random" reflectance is more commonly reported, and is used for the vitrinite data in this study. In polarized light, random reflectance can be determined from 1) measuring the reflectance with no stage rotation (and then calculating mean from many measured points); or 2) finding the average of the maximum and minimum values from stage rotation on a point. Random reflectance is frequently measured in non-polarized light that theoretically yields the average of the range of reflectances on the particle surface. All three methods for determining random vitrinite reflectance were used here, depending on the available microscope set-up.

RESULTS

Lower Paleozoic graptolite reflectance, northeastern Maine. The general trend of graptolite reflectance (GR) data in pre-Acadian rocks mimics the trend of the prehnite-pumpellyite facies and CAI increasing from northwest to southeast across the study area (Fig. 2). The lowest GR values in pre-Acadian (pre-Pragian) rocks are in the Ordovician Winterville Formation in the western arm of the Pre-Taconic Winterville inlier and in Silurian formations along strike to the north. This low trend increases slightly along strike northeast into New Brunswick (Bertrand and Malo, 2005). The highest GR values straddle the western boundary of the Ordovician-Silurian Carys Mills Formation and adjacent Silurian formations just west of Caribou.

Winterville and Munsungun inliers. These pre-Salinic inliers are part of the Middle Ordovician Bronson Hill/Popelogan belt that runs from western Massachusetts to New Brunswick. Major rock types are mafic volcanics, but graptolite-bearing marine black shales are also present in Upper Ordovician sedimentary rocks (Roy, 1970; Wang et al., 2022a). The Munsungun inlier is found to the southwest of the Winterville inlier (Fig. 2). The Winterville inlier has two fault-bounded arms (western and eastern) (Fig. 2) (Wang et al., 2022b; the eastern arm is referred to "Portage inlier" in Wang's Trip B3). The western arm is within the prehnite-analcime zone of Richter and Roy (1976) and the two GR values there (1.6%, 3.0%) are the lowest pre-Taconic values. (The CAI 3 data point at Fish River Lake is in the Lower Devonian Seboomook Group). There is a jump in metamorphism to values 3.4–4.4% GR in the eastern arm and in the northern Munsungun inlier (Fig. 2).

Aroostook-Matapedia basin. The Aroostook-Matapedia basin is a Late Ordovician-Early Devonian basin fed axially from the northeast with calcareous-rich sediment from the Matapedia platform and laterally with more pelitic sediment from adjacent highlands (Ludman et al., 2017; Ludman et al., 2020). The lowest Late-Ordovician to Silurian GR data ($\leq$ 2.0%) in the basin are found northeast along strike from the western arm (prehnite-analcime zone) of the Winterville inlier (Fig. 2). Indeed, the lowest pre-Acadian thermal indicators in the region are the 1.1% GR value in the Jemtland Formation at Guerette, plus the CAI 1.5 in the Lower Devonian Seboomook Group at Square Lake (actually part of the Connecticut-Gaspé basin to the west). GR values less than 3.0% trend south toward Ashland along the western border of the Aroostook-Matapedia basin, east of the Winterville inlier. Graptolite reflectance and CAI increase to the east with values of > 4.0% GR and 3.5–4 CAI around Presque Isle. Within this region, high GR values (>5.0%), with CAI = 5, form a north-northeast-trending wedge west and north of Caribou that widens northward into Canada. Although this metamorphic high crosses formational contacts, superposition of iso-reflectance contours on structural cross-sections (Fig. 3), suggests metamorphic trends were deformed with the stratigraphy during the Early Devonian Acadian orogeny. The highest mean maximum GR value (7.2%) at Colby, northwest of Caribou, may be due to strain since the graptolites in the outcrop are obviously and significantly deformed (Rickards and Riva, 1981).

Graptolite reflectance with other regional metamorphic indicators. The correlation of the Maine percent-mean-maximum graptolite reflectance data to coal rank and vitrinite reflectance was done through the co-existing metamorphic facies and CAI data of the region (Fig. 4).

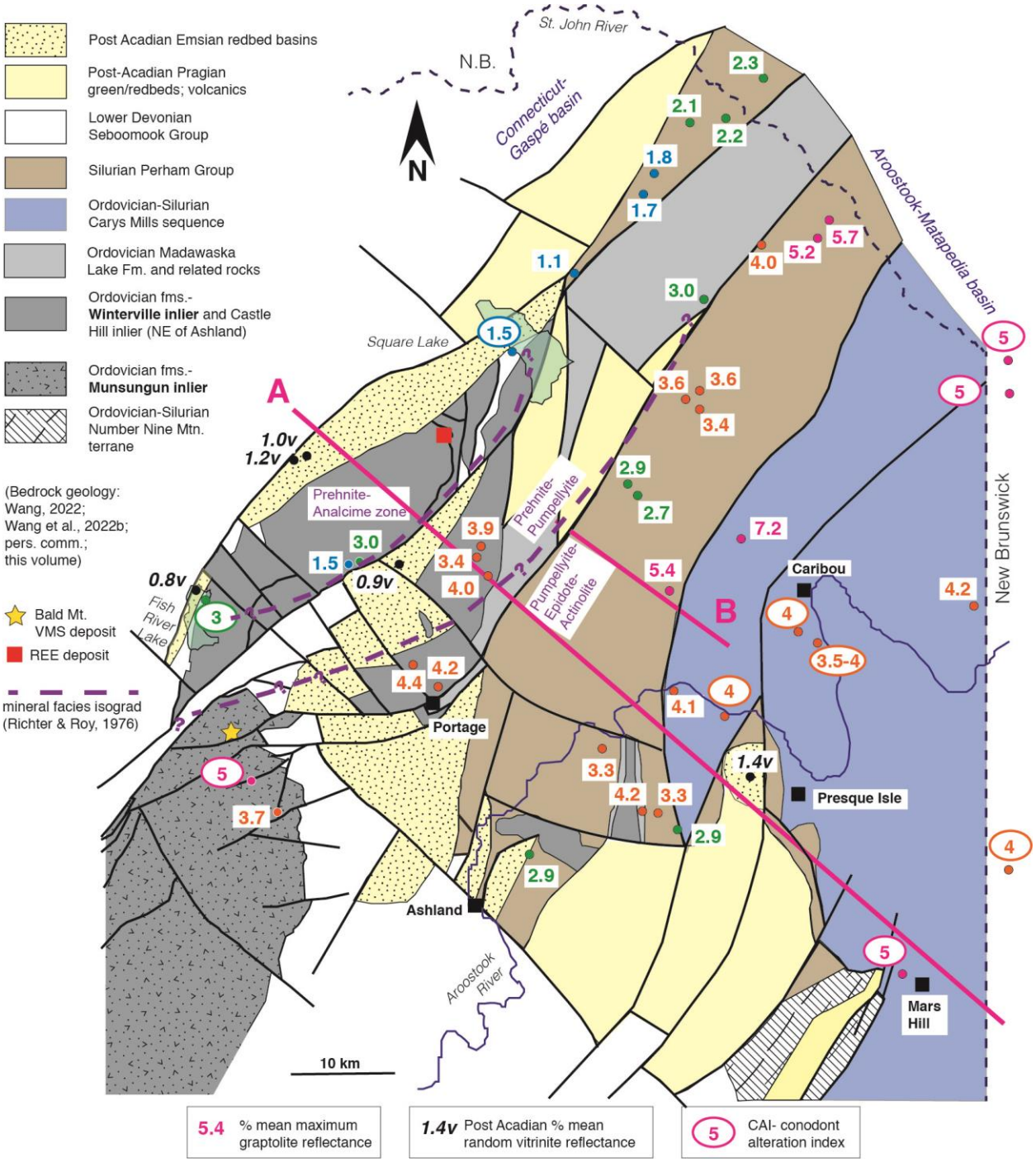

Figure 2. Prehnite-pumpellyite metamorphism isograds, conodont alteration indices (CAI), and graptolite and vitrinite reflectance in northeast Aroostook County. See text for data sources. Colors of data points indicate similar level of metamorphism and correspond to the colored panels in Figure 4, showing correlation of various diagenetic to very-low-grade metamorphic indicators. Cross-section lines A and B, with iso-reflectance contours, in Figure 3.

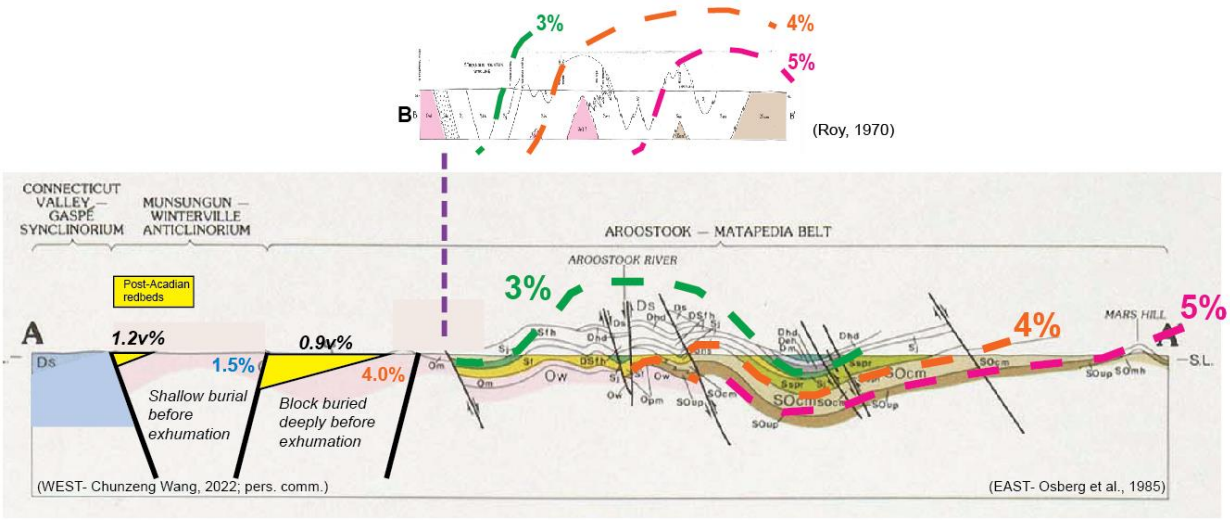

Figure 3. Cross-sections for lines A (south) and B (north) in Figure 2, showing folded iso-reflectance contours in Aroostook-Matapedia basin.

metamorphic grade	mineral facies	coal rank, vitrinite reflectance R_{random}%	conodont alteration index (CAI) (Repetski et al., 2008)	graptolite reflectance $R_{maximum}$% (Malinconico, 1992, 1993, unpubl.)
diagenesis			1	
	zeolite facies	0.6%	1.5	1.1%
		1.3% bituminous coal	2	2.0%
			3	
	prehnite-pumpellyite facies	2.0%		3.0%
very low-grade		semi-anthracite 2.5%		3.5%
	subgreenschist facies		4	
	prehnite-actinolite facies *pumpellyite-actinolite facies*	3.0% anthracite		
		4-5%		5%
			5	~9%
low-grade	greenschist facies	meta-anthracite graphite		

Figure 4. Correlation of NE Maine graptolite reflectance with other diagenetic and very-low-grade metamorphic indicators (Malinconico, 2016): metamorphic grade, mineral facies, coal rank, vitrinite reflectance from the IUGS Subcommission on the Systematics of Metamorphic Rocks (Árkai et al., 2007); general boundaries of zeolite facies to vitrinite reflectance (Kisch, 1981); CAI (conodont alteration index) to vitrinite reflectance (Repetski et al., 2008); mean maximum graptolite reflectance to CAI (see text for NE Maine CAI references) and metamorphic facies (Richter and Roy, 1976) of northern Maine (Malinconico, 1992, 1993, unpublished data). Colored blocks coordinate to data point colors of Figure 2.

Post-Acadian vitrinite (VR). Recent mapping by Chunzeng Wang has importantly identified or reassigned various areas of named and unnamed Lower Devonian formations to the post-Acadian (Early Devonian Pragian and younger) (Wang et al., 2020; Wang et al., 2022b). He has also found new outcrops bearing obvious plant debris. The VR (1.4%) of the post-orogenic Emsian Mapleton Formation near Presque Isle is much lower relative than the enclosing Ordovician-Silurian formations. However, the available post-Acadian VR data at this time, enclosing the western arm of the Winterville inlier, show that those data are similar metamorphic grade (based on correlation chart of Figure 3) to the pre-Acadian GR and CAI there (Figs. 2 and 3A). This indicates little to no erosion of those pre-Acadian Lower Ordovician to lowest Devonian (Lockhovian) formations before post-Acadian Devonian deposition. The mean-random vitrinite reflectance (not contact metamorphosed) of the similar-aged post-Acadian Emsian-Eifelian Trout Valley Formation (Gastaldo, 2016), about 110 km to the south, ranges from 1.4-1.7%.

What temperatures are implied? The minimum metamorphic temperature for the Silurian-Devonian samples at Square Lake (CAI 1.5) and Guerette (1.1% GR), northeast of the western edge of the Winterville inlier would be 80˚C if the rocks were held at maximum temperature until the late Permian, based on kinetic modeling of the equivalent vitrinite reflectance (0.6%) (Sweeney and Burnham, 1990). The minimum temperature of the range for a CAI of 1.5 (50˚C) is not possible since that requires a maximum heating duration of 500 million years (Epstein et al., 1977).

Graptolite and vitrinite reflectance in pre-Acadian formations in the rest of Maine. Although GR data is limited to the south of Mars Hill, they do show a predictable increase towards, and into, the greenschist zone marked by the chlorite isograd on Figure 5. The one isolated VR value, from plant remains in the pre-Acadian Lower Devonian Seboomook Group (mean random reflectance 5.2%) in northwestern Maine, indicates that metamorphic grade also increases to the west of the Winterville-Munsungun inliers. Therefore, the very-low-grade metamorphic rocks along, and northeast of, the western arm of the Winterville inlier, are the least metamorphosed pre-Acadian strata in Maine.

CONCLUSIONS FROM METAMORPHIC TRENDS

- The western limb of the Winterville inlier was not as deeply buried as the eastern arm. Identification of extensive faulting in and around the inlier by Chunzeng Wang (Wang et al., 2022b; pers. comm.), combined with the metamorphic data, suggests the eastern arm ("Portage inlier") was significantly down-faulted before or during the Late Ordovician- Late Silurian infilling of the Aroostook-Matapedia basin to the east. The western limb remained a shallow topographic buttress with limited sedimentary deposition draping over it.
- The general folding of the graptolite iso-reflectance contours in the Late Ordovician-Silurian Aroostook-Matapedia basin (Fig. 3) suggests the maximum reflectance/metamorphism trends are due to deep depositional basin burial ("burial metamorphism"), later folded during Acadian orogenesis (Fig. 3). Appropriate basin depths of ~10 km to produce that level of metamorphism currently exist in the Gulf of Mexico. There should be a transition to the south of Presque Isle/Mars Hill where original sedimentary burial metamorphism is overprinted by higher-grade metamorphism due to tectonic burial.
- The metamorphic contrast between the post-Acadian Lower Devonian Mapleton Formation and adjacent higher-grade pre-Acadian rocks, in the eastern portion of the study area near Presque Isle, indicates an erosive and angular unconformity. However, the similar level of diagenesis/metamorphism of Ordovician to post-Acadian Lower Devonian rocks along the western edge of the Winterville inlier suggests limited but similar maximum depths of burial for all those stratigraphic units. The minimum depth of burial under now-eroded cover strata, based on the very-low-grade metamorphic data here along the western edge of the Winterville inlier and in the post-Acadian Lower Devonian St. Froid Lake Formation is at least 2.5 km, based on comparison with the downhole vitrinite reflectance trend in the deep onshore Hatteras #1 well, North Carolina (geothermal gradient ~25˚C/km) (Malinconico, 2011).
- **Next Questions**: Given that there were a few to several kilometers of now-missing strata over the youngest extant formations, what was that cover? Devonian and/or Carboniferous? Ryan et al. (1993) suggest Carboniferous strata of the Maritimes basin extended across Maine. When was the now-missing cover strata eroded and the current surface exhumed? The closest apatite-fission-track data along strike or structural trend is to the northeast in the Gaspé Peninsula which have cooling ages of 300-260 Ma (Permian) (Pinet and Brake, 2018).

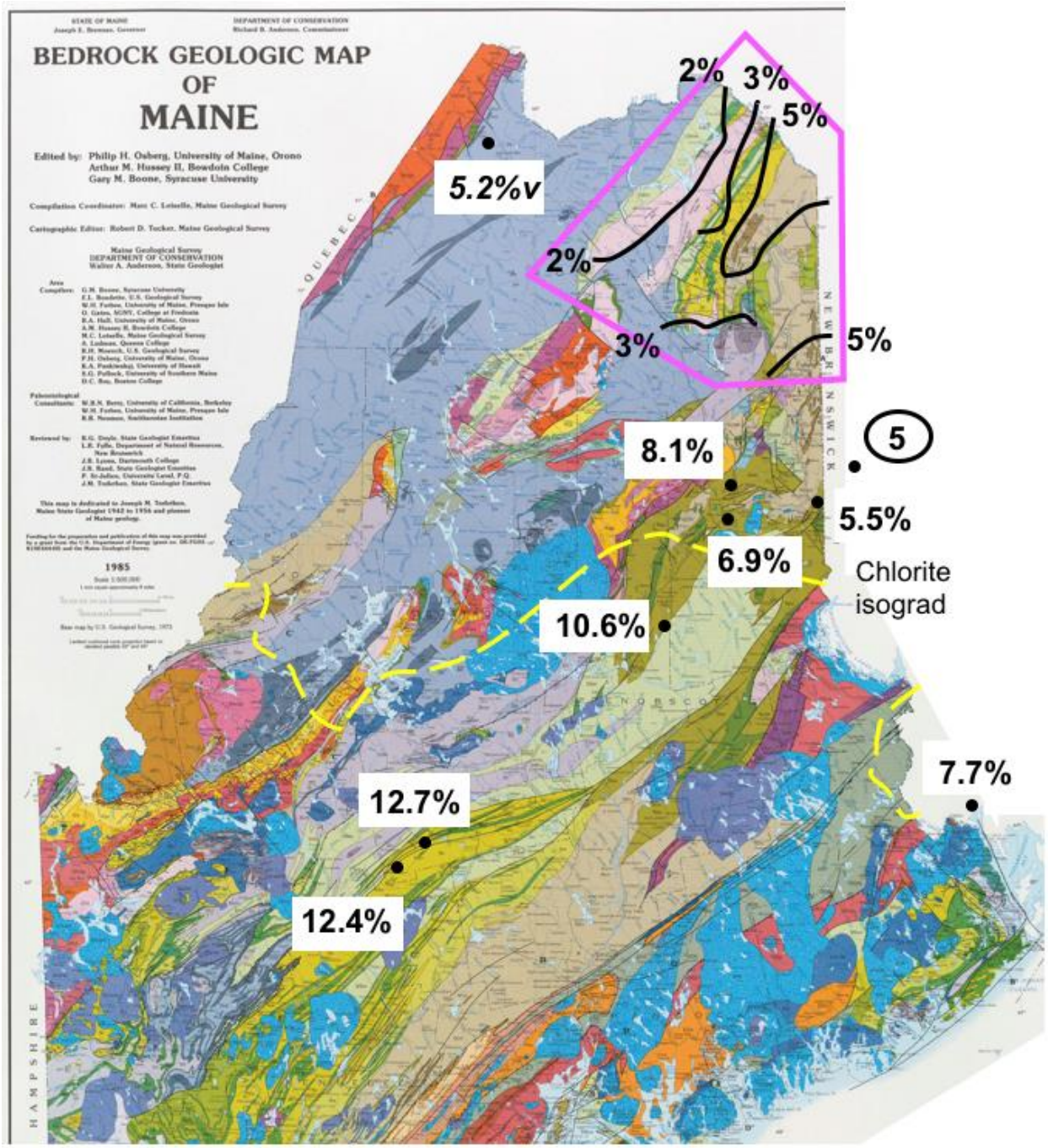

Figure 5. Graptolite (% mean maximum) and vitrinite (% mean random) reflectance in pre-Acadian Ordovician to Lower Devonian (Lockhovian) formations in Maine (base map by Osberg et al., 1985). Data in northeastern Maine, in outlined polygon, are contoured data of Figure 2. Chlorite isograd from subgreenschist-greenschist boundary from Ludman et al. (2020).

ACKNOWLEDGEMENTS

I especially thank David Roy (fossil locality data, great discussions on regional geology) and Bill Forbes (fossil locality information, vehicle loan, trips to a few locales) for their help in the early years of this study. Those who provided samples (mentioned in text) were invaluable, but especially William Berry for access to his entire collection of Maine graptolites; Woody Thompson (Maine Geological Survey) generously served as the contact for delivery of

all the Berkeley sample boxes. Microscope access was generously provided by John C. Crelling (SIU), Susan Rimmer (Kentucky), and Paul Hackley (USGS; Malinconico as visiting scientist succeeding a USGS postdoc). Finally, Chunzeng Wang (UMPI), besides reviewing and providing useful advice on this entry, has generously shared his new maps and structural interpretations which has made the understanding of the metamorphic trends so much more reasonable.

REFERENCES

Árkai, P., Sassi, F., Desmons, J., 2007, Very low- to low-grade metamorphic rocks (Chapter 2.5), in Fettes, D., and Desmons, J., eds., Metamorphic Rocks: A Classification and Glossary of Terms (Recommendations of the International Union of Geological Sciences Subcommission on the Systematics of Metamorphic Rocks): Cambridge, UK, Cambridge University Press, p. 36-42.

Berry, W. B.N., 1964, Early Ludlow graptolites from the Presque Isle quadrangle, Maine: Journal of Paleontology, v. 38, no. 3, p, 587-599.

Bertrand, R., and Malo, M., 2005, Maturation thermique, potentiel roche mère des roches ordoviciennes à dévoniennes du Nord-Ouest du Nouveau-Brunswick (in French): Geological Survey of Canada, Open File 4886, 85 pages and 13 figures.

Boucot, A. J., Field, M. T., Fletcher, R., Forbes, W. H., Naylor, R. S., Pavlides, L., 1964 Reconnaissance bedrock geology of the Presque Isle quadrangle, Maine: Maine Geological Survey (Department of Economic Development), Bulletin 15 (Quadrangle Mapping Series 2), 123 p., illus., geologic maps.

Bradley, D. C., Tucker, R. D., Lux, D.; Harris, A. G., and McGregor, D. C., 2000, Migration of the Acadian orogen and foreland basin across the northern Appalachians of Maine and adjacent areas: U.S. Geological Survey Professional Paper 1624, 49 p.

Burgess, J. D., 1977, Historical review and methods of determining thermal alteration of organic materials: Palynology, v. 1., p. 1-7.

Coombs, D. S., Horodyski, R. J., and Naylor, R. S., 1970, Occurrence of prehnite-pumpellyite facies metamorphism in northern Maine: American Journal of Science, v. 268, p. 142-156.

Epstein, A. G., Epstein, J. B., Harris, L. D., 1977, Conodont color alteration- an index to organic metamorphism: U. S. Geological Survey Professional Paper 995, 27 pages.

Foose, M. P., Slack, J. F., Busby, C. J., Schulz, K. J., Scully, M. V., 2003, Geologic and structural setting of the Bald Mountain volcanogenic massive sulfide deposit, northern Maine: Cu-Sn-Au-Ag mineralization in a synvolcanic sea-floor graben: Economic Geology, Monograph 11, p. 497-512.

Gastaldo, R. A., 2016, New paleontological insights into the Emsian-Eifelian Trout Valley Formation, Baxter State Park's Scientific Forest Management Area, Aroostook County, Maine: Palaios, v. 31, p. 1-8.

Kisch, H. J., 1981, Coal rank and illite crystallinity associated with the zeolite facies of Southland and the pumpellyite-bearing facies of Otago, southern New Zealand: New Zealand Journal of Geology and Geophysics, v. 24, p. 349-360.

Ludman, A., Hopeck, J., Berry, H. N. IV, 2017, Provenance and paleogeography of post-Middle Ordovician, pre-Devonian sedimentary basins on the Gander composite terrane, eastern and east-central Maine: implications for Silurian tectonics in the northern Appalachians: Atlantic Geology, v. 53, p. 63-85.

Ludman, A., Machado, G., Fernandes, P., 2020, Palynological dating of low-grade metamorphosed rocks: Applications to early Paleozoic rocks of the Central Maine/Aroostook-Matapedia basins and Fredericton trough (Northern Appalachians) in eastern and east-central Maine, U.S.A.: American Journal of Science, v. 320, p. 280-312 https://doi.org/10.2475/03.2020.03

Luo, Q., Goodarzi, F., Zhong, N., Wang, Y., Qiu, N., Skovsted, C. B., Suchy, V., Schovsbo, N. H., Morga, R., Xu, Y., Hao, J., Liu, A., Wu, J., Cao, W., Min, X., Wu, J., 2020, Graptolites as fossil geo-thermometers and source material of hydrocarbons: An overview of four decades of progress: Earth-Science Reviews, v. 200, Article 103000. doi:10.1016/j.earscirev.2019.103000

Malinconico, M. L., 1992, Graptolite reflectance in the prehnite- pumpellyite zone, northern Maine, U.S.A.: Organic Geochemistry, v. 18, p. 263-271.

Malinconico, M. L., 1993, Reflectance cross-plot analysis of graptolites from the anchi-metamorphic region of northern Maine, USA: Organic Geochemistry, v. 20, p. 197-207.

Malinconico, M. L., 2011, Thermal maturity of the U. S. Atlantic Coastal Plain, Maryland to North Carolina, based on legacy exploration and stratigraphic test wells (abs.): American Association of Petroleum Geologists Eastern Section Meeting Program, Arlington, Virginia, September 25-27, 2011. (https://www.searchanddiscovery.com/abstracts/pdf/2011/eastern/abstracts/ndx_malinconico.pdf)

Malinconico, M. L., 2016, Graptolite reflectance and correlation with other diagenetic and very-low-grade metamorphic indicators: http://carbonacea.blogspot.com/2016/05/graptolite-reflectance-and-correlation.html (updated November 2020; accessed April 2022).

Malinconico, M. L., 2022, Trends of very-low-grade metamorphism in the Aroostook-Matapedia belt of northeastern Maine (Aroostook County) using graptolite and vitrinite reflectance: Geological Society of America Abstracts with Programs, v. 54, no. 3, doi: 10.1130/abs/2022NE-374568

Nowlan, G. S., Barnes, C. R., 1987, Thermal maturation of Paleozoic strata in eastern Canada from Conodont Colour Alteration Index (CAI) data with implications for burial history, tectonic evolution, hotspot tracks and mineral and hydrocarbon exploration: Geological Survey of Canada, Bulletin 367, 47 pages, https://doi.org/10.4095/122453.

Osberg, P. H., Hussey, A. M., II, and Boone, G. M. (editors), 1985, Bedrock geologic map of Maine: Maine Geological Survey, scale 1:500,000.

Pavlides, L., 1978, Bedrock geologic map of the Mars Hill quadrangle and vicinity, Aroostook County, Maine: U.S. Geological Survey Miscellaneous Investigations Series, Map I-1064.

Pinet, N., and Brake, V., 2018, Preliminary compilation of apatite fission-track data in Canada: Geological Survey of Canada, Open File 8454, 1 poster. https://doi.org/10.4095/308442

Rejebian, V. A., Harris, A. G., and Huebner, J. S., 1987, Conodont color and textural alteration: an index to regional metamorphism, contact metamorphism, and hydrothermal alteration: Geological Society of America Bulletin, v. 99, p. 471-479.

Repetski, J. E., Ryder, R. T., Weary, D. J., Harris, A. G, and Trippi, M. H., 2008, Thermal maturity patterns (CAI and $\%R_o$) in Upper Ordovician and Lower-Middle Devonian rocks of the Appalachian basin: A major revision of USGS Map I-917-E using new subsurface collections: U.S. Geological Survey Scientific Investigations Map 3006, one CD-ROM.

Richter, D. A., and Roy, D. C., 1974, Sub-greenschist metamorphic assemblages in northern Maine: Canadian Mineralogist, v. 12, p. 469-472.

Richter, D. A., and Roy, D. C., 1976, Prehnite-pumpellyite facies metamorphism in central Aroostook County, Maine, *in* Lyons, P. C., and Brownlow, A. H., eds., Studies in New England geology: Geological Society of America Memoir 146, p. 239-261.

Rickards, R. B., and Riva, J., 1981, *Glyptograptus? persculptus* (Salter), its tectonic deformation, and its stratigraphic significance for the Carys Mills Formation of N. E. Maine, USA: Geological Journal, v. 16, p. 219-235.

Roy, D. C., 1970, The Silurian of Northeastern Aroostook County, Maine [Ph.D. dissertation]: Cambridge, Massachusetts, Massachusetts Institute of Technology, 485 pages. (https://dspace.mit.edu/handle/1721.1/44448)

Ryan, R. J., and Zentilli, M., 1993, Allocyclic and thermochronological constraints on the evolution of the Maritimes Basin of eastern Canada: Atlantic Geology, v. 29, p. 187-197.

Slack, J., Flohr, M. J. K., Scully, M. V., 1997, Hypogene mineralogy and paragenesis of the Bald Mountain massive sulfide deposit, Aroostook County, Maine: U. S. Geological Survey, Open File Report, 97-746, 29 pages.

Sweeney, J. J. and Burnham, A. K., 1990, Evaluation of a simple model of vitrinite reflectance based on chemical kinetics: American Association of Petroleum Geologists Bulletin, v. 74, p. 1559-70.

Walker, J. R., 1989, Polytypism of chlorite in very low-grade metamorphic rocks: American Mineralogist, v. 74, p. 738-743.

Wang, C., 2022, Bedrock geology of the Fish River Lake quadrangle, Maine: Maine Geological Survey, Geologic Map 22-5, scale 1:24,000.

Wang, C., Marvinney, R., Putnam, D., Bagley, E., Belair, S., 2020, The newly discovered, giant Fish River post-Acadian rift system in the northern Appalachians of Maine: Geological Society of America Abstracts with Programs, v. 52, no. 6, doi: 10.1130/abs/2020AM-356952.

Wang, C., Marvinney, R., Whittaker, A. H., Pollock, S. G., Putnam, D., 2022a, Advances in understanding the complex and protracted tectonic and deformational history of the Munsungun-Winterville belt in the Maine Appalachians: Geological Society of America Abstracts with Programs, v. 54, no. 3, doi: 10.1130/abs/2022NE-374935

Wang, C., Slack, J., Shah, A. K., Yates, M. G., Lentz, D. R., Whittaker, A. T. H., Marvinney, R. G., 2022b, A recently discovered trachyte-hosted rare earth element-niobium-zirconium occurrence in northern Maine, USA: Economic Geology, doi:10.5382/econgeo.4993

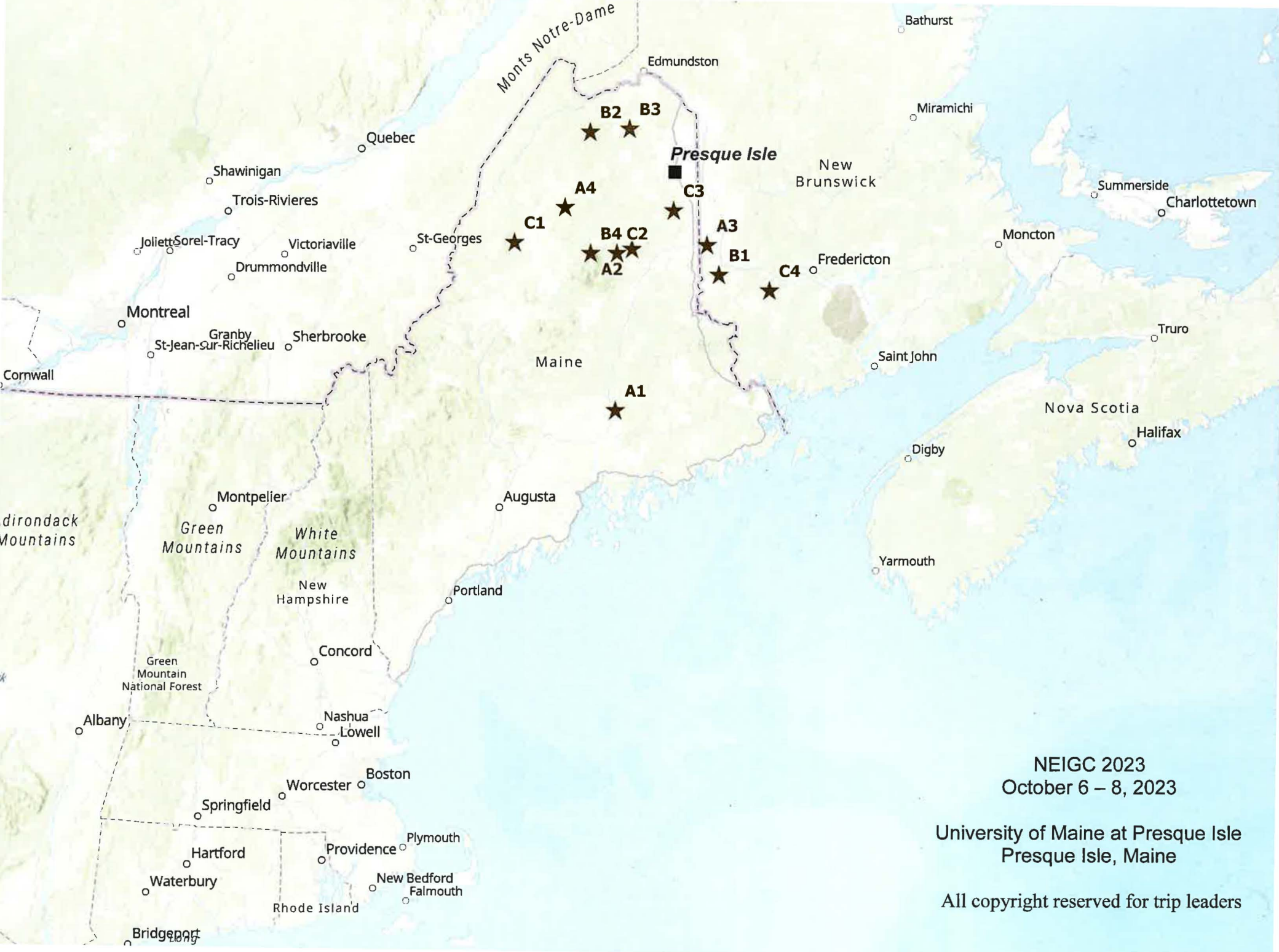

NEIGC 2023
October 6 – 8, 2023

University of Maine at Presque Isle
Presque Isle, Maine